Aus dem Adolf-Butenandt-Institut
der Ludwig-Maximilians-Universität München
Vorstand: Prof. Dr. rer. nat. Dr. h. c. Christian Haass
Lehrstuhl: Stoffwechselbiochemie

STRESS GRANULE RECRUITMENT AND DEPOSITON OF PROTEINS OF THE FET FAMILY AND TDP-43 IN ALS AND FTD

Dissertation zum Erwerb des Doktorgrades der Naturwissenschaften an der Medizinischen Fakultät der Ludwig-Maximilians-Universität München

Vorgelegt von
Eva Brigitte Elisabeth Bentmann

2013

Gedruckt mit Genehmigung der Medizinischen Fakultät
der Ludwigs-Maximilians-Universität München

Dissertation eingereicht am 22. Oktober 2013

Betreuer:	Prof. Dr. rer. nat. Dr. h.c. Christian Haass
Zweitgutachter:	Prof. Dr. rer. nat. Michael Kiebler
Dekan:	Prof. Dr. med. Dr. h.c. Maximilian Reiser, FACR, FRCR

Tag der mündlichen Prüfung: 20. März 2014

Eidesstattliche Versicherung

Ich erkläre hiermit an Eides statt, dass ich die vorliegende Dissertation selbstständig verfasst, mich außer der angegebenen keiner weiteren Hilfsmittel bedient und alle Erkenntnisse, die aus dem Schrifttum ganz oder annähernd übernommen sind, als solche kenntlich gemacht und nach ihrer Herkunft unter Bezeichnung der Fundstelle einzeln nachgewiesen habe.

Ich erkläre des Weiteren, dass die hier vorgelegte Dissertation nicht in gleicher oder ähnlicher Form bei einer anderen Stelle zur Erlangung eines akademischen Grades eingereicht wurde.

München, den 22. Oktober 2013

(Eva Bentmann)

Meinen Eltern und meiner Oma

Table of content

Summary

Neurodegenerative diseases such as Alzheimer´s disease, amyotrophic lateral sclerosis (ALS) and frontotemporal dementia (FTD) are defined by progressive and selective loss of neurons. With increasing age the risk of developing a neurodegenerative disease exponentially rises. To date these diseases are untreatable, imposing a significant medical, social and financial burden onto our ageing society. Typical features of neurodegenerative diseases are abnormal aggregation of a disease characterizing protein and its deposition in pathological inclusions. A unifying feature in the majority of ALS cases and several subtypes of FTD is the pathological deposition of the TAR DNA-binding protein of 43kDa (TDP-43) or the Fused in Sarcoma (FUS) protein. Furthermore, stress granule (SG) marker proteins are consistently detected in FUS inclusions, suggesting that SGs might be involved in the formation of FUS inclusions. However, whether pathologic TDP-43 inclusions contain SG marker proteins is still controversially discussed.

In this thesis I demonstrate that cytosolically mislocalized full-length TDP-43 is recruited into SGs, whereas C-terminal fragments of TDP-43 (TDP-CTFs) fail to localize to SGs. In accordance with these cell culture data, spinal cord inclusions in ALS and FTD patients contain full-length TDP-43 and SG marker proteins. In contrast, hippocampal inclusions are enriched for TDP-CTFs but are SG marker-negative. Thus, the protein composition of TDP-43 inclusions determines whether SG marker proteins are co-deposited in TDP-43 inclusions or not. By analyzing the prerequisites for SG recruitment of TDP-43 and FUS, I demonstrate that cytosolic mislocalization of TDP-43 and FUS is required for their localization in SGs. Additionally, I found that both proteins have the same requirements for SG recruitment, as their main RNA-binding domain and a glycine-rich domain are essential for SG localization.

A detailed analysis of the protein composition of FUS inclusions in ALS and FTD cases unveiled that FUS inclusions in FTD cases contain not only FUS, but all FET (FUS, Ewing sarcoma protein (EWS), TATA binding protein-associated factor 15 (TAF15)) family proteins. Here, I provide evidence that this cytosolic deposition of FET proteins can be mimicked in cultured cells by inhibition of Transportin-mediated nuclear import, which causes cytosolic mislocalization of all FET proteins and recruitment of these proteins in SGs. In contrast to FTD cases, FUS inclusions in ALS cases contain only FUS, but not EWS and TAF15. In line with that, I show that ALS-

associated *FUS* mutations result in cytosolic mislocalization of FUS that is upon subsequent cellular stress sequestered into SGs. These SGs then contain only FUS but not EWS or TAF15, demonstrating that mutant FUS is unable to co-sequester EWS or TAF15.

In addition, I contributed to two studies that revealed that nuclear import defects are involved in the pathogenesis of ALS and FTD. ALS associated *FUS* mutations are frequently located within the proline-tyrosine nuclear localization signal (PY-NLS) of FUS and thus disrupt Transportin-mediated nuclear import and cause cytosolic mislocalization of FUS. EWS and TAF15 also contain a PY-NLS and thus are imported into the nucleus via Transportin. This interaction between Transportin and FET proteins can be modulated by arginine methylation that reduces Transportin binding. In FTD patients with FUS inclusions, this post-translational modification seems to be defective, as FUS inclusions in these cases contain hypomethylated FUS.

Taken together, these data provide evidence that nuclear import defects and sequestration of FUS and TDP-43 in SGs are consecutive steps in the pathogenesis of ALS and several subtypes of FTD.

Zusammenfassung

Neurodegenerative Erkrankungen wie die Alzheimer-Erkrankung, die Amyotrophe Lateralsklerose (ALS) und die Frontotemporale Demenz (FTD) sind durch den progressiven und selektiven Verlust von Neuronen gekennzeichnet. Mit steigendem Alter nimmt das Risiko eine neurodegenerative Erkrankung zu entwickeln exponentiell zu. Bislang gelten diese Krankheiten als nicht behandelbar, was eine signifikante medizinische, soziale und finanzielle Belastung für unsere alternde Gesellschaft darstellt. Typische Charakteristika neurodegenerativer Erkrankungen sind die abnormale Aggregation eines Krankheits-assoziierten Proteins, sowie dessen Anhäufung in pathologischen Ablagerungen. Gemeinsames Merkmal der meisten ALS Fälle und bestimmter Untergruppen von FTD sind pathologische Ablagerungen, die hauptsächlich das TAR DNA-binding protein of 43kDa (TDP-43) oder das Fused in Sarcoma (FUS) Protein enthalten. In FUS Ablagerungen werden stets auch Markerproteine für Stress-Körnchen (engl. *stress granules*, SG) detektiert, was darauf schließen lässt, dass SGs an der Bildung von FUS Ablagerungen beteiligt sein könnten. Bei pathologischen TDP-43 Ablagerungen ist hingegen immer noch umstritten ob diese SG Markerproteine enthalten.

In der vorliegenden Arbeit konnte ich zeigen, dass zytosolisch mislokalisiertes, unfragmentiertes TDP-43 in SGs rekrutiert wird, wohingegen C-terminale Fragmente von TDP-43 (TDP-CTFs) nicht in SGs lokalisieren. Diese Ergebnisse stimmen mit den Beobachtungen in ALS und FTD Patienten überein, wo TDP-43 Ablagerungen im Rückenmark unfragmentiertes TDP-43 und SG Markerproteine enthalten. Im Gegensatz dazu sind hippocampale Ablagerungen mit TDP-CTFs angereichert, enthalten jedoch keine SG Marker. Die Proteinzusammensetzung der TDP-43 Ablagerungen bestimmt also, ob SG Markerproteine darin abgelagert werden oder nicht. Bei der Bestimmung von Voraussetzungen für die Rekrutierung von TDP-43 und FUS in SGs konnte ich feststellen, dass eine zytosolische Umverteilung notwendig ist, damit TDP-43 und FUS in SGs sequestriert werden können. Des Weiteren konnte ich zeigen, dass beide Proteine ihre Haupt-RNA-bindende Domäne, sowie die Glycin-reiche Domäne für die Lokalisierung in SGs benötigen.

Eine detaillierte Analyse der Proteinzusammensetzung von FUS Ablagerungen in ALS und FTD hat aufgedeckt, dass FUS Ablagerungen in FTD-Patienten nicht nur

FUS, sondern alle FET (FUS, Ewing sarcoma protein (EWS), TATA binding protein-associated factor 15 (TAF15)) Familienproteine beinhalten. Ich konnte zeigen, dass diese cytosolische Ablagerung von FET Proteinen in Zellkultur durch eine Hemmung des Transportin-vermittelten Kerntransports nachgestellt werden kann, da dies zur zytosolischen Anhäufung aller FET Proteine und deren Rekrutierung in SGs führt. Im Gegensatz zu FTD Fällen enthalten FUS Ablagerungen in ALS nur FUS, nicht aber EWS und TAF15. In Zellkultur-Experimenten konnte ich zeigen, dass ALS-assoziierte *FUS* Mutationen zur zytosolischen Umverteilung von FUS führen, welches dann durch nachfolgenden zellulären Stress in SGs rekrutiert wird. Diese SGs enthalten FUS, jedoch nicht EWS oder TAF15, was beweist, dass mutiertes FUS nicht wildtypisches EWS oder TAF15 sequestrieren kann.

Darüber hinaus habe ich an zwei Publikationen mitgearbeitet, in denen gezeigt wurde, dass Defekte im Kernimport an der Pathogenese von ALS und FTD beteiligt sind. ALS-assoziierte *FUS* Mutationen sind häufig im Prolin-Tyrosin Kernlokalisierungs-Signal (PY-NLS) lokalisiert und zerstören so den Transportin-vermittelten Kernimport und führen zur zytosolischen Misslokalisierung von FUS. EWS und TAF15 enthalten ebenfalls ein PY-NLS und werden daher über Transportin in den Kern importiert. Die Interaktion zwischen Transportin und den FET Proteinen kann durch Arginin-Methylierung moduliert werden, welche die Transportin-Bindung reduziert. In FTD Patienten mit FUS Ablagerungen scheint diese post-translationale Modifikation gestört zu sein, da FUS Ablagerungen in diesen Fällen hypomethyliertes FUS enthalten.

Diese Daten liefern Beweise dafür, dass Defekte im Kernimport und die Sequestrierung von FUS und TDP-43 in SGs aufeinanderfolgende Schritte in der Pathogenese von ALS und verschiedenen Varianten von FTD sind.

1 Introduction

Neurodegenerative diseases are characterized by progressive neuronal dysfunction and selective loss of neurons. During neurodegeneration structural changes in different proteins impair the function of neurons and eventually result in neuronal cell death. Characteristic features of neurodegenerative diseases such as Alzheimer´s disease, Parkinson´s disease, Amyotrophic lateral sclerosis (ALS) and Frontotemporal dementia (FTD) are aberrant protein aggregates. These aggregates are reminiscent of prion aggregates as they contain misfolded proteins, seed aggregation *in vitro* and *in vivo,* and spread within and/or among brain regions (Goedert et al., 2010; Jucker and Walker, 2013). Furthermore, proteins aggregating in neurodegenerative diseases often contain domains that are under physiological conditions unfolded but aggregation-prone once aggregation is seeded and are hence termed as "prion-like" (Cushman et al., 2010; King et al., 2012). However, in contrast to the prion protein (Prp) these proteins are not infectious. The identification of the aggregated protein(s) in the different neurodegenerative diseases has marked a breakthrough in these fatal disorders as this provided further insight into underlying pathomechanisms (Haass and Selkoe, 2007). Accordingly, the identification of the RNA-binding proteins TDP-43 or FUS, which both contain a prion-like domain, as major component of pathological aggregates in the majority of ALS- and FTD-patients has been a seminal discovery (Arai et al., 2006; Neumann et al., 2006; Neumann et al., 2009a).

1.1 ALS and FTD – related diseases sharing molecular pathology and genetics

ALS and FTD are related neurodegenerative diseases with overlapping clinical phenotypes, pathology and genetics. ALS, also known as Lou Gehrig´s disease, is an incurable disease caused by selective degeneration of upper and lower motor neurons. Due to decreased innervation, muscles progressively weaken and ALS patients develop restrictions in motion, swallowing, speaking, and breathing. Between 1 and 5 years after disease onset, respiratory failure and infections weaken the patient and increase the vulnerability to pneumonia, which then usually causes death (Mackenzie et al., 2010; Kiernan et al., 2011). Approximately 5-10% of ALS are inherited and classified as

familial ALS (fALS), whereas in the vast majority no family history of ALS is documented (sporadic ALS, sALS) (Kiernan et al., 2011).

FTD is the second most common presenile dementia after Alzheimer's disease (Pan and Chen, 2013). The related term Frontotemporal lobar degeneration (FTLD) describes the neuropathological features of FTD (in the following text FTLD is used to designate both, disease and neuropathology), as the disease is characterized by an atrophy of the frontal and temporal cerebral lobes (Pan and Chen, 2013). These brain regions regulate behavior and cognitive functions and thus FTLD patients can exhibit apathy, disinhibition, lack of empathy and/or language dysfunction (McKhann et al., 2001; Snowden et al., 2002; Pan and Chen, 2013). Swallowing difficulties and loss of personal hygiene facilitate infections and pneumonia, ultimately leading to death due to respiratory failure after 4 to 14 years on average (Garcin et al., 2009; Kiernan et al., 2011). About 60% of FTLD patients have a family history of the disease and the remaining FTLD cases are sporadic (Pan and Chen, 2013).

Interestingly, ALS and FTLD seem to be related, as frequently patients present overlapping phenotypes (Robberecht and Philips, 2013). About half of the ALS patients display at least mild cognitive and behavioral changes during disease progression (Ringholz et al., 2005; Consonni et al., 2013). In addition, about 30% of patients with FTLD exhibit some features of motor neuron dysfunction or even concomitant ALS symptoms (Lomen-Hoerth et al., 2002; Burrell et al., 2011). These overlapping phenotypes indicate that ALS and FTLD form a disease continuum with pure forms of ALS and FTLD at the extreme ends and overlapping phenotypes in between (Table 1).

1.1.1 Molecular pathology and genetics of ALS and FTLD

Over the last decade, important discoveries in the neuropathology and genetics of ALS and FTLD have started to reveal the molecular basis for this clinical overlap. ALS and FTLD are categorized in different subtypes depending on the major aggregated protein in the pathological inclusions (Table 1). In most ALS patients TAR DNA-binding protein of 43 kDa (TDP-43) or Superoxide dismutase 1 (SOD1) inclusions are detected. The vast majority of patients with an overlapping ALS/FTLD phenotype present inclusions containing TDP-43 and dipeptide repeat (DPR) proteins, which are translated from an associated repeat expansion in the *C9orf72* gene (Dejesus-Hernandez et al., 2011; Renton et al., 2011; Mori et al., 2013). In FTLD, about 40% of the patient show ubiquitin-negative, Tau-positive inclusions (Joachim et al., 1987; Pan and Chen, 2013).

The remaining 60% of the FTLD cases have ubiquitin-positive inclusions (Mackenzie and Rademakers, 2007). Most of these cases contain either TDP-43 (Neumann et al., 2006) or FET (FUS, Ewing sarcoma protein (EWS), TATA-binding protein associated factor 15 (TAF15)) proteins in pathological inclusions (Munoz et al., 2009; Neumann et al., 2009a; Brelstaff et al., 2011; Neumann et al., 2011). Moreover, in a small proportion of FTLD cases with ubiquitin- and p62-positive inclusions the deposited protein remains to be identified. In my thesis I concentrated on TDP-43 and FUS. Further details on the pathomechanisms of Superoxide dismutase 1 (SOD1) (Ilieva et al., 2009), C9orf72 (Ling et al., 2013), microtubule associated protein Tau (MAPT) (Spillantini and Goedert, 2013), Progranulin (PGRN) (Sieben et al., 2012), Valosin-containing protein (VCP) (Sieben et al., 2012) and charged multivesicular body protein 2B (CHMP2B) (Sieben et al., 2012) are described in several recent review articles.

In most ALS patients the major component of the neuronal, cytosolic ubiquitin-positive inclusions is TDP-43 (Fig. 1, first panel) and these cases are termed ALS-TDP (Table 1) (Arai et al., 2006; Neumann et al., 2006). Additionally, TDP-43- and ubiquitin-positive inclusions were found in about 50% of FTLD patients (FTLD-TDP, Table 1; Fig.1, second panel) (Arai et al., 2006; Neumann et al., 2006) and ALS-TDP and FTLD-TDP are also referred to as TDP-proteinopathies. Specific biochemical characteristics of TDP-43 inclusions include hyperphosphorylation and ubiquitination of deposited TDP-43 and the accumulation of C-terminal fragments of TDP-43 (TDP-CTFs) in hippocampal TDP-43 inclusions (Lee et al., 2012). TDP-CTFs can arise by caspase-cleavage of full-length TDP-43 (Zhang et al., 2007; Dormann et al., 2009) or could reflect an alternative splicing product or a cryptic transcription start (Nishimoto et al., 2010; Lee et al., 2012). The identification of TDP-43 pathology in ALS and FTLD patients motivated screening for disease-associated mutations in *TARDBP*, the gene encoding TDP-43. To date, over 40 *TARDBP* mutations have been identified, mainly in ALS patients and very rarely in FTLD patients (Table 1) (Gitcho et al., 2008; Kabashi et al., 2008; Sreedharan et al., 2008; Van Deerlin et al., 2008; Robberecht and Philips, 2013)

Table 1. Revised classification of ALS and FTLD

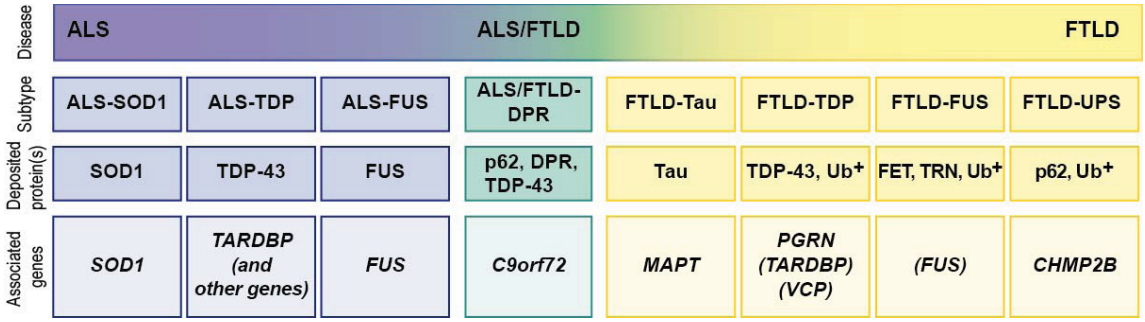

ALS (blue) and FTLD (yellow) are shown as the extreme ends of a disease continuum with ALS/FTLD (green) as overlapping phenotype. Both diseases are divided into different clinical subtypes depending on the deposited protein. Gene mutations associated with the different subtypes are indicated in italic and mutations only detected in rare cases are indicated in parenthesis. Mutations in the *SOD1* gene resulting in SOD1 inclusions were the first mutations found to be associated with fALS (Rosen et al., 1993). In most ALS patients TDP-43-positive inclusions are detected (Neumann et al., 2006) and can arise sporadically or can be caused by mutations in *TARDBP*, the gene encoding TDP-43, (Gitcho et al., 2008; Kabashi et al., 2008; Sreedharan et al., 2008; Van Deerlin et al., 2008) or other genes. FUS inclusions in ALS patients are caused by mutations in *FUS* (Kwiatkowski et al., 2009; Vance et al., 2009). In the vast majority of families with ALS-FTLD an abnormal repeat expansion in the *C9orf72* gene was identified (Dejesus-Hernandez et al., 2011; Renton et al., 2011) which is translated into dipeptide-repeat (DPR) proteins (Mori et al., 2013) that are deposited in ALS/FTLD-DPR patients. In FTLD, mutations in the *MAPT* gene result in FTLD with Tau-positive, ubiquitin-negative inclusions (Hutton et al., 1998). The majority of FTLD patients have ubiquitin-positive inclusions (Pan and Chen, 2013) and in about 80 – 90% of these patients TDP-43 is the major constituent of these inclusions (FTLD-TDP) (Neumann et al., 2006). FTLD-TDP can occur sporadically or can be caused by mutations in *PGRN* (Baker et al., 2006; Cruts et al., 2006) or rarely in *TARDBP* (Van Deerlin et al., 2008; Kovacs et al., 2009) or *VCP* (Watts et al., 2004). In about 10-20 % of the FTLD patients with ubiquitin-positive inclusions, FUS, EWS and TAF15 (FET proteins) are deposited together with Transportin (TRN) (Munoz et al., 2009; Neumann et al., 2009a; Brelstaff et al., 2011; Neumann et al., 2011; Troakes et al., 2013) and mutations in FUS are only rarely found in these patients (Van Langenhove et al., 2010; Van Langenhove et al., 2012). In addition, rare cases of FTLD are genetically linked to mutations in the *CHMP2B* gene (Skibinski et al., 2005) and pathological inclusions contain components of the ubiquitin-proteasome system (ubiquitin and p62,(FTLD-UPS)) (Holm et al., 2007). Table modified from (Dormann and Haass, 2013).

In 2009, FUS was found in pathological inclusions in rare cases of ALS (ALS-FUS, Table 1) (Kwiatkowski et al., 2009; Vance et al., 2009) and FTLD (FTLD-FUS, Table 1) (Munoz et al., 2009; Neumann et al., 2009a; Neumann et al., 2009b) that do not contain TDP-43 or SOD1 in pathological inclusions (Fig. 1, right panels). ALS-FUS and FTLD-FUS are together referred to as FUS-proteinopathies. Like TDP-43, FUS is a DNA/RNA-binding protein and mutations in the *FUS* gene are predominantly found in ALS patients (Kwiatkowski et al., 2009; Vance et al., 2009) and rarely in FTLD patients (Table 1) (Van Langenhove et al., 2010; Van Langenhove et al., 2012), indicating that mutations in TDP-43 or FUS cause ALS rather than FTLD. Recent analysis determining

the composition of pathological FUS inclusions revealed that FUS inclusions in FTLD-FUS also contain EWS and TAF15 (Table 1) (Neumann et al., 2011; Davidson et al., 2013). In contrast, ALS-FUS cases are negative for EWS and TAF15, thereby suggesting that ALS-FUS and FTLD-FUS might be caused by different pathomechanisms (Neumann et al., 2011).

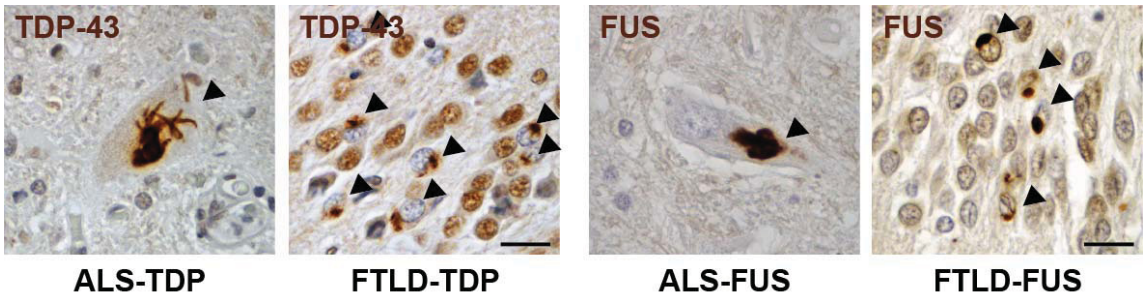

Fig. 1. Cytoplasmic TDP-43 and FUS inclusions in ALS and FTLD patients. The characteristic ubiquitinated TDP-43-inclusions are frequently observed in spinal cord motor neurons in ALS-TDP and in dentae granule cells in the hippocampus of FTLD-TDP cases (left panels). FUS inclusions are detected in motor neurons of ALS-FUS cases with *FUS* mutations and rarely in FTLD-FUS (right panels). Note the larger size of motor neurons compared to dentae granules cells in the hippocampus. Arrowheads mark cells with TDP-43 or FUS inclusions. Scale bar: 20µm. Figure adapted from (Dormann and Haass, 2011).

1.2 TDP-43 - DNA/RNA-binding protein with pivotal roles in neurodegeneration

TDP-43 was originally identified as a transcriptional repressor that binds to the TAR regulatory element in the HIV long terminal repeat (Ou et al., 1995). However, the identification of TDP-43 inclusions in FTLD patients and in the majority of ALS patients (Arai et al., 2006; Neumann et al., 2006), together with the association of *TARDBP* mutations in ALS (Gitcho et al., 2008; Kabashi et al., 2008; Sreedharan et al., 2008; Van Deerlin et al., 2008) dramatically increased the interest in this protein.

1.2.1 Role of TDP-43 in RNA metabolism

TDP-43 is a predominantly nuclear protein with multiple functions in RNA metabolism (Winton et al., 2008a; Buratti and Baralle, 2012). Several splicing factors such as members of the heterogeneous nuclear ribonucleoprotein (hnRNP) family (Buratti et al., 2005; Freibaum et al., 2010), Survial of motorneuron (SMN) (Tsuiji et al., 2013) and other proteins involved in splicing (Elden et al., 2010; Freibaum et al., 2010; Ling et al., 2010) interact with TDP-43. Moreover, the interaction between TDP-43 and SMN is

essential for SMN-containing nuclear Gem bodies and proper levels of U-rich small nuclear ribonucleoproteins (U snRNPs), which are central components of the spliceosome (Tsuiji et al., 2013).

TDP-43 binds about one third of the total transcriptome (Ling et al., 2013) and RNA targets of TDP-43 have been identified in mouse brain (Polymenidou et al., 2011), human brain (Tollervey et al., 2011), primary neurons (Sephton et al., 2011) and cell lines (Xiao et al., 2011; Colombrita et al., 2012). Additionally, splicing pattern changes in thousands of specific targets upon depletion of TDP-43 in adult mouse brains (Polymenidou et al., 2011) support the notion that TDP-43 is an essential regulator of RNA processing. TDP-43 can affect alternative splicing positively as it promotes for example exon skipping in Cystic fibrosis transmembrane conductance regulator (CFTR) mRNA (Buratti and Baralle, 2001; Buratti et al., 2001) and negatively as it inhibits splicing of the human splicing factor SC35 mRNA (Dreumont et al., 2010). In neurons, TDP-43 is part of a protein complex that is involved in alternative splicing of mRNAs associated with synapse formation, neuronal development and RNA metabolism (Sephton et al., 2011; Tollervey et al., 2011; Colombrita et al., 2012). Besides its role in mRNA splicing, TDP-43 modifies mRNA stability of several mRNA such as HDAC 6 (Fiesel et al., 2010), NFL (Strong et al., 2007) and others (Ayala et al., 2008a; Colombrita et al., 2012), including its own mRNA (see below).

1.2.2 Autoregulation of TDP-43

As TDP-43 is such an essential regulator of RNA metabolism, its own levels have to be accurately controlled. Therefore, TDP-43 controls its own mRNA stability via a negative feedback mechanism, which involves binding of TDP-43 to its own 3´UTR, resulting in TDP-43 mRNA instability and degradation (Ayala et al., 2011; Polymenidou et al., 2011; Sephton et al., 2011; Tollervey et al., 2011). This autoregulatory mechanism, which ensures proper levels of TDP-43, is also observed in TDP-43 animal models. Heterozygous TDP-43 knockout mice increase mRNA levels of the remaining TDP-43 allele to compensate for the loss of one allele and have similar TDP-43 levels as their wildtype littermates (Kraemer et al., 2010; Sephton et al., 2010; Wu et al., 2010).

1.2.3 Cytosolic functions of TDP-43

Although TDP-43 is a nuclear protein, it undergoes nucleocytoplasmic shuttling (Ayala et al., 2008b; Winton et al., 2008a). In the cytoplasm, TDP-43 interacts with stress

granule (SG) proteins (Freibaum et al., 2010) and in neurons it is detected in neuronal RNA transport granules (Elvira et al., 2006; Wang et al., 2008; Fallini et al., 2012). Upon neuronal activity TDP-43 is enriched within RNA transport granules, suggesting a role of TDP-43 in RNA transport and local translation at the synapse (Wang et al., 2008; Liu-Yesucevitz et al., 2011). Moreover, increased levels of TDP-43 impair axonal outgrowth (Fallini et al., 2012), which is in line with the notion that TDP-43 has several RNA targets that are essential for neuronal development (Tollervey et al., 2011; Colombrita et al., 2012).

1.2.4 Animal models of TDP-43

Overexpression of TDP-43 in several animal models, such as worms (Ash et al., 2010; Liachko et al., 2010), flies (Hanson et al., 2010; Li et al., 2010; Voigt et al., 2010), zebrafish (Kabashi et al., 2010), rats (Zhou et al., 2010) and mice (Tatom et al., 2009; Wegorzewska et al., 2009; Tsai et al., 2010; Wils et al., 2010; Xu et al., 2010) is not tolerated and results in neurodegeneration and reduced life span. Nevertheless, in most of these animal models wildtype TDP-43 is neurotoxic and sometimes wildtype TDP-43 has a more severe phenotype than TDP-43 mutants (Voigt et al., 2010). These models, however, only partially recapitulate the disease, as no gene duplication mutations have been found in ALS patients. Interestingly, when human TDP-43 is expressed at the same level as endogenous TDP-43 in the central nervous system of mice, only mutant, but not wildtype, TDP-43 provokes progressive neurodegeneration (Arnold et al., 2013). Thus, such an animal model might better reflect the pathomechanisms of *TARDBP* mutations.

Similar to overexpression, depletion of TDP-43 in flies is detrimental for neurons (Feiguin et al., 2009). In homozygous knockout mice embryonic lethality becomes evident after embryonic day 3.5 (Kraemer et al., 2010; Sephton et al., 2010; Wu et al., 2010) and possibly until this stage maternal TDP-43 mRNA can compensate the loss of TDP-43 (Wu et al., 2010). The inner cell mass of these embryos shows a defect in outgrowth *in vitro* (Sephton et al., 2010; Wu et al., 2010), demonstrating that TDP-43 is essential during embryogenesis. Thus, conditional knockout mice are necessary to study loss of TDP-43. Conditional knockout of TDP-43 in murine spinal cord neurons causes an ALS phenotype with progressive neurodegeneration and muscle atrophy (Wu et al., 2012) as seen for TDP-43 overexpression, again proving that disturbing the carefully titrated TDP-43 levels in either direction cause

neurodegeneration. A postnatal, ubiquitous TDP-43 knockout mouse model revealed a novel role of TDP-43 in fat metabolism, as these mice present high fatty acid oxidation and a dramatic loss of body weight (Chiang et al., 2010). This phenotype might be due to reduced protein levels of Tbc1d1, a gene associated with obesity in humans (Chiang et al., 2010). In line with this, postnatal conditional overexpression of an ALS-associated TDP-43 mutant (A315T) presents an inverse phenotype with increased Tbc1d1 levels, impaired glucose uptake and increased fat deposition (Stallings et al., 2013).

In zebrafish, two orthologues of the human TDP-43 were identified and one of these orthologues (*tardbp-like*) lacks the C-terminal domain, which habors almost all ALS-associated pointmutations (see 1.2.5 and Fig. 2). Upon TDP-43 depletion, the *tardbp-like* pre-mRNA is alternatively spliced to a variant that contains the C-terminal domain and compensates the loss of TDP-43, which indicates the importance of the C-terminal domain (Schmid et al., 2013). Knockout of both orthologues of TDP-43 in zebrafish leads to shorter motor neurons, mispatterning of the vasculature and muscle degeneration resulting in pre-mature lethality (Schmid et al., 2013).

1.2.5 Specific functions of different TDP-43 domains

TDP-43 is a member of the hnRNP family and contains a classical nuclear localization signal (NLS), two RNA-recognition motifs (RRMs) and a C-terminal glycine-rich domain (G-rich) (Fig. 2).

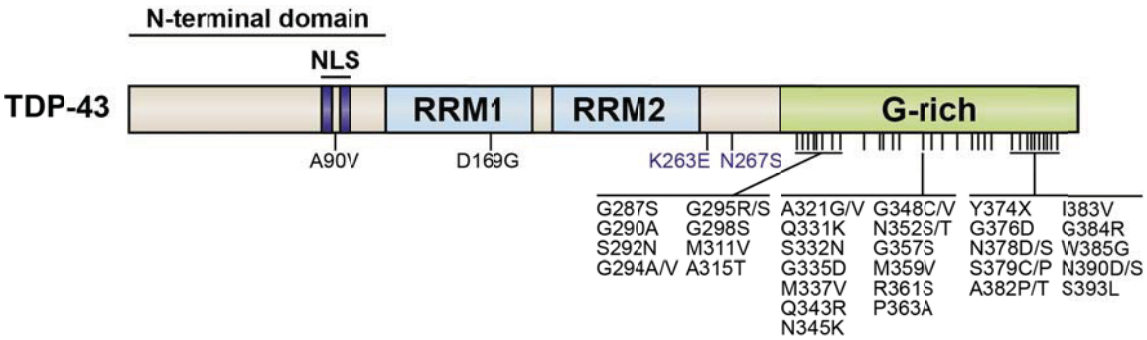

Fig. 2. Domain structure of TDP-43 and disease-associated TDP-43 mutations. The N-terminal domain of TDP-43 is largely uncharacterized and contains a classic bipartite NLS. In addition, TDP-43 has two RRMs and a C-terminal G-rich domain with prion-like properties. To date, 43 TDP-43 missense mutations and one truncation mutation (Y374X) have been identified in ALS patients (black) and FTLD patient (blue), with most mutations clustering in the C-terminal G-rich domain. Figure taken from (Bentmann et al., 2013).

N-terminal domain

Structural features of the N-terminal domain are β-strands, which facilitate DNA-binding properties of TDP-43 (Chang et al., 2012) and are essential for splicing of CFTR mRNA (Zhang et al., 2013). In addition, this domain mediates homodimerization (Kuo et al., 2009) and aggregation of TDP-43 (Zhang et al., 2013). Within the N-terminal domain of TDP-43 is a bipartite classic NLS. Usually, classic NLSs are recognized by the nuclear import factor Importin α/β, which cooperatively binds NLS-containing proteins and promotes their nuclear import (Wente and Rout, 2010) (see also section 1.4). Replacing basic key residues of the TDP-43 NLS by alanine results in cytoplasmic mislocalization of TDP-43 (Ayala et al., 2008b; Winton et al., 2008a).

RNA-binding domains

Two RRMs mediate TDP-43 DNA- and RNA-binding to TG- and UG-rich motifs, respectively, and TDP-43 preferentially binds within long introns, 3´UTRs and to non-coding RNAs (Buratti and Baralle, 2001; Polymenidou et al., 2011; Sephton et al., 2011; Tollervey et al., 2011). RRM1 is necessary and sufficient for binding to UG-rich RNAs (Buratti and Baralle, 2001). In contrast, RRM2 is not essential for RNA-binding (Buratti and Baralle, 2001), but for splicing activity of TDP-43 and possibly plays a role in chromatin organization (Ayala et al., 2005; Ayala et al., 2008b; Fiesel et al., 2010).

Glycine-rich domain

The intrinsically disordered C-terminal G-rich domain in TDP-43 is a prion-like domain with homology to the yeast prion protein Sup35p (King et al., 2012) and this domain mediates sequestration of TDP-43 into polyglutamine (polyQ) aggregates (Fuentealba et al., 2010). Furthermore, residues 318-343 form an amyloidogenic core essential for TDP-43 aggregation (Jiang et al., 2013). The interaction with the hnRNP family members hnRNP A1 and hnRNP A2/B1 mediated by this domain inhibits CFTR splicing and regulates splicing in human and fly (Ayala et al., 2005; Buratti et al., 2005). However, ALS-associated mutations in this region do not alter the interaction with hnRNP A2 (D'Ambrogio et al., 2009).

1.2.6 ALS-associated mutations cluster in the Glycine-rich domain

Nearly all ALS-associated *TARDBP* mutations cluster in the C-terminal G-rich domain (Fig. 2) and several different pathomechanisms have been suggested. Some studies reported cytosolic mislocalization of mutant TDP-43 (Barmada et al., 2010; Ritson et al., 2010) (Liu-Yesucevitz et al., 2010), however, other studies showed that mutant TDP-43 remain nuclear (Kabashi et al., 2010; Ling et al., 2010; Voigt et al., 2010). Furthermore, it was suggested that *TARDBP* mutations enhance and accelerate aggregation and toxicity of TDP-43 (Johnson et al., 2009; Nonaka et al., 2009; Arai et al., 2010; Barmada et al., 2010; Kabashi et al., 2010; Liachko et al., 2010; Liu-Yesucevitz et al., 2010; Ritson et al., 2010; Zhou et al., 2010). In addition, it has been reported that *TARDBP* mutations increase the propensity to interact with FUS (Ling et al., 2010), which is somewhat at odds with other studies (Freibaum et al., 2010; Kim et al., 2010). Thus, despite extensive research over the past few years, it still needs to be clarified, whether *TARDBP* mutations cause neurodegeneration by loss of nuclear TDP-43 (loss-of-function) or by aberrant aggregation and toxicity (toxic gain-of-function) or a combination of both.

Taken together, TDP-43 is an aggregation-prone DNA/RNA-binding protein with a pivotal role in transcription and splicing of several thousand genes. The functional consequences of *TARDBP* mutations, although extensively studied in the past, still remain to be elucidated.

1.3 FUS, EWS und TAF15 (FET proteins) - multifunctional DNA/RNA-binding proteins linked to neurodegeneration

About 20 years ago the DNA/RNA-binding protein FUS, also known as Translocated in sarcoma (TLS), was identified as part of fusion oncogenes in various cancers, including liposarcoma and myeloid leukemia (Crozat et al., 1993; Rabbitts et al., 1993; Ichikawa et al., 1994; Bertolotti et al., 1999). FUS is a member of the FET protein family together with EWS and TAF15, which were also identified as fusion oncogenes in different types of cancer (Delattre et al., 1992; May et al., 1993; Attwooll et al., 1999; Panagopoulos et al., 1999; Martini et al., 2002; Tan and Manley, 2009). In these cancers, the N-terminal half of the FET proteins is fused to the DNA-binding domain of a transcription factor, e.g. of C/EBP homologous protein (CHOP) or erythroblastosis

virus E26 oncogene homologue (ERG), giving rise to a fusion oncogene that acts as abnormal transcription factor (Crozat et al., 1993; Rabbitts et al., 1993; Sanchez-Garcia and Rabbitts, 1994). This abnormal transcription factor causes misregulation of several target genes and results in cell growth disturbances and tumor formation (Zinszner et al., 1994; Schwarzbach et al., 2004).

However, FET proteins are not only implicated in various types of cancer, but also in the neurodegenerative diseases ALS and FTLD. *FUS* mutations associated with ALS-FUS and very rarely EWS and TAF15 mutations are detected in ALS patients (Table 1, Fig. 3) (Kwiatkowski et al., 2009; Vance et al., 2009; Couthouis et al., 2011; Ticozzi et al., 2011; Couthouis et al., 2012). Moreover, all FET proteins are co-deposited in FTLD-FUS (Neumann et al., 2011; Davidson et al., 2013).

1.3.1 Role of FET proteins in transcription and splicing

FET proteins are predominantly nuclear proteins involved in a multitude of nuclear processes (Dormann and Haass, 2013). All FET proteins co-purify with the general transcription factor IID (TFIID) and the RNA-Polymerase II (Bertolotti et al., 1996; Tan and Manley, 2009). Furthermore, FUS and TAF15 are transcription factors that can regulate their target genes both positively and negatively (Tan et al., 2012; Ballarino et al., 2013). Besides these shared targets, FUS is specifically enriched at the promoters of genes encoding proteins with nuclear or cytoplasmic function and those involved in gene expression (Tan et al., 2012), whereas TAF15 controls expression of an miRNA cluster and of genes involved cell cycle regulation and cell death (Ballarino et al., 2013).

All FET proteins contain multiple RNA-binding motifs, which bind mRNAs with AU-rich stem-loop structures (Hoell et al., 2011; Ishigaki et al., 2012) and G-rich motifs such as GGU, GUGGU and GGUG (Lerga et al., 2001; Iko et al., 2004; Lagier-Tourenne et al., 2012; Rogelj et al., 2012). Furthermore, FUS has several thousand pre-mRNA targets and interacts with intronic RNA regions and long non-coding RNAs (Lagier-Tourenne et al., 2012; Rogelj et al., 2012). Upon FUS depletion in either *Xenopus laevis* embryos or mouse brains, several hundred splice changes are detected, corroborating the role of FUS as general splice regulator (Dichmann and Harland, 2012; Lagier-Tourenne et al., 2012; Rogelj et al., 2012). Although there is little overlap between these studies, splicing of the *MAPT* mRNA is altered consistently in all studies upon FUS depletion. This is in accordance with another study, which demonstrated that

upon FUS depletion in primary neurons *MAPT* exons 3 and 10 are included (Orozco et al., 2012). This results in a longer Tau isoform that has also been found to be increased in patients with FTLD and Parkinsonism (Hutton et al., 1998). Additionally, FET proteins are together with SMN part of the spliceosome (Zhou et al., 2002; Yamazaki et al., 2012; Tsuiji et al., 2013), regulating pre-mRNA splicing in general and splice site selection specifically (Bertolotti et al., 1996; Bertolotti et al., 1998; Zhang et al., 1998; Kameoka et al., 2004). Since FET proteins interact with RNA polymerase II, pre-mRNAs and splicing factors (Zinszner et al., 1994; Yang et al., 1998), another putative role of these proteins is to link transcription and splicing (Tan and Manley, 2009).

1.3.2 Autoregulation of FET protein

Some recent findings, e.g. that FUS associates with its own mRNA in a conserved region, which might be either a 3´UTR or a retained intron (Hoell et al., 2011; Lagier-Tourenne et al., 2012; Orozco et al., 2012), indicate that FUS is autoregulated. Moreover, in mouse and human brain an alternative isoform of FUS is detected, that is likely to be degraded via nonsense mediated decay (Lagier-Tourenne et al., 2012) Analysis of mice expressing human FUS further corroborates the idea of FUS autoregulation as these mice show a dose-dependent decrease of endogenous FUS (Mitchell et al., 2013). But FUS does not only regulate its own levels, but also seems to regulate EWS levels. FUS binds EWS mRNA (Hoell et al., 2011; Lagier-Tourenne et al., 2012) and upon transient knockdown of FUS, EWS protein levels show an about 2-fold increase (Han et al., 2012). However, EWS proteins levels are not elevated in heterozygous or homozygous FUS knockout mice (Kuroda et al., 2000), which might be due to an unknown compensatory mechanism upon stable knockout. Thus, how FUS is autoregulated as well as if and how FUS and EWS cross-regulate or compensate each other needs to be further elucidated.

1.3.3 Cytosolic functions of FET proteins

Although FUS is found in the nucleus in the steady state, it continuously shuttles between the nucleus and cytoplasm (Zinszner et al., 1997). In neurons, FUS is part of RNA transport granules which transport mRNAs to dendritic spines for local translation (Kanai et al., 2004; Fujii and Takumi, 2005; Elvira et al., 2006). FUS interacts with the motor proteins Kinesin (Kanai et al., 2004) and Actin (Yoshimura et al., 2006) and is essential for spine morphology (Fujii et al., 2005). Moreover, FUS and TAF15 localize together with other RNA-binding proteins and RNAs to spreading initiation centers (de

Hoog et al., 2004) (Andersson et al., 2008), although their exact function in these centers remains to be investigated. Thus, FUS appears to have important functions not only in the nucleus but also in the cytoplasm (Dormann and Haass, 2013).

1.3.4 Animal models of FET proteins

Overexpression of FUS in worms (Vaccaro et al., 2012), flies (Chen et al., 2011; Wang et al., 2011), mice (Mitchell et al., 2013) and rats (Huang et al., 2011) causes progressive neurodegeneration and recapitulates key features of FUS-proteinopathies. Ectopic expression of human FUS in flies shows that human wildtype FUS localizes in the nucleus, whereas mutant FUS is cytosolic (Chen et al., 2011; Lanson et al., 2011; Murakami et al., 2012) and result in degeneration of motor neurons and reduced life span (Chen et al., 2011; Lanson et al., 2011). Strikingly, eye degeneration is less severe in flies overexpressing wildtype FUS compared to flies overexpressing ALS-associated FUS mutants, indicating that mutant FUS is more toxic than wildtype FUS (Lanson et al., 2011). Similar, overexpressing ALS-associated FUS mutants in rats causes broad neurodegeneration and progressive paralysis (Huang et al., 2011).

Analysis of FUS knockout mice and EWS knockout mice revealed that maintenance of genomic integrity and DNA repair is a common function of FET proteins, as resistance of radiation if impaired in these mice (Hicks et al., 2000; Kuroda et al., 2000; Li et al., 2007). In these studies no obvious neurodegeneration was observed (Hicks et al., 2000; Kuroda et al., 2000), but another group analyzed primary neurons derived from FUS knockout mice and reported that these neurons present a lower spine density and abnormal spine morphology (Fujii et al., 2005). Additionally, knockdown of FUS in flies (Sasayama et al., 2012) or zebrafish (Kabashi et al., 2011) leads to shortening of the axon length and behavioral abnormalities, indicating that FUS is needed for proper neuronal development.

1.3.5 Specific functions of different FET protein domains

FET proteins are structurally related multifunctional proteins with an N-terminal transcriptional activation domain, several nucleic acid-binding domains and a C-terminal NLS (Fig. 3).

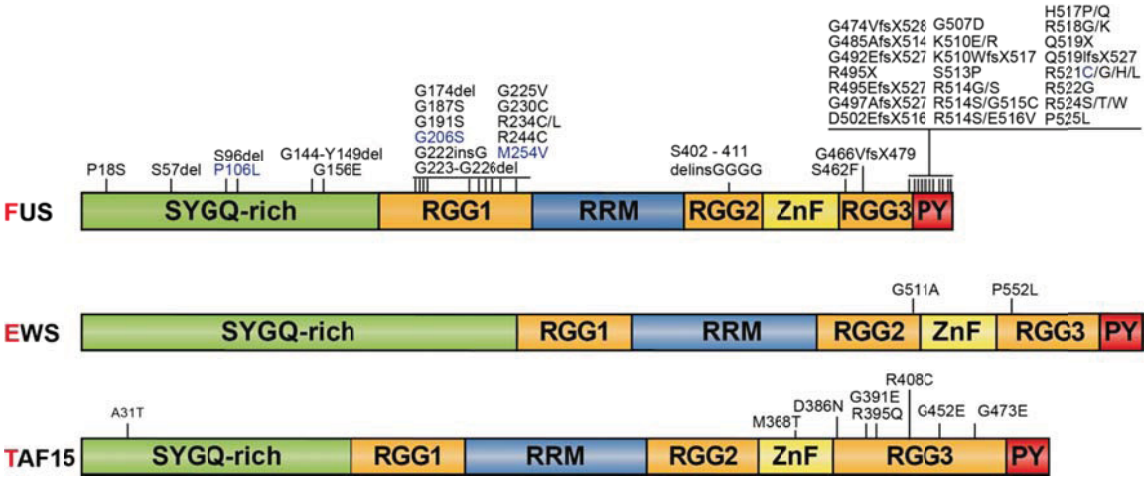

Fig. 3. Domain structure of FET family proteins and disease-associated mutations in FET proteins. All FET proteins share a similar domain structure with a prion-like serine-tyrosine-glycine-glutamine-rich (SYGQ-rich) domain, three arginine-glycine-glycine (RGG) boxes, an RRM, a zinc-finger (ZnF) and a PY-motif which serves as nuclear localization signal (NLS). For FUS, 53 mutations (including missense, frameshift (fs), deletion (del), insertion (ins) and truncating (X) mutations) have been identified in ALS (black) and FTLD (blue) patients with most mutations clustering in the last 17 amino acids and in the RGG1 domain (Kwiatkowski et al., 2009; Vance et al., 2009; Dormann and Haass, 2013). Also EWS and TAF15 have been reported to be mutated in ALS patients (Couthouis et al., 2011; Ticozzi et al., 2011; Couthouis et al., 2012). However, these mutations are very rare and have been found in single cases only. It remains to be shown whether EWS and TAF15 mutations are true disease-causing mutations that segregate with ALS. Figure modified from (Bentmann et al., 2013).

Serine-tyrosine-glycine-glutamine (SYGQ)-rich domain

The N-terminal SYGQ-rich domain of FUS, EWS and TAF15 acts as a potent transcriptional activator when fused to the DNA-binding domain of a transcription factor (May et al., 1993; Ohno et al., 1993; Sanchez-Garcia and Rabbitts, 1994; Zinszner et al., 1994; Bertolotti et al., 1999; Rossow and Janknecht, 2001). As this domain has homology to prion proteins, it is also considered to be "prion-like" (Cushman et al., 2010; Gitler and Shorter, 2011; Udan and Baloh, 2011). Additionally, low complexity sequences (i.e. sequences that have little diversity in the amino acid composition) within the SYGQ-rich domain mediate aggregation of FUS in a cell-free system and in yeast (Fushimi et al., 2011; Sun et al., 2011; Kato et al., 2012). Furthermore, the SYGQ-rich domain of FUS is necessary for the interaction with polyQ-aggregates (Doi et al., 2008) and for self-association of FUS (Yamazaki et al., 2012).

RNA-binding domains of FET proteins

FET proteins contain an RRM and in FUS this domain alone is sufficient to bind RNAs with GGUG motifs (Lerga et al., 2001). A positively charged loop in this domain confers DNA- and RNA-binding properties to FUS (Crozat et al., 1993; Prasad et al., 1994; Baechtold et al., 1999; Liu et al., 2013). Nevertheless, the RRM domain is not the only RNA-binding domain in FET proteins, as it was shown, that the RGG2-ZnF-RGG3 domain has also RNA-binding properties (Ohno et al., 1994; Zinszner et al., 1997; Iko et al., 2004). Especially the ZnF between the RGG motifs seems to be responsible for binding single stranded RNAs containing a GGU motif with micromolar affinity (Nguyen et al., 2011). In addition, the RGG2-ZnF-RGG3 domain of FUS is required for interaction with SMN, which is essential for spliceosome integrity and formation of nuclear foci termed "Gems" that are essential for pre-mRNA splicing (Yamazaki et al., 2012; Tsuiji et al., 2013). In contrast, EWS interacts with SMN via its RGG1 domain (Young et al., 2003).

C-terminal PY-NLS

Finally, all FET proteins contain in their most C-terminal region a non-classical PY-NLS (Lee et al., 2006; Zakaryan and Gehring, 2006; Marko et al., 2012). Interestingly, most of the ALS-associated FUS mutations are clustered in this region (Fig. 3) and result in cytosolic accumulation of mutant FUS (Kwiatkowski et al., 2009; Vance et al., 2009; Dormann et al., 2010).

In summary, all FET proteins are multifunctional DNA/RNA-binding proteins with domains specifically mediating essential roles in RNA metabolism, such as regulating transcription and pre-mRNA splicing or linking transcription and splicing co-transcriptionally (Paronetto et al., 2011; Dormann and Haass, 2013).

1.4 Impairment of nuclear transport in ALS and FTLD

Characteristic features of ALS and FTLD are the cytosolic deposition and nuclear depletion of the normally predominantly nuclear proteins TDP-43 and FUS, pointing to a nuclear transport defect as a key step in the pathological cascade in these diseases (Dormann and Haass, 2011). This is reinforced by the identification of ALS-associated mutations in the NLS of FUS, which cause cytosolic mislocalization (Kwiatkowski et

al., 2009; Vance et al., 2009; Dormann et al., 2010). In contrast, none of the ALS-associated *TARDBP* mutations affects the NLS of TDP-43 and a more general dysfunction in nuclear transport has to be envisaged in TDP-proteinopathies.

1.4.1 Nuclear transport – transport factors and basic mechanisms

The compartmentalization between nucleus and cytoplasm in eukaryotic organisms provokes the demand for transport mechanisms between these two compartments. In eukaryotic organisms translation occurs in the cytoplasm, thus mechanisms evolved by which proteins with nuclear fate can be selectively imported into the nucleus. Nuclear pore complexes (NPCs) span the nuclear envelope (NE) (Fig. 4) and are essential for a controlled and selective nucleocytoplasmic transport. The NPC builds a physical barrier for proteins above 40 kDa, but allows free diffusion of water, ions and small molecules below 40 kDa (Keminer and Peters, 1999; Wente and Rout, 2010). Proteins destined for the nucleus possess a NLS, whereas proteins that need to exit the nucleus contain a nuclear export signal (NES) (Izaurralde and Adam, 1998). To decode the cellular fate of a given protein, transport receptors specifically recognize and interact with the NES and/or NLS in their cargo proteins. These transport receptors are responsible for translocation of their cargo protein through the NPC and are part of the karyopherin protein family. Well-studied examples are the heterodimeric Importin α/β transport receptor complex, which recognizes classical mono- and bipartite NLS sequences and Transportin, which recognizes a PY-NLS present in many RNA-binding proteins (Cook et al., 2007). PY-NLSs have an N-terminal hydrophobic or basic motif, a basic residue and a PY-motif at the C-terminus. The overall basic character of this type of NLS allows binding to negatively charged residues in Transportin (Lee et al., 2006; Cook et al., 2007).

1.4.2 Regulation of nuclear transport by Ran

During nuclear import, the transport receptor, hereafter referred to as receptor, (e.g. Importin α/β or Transportin) binds the NLS of a cargo protein. Afterwards, the receptor-cargo complex interacts transiently with and translocates through the NPC into the nucleus (Wente and Rout, 2010) (Fig. 4). In the nucleoplasm, the small Ras-like GTPase Ran (RanGTP) binds to the allosteric site of the receptor, which induces a conformational change in the cargo-binding pocket of the receptor, resulting in dissociation of the receptor-cargo complex and release of the cargo protein in the nucleoplasm (Rexach and Blobel, 1995; Gorlich et al., 1996; Lee et al., 2005) (Fig. 4).

Receptor and bound RanGTP then recycle through the NPC into the cytoplasm. Upon hydrolysis of RanGTP to RanGDP in the cytosol, the receptor–RanGDP complex falls apart, thereby releasing the transport receptor for a further round of nuclear transport (Cook et al., 2007; Wente and Rout, 2010).

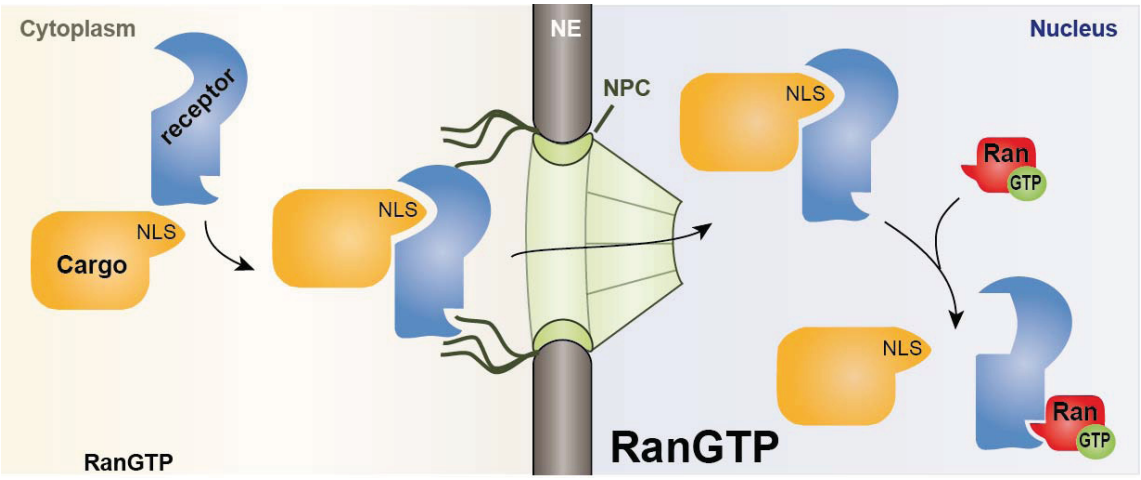

Fig. 4. Nuclear import of transport receptors and their cargo proteins. In the cytoplasm the transport receptor (receptor) interacts with the NLS of a cargo protein (cargo). This interaction enables translocation of the receptor-cargo complex through the NPC, which spans the NE. In the nucleus the level of RanGTP is high and binding of RanGTP to the receptor induces a conformational change in the cargo-binding pocket of the receptor. This conformational change weakens its interaction with the cargo, thus dissociating the receptor cargo complex and releasing the cargo in the nucleus.

Directionality of nuclear transport is mediated by a concentration gradient of RanGTP and its regulators (Fig. 4). Cytosolic RanGTPase activating protein (RanGAP) hydrolyses GTP to GDP, sustaining low levels of RanGTP in the cytoplasm (Bischoff et al., 1995; Yoneda et al., 1999). In contrast, RanGuanine nucleotide exchange factor (RanGEF) is mainly nuclear and yields high levels of RanGTP in the nucleus by converting RanGDP to RanGTP (Bischoff and Ponstingl, 1991; Yoneda et al., 1999). Low RanGTP concentrations in the cytoplasm allow the formation of the receptor-cargo complex, whereas high RanGTP concentrations in the nucleus facilitate the dissociation of the cargo protein from the transport receptor (Izaurralde and Adam, 1998; Cook et al., 2007; Wente and Rout, 2010). Transport receptors that mediate nuclear export use an analogous but inverted process. Here, high RanGTP levels in the nucleus facilitate export-receptor-cargo binding, while low cytoplasmic RanGTP levels allow dissociation of the exported cargo from the export-receptor (Izaurralde and Adam, 1998; Cook et al., 2007; Wente and Rout, 2010).

1.4.3 Arginine methylation fine-tunes nuclear transport of RNA-binding proteins

Nuclear transport can be fine-tuned at several levels, including post-translational modification of cargo proteins (Terry et al., 2007). Post-translational modifications such as phosphorylation, ubiquitination, SUMOylation and arginine methylation can induce a conformational change that alters the accessibility of the NLS or alter the binding affinities between cargo proteins and transport receptors (Terry et al., 2007; Nicholson et al., 2009; Nardozzi et al., 2010).

Arginine methylation is a post-translational modification abundant in RNA-binding proteins, as it can affect not only subcellular localization but also RNA-binding properties (Pahlich et al., 2006). This post-translational modification does not change the charge of the modified arginine, but increases its bulkiness and hydrophobicity. In contrast to other post-translational modifications, arginine methylation is considered very stable. However, some studies point to regulated methylation/demethylation cycles (Metivier et al., 2003; Sakabe and Hart, 2010), although no demethylases have been identified convincingly (Yang and Bedford, 2013).

Protein arginine methyltransferases (PRMTs) catalyze arginine methylation and promote transfer of a methyl group (CH_3^-) from S-adenosyl methionine (SAM) to the guanidino ($CH_6N_3^+$) nitrogen of an arginine (Nicholson et al., 2009; Yang and Bedford, 2013). Three types of arginine methylation are known: monomethylation, symmetric dimethylation, and asymmetric dimethylation (Yang and Bedford, 2013).

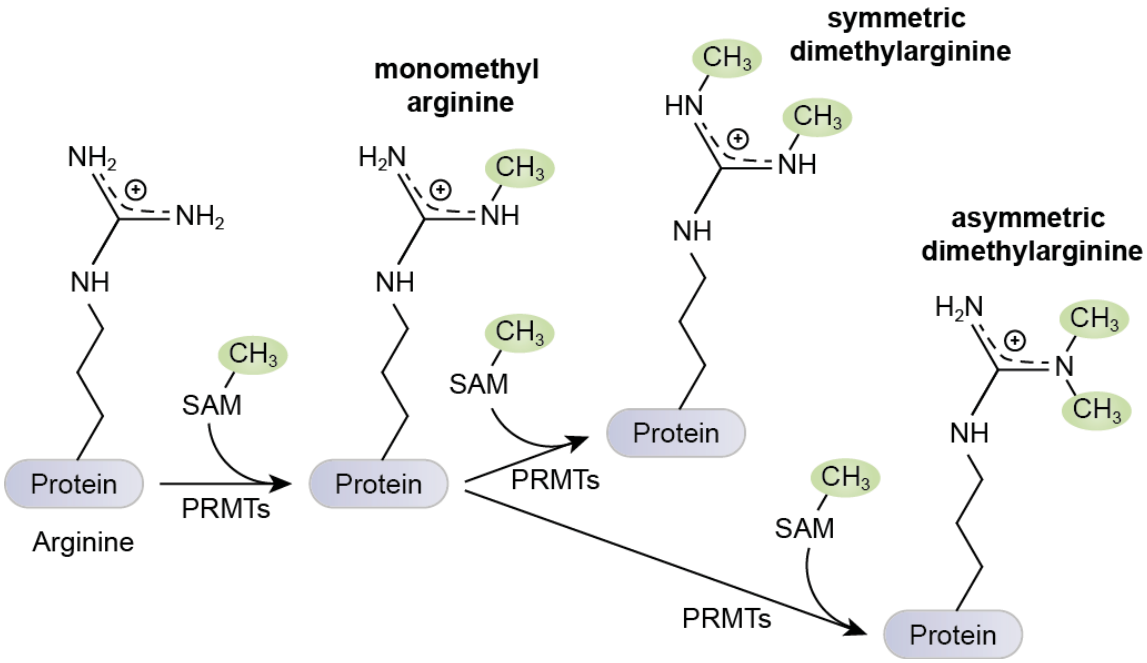

Fig. 5. Different types of arginine methylation. PRMTs first catalyze the transfer of a methyl group from SAM to one of the terminal guanidino nitrogens of an arginine, thereby generating monomethyl arginine. Subsequent addition of a second methyl group to the same terminal guanidino nitrogen results in asymmetric dimethylarginine. In contrast, symmetric dimethylarginine is formed when a second methyl group is added to the other guanidino nitrogen.

PRMT1 is responsible for the majority of total protein arginine methylation in cells. It catalyzes monomethylation and asymmetric dimethylation and has a broad substrate specificity (Tang et al., 2000; Zhang and Cheng, 2003; Bedford and Clarke, 2009). Known PRMT1 substrates are proteins involved in transcription, splicing and signal transduction. The methylated arginine is often, but not always flanked by one or more glycines forming a RGG or glycine- and arginine-rich (GAR) motif (Nicholson et al., 2009; Thandapani et al., 2013; Yang and Bedford, 2013). Interestingly, all FET proteins have been described to be asymmetrically dimethylated in their RGG domains (Belyanskaya et al., 2001; Rappsilber et al., 2003; Ong et al., 2004; Jobert et al., 2009; Du et al., 2011). PRMT1-mediated asymmetric dimethylation of EWS and TAF15 has been described to alter their subcellular localization, their activity as transcription factors and protein-protein interactions (Young et al., 2003; Araya et al., 2005; Jobert et al., 2009; Shaw et al., 2009). However, the functional consequences of asymmetric dimethylation of FUS remain to be elucidated.

1.5 RNA-binding proteins in stress granules (SGs)

1.5.1 SGs in neurodegeneration

Over the last few years, much attention has been drawn to the connection between SGs and neurodegenerative diseases. SGs store mRNAs during cellular stress and RNA-binding proteins attached to these mRNAs are essential components of SGs. Interestingly, several RNA-binding proteins that localize to SGs have recently been linked to neurodegenerative diseases.

First, FUS and TDP-43 and were found to localize in SGs (Andersson et al., 2008; Colombrita et al., 2009; Dormann et al., 2010; Bentmann et al., 2012). Second, repeat expansion in the *ATXN2* gene, encoding the RNA-binding protein Ataxin-2, can cause spinocerebellar ataxia type 2 and ALS-TDP (Pulst et al., 1996; Elden et al., 2010). Ataxin-2 is recruited into SGs upon exposure to various stressors (Ralser et al., 2005; Ariumi et al., 2011; Nihei et al., 2012) and seems to be important for SG formation, as cells depleted for Ataxin-2 form fewer SGs upon cellular stress (Nonhoff et al., 2007). Third, mutations in the *Angiogenin (ANG)* gene have been associated with ALS-TDP (Greenway et al., 2006; van Blitterswijk and Landers, 2010) and ANG localizes into SGs upon stress (Pizzo et al., 2013). ANG is a ribonuclease and disease-associated mutations in ANG are reported to impair subcellular localization and ribonuclease activity (Greenway et al., 2006; Crabtree et al., 2007). Additionally, cells expressing ANG-K40I, an ALS-associated variant of ANG, form fewer SGs upon cellular stress (Thiyagarajan et al., 2012). These are only three examples of RNA-binding proteins associated with ALS and FTLD that are also detected in SGs, but several recent reviews extensively discuss this connection in further detail (Wolozin, 2012; Bentmann et al., 2013; Li et al., 2013; Thomas et al., 2013).

1.5.2 SGs as storage particles of mRNA and proteins

SGs are cytosolic particles that are rapidly formed in eukaryotic cells exposed to environmental stressors, such as oxidative stress, osmotic shock, thermal stress and viral infection (Kedersha and Anderson, 2007; Spriggs et al., 2010; Emara et al., 2012; Hofmann et al., 2012; Lloyd, 2012). They transiently store and thereby prevent translation of poly(A) mRNA encoding housekeeping genes in order to conserve energy by prioritizing selective translation of proteins necessary for stress adaption (Stohr et al., 2006). Thus, expression of mRNAs encoding heat-shock proteins (HSPs),

chaperones and other stress-response proteins is maintained or enhanced, as these mRNAs use non-canonical translation initiation motifs to circumvent the translational arrest in SGs (Sherrill et al., 2004; Bornes et al., 2007; Spriggs et al., 2010). Upon stress, cells start a customized response dependent on cell type and stressor, therefore mRNA and protein composition of SGs is highly variable (Anderson and Kedersha, 2009b; Emara et al., 2012). Nevertheless, some proteins are core components of SGs and serve as SG marker proteins as they are not found in other messenger ribonucleoproteins (mRNPs) such as processing-bodies (p-bodies) or RNA transport granules (Kedersha et al., 2005; Buchan and Parker, 2009). Some of these SG marker proteins are components of the 48S pre-initiation complexes consisting of small ribosomal subunits, eukaryotic translation initiation factors (e.g. eIF3, eIF4E and eIF4G) and Poly(A)-binding protein 1 (PABP-1) (Kedersha et al., 2002). Furthermore, SGs contain certain RNA-binding proteins, that can promote SG assembly when overexpressed, such as Ras-GTPase-activating protein SH3-domain-binding protein (G3BP) and T cell internal antigen-1 (TIA-1) (Tourriere et al., 2003; Gilks et al., 2004). Three possible fates for mRNAs in SGs are known: (1) translation re-initiation (often for mRNAs encoding stress-adaptive proteins), (2) storage as translationally silenced mRNA or (3) degradation in interacting p-bodies, which contain mRNA decay proteins (Anderson and Kedersha, 2009a; Buchan and Parker, 2009).

1.5.3 SG formation

Upon cellular stress, eukaryotic cells form SGs via an eIF2α-dependent or eIF2α-independent pathway (Fig 6). In the eIF2α-dependent pathway, four different serine/threonine kinases (PKR, PERK, HRI, GCN) serve as sensors for environmental stress (Anderson and Kedersha, 2008; Buchan and Parker, 2009) (Fig. 6). Upon stress, these kinases are activated and in turn phosphorylate the alpha subunit of eIF2 (Anderson and Kedersha, 2008; Buchan and Parker, 2009). Translation initiation usually needs eIF2α in its unphosphorylated state to initiate translation, thus phosphorylation of eIF2α inhibits initiation of a further round of translation.

Alternatively, chemicals such as hippuristanol and pateamine A induce SG-formation via the eIF2α-independent pathway. Direct binding of pateamine A for example diminishes the helicase activity of eIF4A, which results in translation initiation inhibition and SG formation (Low et al., 2005; Dang et al., 2006; Mazroui et al., 2006).When translation initiation is stopped either via the eIF2α-dependent or eIF2α-

independent pathway, ribosomes finish their round on the translated transcript and then "run-off", as a further round of translation cannot be initiated. The remaining 48S pre-initiation complex stays bound to the 5´UTR of the mRNA (Fig. 6) (Anderson and Kedersha, 2008). Although the next step (SG nucleation) is not yet fully understood, it is assumed that aggregation-prone SG proteins, such as TIA-1, TIAR and G3BP, associate with the 48S pre-initiation complex and form mRNP oligomers. Subsequently, crosslinking via PABP-1 and additional protein-protein interactions promote the assembly of mature SGs (Fig. 6, SG assembly) (Anderson and Kedersha, 2008).

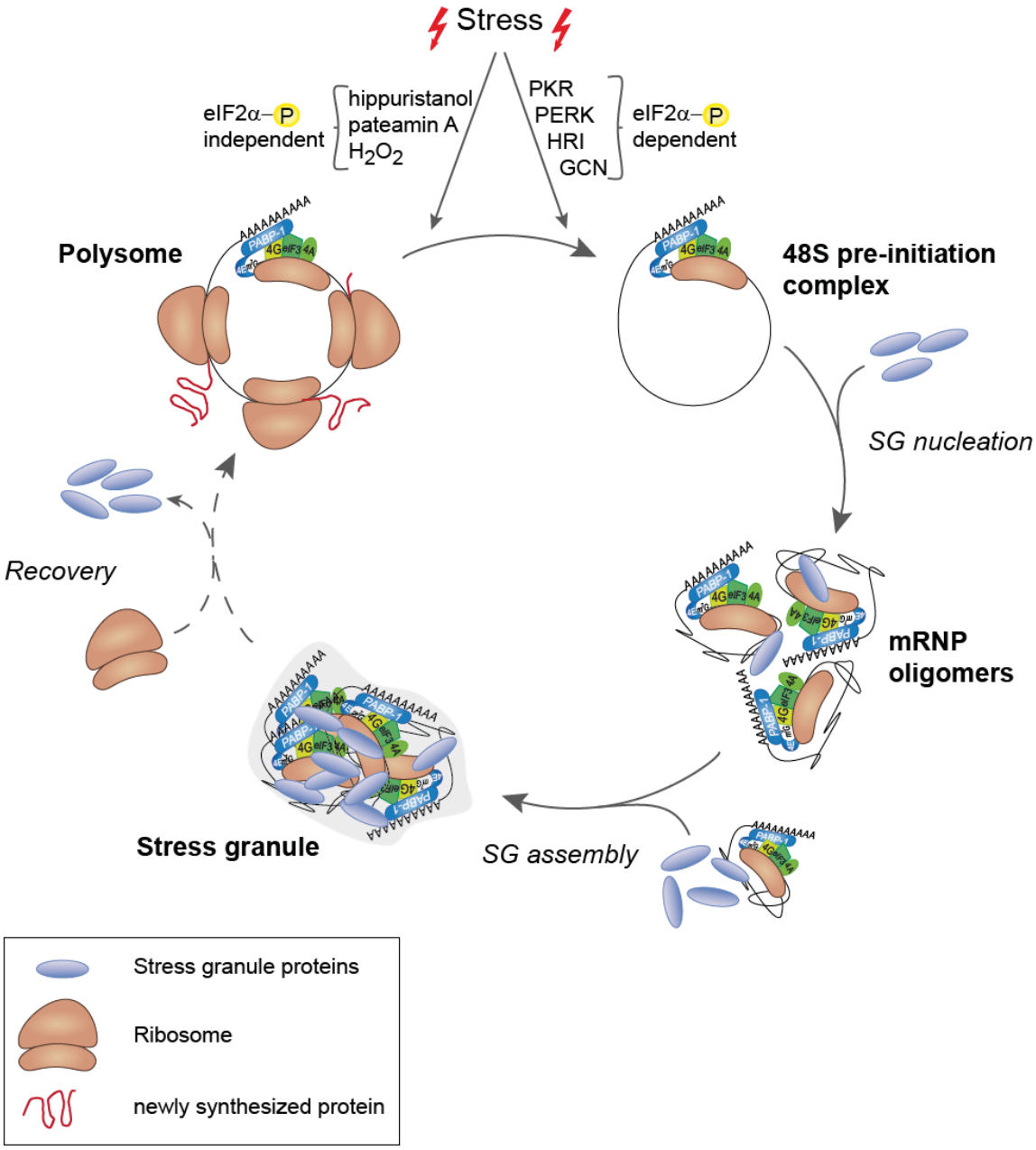

Fig. 6. SG formation and dissolution. Under normal conditions, several ribosomes bind the circularized mRNA and translate the mRNA into newly synthesized protein. Cellular stress results in inhibition of translation initiation and starts SG formation. During SG nucleation, SG proteins (blue) bind to the 48S pre-initiation complex forming mRNP oligomers. The assembly of mRNP oligomers to SGs is promoted by crosslinking via PABP-1 and post-translational modifications such as O-glycosylation. During stress recovery, SG proteins dissociate, ribosomes are recruited to the released mRNA and translation can be re-initiated. Figure modified from (Bentmann et al., 2013).

Post-translational modifications are known to regulate SG assembly. Besides phosphorylation of the α-subunit of eIF2, O-glycosylation of the small ribosomal subunit is involved in SG formation, probably by acting as molecular glue between mRNPs or by facilitating repression of translation initiation by modifying ribosomal

subunits. Furthermore, arginine methylation is necessary for proper SG recruitment of several RNA-binding proteins, as it can modify RNA-binding properties and subcellular localization (see also section 1.5). For example, the RNA-binding proteins Fragile X mental retardation protein (FMRP) and Cold-inducible RNA-binding protein (CIRP) localize to SGs when arginine residues within their RGG domains are methylated (Dolzhanskaya et al., 2006; De Leeuw et al., 2007). Furthermore, PRMT1 itself is also recruited into SGs upon arsenite stress (Yamaguchi and Kitajo, 2012).

1.5.4 SG dissolution

When sublethal stress has passed, SG rapidly dissolve during the recovery phase (Fig. 6) thereby releasing sequestered poly(A) mRNAs and SG proteins (Kedersha et al., 2005). Concomitantly, the large ribosomal subunit binds to the 48S pre-initiation complex and translating polysomes can be re-formed (Fig. 6). Because 48S pre-initiation complexes remain assembled during their storage in SGs, translation rates can rapidly increase upon stress recovery. Dissolution of SGs and recovery of translation is facilitated by chaperones, thus overexpression of HSP70 accelerates SG dissolution and enhances translation rate during recovery (Kedersha and Anderson, 2002; Thomas et al., 2009). Recently, dual specificity tyrosine-phosphorylation-regulated kinase 3 (DYRK3) has been shown to be an important regulator of SG dissolution (Wippich et al., 2013). The active form of DYRK3 promotes SG dissolution, whereas inhibiting the kinase activity of DYRK3 hampers SG dissolution (Wippich et al., 2013). In addition, the dynamic equilibrium between SGs and polysomes becomes evident by the use of drugs (e.g. cycloheximide and emetine) that freeze ribosomes on translating polysomes and thus prevent SG formation upon cellular stress (Kedersha et al., 2000). In contrast, polysome-destabilizing drugs such as puromycin, facilitate SG formation (Kedersha et al., 2000; Chudinova et al., 2012).

2 Aims of the study

The identification of the RNA-binding proteins TDP-43 and FUS in pathological inclusions in ALS and FTLD patients together with the detection of disease-associated mutations in the *TARDBP* and *FUS* genes was a major breakthrough in understanding these devastating neurodegenerative disorders (see also 1.1 – 1.3). As both proteins are under physiological conditions predominantly nuclear, it was surprising to find pathological inclusions containing aggregated FUS and TDP-43 in the cytosol, raising the question how cytosolic TDP-43 and FUS inclusions arise. As both FUS and TDP-43 are detected in SGs upon cellular stress (Colombrita et al., 2009; Dormann et al., 2010), I hypothesized that pathological inclusions might originate from SGs and that a detailed analysis of how FUS and TDP-43 are recruited into SGs might give important insights in the pathomechanisms of FUS- and TDP-proteinopathies.

Thus my major aim was to determine the requirements for SG recruitment of FUS and TDP-43. Therefore, I analyzed which stressors induce the recruitment of FUS and TDP-43 in SGs, whether cytosolic mislocalization of FUS and TDP-43 is a prerequisite for SG localization and whether the sequestration of FUS and TDP-43 can also be observed in primary neurons. Furthermore, I determined which domains of FUS and TDP-43 are essential for their SG recruitment and tested whether SG recruitment correlates with the RNA-binding properties of these domains. Moreover, I examined how ALS-associated *TARDBP* mutations affect SG recruitment of TDP-43 or SG formation in general.

In addition, because FUS inclusions in ALS-FUS contain only FUS, whereas FUS inclusions in FTLD-FUS contain all FET proteins (Neumann et al., 2011), I aimed to model this differential protein composition of FUS inclusions in cell culture, in order to understand the underlying pathomechanisms. To this end, I tested whether general inhibition of Transportin-mediated nuclear import causes accumulation of all FET proteins and whether EWS and TAF15 are co-sequestered with mutant FUS in SGs. As ALS and FTLD patients show a selective degeneration of neurons, I investigated the localization of mutant FUS in also primary rat neurons. Moreover, I established stress conditions that evoke SG formation in HeLa cells and primary neurons. Finally, I determined whether arginine methylation affects nuclear import of EWS and TAF15, as previously shown for FUS (Dormann et al., 2012; Tradewell et al., 2012).

3 Results

This chapter is separated in 4 sections according to the studies published in international, peer-reviewed journals. Each study is summarized independently and if applicable additional information is shown. In addition, a declaration about my contributions within these studies is given.

3.1 Stress granule recruitment of FUS and TDP-43 depends on RNA-binding and protein-protein interactions

Bentmann E, Neumann M, Tahirovic S, Rodde R, Dormann D*, Haass C*
Requirements for Stress Granule Recruitment of Fused in Sarcoma (FUS) and Tar DNA-binding Protein of 43 kDa (TDP-43)
J Biol Chem 2012 Jun 29;287(27):23079-94 Epub 2012 May 4

Several recent studies have demonstrated that FUS and TDP-43 are recruited into SGs upon different types of stress (Colombrita et al., 2009; Moisse et al., 2009a; Bosco et al., 2010; Dormann et al., 2010; Liu-Yesucevitz et al., 2010; Dewey et al., 2011; Gal et al., 2011; Ito et al., 2011; McDonald et al., 2011; Meyerowitz et al., 2011). However, which domains of FUS and TDP-43 are involved in SG recruitment is currently unknown. Two mutually not exclusive mechanisms can be considered. First, FUS and TDP-43 may be recruited to SGs by virtue of their RNA-binding capacity. Second, it is conceivable that protein-protein interactions might be responsible for localizing FUS or TDP-43 into SGs.

3.1.1 Stress granule recruitment of FUS

First, I demonstrated that only the cytosolic ALS-associated *FUS* mutation FUS-P525L but not wildtype FUS (FUS-WT) is recruited into SGs upon treatment with three different stressors (44°C heat shock, sodium arsenite or clotrimazole treatment). Furthermore, I verified that sequestration of FUS-P525L into SGs is not cell type specific, but occurs in HeLa cells, SH-SY5Y cells and primary rat hippocampal neurons. After having determined these general aspects of SG recruitment, I tested which domain(s) of FUS mediate recruitment to SGs.

Upon heat shock, the N-terminal SYGQ-rich domain (termed Q in (Bentmann et al., 2012)), the glycine-rich RGG1 domain (termed G in (Bentmann et al., 2012)) and the RRM domain (termed R in (Bentmann et al., 2012)) remained mainly diffuse cytosolic, but small amounts were recruited into SGs. Only the C-terminal RGG2-ZnF-RGG3 domain (termed Z in (Bentmann et al., 2012)) was efficiently recruited into SGs, although to a lesser extent than full-length FUS. Combining the single domains (RGG1 + RRM + RGG2-ZnF-RGG3) increased the localization to SGs and reached the same levels as full-length FUS-P525L suggesting that all three domains contribute to SG

recruitment. In contrast, the SYGQ-rich domain is dispensable for SG recruitment of FUS, as a construct lacking this domain was recruited into SGs to the same extent as full length FUS-P525L.

Furthermore I examined whether SG recruitment and RNA-binding of individual FUS domains correlate with each other. As expected, UG-rich RNA oligonucleotides were efficiently and selectively bound by full-length FUS. Of the individual domains, only RGG2-ZnF-RGG3-domain-containing constructs showed binding to the UG-rich RNA oligonucleotides. Thus the ability to bind RNA correlates with SG recruitment, suggesting that RNA-binding via the RGG2-ZnF-RGG3 domain plays an important role in SG recruitment of FUS. In contrast, the RGG1 domain and RRM domain, which were unable to bind UG-rich oligonucleotides, facilitate SG recruitment probably via protein-protein interactions.

3.1.2 Stress granule recruitment of TDP-43

To characterize the determinants for SG recruitment of TDP-43, I first examined how nuclear versus cytosolic localization affects its SG recruitment. In contrast to wildtype TDP-43 (TDP-WT), TDP-NLS_{mut}, an artificial cytosolic TDP-43 mutant with a mutated NLS, was sequestered into SGs in HeLa cells, primary rat hippocampal neurons and SH-SY5Y cells, demonstrating that cytosolic mislocalization of TDP-43 is a prerequisite for SG recruitment.

Next I analyzed whether ALS-associated *TARDBP* mutations alter subcellular localization of TDP-43 as previously reported (Barmada et al., 2010; Liu-Yesucevitz et al., 2010). However, three different ALS-associated *TARDBP* mutations (A315T, M337V, G348C) that were analyzed were all nuclear both in unstressed cells and upon heat shock, in line with other studies reporting a nuclear localization of *TARDBP* mutants (Kabashi et al., 2010; Ling et al., 2010; Voigt et al., 2010). To test whether *TARDBP* mutations alter the amount of TDP-43 in SGs once TDP-43 is mislocalized in the cytosol, the same *TARDBP* mutations (A315T, M337V, G348C) were introduced into the TDP-NLS_{mut} construct. However, all double mutant TDP-43 constructs showed similar SG recruitment as TDP-NLS_{mut} without an ALS-associated point mutation.

Whether TDP-43 inclusions contain SG marker proteins was under debate, as in two studies SG marker proteins could not be detected in TDP-43 inclusions (Colombrita et al., 2009; Dormann et al., 2010), whereas two other studies reported that SG marker

proteins co-label TDP-43-inclusions (Volkening et al., 2009; Liu-Yesucevitz et al., 2010). Interestingly, one study demonstrated that depending on the analyzed tissue, different TDP-43 species are present in pathological TDP-43 inclusions: Spinal cord inclusions mainly contain full-length TDP-43 and inclusions in the hippocampus and cortex contain mainly TDP-CTFs (Igaz et al., 2008; Neumann et al., 2009c). By comparing SG marker proteins in TDP-43 inclusions in different tissues, our collaboration partner Prof. Dr. Manuela Neumann, DZNE and University of Tübingen, found that spinal cord TDP-43 inclusions contain full-length TDP-43 and PABP-1, a SG marker protein. In contrast, hippocampal inclusion containing mainly TDP-CTF did not co-label with PABP-1. In line with this finding, a construct encoding a C-terminal fragment of TDP-43 (termed Δ1-173 in (Bentmann et al., 2012)) failed to be recruited into SGs in HeLa cells. In addition, NLS_{mut}-ΔC which lacks the C-terminal G-rich domain (termed G-rich in (Bentmann et al., 2012)), where almost all ALS-associated *TARDBP* mutations cluster, was only poorly sequestered into SGs. Additionally, I tested RNA-binding of different TDP-constructs to possibly correlate RNA-binding with SG-recruitment. In contrast to TDP-CTF, which lacks the RRM1 domain and showed not binding to UG-rich RNA oligonucleotides, NLS_{mut}-ΔC exhibited similar binding to these RNA oligonucleotides as TDP-WT and TDP-NLS_{mut}. The finding that despite normal RNA-binding, NLS_{mut}-ΔC showed reduced SG recruitment indicates that besides RNA-binding TDP-43 requires also other features, probably protein-protein interactions for efficient SG recruitment.

Contribution to this study:

As first author of this manuscript, I had major conceptual and experimental contributions. In detail, I established different stressors (heat shock, arsenite, clotrimazole) in HeLa cells (Fig. 1B; 2 B,C; 4B; 6A; 7A,C; 9B,C; S1, S2A, S4B, S5A, S7B in (Bentmann et al., 2012)) and heat shock as stressor to induce SG formation in SH-SY5Y cells and primary rat hippocampal neurons (Fig. 1C; 4C; S2B; S5B in (Bentmann et al., 2012)). Cloning of TDP-NLS_{mut} constructs carrying ALS-associated *TARDBP* mutations (Fig.7 in (Bentmann et al., 2012)). Transient transfection of FUS or TDP-43 constructs in HeLa cells and SH-SY5Y cells (Fig. 1B; 2 B,C; 4B; 6; 7; 9 in (Bentmann et al., 2012)). Immunofluorescence staining and analysis of SG formation using confocal microscopy in HeLa, SH-SY5Y cells in primary rat hippocampal neurons (Fig. 1, 2, 4, 6, 7, 9 in (Bentmann et al., 2012)). Quantification of SG

recruitment of FUS or TDP-43 deletion constructs to heat shock- or clotrimazole-induced SGs (Fig. 2C; 7C; Fig. 9C in (Bentmann et al., 2012)). Establishment of an RNA-binding assay and *in vitro* transcription and translation of [^{35}S] methionine-labeled FUS or TDP-43 constructs (Fig. 3; 10 in (Bentmann et al., 2012)). Analysis of expression levels and quantification of nuclear and cytosolic fluorescence intensities of TDP-43 constructs carrying ALS-associated point mutations (Fig. 6B,C in (Bentmann et al., 2012)). Drawing of schematic diagrams and a model figure (Fig. 1A; 2A; 4A; 9A; 11 in (Bentmann et al., 2012)).

Additional unpublished data

As a follow-up to our published study, I addressed whether FUS or TDP-43 are necessary for SG formation. Therefore I performed siRNA-mediated knockdown of endogenous FUS (siFUS) or TDP-43 (siTDP) and subjected these cells to clotrimazole stress. Endogenous FUS levels were efficiently reduced with siFUS compared to cells transfected with a control siRNA (NT control) (Fig. 7A), however SGs were still formed normally upon clotrimazole treatment and no obvious difference in SG formation between cells transfected with NT control or siFUS was observed (Fig. 7B). Similarly, TDP-43 knockdown did not change the efficiency of SG formation (Fig. 7C, 7D).

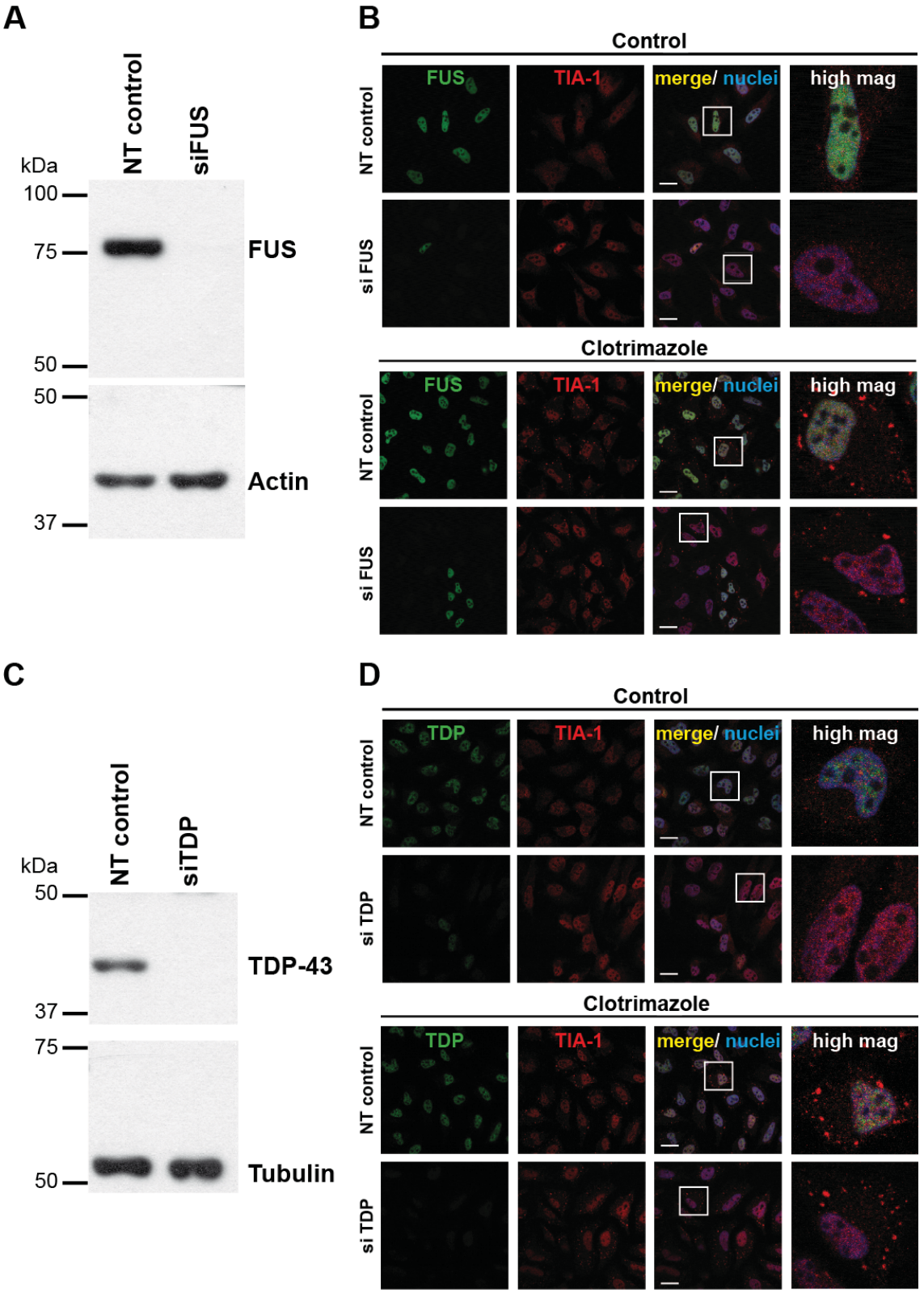

Fig. 7. FUS and TDP-43 are not essential for SG formation. (**A**) Total cell lysates of cells transfected with siFUS or NT control, were analyzed by SDS-PAGE and immunoblotting with a FUS-specific antibody, α-Actin served as a loading control (lower panel). Immunoblots show efficient knockdown of siFUS-transfected cells. (**B**) Endogenous FUS was silenced by siRNA-mediated knockdown (siFUS), non-targeting siRNA (NT control) was used as a negative control; 72 hours post-transfection HeLa cells were incubated with 20μM clotrimazole for 30 min or left untreated (control). Cells were fixed, stained

with FUS (green) and TIA-1 (red)-specific antibodies and nuclei counterstain (DAPI, blue) and analyzed by confocal microscopy. Panels on the right show a higher magnification of the boxed region (high mag). FUS knockdown does not alter the formation of TIA-1 positive SGs induced by clotrimazole. Scale bars: 20 μm. (**C**) Immunoblot of endogenous TDP-43 in HeLa cells following transfection with siTDP or NT control, Tubulin served as a loading control (lower panel). TDP-43 siRNA efficiently silences TDP-43 expression. (**D**) Endogenous TDP-43 was silenced by siRNA-mediated knockdown (siTDP), a control siRNA (NT control) was used as negative control. Prior to fixation, cells were incubated with 20 μM clotrimazole for 30 min or left untreated (control). After staining with TDP-43 (green) and TIA-1 (red) – specific antibodies, SG formation was examined by confocal microscopy. TDP-43 silencing does not inhibit formation of TIA-1 positive-SGs. Note, that endogenous (i.e. nuclear) TDP-43 is not sequestered into clotrimazole-induced SGs. Scale bars: 20 μm.

3.2 TAF15 and EWS are co-deposited with FUS in FTLD-FUS, but not in ALS-FUS

Neumann M, **Bentmann E**, Dormann D, Jawaid A, Dejesus-Hernandez M, Ansorge O, Roeber S, Kretzschmar HA, Munoz DG, Kusaka H, Yokota O, Ang LC, Bilbao J, Rademakers R, Haass C, Mackenzie IRA

FET proteins TAF15 and EWS are selective markers that distinguish FTLD with FUS pathology from amyotrophic lateral sclerosis with FUS mutations.

Brain. 2011 Sep;134(Pt 9):2595-609. Epub 2011 Aug 19.

ALS-associated FUS mutations result in cytosolic mislocalization of mutant FUS (Dormann et al., 2010). In contrast, no genetic alterations have so far been detected in FTLD-FUS patients (Neumann et al., 2009a; Urwin et al., 2010; Snowden et al., 2011), suggesting that mechanisms underlying FUS deposition in FTLD-FUS are distinct from those in ALS-FUS. Within this study, our collaboration partner Prof. Neumann further characterized the composition of FUS inclusions in FTLD-FUS and ALS-FUS patient brain samples. In post-mortem brains of FTLD-FUS patients, TAF15 was consistently detected in FUS-positive inclusions, whereas EWS was variably co-localized in FUS inclusions. In healthy controls, all three FET proteins were predominantly nuclear and no cytoplasmic inclusions were detectable. Interestingly, FUS inclusions in ALS-FUS were devoid of EWS and TAF15 and both proteins were exclusively detected in the nucleus. This striking difference in the composition of FUS inclusions between FTLD-FUS and ALS-FUS corroborates the hypothesis that the two different FUS-proteinopathies have different underlying pathomechanisms.

My contribution to this work was to model Prof. Neumann´s neuropathology data in cultured cells. To this end, I expressed the ALS-associated *FUS* mutation FUS-P525L in HeLa cells and tested whether it could sequester endogenous TAF15 and EWS into SGs. Consistent with the neuropathological findings, recruitment of FUS-P525L into SGs did not change the subcellular localization of endogenous TAF15 and EWS, demonstrating that mislocalized, mutant FUS cannot sequester nuclear EWS and TAF15 to SGs. To test whether a defect in Transportin-mediated import may underlie the pathological co-deposition of all three FET proteins observed in FTLD-FUS patients, I expressed a competitive peptide inhibitor of the Transportin pathway called

M9M (Cansizoglu et al., 2007) in HeLa cells. As all FET proteins contain a PY-NLS, I speculated that GFP-M9M should not only block nuclear import of FUS as shown in (Dormann et al., 2010), but also of EWS and TAF15. Indeed, in GFP-M9M-expressing cells TAF15 and EWS were mislocalized to the cytosol, with EWS being mislocalized to less strongly and TAF15 being more strongly mislocalized than FUS. In addition, TAF15 and EWS formed punctate structures that were confirmed to be *bona fide* SGs by co-labeling with the SG marker protein TIA-1 (see additional unpublished data, Fig. 8, upper rows). In contrast, GFP expression alone did not alter the subcellular localization of TAF15 and EWS, leaving TAF15 and EWS nuclear. This data demonstrates that a dysfunction of Transportin-mediated nuclear import results in cytosolic accumulation of all three FET proteins, supporting the notion that ALS-FUS and FTLD-FUS have distinct underlying pathomechanisms. In ALS-FUS, FUS inclusions are a result of the specific disruption of FUS nuclear import due to a mutation in the PY-NLS of FUS. In FTLD-FUS, all FET proteins appear to be not properly imported into the nucleus, suggesting a general impairment of Transportin-mediated nuclear import. Such a defect could either occur during ageing or could be mediated by a different mechanism (e.g. post-translational modifications) that selectively inhibits nuclear import of FET proteins.

Additional unpublished data

As a follow-up to publication 2, I confirmed that punctate structures observed upon expression of GFP-M9M in HeLa cells were indeed SGs by co-labeling for TIA-1, a SG marker protein.

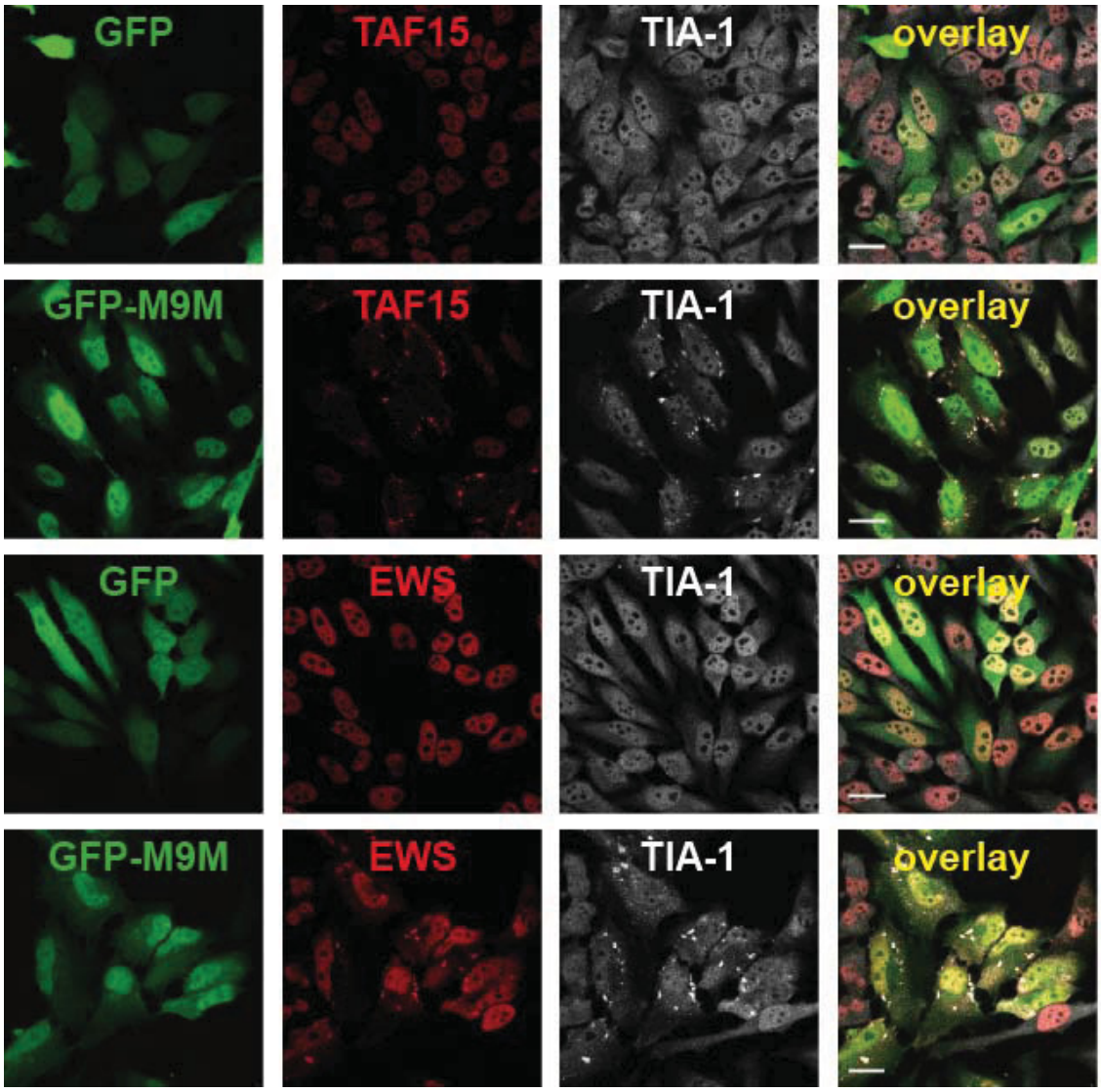

Fig. 8. Expression of GFP-M9M leads to sequestration of EWS and TAF15 into SGs. M9M is a chimeric peptide designed to bind the nuclear import receptor Transportin with unusually high affinity and thus competes with natural Transportin substrates. GFP-tagged M9M (GFP-M9M, green) or GFP alone were expressed in HeLa cells for 24 h. Cells were fixed, stained with EWS or TAF15 (both shown in red) and TIA-1 (white)- specific antibodies and were analyzed using confocal microscopy. Inhibition of Transportin-mediated nuclear import causes localization of TAF15 and EWS into SGs. Note that EWS shows only a mild mislocalization with large amounts of the protein remaining in the nucleus, compared to the striking mislocalization and nuclear depletion of TAF15. Scale bar: 20 μm.

Contribution to this study:

Immunofluorescence and confocal analysis of EWS and TAF15 localization in HeLa cells transiently transfected with either HA-FUS-WT or HA-FUS-P525L after heat shock or control conditions (Fig. 7 A; S3 in (Neumann et al., 2011)). Transient transfection of a Transportin-specific inhibitor (GFP-M9M) in HeLa cells, immunofluorescence staining of FUS, EWS and/or TAF15 and analysis via confocal microscopy (Fig. S3 in (Neumann et al., 2011)).

3.3 C-terminal FUS mutations impair Transportin-mediated nuclear import of FUS

Dormann D, Rodde R, Edbauer D, **Bentmann E**, Fischer I, Hruscha A, Than ME, Mackenzie IR, Capell A, Schmid B, Neumann M, Haass C
ALS-associated fused in sarcoma (FUS) mutations disrupt Transportin-mediated nuclear import.
EMBO J. 2010 Aug 18;29(16):2841-57. Epub 2010 Jul 6.

Most ALS-associated *FUS* mutations cluster in the C-terminal domain of FUS (Fig. 3) and result in cytoplasmic mislocalization of the mutant FUS protein (Kwiatkowski et al., 2009; Vance et al., 2009). Initially, the underlying pathomechanism was unknown.

By investigating the exact pathomechanism of ALS-associated FUS mutations, Dr. Dormann demonstrated that FUS-WT localizes in the nucleus, whereas the four tested C-terminal FUS mutants (R521G, R524S, R522G, P525L) were mislocalized to the cytoplasm in HeLa cells. Intriguingly, the degree of cytosolic mislocalization of mutant FUS inversely correlated with the age of disease-onset in the ALS-patients carrying these mutations. As ALS patients present progressive neuronal degeneration, my contribution to this study was to investigate whether the cytosolic mislocalization of C-terminal FUS mutants observed in HeLa cells can be confirmed in neurons. Therefore, I analyzed the subcellular localization of FUS-WT and FUS-P525L in primary rat hippocampal and cortical neurons using confocal microscopy. In line with the results in HeLa cells, FUS-WT was nuclear, whereas FUS-P525L was redistributed to the cytosol and neuritic processes. Moreover, I showed that N-terminal FUS mutants (G156E, R216C, G225V, R234C, R244C) remained nuclear in HeLa cells and that a combination of N-terminal mutations with the P525L mutation, did not aggravate the cytosolic mislocalization of FUS-P525L.

Furthermore, Dr. Dormann determined that Transportin binds the PY-NLS of FUS and mediates nuclear import of FUS. Notably, upon expression of the Transportin inhibitor GFP-M9M in HeLa cells and primary neurons, FUS was detected in cytosolic, punctate structures. Since FUS is an RNA-binding protein (Zinszner et al., 1997; Iko et al., 2004), we wondered whether the punctate structures are SG and stained with antibodies against SG marker proteins. For further analyses of the punctate structures, I established heat shock as a stressor in HeLa cells and Dr. Dormann confirm that all

cytosolic FUS mutants co-localize with the SG-marker PABP-1. In addition, Prof. Neumann showed that cytosolic, neuronal FUS inclusions in post-mortem brains of ALS and FTLD patients were consistently co-labeled with antibodies against the SG marker proteins PABP-1 and eIF4G.

Nevertheless, it is important to note that cytosolic FUS mutants in the absence of stress show a diffuse cytosolic staining, suggesting that cytosolic mislocalization of FUS does not *per se* induce SG formation, but additional stress is needed to recruit cytosolic FUS in SGs. To test this hypothesis I subjected primary rat hippocampal neurons expressing wildtype FUS or FUS-P525L to heat shock or left them untreated. Indeed, FUS-P525L was recruited into SGs only upon heat shock. FUS-WT remained nuclear after heat shock, even though SGs were formed. These findings suggest that nuclear transport defects and cellular stress are two subsequent hits in the pathological cascade of FUS inclusion formation.

Contribution to this study:

Immunofluorescence staining and confocal analysis of primary rat hippocampal and cortical neurons transiently transfected with HA-FUS-WT, HA-FUS-P525L, GFP or GFP-M9M, respectively (Fig. 3A; 5A; S3A in (Dormann et al., 2010)). Quantification of nuclear and cytosolic HA-FUS-WT and HA-FUS-P525L immunofluorescence intensities (Fig. 3B in (Dormann et al., 2010)). Establishment of heat shock as stressor to induce SGs in transiently transfected HeLa cells and primary neurons (Fig. 8A,B in (Dormann et al., 2010)). Cloning of HA-tagged FUS-P525L carrying additional N-terminal fALS-associated FUS mutation (Fig. S2A in (Dormann et al., 2010)).

3.4 Arginine methylation modulates nuclear import of FET proteins

Dorothee D, Madl T*, Valori CF*, **Bentmann E**, Tahirovic S, Abou-Ajram C, Kremmer E, Ansorge O, Mackenzie IRA , Neumann M, Haass C

Arginine Methylation next to the PY-NLS modulates Transportin Binding and Nuclear Import of FUS

EMBO J. 2012 Nov 14;31(22):4258-75. Epub 2012 Sep 11.

Nuclear import defects seem to be intimately linked to the pathomechanism of ALS-FUS and FTLD-FUS. In ALS-FUS, mutations in the FUS PY-NLS impair the interaction with Transportin, resulting in cytosolic deposition of mutant FUS (Bosco et al., 2010; Dormann et al., 2010). In FTLD-FUS, only rarely mutations in the *FUS* gene are found (Urwin et al., 2010; Snowden et al., 2011; Dormann and Haass, 2013), therefore a mutant PY-NLS cannot be accused for the pathologic mislocalization of FUS, but rather a general transport dysfunction has to be supposed. This notion is supported by the recent detection of the FET proteins EWS and TAF15, two other Transportin-cargo proteins, in FUS inclusions in FTLD-FUS patients (see also Publication 2 (Neumann et al., 2011))(Davidson et al., 2013). Interestingly, all FET proteins were previously shown to be asymmetrically dimethylated in their RGG boxes (Belyanskaya et al., 2001; Rappsilber et al., 2003; Ong et al., 2004; Jobert et al., 2009; Du et al., 2011), but the functional consequences of this posttranslational modification are only poorly understood.

To assess whether arginine methylation affects nuclear transport of FUS, Dr. Dormann treated cells with the broad methylation inhibitor Adenosine-2,3-dialdehyde (AdOx) and analyzed the subcellular localization of HA-tagged FUS-WT and four different ALS-associated FUS mutants. Strikingly, inhibition of arginine methylation with AdOx prevented cytosolic mislocalization of FUS mutants, i.e. these mutants were nuclear in AdOx-treated cells. To test whether nuclear transport of all FET proteins is similarly modulated by arginine methylation, I cloned and expressed wildtype and artificial cytosolic mutants of EWS and TAF15 in untreated and AdOx-treated HeLa cells and analyzed their subcellular localization. In untreated cells, all wildtype FET (FET-WT) proteins were nuclear, whereas the NLS mutants FUS-P525L, EWS-P655L and TAF15-P591L were localized to the cytoplasm. Upon AdOx-treatment, all FET

protein mutants were confined to the nucleus, suggesting that inhibition of methylation affects nuclear import of all FET proteins in a similar manner.

As AdOx is a broad methylation inhibitor, Dr. Dormann aimed to prevent arginine methylation more specifically and silenced PRMT1, the major protein arginine methyltransferase (Bedford and Clarke, 2009; Nicholson et al., 2009) (see also section 1.5). Similar to AdOx, PRMT1 knockdown increased the amount of nuclear FUS-P525L, suggesting that inhibition of arginine methylation restores nuclear import of mutant FUS. To test whether Transportin is responsible for nuclear import of mutant FUS upon inhibition of methylation, Dr. Dormann treated cells expressing GFP-M9M with AdOx. In these cells, FUS-P525L remained cytosolic despite AdOx-treatment, confirming that the nuclear re-localization of FUS-P525L upon inhibition of methylation depends on Transportin. Furthermore, different *in vitro* binding assays revealed that both the PY-NLS and the RGG3 domain interact with Transportin and that arginine methylation in the RGG3 domain of FUS reduces the interaction with Transportin.

To determine if the co-deposition of Transportin with FET proteins in FTLD-FUS could be caused by hypomethylation of FUS, Dr. Dormann raised a monoclonal antibody specific to methylated FUS. Using this antibody, Prof. Neumann determined that FUS inclusions in ALS-FUS contain methylated FUS. In a HeLa cell line stably expressing FUS-P525L, which I generated, Dr. Dormann observed that FUS-P525L is recruited into SGs in the methylated state, thus reflecting the pathology observed in ALS-patients. In contrast, methylated FUS cannot be detected in FUS inclusion in FTLD-FUS patients, suggesting that hypomethylation might be involved in the pathomechanism. This corroborates the hypothesis that both diseases are caused by distinct pathomechanisms.

Contribution to this study:

Cloning of EWS and TAF15 constructs, transient transfection of HA-tagged FUS, EWS or TAF15 (WT or cytosolic mutant) into HeLa cells, immunofluorescence staining, confocal analysis and quantification of nuclear and cytosolic fluorescence intensities (Fig. 2 (Dormann et al., 2012)). Generation of HeLa cell lines stably expressing HA-tagged FUS-WT or FUS-P525L by lentiviral transduction (Fig. 8D (Dormann et al., 2012)). Drawing of a model figure (Fig. 10 B (Dormann et al., 2012)).

Additional unpublished data

Recently, the identification of *TAF15* mutations in sporadic ALS cases was reported (Couthouis et al., 2011). These *TAF15* mutations cluster in the C-terminal ZnF and RGG3 domain but are not located in the PY-NLS (Fig 3). As mainly arginine and glycine residues are mutated, I wondered whether these mutations affect the subcellular localization of TAF15, e.g. by altering arginine methylation of the RGG3 domain and thus disrupting the interaction with Transportin. To test this hypothesis, I cloned and expressed TAF15-WT, TAF15-P591L, and four different ALS-associated *TAF15* mutants (M368T, D386N, G391E, G473E) in untreated or AdOx-treated HeLa cells. As a positive control for AdOx treatment, I used the artificial cytosolic mutant TAF15-P591L, which indeed became nuclear upon AdOx treatment (Fig. 9, right panel). However, ALS-associated *TAF15* mutants remained predominantly nuclear in untreated and AdOx-treated cells (Fig. 9, middle panels), demonstrating that ALS-associated *TAF15* mutations do not alter nuclear import of TAF15 mutants and suggesting an undisturbed interaction with Transportin.

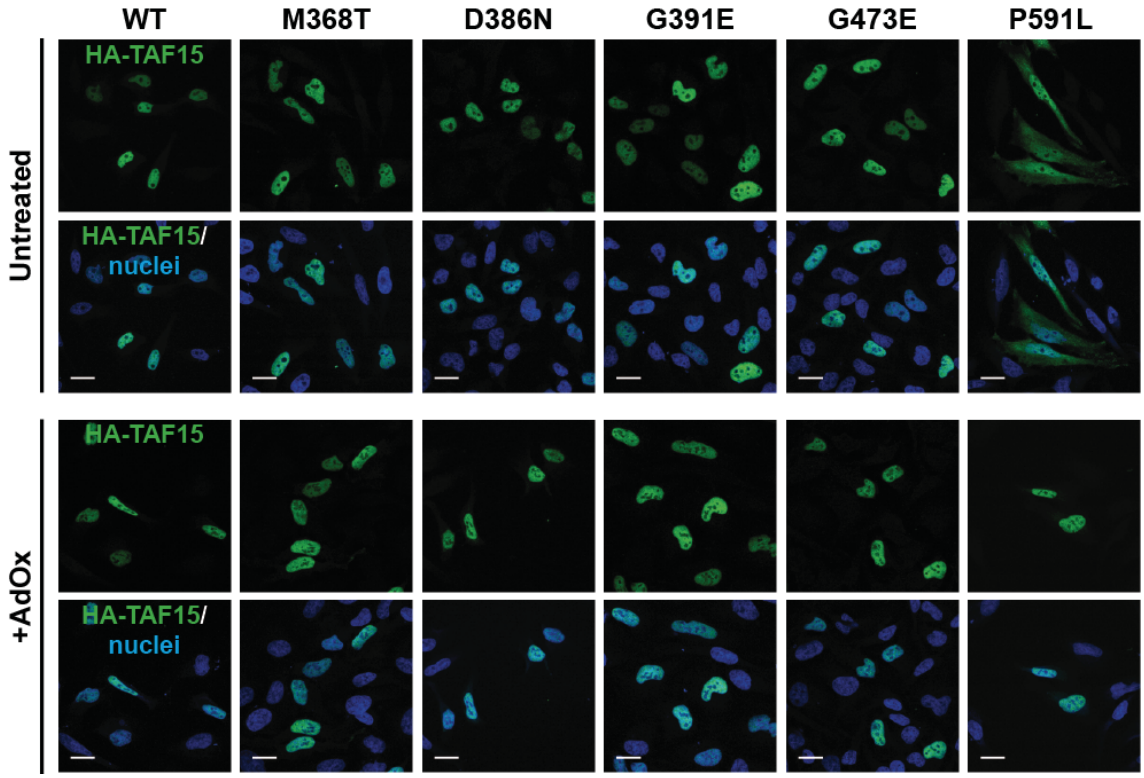

Fig. 9. ALS-associated *TAF15* mutations do not disturb nuclear localization of TAF15. HA-tagged TAF15-WT or TAF15 carrying the indicated ALS-associated mutations or a mutation disrupting the PY-NLS (P591L) were transiently expressed in untreated (upper panels) or AdOx-treated (lower panels) HeLa cells for 24h. Cells were fixed, stained with an HA (green)-specific antibody and a nuclear counter-stain (blue) and analyzed by confocal microscopy. ALS-associated TAF15 mutants are nuclear in both untreated and AdOx-treated cells, suggesting that the mutations do not impair the recognition of the PY-NLS by Transportin. In contrast, the artificial P591L mutation disrupts the PY-NLS and results in cytosolic mislocalization of TAF15; upon AdOx treatment, this mutant is predominantly nuclear, indicating that methylation modulates nuclear import of TAF15. Scale bar: 20 µm.

3.5 Additional Publication:

At the 32nd Blankenese Conference I won the poster prize which came with the invitation to write a review for the FEBS Journal.

Bentmann E, Haass C, Dormann D

Stress Granules in Neurodegeneration – Lessons learnt from TDP-43 and FUS

FEBS J 2013 Sep;280(18):4348-70. Epub 2013 May 9

Contribution:

Content and writing of the manuscript.

4 Discussion

4.1 FUS and TDP-43 have similar requirements for SG recruitment

4.1.1 RNA-binding properties are essential but not sufficient for SG recruitment of FUS

Given the potential importance of SGs in the formation of pathological FUS inclusion, I set out to determine how FUS is recruited into SGs. Some studies report that transient overexpression of ALS-associated cytosolic FUS mutants or even FUS-WT is sufficient to induce SG formation (Andersson et al., 2008; Kino et al., 2010; Gal et al., 2011; Ito et al., 2011). However, I and others found that upon moderate transient or stable expression FUS mutants remain diffusely distributed in the cytosol and that additional stress is needed to induce SG formation (Bosco et al., 2010; Dormann et al., 2010; Bentmann et al., 2012; Kato et al., 2012). These results suggest that formation of SGs upon transient overexpression of mutant FUS is most likely due to transfection stress (Kedersha and Anderson, 2007; Bentmann et al., 2013). Moreover, I tested three different stressors and investigated if one of these stressors would result in the localization of FUS-WT into cytosolic SGs as previously described (Andersson et al., 2008; Blechingberg et al., 2012). However, regardless of which stressor was analyzed, FUS-WT is confined to the nucleus and does not localize to TIA-1 positive SGs (Bentmann et al., 2012). In contrast, the ALS-associated cytosolic mutant FUS-P525L consistently localize in SGs upon treatment with all stressors tested. Thus, cytosolic mislocalization is a prerequisite for SG recruitment of FUS (Bentmann et al., 2012).

Moreover, I set out to determine in detail which domains are required for SG recruitment of FUS. Two mutually non-exclusive mechanisms of SG recruitment are conceivable – (1) RNA-binding and/or (2) protein-protein interactions. My results have shown that FUS is mainly recruited into SGs via RNA-binding mediated by the RGG2-ZnF-RGG3 domain (Bentmann et al., 2012) (see model in Fig. 10). In addition, the RGG1 domain and the RRM domain contribute to SG recruitment of FUS, but show no RNA-binding to UG-rich oligonucleotides. Form these results I conclude that beside RNA-binding mediated by the RGG2-ZnF-RGG3 domain, putative protein-protein interactions mediated by the RGG1 domain and RRM domain facilitate SG recruitment of FUS (Fig. 10) (Bentmann et al., 2012). Consistent with my data, another group reported that the RGG2-ZnF-RGG3 domain is the main RNA-binding domain (Iko et

al., 2004). Nevertheless, it cannot be excluded that the RGG1 and RRM domains bind to other RNAs that are not UG-rich, as several groups identified additional RNA-binding motifs of FUS (Lerga et al., 2001; Hoell et al., 2011). In this case, the RGG1 and RRM domains may contribute to SG recruitment also by binding to RNA.

Surprisingly, the N-terminal prion-like SYGQ-rich domain does not seem to contribute to SG recruitment of FUS, but seems to be entirely dispensable. This is an unexpected result, as it was reported that the prion-like domain of TIA-1, which shows homology to the prion-like domain of FUS (King et al., 2012), facilitates SG formation (Gilks et al., 2004; Furukawa et al., 2009). Moreover, the SYGQ-rich domain of FUS is aggregation-prone and aggregated FUS binds prion-like domains of other RNA-binding proteins that are also SG components (Kato et al., 2012). Artificial tyrosine (Y) to serine (S) mutations within the SYGQ-domain have been reported to disrupt the association of FUS with SGs (Kato et al., 2012), which at first glance seems to contradict my finding that the SYGQ-domain is dispensable for SG recruitment. However, the authors of this study did not co-label for a SG marker protein, so it is impossible to distinguish between two possible scenarios: First, it might be that Y to S mutations prevent the reversible transition from soluble to polymeric FUS. This transition might be essential for the movement in and out of SGs and hence Y to S FUS mutants are not detected in SGs. Second, the Y to S mutations might create a dominant-negative FUS mutant which inhibits SG formation in general and therefore Y to S FUS mutants remain diffusely distributed in the cytosol during cellular stress. My preliminary data provide evidence for the latter scenario, since I found that cells expressing Y to S FUS mutants have a strongly reduced number of SGs (data not shown). Although a detailed analysis would be required to further elucidate the dominant-negative mechanism of these Y to S mutants on SG formation, these results would give an explanation for the conflicting results. Nevertheless, one has to be cautious when comparing deletion mutants with artificial point-mutants, as both deletion of a whole domain and change of several amino acids in a specific domain might change protein folding. However, as deletion of the Q domain did not impair RNA-binding of FUS, it seems likely that this deletion mutant is properly folded and thus comparable to full-length FUS.

Although cytosolic FUS is readily sequestered into SGs, depletion of FUS does not inhibit SG formation *per se* (Fig. 7B). These results are in agreement with two other studies showing that transient FUS knockdown does not change the number of SGs per cell or the size of SGs (Aulas et al., 2012; Blechingberg et al., 2012). Thus, I conclude

that FUS is not an essential SG component whose presence is necessary for SG formation.

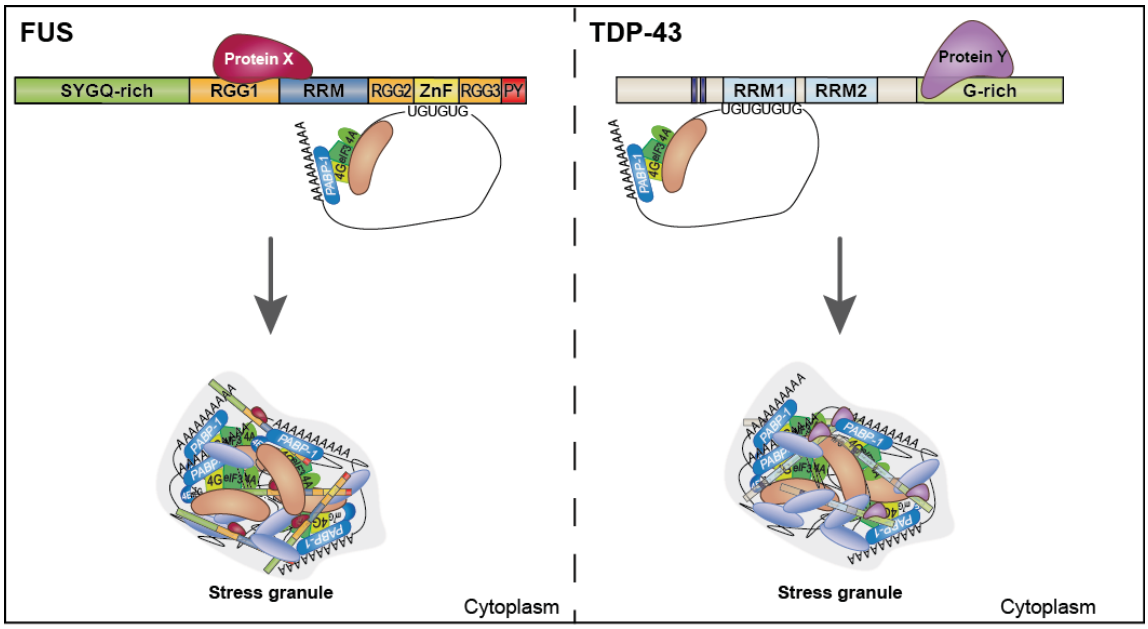

Fig. 10. Model of SG recruitment of FUS and TDP-43. Upon stress, translation is paused and the 48S pre-initiation complex consisting of the small ribosomal subunit, translation initiation factors and PABP-1 bound to mRNA is transiently stored in SGs. I propose that SG recruitment of FUS and TDP-43 involves RNA-binding and protein-protein interactions. Both proteins bind UG-rich RNAs via their major RNA-binding domains (RGG2-ZnF-RGG3 for FUS and RRM1 for TDP-43) and thus might be routed into SG by the associated mRNAs. Yet, additional domains which showed no binding to UG-rich RNAs, enhance recruitment of FUS to SGs. These results suggest that additional protein-protein interaction with the currently unknown proteins X and Y participate in SG recruitment of FUS and TDP-43.

4.1.2 TARDBP *mutations do not affect subcellular localization or SG recruitment of TDP-43*

In contrast to C-terminal ALS-associated *FUS* mutations that are known to disrupt nuclear import of FUS, the mechanism behind *TARDBP* mutations is still puzzling. Some studies claim that *TARDBP* mutations result in cytosolic mislocalization (Barmada et al., 2010; Liu-Yesucevitz et al., 2010; Ritson et al., 2010). However, I did not observe cytosolic accumulation of the three different *TARDBP* mutations (A315T, M337V, G348C) tested (Bentmann et al., 2012), consistent with reports from others (Kabashi et al., 2010; Ling et al., 2010; Voigt et al., 2010; Dewey et al., 2011). These conflicting results might be due the fact that different studies investigated different ALS-associated *TARDBP* mutations or due to different cell types used for the analysis.

Nevertheless, cytosolic mislocalization does not seem to be a general and obvious pathomechanism for *TARDBP* mutations.

As cytosolic mislocalization is a crucial prerequisite for SG recruitment of FUS, I speculated that the recruitment of TDP-43 into SGs might also require cytosolic mislocalization. To test this hypothesis, I analyzed whether TDP-WT localizes in SGs upon cellular stress. Regardless of which stressor is used, TDP-WT remains nuclear, although TIA-1 positive SGs are formed. In contrast, TDP-43 with an artificial NLS mutation (TDP-NLS_{mut}), which is diffusely distributed in the cytosol without stress, is recruited into cytoplasmic SGs upon exposure to different stressors. This demonstrates that similar to FUS, also for TDP-43 cytosolic mislocalization is a prerequisite for SG recruitment.

An alternative pathomechanism of *TARDBP* mutations could be alterations in SG formation and kinetics. One study suggested that the ALS-associated mutation they analyzed (R361S) is a loss-of-function mutation as cells expressing this *TARDBP* mutant formed less SGs during stress (McDonald et al., 2011). However, two other studies reported an increase in SG formation upon overexpression of *TARDBP* mutants, indicating a gain-of-function mechanism (Liu-Yesucevitz et al., 2010; Dewey et al., 2011). Yet, I did not observe such effects for three ALS-associated *TARDBP* mutations examined, as their presence did not alter the amount of TDP-NLS_{mut} sequestered in SGs (Bentmann et al., 2012). Nevertheless, it cannot be excluded that other *TARDBP* mutations, which were not analyzed here, alter SG recruitment of TDP-43 or SG persistence, disassembly or dynamics.

Additionally, I demonstrated that TDP-43 is not essential for SG formation (Fig. 7D) consistent with the results of two other studies (Colombrita et al., 2009; Liu-Yesucevitz et al., 2010). In contrast, two other groups reported that depletion of TDP-43 leads to a reduced number of SGs and that the remaining SGs are smaller, however, the effects are quite small (McDonald et al., 2011; Aulas et al., 2012). Thus, additional detailed investigation of SG formation and kinetics upon TDP-43 depletion are necessary to determine whether or not TDP-43 influences SG formation, size or dynamics.

4.1.3 TDP-43 is recruited into SGs via RNA-binding and additional protein-protein interactions

By analyzing SG recruitment of TDP-43 in further detail, I showed that full-length TDP-43 is rapidly sequestered into SGs upon stress, whereas TDP-CTF is only poorly recruited to SGs (Bentmann et al., 2012). TDP-CTFs lack the RRM1, which is essential for binding of TDP-43 to UG-rich RNA oligonucleotides (Buratti and Baralle, 2001; Bentmann et al., 2012), indicating that RNA-binding is essential for SG recruitment of TDP-43. Nevertheless, protein-protein interactions may also be involved in SG recruitment of TDP-43, as a TDP-43 mutant lacking the G-rich domain ($NLS_{mut-\Delta C}$) is only poorly recruited to SGs. This domain mediates interaction with hnRNP A1 and hnRNP A2/B1 (Buratti et al., 2005) and possibly other unknown proteins, so it might be that these protein-protein interactions facilitate SG recruitment of TDP-43 (Fig. 10).

Furthermore, through my collaboration with Prof. Manuela Neumann, I could resolve controversial results regarding SG markers in pathological TDP-43 inclusions. Two studies reported a lack of SG marker proteins in pathological inclusions (Colombrita et al., 2009; Dormann et al., 2010), whereas two others detected SG marker proteins as consistent components of TDP-43 inclusions (Volkening et al., 2009; Liu-Yesucevitz et al., 2010). I demonstrated that the co-deposition of SG markers depends on the analyzed tissue and thus on the TDP-43 species present in TDP-43 inclusions (Igaz et al., 2008; Neumann et al., 2009c; Bentmann et al., 2012). TDP-43 inclusions in the spinal cord containing mainly full-length TDP-43 are SG-marker positive. In contrast, hippocampal inclusions enriched for TDP-CTFs are SG-marker negative (Bentmann et al., 2012). This is in accordance with my data in HeLa cells (see above) where only full-length TDP-43 was efficiently recruited into SGs.

How differences in the composition of TDP-43 inclusions between tissues arise, why TDP-CTFs are especially enriched in hippocampal inclusions and how TDP-CTFs are generated is still enigmatic. The absence of SG markers from CTF-containing inclusions could have two plausible explanations. First, TDP-CTF might be formed by proteolytic cleavage of full-length TDP-43 present in SGs. Due to lack of RNA-binding of the newly generated TDP-CTFs, they may dissociate and give rise to SG-marker negative inclusions. Second, they might be formed independently of SG recruitment of TDP-43. TDP-CTFs have a higher aggregation propensity than TDP-WT (Li et al., 2011) and TDP-CTFs induce formation of hyperphosphorylated and ubiquitinated TDP-43 inclusions in cultured cells over time (Igaz et al., 2009; Nonaka et al., 2009; Li et al.,

2011). However, further studies are required to unveil which of these scenarios is correct or whether a completely different mechanism is responsible for deposition of TDP-CTFs without SG markers.

4.2 FUS inclusions in ALS-FUS and FTLD-FUS vary in their composition

ALS-FUS and FTLD-FUS are both FUS-proteinopathies with characteristic FUS-positive inclusions and initially it was suggested that they might have a common underlying pathomechanism. However, significant differences in the composition of FUS inclusions in ALS-FUS and FTLD-FUS have provided strong evidence that the two diseases have different underlying pathomechanisms. I demonstrated that upon expression in HeLa cells, only the ALS-associated FUS-P525L mutant, but none of the other FET proteins is cytosolically mislocalized and sequestered in SGs upon cellular stress (Neumann et al., 2011). This can be explained by the fact that only the PY-NLS of FUS is disrupted by ALS-associated mutations and the PY-NLSs of EWS and TAF15 are still intact. Furthermore, the observation that the FET family members EWS and TAF15 remain nuclear in HeLa cells expressing FUS-P525L, demonstrates that cytosolic accumulation of FUS does not co-sequester the other FET family proteins. Consistently, FUS inclusions in ALS-FUS patients, which carry an ALS-associated mutation, contain only FUS but not EWS or TAF15 (Neumann et al., 2011).

In sharp contrast to ALS-FUS, pathological inclusions in FTLD-FUS contain all FET proteins. However, there are some differences between EWS and TAF15. Whereas the latter is detected in all FUS inclusions in FTLD-FUS, EWS is not consistently found in theses inclusions and often to a smaller amount than TAF15 (Neumann et al., 2011). By inhibition of Transportin-mediated nuclear transport in HeLa cells, I could mimic these neuropathological findings. Upon expression of GFP-M9M, all FET proteins accumulate in the cytosol (Neumann et al., 2011), however the co-accumulation of TAF15 with FUS in SGs is much stronger than the co-accumulation of EWS with FUS in SGs, as a substantial proportion of EWS is still detected in the nucleus and only a minor extent is recruited into SGs (Neumann et al., 2011). As inhibition of Transportin-mediated nuclear transport resembles the composition of pathologic inclusions found in FTLD-FUS patients, the pathomechanism of FTLD-FUS may involve a general

dysfunction in nuclear import of FET proteins, followed by their sequestration into SGs (Dormann and Haass, 2011; Neumann et al., 2011; Rademakers et al., 2013).

Interestingly, the nuclear import receptor of FUS, Transportin (Lee et al., 2006; Dormann et al., 2010), is consistently found in FUS inclusions in FTLD-FUS but not in ALS-FUS patients (Brelstaff et al., 2011; Neumann et al., 2012; Davidson et al., 2013). Yet, it is still debated whether Transportin becomes insoluble in FTLD-FUS or not. One study shows that Transportin becomes insoluble in FTLD-FUS patients whereas in control patients Transportin remains soluble (Brelstaff et al., 2011). In contrast, another study could not confirm this result, as they reported that the solubility of Transportin varies in both FTLD-FUS patients and health controls, thus insolubility of Transportin could not be linked to FTLD-FUS (Neumann et al., 2012) Further studies are required to determine whether Transportin is insoluble in FTLD-FUS patients.

The accumulation of Transportin in FUS/FET inclusions might give rise to a vicious circle in which the deposition of Transportin in FUS inclusions decreases the availability of Transportin for FUS and possibly other PY-NLS-containing cargo proteins in the cytosol (Brelstaff et al., 2011). Thus Transportin-mediated nuclear transport may be derogated and cytosolic accumulation of FUS may steadily increase. Recent analysis of 13 additional Transportin cargos demonstrated that these cargos are not co-deposited in FTLD-FUS inclusions. This indicates that a general Transportin defect that affects multiple PY-NLS cargo proteins, e.g. due to age-dependent decline in expression or genetic alterations, is not very likely. The fact that some cargos seems to be correctly imported while others not, rather points to an alternative mechanism, e.g. posttranslational modifications in specific cargo proteins, that specifically alter the interaction of these proteins with Transportin.

4.3 *FUS* mutations in ALS-FUS disrupt nuclear import of FUS

During my collaboration with Dr. Dormann, we were able to unveil that ALS-associated *FUS* mutations result in the cytosolic mislocalization of these FUS mutants by disrupting the interaction between FUS and Transportin in HeLa cells and in primary neurons (Dormann et al., 2010). FUS directly interacts with both Transportin 1 and Transportin 2 (Guttinger et al., 2004) and upon knockdown of either Transportin 1 or

Transportin 2 alone FUS is still efficiently imported (Dormann et al., 2010), suggesting that the two Transportin isoforms are functionally redundant. Several other studies have confirmed that ALS-associated *FUS* mutations cause cytosolic mislocalization of FUS (Bosco et al., 2010; Kino et al., 2010; Gal et al., 2011; Ito et al., 2011) and that mutations in the PY-NLS weaken the Transportin-binding affinity of FUS (Niu et al., 2012; Zhang and Chook, 2012).

Intriguingly, the affinity of FUS mutants with Transportin correlates with the degree of cytosolic mislocalization of FUS and the age of disease-onset and disease duration in FUS mutation carriers (Dormann et al., 2010; Niu et al., 2012; Zhang and Chook, 2012). For example, the P525L mutation, often associated with juvenile-onset ALS and rapid disease progression (Chio et al., 2009b; Kwiatkowski et al., 2009; Baumer et al., 2010; Sproviero et al., 2012) decreases Transportin binding by 9-fold (Zhang and Chook, 2012) and shows a very drastic mislocalization (Dormann et al., 2010). In addition, *FUS* truncation mutations lacking the entire PY-NLS have an unusual early disease-onset and a more severe phenotype compared to most ALS-associated *FUS* missense mutations (Waibel et al., 2010; Yan et al., 2010; Belzil et al., 2011; Yamashita et al., 2012; Waibel et al., 2013), thereby corroborating the correlation between reduced Transportin affinity, cytosolic mislocalization and disease severity. In contrast, *FUS* mutations associated with mid- and late-onset ALS, such as R521C and R524C, decrease Transportin binding affinity by only 3-fold and 1.4-fold, respectively (Zhang and Chook, 2012) and show only a mild cytosolic mislocalization (Dormann et al., 2010). Although FUS mutants have reduced binding affinities compared to FUS-WT, they are still in the nanomolar range which means that they still, albeit weaker, interact with Transportin. These remaining binding affinities of many *FUS* mutants might explain disease manifestation later in life and the fact that cells transfected with FUS mutants (Bosco et al., 2010; Dormann et al., 2010; Gal et al., 2011; Ito et al., 2011; Dormann et al., 2012) or neurons harboring pathological FUS inclusion in FUS-proteinopathies (Neumann et al., 2009a) still have some nuclear FUS.

4.4 Aberrant arginine methylation in FTLD-FUS?

ALS-FUS is caused by mutations in the *FUS* gene; in contrast, *FUS* mutations were detected only very rarely in FTLD-FUS, suggesting that another mechanism might cause cytoplasmic mislocalization of FUS in FTLD-FUS patients. This is also supported by the different composition of FUS inclusions in ALS-FUS and FTLD-FUS (see section 4.2). In my collaboration with Dr. Dormann, we demonstrated that arginine methylation in the RGG3 domain adjacent to the PY-NLS additionally influences the interaction of FUS with Transportin (Dormann et al., 2012). In general, post-translational modifications can alter nuclear transport (see section 1.4) (Terry et al., 2007; Nicholson et al., 2009; Nardozzi et al., 2010), and for example arginine methylation triggers nuclear localization of several RNA-binding proteins (Cote et al., 2003; Aoki et al., 2002; Araya et al., 2005)

Inhibition of arginine methylation reverses the cytosolic mislocalization of several cytosolic ALS-associated *FUS* mutations, e.g. FUS-P525L, by restoring Transportin-mediated nuclear import (Dormann et al., 2012). Likewise, cytosolic mislocalization of artificial cytosolic mutants of EWS and TAF15 is prevented by inhibition of arginine methylation, pointing to a common mechanism in all FET proteins (Dormann et al., 2012).

Analysis of FUS inclusions in ALS-FUS and FTLD-FUS elucidated that antibodies specific for methylated FUS (meFUS) label ALS-FUS inclusions but not FTLD-FUS inclusions (Dormann et al., 2012). This lack of labeling with meFUS specific antibodies in FTLD-FUS prompted us to propose that these FUS inclusions are hypomethylated. As FTLD-FUS inclusions contain all FET proteins (Neumann et al., 2011), we hypothesize that hypomethylation of all FET proteins is responsible for overly tight FET-Transportin-binding and thus selective co-deposition of FET proteins with Transportin in FTLD-FUS. Deposition in the cytoplasm may occur because Transportin-FET complexes may be unable to dissociate in the nucleus, and instead may be re-exported into the cytoplasm. Thus, overly tight binding of FET proteins to Transportin could result to increased levels of FET proteins in the cytosol.

As PRMT1 has been shown to methylate all FET proteins (see section 1.3) (Araya et al., 2005; Pahlich et al., 2005; Jobert et al., 2009; Dormann et al., 2012; Tradewell et al., 2012; Yamaguchi and Kitajo, 2012; Scaramuzzino et al., 2013), it can be speculated that PRMT1 is downregulated or mutated in FTLD-FUS patients.

However, by sequencing PRMT1, PRMT3, and PRMT8 in 20 FTLD-FUS patients, no mutations could be identified, demonstrating that mutations in PRMTs are not a common cause for the hypomethylation of FET proteins in FTLD-FUS (Ravenscroft et al., 2013). Furthermore, another PRMT1-substrate, PABPN1, which has a higher affinity for Transportin in the unmethylated state than in the methylated state (Fronz et al., 2011), is not co-deposited with FET proteins in post-mortem brains of FTLD-FUS patients but shows a normal nuclear staining (Neumann et al., 2012). This suggests that PRMT1 activity and levels are probably not altered in FTLD-FUS, since one would then also expect PABPN1 to be hypomethylated and co-deposited in pathological inclusions. Nevertheless, three different PRMTs (PRMT1, PRMT3, PRMT6) can methylate PABPN1 *in vitro* (Fronz et al., 2008) and it needs to be addressed whether PRMT3 and PRMT6 can compensate for a loss of PRMT1 *in vivo*, explaining why PABPN1 may not be co-deposited in FTLD-FUS inclusions despite a PRMT1 defect.

4.5 Multiple hit-model for the pathogenesis of FUS- and TDP-proteinopathies

The finding that ALS-associated FUS mutations disrupt the protein´s NLS and result in cytosolic mislocalization (Dormann et al., 2010) has been an important step in understanding the pathomechanism of FUS-proteinopathies. However, expression of FUS mutants in different cell lines or primary neurons results in a diffuse cytosolic distribution of these mutants (Bosco et al., 2010; Dormann et al., 2010; Kino et al., 2010; Bentmann et al., 2012) and does not mimic the large pathological FUS-inclusions observed in ALS-FUS or FTLD-FUS patients (Fig. 11)

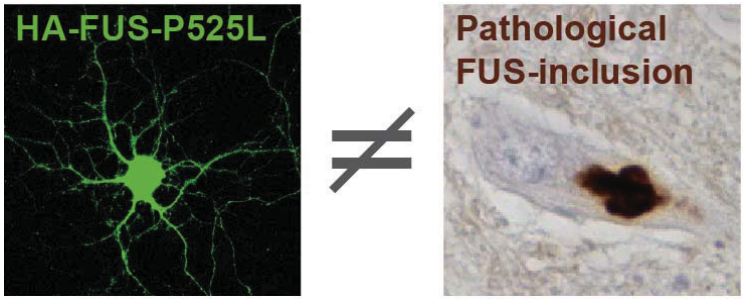

Fig. 11. Diffuse distribution of FUS-P525L in neurons is in stark contrast to aggregated FUS-inclusions. Without additional exposure to cellular stressors, HA-tagged FUS-P525L is diffusely distributed in primary neurons (left). This diffuse distribution is in stark contrast to the large cytosolic aggregates found in patients with FUS-proteinopathies (right). Similar results are also obtained for TDP-43. Figure with pathological inclusion taken from (Dormann and Haass, 2011).

From this result, we concluded that FUS mutations alone might not be sufficient to evoke FUS inclusion formation, but might be rather the first hit in a pathological cascade, which brings a nuclear protein into the cytosol. Furthermore, we hypothesized that cellular stress may be the second hit, which brings cytosolic FUS or TDP-43 into SGs and that SGs might be the origin of the pathological inclusions containing aggregated FUS and TDP-43. Several studies that found SG marker proteins in pathological FUS or TDP-43 inclusions support this hypothesis (Fujita et al., 2008; Volkening et al., 2009; Baumer et al., 2010; Dormann et al., 2010; Elden et al., 2010; Liu-Yesucevitz et al., 2010; Bentmann et al., 2012). Nevertheless, SGs in cultured cells are under all stress conditions tested reversible, as they fully disassemble during the recovery period when cells are not anymore exposed to cellular stress (Fig. 12). Thus, even though the sequestration of cytosolic FUS or TDP-43 into SGs might be the second hit in FUS and TDP-proteinopathies, it still does not fully reflect all events in the pathogenesis of FUS and TDP-43 inclusions.

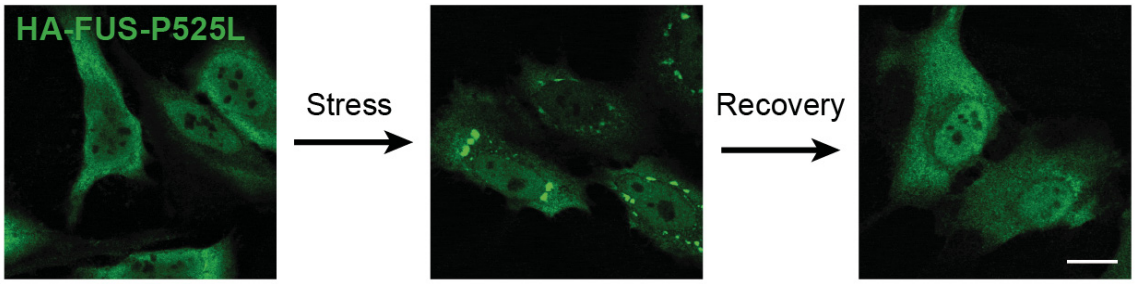

Fig. 12. Upon stress, FUS-P525L is recruited into SGs, however, these FUS-containing SGs dissolve after recovery from stress. Upon low level transient expression HA-tagged FUS-P525L shows a uniform distribution in HeLa cells (left). When cells are exposed to stress, in this case to heat shock, they readily form SGs and FUS-P525L is recruited into these granules (middle). When sublethal stress has passed, SGs disassemble, release their components and FUS is again uniformly distributed in the cell (right). Scale bar: 20 µm. Figures taken from (Bentmann et al., 2012).

The results of our group (Dormann et al., 2010; Bentmann et al., 2012) allowed us to develop a multiple hit model of FUS and TDP-43 inclusion formation (Fig. 13) (Dormann and Haass, 2011). In this model the first hit is the cytosolic mislocalization of FUS or TDP-43. The second hit is the recruitment of cytosolic mislocalized FUS or TDP-43 in SGs upon cellular stress and the third hit is the conversion of reversible SGs into irreversible pathological inclusions.

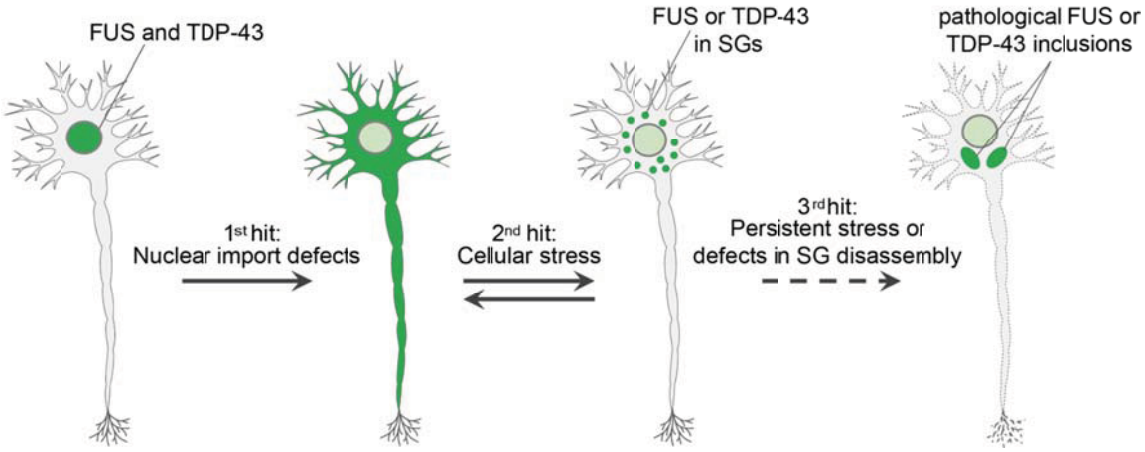

Fig. 13. Multiple hit model of pathogenesis in FUS-proteinopathies and TDP-proteinopathies. Schematic model displaying how multiple steps might result in FUS or TDP-43 pathology. In this model the first hit is a nuclear import defect, e.g. by mutations disrupting the NLS or reduced levels of transport factors, which causes cytosolic mislocalization of FUS or TDP-43. The second hit is cellular stress, e.g. oxidative stress or thermal stress, which recruits cytosolic FUS and TDP-43 into SGs. As SG assembly is reversible, SGs dissociate upon recovery from stress and liberate cytosolic FUS and TDP-43. Persistent stress, dysfunction in SG dissolution or autophagic defects might serve as third hit resulting in insoluble, irreversible pathological inclusions. Figure taken from (Dormann and Haass, 2011).

4.6 Multiple hits in FUS-proteinopathies

4.6.1 First Hit: Distinct nuclear import defects lead to cytosolic FUS in ALS-FUS and FTLD-FUS

ALS-FUS and FTLD-FUS have overlapping clinical phenotypes and are characterized by cytoplasmic and nuclear FUS inclusions that also contain SG marker proteins. However, some striking molecular differences have been unveiled (Table 2).

Table 2. Similarities and differences between ALS-FUS and FTLD-FUS

	ALS-FUS	FTLD-FUS
Disease-associated *FUS* mutations	+	-
Cytosolic and/or nuclear FUS inclusions	+	+
Stress granule markers in FUS inclusions	+	+
Co-deposition of FET proteins and Transportin	-	+
Methylated FUS in FUS inclusions	+	-

Although nuclear and cytosolic FUS inclusions were found in ALS-FUS and FTLD-FUS, the lack of FUS mutations in FTLD-FUS cases and the different protein composition in FUS inclusions in ALS-FUS and FTLD-FUS indicates a different pathomechanism.

In ALS-FUS, mutations disrupt the PY-NLS of FUS, therefore mutant FUS accumulates in the cytoplasm but EWS and TAF15 remain nuclear as their PY-NLS is unaffected (Fig. 16A) (Dormann et al., 2010; Dormann and Haass, 2013). In FTLD-FUS, FUS and presumably the other FET proteins are hypomethylated, which results in an overly tight interaction with Transportin (Dormann et al., 2012). This may cause re-export of the FET proteins together with Transportin from the nucleus to the cytoplasm and deposition of the Transportin-FET complexes in pathological aggregates (Fig. 16B) (Dormann et al., 2010; Dormann and Haass, 2013). Thus, different pathomechanisms result in cytosolic mislocalization of FUS in ALS-FUS and FTLD-FUS. Nevertheless, cytosolic mislocalization of this, under normal conditions predominantly nuclear, protein seems to be an essential first hit in the pathological cascade that leads to FUS and TDP-43 inclusion formation.

4.6.2 Second hit: Recruitment of cytosolic FUS in SGs

The causes for cytosolic mislocalization of FUS in ALS-FUS and FTLD-FUS are different, but the consequence is the same. After this first hit, the pathomechanisms of ALS-FUS and FTLD-FUS converge in the second hit, which is the recruitment of cytosolic FUS in SGs during cellular stress (Fig. 16C). When I transiently transfect ALS-associated FUS mutants in HeLa cells or neurons, I obtained diffusely distributed, cytosolic FUS and no obvious aggregation (Dormann et al., 2010). Additional stress, such as oxidative or thermal stress, is needed to sequester cytosolic FUS into SGs in cell culture and thus serves as a second hit in the cascade that ultimately leads to pathological FUS inclusions (Bosco et al., 2010; Dormann et al., 2010; Bentmann et al., 2012).

In vivo, SGs have been observed upon hypoxia, brain injury and ischemia, e.g. in muscles of Drosophila (van der Laan et al., 2012) and in brains of rats and mice (Kim et al., 2006; Moisse et al., 2009b). Remarkably, oxidative stress (Barber and Shaw, 2010), head injury (Abel, 2007; Chen et al., 2007; Chio et al., 2009a; Gavett et al., 2011), reduced blood flow (Tanaka et al., 1993; Rule et al., 2010) and chronic viral infection (De Chiara et al., 2012) have been associated with an increased risk for motor neuron disease and dementia and might be second hits *in vivo* in the pathogenesis of ALS-FUS and FTLD-FUS, driving diffusely distributed FUS into SGs.

Notably, FUS-positive SGs in cells and FUS inclusions in ALS and FTLD share some important features, corroborating our hypothesis that pathological FUS inclusions

may arise from SGs. Both are composed of granular fibrils of about 10 nm with moderate electron density and are non-membrane bound structures (Munoz-Garcia and Ludwin, 1984; Kedersha and Anderson, 2002; Mosaheb et al., 2005; Souquere et al., 2009). In addition, certain proteins such as PABP-1, eIF4G and TIA-1 and poly(A)-mRNA are characteristic components of SGs in cell culture (Kedersha et al., 2000; Kedersha et al., 2002) and were found to be co-deposited in pathological FUS inclusion in ALS-FUS and FTLD-FUS cases (Fujita et al., 2008; Souquere et al., 2009; Baumer et al., 2010; Dormann et al., 2010). Nevertheless, some differences exist, as SGs are dynamic and reversible structures that dissolve upon stress removal (Kedersha et al., 1999; Bentmann et al., 2012), whereas FUS inclusions are insoluble (Neumann et al., 2009a). SGs in cell culture are usually multiple small granules, whereas FUS inclusions in post-mortem brains are much larger and usually only one inclusion per cell is observed (Neumann et al., 2009a; Dormann et al., 2010). However, during cellular stress SGs can enlarge and coalesce (Kedersha et al., 2000) and it is conceivable that a third hit might promote the fusion of SGs to larger insoluble FUS inclusions (Fig. 16D).

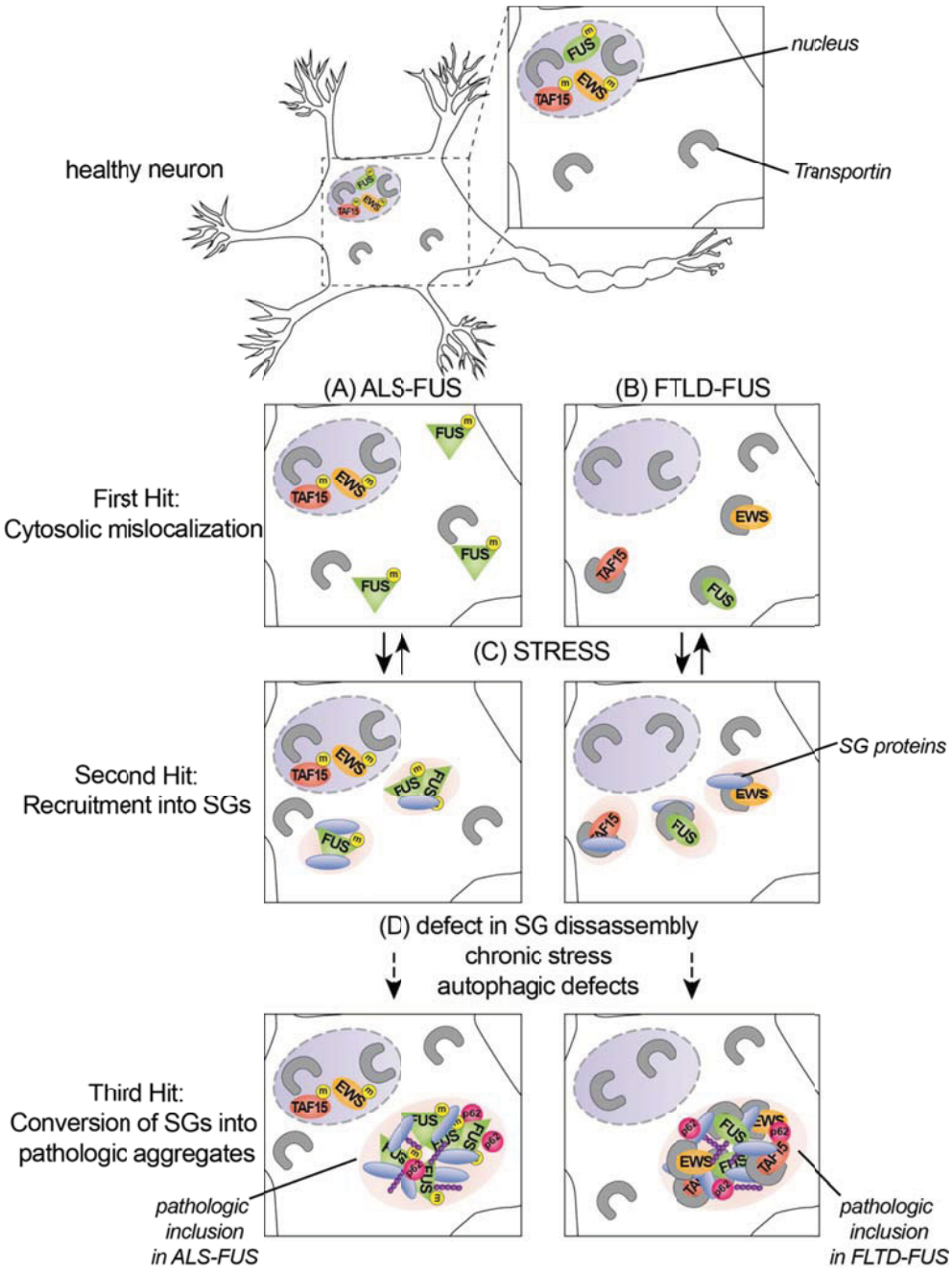

Fig.16. Multiple hit model and distinct pathomechanisms in FUS-proteinopathies. In healthy cells, methylated FET proteins are confined to the nucleus (upper panel, yellow m: arginine methylation). Distinct pathomechanisms are suggested to cause cytosolic mislocalization of FUS and FET proteins, respectively, in ALS-FUS and FTLD-FUS. (**A**) In ALS-FUS, mutations in the PY-NLS of FUS hamper the interaction with Transportin, resulting in the cytosolic mislocalization of methylated mutant FUS. Note that EWS and TAF15 remain in the nucleus. (**B**) In FTLD-FUS, hypomethylated FET proteins have increased binding affinities for Transportin and become cytosolic via an unknown mechanism, possibly by re-export of Transportin-FET complexes to the cytosol. (**C**) Upon cellular stress, cytosolic FUS (left) or all FET proteins (right) are recruited in SGs. (**D**) These SGs are dynamic and fuse. Over time they might become insoluble and irreversible via an unknown mechanism. Defects in SG disassembly e.g. by inhibition of DYRK3, chronic stress or autophagic defects can be considered and need experimental verification.

4.6.3 Third hit: FUS-positive SGs might be converted into pathological inclusions

How reversible FUS-positive SGs can be converted into insoluble pathological inclusions in FUS-proteinopathies remains to be elucidated. Four mutually non-exclusive mechanisms are conceivable.

First, irreversible aggregation of FUS might be induced when critical concentrations of aggregation-prone RNA-binding proteins are reached within SGs. Recently, FUS and other RNA-binding proteins that possess a low complexity domain have been shown to aggregate in a concentration-dependent manner and these aggregates consist of polymerized amyloid-like fibers (Kato et al., 2012). Alternatively, RNA might enhance the aggregation as it was shown for Tau and Prion protein (Kampers et al., 1996; Deleault et al., 2003).

Second, SG dissolution might be impaired, e.g. by chronic inactivation of dual specificity tyrosine-phosphorylation-regulated kinase 3 (DYRK3) (Wippich et al., 2013). Kinase activity of DYRK3 is necessary for SG dissolution and release of mammalian target of rapamycine complex 1 (mTORC1) from SGs. Thus, inactivation of the kinase activity of DYRK3 induces SG formation, SG persistence and inhibition of mTORC1 signaling (Wippich et al., 2013). Furthermore, reduced levels of heat shock proteins (Gilks et al., 2004; Mazroui et al., 2007), cellular acidosis (Chudinova et al., 2012) or chronic stress (Meyerowitz et al., 2011) can impair SG dissolution, resulting in persistent SGs.

Third, phosphorylation of eIF2α is one of the first steps in SG formation and slows down the rate of translation (Kayali et al., 2005; Jamison et al., 2008; Buchan and Parker, 2009; Hofmann et al., 2012). Sustained eIF2α-phosphorylation and hence prolonged inhibition of translation initiation was shown to induce cell death, suggesting that overactive SG formation and/or impairment in SG recovery can cause neurodegeneration (DeGracia and Hu, 2007; DeGracia et al., 2007; Moreno et al., 2012).

Finally, SGs have been reported to be cleared by autophagy, indicating that dysfunction of autophagy might result in persistent SGs (Buchan et al., 2013). VCP is important for autophagosome maturation (Tresse et al., 2010) and mutations in VCP are associated with ALS (Watts et al., 2004; Johnson et al., 2010) and a multisystemic disorder termed inclusion body myophathy, Paget´s disease of bone and frontotemporal dementia (IBMPFD) (Watts et al., 2004). These mutations impair the formation of autophagosomes and result in the accumulation of immature autophagic vesicles and

ubiquitin-positive protein aggregates. Interestingly in cells depleted of VCP, SGs were shown to persist after stress removal (Buchan et al., 2013). This suggests that SGs are not cleared when autophagy is dysfunctional and thus might give rise to pathological inclusions. Interestingly, mutations in proteins with important functions in autophagy e.g. Optineurin (Maruyama et al., 2010), Ubiquilin2 (Deng et al., 2011) and SQSTM1/p62 (Fecto et al., 2011) are detected in rare ALS cases. Thus, several pieces of evidence support a link between autophagic defects and aggregate formation in ALS and FTLD.

4.7 Possible multiple hits in TDP-proteinopathies

Although my work mainly focused on FUS and FET proteins, there is evidence that the same multiple hit model can also be applied for TDP-43, which will be discussed in the following.

4.7.1 First hit: Possible mechanisms that drive TDP-43 into the cytosol

Despite extensive research, the mechanism behind *TARDBP* mutations and the cytosolic deposition of TDP-43 inclusions in TDP-proteinopathies is still puzzling. To date, 43 *TARDBP* missense mutations have been identified and almost all cluster in the C-terminal G-rich domain (Fig. 3) and none of these ALS-associated mutations affects the classic NLS of TDP-43. An Alanine to Valine (A90V) substitution between the bipartite NLSs was reported to disrupt nuclear localization of TDP-43 (Winton et al., 2008b), but this mutation is a genetic polymorphism in TDP-43, as it is also detected in healthy controls (Guerreiro et al., 2008; Kabashi et al., 2008; Sreedharan et al., 2008; Benajiba et al., 2009; Corrado et al., 2009). Although some studies claim that *TARDBP* mutations in the G-rich domain of TDP-43 result in cytosolic mislocalization (Barmada et al., 2010; Liu-Yesucevitz et al., 2010; Ritson et al., 2010), three TARDBP mutations that I investigated (A315T, M337V, G348C) remained nuclear when I expressed them in HeLa cells (Bentmann et al., 2012), consistent with reports from others (Kabashi et al., 2010; Ling et al., 2010; Dewey et al., 2011). Thus, convincing evidence for the idea that *TARDBP* mutations directly disrupt nuclear import of TDP-43 is so far lacking and other mechanisms for cytosolic mislocalization of TDP-43 have to be considered.

A possible mechanism how cytosolic mislocalization of TDP-43 might arise is by dysfunction in the Importin α/β pathway. Indeed, a decrease of the nuclear import

factors cellular apoptosis susceptibility protein (CAS) and Importin α2 was detected in post-mortem brains of ALS-TDP and FTLD-TDP cases (Nishimura et al., 2010). In addition, upon axonal injury or cerebral ischemia, importin β levels are reduced and result in TDP-43 mislocalization to the cytosol in mouse brains (Sato et al., 2009; Shindo et al., 2013).

4.7.2 Second hit: Cytosolic TDP-43 is recruited into SGs upon cellular stress

I found that not only cytosolic FUS, but also cytosolic TDP-43 localizes to SGs upon exposure to various stressors, such as heat shock or oxidative stress (Bentmann et al., 2012) and several SG proteins have been identified as TDP-43 interactors (Freibaum et al., 2010). One study suggested that *TARDBP* mutations cause a loss-of-function with respect to SG formation (McDonald et al., 2011). However, two studies reported more SG formation upon overexpression of TDP-43 mutants, indicating a toxic-gain-of-function (Liu-Yesucevitz et al., 2010; Dewey et al., 2011). In my study, I did not observe increased or reduced localization of mutant TDP-43 in SGs, as the amount of mutant TDP-43 in SGs was not altered compared to controls (Bentmann et al., 2012). Nevertheless, I cannot exclude that other ALS-associated *TARDBP* mutations that I did not examine show an effect on SG recruitment of TDP or SG dynamics.

4.7.3 Third hit: Conversion of SGs into TDP-43 inclusions.

Once cytosolic TDP-43 is recruited into SGs, the same mechanisms as described in 4.6.3 for FUS (e.g. chronic stress, dysfunction in dissolution of SGs or autophagic clearance of SGs) might convert reversible TDP-43-containing SGs into irreversible inclusions composed of aggregated TDP-43.

Moreover, recent studies have demonstrated that TDP-43 forms aggregates *in vitro* through its C-terminal prion-like G-rich domain (Johnson et al., 2009; Furukawa et al., 2011; Guo et al., 2011). Furthermore, intracellular aggregation of TDP-43 can be facilitated by addition of fibrillar TDP-43 aggregates prepared *in vitro* (Furukawa et al., 2011) or by insoluble TDP-43 isolated from ALS or FTLD patient brains (Nonaka et al., 2013). Thus, especially for TDP-43 mechanisms such as the unfolded protein response inhibiting protein misfolding are essential and an age-dependent decline of proteins involved in protein homeostasis might tip the balance towards TDP-43 aggregation. Furthermore, mutations in genes coding for proteins involved in the regulation of the unfolded protein response (Nishimura et al., 2004) or autophagy (Maruyama et al.,

2010; Fecto et al., 2011) have been identified in ALS patients and might contribute to the pathogenesis of TDP-proteinopathies (Ling et al., 2013).

Once TDP-43 is trapped in irreversible aggregates, a vicious circle might exacerbate the situation (Lee et al., 2012). TDP-43 autoregulation is essential to prevent excessive TDP-43 mRNA production and to sustain cell viability (see also 1.2.2). When TDP-43 is trapped in aggregates and is not able to autoregulate its own expression, the consequences are increased TDP-43 levels that in turn might facilitate TDP-43 aggregation. Such a feed forward mechanism might ultimately result in formation of huge TDP-43 aggregates, loss of nuclear TDP-43 and cell death.

4.8 Alternative scenarios of inclusion formation in neurodegenerative diseases

SG marker proteins have been identified in various neurodegenerative diseases. Not only FUS or TDP-43 inclusions in ALS and FTLD contain SG proteins, but SG proteins have been also detected e.g. in Tau or polyQ inclusions in Alzheimer´s disease (Vanderweyde et al., 2012), FTLD-Tau (Vanderweyde et al., 2012) and Huntington´s disease (Waelter et al., 2001). Thus, mounting evidence has implicated SGs as important players in several neurodegenerative diseases. In addition to the multiple hit model I present in this thesis (sections 4.5 - 4.7), other scenarios can be envisioned that will be shortly presented in the following.

4.8.1 Aggregation independent of SGs

In an alternative scenario, mutations or altered post-translational modifications may provoke aggregation of FUS, TDP-43 or other aggregation-prone protein such as Tau, SOD1 or Huntingtin without initial recruitment of these proteins into SGs. *TARDBP* mutations are reported to enhance TDP-43 aggregation in cell culture, yeast and *in vitro* (Johnson et al., 2009; Nonaka et al., 2009; Arai et al., 2010; Liu-Yesucevitz et al., 2010; Guo et al., 2011). In addition, phosphorylation and caspase cleavage further increase the aggregation propensity of TDP-43 (Zhang et al., 2009; Brady et al., 2011). For FUS, alterations in arginine methylation of FUS might increase its aggregation propensity, as shown for other RNA-binding proteins that aggregate and become insoluble when arginine methylation is reduced (Ostareck-Lederer et al., 2006; Perreault et al., 2007). In mice expressing mutant SOD1 show an age-dependent increase of SOD1 aggregation in neuronal tissues that resulted in formation of fibrillar aggregates (Wang et al., 2002a;

Wang et al., 2002b). These aggregates themselves and/or additional cellular stress might then initiate SG formation. Subsequently, SGs might secondarily fuse with already existing protein aggregates and give rise to pathological inclusions containing SG marker proteins.

4.8.2 Sequestration of nuclear transport factors in SGs

Nuclear transport factors such as Transportin (Chang and Tarn, 2009), Importin β1 (Chang and Tarn, 2009), importin α1, α4 and α5 (Fujimura et al., 2010; Mahboubi et al., 2013) have been shown to be components of SGs. This is an interesting finding, as the vast majority of ALS cases and half of the FTLD cases are sporadic and are not caused by mutations in *FUS* or *TARDBP*, thus alternative mechanisms of formation of cytosolic FUS and TDP-43 inclusions have to be supposed. It has been shown that exposure of cells to oxidative stress or heat shock causes sequestration of Transportin, Importin α1, Importin α4 and Importin α5 in SGs (Chang and Tarn, 2009; Fujimura et al., 2010; Mahboubi et al., 2013). This may result in reduced levels of free nuclear transport factors in the cytosol, so that proper nuclear import of FUS and TDP-43 might not be sustained, resulting in cytosolic mislocalization of FUS and TDP-43. Additional cellular stress and/or subsequent protein-protein interactions with transport factors captured in these SGs might recruit cytosolic FUS and TDP-43 into SGs, which then might be converted into irreversible inclusion by mechanisms discussed in 4.6.3 and 4.7.3.

Concluding remarks

Within the last decade our knowledge about key genes and pathomechanisms of ALS and FTLD has dramatically increased and mounting evidence supports the notion that SGs are key players in neurodegeneration. Nevertheless, we are still lacking cell culture and animal models that resemble features of ALS and FTLD with progressive neurodegeneration and pathological inclusions. My studies suggest that it might be important to incorporate different cellular stressors that induce SG formation and are linked to neurodegeneration into these models (Bentmann et al., 2013). In addition, further hits such as defects in autophagy or chronic stress may be required to trigger TDP-43 and FUS pathology and neurodegeneration in existing cell culture and animal models.

References

Abel EL (2007) Football increases the risk for Lou Gehrig's disease, amyotrophic lateral sclerosis. Percept Mot Skills 104:1251-1254.

Anderson P, Kedersha N (2008) Stress granules: the Tao of RNA triage. Trends Biochem Sci 33:141-150.

Anderson P, Kedersha N (2009a) RNA granules: post-transcriptional and epigenetic modulators of gene expression. Nat Rev Mol Cell Biol 10:430-436.

Anderson P, Kedersha N (2009b) Stress granules. Curr Biol 19:R397-398.

Andersson MK, Stahlberg A, Arvidsson Y, Olofsson A, Semb H, Stenman G, Nilsson O, Aman P (2008) The multifunctional FUS, EWS and TAF15 proto-oncoproteins show cell type-specific expression patterns and involvement in cell spreading and stress response. BMC Cell Biol 9:37-53.

Aoki K, Ishii Y, Matsumoto K, Tsujimoto M (2002) Methylation of Xenopus CIRP2 regulates its arginine- and glycine-rich region-mediated nucleocytoplasmic distribution. Nucleic Acids Research 30:5182-5192.

Arai T, Hasegawa M, Akiyama H, Ikeda K, Nonaka T, Mori H, Mann D, Tsuchiya K, Yoshida M, Hashizume Y, Oda T (2006) TDP-43 is a component of ubiquitin-positive tau-negative inclusions in frontotemporal lobar degeneration and amyotrophic lateral sclerosis. Biochem Biophys Res Commun 351:602-611.

Arai T, Hasegawa M, Nonoka T, Kametani F, Yamashita M, Hosokawa M, Niizato K, Tsuchiya K, Kobayashi Z, Ikeda K, Yoshida M, Onaya M, Fujishiro H, Akiyama H (2010) Phosphorylated and cleaved TDP-43 in ALS, FTLD and other neurodegenerative disorders and in cellular models of TDP-43 proteinopathy. Neuropathology 30:170-181.

Araya N, Hiraga H, Kako K, Arao Y, Kato S, Fukamizu A (2005) Transcriptional down-regulation through nuclear exclusion of EWS methylated by PRMT1. Biochem Biophys Res Commun 329:653-660.

Ariumi Y, Kuroki M, Kushima Y, Osugi K, Hijikata M, Maki M, Ikeda M, Kato N (2011) Hepatitis C virus hijacks P-body and stress granule components around lipid droplets. J Virol 85:6882-6892.

Arnold ES, Ling SC, Huelga SC, Lagier-Tourenne C, Polymenidou M, Ditsworth D, Kordasiewicz HB, McAlonis-Downes M, Platoshyn O, Parone PA, Da Cruz S, Clutario KM, Swing D, Tessarollo L, Marsala M, Shaw CE, Yeo GW, Cleveland DW (2013) ALS-linked TDP-43 mutations produce aberrant RNA splicing and adult-onset motor neuron disease without aggregation or loss of nuclear TDP-43. Proceedings of the National Academy of Sciences of the United States of America 110:E736-745.

Ash PE, Zhang YJ, Roberts CM, Saldi T, Hutter H, Buratti E, Petrucelli L, Link CD (2010) Neurotoxic effects of TDP-43 overexpression in C. elegans. Human Molecular Genetics 19:3206-3218.

Attwooll C, Tariq M, Harris M, Coyne JD, Telford N, Varley JM (1999) Identification of a novel fusion gene involving hTAFII68 and CHN from a t(9;17)(q22;q11.2) translocation in an extraskeletal myxoid chondrosarcoma. Oncogene 18:7599-7601.

Aulas A, Stabile S, Vande Velde C (2012) Endogenous TDP-43, but not FUS, contributes to stress granule assembly via G3BP. Mol Neurodegener 7:54.

Ayala YM, Misteli T, Baralle FE (2008a) TDP-43 regulates retinoblastoma protein phosphorylation through the repression of cyclin-dependent kinase 6 expression. Proceedings of the National Academy of Sciences of the United States of America 105:3785-3789.

Ayala YM, Zago P, D'Ambrogio A, Xu YF, Petrucelli L, Buratti E, Baralle FE (2008b) Structural determinants of the cellular localization and shuttling of TDP-43. Journal of Cell Science 121:3778-3785.

Ayala YM, Pantano S, D'Ambrogio A, Buratti E, Brindisi A, Marchetti C, Romano M, Baralle FE (2005) Human, Drosophila, and C.elegans TDP43: nucleic acid binding properties and splicing regulatory function. Journal of Molecular Biology 348:575-588.

Ayala YM, De Conti L, Avendano-Vazquez SE, Dhir A, Romano M, D'Ambrogio A, Tollervey J, Ule J, Baralle M, Buratti E, Baralle FE (2011) TDP-43 regulates its mRNA levels through a negative feedback loop. The EMBO Journal 30:277-288.

Baechtold H, Kuroda M, Sok J, Ron D, Lopez BS, Akhmedov AT (1999) Human 75-kDa DNA-pairing protein is identical to the pro-oncoprotein TLS/FUS and is able to promote D-loop formation. The Journal of Biological Chemistry 274:34337-34342.

Baker M et al. (2006) Mutations in progranulin cause tau-negative frontotemporal dementia linked to chromosome 17. Nature 442:916-919.

Ballarino M, Jobert L, Dembele D, de la Grange P, Auboeuf D, Tora L (2013) TAF15 is important for cellular proliferation and regulates the expression of a subset of cell cycle genes through miRNAs. Oncogene 32:4646-4655.

Barber SC, Shaw PJ (2010) Oxidative stress in ALS: key role in motor neuron injury and therapeutic target. Free Radic Biol Med 48:629-641.

Barmada SJ, Skibinski G, Korb E, Rao EJ, Wu JY, Finkbeiner S (2010) Cytoplasmic mislocalization of TDP-43 is toxic to neurons and enhanced by a mutation associated with familial amyotrophic lateral sclerosis. J Neurosci 30:639-649.

Baumer D, Hilton D, Paine SM, Turner MR, Lowe J, Talbot K, Ansorge O (2010) Juvenile ALS with basophilic inclusions is a FUS proteinopathy with FUS mutations. Neurology 75:611-618.

Bedford MT, Clarke SG (2009) Protein arginine methylation in mammals: who, what, and why. Mol Cell 33:1-13.

Belyanskaya LL, Gehrig PM, Gehring H (2001) Exposure on cell surface and extensive arginine methylation of ewing sarcoma (EWS) protein. The Journal of Biological Chemistry 276:18681-18687.

Belzil VV, Daoud H, St-Onge J, Desjarlais A, Bouchard JP, Dupre N, Lacomblez L, Salachas F, Pradat PF, Meininger V, Camu W, Dion PA, Rouleau GA (2011) Identification of novel FUS mutations in sporadic cases of amyotrophic lateral sclerosis. Amyotroph Lateral Scler 12:113-117.

Benajiba L, Le Ber I, Camuzat A, Lacoste M, Thomas-Anterion C, Couratier P, Legallic S, Salachas F, Hannequin D, Decousus M, Lacomblez L, Guedj E, Golfier V, Camu W, Dubois B, Campion D, Meininger V, Brice A (2009) TARDBP mutations in motoneuron disease with frontotemporal lobar degeneration. Ann Neurol 65:470-473.

Bentmann E, Haass C, Dormann D (2013) Stress granules in neurodegeneration -lessons learnt from TAR DNA binding protein of 43 kDa and fused in sarcoma. The FEBS Journal 280:4348-4370.

Bentmann E, Neumann M, Tahirovic S, Rodde R, Dormann D, Haass C (2012) Requirements for stress granule recruitment of fused in sarcoma (FUS) and TAR DNA-binding protein of 43 kDa (TDP-43). The Journal of Biological Chemistry 287:23079-23094.

Bertolotti A, Bell B, Tora L (1999) The N-terminal domain of human TAFII68 displays transactivation and oncogenic properties. Oncogene 18:8000-8010.

Bertolotti A, Lutz Y, Heard DJ, Chambon P, Tora L (1996) hTAF(II)68, a novel RNA/ssDNA-binding protein with homology to the pro-oncoproteins TLS/FUS and EWS is associated with both TFIID and RNA polymerase II. The EMBO Journal 15:5022-5031.

Bertolotti A, Melot T, Acker J, Vigneron M, Delattre O, Tora L (1998) EWS, but not EWS-FLI-1, is associated with both TFIID and RNA polymerase II: interactions between two members of the TET family, EWS and hTAFII68, and subunits of TFIID and RNA polymerase II complexes. Mol Cell Biol 18:1489-1497.

Bischoff FR, Ponstingl H (1991) Catalysis of guanine nucleotide exchange on Ran by the mitotic regulator RCC1. Nature 354:80-82.

Bischoff FR, Krebber H, Kempf T, Hermes I, Ponstingl H (1995) Human RanGTPase-activating protein RanGAP1 is a homologue of yeast Rna1p involved in mRNA processing and transport. Proceedings of the National Academy of Sciences of the United States of America 92:1749-1753.

Blechingberg J, Luo Y, Bolund L, Damgaard CK, Nielsen AL (2012) Gene expression responses to FUS, EWS, and TAF15 reduction and stress granule sequestration analyses identifies FET-protein non-redundant functions. PloS One 7:e46251.

Bornes S, Prado-Lourenco L, Bastide A, Zanibellato C, Iacovoni JS, Lacazette E, Prats AC, Touriol C, Prats H (2007) Translational induction of VEGF internal ribosome entry site elements during the early response to ischemic stress. Circ Res 100:305-308.

Bosco DA, Lemay N, Ko HK, Zhou H, Burke C, Kwiatkowski TJ, Jr., Sapp P, McKenna-Yasek D, Brown RH, Jr., Hayward LJ (2010) Mutant FUS proteins that cause amyotrophic lateral sclerosis incorporate into stress granules. Human Molecular Genetics 19:4160-4175.

Brady OA, Meng P, Zheng Y, Mao Y, Hu F (2011) Regulation of TDP-43 aggregation by phosphorylation and p62/SQSTM1. Journal of Neurochemistry 116:248-259.

Brelstaff J, Lashley T, Holton JL, Lees AJ, Rossor MN, Bandopadhyay R, Revesz T (2011) Transportin1: a marker of FTLD-FUS. Acta Neuropathologica 122:591-600.

Buchan JR, Parker R (2009) Eukaryotic stress granules: the ins and outs of translation. Mol Cell 36:932-941.

Buchan JR, Kolaitis RM, Taylor JP, Parker R (2013) Eukaryotic Stress Granules Are Cleared by Autophagy and Cdc48/VCP Function. Cell 153:1461-1474.

Buratti E, Baralle FE (2001) Characterization and functional implications of the RNA binding properties of nuclear factor TDP-43, a novel splicing regulator of CFTR exon 9. The Journal of Biological Chemistry 276:36337-36343.

Buratti E, Baralle FE (2012) TDP-43: gumming up neurons through protein-protein and protein-RNA interactions. Trends Biochem Sci 37:237-247.

Buratti E, Dork T, Zuccato E, Pagani F, Romano M, Baralle FE (2001) Nuclear factor TDP-43 and SR proteins promote in vitro and in vivo CFTR exon 9 skipping. The EMBO Journal 20:1774-1784.

Buratti E, Brindisi A, Giombi M, Tisminetzky S, Ayala YM, Baralle FE (2005) TDP-43 binds heterogeneous nuclear ribonucleoprotein A/B through its C-terminal tail: an important region for the inhibition of cystic fibrosis transmembrane conductance regulator exon 9 splicing. The Journal of Biological Chemistry 280:37572-37584.

Burrell JR, Kiernan MC, Vucic S, Hodges JR (2011) Motor neuron dysfunction in frontotemporal dementia. Brain 134:2582-2594.

Cansizoglu AE, Lee BJ, Zhang ZC, Fontoura BM, Chook YM (2007) Structure-based design of a pathway-specific nuclear import inhibitor. Nat Struct Mol Biol 14:452-454.

Chang CK, Wu TH, Wu CY, Chiang MH, Toh EK, Hsu YC, Lin KF, Liao YH, Huang TH, Huang JJ (2012) The N-terminus of TDP-43 promotes its oligomerization and enhances DNA binding affinity. Biochem Biophys Res Commun 425:219-224.

Chang WL, Tarn WY (2009) A role for transportin in deposition of TTP to cytoplasmic RNA granules and mRNA decay. Nucleic Acids Research 37:6600-6612.

Chen H, Richard M, Sandler DP, Umbach DM, Kamel F (2007) Head injury and amyotrophic lateral sclerosis. Am J Epidemiol 166:810-816.

Chen Y, Yang M, Deng J, Chen X, Ye Y, Zhu L, Liu J, Ye H, Shen Y, Li Y, Rao EJ, Fushimi K, Zhou X, Bigio EH, Mesulam M, Xu Q, Wu JY (2011) Expression of human FUS protein in Drosophila leads to progressive neurodegeneration. Protein Cell 2:477-486.

Chiang PM, Ling J, Jeong YH, Price DL, Aja SM, Wong PC (2010) Deletion of TDP-43 down-regulates Tbc1d1, a gene linked to obesity, and alters body fat metabolism. Proceedings of the National Academy of Sciences of the United States of America 107:16320-16324.

Chio A, Calvo A, Dossena M, Ghiglione P, Mutani R, Mora G (2009a) ALS in Italian professional soccer players: the risk is still present and could be soccer-specific. Amyotroph Lateral Scler 10:205-209.

Chio A, Restagno G, Brunetti M, Ossola I, Calvo A, Mora G, Sabatelli M, Monsurro MR, Battistini S, Mandrioli J, Salvi F, Spataro R, Schymick J, Traynor BJ, La Bella V (2009b) Two Italian kindreds with familial amyotrophic lateral sclerosis due to FUS mutation. Neurobiol Aging 30:1272-1275.

Chudinova EM, Nadezhdina ES, Ivanov PA (2012) Cellular acidosis inhibits assembly, disassembly, and motility of stress granules. Biochemistry (Mosc) 77:1277-1284.

Colombrita C, Zennaro E, Fallini C, Weber M, Sommacal A, Buratti E, Silani V, Ratti A (2009) TDP-43 is recruited to stress granules in conditions of oxidative insult. Journal of Neurochemistry 111:1051-1061.

Colombrita C, Onesto E, Megiorni F, Pizzuti A, Baralle FE, Buratti E, Silani V, Ratti A (2012) TDP-43 and FUS RNA-binding proteins bind distinct sets of cytoplasmic messenger RNAs and differently regulate their post-transcriptional fate in motoneuron-like cells. The Journal of Biological Chemistry 287:15635-15647.

Consonni M, Iannaccone S, Cerami C, Frasson P, Lacerenza M, Lunetta C, Corbo M, Cappa SF (2013) The cognitive and behavioural profile of amyotrophic lateral sclerosis: application of the consensus criteria. Behavioural Neurology 27:143-153.

Cook A, Bono F, Jinek M, Conti E (2007) Structural biology of nucleocytoplasmic transport. Annu Rev Biochem 76:647-671.

Corrado L, Ratti A, Gellera C, Buratti E, Castellotti B, Carlomagno Y, Ticozzi N, Mazzini L, Testa L, Taroni F, Baralle FE, Silani V, D'Alfonso S (2009) High frequency of TARDBP gene mutations in Italian patients with amyotrophic lateral sclerosis. Hum Mutat 30:688-694.

Cote J, Boisvert FM, Boulanger MC, Bedford MT, Richard S (2003) Sam68 RNA binding protein is an in vivo substrate for protein arginine N-methyltransferase 1. Mol Biol Cell 14:274-287.

Couthouis J et al. (2012) Evaluating the role of the FUS/TLS-related gene EWSR1 in amyotrophic lateral sclerosis. Human Molecular Genetics 21:2899-2911.

Couthouis J et al. (2011) A yeast functional screen predicts new candidate ALS disease genes. Proceedings of the National Academy of Sciences of the United States of America 108:20881-20890.

Crabtree B, Thiyagarajan N, Prior SH, Wilson P, Iyer S, Ferns T, Shapiro R, Brew K, Subramanian V, Acharya KR (2007) Characterization of human angiogenin variants implicated in amyotrophic lateral sclerosis. Biochemistry 46:11810-11818.

Crozat A, Aman P, Mandahl N, Ron D (1993) Fusion of CHOP to a novel RNA-binding protein in human myxoid liposarcoma. Nature 363:640-644.

Cruts M et al. (2006) Null mutations in progranulin cause ubiquitin-positive frontotemporal dementia linked to chromosome 17q21. Nature 442:920-924.

Cushman M, Johnson BS, King OD, Gitler AD, Shorter J (2010) Prion-like disorders: blurring the divide between transmissibility and infectivity. Journal of Cell Science 123:1191-1201.

D'Ambrogio A, Buratti E, Stuani C, Guarnaccia C, Romano M, Ayala YM, Baralle FE (2009) Functional mapping of the interaction between TDP-43 and hnRNP A2 in vivo. Nucleic Acids Research 37:4116-4126.

Dang Y, Kedersha N, Low WK, Romo D, Gorospe M, Kaufman R, Anderson P, Liu JO (2006) Eukaryotic initiation factor 2alpha-independent pathway of stress granule induction by the natural product pateamine A. The Journal of Biological Chemistry 281:32870-32878.

Davidson YS, Robinson AC, Hu Q, Mishra M, Baborie A, Jaros E, Perry RH, Cairns NJ, Richardson A, Gerhard A, Neary D, Snowden JS, Bigio EH, Mann DMA (2013) Nuclear carrier and RNA-binding proteins in frontotemporal lobar degeneration associated with fused in sarcoma (FUS) pathological changes. Neuropath Appl Neuro 39:157-165.

De Chiara G, Marcocci ME, Sgarbanti R, Civitelli L, Ripoli C, Piacentini R, Garaci E, Grassi C, Palamara AT (2012) Infectious agents and neurodegeneration. Molecular Neurobiology 46:614-638.

de Hoog CL, Foster LJ, Mann M (2004) RNA and RNA binding proteins participate in early stages of cell spreading through spreading initiation centers. Cell 117:649-662.

De Leeuw F, Zhang T, Wauquier C, Huez G, Kruys V, Gueydan C (2007) The cold-inducible RNA-binding protein migrates from the nucleus to cytoplasmic stress granules by a methylation-dependent mechanism and acts as a translational repressor. Exp Cell Res 313:4130-4144.

DeGracia DJ, Hu BR (2007) Irreversible translation arrest in the reperfused brain. J Cereb Blood Flow Metab 27:875-893.

DeGracia DJ, Rudolph J, Roberts GG, Rafols JA, Wang J (2007) Convergence of stress granules and protein aggregates in hippocampal cornu ammonis 1 at later reperfusion following global brain ischemia. Neuroscience 146:562-572.

Dejesus-Hernandez M et al. (2011) Expanded GGGGCC Hexanucleotide Repeat in Noncoding Region of C9ORF72 Causes Chromosome 9p-Linked FTD and ALS. Neuron 72:245-256.

Delattre O, Zucman J, Plougastel B, Desmaze C, Melot T, Peter M, Kovar H, Joubert I, de Jong P, Rouleau G, et al. (1992) Gene fusion with an ETS DNA-binding domain caused by chromosome translocation in human tumours. Nature 359:162-165.

Deleault NR, Lucassen RW, Supattapone S (2003) RNA molecules stimulate prion protein conversion. Nature 425:717-720.

Deng HX et al. (2011) Mutations in UBQLN2 cause dominant X-linked juvenile and adult-onset ALS and ALS/dementia. Nature 477:211-215.

Dewey CM, Cenik B, Sephton CF, Dries DR, Mayer P, 3rd, Good SK, Johnson BA, Herz J, Yu G (2011) TDP-43 Is Directed to Stress Granules by Sorbitol, a Novel Physiological Osmotic and Oxidative Stressor. Mol Cell Biol 31:1098-1108.

Dichmann DS, Harland RM (2012) fus/TLS orchestrates splicing of developmental regulators during gastrulation. Genes Dev 26:1351-1363.

Doi H, Okamura K, Bauer PO, Furukawa Y, Shimizu H, Kurosawa M, Machida Y, Miyazaki H, Mitsui K, Kuroiwa Y, Nukina N (2008) RNA-binding protein TLS is a major nuclear aggregate-interacting protein in huntingtin exon 1 with expanded polyglutamine-expressing cells. The Journal of Biological Chemistry 283:6489-6500.

Dolzhanskaya N, Merz G, Aletta JM, Denman RB (2006) Methylation regulates the intracellular protein-protein and protein-RNA interactions of FMRP. Journal of Cell Science 119:1933-1946.

Dormann D, Haass C (2011) TDP-43 and FUS: a nuclear affair. Trends Neurosci 34:339-348.

Dormann D, Haass C (2013) Fused in sarcoma (FUS): An oncogene goes awry in neurodegeneration. Molecular and Cellular Neurosciences 56:475-486.

Dormann D, Capell A, Carlson AM, Shankaran SS, Rodde R, Neumann M, Kremmer E, Matsuwaki T, Yamanouchi K, Nishihara M, Haass C (2009) Proteolytic processing of TAR DNA binding protein-43 by caspases produces C-terminal fragments with disease defining properties independent of progranulin. Journal of Neurochemistry 110:1082-1094.

Dormann D, Madl T, Valori CF, Bentmann E, Tahirovic S, Abou-Ajram C, Kremmer E, Ansorge O, Mackenzie IR, Neumann M, Haass C (2012) Arginine methylation next to the PY-NLS modulates Transportin binding and nuclear import of FUS. The EMBO Journal 31:4258-4275.

Dormann D, Rodde R, Edbauer D, Bentmann E, Fischer I, Hruscha A, Than ME, Mackenzie IR, Capell A, Schmid B, Neumann M, Haass C (2010) ALS-associated fused in sarcoma (FUS) mutations disrupt Transportin-mediated nuclear import. The EMBO Journal 29:2841-2857.

Dreumont N, Hardy S, Behm-Ansmant I, Kister L, Branlant C, Stevenin J, Bourgeois CF (2010) Antagonistic factors control the unproductive splicing of SC35 terminal intron. Nucleic Acids Research 38:1353-1366.

Du K, Arai S, Kawamura T, Matsushita A, Kurokawa R (2011) TLS and PRMT1 synergistically coactivate transcription at the survivin promoter through TLS arginine methylation. Biochem Biophys Res Commun 404:991-996.

Elden AC et al. (2010) Ataxin-2 intermediate-length polyglutamine expansions are associated with increased risk for ALS. Nature 466:1069-1075.

Elvira G, Wasiak S, Blandford V, Tong XK, Serrano A, Fan X, del Rayo Sanchez-Carbente M, Servant F, Bell AW, Boismenu D, Lacaille JC, McPherson PS, DesGroseillers L, Sossin WS (2006) Characterization of an RNA granule from developing brain. Mol Cell Proteomics 5:635-651.

Emara MM, Fujimura K, Sciaranghella D, Ivanova V, Ivanov P, Anderson P (2012) Hydrogen peroxide induces stress granule formation independent of eIF2alpha phosphorylation. Biochem Biophys Res Commun 423:763-769.

Fallini C, Bassell GJ, Rossoll W (2012) The ALS disease protein TDP-43 is actively transported in motor neuron axons and regulates axon outgrowth. Human Molecular Genetics 21:3703-3718.

Fecto F, Yan J, Vemula SP, Liu E, Yang Y, Chen W, Zheng JG, Shi Y, Siddique N, Arrat H, Donkervoort S, Ajroud-Driss S, Sufit RL, Heller SL, Deng HX, Siddique T (2011) SQSTM1 mutations in familial and sporadic amyotrophic lateral sclerosis. Arch Neurol 68:1440-1446.

Feiguin F, Godena VK, Romano G, D'Ambrogio A, Klima R, Baralle FE (2009) Depletion of TDP-43 affects Drosophila motoneurons terminal synapsis and locomotive behavior. FEBS Lett 583:1586-1592.

Fiesel FC, Voigt A, Weber SS, Van den Haute C, Waldenmaier A, Gorner K, Walter M, Anderson ML, Kern JV, Rasse TM, Schmidt T, Springer W, Kirchner R, Bonin M, Neumann M, Baekelandt V, Alunni-Fabbroni M, Schulz JB, Kahle PJ (2010) Knockdown of transactive response DNA-binding protein (TDP-43) downregulates histone deacetylase 6. The EMBO Journal 29:209-221.

Freibaum BD, Chitta RK, High AA, Taylor JP (2010) Global analysis of TDP-43 interacting proteins reveals strong association with RNA splicing and translation machinery. J Proteome Res 9:1104-1120.

Fronz K, Guttinger S, Burkert K, Kuhn U, Stohr N, Schierhorn A, Wahle E (2011) Arginine methylation of the nuclear poly(a) binding protein weakens the interaction with its nuclear import receptor, transportin. The Journal of Biological Chemistry 286:32986-32994.

Fronz K, Otto S, Kolbel K, Kuhn U, Friedrich H, Schierhorn A, Beck-Sickinger AG, Ostareck-Lederer A, Wahle E (2008) Promiscuous modification of the nuclear poly(A)-binding protein by multiple protein-arginine methyltransferases does not

affect the aggregation behavior. The Journal of Biological Chemistry 283:20408-20420.

Fuentealba RA, Udan M, Bell S, Wegorzewska I, Shao J, Diamond MI, Weihl CC, Baloh RH (2010) Interaction with polyglutamine aggregates reveals a Q/N-rich domain in TDP-43. The Journal of Biological Chemistry 285:26304-26314.

Fujii R, Takumi T (2005) TLS facilitates transport of mRNA encoding an actin-stabilizing protein to dendritic spines. Journal of Cell Science 118:5755-5765.

Fujii R, Okabe S, Urushido T, Inoue K, Yoshimura A, Tachibana T, Nishikawa T, Hicks GG, Takumi T (2005) The RNA binding protein TLS is translocated to dendritic spines by mGluR5 activation and regulates spine morphology. Curr Biol 15:587-593.

Fujimura K, Suzuki T, Yasuda Y, Murata M, Katahira J, Yoneda Y (2010) Identification of importin alpha1 as a novel constituent of RNA stress granules. Biochimica et Biophysica Acta 1803:865-871.

Fujita K, Ito H, Nakano S, Kinoshita Y, Wate R, Kusaka H (2008) Immunohistochemical identification of messenger RNA-related proteins in basophilic inclusions of adult-onset atypical motor neuron disease. Acta Neuropathologica 116:439-445.

Furukawa Y, Kaneko K, Matsumoto G, Kurosawa M, Nukina N (2009) Cross-seeding fibrillation of Q/N-rich proteins offers new pathomechanism of polyglutamine diseases. J Neurosci 29:5153-5162.

Furukawa Y, Kaneko K, Watanabe S, Yamanaka K, Nukina N (2011) A seeding reaction recapitulates intracellular formation of Sarkosyl-insoluble transactivation response element (TAR) DNA-binding protein-43 inclusions. The Journal of Biological Chemistry 286:18664-18672.

Fushimi K, Long C, Jayaram N, Chen X, Li L, Wu JY (2011) Expression of human FUS/TLS in yeast leads to protein aggregation and cytotoxicity, recapitulating key features of FUS proteinopathy. Protein Cell 2:141-149.

Gal J, Zhang J, Kwinter DM, Zhai J, Jia H, Jia J, Zhu H (2011) Nuclear localization sequence of FUS and induction of stress granules by ALS mutants. Neurobiol Aging 32:2323 e2327-2340.

Garcin B, Lillo P, Hornberger M, Piguet O, Dawson K, Nestor PJ, Hodges JR (2009) Determinants of survival in behavioral variant frontotemporal dementia. Neurology 73:1656-1661.

Gavett BE, Stern RA, McKee AC (2011) Chronic traumatic encephalopathy: a potential late effect of sport-related concussive and subconcussive head trauma. Clin Sports Med 30:179-188, xi.

Gilks N, Kedersha N, Ayodele M, Shen L, Stoecklin G, Dember LM, Anderson P (2004) Stress granule assembly is mediated by prion-like aggregation of TIA-1. Mol Biol Cell 15:5383-5398.

Gitcho MA, Baloh RH, Chakraverty S, Mayo K, Norton JB, Levitch D, Hatanpaa KJ, White CL, 3rd, Bigio EH, Caselli R, Baker M, Al-Lozi MT, Morris JC, Pestronk A, Rademakers R, Goate AM, Cairns NJ (2008) TDP-43 A315T mutation in familial motor neuron disease. Ann Neurol 63:535-538.

Gitler AD, Shorter J (2011) RNA-binding proteins with prion-like domains in ALS and FTLD-U. Prion 5:179 - 187.

Goedert M, Clavaguera F, Tolnay M (2010) The propagation of prion-like protein inclusions in neurodegenerative diseases. Trends Neurosci 33:317-325.

Gorlich D, Pante N, Kutay U, Aebi U, Bischoff FR (1996) Identification of different roles for RanGDP and RanGTP in nuclear protein import. The EMBO Journal 15:5584-5594.

Greenway MJ, Andersen PM, Russ C, Ennis S, Cashman S, Donaghy C, Patterson V, Swingler R, Kieran D, Prehn J, Morrison KE, Green A, Acharya KR, Brown RH, Jr., Hardiman O (2006) ANG mutations segregate with familial and 'sporadic' amyotrophic lateral sclerosis. Nat Genet 38:411-413.

Guerreiro RJ, Schymick JC, Crews C, Singleton A, Hardy J, Traynor BJ (2008) TDP-43 is not a common cause of sporadic amyotrophic lateral sclerosis. PloS One 3:e2450.

Guo W et al. (2011) An ALS-associated mutation affecting TDP-43 enhances protein aggregation, fibril formation and neurotoxicity. Nat Struct Mol Biol 18:822-830.

Guttinger S, Muhlhausser P, Koller-Eichhorn R, Brennecke J, Kutay U (2004) Transportin2 functions as importin and mediates nuclear import of HuR. Proceedings of the National Academy of Sciences of the United States of America 101:2918-2923.

Haass C, Selkoe DJ (2007) Soluble protein oligomers in neurodegeneration: lessons from the Alzheimer's amyloid beta-peptide. Nat Rev Mol Cell Biol 8:101-112.

Han TW, Kato M, Xie S, Wu LC, Mirzaei H, Pei J, Chen M, Xie Y, Allen J, Xiao G, McKnight SL (2012) Cell-free formation of RNA granules: bound RNAs identify features and components of cellular assemblies. Cell 149:768-779.

Hanson KA, Kim SH, Wassarman DA, Tibbetts RS (2010) Ubiquilin modifies TDP-43 toxicity in a Drosophila model of amyotrophic lateral sclerosis (ALS). The Journal of Biological Chemistry 285:11068-11072.

Hicks GG, Singh N, Nashabi A, Mai S, Bozek G, Klewes L, Arapovic D, White EK, Koury MJ, Oltz EM, Van Kaer L, Ruley HE (2000) Fus deficiency in mice results in defective B-lymphocyte development and activation, high levels of chromosomal instability and perinatal death. Nat Genet 24:175-179.

Hoell JI, Larsson E, Runge S, Nusbaum JD, Duggimpudi S, Farazi TA, Hafner M, Borkhardt A, Sander C, Tuschl T (2011) RNA targets of wild-type and mutant FET family proteins. Nat Struct Mol Biol.18 1428-1431.

Hofmann S, Cherkasova V, Bankhead P, Bukau B, Stoecklin G (2012) Translation suppression promotes stress granule formation and cell survival in response to cold shock. Mol Biol Cell 23:3786-3800.

Holm IE, Englund E, Mackenzie IR, Johannsen P, Isaacs AM (2007) A reassessment of the neuropathology of frontotemporal dementia linked to chromosome 3. J Neuropathol Exp Neurol 66:884-891.

Huang C, Zhou H, Tong J, Chen H, Liu YJ, Wang D, Wei X, Xia XG (2011) FUS transgenic rats develop the phenotypes of amyotrophic lateral sclerosis and frontotemporal lobar degeneration. PLoS Genet 7:e1002011.

Hutton M et al. (1998) Association of missense and 5'-splice-site mutations in tau with the inherited dementia FTDP-17. Nature 393:702-705.

Ichikawa H, Shimizu K, Hayashi Y, Ohki M (1994) An RNA-binding protein gene, TLS/FUS, is fused to ERG in human myeloid leukemia with t(16;21) chromosomal translocation. Cancer Res 54:2865-2868.

Igaz LM, Kwong LK, Chen-Plotkin A, Winton MJ, Unger TL, Xu Y, Neumann M, Trojanowski JQ, Lee VM (2009) Expression of TDP-43 C-terminal Fragments in Vitro Recapitulates Pathological Features of TDP-43 Proteinopathies. The Journal of Biological Chemistry 284:8516-8524.

Igaz LM, Kwong LK, Xu Y, Truax AC, Uryu K, Neumann M, Clark CM, Elman LB, Miller BL, Grossman M, McCluskey LF, Trojanowski JQ, Lee VM (2008) Enrichment of C-terminal fragments in TAR DNA-binding protein-43 cytoplasmic inclusions in brain but not in spinal cord of frontotemporal lobar degeneration and amyotrophic lateral sclerosis. Am J Pathol 173:182-194.

Iko Y, Kodama TS, Kasai N, Oyama T, Morita EH, Muto T, Okumura M, Fujii R, Takumi T, Tate S, Morikawa K (2004) Domain architectures and characterization of an RNA-binding protein, TLS. The Journal of Biological Chemistry 279:44834-44840.

Ilieva H, Polymenidou M, Cleveland DW (2009) Non-cell autonomous toxicity in neurodegenerative disorders: ALS and beyond. J Cell Biol 187:761-772.

Ishigaki S, Masuda A, Fujioka Y, Iguchi Y, Katsuno M, Shibata A, Urano F, Sobue G, Ohno K (2012) Position-dependent FUS-RNA interactions regulate alternative splicing events and transcriptions. Sci Rep 2:529.

Ito D, Seki M, Tsunoda Y, Uchiyama H, Suzuki N (2011) Nuclear transport impairment of amyotrophic lateral sclerosis-linked mutations in FUS/TLS. Ann Neurol 69:152-162.

Izaurralde E, Adam S (1998) Transport of macromolecules between the nucleus and the cytoplasm. RNA 4:351-364.

Jamison JT, Kayali F, Rudolph J, Marshall M, Kimball SR, DeGracia DJ (2008) Persistent redistribution of poly-adenylated mRNAs correlates with translation arrest

and cell death following global brain ischemia and reperfusion. Neuroscience 154:504-520.

Jiang LL, Che MX, Zhao J, Zhou CJ, Xie MY, Li HY, He JH, Hu HY (2013) Structural transformation of the amyloidogenic core region of TDP-43 protein initiates its aggregation and cytoplasmic inclusion. The Journal of Biological Chemistry 288:19614-19624.

Joachim CL, Morris JH, Kosik KS, Selkoe DJ (1987) Tau antisera recognize neurofibrillary tangles in a range of neurodegenerative disorders. Ann Neurol 22:514-520.

Jobert L, Argentini M, Tora L (2009) PRMT1 mediated methylation of TAF15 is required for its positive gene regulatory function. Exp Cell Res 315:1273-1286.

Johnson BS, Snead D, Lee JJ, McCaffery JM, Shorter J, Gitler AD (2009) TDP-43 is intrinsically aggregation-prone, and amyotrophic lateral sclerosis-linked mutations accelerate aggregation and increase toxicity. The Journal of Biological Chemistry 284:20329-20339.

Johnson JO et al. (2010) Exome sequencing reveals VCP mutations as a cause of familial ALS. Neuron 68:857-864.

Jucker M, Walker LC (2013) Self-propagation of pathogenic protein aggregates in neurodegenerative diseases. Nature 501:45-51.

Kabashi E, Bercier V, Lissouba A, Liao M, Brustein E, Rouleau GA, Drapeau P (2011) FUS and TARDBP but not SOD1 interact in genetic models of amyotrophic lateral sclerosis. PLoS Genet 7:e1002214.

Kabashi E, Lin L, Tradewell ML, Dion PA, Bercier V, Bourgouin P, Rochefort D, Bel Hadj S, Durham HD, Vande Velde C, Rouleau GA, Drapeau P (2010) Gain and loss of function of ALS-related mutations of TARDBP (TDP-43) cause motor deficits in vivo. Human Molecular Genetics 19:671-683.

Kabashi E, Valdmanis PN, Dion P, Spiegelman D, McConkey BJ, Vande Velde C, Bouchard JP, Lacomblez L, Pochigaeva K, Salachas F, Pradat PF, Camu W, Meininger V, Dupre N, Rouleau GA (2008) TARDBP mutations in individuals with sporadic and familial amyotrophic lateral sclerosis. Nat Genet 40:572-574.

Kameoka S, Duque P, Konarska MM (2004) p54(nrb) associates with the 5' splice site within large transcription/splicing complexes. The EMBO Journal 23:1782-1791.

Kampers T, Friedhoff P, Biernat J, Mandelkow EM, Mandelkow E (1996) RNA stimulates aggregation of microtubule-associated protein tau into Alzheimer-like paired helical filaments. FEBS Lett 399:344-349.

Kanai Y, Dohmae N, Hirokawa N (2004) Kinesin transports RNA: isolation and characterization of an RNA-transporting granule. Neuron 43:513-525.

Kato M, Han TW, Xie S, Shi K, Du X, Wu LC, Mirzaei H, Goldsmith EJ, Longgood J, Pei J, Grishin NV, Frantz DE, Schneider JW, Chen S, Li L, Sawaya MR, Eisenberg

D, Tycko R, McKnight SL (2012) Cell-free formation of RNA granules: low complexity sequence domains form dynamic fibers within hydrogels. Cell 149:753-767.

Kayali F, Montie HL, Rafols JA, DeGracia DJ (2005) Prolonged translation arrest in reperfused hippocampal cornu Ammonis 1 is mediated by stress granules. Neuroscience 134:1223-1245.

Kedersha N, Anderson P (2002) Stress granules: sites of mRNA triage that regulate mRNA stability and translatability. Biochem Soc Trans 30:963-969.

Kedersha N, Anderson P (2007) Mammalian stress granules and processing bodies. Methods Enzymol 431:61-81.

Kedersha N, Chen S, Gilks N, Li W, Miller IJ, Stahl J, Anderson P (2002) Evidence that ternary complex (eIF2-GTP-tRNA(i)(Met))-deficient preinitiation complexes are core constituents of mammalian stress granules. Mol Biol Cell 13:195-210.

Kedersha N, Cho MR, Li W, Yacono PW, Chen S, Gilks N, Golan DE, Anderson P (2000) Dynamic shuttling of TIA-1 accompanies the recruitment of mRNA to mammalian stress granules. J Cell Biol 151:1257-1268.

Kedersha N, Stoecklin G, Ayodele M, Yacono P, Lykke-Andersen J, Fritzler MJ, Scheuner D, Kaufman RJ, Golan DE, Anderson P (2005) Stress granules and processing bodies are dynamically linked sites of mRNP remodeling. J Cell Biol 169:871-884.

Kedersha NL, Gupta M, Li W, Miller I, Anderson P (1999) RNA-binding proteins TIA-1 and TIAR link the phosphorylation of eIF-2 alpha to the assembly of mammalian stress granules. J Cell Biol 147:1431-1442.

Keminer O, Peters R (1999) Permeability of single nuclear pores. Biophys J 77:217-228.

Kiernan MC, Vucic S, Cheah BC, Turner MR, Eisen A, Hardiman O, Burrell JR, Zoing MC (2011) Amyotrophic lateral sclerosis. Lancet 377:942-955.

Kim SH, Dong WK, Weiler IJ, Greenough WT (2006) Fragile X mental retardation protein shifts between polyribosomes and stress granules after neuronal injury by arsenite stress or in vivo hippocampal electrode insertion. J Neurosci 26:2413-2418.

Kim SH, Shanware NP, Bowler MJ, Tibbetts RS (2010) Amyotrophic lateral sclerosis-associated proteins TDP-43 and FUS/TLS function in a common biochemical complex to co-regulate HDAC6 mRNA. The Journal of Biological Chemistry 285:34097-34105.

King OD, Gitler AD, Shorter J (2012) The tip of the iceberg: RNA-binding proteins with prion-like domains in neurodegenerative disease. Brain Res 1462:61-80.

Kino Y, Washizu C, Aquilanti E, Okuno M, Kurosawa M, Yamada M, Doi H, Nukina N (2010) Intracellular localization and splicing regulation of FUS/TLS are variably

affected by amyotrophic lateral sclerosis-linked mutations. Nucleic Acids Research 39:2781-2798.

Kovacs GG, Murrell JR, Horvath S, Haraszti L, Majtenyi K, Molnar MJ, Budka H, Ghetti B, Spina S (2009) TARDBP variation associated with frontotemporal dementia, supranuclear gaze palsy, and chorea. Movement disorders : official journal of the Movement Disorder Society 24:1843-1847.

Kraemer BC, Schuck T, Wheeler JM, Robinson LC, Trojanowski JQ, Lee VM, Schellenberg GD (2010) Loss of murine TDP-43 disrupts motor function and plays an essential role in embryogenesis. Acta Neuropathologica 119:409-419.

Kuo PH, Doudeva LG, Wang YT, Shen CK, Yuan HS (2009) Structural insights into TDP-43 in nucleic-acid binding and domain interactions. Nucleic Acids Research 37:1799-1808.

Kuroda M, Sok J, Webb L, Baechtold H, Urano F, Yin Y, Chung P, de Rooij DG, Akhmedov A, Ashley T, Ron D (2000) Male sterility and enhanced radiation sensitivity in TLS(-/-) mice. The EMBO Journal 19:453-462.

Kwiatkowski TJ, Jr. et al. (2009) Mutations in the FUS/TLS gene on chromosome 16 cause familial amyotrophic lateral sclerosis. Science 323:1205-1208.

Lagier-Tourenne C et al. (2012) Divergent roles of ALS-linked proteins FUS/TLS and TDP-43 intersect in processing long pre-mRNAs. Nat Neurosci 15:1488-1497.

Lanson NA, Jr., Maltare A, King H, Smith R, Kim JH, Taylor JP, Lloyd TE, Pandey UB (2011) A Drosophila model of FUS-related neurodegeneration reveals genetic interaction between FUS and TDP-43. Human Molecular Genetics 20:2510-2523.

Lee BJ, Cansizoglu AE, Suel KE, Louis TH, Zhang Z, Chook YM (2006) Rules for nuclear localization sequence recognition by karyopherin beta 2. Cell 126:543-558.

Lee EB, Lee VM, Trojanowski JQ (2012) Gains or losses: molecular mechanisms of TDP43-mediated neurodegeneration. Nat Rev Neurosci 13:38-50.

Lee SJ, Matsuura Y, Liu SM, Stewart M (2005) Structural basis for nuclear import complex dissociation by RanGTP. Nature 435:693-696.

Lerga A, Hallier M, Delva L, Orvain C, Gallais I, Marie J, Moreau-Gachelin F (2001) Identification of an RNA binding specificity for the potential splicing factor TLS. The Journal of Biological Chemistry 276:6807-6816.

Li H, Watford W, Li C, Parmelee A, Bryant MA, Deng C, O'Shea J, Lee SB (2007) Ewing sarcoma gene EWS is essential for meiosis and B lymphocyte development. J Clin Invest 117:1314-1323.

Li HY, Yeh PA, Chiu HC, Tang CY, Tu BP (2011) Hyperphosphorylation as a defense mechanism to reduce TDP-43 aggregation. PloS One 6:e23075.

Li Y, Ray P, Rao EJ, Shi C, Guo W, Chen X, Woodruff EA, 3rd, Fushimi K, Wu JY (2010) A Drosophila model for TDP-43 proteinopathy. Proceedings of the National Academy of Sciences of the United States of America 107:3169-3174.

Li YR, King OD, Shorter J, Gitler AD (2013) Stress granules as crucibles of ALS pathogenesis. J Cell Biol 201:361-372.

Liachko NF, Guthrie CR, Kraemer BC (2010) Phosphorylation promotes neurotoxicity in a Caenorhabditis elegans model of TDP-43 proteinopathy. J Neurosci 30:16208-16219.

Ling SC, Polymenidou M, Cleveland DW (2013) Converging Mechanisms in ALS and FTD: Disrupted RNA and Protein Homeostasis. Neuron 79:416-438.

Ling SC, Albuquerque CP, Han JS, Lagier-Tourenne C, Tokunaga S, Zhou H, Cleveland DW (2010) ALS-associated mutations in TDP-43 increase its stability and promote TDP-43 complexes with FUS/TLS. Proceedings of the National Academy of Sciences of the United States of America 107:13318-13323.

Liu-Yesucevitz L, Bassell GJ, Gitler AD, Hart AC, Klann E, Richter JD, Warren ST, Wolozin B (2011) Local RNA translation at the synapse and in disease. J Neurosci 31:16086-16093.

Liu-Yesucevitz L, Bilgutay A, Zhang YJ, Vanderwyde T, Citro A, Mehta T, Zaarur N, McKee A, Bowser R, Sherman M, Petrucelli L, Wolozin B (2010) Tar DNA binding protein-43 (TDP-43) associates with stress granules: analysis of cultured cells and pathological brain tissue. PloS One 5:e13250.

Liu X, Niu C, Ren J, Zhang J, Xie X, Zhu H, Feng W, Gong W (2013) The RRM domain of human fused in sarcoma protein reveals a non-canonical nucleic acid binding site. Biochimica et Biophysica Acta 1832:375-385.

Lloyd RE (2012) How Do Viruses Interact with Stress-Associated RNA Granules? PLoS Pathog 8:e1002741.

Lomen-Hoerth C, Anderson T, Miller B (2002) The overlap of amyotrophic lateral sclerosis and frontotemporal dementia. Neurology 59:1077-1079.

Low WK, Dang Y, Schneider-Poetsch T, Shi Z, Choi NS, Merrick WC, Romo D, Liu JO (2005) Inhibition of eukaryotic translation initiation by the marine natural product pateamine A. Mol Cell 20:709-722.

Mackenzie IR, Rademakers R (2007) The molecular genetics and neuropathology of frontotemporal lobar degeneration: recent developments. Neurogenetics 8:237-248.

Mackenzie IR, Rademakers R, Neumann M (2010) TDP-43 and FUS in amyotrophic lateral sclerosis and frontotemporal dementia. Lancet Neurol 9:995-1007.

Mahboubi H, Seganathy E, Kong D, Stochaj U (2013) Identification of Novel Stress Granule Components That Are Involved in Nuclear Transport. PloS One 8:e68356.

Marko M, Vlassis A, Guialis A, Leichter M (2012) Domains involved in TAF15 subcellular localisation: dependence on cell type and ongoing transcription. Gene 506:331-338.

Martini A, La Starza R, Janssen H, Bilhou-Nabera C, Corveleyn A, Somers R, Aventin A, Foa R, Hagemeijer A, Mecucci C, Marynen P (2002) Recurrent rearrangement of the Ewing's sarcoma gene, EWSR1, or its homologue, TAF15, with the transcription factor CIZ/NMP4 in acute leukemia. Cancer Res 62:5408-5412.

Maruyama H et al. (2010) Mutations of optineurin in amyotrophic lateral sclerosis. Nature 465:223-226.

May WA, Gishizky ML, Lessnick SL, Lunsford LB, Lewis BC, Delattre O, Zucman J, Thomas G, Denny CT (1993) Ewing sarcoma 11;22 translocation produces a chimeric transcription factor that requires the DNA-binding domain encoded by FLI1 for transformation. Proceedings of the National Academy of Sciences of the United States of America 90:5752-5756.

Mazroui R, Di Marco S, Kaufman RJ, Gallouzi IE (2007) Inhibition of the ubiquitin-proteasome system induces stress granule formation. Mol Biol Cell 18:2603-2618.

Mazroui R, Sukarieh R, Bordeleau ME, Kaufman RJ, Northcote P, Tanaka J, Gallouzi I, Pelletier J (2006) Inhibition of ribosome recruitment induces stress granule formation independently of eukaryotic initiation factor 2alpha phosphorylation. Mol Biol Cell 17:4212-4219.

McDonald KK, Aulas A, Destroismaisons L, Pickles S, Beleac E, Camu W, Rouleau GA, Vande Velde C (2011) TAR DNA-binding protein 43 (TDP-43) regulates stress granule dynamics via differential regulation of G3BP and TIA-1. Human Molecular Genetics 20:1400-1410.

McKhann GM, Albert MS, Grossman M, Miller B, Dickson D, Trojanowski JQ (2001) Clinical and pathological diagnosis of frontotemporal dementia: report of the Work Group on Frontotemporal Dementia and Pick's Disease. Arch Neurol 58:1803-1809.

Metivier R, Penot G, Hubner MR, Reid G, Brand H, Kos M, Gannon F (2003) Estrogen receptor-alpha directs ordered, cyclical, and combinatorial recruitment of cofactors on a natural target promoter. Cell 115:751-763.

Meyerowitz J, Parker SJ, Vella LJ, Ng D, Price KA, Liddell JR, Caragounis A, Li QX, Masters CL, Nonaka T, Hasegawa M, Bogoyevitch MA, Kanninen KM, Crouch PJ, White AR (2011) C-Jun N-terminal kinase controls TDP-43 accumulation in stress granules induced by oxidative stress. Mol Neurodegener 6:57.

Mitchell JC, McGoldrick P, Vance C, Hortobagyi T, Sreedharan J, Rogelj B, Tudor EL, Smith BN, Klasen C, Miller CC, Cooper JD, Greensmith L, Shaw CE (2013) Overexpression of human wild-type FUS causes progressive motor neuron degeneration in an age- and dose-dependent fashion. Acta Neuropathologica 125:273-288.

Moisse K, Mepham J, Volkening K, Welch I, Hill T, Strong MJ (2009a) Cytosolic TDP-43 expression following axotomy is associated with caspase 3 activation in

NFL-/- mice: support for a role for TDP-43 in the physiological response to neuronal injury. Brain Res 1296:176-186.

Moisse K, Volkening K, Leystra-Lantz C, Welch I, Hill T, Strong MJ (2009b) Divergent patterns of cytosolic TDP-43 and neuronal progranulin expression following axotomy: implications for TDP-43 in the physiological response to neuronal injury. Brain Res 1249:202-211.

Moreno JA, Radford H, Peretti D, Steinert JR, Verity N, Martin MG, Halliday M, Morgan J, Dinsdale D, Ortori CA, Barrett DA, Tsaytler P, Bertolotti A, Willis AE, Bushell M, Mallucci GR (2012) Sustained translational repression by eIF2alpha-P mediates prion neurodegeneration. Nature 485:507-511.

Mori K, Weng SM, Arzberger T, May S, Rentzsch K, Kremmer E, Schmid B, Kretzschmar HA, Cruts M, Van Broeckhoven C, Haass C, Edbauer D (2013) The C9orf72 GGGGCC repeat is translated into aggregating dipeptide-repeat proteins in FTLD/ALS. Science 339:1335-1338.

Mosaheb S, Thorpe JR, Hashemzadeh-Bonehi L, Bigio EH, Gearing M, Cairns NJ (2005) Neuronal intranuclear inclusions are ultrastructurally and immunologically distinct from cytoplasmic inclusions of neuronal intermediate filament inclusion disease. Acta Neuropathologica 110:360-368.

Munoz-Garcia D, Ludwin SK (1984) Classic and generalized variants of Pick's disease: a clinicopathological, ultrastructural, and immunocytochemical comparative study. Ann Neurol 16:467-480.

Munoz DG, Neumann M, Kusaka H, Yokota O, Ishihara K, Terada S, Kuroda S, Mackenzie IR (2009) FUS pathology in basophilic inclusion body disease. Acta Neuropathologica 118:617-627.

Murakami T, Yang SP, Xie L, Kawano T, Fu D, Mukai A, Bohm C, Chen F, Robertson J, Suzuki H, Tartaglia GG, Vendruscolo M, Kaminski Schierle GS, Chan FT, Moloney A, Crowther D, Kaminski CF, Zhen M, St George-Hyslop P (2012) ALS mutations in FUS cause neuronal dysfunction and death in Caenorhabditis elegans by a dominant gain-of-function mechanism. Human Molecular Genetics 21:1-9.

Nardozzi JD, Lott K, Cingolani G (2010) Phosphorylation meets nuclear import: a review. Cell Commun Signal 8:32.

Neumann M, Rademakers R, Roeber S, Baker M, Kretzschmar HA, Mackenzie IR (2009a) A new subtype of frontotemporal lobar degeneration with FUS pathology. Brain 132:2922-2931.

Neumann M, Roeber S, Kretzschmar HA, Rademakers R, Baker M, Mackenzie IR (2009b) Abundant FUS-immunoreactive pathology in neuronal intermediate filament inclusion disease. Acta Neuropathologica 118:605-616.

Neumann M, Kwong LK, Lee EB, Kremmer E, Flatley A, Xu Y, Forman MS, Troost D, Kretzschmar HA, Trojanowski JQ, Lee VM (2009c) Phosphorylation of S409/410 of TDP-43 is a consistent feature in all sporadic and familial forms of TDP-43 proteinopathies. Acta Neuropathologica 117(2):137-149.

Neumann M, Valori CF, Ansorge O, Kretzschmar HA, Munoz DG, Kusaka H, Yokota O, Ishihara K, Ang LC, Bilbao JM, Mackenzie IR (2012) Transportin 1 accumulates specifically with FET proteins but no other transportin cargos in FTLD-FUS and is absent in FUS inclusions in ALS with FUS mutations. Acta Neuropathologica 124:705-716.

Neumann M, Bentmann E, Dormann D, Jawaid A, DeJesus-Hernandez M, Ansorge O, Roeber S, Kretzschmar HA, Munoz DG, Kusaka H, Yokota O, Ang LC, Bilbao J, Rademakers R, Haass C, Mackenzie IR (2011) FET proteins TAF15 and EWS are selective markers that distinguish FTLD with FUS pathology from amyotrophic lateral sclerosis with FUS mutations. Brain 134:2595-2609.

Neumann M, Sampathu DM, Kwong LK, Truax AC, Micsenyi MC, Chou TT, Bruce J, Schuck T, Grossman M, Clark CM, McCluskey LF, Miller BL, Masliah E, Mackenzie IR, Feldman H, Feiden W, Kretzschmar HA, Trojanowski JQ, Lee VM (2006) Ubiquitinated TDP-43 in frontotemporal lobar degeneration and amyotrophic lateral sclerosis. Science 314:130-133.

Nguyen CD, Mansfield RE, Leung W, Vaz PM, Loughlin FE, Grant RP, Mackay JP (2011) Characterization of a family of RanBP2-type zinc fingers that can recognize single-stranded RNA. Journal of Molecular Biology 407:273-283.

Nicholson TB, Chen T, Richard S (2009) The physiological and pathophysiological role of PRMT1-mediated protein arginine methylation. Pharmacol Res 60:466-474.

Nihei Y, Ito D, Suzuki N (2012) Roles of ataxin-2 in pathological cascades mediated by TAR DNA-binding protein 43 (TDP-43) and Fused in Sarcoma (FUS). The Journal of Biological Chemistry 287:41310-41323.

Nishimoto Y, Ito D, Yagi T, Nihei Y, Tsunoda Y, Suzuki N (2010) Characterization of alternative isoforms and inclusion body of the TAR DNA-binding protein-43. The Journal of Biological Chemistry 285:608-619.

Nishimura AL, Zupunski V, Troakes C, Kathe C, Fratta P, Howell M, Gallo JM, Hortobagyi T, Shaw CE, Rogelj B (2010) Nuclear import impairment causes cytoplasmic trans-activation response DNA-binding protein accumulation and is associated with frontotemporal lobar degeneration. Brain 133:1763-1771.

Nishimura AL, Mitne-Neto M, Silva HC, Richieri-Costa A, Middleton S, Cascio D, Kok F, Oliveira JR, Gillingwater T, Webb J, Skehel P, Zatz M (2004) A mutation in the vesicle-trafficking protein VAPB causes late-onset spinal muscular atrophy and amyotrophic lateral sclerosis. Am J Hum Genet 75:822-831.

Niu C, Zhang J, Gao F, Yang L, Jia M, Zhu H, Gong W (2012) FUS-NLS/Transportin 1 Complex Structure Provides Insights into the Nuclear Targeting Mechanism of FUS and the Implications in ALS. PloS One 7:e47056.

Nonaka T, Kametani F, Arai T, Akiyama H, Hasegawa M (2009) Truncation and pathogenic mutations facilitate the formation of intracellular aggregates of TDP-43. Human Molecular Genetics 18:3353-3364.

Nonaka T, Masuda-Suzukake M, Arai T, Hasegawa Y, Akatsu H, Obi T, Yoshida M, Murayama S, Mann DM, Akiyama H, Hasegawa M (2013) Prion-like properties of pathological TDP-43 aggregates from diseased brains. Cell Rep 4:124-134.

Nonhoff U, Ralser M, Welzel F, Piccini I, Balzereit D, Yaspo ML, Lehrach H, Krobitsch S (2007) Ataxin-2 interacts with the DEAD/H-box RNA helicase DDX6 and interferes with P-bodies and stress granules. Mol Biol Cell 18:1385-1396.

Ohno T, Rao VN, Reddy ES (1993) EWS/Fli-1 chimeric protein is a transcriptional activator. Cancer Res 53:5859-5863.

Ohno T, Ouchida M, Lee L, Gatalica Z, Rao VN, Reddy ES (1994) The EWS gene, involved in Ewing family of tumors, malignant melanoma of soft parts and desmoplastic small round cell tumors, codes for an RNA binding protein with novel regulatory domains. Oncogene 9:3087-3097.

Ong SE, Mittler G, Mann M (2004) Identifying and quantifying in vivo methylation sites by heavy methyl SILAC. Nat Methods 1:119-126.

Orozco D, Tahirovic S, Rentzsch K, Schwenk BM, Haass C, Edbauer D (2012) Loss of fused in sarcoma (FUS) promotes pathological Tau splicing. EMBO Rep 13:759-764.

Ostareck-Lederer A, Ostareck DH, Rucknagel KP, Schierhorn A, Moritz B, Huttelmaier S, Flach N, Handoko L, Wahle E (2006) Asymmetric arginine dimethylation of heterogeneous nuclear ribonucleoprotein K by protein-arginine methyltransferase 1 inhibits its interaction with c-Src. The Journal of Biological Chemistry 281:11115-11125.

Ou SH, Wu F, Harrich D, Garcia-Martinez LF, Gaynor RB (1995) Cloning and characterization of a novel cellular protein, TDP-43, that binds to human immunodeficiency virus type 1 TAR DNA sequence motifs. J Virol 69:3584-3596.

Pahlich S, Zakaryan RP, Gehring H (2006) Protein arginine methylation: Cellular functions and methods of analysis. Biochimica et Biophysica Acta 1764:1890-1903.

Pahlich S, Bschir K, Chiavi C, Belyanskaya L, Gehring H (2005) Different methylation characteristics of protein arginine methyltransferase 1 and 3 toward the Ewing Sarcoma protein and a peptide. Proteins 61:164-175.

Pan XD, Chen XC (2013) Clinic, neuropathology and molecular genetics of frontotemporal dementia: a mini-review. Transl Neurodegener 2:8.

Panagopoulos I, Mencinger M, Dietrich CU, Bjerkehagen B, Saeter G, Mertens F, Mandahl N, Heim S (1999) Fusion of the RBP56 and CHN genes in extraskeletal myxoid chondrosarcomas with translocation t(9;17)(q22;q11). Oncogene 18:7594-7598.

Paronetto MP, Minana B, Valcarcel J (2011) The Ewing sarcoma protein regulates DNA damage-induced alternative splicing. Mol Cell 43:353-368.

Perreault A, Lemieux C, Bachand F (2007) Regulation of the nuclear poly(A)-binding protein by arginine methylation in fission yeast. The Journal of Biological Chemistry 282:7552-7562.

Pizzo E, Sarcinelli C, Sheng J, Fusco S, Formiggini F, Netti P, Yu W, D'Alessio G, Hu GF (2013) Ribonuclease/angiogenin inhibitor 1 regulates stress-induced subcellular localization of angiogenin to control growth and survival. Journal of Cell Science 126:4308-4319.

Polymenidou M, Lagier-Tourenne C, Hutt KR, Huelga SC, Moran J, Liang TY, Ling SC, Sun E, Wancewicz E, Mazur C, Kordasiewicz H, Sedaghat Y, Donohue JP, Shiue L, Bennett CF, Yeo GW, Cleveland DW (2011) Long pre-mRNA depletion and RNA missplicing contribute to neuronal vulnerability from loss of TDP-43. Nat Neurosci 14:459-468.

Prasad DD, Ouchida M, Lee L, Rao VN, Reddy ES (1994) TLS/FUS fusion domain of TLS/FUS-erg chimeric protein resulting from the t(16;21) chromosomal translocation in human myeloid leukemia functions as a transcriptional activation domain. Oncogene 9:3717-3729.

Pulst SM, Nechiporuk A, Nechiporuk T, Gispert S, Chen XN, Lopes-Cendes I, Pearlman S, Starkman S, Orozco-Diaz G, Lunkes A, DeJong P, Rouleau GA, Auburger G, Korenberg JR, Figueroa C, Sahba S (1996) Moderate expansion of a normally biallelic trinucleotide repeat in spinocerebellar ataxia type 2. Nat Genet 14:269-276.

Rabbitts TH, Forster A, Larson R, Nathan P (1993) Fusion of the dominant negative transcription regulator CHOP with a novel gene FUS by translocation t(12;16) in malignant liposarcoma. Nat Genet 4:175-180.

Rademakers R, Neumann M, Mackenzie IR (2013) Advances in understanding the molecular basis of frontotemporal dementia. Nat Rev Neurol 9:240.

Ralser M, Albrecht M, Nonhoff U, Lengauer T, Lehrach H, Krobitsch S (2005) An integrative approach to gain insights into the cellular function of human ataxin-2. Journal of Molecular Biology 346:203-214.

Rappsilber J, Friesen WJ, Paushkin S, Dreyfuss G, Mann M (2003) Detection of arginine dimethylated peptides by parallel precursor ion scanning mass spectrometry in positive ion mode. Anal Chem 75:3107-3114.

Ravenscroft TA, Baker MC, Rutherford NJ, Neumann M, Mackenzie IR, Josephs KA, Boeve BF, Petersen R, Halliday GM, Kril J, van Swieten JC, Seeley WW, Dickson DW, Rademakers R (2013) Mutations in protein N-arginine methyltransferases are not the cause of FTLD-FUS. Neurobiol Aging 34:2235 e2211-2233.

Renton AE et al. (2011) A hexanucleotide repeat expansion in C9ORF72 is the cause of chromosome 9p21-linked ALS-FTD. Neuron 72:257-268.

Rexach M, Blobel G (1995) Protein import into nuclei: association and dissociation reactions involving transport substrate, transport factors, and nucleoporins. Cell 83:683-692.

Ringholz GM, Appel SH, Bradshaw M, Cooke NA, Mosnik DM, Schulz PE (2005) Prevalence and patterns of cognitive impairment in sporadic ALS. Neurology 65:586-590.

Ritson GP, Custer SK, Freibaum BD, Guinto JB, Geffel D, Moore J, Tang W, Winton MJ, Neumann M, Trojanowski JQ, Lee VM, Forman MS, Taylor JP (2010) TDP-43 mediates degeneration in a novel Drosophila model of disease caused by mutations in VCP/p97. J Neurosci 30:7729-7739.

Robberecht W, Philips T (2013) The changing scene of amyotrophic lateral sclerosis. Nat Rev Neurosci 14:248-264.

Rogelj B, Easton LE, Bogu GK, Stanton LW, Rot G, Curk T, Zupan B, Sugimoto Y, Modic M, Haberman N, Tollervey J, Fujii R, Takumi T, Shaw CE, Ule J (2012) Widespread binding of FUS along nascent RNA regulates alternative splicing in the brain. Sci Rep 2:603.

Rosen DR, Siddique T, Patterson D, Figlewicz DA, Sapp P, Hentati A, Donaldson D, Goto J, O'Regan JP, Deng HX, et al. (1993) Mutations in Cu/Zn superoxide dismutase gene are associated with familial amyotrophic lateral sclerosis. Nature 362:59-62.

Rossow KL, Janknecht R (2001) The Ewing's sarcoma gene product functions as a transcriptional activator. Cancer Res 61:2690-2695.

Rule RR, Schuff N, Miller RG, Weiner MW (2010) Gray matter perfusion correlates with disease severity in ALS. Neurology 74:821-827.

Sakabe K, Hart GW (2010) O-GlcNAc transferase regulates mitotic chromatin dynamics. The Journal of Biological Chemistry 285:34460-34468.

Sanchez-Garcia I, Rabbitts TH (1994) Transcriptional activation by TAL1 and FUS-CHOP proteins expressed in acute malignancies as a result of chromosomal abnormalities. Proceedings of the National Academy of Sciences of the United States of America 91:7869-7873.

Sasayama H, Shimamura M, Tokuda T, Azuma Y, Yoshida T, Mizuno T, Nakagawa M, Fujikake N, Nagai Y, Yamaguchi M (2012) Knockdown of the Drosophila fused in sarcoma (FUS) homologue causes deficient locomotive behavior and shortening of motoneuron terminal branches. PloS One 7:e39483.

Sato T, Takeuchi S, Saito A, Ding W, Bamba H, Matsuura H, Hisa Y, Tooyama I, Urushitani M (2009) Axonal ligation induces transient redistribution of TDP-43 in brainstem motor neurons. Neuroscience 164:1565-1578.

Scaramuzzino C, Monaghan J, Milioto C, Lanson NA, Jr., Maltare A, Aggarwal T, Casci I, Fackelmayer FO, Pennuto M, Pandey UB (2013) Protein arginine methyltransferase 1 and 8 interact with FUS to modify its sub-cellular distribution and toxicity in vitro and in vivo. PloS One 8:e61576.

Schmid B, Hruscha A, Hogl S, Banzhaf-Strathmann J, Strecker K, van der Zee J, Teucke M, Eimer S, Hegermann J, Kittelmann M, Kremmer E, Cruts M,

Solchenberger B, Hasenkamp L, van Bebber F, Van Broeckhoven C, Edbauer D, Lichtenthaler SF, Haass C (2013) Loss of ALS-associated TDP-43 in zebrafish causes muscle degeneration, vascular dysfunction, and reduced motor neuron axon outgrowth. Proceedings of the National Academy of Sciences of the United States of America 110:4986-4991.

Schwarzbach MH, Koesters R, Germann A, Mechtersheimer G, Geisbill J, Winkler S, Niedergethmann M, Ridder R, Buechler MW, von Knebel Doeberitz M, Willeke F (2004) Comparable transforming capacities and differential gene expression patterns of variant FUS/CHOP fusion transcripts derived from soft tissue liposarcomas. Oncogene 23:6798-6805.

Sephton CF, Good SK, Atkin S, Dewey CM, Mayer P, 3rd, Herz J, Yu G (2010) TDP-43 is a developmentally regulated protein essential for early embryonic development. The Journal of Biological Chemistry 285:6826-6834.

Sephton CF, Cenik C, Kucukural A, Dammer EB, Cenik B, Han Y, Dewey CM, Roth FP, Herz J, Peng J, Moore MJ, Yu G (2011) Identification of neuronal RNA targets of TDP-43-containing ribonucleoprotein complexes. The Journal of Biological Chemistry 286:1204-1215.

Shaw DJ, Morse R, Todd AG, Eggleton P, Lorson CL, Young PJ (2009) Identification of a tripartite import signal in the Ewing Sarcoma protein (EWS). Biochem Biophys Res Commun 390:1197-1201.

Sherrill KW, Byrd MP, Van Eden ME, Lloyd RE (2004) BCL-2 translation is mediated via internal ribosome entry during cell stress. The Journal of Biological Chemistry 279:29066-29074.

Shindo A, Yata K, Sasaki R, Tomimoto H (2013) Chronic cerebral ischemia induces redistribution and abnormal phosphorylation of transactivation-responsive DNA-binding protein-43 in mice. Brain Res 1533:131-140.

Sieben A, Van Langenhove T, Engelborghs S, Martin JJ, Boon P, Cras P, De Deyn PP, Santens P, Van Broeckhoven C, Cruts M (2012) The genetics and neuropathology of frontotemporal lobar degeneration. Acta Neuropathologica 124:353-372.

Skibinski G, Parkinson NJ, Brown JM, Chakrabarti L, Lloyd SL, Hummerich H, Nielsen JE, Hodges JR, Spillantini MG, Thusgaard T, Brandner S, Brun A, Rossor MN, Gade A, Johannsen P, Sorensen SA, Gydesen S, Fisher EM, Collinge J (2005) Mutations in the endosomal ESCRTIII-complex subunit CHMP2B in frontotemporal dementia. Nat Genet 37:806-808.

Snowden JS, Neary D, Mann DM (2002) Frontotemporal dementia. Br J Psychiatry 180:140-143.

Snowden JS, Hu Q, Rollinson S, Halliwell N, Robinson A, Davidson YS, Momeni P, Baborie A, Griffiths TD, Jaros E, Perry RH, Richardson A, Pickering-Brown SM, Neary D, Mann DM (2011) The most common type of FTLD-FUS (aFTLD-U) is associated with a distinct clinical form of frontotemporal dementia but is not related to mutations in the FUS gene. Acta Neuropathologica 122:99-110.

Souquere S, Mollet S, Kress M, Dautry F, Pierron G, Weil D (2009) Unravelling the ultrastructure of stress granules and associated P-bodies in human cells. Journal of Cell Science 122:3619-3626.

Spillantini MG, Goedert M (2013) Tau pathology and neurodegeneration. Lancet Neurol 12:609-622.

Spriggs KA, Bushell M, Willis AE (2010) Translational regulation of gene expression during conditions of cell stress. Mol Cell 40:228-237.

Sproviero W, La Bella V, Mazzei R, Valentino P, Rodolico C, Simone IL, Logroscino G, Ungaro C, Magariello A, Patitucci A, Tedeschi G, Spataro R, Condino F, Bono F, Citrigno L, Monsurro MR, Muglia M, Gambardella A, Quattrone A, Conforti FL (2012) FUS mutations in sporadic amyotrophic lateral sclerosis: clinical and genetic analysis. Neurobiol Aging 33:837 e831-835.

Sreedharan J, Blair IP, Tripathi VB, Hu X, Vance C, Rogelj B, Ackerley S, Durnall JC, Williams KL, Buratti E, Baralle F, de Belleroche J, Mitchell JD, Leigh PN, Al-Chalabi A, Miller CC, Nicholson G, Shaw CE (2008) TDP-43 mutations in familial and sporadic amyotrophic lateral sclerosis. Science 319:1668-1672.

Stallings NR, Puttaparthi K, Dowling KJ, Luther CM, Burns DK, Davis K, Elliott JL (2013) TDP-43, an ALS Linked Protein, Regulates Fat Deposition and Glucose Homeostasis. PloS One 8:e71793.

Stohr N, Lederer M, Reinke C, Meyer S, Hatzfeld M, Singer RH, Huttelmaier S (2006) ZBP1 regulates mRNA stability during cellular stress. J Cell Biol 175:527-534.

Strong MJ, Volkening K, Hammond R, Yang W, Strong W, Leystra-Lantz C, Shoesmith C (2007) TDP43 is a human low molecular weight neurofilament (hNFL) mRNA-binding protein. Molecular and Cellular Neurosciences 35:320-327.

Sun Z, Diaz Z, Fang X, Hart MP, Chesi A, Shorter J, Gitler AD (2011) Molecular determinants and genetic modifiers of aggregation and toxicity for the ALS disease protein FUS/TLS. PLoS Biol 9:e1000614.

Tan AY, Manley JL (2009) The TET family of proteins: functions and roles in disease. J Mol Cell Biol 1:82-92.

Tan AY, Riley TR, Coady T, Bussemaker HJ, Manley JL (2012) TLS/FUS (translocated in liposarcoma/fused in sarcoma) regulates target gene transcription via single-stranded DNA response elements. Proceedings of the National Academy of Sciences of the United States of America 109:6030-6035.

Tanaka M, Kondo S, Hirai S, Sun X, Yamagishi T, Okamoto K (1993) Cerebral blood flow and oxygen metabolism in progressive dementia associated with amyotrophic lateral sclerosis. Journal of the Neurological Sciences 120:22-28.

Tang J, Frankel A, Cook RJ, Kim S, Paik WK, Williams KR, Clarke S, Herschman HR (2000) PRMT1 is the predominant type I protein arginine methyltransferase in mammalian cells. The Journal of Biological Chemistry 275:7723-7730.

Tatom JB, Wang DB, Dayton RD, Skalli O, Hutton ML, Dickson DW, Klein RL (2009) Mimicking aspects of frontotemporal lobar degeneration and Lou Gehrig's disease in rats via TDP-43 overexpression. Mol Ther 17:607-613.

Terry LJ, Shows EB, Wente SR (2007) Crossing the nuclear envelope: hierarchical regulation of nucleocytoplasmic transport. Science 318:1412-1416.

Thandapani P, O'Connor TR, Bailey TL, Richard S (2013) Defining the RGG/RG Motif. Mol Cell 50:613-623.

Thiyagarajan N, Ferguson R, Subramanian V, Acharya KR (2012) Structural and molecular insights into the mechanism of action of human angiogenin-ALS variants in neurons. Nat Commun 3:1121.

Thomas M, Alegre-Abarrategui J, Wade-Martins R (2013) RNA dysfunction and aggrephagy at the centre of an amyotrophic lateral sclerosis/frontotemporal dementia disease continuum. Brain 136:1345-1360.

Thomas MG, Martinez Tosar LJ, Desbats MA, Leishman CC, Boccaccio GL (2009) Mammalian Staufen 1 is recruited to stress granules and impairs their assembly. Journal of Cell Science 122:563-573.

Ticozzi N, Vance C, Leclerc AL, Keagle P, Glass JD, McKenna-Yasek D, Sapp PC, Silani V, Bosco DA, Shaw CE, Brown RH, Jr., Landers JE (2011) Mutational analysis reveals the FUS homolog TAF15 as a candidate gene for familial amyotrophic lateral sclerosis. Am J Med Genet B Neuropsychiatr Genet 156B:285-290.

Tollervey JR, Curk T, Rogelj B, Briese M, Cereda M, Kayikci M, Konig J, Hortobagyi T, Nishimura AL, Zupunski V, Patani R, Chandran S, Rot G, Zupan B, Shaw CE, Ule J (2011) Characterizing the RNA targets and position-dependent splicing regulation by TDP-43. Nat Neurosci 14:452-458.

Tourriere H, Chebli K, Zekri L, Courselaud B, Blanchard JM, Bertrand E, Tazi J (2003) The RasGAP-associated endoribonuclease G3BP assembles stress granules. J Cell Biol 160:823-831.

Tradewell ML, Yu Z, Tibshirani M, Boulanger MC, Durham HD, Richard S (2012) Arginine methylation by PRMT1 regulates nuclear-cytoplasmic localization and toxicity of FUS/TLS harbouring ALS-linked mutations. Human Molecular Genetics 21:136-149.

Tresse E, Salomons FA, Vesa J, Bott LC, Kimonis V, Yao TP, Dantuma NP, Taylor JP (2010) VCP/p97 is essential for maturation of ubiquitin-containing autophagosomes and this function is impaired by mutations that cause IBMPFD. Autophagy 6:217-227.

Troakes C, Hortobagyi T, Vance C, Al-Sarraj S, Rogelj B, Shaw CE (2013) Transportin 1 colocalization with Fused in Sarcoma (FUS) inclusions is not characteristic for amyotrophic lateral sclerosis-FUS confirming disrupted nuclear import of mutant FUS and distinguishing it from frontotemporal lobar degeneration with FUS inclusions. Neuropathol Appl Neurobiol 39:553-561.

Tsai KJ, Yang CH, Fang YH, Cho KH, Chien WL, Wang WT, Wu TW, Lin CP, Fu WM, Shen CK (2010) Elevated expression of TDP-43 in the forebrain of mice is sufficient to cause neurological and pathological phenotypes mimicking FTLD-U. J Exp Med 207:1661-1673.

Tsuiji H, Iguchi Y, Furuya A, Kataoka A, Hatsuta H, Atsuta N, Tanaka F, Hashizume Y, Akatsu H, Murayama S, Sobue G, Yamanaka K (2013) Spliceosome integrity is defective in the motor neuron diseases ALS and SMA. EMBO Mol Med 5:221-234.

Udan M, Baloh RH (2011) Implications of the prion-related Q/N domains in TDP-43 and FUS. Prion 5:1-5.

Urwin H et al. (2010) FUS pathology defines the majority of tau- and TDP-43-negative frontotemporal lobar degeneration. Acta Neuropathologica 120:33-41.

Vaccaro A, Tauffenberger A, Aggad D, Rouleau G, Drapeau P, Parker JA (2012) Mutant TDP-43 and FUS cause age-dependent paralysis and neurodegeneration in C. elegans. PloS One 7:e31321.

van Blitterswijk M, Landers JE (2010) RNA processing pathways in amyotrophic lateral sclerosis. Neurogenetics 11:275-290.

Van Deerlin VM et al. (2008) TARDBP mutations in amyotrophic lateral sclerosis with TDP-43 neuropathology: a genetic and histopathological analysis. Lancet Neurol 7:409-416.

van der Laan AM, van Gemert AM, Dirks RW, Noordermeer JN, Fradkin LG, Tanke HJ, Jost CR (2012) mRNA cycles through hypoxia-induced stress granules in live Drosophila embryonic muscles. Int J Dev Biol 56:701-709.

Van Langenhove T, van der Zee J, Van Broeckhoven C (2012) The molecular basis of the frontotemporal lobar degeneration-amyotrophic lateral sclerosis spectrum. Annals of Medicine 44:817-828.

Van Langenhove T, van der Zee J, Sleegers K, Engelborghs S, Vandenberghe R, Gijselinck I, Van den Broeck M, Mattheijssens M, Peeters K, De Deyn PP, Cruts M, Van Broeckhoven C (2010) Genetic contribution of FUS to frontotemporal lobar degeneration. Neurology 74:366-371.

Vance C et al. (2009) Mutations in FUS, an RNA processing protein, cause familial amyotrophic lateral sclerosis type 6. Science 323:1208-1211.

Vanderweyde T, Yu H, Varnum M, Liu-Yesucevitz L, Citro A, Ikezu T, Duff K, Wolozin B (2012) Contrasting Pathology of the Stress Granule Proteins TIA-1 and G3BP in Tauopathies. J Neurosci 32:8270-8283.

Voigt A, Herholz D, Fiesel FC, Kaur K, Muller D, Karsten P, Weber SS, Kahle PJ, Marquardt T, Schulz JB (2010) TDP-43-mediated neuron loss in vivo requires RNA-binding activity. PloS One 5:e12247.

Volkening K, Leystra-Lantz C, Yang W, Jaffee H, Strong MJ (2009) Tar DNA binding protein of 43 kDa (TDP-43), 14-3-3 proteins and copper/zinc superoxide dismutase

(SOD1) interact to modulate NFL mRNA stability. Implications for altered RNA processing in amyotrophic lateral sclerosis (ALS). Brain Res 1305:168-182.

Waelter S, Boeddrich A, Lurz R, Scherzinger E, Lueder G, Lehrach H, Wanker EE (2001) Accumulation of mutant huntingtin fragments in aggresome-like inclusion bodies as a result of insufficient protein degradation. Mol Biol Cell 12:1393-1407.

Waibel S, Neumann M, Rabe M, Meyer T, Ludolph AC (2010) Novel missense and truncating mutations in FUS/TLS in familial ALS. Neurology 75:815-817.

Waibel S, Neumann M, Rosenbohm A, Birve A, Volk AE, Weishaupt JH, Meyer T, Muller U, Andersen PM, Ludolph AC (2013) Truncating mutations in FUS/TLS give rise to a more aggressive ALS-phenotype than missense mutations: a clinico-genetic study in Germany. Eur J Neurol 20:540-546.

Wang IF, Wu LS, Chang HY, Shen CK (2008) TDP-43, the signature protein of FTLD-U, is a neuronal activity-responsive factor. Journal of Neurochemistry 105:797-806.

Wang J, Xu G, Borchelt DR (2002a) High molecular weight complexes of mutant superoxide dismutase 1: age-dependent and tissue-specific accumulation. Neurobiol Dis 9:139-148.

Wang J, Xu G, Gonzales V, Coonfield M, Fromholt D, Copeland NG, Jenkins NA, Borchelt DR (2002b) Fibrillar inclusions and motor neuron degeneration in transgenic mice expressing superoxide dismutase 1 with a disrupted copper-binding site. Neurobiol Dis 10:128-138.

Wang JW, Brent JR, Tomlinson A, Shneider NA, McCabe BD (2011) The ALS-associated proteins FUS and TDP-43 function together to affect Drosophila locomotion and life span. J Clin Invest 121:4118-4126.

Watts GD, Wymer J, Kovach MJ, Mehta SG, Mumm S, Darvish D, Pestronk A, Whyte MP, Kimonis VE (2004) Inclusion body myopathy associated with Paget disease of bone and frontotemporal dementia is caused by mutant valosin-containing protein. Nat Genet 36:377-381.

Wegorzewska I, Bell S, Cairns NJ, Miller TM, Baloh RH (2009) TDP-43 mutant transgenic mice develop features of ALS and frontotemporal lobar degeneration. Proceedings of the National Academy of Sciences of the United States of America 106:18809-18814.

Wente SR, Rout MP (2010) The nuclear pore complex and nuclear transport. Cold Spring Harb Perspect Biol 2:a000562.

Wils H, Kleinberger G, Janssens J, Pereson S, Joris G, Cuijt I, Smits V, Ceuterick-de Groote C, Van Broeckhoven C, Kumar-Singh S (2010) TDP-43 transgenic mice develop spastic paralysis and neuronal inclusions characteristic of ALS and frontotemporal lobar degeneration. Proceedings of the National Academy of Sciences of the United States of America 107:3858-3863.

Winton MJ, Igaz LM, Wong MM, Kwong LK, Trojanowski JQ, Lee VM (2008a) Disturbance of nuclear and cytoplasmic TAR DNA-binding protein (TDP-43)

induces disease-like redistribution, sequestration, and aggregate formation. The Journal of Biological Chemistry 283:13302-13309.

Winton MJ, Van Deerlin VM, Kwong LK, Yuan W, Wood EM, Yu CE, Schellenberg GD, Rademakers R, Caselli R, Karydas A, Trojanowski JQ, Miller BL, Lee VM (2008b) A90V TDP-43 variant results in the aberrant localization of TDP-43 in vitro. FEBS Lett 582:2252-2256.

Wippich F, Bodenmiller B, Trajkovska MG, Wanka S, Aebersold R, Pelkmans L (2013) Dual Specificity Kinase DYRK3 Couples Stress Granule Condensation/Dissolution to mTORC1 Signaling. Cell 152:791-805.

Wolozin B (2012) Regulated protein aggregation: stress granules and neurodegeneration. Mol Neurodegener 7:56.

Wu LS, Cheng WC, Shen CK (2012) Targeted depletion of TDP-43 expression in the spinal cord motor neurons leads to the development of amyotrophic lateral sclerosis-like phenotypes in mice. The Journal of Biological Chemistry 287:27335-27344.

Wu LS, Cheng WC, Hou SC, Yan YT, Jiang ST, Shen CK (2010) TDP-43, a neuro-pathosignature factor, is essential for early mouse embryogenesis. Genesis 48:56-62.

Xiao S, Sanelli T, Dib S, Sheps D, Findlater J, Bilbao J, Keith J, Zinman L, Rogaeva E, Robertson J (2011) RNA targets of TDP-43 identified by UV-CLIP are deregulated in ALS. Molecular and Cellular Neurosciences 47:167-180.

Xu YF, Gendron TF, Zhang YJ, Lin WL, D'Alton S, Sheng H, Casey MC, Tong J, Knight J, Yu X, Rademakers R, Boylan K, Hutton M, McGowan E, Dickson DW, Lewis J, Petrucelli L (2010) Wild-type human TDP-43 expression causes TDP-43 phosphorylation, mitochondrial aggregation, motor deficits, and early mortality in transgenic mice. J Neurosci 30:10851-10859.

Yamaguchi A, Kitajo K (2012) The effect of PRMT1-mediated arginine methylation on the subcellular localization, stress granules, and detergent-insoluble aggregates of FUS/TLS. PloS One 7:e49267.

Yamashita S, Mori A, Sakaguchi H, Suga T, Ishihara D, Ueda A, Yamashita T, Maeda Y, Uchino M, Hirano T (2012) Sporadic juvenile amyotrophic lateral sclerosis caused by mutant FUS/TLS: possible association of mental retardation with this mutation. J Neurol 259:1039-1044.

Yamazaki T, Chen S, Yu Y, Yan B, Haertlein TC, Carrasco MA, Tapia JC, Zhai B, Das R, Lalancette-Hebert M, Sharma A, Chandran S, Sullivan G, Nishimura AL, Shaw CE, Gygi SP, Shneider NA, Maniatis T, Reed R (2012) FUS-SMN protein interactions link the motor neuron diseases ALS and SMA. Cell Rep 2:799-806.

Yan J, Deng HX, Siddique N, Fecto F, Chen W, Yang Y, Liu E, Donkervoort S, Zheng JG, Shi Y, Ahmeti KB, Brooks B, Engel WK, Siddique T (2010) Frameshift and novel mutations in FUS in familial amyotrophic lateral sclerosis and ALS/dementia. Neurology 75:807-814.

Yang L, Embree LJ, Tsai S, Hickstein DD (1998) Oncoprotein TLS interacts with serine-arginine proteins involved in RNA splicing. The Journal of Biological Chemistry 273:27761-27764.

Yang Y, Bedford MT (2013) Protein arginine methyltransferases and cancer. Nat Rev Cancer 13:37-50.

Yoneda Y, Hieda M, Nagoshi E, Miyamoto Y (1999) Nucleocytoplasmic protein transport and recycling of Ran. Cell Struct Funct 24:425-433.

Yoshimura A, Fujii R, Watanabe Y, Okabe S, Fukui K, Takumi T (2006) Myosin-Va facilitates the accumulation of mRNA/protein complex in dendritic spines. Curr Biol 16:2345-2351.

Young PJ, Francis JW, Lince D, Coon K, Androphy EJ, Lorson CL (2003) The Ewing's sarcoma protein interacts with the Tudor domain of the survival motor neuron protein. Brain Res Mol Brain Res 119:37-49.

Zakaryan RP, Gehring H (2006) Identification and characterization of the nuclear localization/retention signal in the EWS proto-oncoprotein. Journal of Molecular Biology 363:27-38.

Zhang D, Paley AJ, Childs G (1998) The transcriptional repressor ZFM1 interacts with and modulates the ability of EWS to activate transcription. The Journal of Biological Chemistry 273:18086-18091.

Zhang X, Cheng X (2003) Structure of the predominant protein arginine methyltransferase PRMT1 and analysis of its binding to substrate peptides. Structure 11:509-520.

Zhang YJ, Xu YF, Dickey CA, Buratti E, Baralle F, Bailey R, Pickering-Brown S, Dickson D, Petrucelli L (2007) Progranulin mediates caspase-dependent cleavage of TAR DNA binding protein-43. J Neurosci 27:10530-10534.

Zhang YJ, Caulfield T, Xu YF, Gendron TF, Hubbard J, Stetler C, Sasaguri H, Whitelaw EC, Cai S, Lee WC, Petrucelli L (2013) The dual functions of the extreme N-terminus of TDP-43 in regulating its biological activity and inclusion formation. Human Molecular Genetics 22:3112-3122.

Zhang YJ, Xu YF, Cook C, Gendron TF, Roettges P, Link CD, Lin WL, Tong J, Castanedes-Casey M, Ash P, Gass J, Rangachari V, Buratti E, Baralle F, Golde TE, Dickson DW, Petrucelli L (2009) Aberrant cleavage of TDP-43 enhances aggregation and cellular toxicity. Proceedings of the National Academy of Sciences of the United States of America 106:7607-7612.

Zhang ZC, Chook YM (2012) Structural and energetic basis of ALS-causing mutations in the atypical proline-tyrosine nuclear localization signal of the Fused in Sarcoma protein (FUS). Proceedings of the National Academy of Sciences of the United States of America 109:12017-12021.

Zhou H, Huang C, Chen H, Wang D, Landel CP, Xia PY, Bowser R, Liu YJ, Xia XG (2010) Transgenic rat model of neurodegeneration caused by mutation in the TDP gene. PLoS Genet 6:e1000887.

Zhou Z, Licklider LJ, Gygi SP, Reed R (2002) Comprehensive proteomic analysis of the human spliceosome. Nature 419:182-185.

Zinszner H, Albalat R, Ron D (1994) A novel effector domain from the RNA-binding protein TLS or EWS is required for oncogenic transformation by CHOP. Genes Dev 8:2513-2526.

Zinszner H, Sok J, Immanuel D, Yin Y, Ron D (1997) TLS (FUS) binds RNA in vivo and engages in nucleo-cytoplasmic shuttling. Journal of Cell Science 110 (Pt 15):1741-1750.

Acknowledgements

Vielen Dank

… Prof. Dr. Dr. Christian Haass für die wissenschaftliche Betreuung meiner Doktorarbeit und die große Unterstützung in den letzten vier Jahren. Ihr Enthusiasmus sowie Ihre endlose Energie und ansteckende Freude an der Wissenschaft waren immer sehr inspirierend für mich. Vielen Dank, dass Sie mir die Möglichkeit gegeben haben auf zahlreichen internationalen Konferenzen meinen wissenschaftlichen und persönlichen Horizont zu erweitern.

… Dr. Dorothee Dormann für die hervorragende Betreuung meiner Doktorarbeit. Du hast mir nicht nur alle Techniken beigebracht, sondern warst auch immer bereit mit mir aktuelle Ergebnisse und Hypothesen zu diskutieren. Vielen Dank, dass Du mich ermutigt hast unabhängig Projekte zu entwickeln und zu hinterfragen. Für deine Geduld und Hilfestellung beim gemeinsamen Schreiben von Publikationen (manchmal auch bis spät in die Nacht!) möchte ich mich ganz besonders bedanken. Danke auch, dass Du selbst nach der X-ten Korrektur-Runde einen Blick für alle winzigen Details hattest.

… Prof. Dr. Michael Kiebler für die Übernahme des Zweitgutachtens und guten Ratschläge zum weiteren Karriereweg.

... PD Dr. Ingrid Boekhoff und **PD Dr. Peter Zill** für die Begutachtung und Prüfung meiner Dissertation.

… Prof. Dr. Konstanze Winklhofer und **Prof. Dr. Stefan Lichtenthaler** für die hilfreichen Ratschläge in meinem TAC-Meeting.

… allen Kollaborationspartnern, besonders **Prof. Dr. Manuela Neumann, Dr. Sabina Tahirovic** und **Denise Orozco** für die produktiven und angenehmen Kollaborationen.

… Ramona Rodde, die meine ersten Schritte im Haass-Labor mit viel Geduld begleitet hat und auch danach eine hervorragende technische Unterstützung war.

… Claudia Abou-Ajram, die mir stets mit Rat und Tat zu Seite stand. Besonders schön fand ich, dass wir so viel Spaß im Labor hatten und uns manchmal wortlos verstanden.

… allen aktuellen und ehemaligen Mitgliedern des Haass Labors für ihre Hilfsbereitschaft und die angenehme Atmosphäre im Labor. Besonderer Dank geht an die Mittags-Runde mit oftmals hitzigen aber trotzdem immer lustigen Diskussionen, der Kicker-Runde die mich trotz stagnierender Kicker-Fertigkeiten immer hat mitspielen lassen und besonders **Matthias Voss,** der wahrscheinlich am meisten darunter zu leiden

hatte, mich aber auch bei einem 0:8 Rückstand noch versucht hat zum Sieg zu motivieren.
… Daniel Fleck und **Benni Schwenk** für Serien- und Musik-Empfehlungen.
… Teresa Bachhuber und **Steffi May** fürs Zuhören wenn es mal wieder nicht mit dem Schreiben voranging und **Joanna Carter** für kompetente Hilfe bei Fragen rund um die englische Grammatik.

… den Winklhofer-Girls für gemeinsame Kaffeepausen, Mädels-Abende und für die Aufrechterhaltung meines Blutzuckerspiegels. Besonderer Dank gilt **Caro Schweimer** für grenzenlose Hilfsbereitschaft, die „Superpolymerase“ und tolle Tage an der Ruderregatta; **Maria Sadic** fürs Korrekturlesen, Ratschläge rund ums Klonieren und emotionale Unterstützung bei so mancher Labor-Krise; **Kathrin Müller-Rischart** fürs Korrekturlesen, Tipps und Tricks für verschiedene Zelllinien, IPs und Adobe Illustrator sowie eine tolle Zeit in Amsterdam.
Maria und Kathrin, ich danke euch für eure Ermutigungen und genieße sehr unsere gemeinsamen Abende!

… Dr. Sven Lammich und **Dr. Anja Capell** für die Betreuung des Radioaktiv-Labors, viele gute Ratschläge und das Teilen von Reagenzien.

… Sabine Odoy und **Barbara Kassner** dafür, dass ihr den ganzen Laden so hervorragend am Laufen haltet.

… ENB für die finanzielle Unterstützung, die mir den Besuch von einigen Konferenzen ermöglicht hat. Danke auch für die brillanten und lehrreichen Workshops, Retreats mit interessanten wissenschaftlichen und nicht-wissenschaftlichen Diskussionen, sowie viel gemeinsamen Spaß.

… den Würzburg-Mädels durch die ich eine unvergessliche Studienzeit hatte und die mit mir währenddessen und danach Freud und Leid durchgestanden haben. Auch den **Mädels aus meiner alten Heimat** möchte ich meinen besonderen Dank aussprechen – die unsere mittlerweile über 13-jährige Freundschaft bedeutet mir sehr viel und es ist schön zu wissen, dass ich auch noch in den kommenden Jahrzehnten auf euch bauen kann.

… meinen Eltern, die mir so Vieles im Leben ermöglichen und mir stets Rückhalt geben. Liebe **Mama**, danke für deine schier unendliche Unterstützung, dass Du meinen Ehrgeiz immer gefördert hast und dass du mir stets dein Vertrauen schenkst. Lieber **Papulino**, danke für dein Interesse an meiner Arbeit und das Du mir das Gefühl gibst stolz auf mich zu sein.

… Philipp für andauernde Unterstützung, Geduld auch wenn es mal wieder später wurde und so viel mehr…Es bedeutet mir viel, dass Du immer an meiner Seite bist!

Curriculum vitae

Die privaten Informationen aus dem Lebenslauf sind aus Gründen des Datenschutzes in der Online-Version nicht enthalten.

Die privaten Informationen aus dem Lebenslauf sind aus Gründen des Datenschutzes in der Online-Version nicht enthalten.

Die privaten Informationen aus dem Lebenslauf sind aus Gründen des Datenschutzes in der Online-Version nicht enthalten.

Abbreviations

µm	Micrometer
AdOx	Adenosine-2,3-dialdehyde
A	Adenine
ALS	Amyotrophic lateral sclerosis
ANG	Angiogenin
ATXN-2	Ataxin-2
AU-rich	Adenine uracil
C	Cytosine
CAS	Cellular apoptosis suceptibility protein
CFTR	Cystic fibrosis transmembrane conductance regulator
CHMP2B	Charged multivesicular body protein 2B
CHOP	C/EBP homologous protein
CIRP	Cold-inducible RNA-binding protein
C-terminal	Carboxy-terminal end of a protein
CTF	C-terminal fragment
DAPI	4',6'-diamidino-2-phenylindole
DNA	Deoxyribonucleic acid
DPR	Dipeptide-repeat proteins
DYRK3	Dual specificity tyrosine-phosphorylation-regulated kinase 3
e.g.	Exempli gratia
eIF	Eukaryotic translation initiation factor
ERG	Erythroblastosis virus E26 oncogene homologue
EWS	Ewing sarcoma protein
fALS	familial ALS
Fig.	Figure
FMRP	Fragile X mental retardation protein
FTD	Frontotemporal dementia
FTLD	Frontotemporal lobar degeneration
FUS	Fused in sarcoma
G	Guanosine
G3BP	Ras-GTPase-activating protein SH3-domain-binding protein

GAR motif	Glycine- and arginine-rich motif
GCN	General control nonderepressible
GDP	Guanosine-5'-diphosphate
GFP	Green fluorescent protein
GTP	Guanosine-5'-triphosphate
HA	Hemagglutinin
HeLa	Cell line derived from a human cervical carcinoma of Henrietta Lacks
high mag	High magnification
hnRNP	Heterogeneous nuclear ribonucleoprotein
HRI	Heme-regulated initiation factor 2a kinase
HSPs	Heat shock proteins
i.e.	Lat. *Id est*,
kDa	Kilodalton
Kd_{ITC}	Dissociation constant isothermal titration calorimetry
MAPT	Microtubule-associated protein Tau
meFUS	Methylated FUS
min	Minute
mRNP	Messenger ribonucleoprotein
mTORC1	Mammalian target of rapamycine complex 1
NE	Nuclear envelope
NES	Nuclear export signal
NLS	Nuclear localization signal
NPC	Nuclear pore complex
NT control	Non-targeting control
OPTN	Optineurin
PABP-1	Poly(A)-binding protein 1
PABPN1	Nuclear poly(A) binding protein
p-bodies	Processing bodies
PERK	PKR-like endoplasmic reticulum kinase
PFN1	Profilin1
PGRN	Progranulin
PKR	Protein kinase R
polyQ	PolyGlutamine

PRMTs	Protein arginine methyltransferases
PrP	Prion protein
PTMs	Post-translational modifications
PY-NLS	Proline-tyrosine nuclear localization signal
Ran	Ras-related Nuclear protein/ small Ras-like GTPase
RanGAP	RanGTPase activating protein
RanGEF	RanGuanine nucleotide exchange factor
RGG	Arginine-glycine-glycine
RNA	Ribonucleic acid
RRM	RNA recognition motif
sALS	sporadic ALS
SAM	S-adenosylmethionine
Sam68	Src substrate associated in mitosis of 68 kDa
SDS-PAGE	Sodium Dodecyl Sulfate Polyacrylamide Gel Electrophoresis
SGs	Stress granules
siFUS	Small interfering RNA against FUS
siRNA	Small interfering RNA
siTDP	Small interfering RNA against TDP-43
SKAR	Ribosomal S6 kinase 1 Aly/REF-like target
SMN	Survival of motor neuron
SOD1	Superoxide dismutase 1
SQSTM1	Sequestosome 1/p62
SR protein	Serine-arginine protein
SYGQ	Serine-tyrosine-glycine-glutamine
T	Thymine
TAF15	TATA binding protein-associated factor 15
TDP-43	Trans-activation response DNA-binding protein of 43 kDa
TFIID	Transcription factor II D
TG-rich	Thymine guanosine-rich
TIA-1	T cell internal antigen-1
TIAR	TIA-1-related
TLS	Translocated in sarcoma
TLS	Translocated in sarcoma

U snRNPs	U-rich small nuclear ribonucleoproteins
UBQLN2	Ubiquilin2
UG-rich	Uracil guanosine-rich
UTR	Untranslated region
VAPB	VAMP-associated protein type B
VCP	Valosin-containing protein
WT	Wildtype

Publications

Neurobiology:

Requirements for Stress Granule Recruitment of Fused in Sarcoma (FUS) and TAR DNA-binding Protein of 43 kDa (TDP-43)

Eva Bentmann, Manuela Neumann, Sabina Tahirovic, Ramona Rodde, Dorothee Dormann and Christian Haass

J. Biol. Chem. 2012, 287:23079-23094.
doi: 10.1074/jbc.M111.328757 originally published online May 4, 2012

THE JOURNAL OF BIOLOGICAL CHEMISTRY VOL. 287, NO. 27, pp. 23079–23094, June 29, 2012

Requirements for Stress Granule Recruitment of Fused in Sarcoma (FUS) and TAR DNA-binding Protein of 43 kDa (TDP-43)*[S]

Received for publication, November 30, 2011, and in revised form, April 18, 2012 Published, JBC Papers in Press, May 4, 2012, DOI 10.1074/jbc.M111.328757

Eva Bentmann[‡], Manuela Neumann[§], Sabina Tahirovic[¶], Ramona Rodde[‡], Dorothee Dormann[‡1], and Christian Haass[‡¶2]

From the [‡]Adolf-Butenandt-Institute, Biochemistry, Ludwig-Maximilians-University and [¶]DZNE-German Center for Neurodegenerative Diseases, Schillerstrasse 44, 80336 München, Germany and [§]Institute of Neuropathology, University Hospital Zurich, Schmelzbergstrasse 12, 8091 Zurich, Switzerland

Background: Stress granules (SG) have been implicated in the formation of pathological FUS and TDP-43 inclusions.
Results: SG recruitment of FUS and TDP-43 requires cytosolic mislocalization and their main RNA binding domain and glycine-rich domain.
Conclusion: FUS and TDP-43 have similar requirements for SG recruitment.
Significance: Understanding how FUS and TDP-43 are recruited to SG is critical for understanding FTLD/ALS pathology.

Cytoplasmic inclusions containing TAR DNA-binding protein of 43 kDa (TDP-43) or Fused in sarcoma (FUS) are a hallmark of amyotrophic lateral sclerosis (ALS) and several subtypes of frontotemporal lobar degeneration (FTLD). FUS-positive inclusions in FTLD and ALS patients are consistently co-labeled with stress granule (SG) marker proteins. Whether TDP-43 inclusions contain SG markers is currently still debated. We determined the requirements for SG recruitment of FUS and TDP-43 and found that cytoplasmic mislocalization is a common prerequisite for SG recruitment of FUS and TDP-43. For FUS, the arginine-glycine-glycine zinc finger domain, which is the protein's main RNA binding domain, is most important for SG recruitment, whereas the glycine-rich domain and RNA recognition motif (RRM) domain have a minor contribution and the glutamine-rich domain is dispensable. For TDP-43, both the RRM1 and the C-terminal glycine-rich domain are required for SG localization. ALS-associated point mutations located in the glycine-rich domain of TDP-43 do not affect SG recruitment. Interestingly, a 25-kDa C-terminal fragment of TDP-43, which is enriched in FTLD/ALS cortical inclusions but not spinal cord inclusions, fails to be recruited into SG. Consistently, inclusions in the cortex of FTLD patients, which are enriched for C-terminal fragments, are not co-labeled with the SG marker poly(A)-binding protein 1 (PABP-1), whereas inclusions in spinal cord, which contain full-length TDP-43, are frequently positive for this marker protein.

Amyotrophic lateral sclerosis (ALS)[3] and frontotemporal lobar degeneration (FTLD) are related neurodegenerative diseases in which the majority of cases are characterized by the pathological accumulation of the TAR DNA-binding protein 43 (TDP-43) or the Fused in sarcoma (FUS) protein (1). TDP-43 and FUS are DNA/RNA-binding proteins that are involved in transcriptional regulation, pre-mRNA splicing, microRNA processing, and mRNA transport (for review, see in Refs. 2 and 3). Although both proteins exert their function predominantly in the nucleus, pathological TDP-43 and FUS inclusions are mostly observed in the cytoplasm. Strikingly, inclusion-bearing cells often show a loss or reduction of nuclear TDP-43 or FUS staining (4–11). This has led to the hypothesis that loss of nuclear TDP-43 or FUS is a crucial step in disease progression.

Both proteins have multiple RNA binding domains as well as a protein interaction domain predicted to have prion-like properties. TDP-43 has two RNA recognition motif (RRM) domains, RRM1 and RRM2, with RRM1 being the predominant functional RNA binding domain (12). In addition, TDP-43 contains a C-terminal glycine-rich domain that mediates interactions with other heterogeneous nuclear ribonucleoproteins and is required for splicing regulation (13). This domain is highly aggregation-prone (14–18) and due to its amino acid composition has been suggested to have prion-like properties (19–22). FUS has multiple RNA binding domains with arginine-glycine-glycine (RGG) motifs, a RRM domain, and a zinc finger domain shown to mediate RNA binding (23, 24). In addition, FUS con-

* This work was supported by the Sonderforschungsbereich Molecular Mechanisms of Neurodegeneration (SFB 596), the Competence Network for Neurodegenerative Diseases (KNDD) of the Bundesministerium für Bildung und Forschung (BMBF), and an EMBO post-doctoral fellowship (to D. D.).

[S] This article contains supplemental Figs. S1–S7.

[1] Supported by the Robert Bosch Foundation. To whom correspondence may be addressed: Adolf-Butenandt-Institute, Biochemistry, Ludwig-Maximilians-University, Schillerstrasse 44, 80336 Munich, Germany. Tel.: 49-89-2180-75471; Fax: 49-89-2180-75415; E-mail: dorothee.dormann@dzne.lmu.de.

[2] Supported by a "Forschungsprofessur" of the Ludwig-Maximilians University. To whom correspondence may be addressed: Adolf-Butenandt-Institute, Biochemistry, Ludwig-Maximilians-University and DZNE-German Center for Neurodegenerative Diseases, Munich, Schillerstrasse 44, 80336 Munich, Germany. Tel.: 49-89-2180-75471; Fax: 49-89-2180-75415; E-mail: christian.haass@dzne.lmu.de.

[3] The abbreviations used are: ALS, amyotrophic lateral sclerosis; TDP-43, TAR DNA-binding protein of 43 kDa; FUS, Fused in sarcoma; FTLD, frontotemporal lobar degeneration; SG, stress granule; RRM, RNA recognition motif; CTF, C-terminal fragment; PY-NLS, proline-tyrosine nuclear localization signal; PABP-1, poly(A)-binding protein 1; TIA-1, T cell intracellular antigen 1; DIV, days *in vitro*.

tains an N-terminal glutamine-rich domain that functions as a potent transcriptional activation domain (25) and was predicted to be a prion-like domain (19–21).

The relevance of TDP-43 and FUS in the pathogenesis of ALS and FTLD was strongly supported by the discovery of autosomal dominant mutations within *TARDBP* (the gene encoding TDP-43) and *FUS* in familial forms of ALS (6, 7, 26). So far, almost 40 different *TARDBP* mutations have been reported; most of them are missense mutations in the glycine-rich C-terminal domain. Although it has been claimed that *TARDBP* mutations increase aggregation tendency (14, 15, 27, 28), alter the protein cellular localization (29–31), or alter the protein half-life and interactions with other proteins (32), the pathogenic mechanism of these mutations is still unclear, as many inconsistencies among different studies have been reported. Pathogenic mutations in the *FUS* gene are mostly clustered in the C-terminal proline-tyrosine nuclear localization signal (PY-NLS) and impair Transportin-mediated nuclear import of FUS (33–36). Interestingly, mutations that show a very severe nuclear import defect, such as P525L, cause an unusually early disease onset and rapid disease progression (37–39), suggesting that impaired nuclear import of FUS is causally linked to the disease (33, 40). Even though it is still unclear how reduced nuclear import of FUS leads to neurodegeneration, it has been shown that blockade of Transportin-mediated nuclear import or *FUS* mutations leads to recruitment of FUS into stress granules (SG), implicating SG and reduced nuclear transport in disease pathogenesis (33, 34, 36, 40, 41). This is supported by the presence of SG markers in inclusions in ALS/FTLD-FUS patients (33, 42).

SG are cytosolic structures that form transiently upon exposure of cells to environmental stress, such as heat, viral infection, oxidative stress, or hypoxia (43). They arise from polysomes and store mRNAs encoding housekeeping proteins but exclude mRNAs encoding chaperones and enzymes involved in damage repair. In addition to mRNAs, SG contain many RNA-binding proteins, such as poly(A)-binding protein 1 (PABP-1) and T cell intracellular antigen 1 (TIA-1), which serve as specific markers for SG (44). In cultured cells, SG formation can be elicited with a variety of stress treatments, such as heat shock (42–44 °C), osmotic shock, UV irradiation, or substances that elicit mitochondrial and/or oxidative stress (44). SG have also been observed *in vivo* (41, 45–47), and SG marker proteins were found to label the pathological FUS inclusions in post mortem brains of ALS/FTLD patients (33, 42). Thus, it has been suggested that SG might be the precursors of the pathological FUS inclusions in ALS/FTLD-FUS patients (33).

How FUS is recruited to SG is currently unknown. Because FUS is an RNA-binding protein, it is conceivable that it is recruited into these structures via its associated mRNAs. Alternatively, protein-protein interactions might be involved in localization of FUS to SG. Interestingly, TIA-1 contains a prion-like glutamine-rich domain that has homology to the N-terminal glutamine-rich domain of FUS and promotes SG assembly by a prion-like aggregation mechanism (48, 49). Whether this domain of FUS is required for SG recruitment or aggregation is still unknown.

TDP-43 has also been described to be recruited to SG under various stress conditions (31, 50–55), and SG-associated proteins have been identified as TDP-43-interacting proteins (56). However, it is still controversial whether TDP-43 inclusions in human patients contain SG markers. Two studies found a lack of SG markers in TDP-43 inclusions of ALS/FTLD-TDP patients (33, 50), whereas two other studies reported co-labeling of TDP-43 inclusions with SG markers (31, 57). Furthermore, it is still not clear if or how *TARDBP* mutations affect SG recruitment. One cell culture study reported that *TARDBP* mutations increase the number of cells with TDP-43 inclusions in response to stress (31), whereas another group found that mutant (R361S) TDP-43 impairs SG formation (54), and a third study reported that overexpression of mutant (G348C) TDP-43 leads to larger SG (51).

To address how FUS and TDP-43 are recruited into SG, we mapped the domains required for SG recruitment of FUS and TDP-43. In addition, we analyzed the effect of various forms of ALS-associated *TARDBP* mutations on SG recruitment of TDP-43 and further investigated the presence of SG marker proteins in TDP-43 inclusions in ALS/FTLD-TDP cortex and spinal cord.

EXPERIMENTAL PROCEDURES

Cell Culture and Transfection—Human cervical carcinoma cells (HeLa) were cultured in Dulbecco's modified Eagle's medium with Glutamax (Invitrogen) supplemented with 10% (v/v) fetal calf serum (Invitrogen) and penicillin/streptomycin (PAA Laboratories). Transfection of HeLa cells was carried out with FuGENE 6 (Roche Applied Science) or Lipofectamine 2000 (Invitrogen) according to the manufacturer's instructions. Hippocampal neurons were isolated from embryonic day 18 rats as described previously (58). Neurons were plated at densities of 18,000 cells/cm^2 in 6-cm tissue culture dishes containing poly-L-lysine (1 mg/ml; Sigma)-coated glass coverslips and Neurobasal medium supplemented with 2% B27 and 0.5 mM glutamine (all from Invitrogen). On day *in vitro* 7 (DIV 7), cultured neurons were transfected with FUS or TDP-43 constructs using Lipofectamine 2000 (Invitrogen) and were analyzed on DIV 9.

Stress and Inhibitor Treatment—Heat shock was performed by incubating cells for 1 h in a tissue culture incubator heated to 44 °C. For recovery experiments, cells were shifted back to 37 °C and incubated another 60 min. Where indicated, cycloheximide (Sigma) was added at a concentration of 20 μg/ml immediately before shifting cells to 44 °C. Clotrimazole (Sigma C6019) was dissolved in DMSO (20 mM stock) and was added to cells under serum-free conditions in Opti-MEM (Invitrogen) at a final concentration of 20 μM for 30 min. Sodium (meta)arsenite (Sigma S71287) was dissolved in water (100 mM stock) and added to cells at a final concentration of 0.5 mM for 30 min.

Antibodies—The following antibodies were used: β-actin-specific mouse monoclonal antibody clone AC-74 (Sigma); GFP-specific rabbit polyclonal antibody (BD Living Colors); HA-specific mouse monoclonal antibody HA.11 (Covance); horseradish peroxidase (HRP)-coupled rat monoclonal anti-HA antibody 3F10 (Roche Applied Science); myc-specific mouse monoclonal antibody 9E10 (sc-40, Santa Cruz); PABP-

1-specific rabbit polyclonal antibody (Cell Signaling); TDP-43-specific rabbit polyclonal antibody TARDBP (Proteintech); polyclonal antibodies raised against amino acid residues 6–24 of TDP-43 (N-t TDP-43) and amino acid residues 394–414 of TDP-43 (C-t TDP-43) (59); phosphoserine 409/410-specific TDP-43 rat monoclonal antibody clone 1D3 (60); TIA-1-specific goat polyclonal antibody (C-20, Santa Cruz); α-tubulin-specific mouse monoclonal antibody clone B-5–1-2 (Sigma); βIII-tubulin-specific rabbit polyclonal antibody clone Tuj1 (Sigma); V5-specific mouse monoclonal antibody (R960–25, Invitrogen). Secondary antibodies for immunoblotting were HRP-coupled goat anti-mouse or anti-rabbit IgGs (Promega). For immunofluorescence stainings, Alexa-488, Alexa-555, Alexa-594, and Alexa-647-conjugated donkey anti-mouse, anti-rabbit, anti-rat or anti-goat IgG (Invitrogen) were used.

cDNA Constructs and Primers—HA-FUS-WT, HA-FUS-P525L, and GFP-Bimax were described in Dormann *et al.* (33). For FUS deletion constructs, the individual domains of FUS were amplified by PCR, and PCR products were cloned into the pcDNA3.1/Hygro(−) vector (Invitrogen) via BamHI/XhoI restriction digest. TDP-WT-V5, myc-TDP-WT, and TDP-Δ1–173-V5 were described in Dormann *et al.* (61). For TDP-NLSmut, amino acids 82–84 of TDP-WT-V5 were mutated to alanine by QuikChange mutagenesis (Stratagene) as described by Winton *et al.* (62). ALS-associated point mutations (A315T, M337V, and G348C) were introduced into myc-TDP-WT or TDP-NLSmut-V5 by QuikChange mutagenesis (Stratagene). NLSmut-ΔC encoding amino acids 1–273 of human TDP-43 was amplified by PCR and after BamHI/XbaI restriction digest was cloned into the pcDNA6/V5-His vector (Invitrogen) that contained a stop codon between the V5 and the polyhistidine tag sequence. GFP-tagged constructs were generated by subcloning the respective sequences into pEGFP-C1 (Clontech). For all constructs, sequence integrity was verified by sequencing. Oligonucleotides sequences are available upon request.

Human Post Mortem Tissue—Histological analysis included five cases of FTLD-TDP (FTLD-TDP subtype A ($n = 2$), subtype B ($n = 2$), and subtype C ($n = 1$) according to Mackenzie *et al.* (63)) and four ALS cases with TDP-43 pathology.

Immunocytochemistry and Immunohistochemistry—For immunocytochemistry of HeLa cells, cells were fixed for 15 min in 4% paraformaldehyde in PBS, permeabilized for 5 min in 0.2% Triton X-100 with 50 mM NH_4Cl, and subsequently blocked for 20–30 min in 5% donkey serum in PBSS (PBS with 0.1% saponin). Cells were stained with the indicated primary and secondary antibodies diluted in 5% donkey serum in PBSS for 30 min and washed 3–5 times in PBSS. To visualize nuclei, cells were stained with TO-PRO-3 iodide (Invitrogen, 1:500 in PBS) for 15 min and washed 3 times in PBS. Coverslips were mounted onto glass slides using ProLong Gold Antifade Reagent (Invitrogen).

For immunocytochemistry of hippocampal neurons, neurons were fixed with 4% paraformaldehyde on DIV 9, quenched in 50 mM ammonium chloride for 10 min, and permeabilized with 0.1% Triton X-100 for 3 min. After blocking with 2% fetal bovine serum (Invitrogen), 2% bovine serum albumin (Sigma), and 0.2% fish gelatin (Sigma) dissolved in PBS, neurons were incubated with respective primary and secondary antibodies diluted in 10% blocking solution. 4′-6-Diamidino-2-phenyl-indol (DAPI, Invitrogen) was used as a nuclear counterstain.

Immunohistochemistry on human post mortem material was performed on 5-μm-thick sections of formalin-fixed, paraffin-embedded sections from spinal cord or hippocampus with the N- and C-terminal TDP-43-specific antibodies and anti-PABP-1 using the NovoLink™ Polymer Detection kit (Novocastra) and developed with 3,3′-diaminobenzidine. Microwave antigen retrieval was performed for all stainings. Double-label immunofluorescence for PABP-1 and pTDP-43 was performed using Alexa-488- and -594-conjugated secondary antibodies. DAPI (Vector Laboratories) was used for nuclear counterstaining.

Image Acquisition and Quantification—Confocal images were obtained with an inverted laser scanning confocal microscope (Zeiss Axiovert 200 M) with a 63×/1.4 N.A. oil immersion lens using a pinhole diameter of 1 Airy unit in the red channel. Pictures were taken and analyzed with the LSM 510 confocal software (Zeiss). For HeLa cells, single confocal images were taken in the plane of the largest cytosolic area. For neurons, a series of images along the *z* axis was taken and projected into a single image using the maximal projection tool of the LSM 510 software. Immunofluorescence images of brain sections were obtained by wide-field fluorescence microscopy (BX61 Olympus with digital camera F-view, Olympus).

Nuclear and cytosolic localization was quantified with the LSM 510 colocalization tool as described in Dormann *et al.* (33). Stress granule localization was quantified with Image J as follows. Image identity was blinded, and FUS or TDP-43 (green)/TIA-1 (red) double positive cytoplasmic granules as well as the entire cell were manually encircled to measure fluorescence intensities of the green channel. After background subtraction, the percentage of FUS or TDP-43 in SG was calculated. For each condition, 10–20 cells were analyzed. Means across all cells and standard deviations were calculated.

Cell Lysates and Immunoblotting—Total cell lysates were prepared in ice cold radioimmune precipitation assay (RIPA) buffer freshly supplemented with complete EDTA-free protease inhibitor mixture (Roche Applied Science) for 15 min on ice. Lysates were sonicated in a bioruptor (Diagenode, 45 s on high), and protein concentration was determined by BCA protein assay (Pierce). Equal amounts of protein were separated by SDS-PAGE, transferred onto a PVDF membrane (Immobilon-P, Millipore), and analyzed by immunoblotting using the indicated antibodies. Bound antibodies were detected with the chemiluminescence detection reagents ECL (Amersham Biosciences) or Immobilon (Millipore).

RNA Binding Assay—RNA binding of FUS and TDP-43 domains was determined in an *in vitro* RNA binding assay according to Lerga *et al.* (24). Briefly, proteins were *in vitro* transcribed and translated using the TNT T7 Coupled Reticulocyte Lysate System (Promega) and labeled with 20 μCi of [^{35}S]methionine (Amersham Biosciences). Strep-Tactin-Sepharose (IBA) was blocked with 200 μg/ml yeast tRNA (Roche Applied Science) and 0.125 mg/ml bovine serum albumin (BSA, New England Biolabs) in wash buffer (10 mM Tris-HCl, pH 7.4, 100 mM NaCl, 2.5 mM $MgCl_2$, 0.5 mM DTT, 0.5 mM EGTA, 0.5% Triton X-100, 10% glycerol) for 30 min at 4 °C. Afterward, bioti-

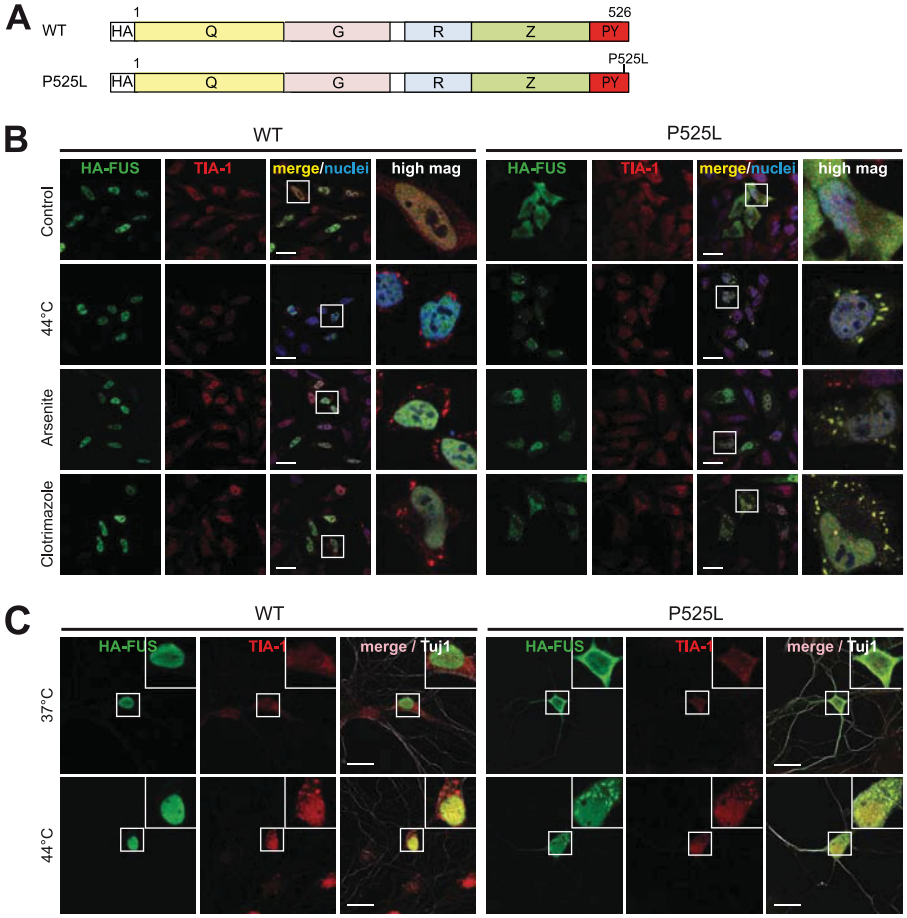

FIGURE 1. **Cytosolic FUS is recruited to SG upon treatment with various stressors.** *A*, shown is a schematic diagram of FUS wild-type (*WT*) and P525L mutant used for transient transfection in HeLa cells. *HA*, HA epitope tag; *Q*, glutamine-rich domain; *G*, glycine-rich domain; *R*, RRM domain; *Z*, arginine-glycine-glycine (RGG) zinc finger domain. *B*, HeLa cells were transiently transfected with N-terminal-HA-tagged FUS-WT or FUS-P525L. 24 h after transfection cells were subjected to heat shock (44 °C for 1 h), sodium arsenite (0.5 mM for 30 min), or clotrimazole (20 μM for 30 min) or were left untreated (*Control*). Cells were fixed, stained with an HA-specific antibody (*green*), a TIA-1-specific antibody (*red*), and a nuclear counterstain (*blue*) and analyzed by confocal microscopy. *Panels to the right* show a higher magnification of the *boxed region*. Although FUS-WT remained nuclear, FUS-P525L was sequestered into SG under all stress conditions examined. *Scale bars*, 20 μm. *C*, primary rat hippocampal neurons were transiently transfected with HA-FUS-WT or P525L on DIV 7. 48 h after transfection, neurons were subjected to heat shock (44 °C) for 1 h or left untreated (37 °C). Neurons were fixed and stained with an HA-specific antibody (*green*), a TIA-1-specific antibody (*red*), and the neuronal marker antibody Tuj1 (*white*) to visualize neuronal morphology. FUS-P525L showed cytoplasmic mislocalization and was recruited to TIA-1-positive SG upon heat stress. *Insets in the upper right corner* show a higher magnification of the *boxed region*. *Scale bars*, 20 μm.

nylated RNA oligonucleotides (UG_{12}, UGUGUGUGUGUGUGUGUGUGUG; GGUG, UUGUAUUUUGAGCUAGUUUGGUGAU; CCUC, UUGUAUUUUGAGCUAGUUUCCUCAU, all from Thermo Fisher Scientific) were bound to the preblocked Sepharose beads. Beads were rinsed twice with wash buffer and incubated with radiolabeled samples for 10 min at 4 °C in blocking buffer. Beads were washed 5 times in wash buffer and boiled 5 min in Laemmli buffer. Bound radiolabeled proteins were separated by SDS-PAGE and visualized by fluorography. 10% of the radiolabeled sample was directly used for SDS-PAGE and fluorography to visualize the input of radiolabeled protein.

RESULTS

RGG-Zinc Finger Domain of FUS Is Most Important for SG Recruitment, Whereas Glutamine-rich Domain Is Dispensable—We and others previously found that cytosolically mislocalized FUS is recruited to SG upon cellular stress (33, 34, 41). It is, however, still unknown whether cytosolic FUS is recruited into SG via its bound mRNAs or via protein-protein interactions, involving for example its TIA-1-related N-terminal domain or even both. To determine which domains are responsible for recruitment of FUS to SG, we expressed individual FUS domains in HeLa cells with an N-terminal HA tag and analyzed their SG recruitment in comparison to full-length FUS (see Fig. 1*A* for a schematic diagram). To this end we introduced the P525L mutation into the PY-NLS of the respective constructs, because this mutation causes cytosolic retention of FUS and allows its efficient recruitment to TIA-1-positive SG (33). In contrast, constructs carrying a wild-type (WT) PY-NLS were almost exclusively nuclear and, hence, were not recruited to SG upon cellular stress (supplemental Fig. S1).

Initially, we investigated a variety of stress conditions such as heat shock (44 °C), oxidative stress caused by sodium arsenite treatment, and mitochondrial stress caused by clotrimazole treatment for their ability to induce SG formation. Consistent with our previous findings (33), FUS-WT was located in the nucleus and, therefore, was not recruited to SG upon cellular

stress (Fig. 1*B*, *upper panels*). In contrast, FUS-P525L was efficiently recruited into SG under all stress conditions examined (Fig. 1*B*, *lower panels*). FUS-P525L-positive granules were *bona fide* stress granules, as they were co-localized with the SG marker TIA-1 and disassembled upon cycloheximide treatment or recovery from heat stress (supplemental Fig. S2*A*). SG recruitment of FUS-P525L was not a cell type-specific phenomenon, as it could also be observed in primary hippocampal neurons (Fig. 1*C*) and in SH-SY5Y neuroblastoma cells (supplemental Fig. S2*B*).

Using heat shock as stress condition, we next examined how well the individual domains of FUS are recruited to SG (see the schematic diagram in Fig. 2*A*). To obtain quantitative information, we measured the percentage of FUS protein localized in TIA-1-positive SG (see "Experimental Procedures" for details). In contrast to full-length FUS-P525L, the glutamine-rich domain (Q) remained diffusely distributed in the cytosol after heat shock, and no granular localization became evident even though TIA-1-positive SG formed in transfected cells (Fig. 2, *B* and *C*). Thus, despite its homology to the prion-like domain of TIA-1 (48, 49), the Q domain of FUS does not seem to be involved in SG recruitment. The glycine-rich domain (G) and the RRM domain (R) remained predominantly diffusely cytosolic, but small amounts were found in TIA-1-positive SG (Fig. 2, *B* and *C*). Finally, the C-terminal RGG-zinc finger domain (Z), which was rendered cytosolic by addition of the P525L mutation (Z_{P525L}), showed more SG recruitment than all other domains examined. Because the HA-tagged Q and Z_{P525L} domain showed very weak expression compared with the other constructs and could not be detected by Western blot (supplemental Fig. S3), we expressed these apparently unstable domains as GFP fusion proteins along with GFP-FUS_{P525L} as a control. This yielded higher expression levels (supplemental Fig. S4*A*) and confirmed that the Z_{P525L} domain shows SG association, whereas the Q domain does not (supplemental Fig. S4*B*).

Because our quantitative analysis revealed that none of the individual domains was recruited to SG to the same extent as the full-length protein (Fig. 2*C*), we analyzed combinations of the three domains (RZ_{P525L}, GRZ_{P525L}, and GR) and asked if this would enhance SG recruitment. Indeed, the combination of these domains showed an additive effect compared with the individual domains (Fig. 2, *B* and *C*), suggesting that all three domains contribute to SG recruitment. Finally, we analyzed combinations of the Q domain with other domains (QGR, QG), to exclude that the Q domain might have a different effect in the context of the other domains. However, QGR and QG did not differ in their SG localization from GR and G, respectively, demonstrating that the Q domain is indeed dispensable for SG recruitment. Consistently, the GRZ_{P525L} protein, which lacks the Q domain, was recruited to SG equally well as full-length FUS-P525L. Furthermore, the relatively weak SG recruitment efficiency of the QGR protein confirms that the C-terminal Z domain plays the most important role for SG association of FUS.

In summary, the RGG-zinc finger domain (Z) is the most important domain for SG recruitment of FUS. The glycine-rich domain (G) and to a minor extent the RRM domain (R) also contribute to SG recruitment, whereas the prion-like glutamine-rich domain (Q) is dispensable.

RGG-Zinc Finger Domain Is Main RNA Binding Domain of FUS—To explore if SG recruitment of the different FUS domains can be correlated with their ability to bind RNA, we examined their RNA binding capacity in an RNA binding assay. To this end we *in vitro* translated the same FUS constructs and performed a pulldown assay with biotinylated RNA oligonucleotides immobilized on streptavidin beads. Because FUS is known to preferentially bind to UG-rich sequences, specifically to oligonucleotides containing a GGUG motif (24), we first tested the ability of FUS-WT to bind to UG_{12} or a GGUG-containing oligonucleotide (UUGUAUUUUGAGCUAGUUU-GGUGAU, named GGUG). The same oligonucleotide with a CCUC motif (named CCUC) was used as a negative control. Consistent with the previously reported finding that FUS binds to UG-rich sequences, FUS-WT was efficiently pulled down by UG_{12} and to a lesser extent by GGUG but not CCUC (Fig. 3*A*).

Using UG_{12} as RNA bait, we next examined the RNA binding capacity of the individual FUS domains and combinations thereof (Fig. 3*B*). This demonstrated that only proteins containing the Z domain (Z_{P525L}, RZ_{P525L}, and GRZ_{P525L}) showed efficient and selective binding to UG_{12} RNA (note that compared with Z_{P525L}, RZ_{P525L} and GRZ_{P525L} showed stronger signals already in the input gel, and therefore, signals obtained in the pulldown assay cannot be compared directly). In contrast, the Q, G, and R domain and different combinations thereof (GR, QGR, QG) were not pulled down in our RNA binding assay, demonstrating that Q, G, and R show no or only weak binding to UG_{12} RNA. Thus, the C-terminal Z domain seems to be responsible for the preferential binding to UG-rich RNA. Interestingly, the domain with the highest RNA binding capacity (Z) was the one most important for SG recruitment (Fig. 2). This correlation suggests that FUS might be recruited to SG by virtue of its RNA binding capacity. The domains that contribute to SG recruitment to a lesser extent (G and R) showed no RNA binding capacity in our *in vitro* binding assay, suggesting that they might contribute to SG recruitment through other means, possibly protein-protein interactions.

Cytosolic Mislocalization Is Prerequisite for SG Recruitment of TDP-43—Similar to FUS, TDP-43 has been described to be localized in SG under various experimental conditions (31, 50–55). Because cytosolic mislocalization is a prerequisite for efficient SG recruitment of FUS (Fig. 1 and Refs 33 and 41), we speculated that this might also be the case for TDP-43. To test this hypothesis, we mutated three essential amino acids of the classical bipartite nuclear localization signal (62) and analyzed SG recruitment of this artificial NLS mutant (*NLSmut*, see Fig. 4*A* for a schematic diagram) in comparison to wild-type TDP-43 (TDP-WT) upon exposure to different stressors. TDP-WT was predominantly nuclear with and without stress and was not detectable in cytoplasmic granules (Fig. 4*B*, *upper panels*). In contrast, the partially cytosolic NLSmut protein was readily detectable in TIA-1-positive SG upon heat shock, clotrimazole treatment, and sodium arsenite treatment (Fig. 4*B*, *lower panels*). TDP-43-positive granules dissolved upon cycloheximide treatment or recovery from heat stress (supplemental Fig. S5*A*), demonstrating that they are indeed SG and not pro-

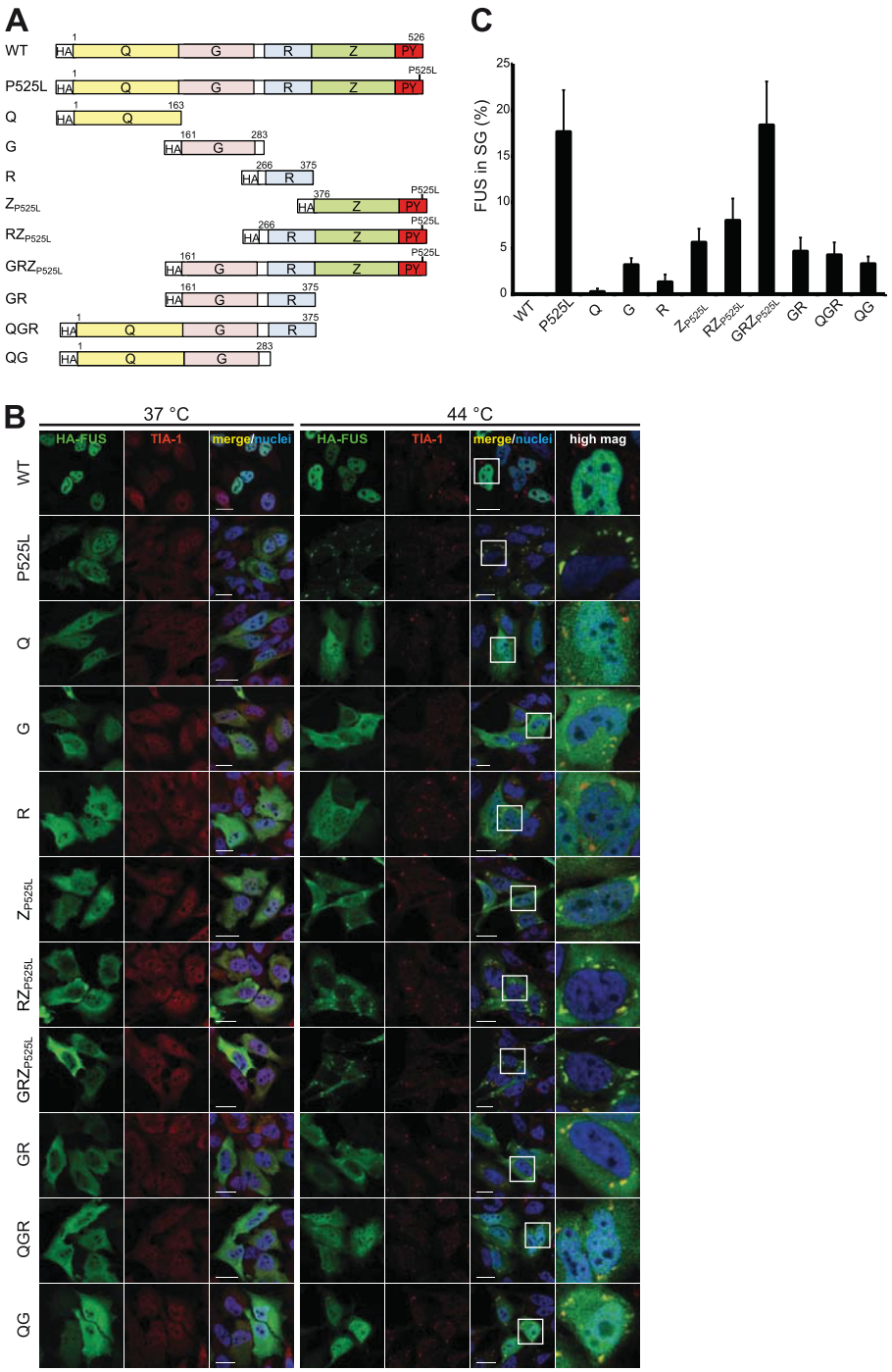

FIGURE 2. **The C-terminal RGG-zinc finger domain of FUS is the most important domain for SG recruitment.** *A*, shown is a schematic diagram of different FUS constructs analyzed for SG recruitment. The P525L mutation was introduced into the PY-NLS to obtain proteins mislocalized in the cytosol. *B*, shown is immunocytochemistry of HeLa cells expressing the different FUS constructs shown in *A*. Before fixation, cells were subjected to heat shock (44 °C for 1 h) or left untreated (37 °C). Cells were stained with an HA-specific antibody (*green*), a TIA-1-specific antibody (*red*), and a nuclear counterstain (*blue*) and analyzed by confocal microscopy. *Panels to the right* show a higher magnification of the *boxed region*. The Z domain is most important for SG recruitment, whereas the Q domain is dispensable. The G and R domains also contribute to SG recruitment but to a lesser extent than Z. *Scale bars* = 20 μm. *C*, the percentage of FUS localized in TIA-1-positive SG was quantified using ImageJ. 10–20 cells were analyzed in a blinded manner, means across all cells were calculated, and S.D. are indicated by *error bars*. Note that the percentage of FUS-P525L in SG seems surprisingly low when looking at the corresponding confocal images in *B*. However, SG are very small compared with the remaining cellular volume, and therefore, FUS-P525L diffusely distributed in the cytosol and nucleus amounts to a significant percentage of the total protein (more than 80%).

tein aggregates. Moreover, SG recruitment of NLSmut but not TDP-WT was observed in primary hippocampal neurons (Fig. 4*C*) and SH-SY5Y cells (supplemental Fig. S5*B*). Thus, in all cell types examined, only cytosolic but not nuclear TDP-43 is efficiently recruited to SG.

To corroborate this finding, we expressed an Importin α/β inhibitor peptide fused to GFP (GFP-Bimax) (64) in HeLa cells. Consistent with our previous findings (33), this caused endogenous TDP-43 to accumulate in the cytosol (Fig. 5). In line with the view that cytosolic mislocalization of TDP-43 is required for

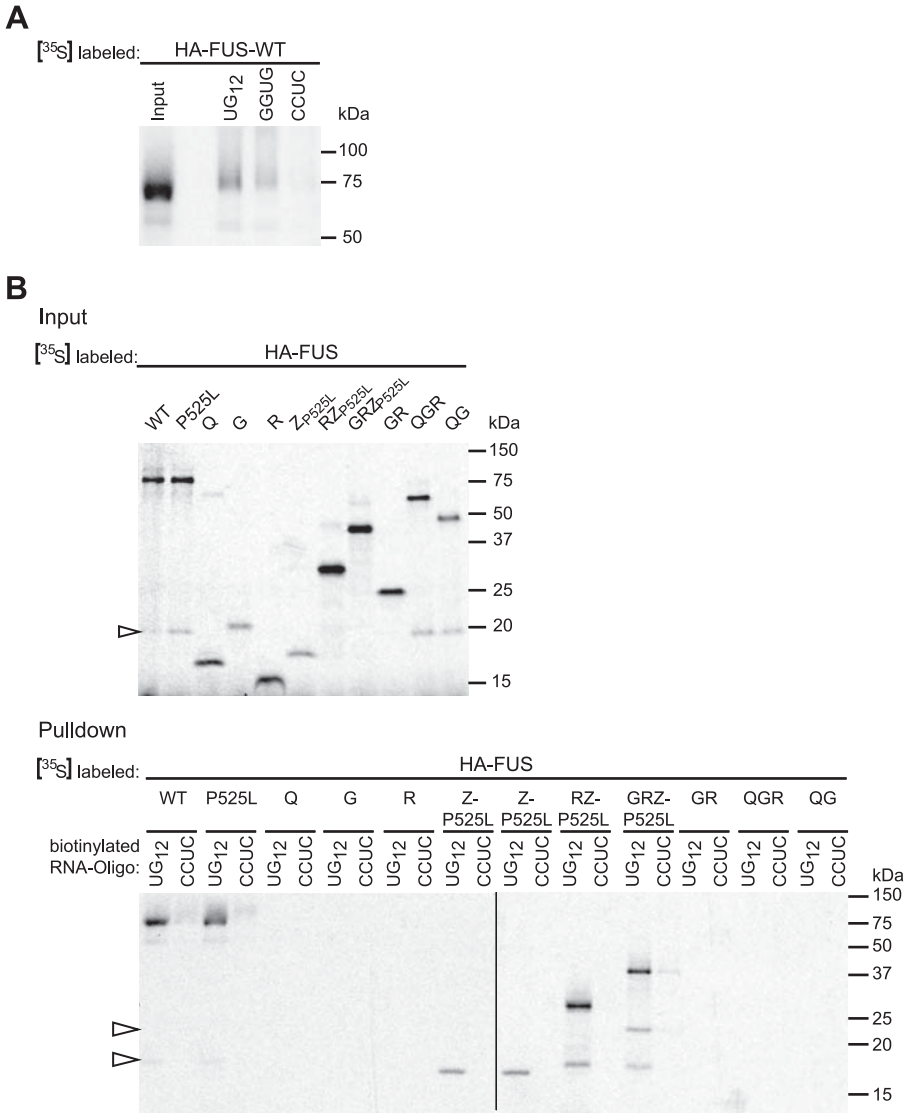

FIGURE 3. **The RGG-zinc finger domain of FUS binds to UG-rich RNA.** *A*, FUS-WT was *in vitro* translated in the presence of [^{35}S]methionine (*left lane*, *input*) and was analyzed for binding to different RNA oligonucleotides immobilized on streptavidin beads (*right lanes*, *UG$_{12}$*, UGUGUGUGUGUGUGUGUGUGUG; *GGUG*, UUGUAUUUUGAGCUAGUUUGGUGAU; *CCUC*, UUGUAUUUUGAGCUAGUUUCCUCAU). FUS was pulled down most efficiently by UG$_{12}$ and to a lesser extent by GGUG RNA. *B*, the indicated FUS constructs were *in vitro* translated in the presence of [^{35}S]methionine (*upper panel*, *Input*). Biotinylated UG$_{12}$ RNA immobilized on streptavidin beads was used to pull down radioactively labeled proteins (*lower panel*, *Pulldown*). CCUC RNA was used as a negative control. FUS-WT and P525L and all proteins comprising the Z$_{P525L}$ domain were specifically pulled down by UG$_{12}$ RNA, whereas the other proteins did not show detectable RNA binding. *Open arrowheads* indicate degradation products.

SG recruitment, endogenous TDP-43 was detectable in heat shock-induced SG only when its nuclear import was blocked by expression of the GFP-Bimax inhibitor (Fig. 5). In contrast, in control (GFP)-transfected cells, TDP-43 remained nuclear and was not detectable in SG upon heat shock. Together these findings demonstrate that similar to FUS, SG recruitment of TDP-43 requires at least a partial mislocalization of the nuclear protein to the cytosol.

ALS-associated TARDBP Mutations Do Not Affect Nuclear Localization or SG Recruitment—Despite extensive research over the last few years, the pathogenic mechanism of ALS-associated *TARDBP* mutations remains unclear. Some *TARDBP* mutations have been reported to cause cytosolic missorting of the protein (30, 31); however, this could not be confirmed in other studies (28, 32, 51). Furthermore, it is still not clear if and how *TARDBP* mutations affect SG recruitment, as controversial findings have been reported (31, 51, 54).

Because our data above imply that SG recruitment could be indicative of cytosolic mislocalization, we examined the localization of three well studied ALS-associated *TARDBP* mutations (A315T, M337V, and G348C) upon heat shock to see if these mutants would be preferentially detected in SG. However, none of the three examined ALS-associated point mutants showed detectable localization in TIA-1-positive SG upon heat shock (44 °C); instead, they were located entirely in the nucleus like TDP-WT (Fig. 6*A*; for expression levels see Fig. 6*B*). Consistently, a quantification of the amount of nuclear/cytosolic TDP-43 in cells cultured under normal culture conditions (37 °C) demonstrated that the three point mutants had an almost exclusive nuclear local-

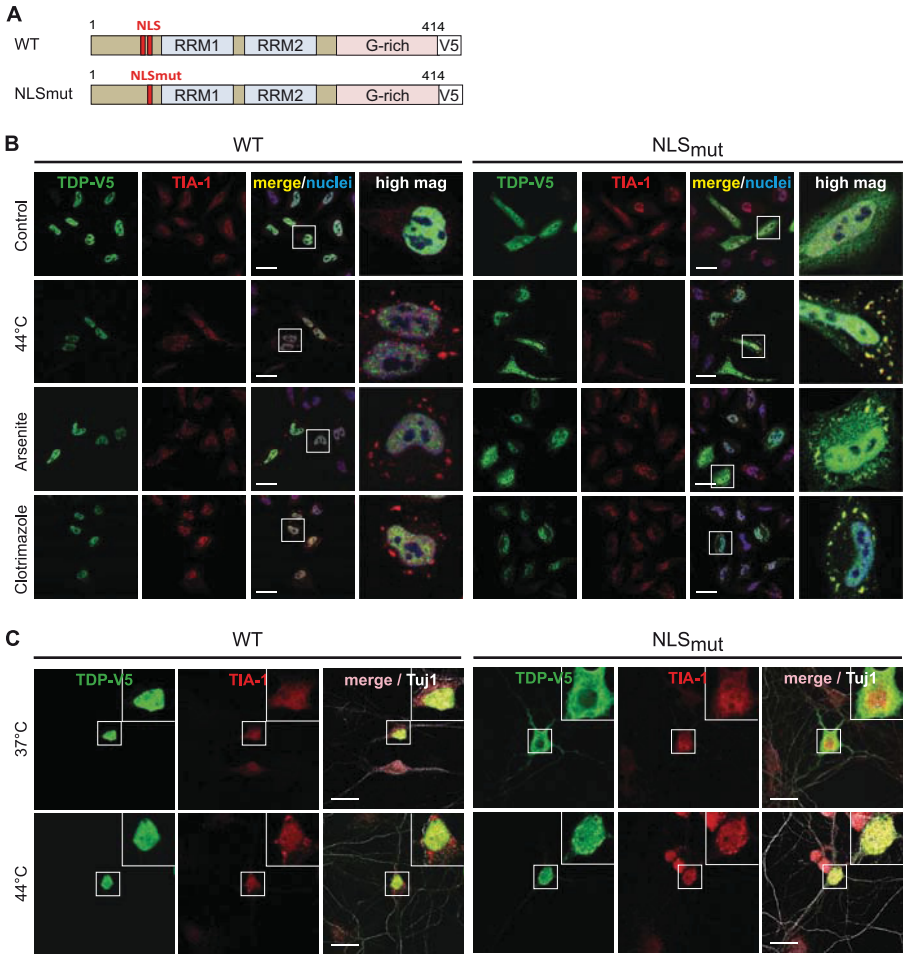

FIGURE 4. **Cytosolic mislocalization is a prerequisite for SG recruitment of TDP-43.** *A*, shown is a schematic diagram of TDP-43 wild-type (*WT*) and NLS mutant (*NLSmut*). *NLSmut*, triple point mutation in the classical nuclear localization signal (K83A/R84A/K85A); *G-rich*, glycine-rich domain; *V5*, V5 epitope tag. *B*, C-terminal-V5-tagged TDP-WT or NLSmut were transiently transfected into HeLa cells and 24 h later were subjected to heat shock (44 °C for 1 h), sodium arsenite (0.5 mM for 30 min), or clotrimazole (20 μM for 30 min) treatment or were left untreated (*Control*). Cells were fixed, stained with a V5 (*green*) and TIA-1 (*red*)-specific antibody and a nuclear counterstain (*blue*), and analyzed by confocal microscopy. *Panels to the right* show a higher magnification of the boxed region. Although the cytosolic NLS mutant was sequestered into SG, TDP-WT remained nuclear under all stress conditions examined. *Scale bars* = 20 μm. *C*, primary rat hippocampal neurons were transiently transfected with V5-tagged TDP-WT or NLSmut. 48 h post-transfection, neurons were subjected to heat shock (44 °C) for 1 h or left untreated (37 °C). Neurons were fixed and stained with a V5-specific antibody (*green*), a TIA-1-specific antibody (*red*), and the neuronal marker antibody Tuj1 (*white*) to visualize neuronal morphology. NLSmut showed partial cytoplasmic mislocalization and was recruited to TIA-1-positive SG upon heat stress. *Insets in the upper right corner* show a higher magnification of the boxed region. *Scale bars*, 20 μm.

ization and did not differ from the WT protein (Fig. 6*C*). Thus, the examined ALS-associated *TARDBP* mutations (A315T, M337V, and G348C) do not cause cytoplasmic mislocalization or SG recruitment of TDP-43.

Because it is possible that *TARDBP* mutations may affect SG recruitment once the protein has accumulated in the cytosol, for example as a consequence of axonal injury (65) or reduced expression of nuclear import factors (66), we introduced the same ALS-associated *TARDBP* mutations into the NLS mutant of TDP-43 to see if the mutations would impair or enhance SG recruitment of cytosolic TDP-43. As expected, TDP-$NLSmut_{A315T}$, $NLSmut_{M337V}$, and $NLSmut_{G348C}$ showed the same cytosolic mislocalization as NLSmut (Fig. 7*A*, *left panels*) and similar expression levels (Fig. 7*B*). Upon cellular stress elicited by clotrimazole treatment, all mutants were readily detectable in TIA-1-positive SG (Fig. 7*A*, *right panels*). A quantitative analysis of SG recruitment showed that the ALS-associated *TARDBP* mutants were incorporated into SG to a similar degree as NLSmut (Fig. 7*C*). Taken together, the examined ALS-associated point mutations in the glycine-rich C-terminal domain of TDP-43 (A315T, M337V, and G348C) neither cause cytosolic mislocalization of nuclear TDP-43 nor do they affect SG recruitment of cytosolic TDP-43.

TDP-43 Inclusions in Spinal Cord but Not in Cortex Contain SG Marker PABP-1—Even though TDP-43 can be recruited to SG under various experimental conditions (this study and Refs. 31, 50, 51, 53, and 56), it is still controversial whether TDP-43 inclusions in ALS/FTLD patients contain SG marker proteins. Two studies showed a lack of SG markers in TDP-43 inclusions (33, 50), whereas two other studies reported co-labeling of TDP-43 inclusions with SG markers (31, 57). We reasoned that these discrepancies might be due to the fact that TDP-43 inclusions differ in their TDP-43 species composition, with inclusions in the spinal cord of ALS and FTLD patients containing predominantly full-length TDP-43 and inclusions in the cortex and hippocampus of ALS and FTLD patients being highly

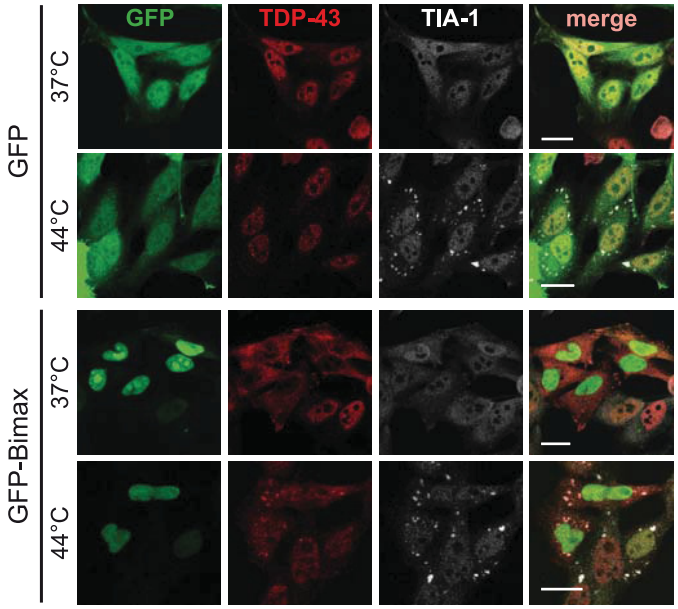

FIGURE 5. **Endogenous TDP-43 is sequestered into heat shock-induced SG upon inhibition of Importin α/β-dependent nuclear import.** HeLa cells were transfected with an Importin α/β-specific peptide inhibitor fused to GFP (*GFP-Bimax*) or GFP as a control (*green*). 24 h post-transfection cells were subjected to heat shock (44 °C for 1 h) or kept at control temperature (37 °C) before fixation. Cells were co-stained for endogenous TDP-43 (*red*) and TIA-1 (white) and analyzed by confocal microscopy. Expression of GFP-Bimax resulted in cytosolic mislocalization of endogenous TDP-43 and recruitment into SG upon heat shock. Under control conditions (GFP), TDP-43 was predominantly nuclear and did not colocalize with SG after heat shock. *Scale bars* = 20 μm.

enriched for C-terminal fragments (CTFs) of ~25 kDa (59, 60).

To see if differences in the TDP-43 species composition might account for the different results regarding co-labeling of TDP-43 inclusions with SG markers, we stained sections of spinal cord or cortex (hippocampus) from ALS-TDP and FTLD-TDP cases with N- and C-terminal TDP-43 antibodies as well as antibodies specific for the SG marker protein PABP-1. Inclusions in the spinal cord were consistently labeled with both N- and C-terminal TDP-43 antibodies, whereas inclusions in the cortex, including those in dentate granule neurons, were only labeled with the C-terminal antibody (Fig. 8), confirming previous results (59). Cortical TDP-43 inclusions were not immunoreactive for PABP-1, confirming our previous results (33). However, we revealed PABP-1 positivity in a subset (~66%) of TDP-43-positive inclusions in the spinal cord, as demonstrated by double-label immunofluorescence (Fig. 8 and supplemental Fig. S6). Thus, TDP-43 inclusions in spinal cord and cortex show a differential co-labeling for the SG marker protein PABP-1.

25-kDa CTF of TDP-43 Is Not Recruited to SG—We speculated that the differences in SG marker co-labeling of TDP-43 inclusions in different tissues may be due to the presence of different TDP-43 species, with distinct abilities to be recruited to SG. Because inclusions in cortex are highly enriched in CTFs of TDP-43 (59, 60) and are negative for PABP-1 (Fig. 8), we wondered if CTFs may be unable to associate with SG. To test this hypothesis, we expressed a CTF of ~25 kDa (TDPΔ1–173, see Fig. 9*A* for a schematic diagram) in HeLa cells and analyzed its recruitment to TIA-1-positive SG upon cellular stress. Like NLSmut, TDPΔ1–173 was partially localized in the cytosol under control conditions (Fig. 9*B*, *left panels*), as it lacks the N-terminal domain including the protein NLS (Fig. 9*A*). However, in contrast to NLSmut, TDPΔ1–173 remained diffusely distributed in the cytosol upon clotrimazole treatment and, consistent with our hypothesis, was very poorly incorporated into TIA-1-positive SG (Fig. 9, *B*, *right panels*, and *C*). Because TDPΔ1–173 showed very low expression levels compared with NLSmut (Fig. 9*D*), we repeated the experiment with GFP-tagged TDPΔ1–173 to exclude that the lack of SG association was simply due to low protein levels. Similar to V5-tagged TDPΔ1–173, the highly expressed GFP-tagged TDPΔ1–173 remained diffusely distributed upon cellular stress (supplemental Fig. S7, *A* and *B*). Thus, independent of expression levels, the 25-kDa CTF fails to associate with SG. This might explain why cortical TDP-43 inclusions, which are highly enriched in CTFs and contain little full-length TDP-43 (Fig. 8 and Refs. 59 and 60) are not co-labeled with SG marker proteins.

C-terminal Glycine-rich Domain of TDP-43 Is Required for Efficient SG Recruitment—Surprisingly, not only deletion of amino acids 1–173 but also deletion of the C-terminal glycine-rich domain from TDP-43 NLSmut (NLSmut-ΔC, see the schematic diagram in Fig. 9*A*) led to a strong reduction in SG recruitment, as NLSmut-ΔC remained mostly diffusely distributed in the cytoplasm upon cellular stress (Fig. 9, *B* and *C*). Expression level differences could not account for this effect, as NLSmut-ΔC was at least as well expressed as NLSmut (Fig. 9*D*). To test whether reduced RNA binding may be responsible for reduced SG recruitment of NLSmut-ΔC, we performed an RNA binding assay using UG_{12} RNA as a TDP-43-specific target sequence (12). As expected, TDP-WT was efficiently pulled down by UG_{12} (Fig. 10*A*). Interestingly, TDP-WT bound equally well to GGUG but not the corresponding CCUC oligonucleotide, consistent with the recent finding that TDP-43 can bind to sequences other than UG repeats (67).

Using UG_{12} as the RNA bait, we next compared the RNA binding capacity of full-length TDP-43 (WT and NLSmut) and the two deletion mutants NLSmutΔC and Δ1–173. The full-length proteins were specifically pulled down in our RNA binding assay, whereas TDP-Δ1–173, which lacks the protein main RNA recognition motif (RRM1) (12), failed to bind to UG_{12} RNA (Fig. 10*B*), which might explain why this fragment is not recruited to SG in FTLD/ALS patients (Fig. 8) and in cultured cells (Fig. 9). In contrast, NLSmut-ΔC bound to UG_{12} RNA as efficiently as full-length TDP-43 (Fig. 10*B*), demonstrating that the reduced SG recruitment capacity of this deletion mutant cannot be explained by reduced RNA binding. Thus, the glycine-rich domain seems to possess other, so far unknown features that are important for SG recruitment.

In summary, RNA binding of TDP-43 depends on the N-terminal RRM1 domain but not the C-terminal glycine-rich domain. Because both domains are required for SG recruitment of TDP-43, we suggest that RNA binding plus additional features encoded in the C-terminal glycine-rich domain such as protein-protein interactions might contribute to SG recruitment of TDP-43.

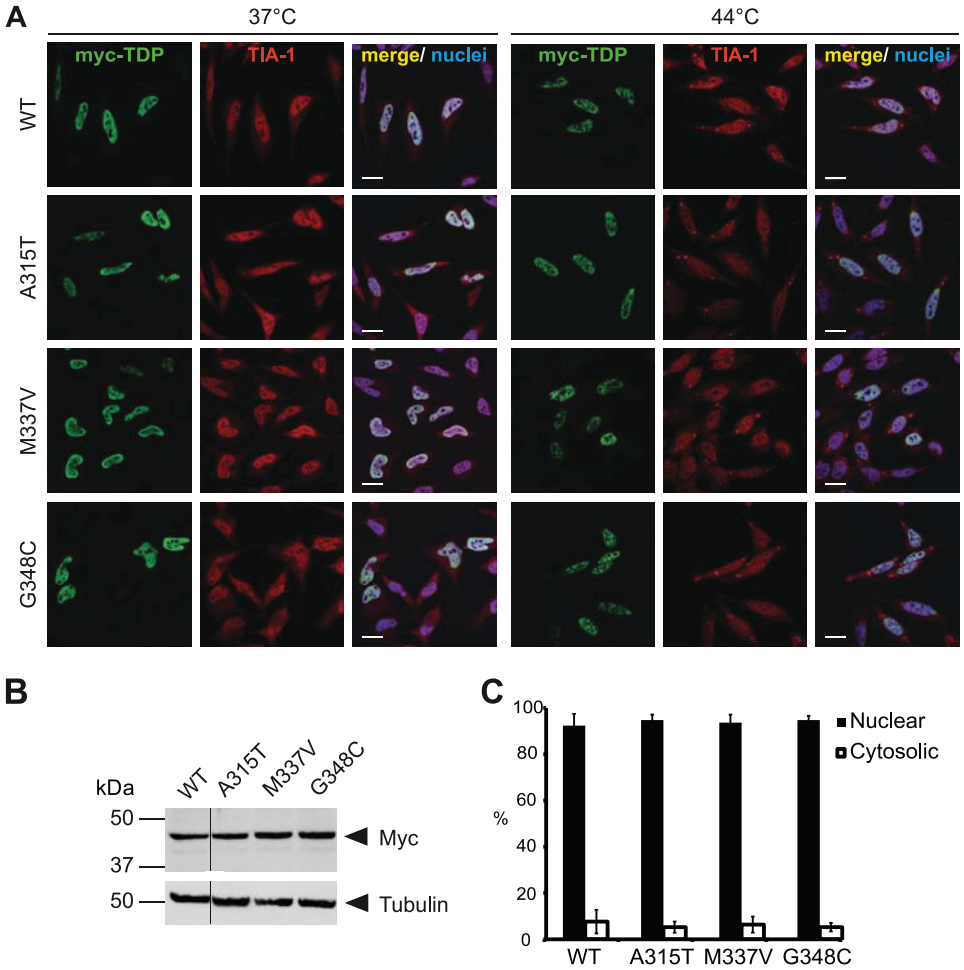

FIGURE 6. **ALS-associated *TARDBP* mutations do not alter the cellular localization of TDP-43.** *A*, Myc-tagged wild-type TDP-WT or TDP-43 carrying the indicated ALS-associated point mutations (A315T, M337V, or G348C) were transiently transfected into HeLa cells. 24 h post-transfection cells were subjected to heat shock (44 °C for 1 h) or kept at control temperature (37 °C). Afterward cells were fixed, stained with a myc (*green*) and TIA-1 (*red*)-specific antibody and a nuclei counterstain (*blue*), and analyzed by confocal microscopy. Both TDP-WT and the ALS-associated point mutants were nuclear under control conditions and remained nuclear upon heat shock. *Scale bars* = 20 μm. *B*, shown are expression levels of TDP-43 constructs used in *A*. Total cell lysates were analyzed by immunoblotting with a myc-specific antibody (*upper panel*). Tubulin served as a loading control (*lower panel*). All lanes were from the same exposure of the same blot. *C*, quantification of nuclear and cytosolic fluorescence intensities of myc staining at 37 °C is shown. *Error bars* indicate S.D.

DISCUSSION

Two different mechanisms of how FUS and TDP-43 are recruited to SG can be envisaged. First, because both proteins have multiple RNA binding motifs (12, 24, 68), it is conceivable that they are recruited into SG via bound mRNAs. Second, protein-protein interactions with other SG-associated proteins could be involved. Our results suggest that RNA binding plays a crucial role for SG recruitment of both FUS and TDP-43, as deletion mutants lacking the principal RNA binding domains (Z domain of FUS and RRM1 domain of TDP-43) showed poor recruitment to SG. This correlation between RNA binding and SG recruitment suggests that FUS and TDP-43 might be recruited into SG through binding to UG-rich RNA sequences (see the model in Fig. 11), although we cannot exclude that protein-protein interactions mediated by the Z and RRM1 domain are involved as well.

In addition, domains that did not bind to UG-rich RNA in our *in vitro* assay (G and R domain of FUS and the C-terminal glycine-rich domain of TDP-43) seem to contribute to SG recruitment as well, as deletion of these domains impaired SG recruitment. Given their lack of RNA binding, these domains may contribute to SG recruitment by providing protein-protein interactions with other SG proteins (symbolized by protein X and Y in Fig. 11). However, we cannot exclude that these putative protein-interacting domains bind to RNA sequences not represented in our *in vitro* binding assay and that these protein-RNA interactions contribute to SG recruitment. Indeed, recent cross-linking and immunoprecipitation (CLIP) experiments have shown that FUS can bind to AU-rich stem loop structures (69) and TDP-43 can bind to sequences other than UG repeats (67). Which domain(s) of FUS and TDP-43 mediates binding to these alternative target sequences remains to be investigated.

Our finding that the C-terminal glycine-rich domain of TDP-43 (amino acid residues 274–414) is required for efficient SG recruitment is consistent with previously published data showing that residues 268–315 are necessary for localization of TDP-43 within SG (50, 51). Because the C-terminal domain has been reported to mediate protein-protein interactions, such as interactions with other heterogeneous nuclear ribonucleoproteins (13) including FUS (70), it seems likely that protein-pro-

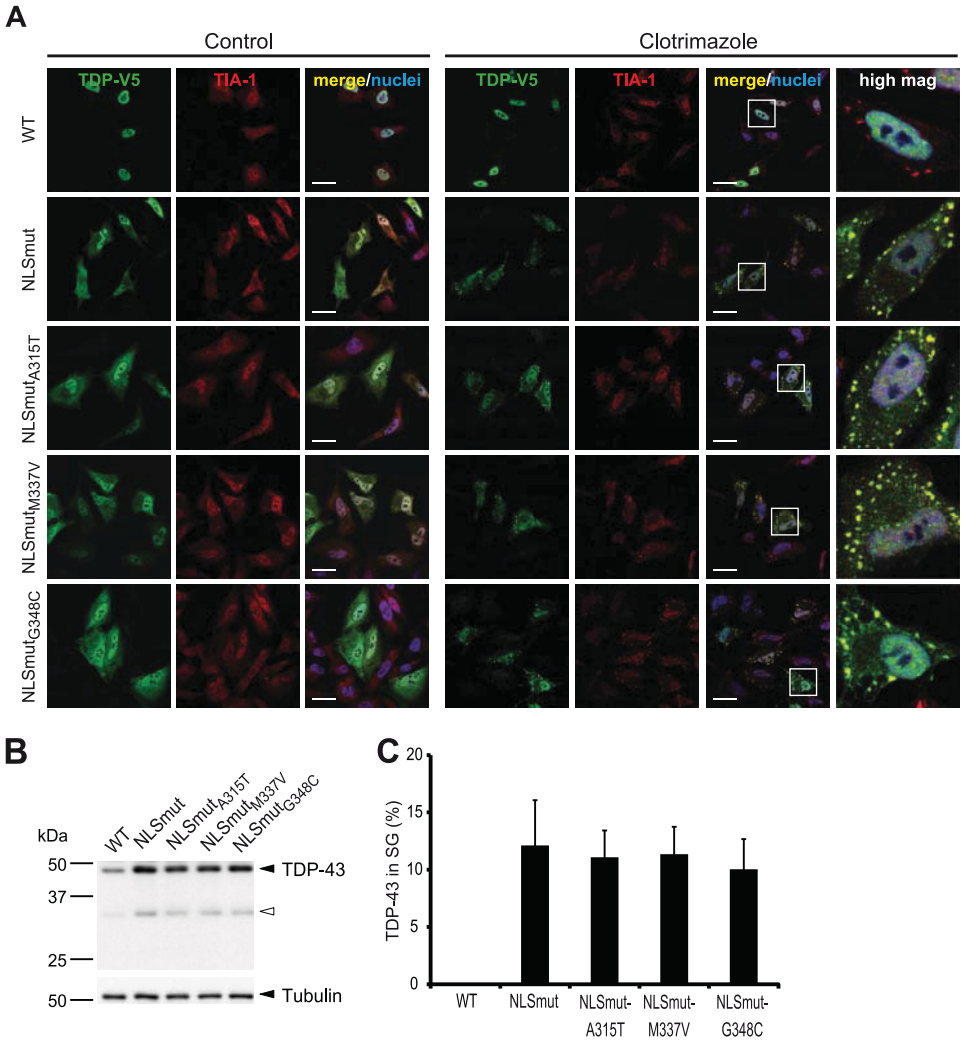

FIGURE 7. **ALS-associated *TARDBP* mutations do not affect SG recruitment of cytosolic TDP-43.** ALS-associated point mutations (A315T, M337V, G348C) were introduced into the TDP-43 NLS mutant (NLSmut$_{A315T}$, NLSmut$_{M337V}$, NLSmut$_{G348C}$), and the effect of mutations on SG recruitment was analyzed. *A*, HeLa cells transiently transfected with the indicated TDP-43 constructs were incubated with clotrimazole for 30 min or left untreated (*Control*). Cells were fixed, stained with a V5 (*green*) and TIA-1 (*red*)-specific antibody and a nuclear counterstain (*blue*), and analyzed by confocal microscopy. ALS-associated point mutations did not affect SG recruitment of cytosolic TDP-43. *Scale bars* = 20 μm. *B*, protein levels in total cell lysates were analyzed by immunoblotting with a V5-specific antibody (*upper panel*), and tubulin served as a loading control (*lower panel*). The *black arrowhead* indicates full-length TDP-43, and the *white arrowhead* indicates caspase-generated 35-kDa CTF frequently observed under transient transfection conditions (61, 75). *C*, the percentage of TDP-43 localized in TIA-1-positive SG was quantified using ImageJ. 15–20 cells were analyzed in a blinded manner, means across all cells were calculated, and S.D. are indicated by *error bars*.

tein interactions contribute to SG recruitment of TDP-43, although the protein(s) involved remains to be identified (protein X in Fig. 11). Freibaum *et al.* (56) identified numerous proteins involved in translation and SG-associated proteins as TDP-43-interacting proteins. Furthermore, TDP-43 and TIA-1 were found to interact in co-immunoprecipitation assays; however, this was only seen upon overexpression of both proteins (31). Nevertheless, TIA-1 and other SG-associated proteins are obvious candidates for proteins that recruit TDP-43 into SG via its C-terminal domain.

Although we did not observe myc- or V5-tagged TDP-WT or endogenous TDP-43 in SG after various stress treatments (Fig. 4–7), it is possible that very small amounts of TDP-43, undetectable by our antibodies, are present in SG under these conditions. That this might be the case is suggested by several reports describing at least small amounts of wild-type TDP-43 in SG upon various stress treatments (31, 50, 51, 53, 54, 56). Nevertheless, we could show that an artificial mutation in the TDP-43 NLS (NLSmut) or inhibition of Importin α/β-mediated nuclear import readily caused SG localization of TDP-43 upon cellular stress. We, therefore, suggest that cytosolic mislocalization is a prerequisite for recruitment of TDP-43 into SG. Cytosolic mislocalization may be artificially caused by high expression levels of TDP-WT and thus may allow unphysiological SG recruitment. Under physiological expression levels, we suggest that a nuclear import defect as the primary hit and cellular stress as the second hit are required for SG recruitment of TDP-43 (33, 40). *In vivo*, axonal injury (65) or reduced expression of nuclear transport factors, such as cellular apoptosis susceptibility protein (CAS) and Importin-α2 (66), might constitute such a primary hit leading to the cytoplasmic mislocalization of TDP-43 in ALS/FTLD-TDP patients.

What remains enigmatic is the cellular mechanism of ALS-associated *TARDBP* mutations. In contrast to ALS-associated

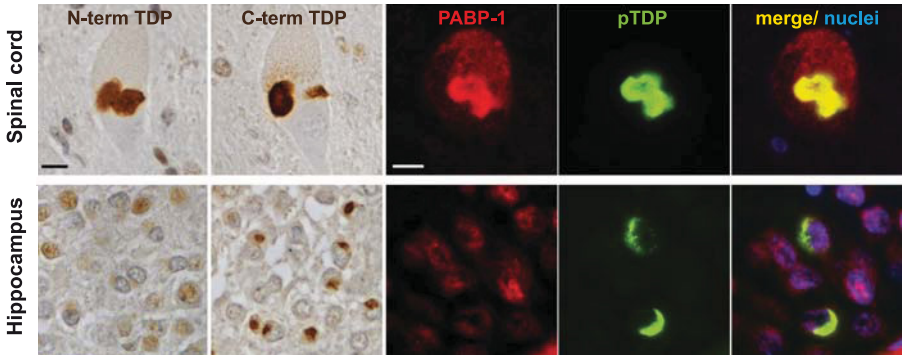

FIGURE 8. **TDP-43 inclusions in spinal cord but not hippocampus are frequently co-labeled for the SG marker protein PABP-1.** TDP-43 immunohistochemistry performed on formalin-fixed, paraffin-embedded tissue sections of spinal cord (*upper panels*) or hippocampus (*lower panels*) from FTLD-TDP and ALS-TDP cases is shown. Staining with N-terminal and C-terminal TDP-43-specific antibodies demonstrated labeling of neuronal cytoplasmic inclusions in motor neurons in the spinal cord with both antibodies (ALS case #1 shown), whereas inclusions in dentate granule neurons in the hippocampus were labeled only with the C-terminal antibody (FTLD-TDP case #1 shown). Double-label immunofluorescence stainings of the same cases showed co-labeling of phospho-TDP-43 positive inclusions (*green*) with the SG marker protein PABP-1 (*red*) in the spinal cord but not in cortical inclusions. Nuclei were stained with DAPI (*blue*). *Scale bars* = 10 μm.

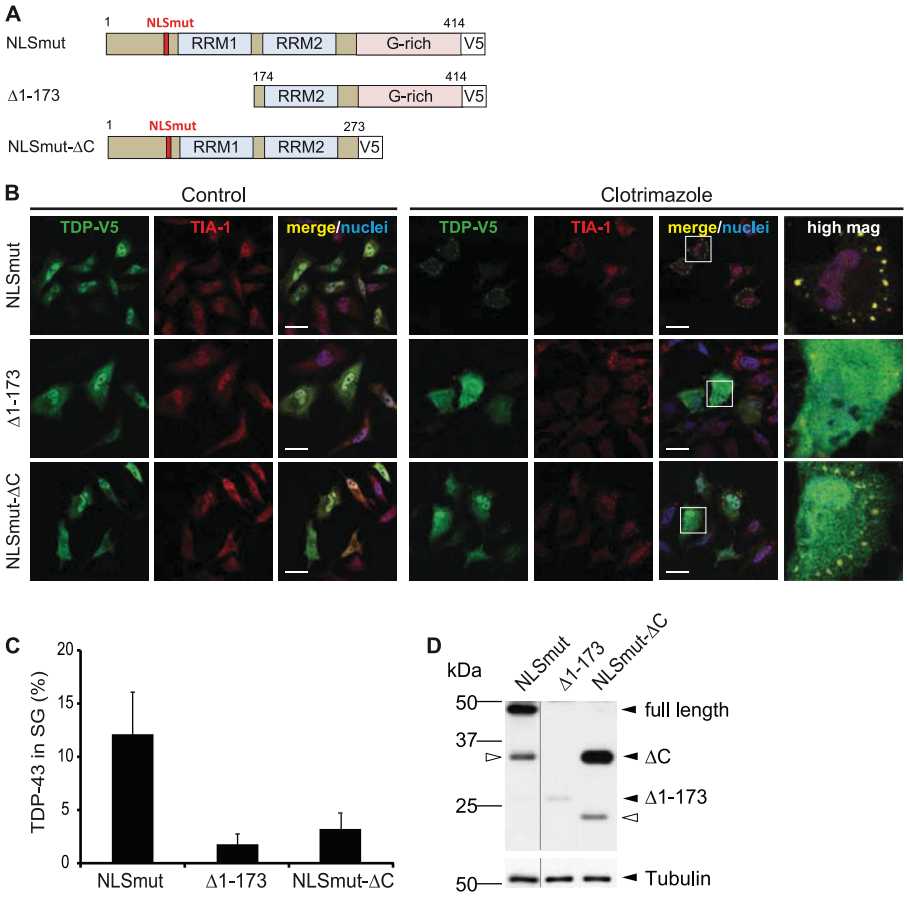

FIGURE 9. **25 kDa C-terminal fragment and a C-terminal deletion mutant of TDP-43 are poorly sequestered into SG.** *A*, shown is a schematic diagram of TDP-43 deletion mutants analyzed for SG recruitment. The deletion mutant Δ1–173 was chosen to mimic the 25-kDa CTF found to be deposited in cortical regions of FTLD-TDP patients (4, 59). The C-terminal deletion mutant (*NLSmutΔC*) lacks the prion-like glycine-rich domain. *B*, the indicated TDP-43 constructs were transiently transfected in HeLa cells. Before fixation, cells were treated with clotrimazole (20 μM, 30 min) or left untreated (control). Subsequently, cells were stained with a V5 (*green*) and TIA-1 (*red*)-specific antibody and a nuclear counterstain (*blue*) and analyzed by confocal microscopy. *Panels to the right* show a higher magnification of the *boxed region*. In contrast to full-length TDP-NLSmut, both deletion mutants remained predominantly diffuse in the cytosol upon heat shock and were poorly recruited to SG. *Scale bars* = 20 μm. *C*, the percentage of TDP-43 localized in TIA-1-positive SG was quantified using ImageJ. 15–20 cells were analyzed in a blinded manner, means across all cells were calculated, and S.D. are indicated by *error bars*. *D*, protein levels in total cell lysates were analyzed by immunoblotting with a V5-specific antibody (*upper panel*); tubulin served as a loading control (*lower panel*). *Black arrowheads* indicate full-length TDP-NLSmut or the two deletion mutants, and *white arrowheads* indicate degradation products. All lanes were from the same exposure of the same blot.

FUS mutations, *TARDBP* mutations in the glycine-rich C-terminal domain (A315T, M337V, and G348C) did not affect nuclear localization in our study, consistent with previous reports (28, 32, 51). Whether ALS-associated *TARDBP* mutations affect SG formation was controversial. Two studies reported that *TARDBP* mutations increase the number or size

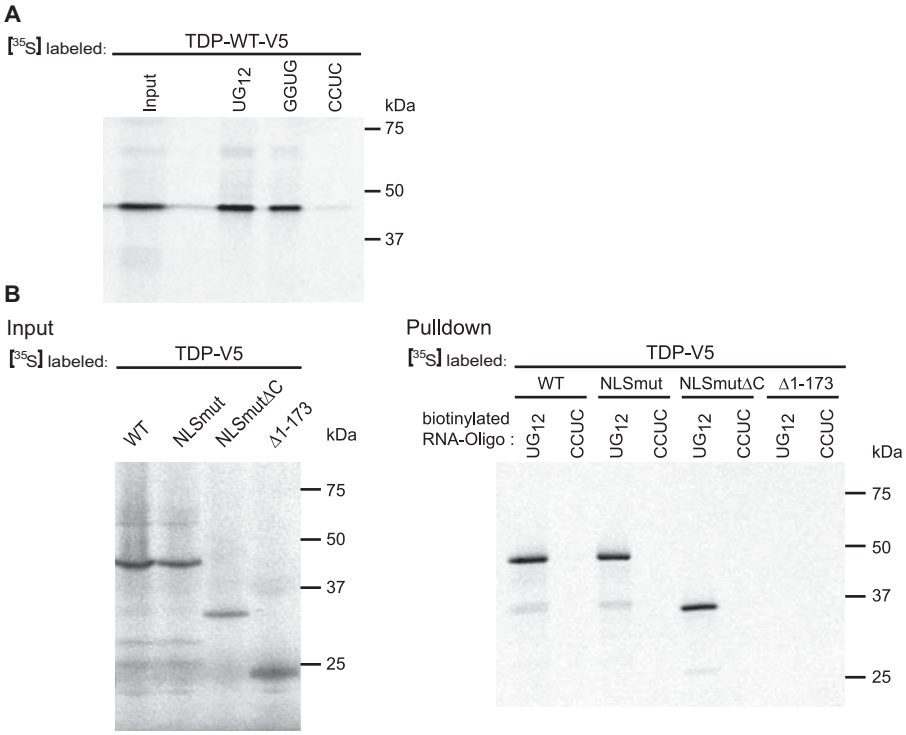

FIGURE 10. **The C-terminal deletion mutant of TDP-43 still binds to UG_{12} RNA.** *A*, TDP-WT was *in vitro* translated in the presence of [^{35}S]methionine (*left lane*, *Input*) and was analyzed for binding to different RNA oligonucleotides immobilized on streptavidin beads (*right lanes*, *UG_{12}*, UGUGUGUGUGUGUGUGUGUGUGUG; *GGUG*, UUGUAUUUUGAGCUAGUUUGGUGAU; *CCUC*, UUGUAUUUUGAGCUAGUUUCCUCAU). TDP-43 bound to both UG_{12} and GGUG RNA but not to CCUC RNA). *B*, the indicated TDP-43 constructs were *in vitro* translated in the presence of [^{35}S]methionine (*upper panel*, *Input*). Biotinylated UG_{12} RNA or CCUC control RNA were immobilized on streptavidin beads and were used to pull down radioactively labeled proteins (*lower panel*, *Pulldown*). TDP-WT and NLSmut as well as the C-terminal deletion mutant NLSmut-ΔC were specifically pulled down by UG_{12} RNA, whereas the Δ1–173 deletion mutant resembling the 25-kDa CTF did not bind to UG_{12} RNA.

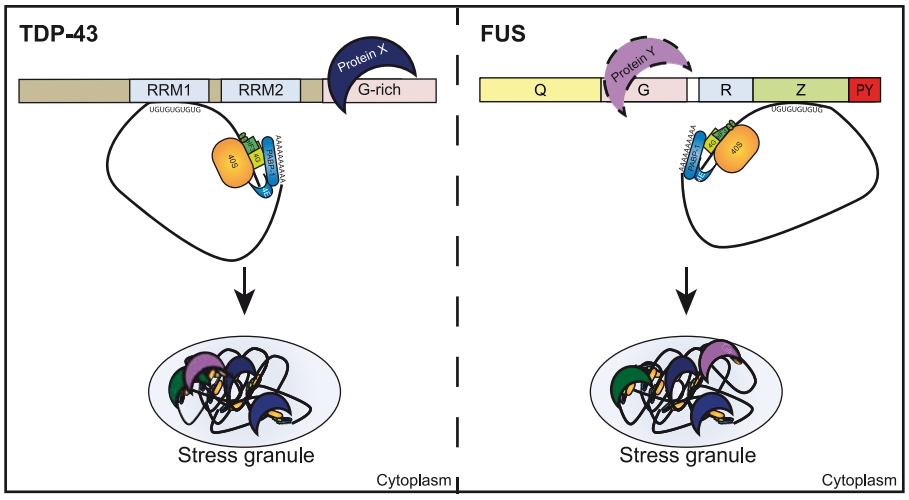

FIGURE 11. **Model of SG recruitment of TDP-43 and FUS.** Upon cellular stress, translation of mRNAs is arrested and translationally silent preinitiation complexes that contain mRNA, the small ribosomal subunit (*40 S*), early initiation factors (*e.g. eIF3*, *eIF4A*, *eIF4G*), and PABP-1 are packaged into SG. We suggest that recruitment of TDP-43 (*left*) or FUS (*right*) into SG involves both protein-RNA and protein-protein interactions. TDP-43 and FUS bind to UG-rich mRNA sequences via their main RNA binding domain (RRM1 in TDP-43 and RGG-zinc finger (Z) domain in FUS, respectively) and thus might be recruited into SG via their associated mRNAs. Because additional domains that did not show binding to UG-rich RNA in our RNA binding assay also contribute to SG recruitment of TDP-43 and FUS, we suggest that additional protein-protein interactions with proteins X and Y are involved in SG recruitment of TDP-43 and FUS.

of SG, suggesting a toxic gain-of-function mechanism (31, 51), whereas another group found that R361S is a loss-of-function mutation with regard to SG formation, leading to fewer SG (54). In our study the percentage of TDP-NLSmut in SG was not significantly altered by the presence of ALS-associated point mutations (A315T, M337V, and G348C) despite the importance of the C-terminal domain for SG recruitment. However, it remains possible that the dynamics of SG formation or dissolution are affected by ALS-associated *TARDBP* mutations, as recently suggested for R361S (54).

Another dispute that has remained unresolved is whether TDP-43 inclusions in FTLD and ALS patients contain SG marker proteins or not. Two studies reported a co-labeling of TDP-43 inclusions with SG markers (31, 57), whereas two other

studies did not find evidence for SG marker co-labeling (33, 50). Our data suggest that SG marker co-labeling is dependent on the presence of full-length TDP-43, which is much more abundant in spinal cord inclusions than in cortical TDP-43 inclusions (this study and Refs. 59 and 60). We, therefore, suggest that the reported discrepancies could be due to the presence of different TDP-43 species in inclusions in different regions of the central nervous system. How CTFs are generated and why cortical TDP-43 inclusions are highly enriched in these fragments is still unclear. The absence of SG markers from CTF-containing inclusions suggests that these inclusions either arise independently of SG or that CTFs dissociate from SG upon proteolytic cleavage of full-length TDP-43, presumably due to its reduced RNA binding capacity. How exactly SG relate to CTF generation and TDP-43 inclusion formation remains to be investigated.

The presence of SG marker proteins and RNA in pathological FUS or TDP-43 inclusions has led to the hypothesis that these inclusions could arise from stress granules (31, 33, 42, 55). Indeed, various forms of stress have been implicated in the pathogenesis of ALS, including oxidative stress, mitochondrial dysfunction, damage to the vasculature, and inflammatory reactions (71–73). Even though it remains to be seen whether SG are actually pathogenic or protective, this model offers a plausible mechanism for how pathological aggregation of cytosolic FUS or TDP-43 might be triggered in response to cellular stress. Recruitment into SG most likely increases the local FUS or TDP-43 concentration, which might seed aggregation of these otherwise soluble proteins in a prion-like manner (74). Whether the prion-like domains of FUS and TDP-43 are secondarily involved in seeding aggregation remains to be seen. We note that so far cellular models were unable to recapitulate *bona fide* FUS or TDP-43 aggregation, as FUS- or TDP-43-containing SG are rapidly disassembled upon stress removal (Ref. 41 and this study). We, therefore, believe that additional hits or chronic stress might be needed for irreversible aggregation of SG-localized proteins (40).

Acknowledgments—We thank Claudia Abou-Ajram, Andrea Seibel, and Stephanie Kunath for technical assistance. We are grateful to the Hans and Ilse Breuer Foundation for the Confocal Microscope.

REFERENCES

1. Mackenzie, I. R., Rademakers, R., and Neumann, M. (2010) TDP-43 and FUS in amyotrophic lateral sclerosis and frontotemporal dementia. *Lancet Neurol.* **9,** 995–1007
2. Buratti, E., and Baralle, F. E. (2008) Multiple roles of TDP-43 in gene expression, splicing regulation, and human disease. *Front. Biosci.* **13,** 867–878
3. Lagier-Tourenne, C., and Cleveland, D. W. (2009) Rethinking ALS: the FUS about TDP-43. *Cell* **136,** 1001–1004
4. Neumann, M., Sampathu, D. M., Kwong, L. K., Truax, A. C., Micsenyi, M. C., Chou, T. T., Bruce, J., Schuck, T., Grossman, M., Clark, C. M., McCluskey, L. F., Miller, B. L., Masliah, E., Mackenzie, I. R., Feldman, H., Feiden, W., Kretzschmar, H. A., Trojanowski, J. Q., and Lee, V. M. (2006) Ubiquitinated TDP-43 in frontotemporal lobar degeneration and amyotrophic lateral sclerosis. *Science* **314,** 130–133
5. Arai, T., Hasegawa, M., Akiyama, H., Ikeda, K., Nonaka, T., Mori, H., Mann, D., Tsuchiya, K., Yoshida, M., Hashizume, Y., and Oda, T. (2006) TDP-43 is a component of ubiquitin-positive Tau-negative inclusions in frontotemporal lobar degeneration and amyotrophic lateral sclerosis. *Biochem. Biophys. Res. Commun.* **351,** 602–611
6. Kwiatkowski, T. J., Jr., Bosco, D. A., Leclerc, A. L., Tamrazian, E., Vanderburg, C. R., Russ, C., Davis, A., Gilchrist, J., Kasarskis, E. J., Munsat, T., Valdmanis, P., Rouleau, G. A., Hosler, B. A., Cortelli, P., de Jong, P. J., Yoshinaga, Y., Haines, J. L., Pericak-Vance, M. A., Yan, J., Ticozzi, N., Siddique, T., McKenna-Yasek, D., Sapp, P. C., Horvitz, H. R., Landers, J. E., and Brown, R. H., Jr. (2009) Mutations in the FUS/TLS gene on chromosome 16 cause familial amyotrophic lateral sclerosis. *Science* **323,** 1205–1208
7. Vance, C., Rogelj, B., Hortobágyi, T., De Vos, K. J., Nishimura, A. L., Sreedharan, J., Hu, X., Smith, B., Ruddy, D., Wright, P., Ganesalingam, J., Williams, K. L., Tripathi, V., Al-Saraj, S., Al-Chalabi, A., Leigh, P. N., Blair, I. P., Nicholson, G., de Belleroche, J., Gallo, J. M., Miller, C. C., and Shaw, C. E. (2009) Mutations in FUS, an RNA processing protein, cause familial amyotrophic lateral sclerosis type 6. *Science* **323,** 1208–1211
8. Neumann, M., Rademakers, R., Roeber, S., Baker, M., Kretzschmar, H. A., and Mackenzie, I. R. (2009) A new subtype of frontotemporal lobar degeneration with FUS pathology. *Brain* **132,** 2922–2931
9. Lashley, T., Rohrer, J. D., Bandopadhyay, R., Fry, C., Ahmed, Z., Isaacs, A. M., Brelstaff, J. H., Borroni, B., Warren, J. D., Troakes, C., King, A., Al-Saraj, S., Newcombe, J., Quinn, N., Ostergaard, K., Schrøder, H. D., Bojsen-Møller, M., Braendgaard, H., Fox, N. C., Rossor, M. N., Lees, A. J., Holton, J. L., and Revesz, T. (2011) A comparative clinical, pathological, biochemical, and genetic study of fused in sarcoma proteinopathies. *Brain* **134,** 2548–2564
10. Mackenzie, I. R., Ansorge, O., Strong, M., Bilbao, J., Zinman, L., Ang, L. C., Baker, M., Stewart, H., Eisen, A., Rademakers, R., and Neumann, M. (2011) Pathological heterogeneity in amyotrophic lateral sclerosis with FUS mutations. Two distinct patterns correlating with disease severity and mutation. *Acta Neuropathol.* **122,** 87–98
11. Mackenzie, I. R., Munoz, D. G., Kusaka, H., Yokota, O., Ishihara, K., Roeber, S., Kretzschmar, H. A., Cairns, N. J., and Neumann, M. (2011) Distinct pathological subtypes of FTLD-FUS. *Acta Neuropathol.* **121,** 207–218
12. Buratti, E., and Baralle, F. E. (2001) Characterization and functional implications of the RNA binding properties of nuclear factor TDP-43, a novel splicing regulator of CFTR exon 9. *J. Biol. Chem.* **276,** 36337–36343
13. Buratti, E., Brindisi, A., Giombi, M., Tisminetzky, S., Ayala, Y. M., and Baralle, F. E. (2005) TDP-43 binds heterogeneous nuclear ribonucleoprotein A/B through its C-terminal tail. An important region for the inhibition of cystic fibrosis transmembrane conductance regulator exon 9 splicing. *J. Biol. Chem.* **280,** 37572–37584
14. Johnson, B. S., Snead, D., Lee, J. J., McCaffery, J. M., Shorter, J., and Gitler, A. D. (2009) TDP-43 is intrinsically aggregation-prone, and amyotrophic lateral sclerosis-linked mutations accelerate aggregation and increase toxicity. *J. Biol. Chem.* **284,** 20329–20339
15. Nonaka, T., Kametani, F., Arai, T., Akiyama, H., and Hasegawa, M. (2009) Truncation and pathogenic mutations facilitate the formation of intracellular aggregates of TDP-43. *Hum. Mol. Genet.* **18,** 3353–3364
16. Furukawa, Y., Kaneko, K., and Nukina, N. (2011) Molecular properties of TAR DNA=binding protein-43 fragments are dependent upon its cleavage site. *Biochim. Biophys. Acta* **1812,** 1577–1583
17. Zhang, Y. J., Xu, Y. F., Cook, C., Gendron, T. F., Roettges, P., Link, C. D., Lin, W. L., Tong, J., Castanedes-Casey, M., Ash, P., Gass, J., Rangachari, V., Buratti, E., Baralle, F., Golde, T. E., Dickson, D. W., and Petrucelli, L. (2009) Aberrant cleavage of TDP-43 enhances aggregation and cellular toxicity. *Proc. Natl. Acad. Sci. U.S.A.* **106,** 7607–7612
18. Yang, C., Tan, W., Whittle, C., Qiu, L., Cao, L., Akbarian, S., and Xu, Z. (2010) The C-terminal TDP-43 fragments have a high aggregation propensity and harm neurons by a dominant-negative mechanism. *PLoS One* **5,** e15878
19. Gitler, A. D., and Shorter, J. (2011) RNA-binding proteins with prion-like domains in ALS and FTLD-U. *Prion* **5,** 179–187
20. Udan, M., and Baloh, R. H. (2011) Implications of the prion-related Q/N domains in TDP-43 and FUS. *Prion* **5,** 1–5
21. Cushman, M., Johnson, B. S., King, O. D., Gitler, A. D., and Shorter, J. (2010) Prion-like disorders. Blurring the divide between transmissibility and infectivity. *J. Cell Sci.* **123,** 1191–1201

22. Fuentealba, R. A., Udan, M., Bell, S., Wegorzewska, I., Shao, J., Diamond, M. I., Weihl, C. C., and Baloh, R. H. (2010) Interaction with polyglutamine aggregates reveals a Q/N-rich domain in TDP-43. *J. Biol. Chem.* **285,** 26304–26314
23. Iko, Y., Kodama, T. S., Kasai, N., Oyama, T., Morita, E. H., Muto, T., Okumura, M., Fujii, R., Takumi, T., Tate, S., and Morikawa, K. (2004) Domain architectures and characterization of an RNA-binding protein, TLS. *J. Biol. Chem.* **279,** 44834–44840
24. Lerga, A., Hallier, M., Delva, L., Orvain, C., Gallais, I., Marie, J., and Moreau-Gachelin, F. (2001) Identification of an RNA binding specificity for the potential splicing factor TLS. *J. Biol. Chem.* **276,** 6807–6816
25. Prasad, D. D., Ouchida, M., Lee, L., Rao, V. N., and Reddy, E. S. (1994) TLS/FUS fusion domain of TLS/FUS-erg chimeric protein resulting from the t(16;21) chromosomal translocation in human myeloid leukemia functions as a transcriptional activation domain. *Oncogene* **9,** 3717–3729
26. Mackenzie, I. R., and Rademakers, R. (2008) The role of transactive response DNA-binding protein-43 in amyotrophic lateral sclerosis and frontotemporal dementia. *Curr. Opin. Neurol.* **21,** 693–700
27. Guo, W., Chen, Y., Zhou, X., Kar, A., Ray, P., Chen, X., Rao, E. J., Yang, M., Ye, H., Zhu, L., Liu, J., Xu, M., Yang, Y., Wang, C., Zhang, D., Bigio, E. H., Mesulam, M., Shen, Y., Xu, Q., Fushimi, K., and Wu, J. Y. (2011) An ALS-associated mutation affecting TDP-43 enhances protein aggregation, fibril formation, and neurotoxicity. *Nat. Struct. Mol. Biol.* **18,** 822–830
28. Kabashi, E., Lin, L., Tradewell, M. L., Dion, P. A., Bercier, V., Bourgouin, P., Rochefort, D., Bel Hadj, S., Durham, H. D., Vande Velde, C., Rouleau, G. A., and Drapeau, P. (2010) Gain and loss of function of ALS-related mutations of TARDBP (TDP-43) cause motor deficits *in vivo*. *Hum. Mol. Genet.* **19,** 671–683
29. Winton, M. J., Van Deerlin, V. M., Kwong, L. K., Yuan, W., Wood, E. M., Yu, C. E., Schellenberg, G. D., Rademakers, R., Caselli, R., Karydas, A., Trojanowski, J. Q., Miller, B. L., and Lee, V. M. (2008) A90V TDP-43 variant results in the aberrant localization of TDP-43 *in vitro*. *FEBS Lett.* **582,** 2252–2256
30. Barmada, S. J., Skibinski, G., Korb, E., Rao, E. J., Wu, J. Y., and Finkbeiner, S. (2010) Cytoplasmic mislocalization of TDP-43 is toxic to neurons and enhanced by a mutation associated with familial amyotrophic lateral sclerosis. *J. Neurosci.* **30,** 639–649
31. Liu-Yesucevitz, L., Bilgutay, A., Zhang, Y. J., Vanderweyde, T., Vanderwyde, T., Citro, A., Mehta, T., Zaarur, N., McKee, A., Bowser, R., Sherman, M., Petrucelli, L., and Wolozin, B. (2010) Tar DNA-binding protein-43 (TDP-43) associates with stress granules. Analysis of cultured cells and pathological brain tissue. *PLoS One* **5,** e13250
32. Ling, S. C., Albuquerque, C. P., Han, J. S., Lagier-Tourenne, C., Tokunaga, S., Zhou, H., and Cleveland, D. W. (2010) ALS-associated mutations in TDP-43 increase its stability and promote TDP-43 complexes with FUS/TLS. *Proc. Natl. Acad. Sci. U.S.A.* **107,** 13318–13323
33. Dormann, D., Rodde, R., Edbauer, D., Bentmann, E., Fischer, I., Hruscha, A., Than, M. E., Mackenzie, I. R., Capell, A., Schmid, B., Neumann, M., and Haass, C. (2010) ALS-associated fused in sarcoma (FUS) mutations disrupt Transportin-mediated nuclear import. *EMBO J.* **29,** 2841–2857
34. Gal, J., Zhang, J., Kwinter, D. M., Zhai, J., Jia, H., Jia, J., and Zhu, H. (2011) Nuclear localization sequence of FUS and induction of stress granules by ALS mutants. *Neurobiol. Aging* **32,** 2323
35. Kino, Y., Washizu, C., Aquilanti, E., Okuno, M., Kurosawa, M., Yamada, M., Doi, H., and Nukina, N. (2011) Intracellular localization and splicing regulation of FUS/TLS are variably affected by amyotrophic lateral sclerosis-linked mutations. *Nucleic Acids Res.* **39,** 2781–2798
36. Ito, D., Seki, M., Tsunoda, Y., Uchiyama, H., and Suzuki, N. (2011) Nuclear transport impairment of amyotrophic lateral sclerosis-linked mutations in FUS/TLS. *Ann. Neurol.* **69,** 152–162
37. Chiò, A., Restagno, G., Brunetti, M., Ossola, I., Calvo, A., Mora, G., Sabatelli, M., Monsurrò, M. R., Battistini, S., Mandrioli, J., Salvi, F., Spataro, R., Schymick, J., Traynor, B. J., La Bella, V., and ITALSGEN Consortium (2009) Two Italian kindreds with familial amyotrophic lateral sclerosis due to FUS mutation. *Neurobiol. Aging* **30,** 1272–1275
38. Huang, E. J., Zhang, J., Geser, F., Trojanowski, J. Q., Strober, J. B., Dickson, D. W., Brown, R. H., Jr., Shapiro, B. E., and Lomen-Hoerth, C. (2010) Extensive FUS-immunoreactive pathology in juvenile amyotrophic lateral sclerosis with basophilic inclusions. *Brain Pathol.* **20,** 1069–1076
39. Bäumer, D., Hilton, D., Paine, S. M., Turner, M. R., Lowe, J., Talbot, K., and Ansorge, O. (2010) Juvenile ALS with basophilic inclusions is a FUS proteinopathy with FUS mutations. *Neurology* **75,** 611–618
40. Dormann, D., and Haass, C. (2011) TDP-43 and FUS. A nuclear affair. *Trends Neurosci.* **34,** 339–348
41. Bosco, D. A., Lemay, N., Ko, H. K., Zhou, H., Burke, C., Kwiatkowski, T. J., Jr., Sapp, P., McKenna-Yasek, D., Brown, R. H., Jr., and Hayward, L. J. (2010) Mutant FUS proteins that cause amyotrophic lateral sclerosis incorporate into stress granules. *Hum. Mol. Genet.* **19,** 4160–4175
42. Fujita, K., Ito, H., Nakano, S., Kinoshita, Y., Wate, R., and Kusaka, H. (2008) Immunohistochemical identification of messenger RNA-related proteins in basophilic inclusions of adult-onset atypical motor neuron disease. *Acta Neuropathol.* **116,** 439–445
43. Anderson, P., and Kedersha, N. (2006) RNA granules. *J. Cell Biol.* **172,** 803–808
44. Kedersha, N., and Anderson, P. (2007) Mammalian stress granules and processing bodies. *Methods Enzymol.* **431,** 61–81
45. Kayali, F., Montie, H. L., Rafols, J. A., and DeGracia, D. J. (2005) Prolonged translation arrest in reperfused hippocampal cornu Ammonis 1 is mediated by stress granules. *Neuroscience* **134,** 1223–1245
46. DeGracia, D. J., Rudolph, J., Roberts, G. G., Rafols, J. A., and Wang, J. (2007) Convergence of stress granules and protein aggregates in hippocampal cornu ammonis 1 at later reperfusion following global brain ischemia. *Neuroscience* **146,** 562–572
47. Moeller, B. J., Cao, Y., Li, C. Y., and Dewhirst, M. W. (2004) Radiation activates HIF-1 to regulate vascular radiosensitivity in tumors. Role of reoxygenation, free radicals, and stress granules. *Cancer Cell* **5,** 429–441
48. Gilks, N., Kedersha, N., Ayodele, M., Shen, L., Stoecklin, G., Dember, L. M., and Anderson, P. (2004) Stress granule assembly is mediated by prion-like aggregation of TIA-1. *Mol. Biol. Cell* **15,** 5383–5398
49. Furukawa, Y., Kaneko, K., Matsumoto, G., Kurosawa, M., and Nukina, N. (2009) Cross-seeding fibrillation of Q/N-rich proteins offers new pathomechanism of polyglutamine diseases. *J. Neurosci.* **29,** 5153–5162
50. Colombrita, C., Zennaro, E., Fallini, C., Weber, M., Sommacal, A., Buratti, E., Silani, V., and Ratti, A. (2009) TDP-43 is recruited to stress granules in conditions of oxidative insult. *J. Neurochem.* **111,** 1051–1061
51. Dewey, C. M., Cenik, B., Sephton, C. F., Dries, D. R., Mayer, P., 3rd, Good, S. K., Johnson, B. A., Herz, J., and Yu, G. (2011) TDP-43 is directed to stress granules by sorbitol, a novel physiological osmotic and oxidative stressor. *Mol. Cell Biol.* **31,** 1098–1108
52. Moisse, K., Volkening, K., Leystra-Lantz, C., Welch, I., Hill, T., and Strong, M. J. (2009) Divergent patterns of cytosolic TDP-43 and neuronal progranulin expression following axotomy. Implications for TDP-43 in the physiological response to neuronal injury. *Brain Res.* **1249,** 202–211
53. Meyerowitz, J., Parker, S. J., Vella, L. J., Ng, D. Ch., Price, K. A., Liddell, J. R., Caragounis, A., Li, Q. X., Masters, C. L., Nonaka, T., Hasegawa, M., Bogoyevitch, M. A., Kanninen, K. M., Crouch, P. J., and White, A. R. (2011) c-Jun N-terminal kinase controls TDP-43 accumulation in stress granules induced by oxidative stress. *Mol. Neurodegener.* **6,** 57
54. McDonald, K. K., Aulas, A., Destroismaisons, L., Pickles, S., Beleac, E., Camu, W., Rouleau, G. A., and Vande Velde, C. (2011) TAR DNA-binding protein 43 (TDP-43) regulates stress granule dynamics via differential regulation of G3BP and TIA-1. *Hum. Mol. Genet.* **20,** 1400–1410
55. Dewey, C. M., Cenik, B., Sephton, C. F., Johnson, B. A., Herz, J., and Yu, G. (2012) TDP-43 aggregation in neurodegeneration. Are stress granules the key? *Brain Res.*, in press
56. Freibaum, B. D., Chitta, R. K., High, A. A., and Taylor, J. P. (2010) Global analysis of TDP-43 interacting proteins reveals strong association with RNA splicing and translation machinery. *J. Proteome Res.* **9,** 1104–1120
57. Volkening, K., Leystra-Lantz, C., Yang, W., Jaffee, H., and Strong, M. J. (2009) Tar DNA binding protein of 43 kDa (TDP-43), 14-3-3 proteins, and copper/zinc superoxide dismutase (SOD1) interact to modulate NFL mRNA stability. Implications for altered RNA processing in amyotrophic lateral sclerosis (ALS). *Brain Res.* **1305,** 168–182
58. Kaech, S., and Banker, G. (2006) Culturing hippocampal neurons. *Nat. Protoc.* **1,** 2406–2415
59. Igaz, L. M., Kwong, L. K., Xu, Y., Truax, A. C., Uryu, K., Neumann, M.,

Clark, C. M., Elman, L. B., Miller, B. L., Grossman, M., McCluskey, L. F., Trojanowski, J. Q., and Lee, V. M. (2008) Enrichment of C-terminal fragments in TAR DNA-binding protein-43 cytoplasmic inclusions in brain but not in spinal cord of frontotemporal lobar degeneration and amyotrophic lateral sclerosis. *Am. J. Pathol.* **173,** 182–194

60. Neumann, M., Kwong, L. K., Lee, E. B., Kremmer, E., Flatley, A., Xu, Y., Forman, M. S., Troost, D., Kretzschmar, H. A., Trojanowski, J. Q., and Lee, V. M. (2009) Phosphorylation of S409/410 of TDP-43 is a consistent feature in all sporadic and familial forms of TDP-43 proteinopathies. *Acta Neuropathol.* **117,** 137–149
61. Dormann, D., Capell, A., Carlson, A. M., Shankaran, S. S., Rodde, R., Neumann, M., Kremmer, E., Matsuwaki, T., Yamanouchi, K., Nishihara, M., and Haass, C. (2009) Proteolytic processing of TAR DNA binding protein-43 by caspases produces C-terminal fragments with disease defining properties independent of progranulin. *J. Neurochem.* **110,** 1082–1094
62. Winton, M. J., Igaz, L. M., Wong, M. M., Kwong, L. K., Trojanowski, J. Q., and Lee, V. M. (2008) Disturbance of nuclear and cytoplasmic TAR DNA-binding protein (TDP-43) induces disease-like redistribution, sequestration, and aggregate formation. *J. Biol. Chem.* **283,** 13302–13309
63. Mackenzie, I. R., Neumann, M., Baborie, A., Sampathu, D. M., Du Plessis, D., Jaros, E., Perry, R. H., Trojanowski, J. Q., Mann, D. M., and Lee, V. M. (2011) A harmonized classification system for FTLD-TDP pathology. *Acta Neuropathol.* **122,** 111–113
64. Kosugi, S., Hasebe, M., Entani, T., Takayama, S., Tomita, M., and Yanagawa, H. (2008) Design of peptide inhibitors for the importin alpha/beta nuclear import pathway by activity-based profiling. *Chem. Biol.* **15,** 940–949
65. Sato, T., Takeuchi, S., Saito, A., Ding, W., Bamba, H., Matsuura, H., Hisa, Y., Tooyama, I., and Urushitani, M. (2009) Axonal ligation induces transient redistribution of TDP-43 in brainstem motor neurons. *Neuroscience* **164,** 1565–1578
66. Nishimura, A. L., Zupunski, V., Troakes, C., Kathe, C., Fratta, P., Howell, M., Gallo, J. M., Hortobágyi, T., Shaw, C. E., and Rogelj, B. (2010) Nuclear import impairment causes cytoplasmic trans-activation response DNA-binding protein accumulation and is associated with frontotemporal lobar degeneration. *Brain* **133,** 1763–1771
67. Polymenidou, M., Lagier-Tourenne, C., Hutt, K. R., Huelga, S. C., Moran, J., Liang, T. Y., Ling, S. C., Sun, E., Wancewicz, E., Mazur, C., Kordasiewicz, H., Sedaghat, Y., Donohue, J. P., Shiue, L., Bennett, C. F., Yeo, G. W., and Cleveland, D. W. (2011) Long pre-mRNA depletion and RNA missplicing contribute to neuronal vulnerability from loss of TDP-43. *Nat. Neurosci.* **14,** 459–468
68. Burd, C. G., and Dreyfuss, G. (1994) Conserved structures and diversity of functions of RNA-binding proteins. *Science* **265,** 615–621
69. Hoell, J. I., Larsson, E., Runge, S., Nusbaum, J. D., Duggimpudi, S., Farazi, T. A., Hafner, M., Borkhardt, A., Sander, C., and Tuschl, T. (2011) RNA targets of wild-type and mutant FET family proteins. *Nat. Struct. Mol. Biol.* **18,** 1428–1431
70. Kim, S. H., Shanware, N. P., Bowler, M. J., and Tibbetts, R. S. (2010) Amyotrophic lateral sclerosis-associated proteins TDP-43 and FUS/TLS function in a common biochemical complex to co-regulate HDAC6 mRNA. *J. Biol. Chem.* **285,** 34097–34105
71. Barber, S. C., and Shaw, P. J. (2010) Oxidative stress in ALS. Key role in motor neuron injury and therapeutic target. *Free Radic. Biol. Med.* **48,** 629–641
72. Saxena, S., and Caroni, P. (2011) Selective neuronal vulnerability in neurodegenerative diseases. From stressor thresholds to degeneration. *Neuron* **71,** 35–48
73. Quaegebeur, A., Lange, C., and Carmeliet, P. (2011) The neurovascular link in health and disease. Molecular mechanisms and therapeutic implications. *Neuron* **71,** 406–424
74. Polymenidou, M., and Cleveland, D. W. (2011) The seeds of neurodegeneration. Prion-like spreading in ALS. *Cell* **147,** 498–508
75. Zhang, Y. J., Xu, Y. F., Dickey, C. A., Buratti, E., Baralle, F., Bailey, R., Pickering-Brown, S., Dickson, D., and Petrucelli, L. (2007) Progranulin mediates caspase-dependent cleavage of TAR DNA binding protein-43. *J. Neurosci.* **27,** 10530–10534

SUPPLEMENTAL DATA

FIGURE S1. **Expression of FUS domain constructs containing the WT PY-NLS.**
Immunocytochemistry of transiently transfected HeLa cells expressing HA-tagged FUS-Z, FUS-RZ and FUS-GRZ, respectively. 24 hours after transfection cells were exposed to heat shock (44°C for 1 hour) or left untreated (37°C). Cells were fixed, stained with an HA-specific antibody (green), a TIA-1–specific antibody (red) and a nuclear counterstain (blue) and were analyzed by confocal microscopy. FUS proteins containing the Z-domain with the WT PY-NLS were nuclear both under control conditions and after heat shock. Scale bars: 20 μm.

FIGURE S2. **Heat shock-induced FUS-positive granules are SG.**
(A) To verify that stress-induced FUS-positive granules are bona fide SG, HeLa cells expressing HA-FUS-P525L were treated with cycloheximide (CHX) during heat shock (44°C + CHX) or were allowed to recover from heat shock (44°C + rec) by incubation at 37°C for 1 hour subsequent to heat shock. Afterwards cells were fixed, stained with an HA-specific antibody (green), a TIA-1-specific antibody (red) and a nuclear counterstain (blue) and were analyzed by confocal microscopy. CHX blocks translational elongation and is a well-known inhibitor of SG assembly. Addition of CHX prevented the formation of TIA-1/FUS-positive SG. Moreover, FUS-positive granules disassembled after recovery from heat stress, confirming their SG identity. Scale bars: 20 μm.
(B) SH-SY5Y neuroblastoma cells were transiently transfected with HA-tagged FUS-WT or FUS-P525L. 24 hours post-transfection cells were subjected to heat shock (44°C for 1 hour) or kept at control temperature (37°C). SH-SY5Y cells were fixed, stained with an HA-specific antibody (green), a TIA-1-specific antibody (red) and a nuclear counterstain (blue) and were analyzed using confocal microscopy. Like in HeLa cells, FUS-WT was nuclear with and without stress, while cytoplasmically mislocalized FUS-P525L was recruited into SG upon cellular stress. Scale bars: 20 μm.

FIGURE S3. **Expression of FUS domain constructs.**
Expression levels of HA-FUS constructs were examined by immunoblot. Total cell lysates were prepared in RIPA buffer and after SDS-PAGE were analyzed by immunoblotting with an HA-specific antibody (upper panel). A longer exposure of the same blot shows the weakly expressed R domain (middle panel). Actin served as a loading control (lower panel). Note that HA-tagged Q and Z_{P525L} were not detectable by HA immunoblot.

FIGURE S4. **GFP-tagged FUS-Z_{P525L} but not Q is recruited to SG.**
Since HA-tagged FUS-Q and Z_{P525L} were poorly expressed and not detectable by HA immunoblot, GFP-Q, GFP-Z_{P525L} and full-length GFP-FUS-P525L were expressed in HeLa cells and analyzed for expression and SG recruitment 24 hours post-transfection.
(A) Protein levels in total cell lysates were analyzed by immunoblotting with a GFP-specific antibody (upper panel). β-Actin served as a loading control (lower panel). Black arrowheads indicate GFP-tagged FUS proteins, white arrowhead indicates a degradation product.
(B) 24 hours post-transfection cells were subjected to heat shock (44°C for 1 hour) or left untreated (37°C). Cells were fixed, stained with a TIA-1-specific antibody (red) and a nuclear counterstain (blue) and analyzed by confocal microscopy. GFP-tagged proteins were visualized in the green channel via GFP fluorescence (green). Note that despite the P525L mutation, GFP-Z_{P525L} showed a more prominent nuclear localization than full-length GFP-FUS-P525L. Nevertheless, GFP-Z_{P525L} can be found to overlap with TIA-1, whereas GFP-Q is poorly recruited to SG and remains mainly diffusely distributed in the cytosol. Scale bars = 20 μm.

FIGURE S5. **Heat shock-induced TDP-43-positive granules are SG.**
(A) To verify that stress-induced TDP-43-positive granules are bona fide SG, HeLa cells expressing V5-tagged TDP-43 NLSmut were treated with cycloheximide (CHX) during heat shock (44°C + CHX) or were

allowed to recover from heat shock (44°C + rec) by incubation at 37°C for 1 hour subsequent to heat shock. Subsequently, cells were fixed, stained with a V5-specific antibody (green), a TIA-1-specific antibody (red) and a nuclear counterstain (blue) and analyzed by confocal microscopy. CHX-treated cells show no SG and TDP-43-positive granular structures resolve after recovery from heat shock, showing that the TDP-43-positive granules are indeed SG and not aggregates due to overexpression of TDP-43. Scale bars: 20 μm.
(B) Immunocytochemistry of SH-SY5Y cells transfected with TDP-WT-V5 or TDP-NLSmut-V5. 24 hours post-transfection, cells were subjected to heat shock (44°C for 1 hour) or left untreated (37°C). Cells were fixed, stained with a V5-specific antibody (green), a TIA-1-specific antibody (red) and a nuclear counterstain and analyzed by confocal microscopy. Like in Hela cells, TDP-WT remained nuclear and NLSmut was sequestered into SG upon heat stress. Scale bars: 20 μm.

FIGURE S6. **Percentage of PABP-1-positive TDP-43 inclusions in the spinal cord of ALS-TDP and FTLD-TDP patients.**
(A) Double-label immunofluorescence stainings for pTDP-43 (green) and the SG marker PABP-1 (red) showing colocalization in inclusions in ALS case #2 (I) and ALS case #3 (II). Notice that a subset of pTDP-43 inclusions in the spinal cord in all cases are only labeled for pTDP-43, as shown here for ALS case #1 (III). Nuclei were stained with DAPI (blue). Scale bar = 10 μM.
(B) pTDP-43 and PABP-1-labeled neuronal cytoplasmic inclusions in the anterior horn on double-label immunofluorescence stainings were counted on 1-2 spinal cord sections from each case. 66 % of the pTDP-43-positive inclusions showed co-labeling with the SG marker protein PABP-1.

FIGURE S7. **GFP-tagged TDP-Δ1-173 is not recruited to SG.**
Since V5-tagged TDP-Δ1-173 was poorly expressed and only gave a weak band in V5 immunoblot, GFP-Δ1-173 and full-length GFP-NLSmut were expressed in HeLa cells and analyzed for expression and SG recruitment 24 hours post-transfection.
(A) Protein levels in total cell lysates were analyzed by immunoblotting with a GFP-specific antibody (upper panel). β-Actin served as a loading control (lower panel). Black arrowheads indicate GFP-tagged TDP-43 proteins, white arrowheads indicate degradation products.
(B) 24 hours post-transfection cells were treated with clotrimazole (20 μM for 30 min) or left untreated (control). Cells were fixed, stained with a TIA-1-specific antibody (red) and a nuclear counterstain (blue) and analyzed by confocal microscopy. GFP-tagged proteins were visualized in the green channel via GFP fluorescence (green). Despite high expression levels, GFP-Δ1-173 did not co-localize with TIA-1-positive granules, whereas full-length GFP-NLSmut was readily recruited to SG. Scale bars = 20 μm.

Fig. S1

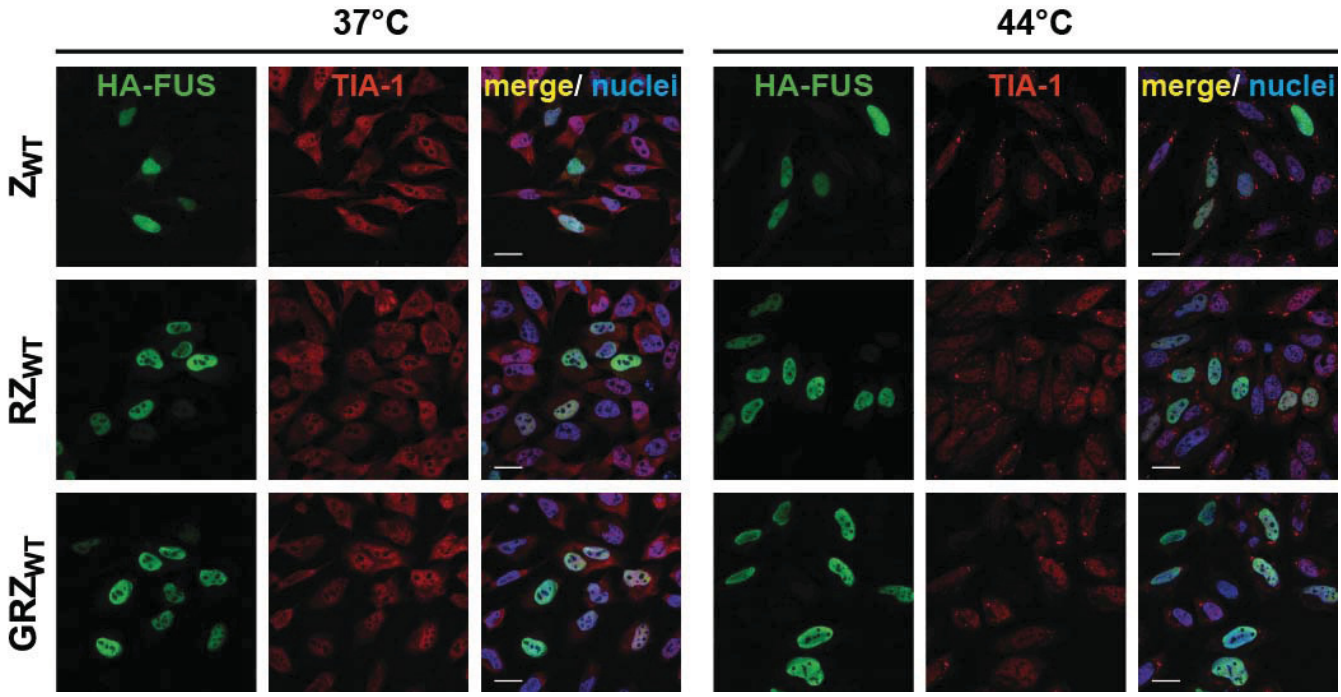
37°C
44°C
HA-FUS
TIA-1
merge/ nuclei
HA-FUS
TIA-1
merge/ nuclei
Z_WT
RZ_WT
GRZ_WT

Fig. S2

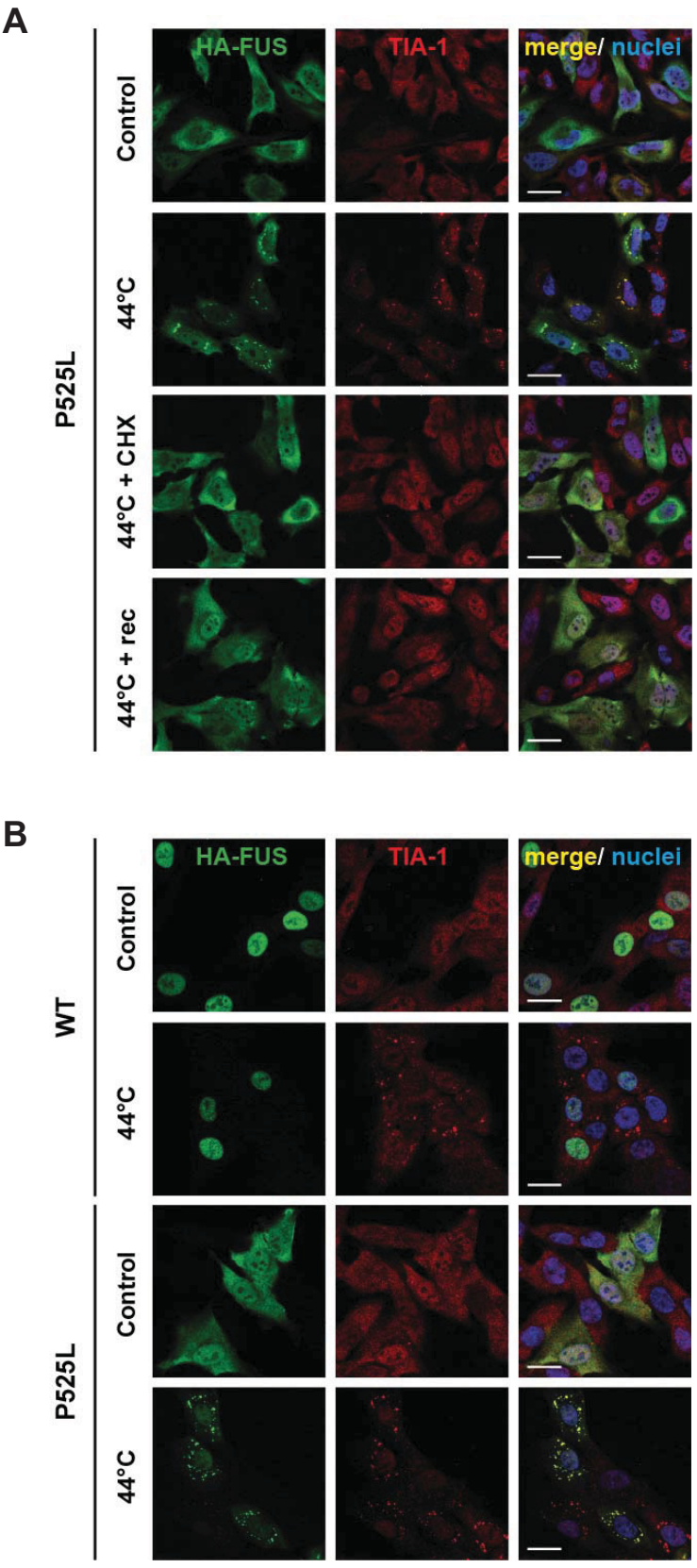
A
HA-FUS
TIA-1
merge/ nuclei
P525L
Control
44°C
44°C + CHX
44°C + rec
B
HA-FUS
TIA-1
merge/ nuclei
WT
Control
44°C
P525L
Control
44°C

Fig. S3

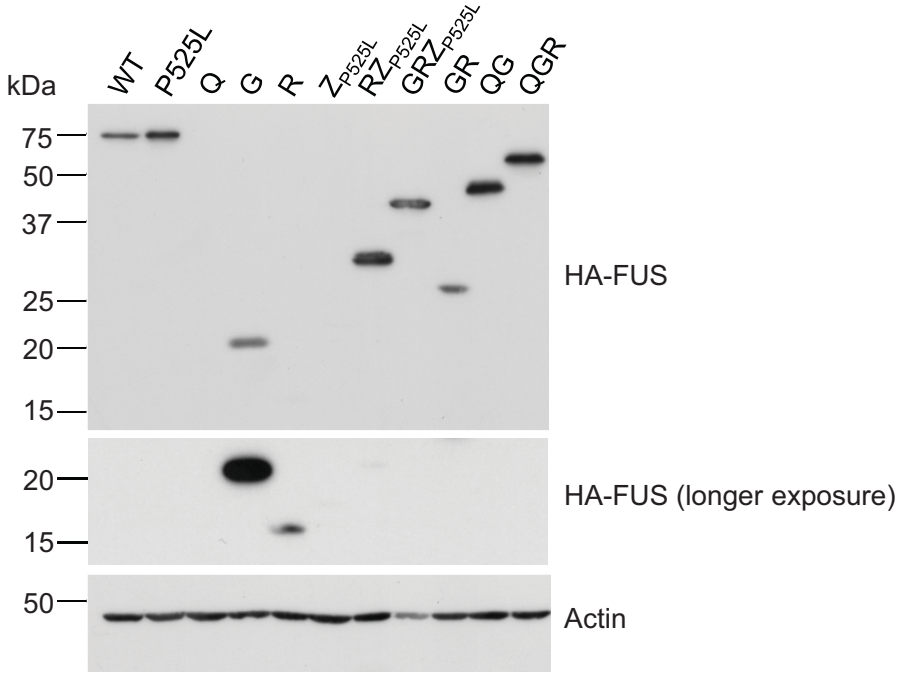
kDa
WT
P525L
Q
G
R
ZP525L
RZP525L
GRZP525L
GR
QG
QGR
75
50
37
25
20
15
HA-FUS
20
15
HA-FUS (longer exposure)
50
Actin

Fig. S4

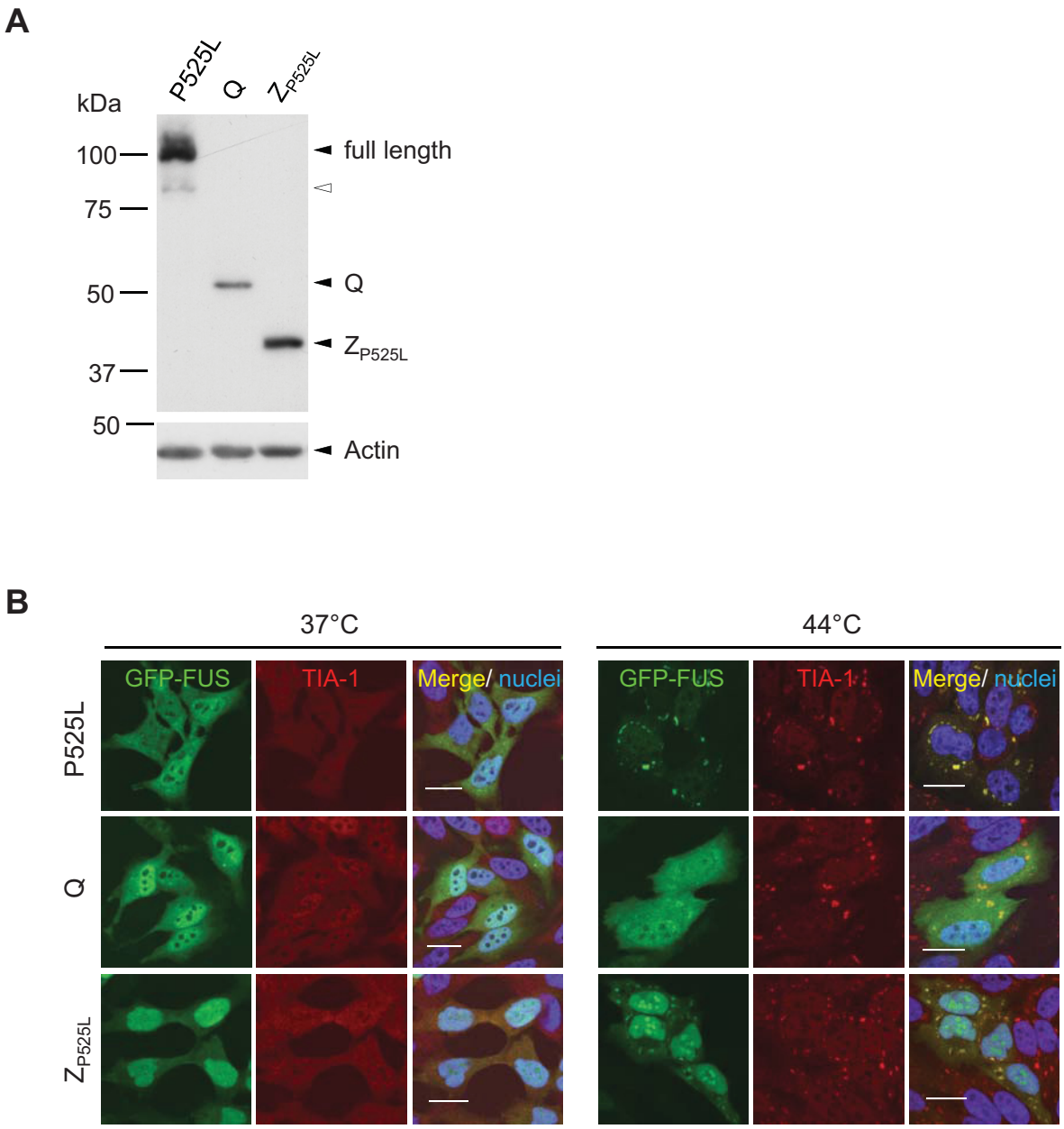
A
P525L
Q
Z_{P525L}
kDa
100
75
50
37
50
full length
Q
Z_{P525L}
Actin
B
37°C
44°C
GFP-FUS
TIA-1
Merge/ nuclei
P525L
Q
Z_{P525L}

Fig. S5

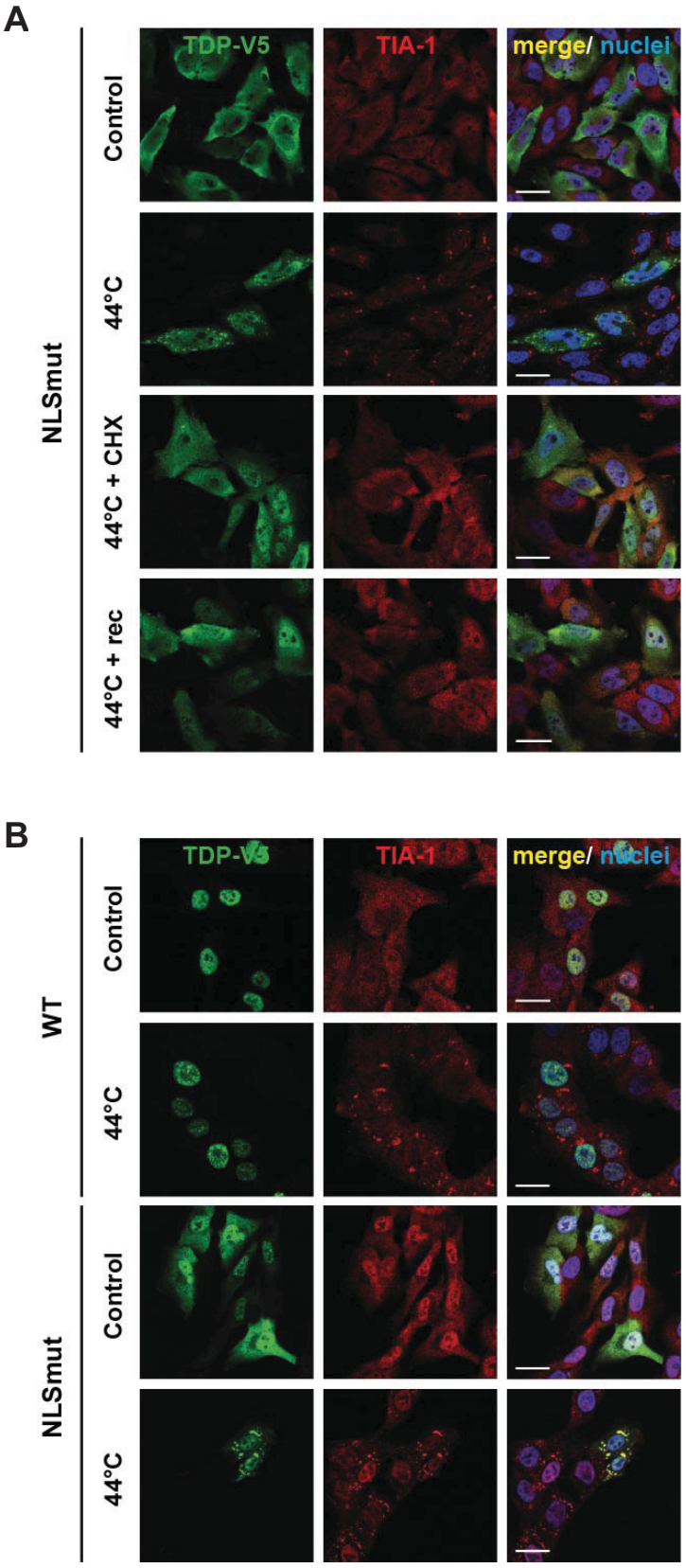
A
NLSmut
Control
44°C
44°C + CHX
44°C + rec
TDP-V5
TIA-1
merge/ nuclei
B
WT
Control
44°C
NLSmut
Control
44°C
TDP-V5
TIA-1
merge/ nuclei

Fig. S6

A

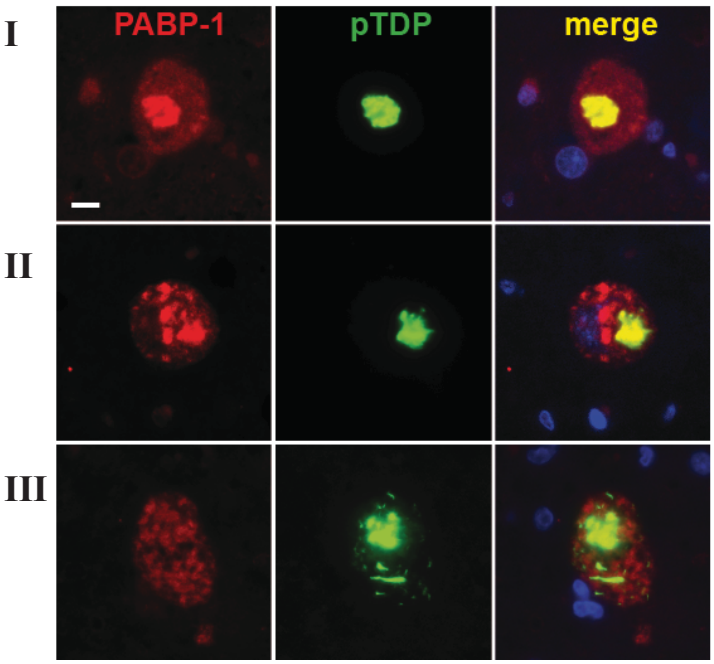

B

	Number of pTDP-43 positive NCI in spinal cord	Number of pTDP-43 and PABP1 positive NCI in spinal cord	Percentage pTDP-43 and PABP1 positive NCI in spinal cord
ALS #1	7	4	57.14%
ALS #2	9	7	77.78%
ALS #3	3	2	66.67%
ALS #4	4	3	75.00%
FTLD-TDP #1	11	7	63.64%
FTLD-TDP #2	5	3	60.00%
Total	**39**	**26**	**66.67%**

Fig. S7

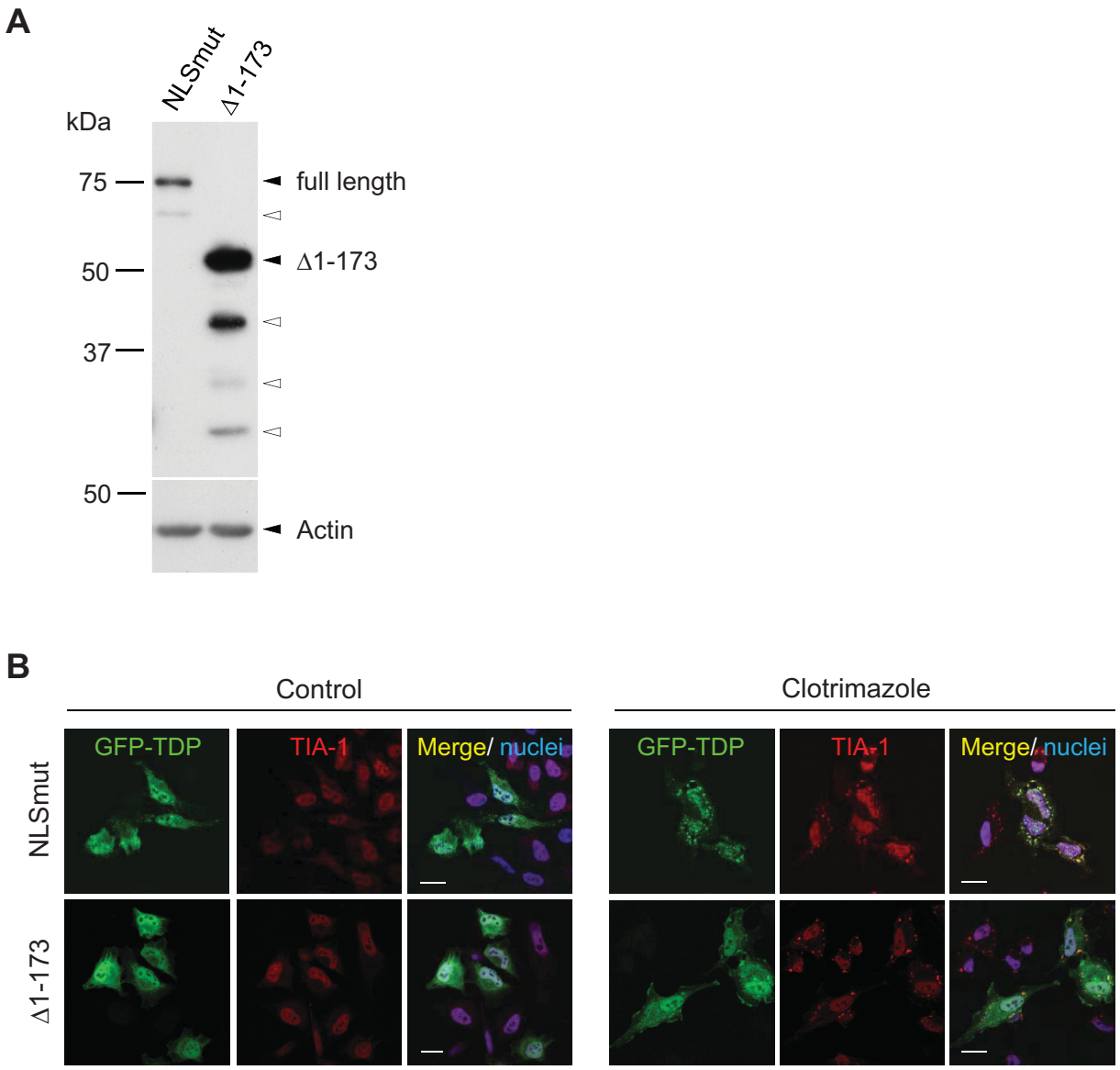
A
NLSmut
Δ1-173
kDa
75
50
37
50
full length
Δ1-173
Actin
B
Control
Clotrimazole
GFP-TDP
TIA-1
Merge/ nuclei
NLSmut
Δ1-173

doi:10.1093/brain/awr201 Brain 2011: 134; 2595–2609 | 2595

BRAIN
A JOURNAL OF NEUROLOGY

FET proteins TAF15 and EWS are selective markers that distinguish FTLD with FUS pathology from amyotrophic lateral sclerosis with *FUS* mutations

Manuela Neumann,[1] Eva Bentmann,[2,3] Dorothee Dormann,[2,3] Ali Jawaid,[1] Mariely DeJesus-Hernandez,[4] Olaf Ansorge,[5] Sigrun Roeber,[6] Hans A. Kretzschmar,[6] David G. Munoz,[7] Hirofumi Kusaka,[8] Osamu Yokota,[9] Lee-Cyn Ang,[10] Juan Bilbao,[11] Rosa Rademakers,[4] Christian Haass[2,3] and Ian R. A. Mackenzie[12]

1 Institute of Neuropathology, University Hospital Zurich, Zurich, Switzerland
2 Adolf-Butenandt-Institute, Biochemistry, Ludwig-Maximilians-University, Munich, Germany
3 DZNE–German Centre for Neurodegenerative Diseases, Munich, Germany
4 Department of Neuroscience, Mayo Clinic, Jacksonville, FL, USA
5 Department of Neuropathology, John Radcliffe Hospital, Oxford, UK
6 Centre for Neuropathology and Prion Research, Ludwig-Maximilians-University, Munich, Germany
7 Department of Laboratory Medicine and Pathobiology, University of Toronto and St. Michael's Hospital, Toronto, ON, Canada
8 Department of Neurology, Kansai Medical University, Osaka, Japan
9 Department of Neuropsychiatry, Okayama University Graduate School of Medicine, Dentistry and Pharmaceutical Sciences, Okayama, Japan
10 Department of Pathology, London Health Sciences Centre, London, ON, Canada
11 Department of Pathology, Sunnybrook Health Sciences Centre, Toronto, ON, Canada
12 Department of Pathology, University of British Columbia and Vancouver General Hospital, Vancouver, BC, Canada

Correspondence to: Manuela Neumann,
Institute of Neuropathology,
Schmelzbergstr. 12, 8091 Zurich,
Switzerland
E-mail: manuela.neumann@usz.ch

Accumulation of the DNA/RNA binding protein fused in sarcoma as cytoplasmic inclusions in neurons and glial cells is the pathological hallmark of all patients with amyotrophic lateral sclerosis with mutations in *FUS* as well as in several subtypes of frontotemporal lobar degeneration, which are not associated with *FUS* mutations. The mechanisms leading to inclusion formation and fused in sarcoma-associated neurodegeneration are only poorly understood. Because fused in sarcoma belongs to a family of proteins known as FET, which also includes Ewing's sarcoma and TATA-binding protein-associated factor 15, we investigated the potential involvement of these other FET protein family members in the pathogenesis of fused in sarcoma proteinopathies. Immunohistochemical analysis of FET proteins revealed a striking difference among the various conditions, with pathology in amyotrophic lateral sclerosis with *FUS* mutations being labelled exclusively for fused in sarcoma, whereas fused in sarcoma-positive inclusions in subtypes of frontotemporal lobar degeneration also consistently immunostained for TATA-binding protein-associated factor 15 and variably for Ewing's sarcoma. Immunoblot analysis of proteins extracted from post-mortem tissue of frontotemporal lobar degeneration with fused in sarcoma pathology demonstrated a relative shift of all FET proteins towards insoluble protein fractions, while genetic analysis of the *TATA-binding protein-associated factor 15* and *Ewing's sarcoma* gene did not identify any pathogenic variants. Cell culture experiments replicated the findings of amyotrophic lateral sclerosis with *FUS* mutations by confirming the absence of TATA-binding protein-associated factor 15 and Ewing's sarcoma alterations upon expression of mutant fused in sarcoma. In contrast, all endogenous FET proteins were

Received May 25, 2011. Revised July 13, 2011. Accepted July 20, 2011

recruited into cytoplasmic stress granules upon general inhibition of Transportin-mediated nuclear import, mimicking the findings in frontotemporal lobar degeneration with fused in sarcoma pathology. These results allow a separation of fused in sarcoma proteinopathies caused by *FUS* mutations from those without a known genetic cause based on neuropathological features. More importantly, our data imply different pathological processes underlying inclusion formation and cell death between both conditions; the pathogenesis in amyotrophic lateral sclerosis with *FUS* mutations appears to be more restricted to dysfunction of fused in sarcoma, while a more global and complex dysregulation of all FET proteins is involved in the subtypes of frontotemporal lobar degeneration with fused in sarcoma pathology.

Keywords: FUS; TAF15; EWS; amyotrophic lateral sclerosis; frontotemporal dementia

Abbreviations: ALS = amyotrophic lateral sclerosis; BIBD = basophilic inclusion body disease; EWS = Ewing's sarcoma protein; FUS = fused in sarcoma; FTLD = frontotemporal lobar degeneration; FTLD-U = frontotemporal lobar degeneration with ubiquitin-positive inclusions; NIFID = neuronal intermediate filament inclusion body disease; TAF15 = TATA-binding protein-associated factor 15; TDP-43 = TAR-DNA binding protein 43 kDa

Introduction

The identification of the DNA/RNA binding protein TAR-DNA binding protein 43 kDa (TDP-43) as the disease protein in most forms of amyotrophic lateral sclerosis (ALS) and in the most common form of frontotemporal lobar degeneration (FTLD), confirmed that these two neurodegenerative conditions belong to a clinicopathological spectrum of diseases and initiated the concept of RNA dysmetabolism as a crucial event in disease pathogenesis (Neumann et al., 2006; Mackenzie *et al.*, 2010*a*). This idea was corroborated with the subsequent discovery of another DNA/RNA binding protein fused in sarcoma (FUS), as the pathological protein in many remaining TDP-43-negative cases with ALS and FTLD.

Briefly, the finding of mutations in the *FUS* gene as cause of familial ALS (Kwiatkowski *et al.*, 2009; Vance *et al.*, 2009) was rapidly confirmed in genetic screenings of large ALS cohorts throughout the world and were found to account for ~3% of familial ALS and ~1% of sporadic ALS (Mackenzie *et al.*, 2010*a*). The majority of *FUS* mutations cluster in the C-terminus of the protein that encodes for a non-classical nuclear localization sequence (Lee *et al.*, 2006; Dormann *et al.*, 2010). *FUS* mutations have been shown to disrupt this motif, resulting in impaired Transportin-mediated nuclear import of FUS and increased concentrations of cytoplasmic FUS (Dormann *et al.*, 2010; Ito *et al.*, 2011; Kino *et al.*, 2011). In line with the idea that altered nuclear import is a key event in disease pathogenesis, the neuropathology associated with ALS with *FUS* mutations (ALS-*FUS*) is characterized by abnormal cytoplasmic neuronal and glial inclusions that are immunoreactive for FUS (Kwiatkowski *et al.*, 2009; Vance *et al.*, 2009; Blair *et al.*, 2010; Groen *et al.*, 2010; Hewitt *et al.*, 2010; Rademakers *et al.*, 2010; Mackenzie *et al.*, 2011*b*).

Subsequently, FUS was studied in other neurodegenerative diseases and identified as a component of the inclusions in several subtypes of FTLD, now subsumed as FTLD-FUS (Mackenzie *et al.*, 2010*b*). This group includes cases initially designated as atypical FTLD with ubiquitin-positive inclusions (FTLD-U) (Neumann *et al.*, 2009*b*), neuronal intermediate filament inclusion disease (NIFID) (Neumann *et al.*, 2009*a*) and basophilic inclusion body disease (BIBD) (Munoz *et al.*, 2009). In contrast to cases presenting with pure ALS, which are almost always associated with mutations in *FUS*, no genetic alterations of *FUS* have been reported to date for cases within the FTLD-FUS group (Neumann *et al.*, 2009*a*, *b*; Rohrer *et al.*, 2010; Urwin *et al.*, 2010; Snowden *et al.*, 2011). Thus, the mechanisms underlying FUS accumulation in FTLD-FUS as well as an explanation for the different patterns of FUS pathology in the distinct FTLD-FUS subtypes awaits further clarification (Mackenzie *et al.*, 2011*a*).

FUS is a multifunctional DNA/RNA binding protein and belongs to the FET family of proteins that also includes Ewing's sarcoma protein (EWS), TATA-binding protein-associated factor 15 (TAF15) and the *Drosophila* orthologue Cabeza (Law *et al.*, 2006; Kovar 2011). The FET proteins were initially discovered as components of fusion oncogenes that cause human cancers. Their normal function is predicted to include roles in RNA transcription, processing, transport, microRNA processing and DNA repair (Law *et al.*, 2006; Tan and Manley, 2009; Kovar, 2011). In most cell types, all of the FET proteins are predominantly localized to the nucleus, but they are able to continuously shuttle between the nucleus and cytoplasm (Zinszner *et al.*, 1997; Zakaryan and Gehring 2006; Jobert *et al.*, 2009). Protein-interaction studies have revealed that FET proteins are able to interact with each other, suggesting that they may form protein complexes (Pahlich *et al.*, 2008; Kovar, 2011). This raises the possibility that alterations of TAF15 and EWS might also be involved in the pathogenesis of FUS-opathies.

In order to address this hypothesis we performed detailed immunohistochemical, biochemical and genetic analyses of TAF15 and EWS in a range of cases with FTLD-FUS and ALS-*FUS* that covers the complete spectrum of FUS-opathies. Our data revealed striking differences in FET protein alterations between ALS-*FUS* and FTLD-FUS, thereby strongly suggesting different disease mechanisms underlying these conditions.

Materials and methods

Case selection

Cases with FUS pathology, including atypical FTLD-U ($n = 15$), BIBD ($n = 7$), NIFID ($n = 4$) and ALS-*FUS* ($n = 6$), were selected from previous studies (Munoz *et al.*, 2009; Neumann *et al.*, 2009*a*, *b*; Mackenzie *et al.*, 2011*a*, *b*). Detailed clinical and pathological description of each

of the FTLD-FUS and ALS-*FUS* cases has been published previously and is summarized in Supplementary Table 1.

Neurological control cases for immunohistochemistry included FTLD with TDP-43 pathology [($n = 17$); including sporadic subtype 1 ($n = 3$), subtype 2 ($n = 2$), subtype 3 ($n = 6$), according to Mackenzie *et al*. 2006, familial with *GRN* mutations ($n = 2$), familial with *VCP* mutations ($n = 2$) and familial linked to chromosome 9p ($n = 2$)], FTLD with tau pathology ($n = 8$; including two each of Pick's disease, progressive supranuclear palsy, corticobasal degeneration and argyrophilic grain disease), FTLD with *CHMP2B* mutations ($n = 2$), sporadic ALS with TDP-43 pathology ($n = 8$), familial ALS with *SOD1* mutations ($n = 2$), Alzheimer's disease ($n = 4$), Lewy body disease ($n = 4$), multiple system atrophy ($n = 2$), Huntington's disease ($n = 2$), spinocerebellar ataxia ($n = 3$) and neuronal intranuclear inclusion body disease ($n = 1$). Normal control tissue ($n = 4$) was from elderly patients with no history of neurological disease.

Antibodies

A number of commercially available anti-TAF15 and anti-EWS antibodies were tested by immunohistochemistry on formalin-fixed paraffin-embedded brain tissue and by immunoblot. Results are summarized in Supplementary Table 2. Three TAF15 antibodies revealed physiological staining in tissue sections. The polyclonal antibody TAF15-IHC-00094-1 (Bethyl) was used for staining of all cases and for immunofluorescence. TAF15-309A and 308A (Bethyl) were used for confirmation in selected sections and for immunoblots; TAF15-308A was used in cell culture experiments. For EWS, four antibodies revealed physiological staining in tissue sections. The monoclonal antibody EWS-G5 (Santa Cruz) was used for staining of all cases, immunofluorescence, immunoblotting and cell culture experiments. Selected sections were stained with EWS-IHC-00086 (Bethyl), EWS-3319-1 and EWS-3320-1 (Epitomics) for confirmation. Given the homology of FET proteins, possible cross-reactivity of the TAF15 and EWS antibodies with FUS was excluded by immunoblot analysis (Supplementary Fig. 1).

Other primary antibodies employed included polyclonal anti-FUS HPA008784 (Sigma-Aldrich, 1 : 2000), FUS-302A (Bethyl, 1 : 10 000), monoclonal anti-FUS (ProteintechGroup, 1 : 1000), monoclonal anti-α-internexin (Zymed, 1 : 500), monoclonal anti-haemagglutinin (Sigma, 1 : 500), and polyclonal anti-haemagglutinin (Sigma, 1 : 200).

Immunohistochemistry and immunofluorescence

Immunohistochemistry was performed on 5-μm thick paraffin sections using the Ventana BenchMark XT automated staining system (Ventana) and developed with aminoethylcarbizole or using the NovoLink™ Polymer Detection Kit and developed with 3,3′-diaminobenzidine. Microwave antigen retrieval was performed for all stainings.

FUS, TAF15 and EWS pathology was evaluated using a semi-quantitative grading system, similar to that used in previous studies in which the pathological lesions are scored as absent (−), rare (+), occasional (++), common (+++) or numerous (++++). A grading of 'rare' indicates that extensive survey of the tissue section is required for identification. 'Occasional' means that the lesions are easy to find but not present in every microscopic field. The pathology is considered 'common' when at least one example is present in most high-power fields. When many lesions are present in every high-power field, then the lesions are considered to be 'numerous'.

Double-label immunofluorescence was performed on selected cases for FUS and TAF15 or EWS, and α-internexin and TAF15 or EWS. The secondary antibodies were Alexa Fluor 594 and Alexa Fluor 488 conjugated anti-mouse and anti-rabbit IgG (Invitrogen, 1 : 500). 4′-6-diamidino-2-phenylindol was used for nuclear counterstaining. Immunofluorescence images of brain sections were obtained by wide-field fluorescence microscopy (BX61 Olympus with digital camera F-view, Olympus).

Biochemical analysis

Fresh-frozen post-mortem frontal grey matter from atypical FTLD-U ($n = 5$), BIBD ($n = 1$), NIFID ($n = 1$), FTLD with TDP-43 pathology ($n = 5$), Alzheimer's disease ($n = 2$) and normal controls ($n = 4$) was used for the sequential extraction of proteins with buffers of increasing stringency, using a protocol described previously (Neumann *et al*., 2009*b*). Briefly, grey matter was extracted at 2 ml/g (v/w) by repeated homogenization and centrifugation steps (120 000 *g*, 30 min, 4°C) with high-salt buffer (50 mM Tris–HCl, 750 mM NaCl, 10 mM NaF, 5 mM EDTA, pH 7.4), 1% Triton-X 100 in high-salt buffer, radioimmunoprecipitation assay buffer (50 mM Tris–HCl, 150 mM NaCl, 5 mM EDTA, 1% NP-40, 0.5 % sodium deoxycholate, 0.1% sodium dodecyl sulphate) and 2% sodium dodecyl sulphate buffer. To prevent carry over, each extraction step was performed twice. Supernatants from the first extraction steps were analysed while supernatants from the wash steps were discarded. The 2% sodium dodecyl sulphate insoluble pellet was extracted in 70% formic acid at 0.5 ml/g (v/w), evaporated in a SpeedVac system. The dried pellet was resuspended in sample buffer and the pH adjusted with NaOH. Protease inhibitors were added to all buffers prior to use. For immunoblot analysis, fractions were resolved by 7.5% sodium dodecyl sulphate–polyacrylamide gel electrophoresis and transferred to polyvinylidene difluoride membranes (Millipore). Membranes were blocked with Tris-buffered saline containing 3% powdered milk and probed with anti-FUS, anti-TAF-15 or anti-EWS antibodies. Primary antibodies were detected with horseradish peroxidase-conjugated anti-rabbit or anti-mouse IgG (Jackson ImmunoResearch), signals were visualized by a chemiluminescent reaction (Pierce) and the Chemiluminescence Imager Stella 3200 (Raytest). Quantification of band intensities was performed with AIDA software. The Mann–Whitney U-test was used for statistical analysis of insoluble/soluble ratios with significance level set as $P < 0.05$.

Cell culture experiments

HeLa cells were cultured in Dulbecco's modified Eagle's medium with Glutamax (Invitrogen) supplemented with 10% (v/v) foetal calf serum (Invitrogen) and penicillin/streptomycin. Transfection of HeLa cells was carried out with Fugene 6 (Roche) or Lipofectamine 2000 (Invitrogen) according to the manufacturer's instructions. Expression vectors with haemagglutinin-tagged human FUS with the p.P525L mutation and with the Transportin-specific inhibitor peptide M9M fused to green fluorescent protein were generated as described previously (Dormann *et al*., 2010). In some experiments, cells were subjected to heat shock (1 h at 44°C) 24 h after transfection. For immunofluorescence, HeLa cells were fixed for 15 min in 4% paraformaldehyde in phosphate-buffered saline, permeabilized for 5 min in 0.2% Triton X-100 with 50 mM NH_4Cl and subsequently blocked for 20–30 min in 5% goat serum. Cells were stained with the indicated primary and secondary antibodies, diluted in blocking buffer for 30 min. Alexa Fluor 488, 555 and 647 conjugated goat anti-mouse and goat anti-rabbit IgGs were used as secondary antibodies. To visualize nuclei,

cells were stained with TO-PRO-3 iodide (Invitrogen) for 15 min. Confocal images were obtained with an inverted laser scanning confocal microscope (Zeiss Axiovert 200M).

Genetic analysis

DNA was available from six atypical FTLD-U, one NIFID and one BIBD case. *EWS breakpoint region 1 (EWSR1)* exons 1–18 and *TAF15* exons 1–16 were polymerase chain reaction amplified using primers designed to flanking intronic sequences using Qiagen products (Qiagen). Polymerase chain reaction conditions and primer sequences available on request. Polymerase chain reaction products were purified using the Ampure system (Agencourt Bioscience Corporation) and sequenced using Big Dye terminator V.3.1 products (Applied Biosystems). Sequencing products were purified using the CleanSEQ method (Agencourt) and analysed on an ABI 3730 DNA analyser (Applied Biosystems). Sequence analysis was performed using Sequencher software (Gene Codes).

Results

Detailed clinical and pathological descriptions of each of the cases with FTLD-FUS and ALS-*FUS* have been published previously and are summarized in Supplementary Table 1. TAF15 and EWS pathology was evaluated in neuroanatomical regions previously shown to be most affected by FUS pathology in each condition and results are summarized in Table 1.

TAF15 and EWS pathology is present in all subtypes of frontotemporal lobar degeneration with FUS pathology

Immunohistochemistry for TAF15 revealed robust physiological staining of neuronal nuclei and weaker and more variable staining of glial nuclei in all cases and controls (Fig. 1A). All subtypes of FTLD-FUS showed strong TAF15 immunoreactivity in neuronal and glial inclusions that were of similar morphology, number and anatomical distribution as demonstrated with FUS antibodies (Fig. 1 and Table 1). Specifically, atypical FTLD-U cases showed TAF15-positive round neuronal cytoplasmic inclusions in hippocampus, neocortex and lower motor neurons, as well as vermiform or round neuronal intranuclear inclusions predominantly in the dentate gyrus (Fig. 1B–E). NIFID and BIBD cases were found to have numerous round or tangle-like inclusions throughout cortical, subcortical, brainstem and spinal cord regions (Fig. 1F–H). In addition to neuronal inclusions, all subtypes of FTLD-FUS revealed at least some TAF15-positive dystrophic neurites and glial cytoplasmic inclusions (Fig. 1I, J) that were more numerous in NIFID and BIBD than in atypical FTLD-U. Notably, most inclusion bearing cells in FTLD-FUS showed a striking reduction of the physiological nuclear staining for TAF15 (Fig. 1B and C). Similar results were observed using TAF15 antibodies recognizing different epitopes, including the mid-region and C-terminus.

Double-label immunofluorescence confirmed co-localization of FUS and TAF15 in almost all inclusions in FTLD-FUS cases (Fig. 2). There was a tendency for intranuclear inclusions in atypical FTLD-U and NIFID to be more strongly labelled for FUS compared with TAF15 and they were rarely found to be only FUS positive (Fig. 2B). In NIFID cases, TAF15 and α-internexin labelled discrete inclusions in the same neurons (Supplementary Fig. 2A), a finding similar to our previous results for FUS and α-internexin (Neumann *et al.*, 2009*a*).

Antibodies against EWS revealed nuclear and diffuse cytoplasmic staining of neuronal and glial cells as the normal physiological staining pattern (Fig. 3A). However, EWS staining was more variable among cases compared with TAF15 with some sections completely lacking physiological staining while others revealed strong background staining making the scoring of EWS pathology in some cases more uncertain. Nevertheless, all subtypes of FTLD-FUS revealed at least some EWS-positive inclusions (Fig. 3 and Table 1) and similar results were obtained with four EWS antibodies recognizing different epitopes at the N-terminal and mid-region. Importantly, notable differences were observed between the distinct FTLD-FUS subtypes. In atypical FTLD-U, EWS-positive neuronal cytoplasmic and intranuclear inclusions were less numerous than those labelled with FUS, being rare to moderate in neocortical regions and lower motor neurons (Fig. 3B–D and G) and the staining intensity tended to be rather weak. In contrast, inclusions in NIFID and BIBD revealed a much more robust EWS staining intensity and the frequency of pathology in cortical, subcortical, brainstem and spinal cord regions was comparable with that seen with FUS (Fig. 3E, F and H). Due to the variability in staining intensity among cases, analysis of the normal physiological staining pattern of EWS was more difficult to assess; however, nuclear EWS staining was retained in at least some inclusion bearing cells.

Double-label immunofluorescence for EWS and FUS confirmed that in atypical FTLD-U only a subset of FUS-positive inclusions also labelled for EWS (Fig. 4A), while most FUS pathology in NIFID and BIBD revealed clear EWS co-localization (Fig. 4B–E). EWS and α-internexin labelled discrete inclusions in the same neurons in NIFID (Supplementary Fig. 2B) in accordance with the FUS and TAF15 results.

Absence of TAF15 and EWS pathology in amyotrophic lateral sclerosis with FUS mutations

Next, we analysed the pattern of TAF15 and EWS staining in six ALS-*FUS* cases, which included four different *FUS* mutations. All cases showed robust FUS pathology, particularly in the spinal cord and motor cortex, with neuronal cytoplasmic inclusions (including basophilic inclusions) as well as variable presence of glial inclusions (Mackenzie *et al.*, 2011*b*). Interestingly, and in striking contrast to FTLD-FUS, neither TAF15 nor EWS immunohistochemistry demonstrated any neuronal or glial inclusions in cortical, subcortical, brainstem or spinal cord regions in any of the ALS-*FUS* cases (Fig. 5). The absence of TAF15 and EWS immunoreactivity of FUS-positive inclusions in ALS-*FUS* was further confirmed by double-label immunofluorescence (Fig. 5G–L). Notably, cells with FUS-immunoreactive inclusions retained their physiological nuclear staining for TAF15 and EWS.

Table 1 Summary of immunoreactivity for FET proteins in FTLD-FUS subtypes and ALS-*FUS*

	FUS					TAF15					EWS				
	FC	HC	BG	BS	LMN	FC	HC	BG	BS	LMN	FC	HC	BG	BS	LMN
Atypical FTLD-U															
1	+ +	+ + + +	+ + +	+ + +	+ +	+ + +	+ + + +	ND	ND	+ + +	+	+ + +	ND	ND	NA
2	+ + +	NA	+ + +	+ + +	+ +	+ + +	NA	ND	ND	+ +	+ + +	NA	ND	ND	(+)
3	+ +	+ + +	+ + +	+ +	+ + +	+ +	+ + +	ND	ND	+ + +	+ +	+ +	ND	ND	+ +
4	+ +	+ +	+ +	NA	NA	+ + +	+ +	ND	NA	NA	+ +	(+)	ND	NA	NA
5	+ + +	+ + + +	+ + +	+ + +	+ + +	+ + +	+ + + +	ND	ND	+ + + +	+ +	+ + +	ND	ND	(+ +)
6	+ + +	+ + + +	+ + +	+ + +	+	+ + + +	+ + + +	ND	ND	+ +	+ +	+ + +	ND	ND	(+)
7	+ + +	+ + + +	NA	NA	+	+ + +	+ + + +	NA	NA	+	+	+ +	NA	NA	–
8	+ + + +	+ + + +	+ + + +	+ +	+ +	+ + + +	+ + + +	ND	ND	+ +	+	+ + +	ND	ND	+
9	+ +	+ + +	NA	NA	+ +	+ +	NA	NA	NA	+ +	+	NA	NA	NA	+
10	+ +	+ + +	+ +	+ +	+ +	+ +	+ + +	ND	ND	+ +	+	+	ND	ND	+
11	+ +	+ +	+ +	+ +	+	+ +	NR	ND	ND	+ +	+	NR	ND	ND	+
12	+ +	+ +	+ +	+	+ +	+ + +	+ +	ND	ND	+ +	+	(+)	ND	ND	+
13	+ + +	+ +	+ +	+ +	+ +	+ + +	+ +	ND	ND	+ +	+	+	ND	ND	+
14	+ + +	+ + + +	+ + +	+ + +	+ +	+ + +	+ + + +	ND	ND	+ + +	+	+	ND	ND	+
15	+	+ +	+ + +	+	+	+	+ +	ND	ND	+	(+)	+ +	ND	ND	+
Intensity NCI	Strong					Strong					Weak/Moderate				
NIFID															
1	+ + + +	+ + + +	+ + + +	+ + + +	+ + + +	+ + + +	+ + + +	+ + + +	ND	+ + + +	+ + + +	+ + + +	+ + + +	ND	+ + +
2	+ + + +	+ + + +	+ + + +	+ + + +	+ + + +	+ + + +	+ + + +	+ + + +	ND	+ + + +	+ + + +	+ + + +	+ + +	ND	+ + +
3	+ + + +	+ + + +	+ + + +	+ + + +	+ + + +	+ + + +	+ + + +	+ + + +	ND	+ + + +	+ + + +	+ + + +	+ + + +	ND	+ + + +
4	+ + + +	+ + + +	+ + + +	+ + + +	+	+ + + +	+ + + +	+ + + +	ND	+	+ + + +	+ + + +	+ + + +	ND	NA
Intensity NCI	Strong					Strong					Strong				
BIBD															
1	+ + + +	+ + + +	+ + +	+ + + +	+ + +	+ + + +	+ + + +	+ + +	ND	+ + + +	(+ + + +)	(+ + +)	(+ + +)	ND	(+)
2	+ + + +	+ + + +	+ + + +	+ + + +	+ +	+ + + +	+ + + +	ND	+ + + +	+ + +	(+ +)	(+ +)	ND	(+)	(+)
3	+ + + +	+ + + +	+ + + +	+ + + +	+ + + +	+ + + +	NR	+ + + +	ND	NR	(+ + + +)	NR	(+)	ND	(+ +)
4	+ + + +	+	NA	+ + + +	+ + + +	+ + + +	+	NA	+ + + +	+ + + +	+ + + +	(+)	NA	(+ + + +)	NR
5	+ + + +	+ +	+ +	+ + + +	+ + + +	NR	+	+ + +	+ + +	+ + + +	NR	NA	ND	(+ + +)	(+)
6	+ + + +	+ + +	+ + +	+ + + +	+ + + +	+ + +	+ + +	+ + +	+ + + +	+ + +	+ + +	+ +	+ + +	+ + +	+ + +
7	+ + + +	+ + +	+ + + +	+ + + +	+ +	+ + + +	+ + +	+ + + +	ND	+ +	+ + + +	+ + +	+ + + +	ND	+
Intensity NCI	Strong					Strong					Strong				
ALS-*FUS*															
1 p.R521C	+	–	+ +	+	+ + +	–	ND	–	–	–	–	ND	–	–	–
2 p.R521C	+ +	–	+ +	–	+ + +	–	ND	–	NA	–	NA	ND	NA	NA	–
3 p.R514S/E516V	+ + +	–	+ + +	+ +	+ + +	–	ND	–	–	–	–	ND	–	–	–
4 p.P525L	+ + +	–	–	+	+ + + +	NA	ND	–	–	–	NA	ND	–	–	–
5 p.P525L	+ + +	–	–	+ + +	+ + + +	–	ND	–	–	–	–	ND	–	–	–
6 p.Q519lfsX9	+ + +	–	+	+ + +	+ + +	–	ND	–	–	–	–	ND	–	–	–
Intensity NCI	Strong					Absent					Absent				

Semiquantitative grading: – = absent; + = rare; + + = occasional; + + + = moderate; + + + + = numerous. Scores in parentheses indicate sections where the quality of the immunostaining makes the accuracy of the scoring uncertain. BG = basal ganglia; BS = upper brainstem; FC = frontal cortex (mid-frontal gyrus for atypical FTLD-U, NIFID and BIBD; precentral gyrus for ALS-*FUS*); HC = hippocampus; LMN = lower motor neurons of spinal cord or hypoglossal nucleus; NA = not available; NCI = neuronal cytoplasmic inclusion; ND = staining not done; NR = no immunoreactivity, neither physiological nor pathological in the entire section.

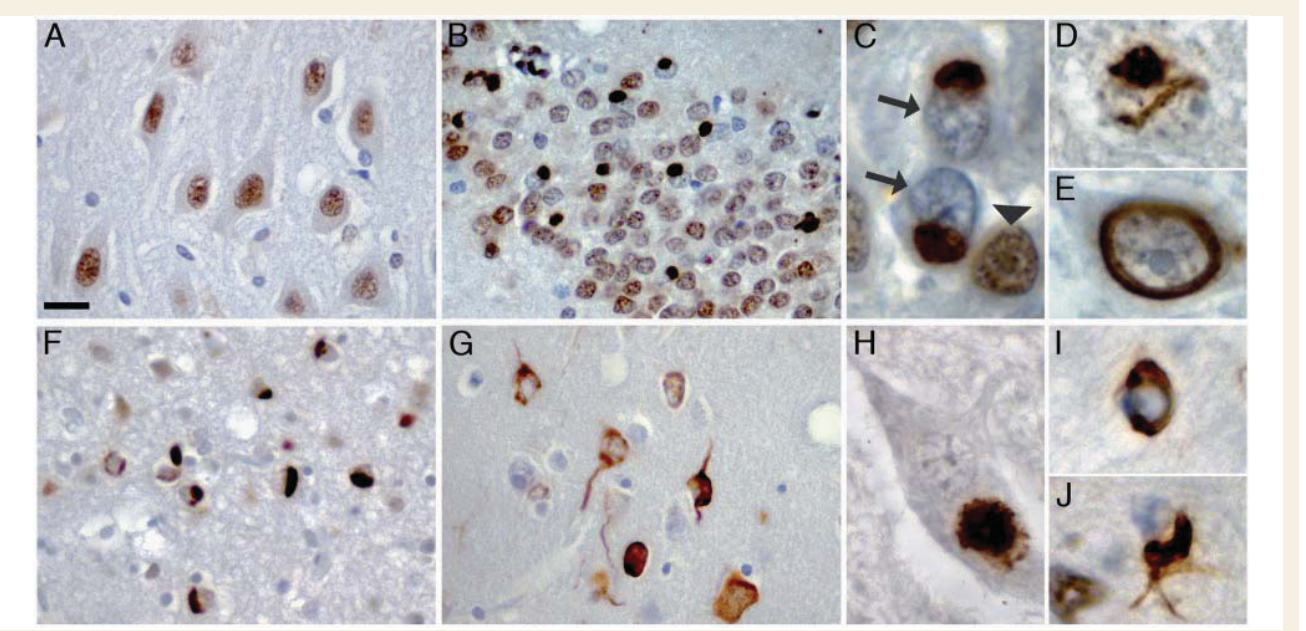

Figure 1 TAF15 pathology in FTLD-FUS. TAF15 immunohistochemisty performed on sections of post-mortem brain tissue from normal control (**A**), atypical FTLD-U (**B–E**), NIFID (**F**) and BIBD (**G–J**). Normal physiological staining pattern, consisting of strong immunoreactivity of neuronal nuclei was seen in normal controls (**A**) and FTLD-FUS subjects (**B**). In atypical FTLD-U numerous round neuronal cytoplasmic inclusions were seen in the dentate granule cells (**B** and **C**). Note the dramatically reduced nuclear staining in inclusion bearing cells (arrows in **C**) compared with adjacent cells without inclusions (arrowhead in **C**). Neuronal intranuclear inclusions with vermiform (**D**) or ring-like morphology (**E**) were a consistent finding in the dentate granule and pyramidal cells of the hippocampus in all subjects with atypical FTLD-U. Numerous cytoplasmic inclusions with variable morphology ranging from round, crescentic, globular and tangle-like were present in neurons in NIFID (**F**) and BIBD (**G**) as shown here in frontal cortex. All FTLD-FUS cases revealed at least rare inclusions in lower motor neurons (**H**) as well as variable numbers of glial cytoplasmic inclusions in the white matter of affected brain regions (**I, J**). Scale bar: **A**, **B**, **F** and **G** = 25 μm; **C–E**, **I** and **J** = 5 μm; **H** = 10 μm.

TAF15 and EWS immunoreactivity in neurological controls

The normal controls and the majority of neurological controls did not reveal any TAF or EWS pathology (Table 2). Specifically, there was no labelling of the characteristic inclusions in Alzheimer's disease, Lewy body disease, FTLD with tau pathology, ALS with TDP-43 pathology or ALS due to *SOD1* mutations. Inclusions in FTLD with TDP-43 pathology were negative, with the exception of one case that showed a small number of TAF15-positive cortical neurites and EWS staining of a minority of inclusions in the hippocampal dentate granule cells. Glial inclusions in multiple system atrophy were negative for FUS and TAF15; however, one case showed weak EWS labelling. Interestingly, intranuclear inclusions in spinocerebellar ataxia and Huntington's disease, previously shown to be FUS positive (Doi *et al.*, 2010; Woulfe *et al.*, 2010), were consistently labelled for EWS but not TAF15, while the FUS-positive inclusions in neuronal intranuclear inclusion body disease were negative for both. These findings for intranuclear inclusions are noteworthy in suggesting that different combinations of FET proteins are involved in inclusion formation in a disease-specific fashion and that co-aggregation of all three FET proteins is a specific feature of FTLD-FUS.

Biochemical analysis of TAF15 and EWS in frontotemporal lobar degeneration with FUS pathology

A change in the solubility of FUS protein has previously been shown to be a consistent biochemical alteration in atypical FTLD-U (Neumann *et al.*, 2009*b*) and NIFID (Page *et al.*, 2011). To gain further insight into potential biochemical alterations of TAF15 and EWS, proteins were sequentially extracted from frozen brain tissue from FTLD-FUS, as well as normal and neurological controls, using a series of buffers containing detergents and acids with an increasing ability to solubilize proteins. Unfortunately, sufficient amounts of frozen tissue from ALS-*FUS* cases were not available for analysis.

TAF15, EWS and FUS could be detected as major bands at the expected molecular mass of ~75, ~90 and ~73 kDa, respectively, in the high salt (soluble proteins) and sodium dodecyl sulphate (enriched for insoluble proteins) fractions from FTLD-FUS, as well as controls (Fig. 6A). However, remarkable differences were observed in the amount of the proteins in the distinct fractions in FTLD-FUS compared with controls. In accordance with previous findings, a clear shift of FUS towards the insoluble fraction was

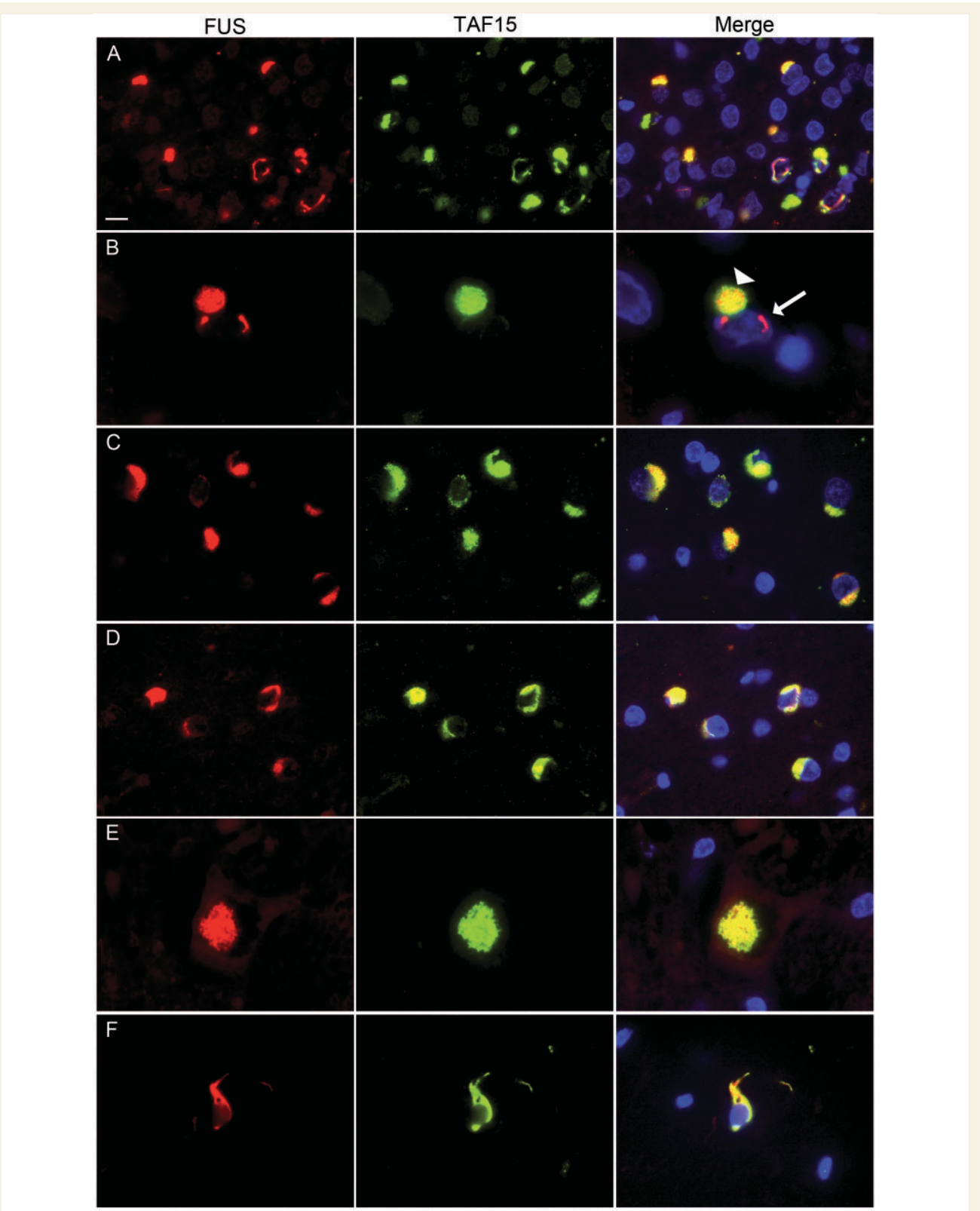

Figure 2 Co-localization of TAF15 and FUS in FTLD-FUS inclusions. Double-label immunofluorescence for FUS (red) and TAF15 (green), with DAPI staining of nuclei in the merged images. (**A**) In atypical FTLD-U the vast majority of inclusions showed co-localization of FUS and TAF15. (**B**) However, note that single neuronal intranuclear inclusions in atypical FTLD-U were not labelled for TAF15 (arrow) while the cytoplasmic inclusion in the same cell shows co-localization (arrowhead). Consistent co-labelling for TAF15 was revealed for FUS pathology in NIFID (**C**) and BIBD (**D**). Inclusions in the lower motor neurons (**E**, atypical FTLD-U case) and glial cytoplasmic inclusions (**F**, BIBD case), also showed colocalization. Scale bar: **A**, **C** and **D** = 10 μm; **B** = 4 μm; **E** and **F** = 6.5 μm.

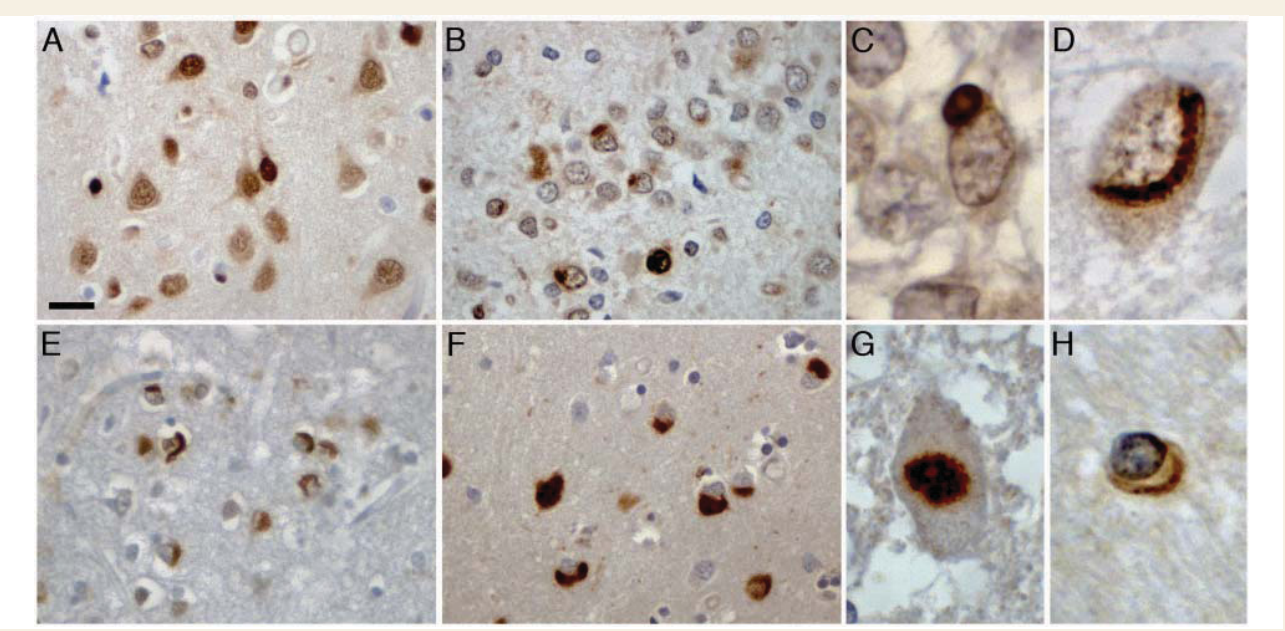

Figure 3 EWS pathology in FTLD-FUS. EWS immunohistochemistry performed on sections of post-mortem brain tissue from normal control (**A**), atypical FTLD-U (**B–D**, **G**), NIFID (**E**) and BIBD (**F** and **H**). Normal physiological staining pattern of nuclei and diffuse cytoplasmic labelling (**A**). In atypical FTLD-U, round cytoplasmic and intranuclear inclusions were observed in the dentate granule cells with variable labelling intensity (**B**). Higher magnification of cytoplasmic (**C**) and vermiform intranuclear inclusion (**D**) in atypical FTLD-U. Numerous neuronal cytoplasmic inclusions with variable morphology including round, crescentic, globular and tangle-like showed strong immunoreactivity in NIFID (**E**) and BIBD (**F**) as shown here in frontal cortex. Most cases with FTLD-FUS revealed at least rare inclusions in lower motor neurons (**G**) as well as variable numbers of glial cytoplasmic inclusions in the white matter of affected brain regions (**H**). Scale bar: **A**, **B**, **E** and **F** = 25 μm; **C**, **D** and **H** = 5 μm; **G** = 10 μm.

seen in all FTLD-FUS cases resulting in a significantly higher insoluble : soluble ratio (median 0.58, mean 2.51 ± 3.54), compared with controls (median 0.13, mean 0.17 ± 0.17, $P = 0.0038$) (Fig. 6B). A similar change in solubility was observed for TAF15 with a significantly higher insoluble : soluble ratio for FTLD-FUS cases (median 2.47, mean 4.09 ± 3.70) compared with controls (median 0.50, mean 0.36 ± 0.21, $P = 0.0006$). Notably, in some FTLD-FUS cases the shift in solubility was even more pronounced for TAF15 than that observed for FUS (e.g. atypical FTLD-U Case 14 and NIFID Case 2). For EWS, there was a similar tendency for higher levels in the insoluble protein fraction in cases with FTLD-FUS (median 1.55, mean 1.5 ± 0.78) compared with controls (median 0.80, mean ratio = 0.8 ± 0.44); however, the difference did not reach significance.

Despite the change in solubility, there was no evidence of other biochemical alterations of TAF15 and EWS, as indicated by abnormal molecular weight species, using antibodies specific for different TAF15 and EWS epitopes.

Genetic analysis of TAF15 and EWSR1 in frontotemporal lobar degeneration with FUS pathology

Sequence analyses of *EWSR1* and *TAF15* did not identify any novel coding variants in the eight FTLD-FUS cases with DNA available, with the exception of a 24 base pair deletion in *TAF15* exon 15 in atypical FTLD-U Case 13 (c.1674_1697del), predicted to delete eight amino acids (p.G559_Y566del). This particular deletion has not been reported previously; however, similar deletions have been found in controls, suggesting it is likely a benign polymorphism (Ticozzi *et al.*, 2011). Novel non-coding variants identified are summarized in Supplementary Table 3.

Characteristic features of human FUS-opathies are recapitulated in cultured cells

The strikingly different patterns of FET protein immunoreactivity in the pathology of FTLD-FUS versus ALS-*FUS*, suggest different mechanisms underlying inclusion body formation. To further address this issue we investigated whether the absence of TAF15 and EWS alterations seen in ALS-*FUS* would be recapitulated in cultured cells expressing mutant FUS.

In accordance with previous results (Dormann *et al.*, 2010), HeLa cells expressing FUS with the p.P525L mutation (a mutation present in two of our studied cases with ALS) showed a robust increase of cytoplasmic FUS compared with cells expressing wild-type FUS (Fig. 7A and Supplementary Fig. 3). Under stress conditions of heat shock, cells expressing mutant FUS showed recruitment of FUS into punctuate cytoplasmic structures,

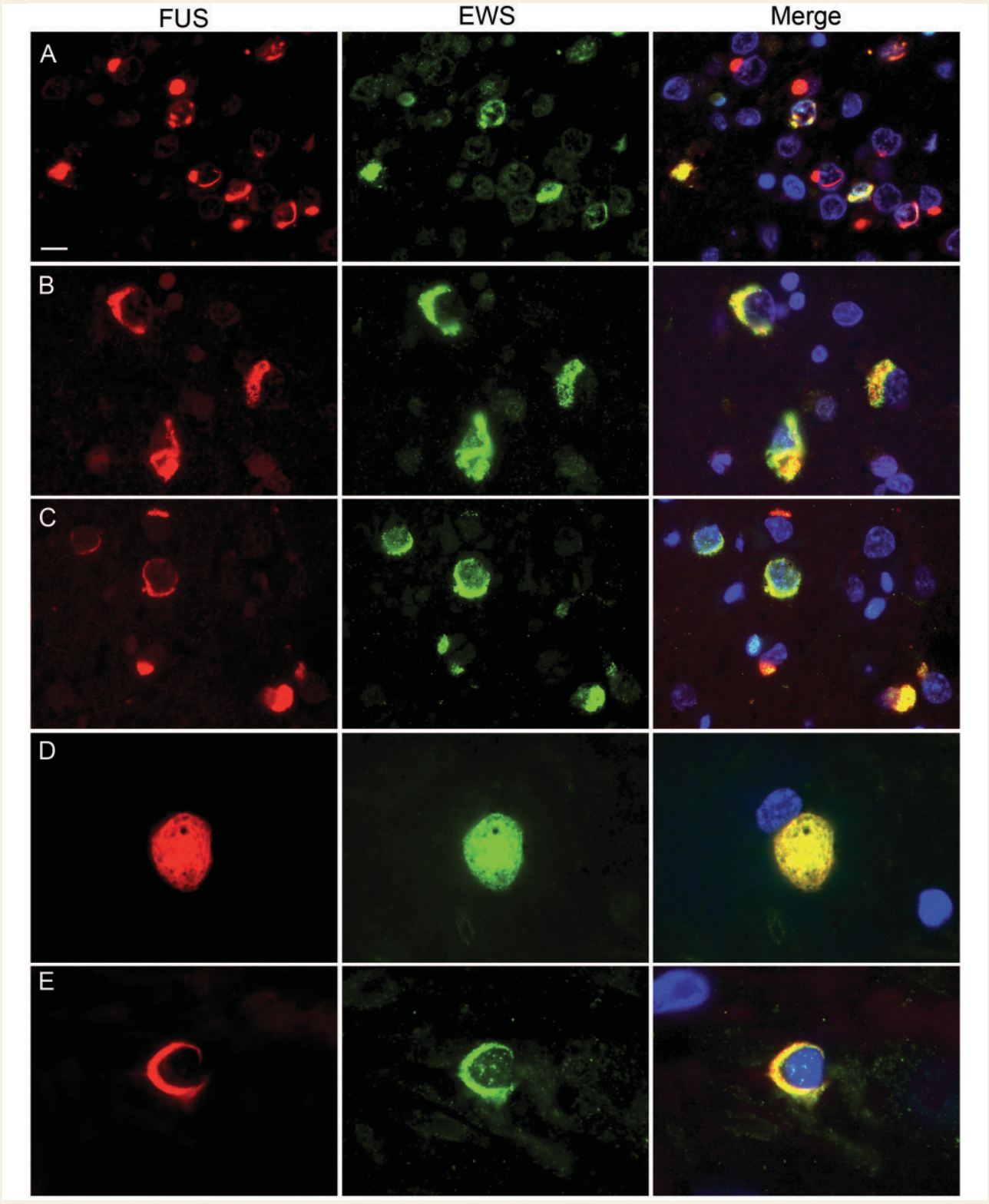

Figure 4 Co-localization of EWS and FUS in FTLD-FUS inclusions. Double-label immunofluorescence for FUS (red) and EWS (green), with DAPI staining of nuclei in the merged images. In atypical FTLD-U, only a subset of FUS-positive neuronal cytoplasmic and intranuclear inclusions were stained for EWS (**A**). In contrast, robust co-labelling for EWS and FUS was observed in most inclusions in NIFID (**B**) and BIBD (**C**). Inclusions in the lower motor neurons (**D,** BIBD case) as well as glial cytoplasmic inclusions (**E,** BIBD case) also showed co-localization. Scale bar: **A–C** = 10 μm; **D** = 6.5 μm; **E** = 4 μm.

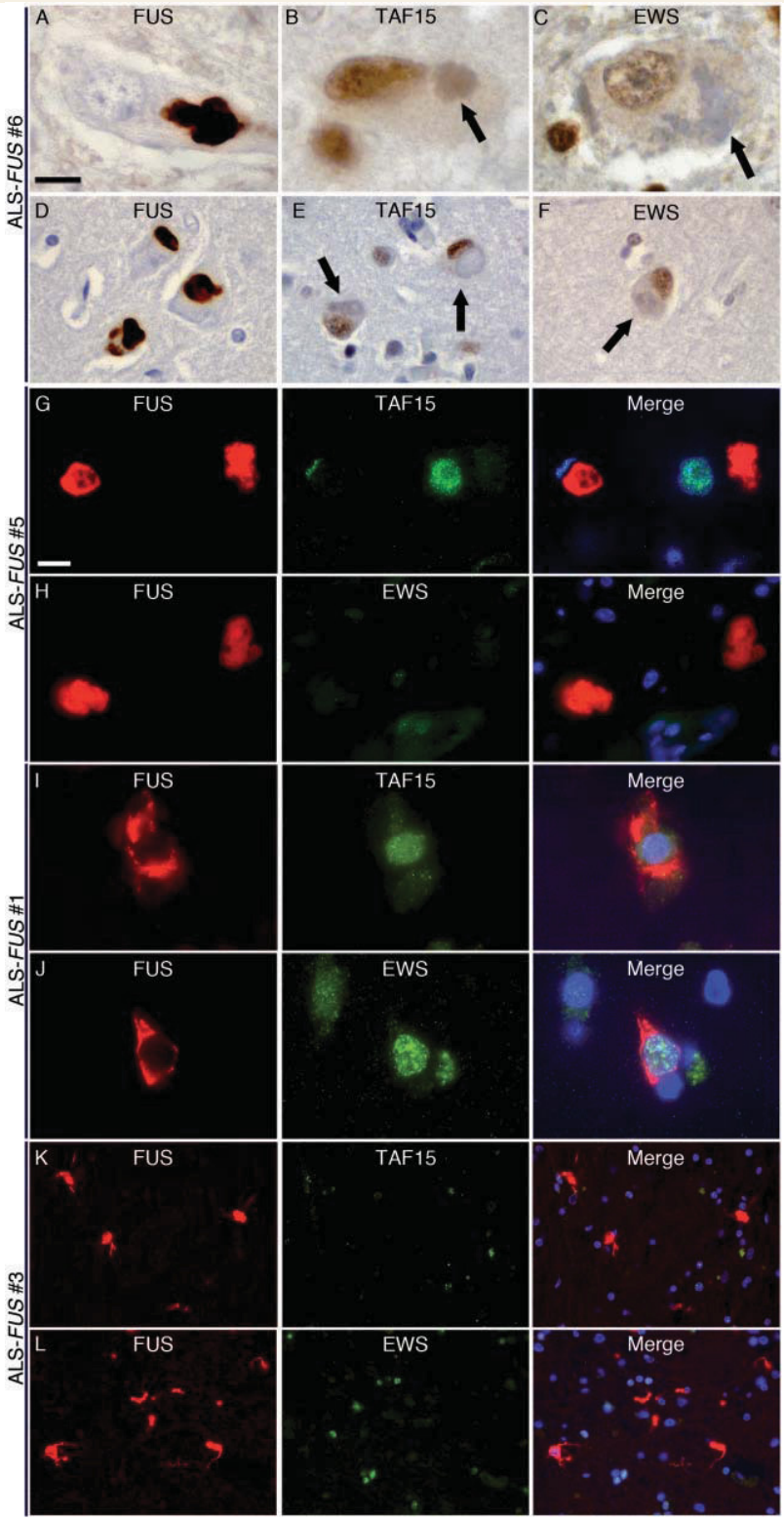

Figure 5 Absence of TAF15 and EWS pathology in ALS-*FUS*. Lower (**A**) and upper (**D**) motor neurons in all ALS-*FUS* cases contained at least some cytoplasmic inclusions strongly labelled for FUS; however, no inclusions (including basophilic inclusions, arrows) were labelled for TAF15 (**B**, lower motor neuron; **E**, upper motor neuron) or EWS (**C**, lower motor neuron; **F**, upper motor neuron). Note the regular nuclear staining for both TAF15 (**B** and **E**) and EWS (**C** and **F**) in inclusion-bearing cells (arrows). The absence of TAF15 and EWS pathology in ALS-*FUS* was confirmed by double-label immunofluorescence that showed robust FUS-immunoreactivity of round and tangle-like neuronal inclusions in the spinal cord (red, **G–J**) that were not labelled for TAF15 (green in **G** and **I**) or EWS (green in **H** and **J**). In addition, FUS-positive glial cytoplasmic inclusions present in a subset of cases (red, **K** and **L**, basal ganglia) showed no co-localization for TAF15 (green, **K**) or EWS (green, **L**). Scale bar in **A**: **A–C** = 10 μm; **D–F** = 22 μm. Scale bar in **G**: **G–J** = 10 μm; **K** and **L** = 30 μm.

Table 2 Immunoreactivity for FET proteins in other neurodegenerative diseases

Diagnosis	FUS	TAF15	EWS
AD	0/4	0/4	0/4
FTLD-TDP	0/17	1/17[a]	1/17[a]
FTLD with *CHMP2B*	0/2	0/2	0/2
FTLD-tau	0/8	0/8	0/8
ALS-TDP	0/8	0/8	0/8
ALS with *SOD1*	0/2	0/2	0/2
MSA	0/2	0/2	1/2[b]
LBD	0/2	0/2	0/2
SCA	3/3	0/3	3/3
HD	2/2	0/2	2/2
NIIBD	1/1	0/1	0/1

a One FTLD-TDP subtype 2 case [according to (Mackenzie *et al*., 2006)] with semantic dementia showed moderated EWS-immunoreactivity in a subset of neuronal cytoplasmic inclusions in the dentate gyrus and TAF15-immunoreactivity in a small proportion of long neurites.
b One case showed EWS-immunoreactivity in a small proportion of glial cytoplasmic inclusions.
AD = Alzheimer's disease; ALS-TDP, amyotrophic lateral sclerosis with TDP-43 pathology; ALS with *SOD1* = amyotrophic lateral sclerosis due to mutations in SOD1 gene; FTLD-TDP = frontotemporal lobar degeneration with TDP-43 pathology; FTLD-tau, frontotemporal lobar degeneration with tau pathology; FTLD with *CHMP2B* = frontotemporal lobar degeneration with mutations in *CHMP2B* gene; HD = Huntington's disease; LBD = Lewy body disease; MSA = multiple system atrophy; NIIBD = neuronal intranuclear inclusion body disease; SCA = spinocerebellar ataxia.

corresponding to stress granules. In contrast, these same conditions resulted in no changes in the subcellular distribution of endogenous TAF15 or EWS. Specifically, both proteins remained almost exclusively within the nucleus and there was no recruitment of TAF15 or EWS into FUS-positive stress granules. In this way, cells expressing an ALS-associated *FUS* mutation recapitulate our findings in human ALS-*FUS*, demonstrating the absence of other FET protein members in cytoplasmic FUS inclusions.

To investigate whether the accumulation of all FET proteins in FTLD-FUS might reflect a more general problem of Transportin-mediated nuclear import, we studied the effect on TAF15 and EWS by transfecting HeLa cells with a Transportin-specific competitive inhibitor peptide (M9M) fused to green fluorescent protein (Fig. 7B). Similar to what has been shown previously for FUS (Dormann *et al*., 2010), a striking redistribution of endogenous TAF15 and EWS proteins to the cytoplasm was observed, that was associated with the formation of stress granules with co-localization of all FET proteins. Notably, recruitment of FUS and TAF15 into stress granules in this system seemed to be more efficient compared with EWS, based on staining intensities of stress granules, recapitulating the differences we observed in the staining intensities of inclusions for FET proteins in atypical FTLD-U. Furthermore, the most obvious reduction of normal nuclear protein levels was found for TAF15, similar to the dramatic decrease in nuclear staining intensity in inclusion bearing cells in FTLD-FUS. Thus, inhibition of Transportin-mediated nuclear import in cultured cells mimics characteristic alterations of FET proteins found in human FTLD-FUS.

Discussion

FUS accumulates in the pathological cellular inclusions that characterize all cases of ALS with *FUS* mutations and a variety of FTLD subtypes, collectively referred to as FTLD-FUS (Kwiatkowski *et al*., 2009; Munoz *et al*., 2009; Neumann *et al*., 2009*a*, *b*; Vance *et al*., 2009; Mackenzie *et al*., 2010*b*). Our knowledge of the underlying mechanisms leading to FUS accumulation and FUS-mediated cell death is still limited. So far, most insights come from studies analysing the functional consequences of *FUS* mutations. As demonstrated in cell culture experiments, pathogenic *FUS* mutations interfere with the Transportin-mediated nuclear import, leading to increased levels of cytoplasmic FUS where it is recruited into stress granules upon stress conditions (Dormann *et al*., 2010; Ito *et al*., 2011; Kino *et al*., 2011). Since stress granule markers have been found in FUS-positive inclusions in FTLD-FUS and ALS-*FUS*, it has been suggested that stress granules might be the precursors of pathological FUS-inclusions (Dormann *et al*., 2010; Dormann and Haass, 2011).

Although there is some clinical and pathological overlap between ALS-*FUS* and FTLD-FUS, the presence of significant differences in the phenotypes and the morphological patterns of FUS pathology (Mackenzie *et al*., 2011*b*) and the fact that no FTLD-FUS case has yet been associated with a *FUS* mutation (Neumann *et al*., 2009*a*, *b*; Rohrer *et al*., 2010; Urwin *et al*., 2010; Snowden *et al*., 2011), raise questions as to whether these conditions represent a clinicopathological spectrum of diseases with a shared pathomechanism or whether the pathogenic pathways triggered by *FUS* mutations may be different from those involved in FTLD-FUS.

In the present study, we performed a detailed analysis of the role of the FUS homologues TAF15 and EWS in the spectrum of FUS-opathies and identified remarkable differences in the protein composition of inclusions between FTLD-FUS and ALS-*FUS*. These findings strongly support the idea that the pathological processes underlying cell death in ALS-*FUS* might be different from those in FTLD-FUS.

None of the ALS-*FUS* cases investigated, including six cases with four different *FUS* mutations, showed any alteration in the subcellular distribution of TAF15 or EWS and no evidence of co-accumulation of these proteins in the FUS-positive pathological inclusions. Importantly, we confirmed retention of the normal physiological staining pattern and the absence of TAF15 and EWS co-localization in the cytoplasmic FUS pathology (i.e. stress granules) that develops in cultured cells expressing ALS-associated *FUS* mutations (Dormann *et al*., 2010). Thus, cytoplasmic accumulation of FUS *per se* does not trigger an alteration in the subcellular distribution of its homologues and does not lead to sequestration of TAF15 and EWS into FUS inclusions as a secondary phenomenon. This strongly implies that the pathological processes in ALS-*FUS* are restricted to dysfunctions of FUS. Since the ALS-*FUS* cases we studied do not cover the entire spectrum of reported *FUS* mutations, we cannot exclude the possibility that other *FUS* mutations, particularly those reported in exons 3, 5 or 6 (Mackenzie *et al*., 2010*a*) might be associated with TAF15 and/or EWS pathology. However, since our analysis did include two

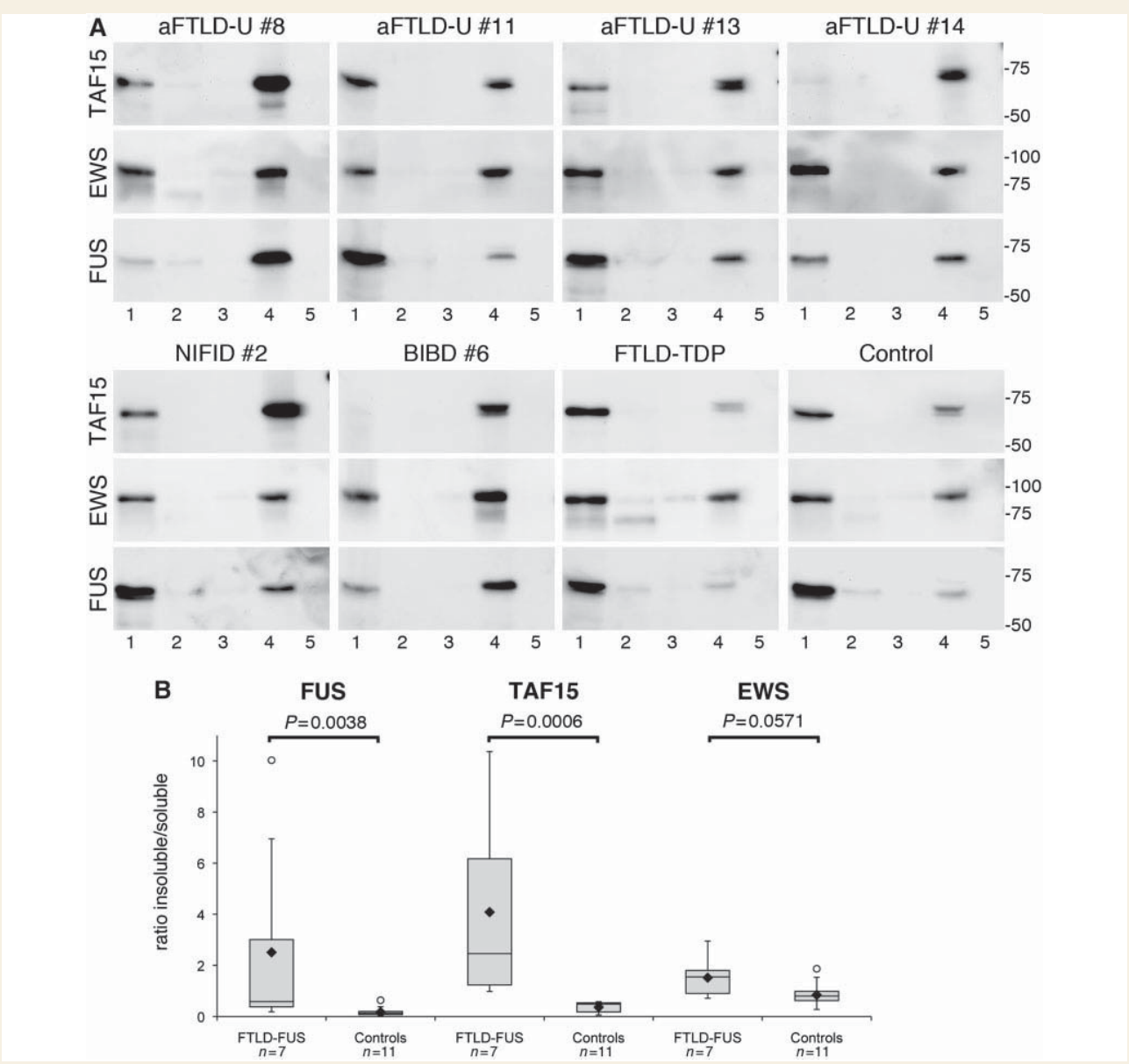

Figure 6 Biochemical analysis of FET proteins in FTLD-FUS. (**A**) Proteins were sequentially extracted from frontal cortex of atypical FTLD-U, NIFID, BIBD, normal as well as neurological controls. High salt (Lane 1), Triton-X-100 (Lane 2), radioimmunoprecipitation assay buffer (Lane 3), 2% sodium dodecyl sulphate (Lane 4) and formic acid (Lane 5) protein fractions were separated by sodium dodecyl sulphate–polyacrylamide gel electrophoresis and immunoblotted with anti-TAF15 (TAF15-309A), EWS (G5) and FUS (FUS-302A). All proteins were present in the soluble high salt fraction and sodium dodecyl sulphate fraction in each case as one major band at the expected molecular size for the full-length proteins. However, the amount of TAF15 and FUS in the sodium dodecyl sulphate fraction was much higher in FTLD-FUS compared with controls, while the shift towards the sodium dodecyl sulphate fraction was less obvious for EWS. (**B**) Densitometric quantification of band intensities of FUS, TAF15 and EWS in the soluble (high salt) and insoluble (sodium dodecyl sulphate) fraction was performed. Calculated insoluble/soluble ratios for each protein in the FTLD-FUS ($n = 7$) and control group ($n = 11$, including four normal controls, five FTLD with TDP-43 pathology and two cases with Alzheimer's disease) are shown as box plot showing the range of values, with the box being subdivided by the median into the 25th and 75th percentiles. Filled rhombus represents the mean; circles represent outliers. aFTLD-U = atypical FTLD-U.

cases with the most common *FUS* mutation (p.R521C), this is unlikely to be a frequent finding.

In sharp contrast to ALS-*FUS*, abnormal co-accumulation of all three FET proteins into pathological inclusions was a consistent and specific feature of all subtypes of FTLD-FUS. This finding further extends the similarities between the various subtypes of FTLD-FUS, thereby strongly supporting the idea, that atypical FTLD-U, NIFID and BIBD are closely related disease entities

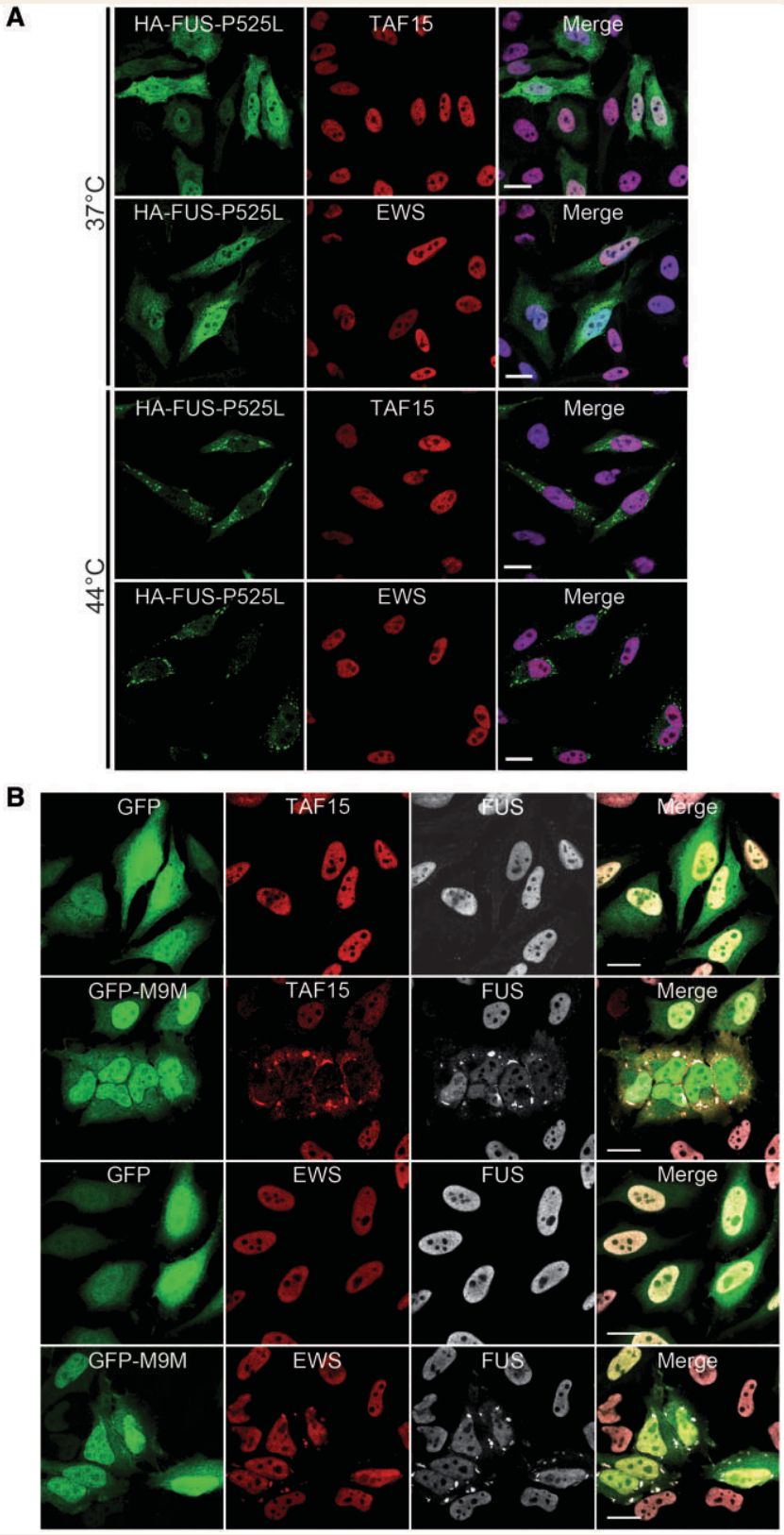

Figure 7 Analysis of FET proteins in cell culture systems. (**A**) Cytoplasmically mislocalized mutant FUS does not sequester TAF15 or EWS into stress granules upon heat shock. HeLa cells transiently transfected with haemagglutinin-tagged human FUS with the P525L mutation (HA-FUS-P525L) were left untreated (37°C, *top*) or subjected to heat shock (1 h at 44°C, *bottom*) 24 h after transfection. Cells were stained with antibodies against haemagglutinin (green) and EWS (red) or TAF15 (red) and analysed by confocal microscopy. Under control

(continued)

(Mackenzie *et al*., 2011*a*). However, our results also suggest some important differences among distinct FET family members in the different FTLD-FUS subtypes. While antibodies against TAF15 robustly labelled virtually all FUS pathology in atypical FTLD-U, NIFID and BIBD, subtle disease-specific differences were observed for EWS. Only a proportion of inclusions in atypical FTLD-U cases labelled for EWS and the staining intensity was often weak. In contrast, inclusions in NIFID and BIBD were more consistently and robustly labelled for EWS. Because the quality of immunostaining obtained with the commercial EWS antibodies employed was not felt to be optimal in all sections, we are cautious in interpreting these results. However, they raise the possibility of subtle differences in the pathogenic pathways involved in the different FTLD-FUS subtypes, that may underlie the distinct clinicopathological phenotypes previously described (Mackenzie *et al*., 2011*a*).

Another difference in the pattern of immunostaining among the FET proteins in FTLD-FUS is worth noting for its potential functional significance. Whereas inclusion bearing cells often demonstrated at least partial retention of nuclear FUS and EWS localization, a dramatic and consistent reduction of physiological nuclear staining was observed for TAF15, suggesting a possible loss-of-function mechanism.

The mechanisms leading to the accumulation of all FET proteins in FTLD-FUS remain unclear. The results in human ALS-*FUS* and in cultured cells expressing mutant FUS indicates that other FET proteins are not secondarily entrapped within FUS inclusions. An alternate mechanism is suggested by our cell culture data in which inhibition of Transportin-mediated nuclear import resulted in recruitment and co-localization of all FET proteins into stress granules. This favours a scenario in which a broader nuclear import defect in FTLD-FUS leads to increased cytoplasmic levels of all FET proteins (and possibly other proteins), which then predisposes to their abnormal accumulation. Although the underlying defect in nuclear import could reflect a direct dysfunction of the Transportin import machinery, preliminary studies in which we found no alterations in the subcellular distribution of other Transportin cargos, such as hnRNPA1, makes this mechanism more unlikely. Alternatively, altered post-translational modifications of FET proteins, such as phosphorylation or arginine methylation, might affect their subcellular localization and nuclear import in FTLD-FUS (Tan and Manley, 2009; Kovar, 2011). While biochemical analysis has so far revealed only a relative change in solubility for FET proteins (Neumann *et al*., 2009*b* and this study), the presence of potential disease-associated post-translational modifications as well as alterations of the transportin machinery requires further studies.

Our findings in FTLD-FUS add TAF15 and EWS to the growing list of DNA/RNA binding proteins involved in neurodegenerative diseases. Despite the fact that we have not detected any pathogenic mutations in *TAF15* and *EWSR1* in our FTLD-FUS cases, both genes are considered promising candidates for genetic screens in FTLD and ALS and a very recent report has described coding variants in *TAF15* in ALS, although their pathogenicity remains to be confirmed (Ticozzi *et al*., 2011).

In summary, this study demonstrates the co-accumulation of all members of the FET protein family in the characteristic inclusions as specific feature of FTLD-FUS but not of ALS-*FUS*, thus allowing a clear separation between genetic and non-genetic forms of FUS-opathies by neuropathological features. More importantly, these findings imply that different pathomechanisms underlie inclusion body formation and cell death in ALS-*FUS* versus FTLD-FUS. Our data indicate that neurodegeneration associated with *FUS* mutations is probably the result of a restricted dysfunction of FUS, whereas a more complex dysregulation of all FET family members seems to be involved in FTLD-FUS pathogenesis. While the relative roles of the different FET proteins in the disease pathogenesis of FTLD-FUS remain to be determined in future studies, our data suggest that the conditions currently subsumed within the FTLD-FUS molecular subgroup might be more appropriately designated as FTLD-FET, in accordance with the recently proposed system of FTLD nomenclature (Mackenzie *et al*., 2009).

Supplementary material

Supplementary material is available at *Brain* online.

Funding

The Swiss National Science Foundation (31003A-132864, M.N.); the Synapsis Foundation (M.N.); the Canadian Institutes of Health Research (74580, I.R.A.M.); the Pacific Alzheimer Research Foundation (I.R.A.M.); the National Institutes of Health (R01 AG26251; R.R.); the ALS Association (R.R.); the Center for Integrated Protein Science Munich (CIPSM; C.H.), the German Federal Ministry of Education and Research (01GI1005B; C.H., M.N.), the Sonderforschungsbereich Molecular Mechanisms of

Figure 7 Continued
conditions, HA-FUS-P525L is diffusely distributed in the cytoplasm, and endogenous TAF15 and EWS is localized in the nucleus. Upon heat shock, HA-FUS-P525L is recruited into cytoplasmic stress granules, while TAF15 and EWS remain predominantly nuclear and are not entrapped into FUS-positive stress granules. Scale bar = 20 μm. (**B**) Inhibition of the Transportin pathway leads to cytoplasmic mislocalization of TAF15, EWS and FUS into stress granules. The Transportin-specific peptide inhibitor M9M fused to green fluorescent protein (GFP-M9M, green) or GFP alone was expressed in HeLa cells for 24 h. Cells were stained with antibodies against TAF15, EWS (both shown in red) and FUS (white) and were analysed using confocal microscopy. Upon inhibition of Transportin-mediated nuclear import by the GFP-M9M peptide, TAF15 and EWS are recruited into cytoplasmic stress granules, where they co-localize with FUS. Note that EWS shows only mild cytoplasmic mislocalization, while FUS and especially TAF15 show a marked cytoplasmic redistribution with a nuclear depletion of these proteins. Scale bar = 20 μm.

Neurodegeneration (SFB 596; C.H.); and the National Institute for Health Research, Oxford Biomedical Research Centre (O.A.).

Acknowledgements

We thank Margaret Luk and Mareike Schroff for their excellent technical assistance.

References

Blair IP, Williams KL, Warraich ST, Durnall JC, Thoeng AD, Manavis J, et al. FUS mutations in amyotrophic lateral sclerosis: clinical, pathological, neurophysiological and genetic analysis. J Neurol Neurosurg Psychiatry 2010; 81: 639–45.

Doi H, Koyano S, Suzuki Y, Nukina N, Kuroiwa Y. The RNA-binding protein FUS/TLS is a common aggregate-interacting protein in polyglutamine diseases. Neurosci Res 2010; 66: 131–3.

Dormann D, Rodde R, Edbauer D, Bentmann E, Fischer I, Hruscha A, et al. ALS-associated fused in sarcoma (FUS) mutations disrupt Transportin-mediated nuclear import. EMBO J 2010; 29: 2841–57.

Dormann D, Haass C. TDP-43 and FUS – a nuclear affair. Trends Neuroscience 2011; 34: 339–48.

Groen EJ, van Es MA, van Vught PW, Spliet WG, van Engelen-Lee J, de Visser M, et al. FUS mutations in familial amyotrophic lateral sclerosis in the Netherlands. Arch Neurol 2010; 67: 224–30.

Hewitt C, Kirby J, Highley JR, Hartley JA, Hibberd R, Hollinger HC, et al. Novel FUS/TLS mutations and pathology in familial and sporadic amyotrophic lateral sclerosis. Arch Neurol 2010; 67: 455–61.

Ito D, Seki M, Tsunoda Y, Uchiyama H, Suzuki N. Nuclear transport impairment of amyotrophic lateral sclerosis-linked mutations in FUS/TLS. Ann Neurol 2011; 69: 152–62.

Jobert L, Argentini M, Tora L. PRMT1 mediated methylation of TAF15 is required for its positive gene regulatory function. Exp Cell Res 2009; 315: 1273–86.

Kino Y, Washizu C, Aquilanti E, Okuno M, Kurosawa M, Yamada M, et al. Intracellular localization and splicing regulation of FUS/TLS are variably affected by amyotrophic lateral sclerosis-linked mutations. Nucleic Acids Res 2011; 39: 2781–98.

Kovar H. Dr. Jekyll and Mr. Hyde: the two faces of the FUS/EWS/TAF15 protein family. Sarcoma 2011; 2011: 837474.

Kwiatkowski TJ Jr, Bosco DA, Leclerc AL, Tamrazian E, Vanderburg CR, Russ C, et al. Mutations in the FUS/TLS gene on chromosome 16 cause familial amyotrophic lateral sclerosis. Science 2009; 323: 1205–8.

Law WJ, Cann KL, Hicks GG. TLS, EWS and TAF15: a model for transcriptional integration of gene expression. Brief Funct Genomic Proteomic 2006; 5: 8–14.

Lee BJ, Cansizoglu AE, Suel KE, Louis TH, Zhang Z, Chook YM. Rules for nuclear localization sequence recognition by karyopherin beta 2. Cell 2006; 126: 543–58.

Mackenzie IR, Baborie A, Pickering-Brown S, Plessis DD, Jaros E, Perry RH, et al. Heterogeneity of ubiquitin pathology in frontotemporal lobar degeneration: classification and relation to clinical phenotype. Acta Neuropathol 2006; 112: 539–49.

Mackenzie IR, Neumann M, Bigio EH, Cairns NJ, Alafuzoff I, Kril J, et al. Nomenclature for neuropathologic subtypes of frontotemporal lobar degeneration: consensus recommendations. Acta Neuropathol 2009; 117: 15–8.

Mackenzie IR, Rademakers R, Neumann M. TDP-43 and FUS in amyotrophic lateral sclerosis and frontotemporal dementia. Lancet Neurol 2010a; 9: 995–1007.

Mackenzie IR, Neumann M, Bigio EH, Cairns NJ, Alafuzoff I, Kril J, et al. Nomenclature and nosology for neuropathologic subtypes of frontotemporal lobar degeneration: an update. Acta Neuropathol 2010b; 119: 1–4.

Mackenzie IR, Munoz DG, Kusaka H, Yokota O, Ishihara K, Roeber S, et al. Distinct pathological subtypes of FTLD-FUS. Acta Neuropathol 2011a; 121: 207–18.

Mackenzie IRA, Ansorge O, Strong M, Bilbao J, Zinman L, Ang LC, et al. Pathological heterogeneity in amyotrophic lateral sclerosis with FUS mutations: two distinct patterns correlating with disease severity and mutation. Acta Neuropathol 2011b; 122: 87–98.

Munoz DG, Neumann M, Kusaka H, Yokota O, Ishihara K, Terada S, et al. FUS pathology in basophilic inclusion body disease. Acta Neuropathol 2009; 118: 617–27.

Neumann M, Sampathu DM, Kwong LK, Truax AC, Micsenyi MC, Chou TT, et al. Ubiquitinated TDP-43 in frontotemporal lobar degeneration and amyotrophic lateral sclerosis. Science 2006; 314: 130–3.

Neumann M, Roeber S, Kretzschmar HA, Rademakers R, Baker M, Mackenzie IR. Abundant FUS-immunoreactive pathology in neuronal intermediate filament inclusion disease. Acta Neuropathol 2009a; 118: 605–16.

Neumann M, Rademakers R, Roeber S, Baker M, Kretzschmar HA, Mackenzie IR. A new subtype of frontotemporal lobar degeneration with FUS pathology. Brain 2009b; 132: 2922–31.

Page T, Gitcho MA, Mosaheb M, Carter D, Chakraverty S, Perry RH, et al. FUS immunogold labelling TEM analysis of the neuronal cytoplasmic inclusions of neuronal intermediate filament inclusion disease: a frontotemporal lobar degeneration with FUS proteinopathy. J Mol Neurosci 2011. [Epub ahead of print] advance access date: May 21, doi:10.1007/s12031-011-9549-8.

Pahlich S, Zakaryan RP, Gehring H. Identification of proteins interacting with protein arginine methyltransferase 8: the Ewing sarcoma (EWS) protein binds independent of its methylation state. Proteins 2008; 72: 1125–37.

Rademakers R, Stewart H, DeJesus-Hernandez M, Krieger C, Graff-Radford N, Fabros M, et al. FUS gene mutations in familial and sporadic amyotrophic lateral sclerosis. Muscle Nerve 2010; 42: 170–6.

Rohrer JD, Lashley T, Holton J, Revesz T, Urwin H, Isaacs AM, et al. The clinical and neuroanatomical phenotype of FUS associated frontotemporal lobar degeneration. J Neurol Neurosurg Psychiatry 2010. [Epub ahead of print] advance access date: July 16, doi:10.1136/jnnp.2010.214437.

Snowden JS, Hu Q, Rollinson S, Halliwell N, Robinson A, Davidson YS, et al. The most common type of FTLD-FUS (aFTLD-U) is associated with a distinct clinical form of frontotemporal dementia but is not related to mutations in the FUS gene. Acta Neuropathol 2011; 122: 99–110.

Tan AY, Manley JL. The TET family of proteins: functions and roles in disease. J Mol Cell Biol 2009; 1: 82–92.

Ticozzi N, Vance C, Leclerc AL, Keagle P, Glass JD, McKenna-Yasek D, et al. Mutational analysis reveals the FUS homolog TAF15 as a candidate gene for familial amyotrophic lateral sclerosis. Am J Med Genet B Neuropsychiatr Genet 2011; 156: 285–90.

Urwin H, Josephs KA, Rohrer JD, Mackenzie IR, Neumann M, Authier A, et al. FUS pathology defines the majority of tau- and TDP-43-negative frontotemporal lobar degeneration. Acta Neuropathol 2010; 120: 33–41.

Vance C, Rogelj B, Hortobagyi T, De Vos KJ, Nishimura AL, Sreedharan J, et al. Mutations in FUS, an RNA processing protein, cause familial amyotrophic lateral sclerosis type 6. Science 2009; 323: 1208–11.

Woulfe J, Gray DA, Mackenzie IR. FUS-immunoreactive intranuclear inclusions in neurodegenerative disease. Brain Pathol 2010; 20: 589–97.

Zakaryan RP, Gehring H. Identification and characterization of the nuclear localization/retention signal in the EWS proto-oncoprotein. J Mol Biol 2006; 363: 27–38.

Zinszner H, Sok J, Immanuel D, Yin Y, Ron D. TLS (FUS) binds RNA in vivo and engages in nucleo-cytoplasmic shuttling. J Cell Sci 1997; 110: 1741–50.

Supplementary Online Material:

Supplementary Table 1: Demographic and clinical features of FTLD-FUS and ALS-*FUS* cases.

NP diagnosis	Case No	Sex	Family history	Onset (y)	Duration (y)	Dementia	Park	ALS	References
aFTLD-U	1	F	no	38	11	bvFTD	no	no	(Mackenzie *et al.*, 2008; Neumann *et al.*, 2009a)
aFTLD-U	2	F	no	37	8	bvFTD	no	no	(Mackenzie *et al.*, 2008; Neumann *et al.*, 2009a)
aFTLD-U	3	F	no	40	11	bvFTD	no	no	(Mackenzie *et al.*, 2008; Neumann *et al.*, 2009a)
aFTLD-U	4	F	no	32	7	bvFTD	no	no	(Mackenzie *et al.*, 2008; Neumann *et al.*, 2009a)
aFTLD-U	5	M	no	29	7	bvFTD	no	no	(Mackenzie *et al.*, 2008; Neumann *et al.*, 2009a)
aFTLD-U	6	F	no	36	6	bvFTD	no	no	(Mackenzie *et al.*, 2008; Neumann *et al.*, 2009a)
aFTLD-U	7	M	no	na	na	bvFTD	no	no	(Neumann *et al.*, 2009a)
aFTLD-U	8	F	no	46	4	bvFTD	no	no	(Neumann *et al.*, 2009a; Roeber *et al.*, 2008)
aFTLD-U	9	M	no	36	5	bvFTD	no	no	(Neumann *et al.*, 2009a; Roeber *et al.*, 2008)
aFTLD-U	10	M	no	41	5	bvFTD	no	no	(Neumann *et al.*, 2009a; Roeber *et al.*, 2008)
aFTLD-U	11	F	no	39	9	bvFTD	no	no	(Neumann *et al.*, 2009a; Roeber *et al.*, 2008)
aFTLD-U	12	F	no	35	5	bvFTD	no	no	(Neumann *et al.*, 2009a; Roeber *et al.*, 2008)
aFTLD-U	13	M	no	na	na	bvFTD	no	no	(Neumann *et al.*, 2009a; Roeber *et al.*, 2008)
aFTLD-U	14	M	no	28	5	bvFTD	no	no	(Neumann *et al.*, 2009a; Roeber *et al.*, 2008)
aFTLD-U	15	F	no	39	15	bvFTD	no	no	(Neumann *et al.*, 2009a; Roeber *et al.*, 2008)
NIFID	1	F	no	25	4	PPA, bvFTD	no	yes	(Cairns *et al.*, 2004; Mackenzie and Feldman 2004; Neumann *et al.*, 2009b)
NIFID	2	F	no	34	7	PPA, bvFTD	no	yes	(Neumann *et al.*, 2009b)
NIFID	3	M	no	58	3	PPA	no	no	(Neumann *et al.*, 2009b)
NIFID	4	F	no	53	3	bvFTD	yes	no	(Neumann *et al.*, 2009b)
BIBD	1	M	no	29	10	bvFTD	no	yes	(Munoz *et al.*, 2009; Munoz-Garcia and Ludwin 1984)
BIBD	2	M	no	57	6	bvFTD	yes	no	(Munoz *et al.*, 2009; Yokota *et al.*, 2008)
BIBD	3	F	no	56	11	bvFTD	no	no	(Munoz *et al.*, 2009; Yokota *et al.*, 2008)
BIBD	4	M	no	36	6	no	no	yes	(Kusaka *et al.*, 1990; Munoz *et al.*, 2009)
BIBD	5	M	no	53	5	no	no	yes	(Kusaka *et al.*, 1990; Munoz *et al.*, 2009)
BIBD	6	F	no	43	8	no	yes	no	(Munoz *et al.*, 2009)
BIBD	7	M	no	46	5	yes	yes	no	(Behring *et al.*, 1998)
ALS-*FUS* (p.R521C)	1	F	yes	62	4	no	no	yes	(Mackenzie *et al.*, 2011; Rademakers *et al.*, 2010)
ALS-*FUS* (p.R521C)	2	F	yes	44	2	no	no	yes	(Mackenzie *et al.*, 2011)
ALS-*FUS* (p.R514S/E516V)	3	M	no	44	3	no	no	yes	(Mackenzie *et al.*, 2011; Robertson *et al.*, 2011)
ALS-*FUS* (p.P525L)	4	F	no	22	< 1	no	no	yes	(Baumer *et al.*, 2010; Mackenzie *et al.*, 2011)
ALS-*FUS* (p.P525L)	5	F	no	18	< 1	no	no	yes	(Baumer *et al.*, 2010; Mackenzie *et al.*, 2011)
ALS-*FUS* (p.Q519lfsX9)	6	M	no	18	< 1	mild learning difficulty	no	yes	(Baumer *et al.*, 2010; Mackenzie *et al.*, 2011)

aFTLD-U, atypical frontotemporal lobar degeneration with ubiquitinated inclusions; ALS, amyotrophic lateral sclerosis, ALS-*FUS*, Amyotrophic lateral sclerosis with mutations in *FUS* gene; BIBD, basophilic inclusion body disease; bvFTD, behavioural variant of frontotemporal dementia; na, not available; NIFID, neuronal intermediate filament inclusion body disease; Park, parkinsonism; PPA primary progressive aphasia.

Supplementary Table 2: Summary of TAF15 and EWS antibodies tested

Company	Product No	Species	Epitope	IHC	WB
TAF15					
Bethyl	IHC-00094-1	RP	200-250	1:200-1:400	1:1000
Bethyl	A300-308A	RP	200-250	1:1000-1:2000	1:5000
Bethyl	A300-309A	RP	550-592	1:1000-1:2000	1:5000
Abnova	H00008148-B01P	MP	na	no	no
Abcam	TAF15B11A6	MM	na	no	no
EWS					
Santa Cruz	G5-sc28327	MM	2-43	1:100-1:300	1:500
Bethyl	IHC-00086	RP	100-150	1:200	nd
Epitomics	3319-1	RP	130 - 155	1:100	nd
Epitomics	3320-1	RP	345 - 370	1:1000	nd
Amsbio	M01, clone 5C10	MM	358-454	no	1:200*

IHC, immunohistochemistry; MM, mouse monoclonal; MP, mouse polyclonal; na, not available; nd, not determined; RP, rabbit polyclonal; WB, Western blotting.
* Additional staining of band ~75 kD, suggesting cross-reactivity with TAF15 (see Supplementary Fig. 1).

Supplementary Table 3.

Non-coding variants identified in *EWSR1* and *TAF15* in FTLD-FUS

Gene	Region	Nucleotide Change	FTLD-FUS
EWSR1	Intron 3	c.102+14_21delTAATTACA	1/8
TAF15	3'UTR	c.*19C>T	1/8
TAF15	Intron 10	c.783+142G>C	5/8

Supplementary Figure 1

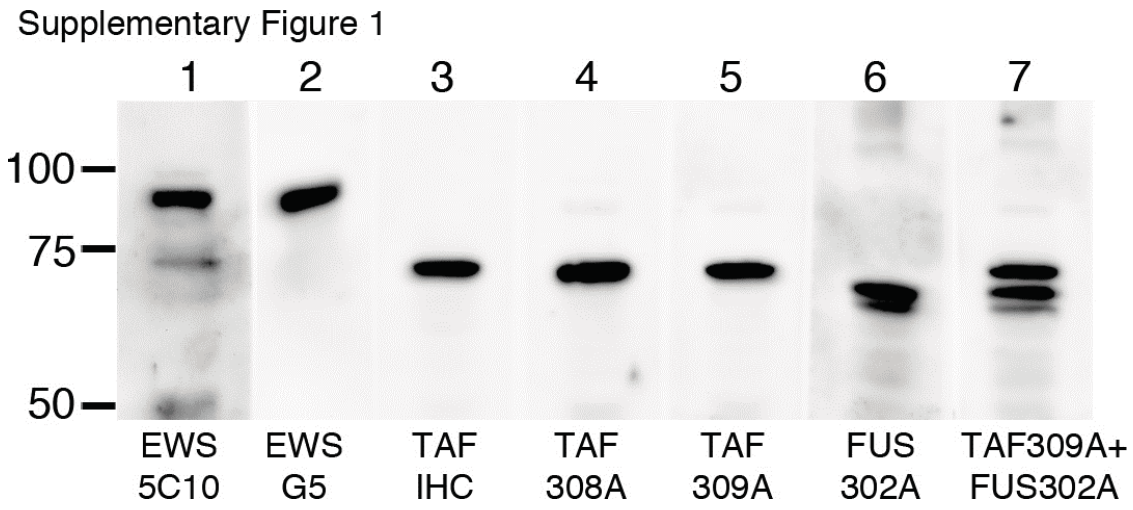

Specificity testing of used TAF15 and EWS antibodies by immunoblot.

High-salt fraction extracted from frontal cortex of patient with FTLD-FUS subjected to 7.5% SDS-PAGE and blotted onto PVDF membrane. Membrane was cut into strips that were immunolabeled with the indicated primary antibodies against EWS (lane 1 and 2), TAF15 (lane 3-5) and FUS (lane 6). Note that all antibodies recognize a single band of the expected molecular size, only EWS-5C10 showed additional weak labeling of a band at the similar size of TAF15 suggesting weak cross reactivity to TAF15. One strip (lane 7) was probed for TAF15 and FUS to clearly demonstrate that distinct bands are recognized by TAF15 and FUS antibodies.

Supplementary Figure 2:

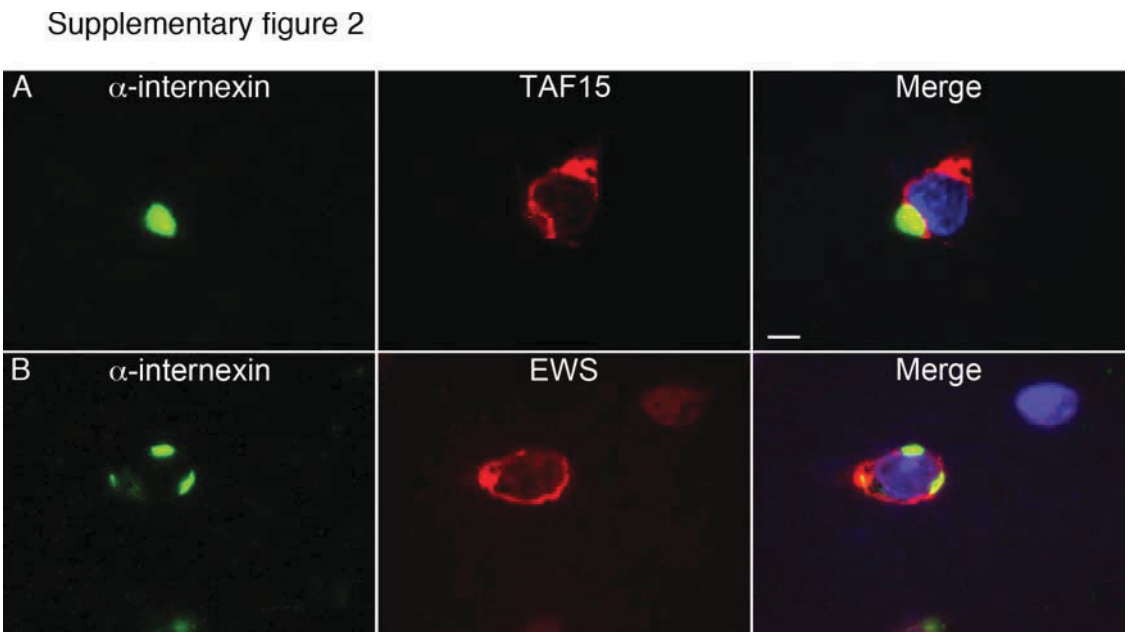

Double-label immunofluorescence for TAF15, EWS and α-internexin in NIFID: Neurons in NIFID with compact α-internexin-positive inclusions (**A** and **B**, green) always revealed additional TAF15 (**A**, red) and EWS (**B**, red) pathology. Note that separate, discrete inclusions are labeled for TAF15 and α-internexin (**A**) and EWS and α-internexin (**B**) in the same neuron. Scale bar: 4 μm.

Supplementary Figure 3:

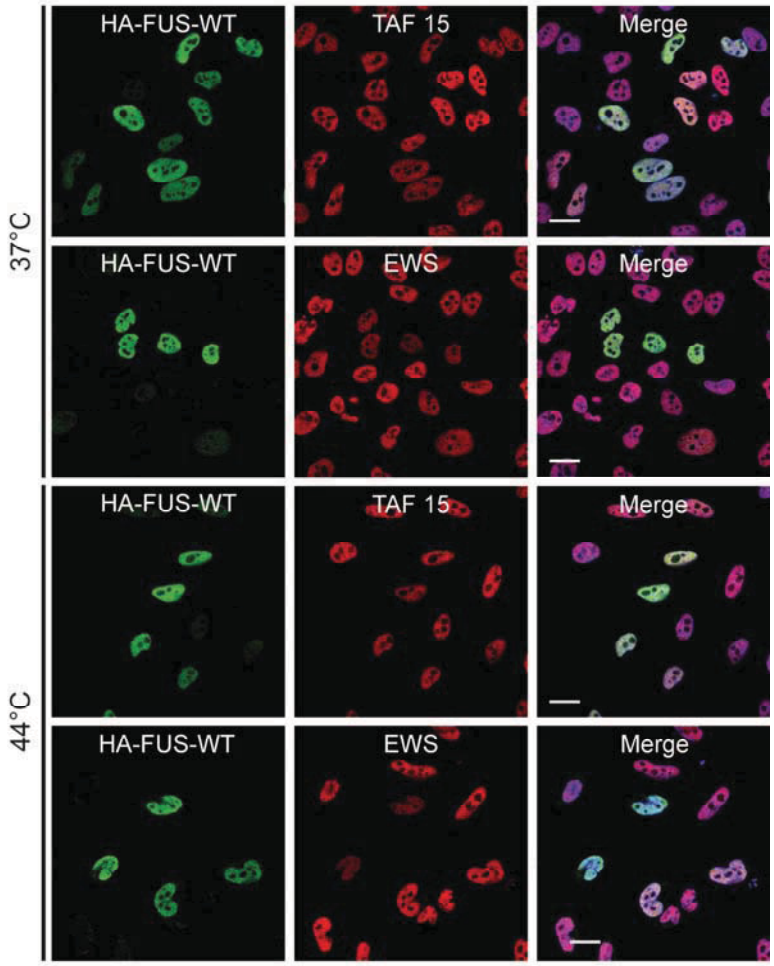

Analysis of FET proteins in cells overexpressing wildtype FUS

HeLa cells were transiently transfected with hemagglutinin-tagged human wildtype FUS (HA-FUS-WT) and left untreated (37°C, upper panel) or subjected to heat shock (1h at 44°C, lower panel) 24h after transfection. Cells were stained with antibodies against HA (green) and EWS (red) or TAF15 (red) and analyzed by confocal microscopy. Under both conditions, HA-FUS-WT as well as endogenous TAF15 and EWS are localized in the nucleus. Scale bar: 20µm.

References:

Baumer D, Hilton D, Paine SM, Turner MR, Lowe J, Talbot K, et al. Juvenile ALS with basophilic inclusions is a FUS proteinopathy with FUS mutations. Neurology. 2010; 75: 611-8.

Behring B, Beuche W, Kretzschmar HA. Progressive dementia with parkinsonism in corticobasal degeneration and brainstem degeneration with neuronal inclusions. Neurology. 1998; 51: 288.

Cairns NJ, Grossman M, Arnold SE, Burn DJ, Jaros E, Perry RH, et al. Clinical and neuropathologic variation in neuronal intermediate filament inclusion disease. Neurology. 2004; 63: 1376-84.

Kusaka H, Matsumoto S, Imai T. An adult-onset case of sporadic motor neuron disease with basophilic inclusions. Acta Neuropathol. 1990; 80: 660-5.

Mackenzie IR, Feldman H. Neurofilament inclusion body disease with early onset frontotemporal dementia and primary lateral sclerosis. Clin Neuropathol. 2004; 23: 183-93.

Mackenzie IR, Foti D, Woulfe J, Hurwitz TA. Atypical frontotemporal lobar degeneration with ubiquitin-positive, TDP-43-negative neuronal inclusions. Brain. 2008; 131: 1282-93.

Mackenzie IRA, Ansorge O, Strong M, Bilbao J, Zinman L, Ang LC, et al. Pathological heterogeneity in amyotrophic lateral sclerosis with *FUS* mutations Acta Neuropathol. 2011; [Epub ahead of print].

Munoz DG, Neumann M, Kusaka H, Yokota O, Ishihara K, Terada S, et al. FUS pathology in basophilic inclusion body disease. Acta Neuropathol. 2009; 118: 617-27.

Munoz-Garcia D, Ludwin SK. Classic and generalized variants of Pick's disease: a clinicopathological, ultrastructural, and immunocytochemical comparative study. Ann Neurol. 1984; 16: 467-80.

Neumann M, Rademakers R, Roeber S, Baker M, Kretzschmar HA, Mackenzie IR. A new subtype of frontotemporal lobar degeneration with FUS pathology. Brain. 2009a; 132: 2922-31.

Neumann M, Roeber S, Kretzschmar HA, Rademakers R, Baker M, Mackenzie IR. Abundant FUS-immunoreactive pathology in neuronal intermediate filament inclusion disease. Acta Neuropathol. 2009b; 118: 605-16.

Rademakers R, Stewart H, DeJesus-Hernandez M, Krieger C, Graff-Radford N, Fabros M, et al. FUS gene mutations in familial and sporadic amyotrophic lateral sclerosis. . Muscle Nerve. 2010; 42: 170-6.

Robertson J, Bilbao J, Zinman L, Hazrati LN, Tokuhiro S, Sato C, et al. A novel double mutation in FUS gene causing sporadic ALS. Neurobiol Aging. 2011; 32: 553 e27-30.

Roeber S, Mackenzie IR, Kretzschmar HA, Neumann M. TDP-43-negative FTLD-U is a significant new clinico-pathological subtype of FTLD. Acta Neuropathol. 2008; 116: 147-57.

Yokota O, Tsuchiya K, Terada S, Ishizu H, Uchikado H, Ikeda M, et al. Basophilic inclusion body disease and neuronal intermediate filament inclusion disease: a comparative clinicopathological study. Acta Neuropathol. 2008; 115: 561-75.

The EMBO Journal (2010) 29, 2841–2857 | © 2010 European Molecular Biology Organization | All Rights Reserved 0261-4189/10
www.embojournal.org

THE EMBO JOURNAL

ALS-associated fused in sarcoma (*FUS*) mutations disrupt Transportin-mediated nuclear import

Dorothee Dormann[1,2], Ramona Rodde[1,2], Dieter Edbauer[1], Eva Bentmann[1,2], Ingeborg Fischer[3], Alexander Hruscha[1], Manuel E Than[4], Ian RA Mackenzie[5], Anja Capell[1,2], Bettina Schmid[1], Manuela Neumann[3] and Christian Haass[1,2,*]

[1]DZNE–German Center for Neurodegenerative Diseases, Munich, Germany, [2]Adolf-Butenandt-Institute, Biochemistry, Ludwig-Maximilians-University, Munich, Germany, [3]Institute of Neuropathology, Zurich, Switzerland, [4]Leibniz Institute for Age Research, Fritz-Lipmann Institute (FLI), Protein Crystallography Group, Jena, Germany and [5]Department of Pathology, Vancouver General Hospital, Vancouver, British Columbia, Canada

Mutations in fused in sarcoma (*FUS*) are a cause of familial amyotrophic lateral sclerosis (fALS). Patients carrying point mutations in the C-terminus of *FUS* show neuronal cytoplasmic FUS-positive inclusions, whereas in healthy controls, FUS is predominantly nuclear. Cytoplasmic FUS inclusions have also been identified in a subset of frontotemporal lobar degeneration (FTLD-FUS). We show that a non-classical PY nuclear localization signal (NLS) in the C-terminus of FUS is necessary for nuclear import. The majority of fALS-associated mutations occur within the NLS and impair nuclear import to a degree that correlates with the age of disease onset. This presents the first case of disease-causing mutations within a PY-NLS. Nuclear import of FUS is dependent on Transportin, and interference with this transport pathway leads to cytoplasmic redistribution and recruitment of FUS into stress granules. Moreover, proteins known to be stress granule markers co-deposit with inclusions in fALS and FTLD-FUS patients, implicating stress granule formation in the pathogenesis of these diseases. We propose that two pathological hits, namely nuclear import defects and cellular stress, are involved in the pathogenesis of FUS-opathies.

The EMBO Journal (2010) **29,** 2841–2857. doi:10.1038/emboj.2010.143; Published online 6 July 2010
Subject Categories: neuroscience; molecular biology of disease
Keywords: amyotrophic lateral sclerosis (ALS); frontotemporal lobar degeneration (FTLD); fused in sarcoma (FUS); stress granules; Transportin

*Corresponding author. DZNE–German Center for Neurodegenerative Diseases and Adolf-Butenandt-Institute, Biochemistry, Ludwig-Maximilians-University, Schillerstrasse 44, Munich 80336, Germany. Tel.: +4 98 921 807 5471; Fax: +4 98 921 807 5415; E-mail: chaass@med.uni-muenchen.de

Received: 26 March 2010; accepted: 7 June 2010; published online: 6 July 2010

Introduction

ALS, also known as Lou Gehrig's disease, is an incurable, severely disabling condition that is characterized by the degeneration of both upper and lower motor neurons. Loss of motor neurons leads to progressive muscle weakening, atrophy and spasticity. The majority of patients succumb to the disease within 1–5 years after disease onset, typically because of respiratory failure (Boillee *et al*, 2006). Although the majority of ALS cases are sporadic (sALS), about 10% are inherited in a dominant manner (fALS) (Boillee *et al*, 2006; Valdmanis and Rouleau, 2008). Of these, about 5–10% are caused by mutations in the *TAR DNA-binding protein 43* (*TDP-43*) gene on chromosome 1 (Gitcho *et al*, 2008; Kabashi *et al*, 2008; Mackenzie and Rademakers, 2008; Sreedharan *et al*, 2008) or the *FUS* gene on chromosome 16 (Kwiatkowski *et al*, 2009; Vance *et al*, 2009). Although these genes account for only a small number of fALS cases, their gene products seem to have a crucial function in the pathogenesis of the majority of ALS cases, including sALS, as well as the related disorder frontotemporal lobar degeneration with ubiquitin-positive inclusions (FTLD-U). Both neurodegenerative diseases are characterized by the presence of neuronal and/or glial TDP-43 or FUS inclusions. TDP-43 inclusions are found in most ALS cases, with the exception of fALS caused by mutations in the *Cu/Zn superoxide dismutase* (*SOD1*) gene (Mackenzie *et al*, 2007). Moreover, TDP-43-positive inclusions are also found in >90% of FTLD-U patients (Arai *et al*, 2006; Neumann *et al*, 2006), now renamed as FTLD-TDP (Mackenzie *et al*, 2010). FUS inclusions are present in the remaining 10% of atypical TDP-43-negative FTLD-U cases (aFTLD-U) (Neumann *et al*, 2009a) and in other rare cases of FTLD, such as basophilic inclusion body disease (BIBD) (Munoz *et al*, 2009) and neuronal intermediate filament inclusion disease (NIFID) (Neumann *et al*, 2009b), now subsumed as FTLD-FUS (Mackenzie *et al*, 2010), as well as in fALS patients carrying *FUS* mutations (Kwiatkowski *et al*, 2009; Vance *et al*, 2009). These diseases are now commonly termed FUS-opathies (Munoz *et al*, 2009). The discovery of TDP-43 and FUS inclusions in both ALS and FTLD has led to the concept that ALS and FTLD are related diseases and that the same proteins are involved in their pathogenesis (Neumann *et al*, 2009a). This is further supported by the fact that up to 50% of ALS patients show cognitive impairment and a significant portion of FTLD patients develop motor neuron disease (Talbot and Ansorge, 2006).

Both FUS and TDP-43 are DNA- and RNA-binding proteins that shuttle continuously between the nucleus and cytoplasm (Zinszner *et al*, 1997b; Ayala *et al*, 2008) and are involved in multiple steps of gene expression, such as transcriptional regulation, pre-mRNA splicing and microRNA processing (Buratti and Baralle, 2008; Lagier-Tourenne and Cleveland, 2009). In addition, FUS has been implicated in mRNA export and mRNA transport to neuronal dendrites

(Fujii and Takumi, 2005; Fujii *et al*, 2005). Although FUS and TDP-43 normally reside and function predominantly in the nucleus, pathological FUS and TDP-43 inclusions are mostly observed in the cytosol, and inclusion-bearing cells often show a reduction of nuclear staining (Arai *et al*, 2006; Neumann *et al*, 2006, 2009a; Kwiatkowski *et al*, 2009; Vance *et al*, 2009). It is completely unclear, how cytosolic FUS and TDP-43 inclusions arise and apart from p62 and ubiquitin, no other cellular markers or co-aggregating proteins have been detected within these inclusions (Neumann *et al*, 2006, 2007, 2009a; Kwiatkowski *et al*, 2009; Vance *et al*, 2009). As the inclusions occur predominantly in the cytosol, defects in nucleocytoplasmic transport or enhanced aggregation in the cytosol may lead to cytoplasmic mislocalization of TDP-43 and FUS. This may interfere with their physiological nuclear function or cause a toxic gain-of-function because of excessive accumulation in the cytoplasm.

For TDP-43, a classical NLS in the N-terminal domain has been identified and experimentally confirmed (Winton *et al*, 2008). However, none of the over 30 mutations identified in TDP-43 so far affect the NLS, and it is still unclear whether any of the mutations functionally affect nucleocytoplasmic transport. Moreover, expression of TDP-43 in yeast and neuroblastoma cells suggested that the fALS-associated mutations might increase the aggregation propensities of TDP-43 rather than impairing its nuclear transport (Johnson *et al*, 2009; Nonaka *et al*, 2009). For FUS, it has been described that some of the fALS-associated mutations in the C-terminal region lead to an accumulation of the protein in the cytosol (Kwiatkowski *et al*, 2009; Vance *et al*, 2009). However, the underlying cellular mechanism is unknown, and it is not clear whether disturbed nuclear transport or aberrant cytoplasmic aggregation of mutant proteins leads to the cytosolic redistribution of mutant FUS. A non-classical $R/H/KX_{2-5}PY$-NLS has been predicted in the FUS C-terminal region (Lee *et al*, 2006). However, experimental evidence is missing that this sequence is required for nuclear import of FUS and the function of the predicted NLS is controversial. For example, a homologous motif in the related Ewing sarcoma protein (EWS), which belongs to the same transcription factor family (Law *et al*, 2006; Zakaryan and Gehring, 2006), was shown to be necessary, but not sufficient for nuclear import of EWS (Zakaryan and Gehring, 2006). Furthermore, an N-terminal fragment, but not a C-terminal fragment of FUS has earlier been shown to localize to the nucleus (Zinszner *et al*, 1997b). Nevertheless, 12 out of 22 *FUS* mutations identified in fALS patients are concentrated within the predicted NLS (Figure 1A) (Belzil *et al*, 2009; Chio *et al*, 2009; Kwiatkowski *et al*, 2009; Ticozzi *et al*, 2009; Vance *et al*, 2009; Corrado *et al*, 2010) and the motif is highly conserved during evolution (Figure 1B). We, therefore, assessed whether the predicted NLS was functionally relevant and whether it would be impaired by fALS-associated *FUS* mutations.

Results

C-terminal region of FUS is necessary and sufficient for nuclear import

To test whether the C-terminal domain of FUS is required for nuclear import, we generated a deletion mutant lacking the C-terminal 13 amino acids (Δ514–526) (Figure 1A) and analysed its localization in HeLa cells. In contrast to wild-type (WT) FUS, which was located almost exclusively in the nucleus, the deletion mutant showed a predominantly (72 ± 4%) cytoplasmic localization (Figure 1C, see D for quantification). This shows that the C-terminal domain (amino acids 514–526) is necessary for efficient nuclear import of FUS. We next investigated whether the three arginine residues most frequently mutated in FUS-positive fALS patients (R521, R522, R524; see Figure 1A) are critical for nuclear import. When we changed these three arginines to alanine (R521A/R522A/R524A), the localization of the triple point mutant was indistinguishable from that of the deletion mutant (73 ± 3% cytosolic; Figure 1C and D), showing that at least one of these arginines is essential for nuclear localization of FUS (for individual arginine mutations, see Figure 2). In addition, the two arginine residues further upstream (R514 and R518) are also required for nuclear import, as an R514A/R518A mutant showed a predominantly (65 ± 5%) cytosolic localization (Figure 1C and D). These findings suggest that fALS-associated mutations may affect a functionally active NLS located in the C-terminus of FUS.

To test whether the C-terminal tail of FUS is not only necessary but also sufficient for active nuclear import, we transplanted this domain onto the C-terminus of the cytosolic reporter protein GST-GFP. Owing to its size (55 kDa), the GST-GFP fusion protein is largely excluded from the nucleus (Figure 1E) and requires active nuclear import mediated by an NLS (Iijima *et al*, 2006; Terry *et al*, 2007). Similar to the well-characterized classical NLS of the SV40 large T antigen (SV40-NLS) (Kalderon *et al*, 1984), the C-terminal 13 amino acids of FUS ($FUS_{514-526}$) mediated an almost exclusive nuclear localization of the reporter protein (Figure 1E, see F for quantification). In contrast, the same amino acids arranged in random order ($FUS_{514-526}$ scrambled) were not able to mediate import of GST-GFP (Figure 1E and F), showing that the FUS NLS activity requires a specific sequence motif rather than the random presence of several positively charged arginines. Taken together, these experiments demonstrate that the C-terminal tail of FUS is necessary and sufficient for active nuclear import and thus constitutes a bona fide NLS.

fALS-associated point mutations in the C-terminal domain disrupt nuclear import of FUS

After functionally identifying the NLS of FUS, we analysed four fALS-associated point mutations that occur within this domain at evolutionarily conserved residues (R521G, R522G, R524S, P525L; see Figure 1B) (Chio *et al*, 2009; Kwiatkowski *et al*, 2009) and asked whether they may disrupt nuclear import. Indeed, all four point mutations showed a varying degree of cytosolic accumulation, ranging from a mild mislocalization for R521G and R524S (16 ± 10% and 21 ± 7% cytosolic, respectively) over an intermediate phenotype for R522G (45 ± 9% cytosolic) to a severe mislocalization for P525L (65 ± 5% cytosolic) (Figure 2A, see B for quantification, note that mutations were ordered according to their strength/age of onset). R521H and R521C, the fALS-associated *FUS* mutations identified most frequently (Belzil *et al*, 2009; Drepper *et al*, 2009; Kwiatkowski *et al*, 2009; Ticozzi *et al*, 2009; Vance *et al*, 2009; Corrado *et al*, 2010; Lai *et al*, 2010; Suzuki *et al*, 2010), also caused a mild nuclear import defect, similar to R521G (Supplementary Figure S1A

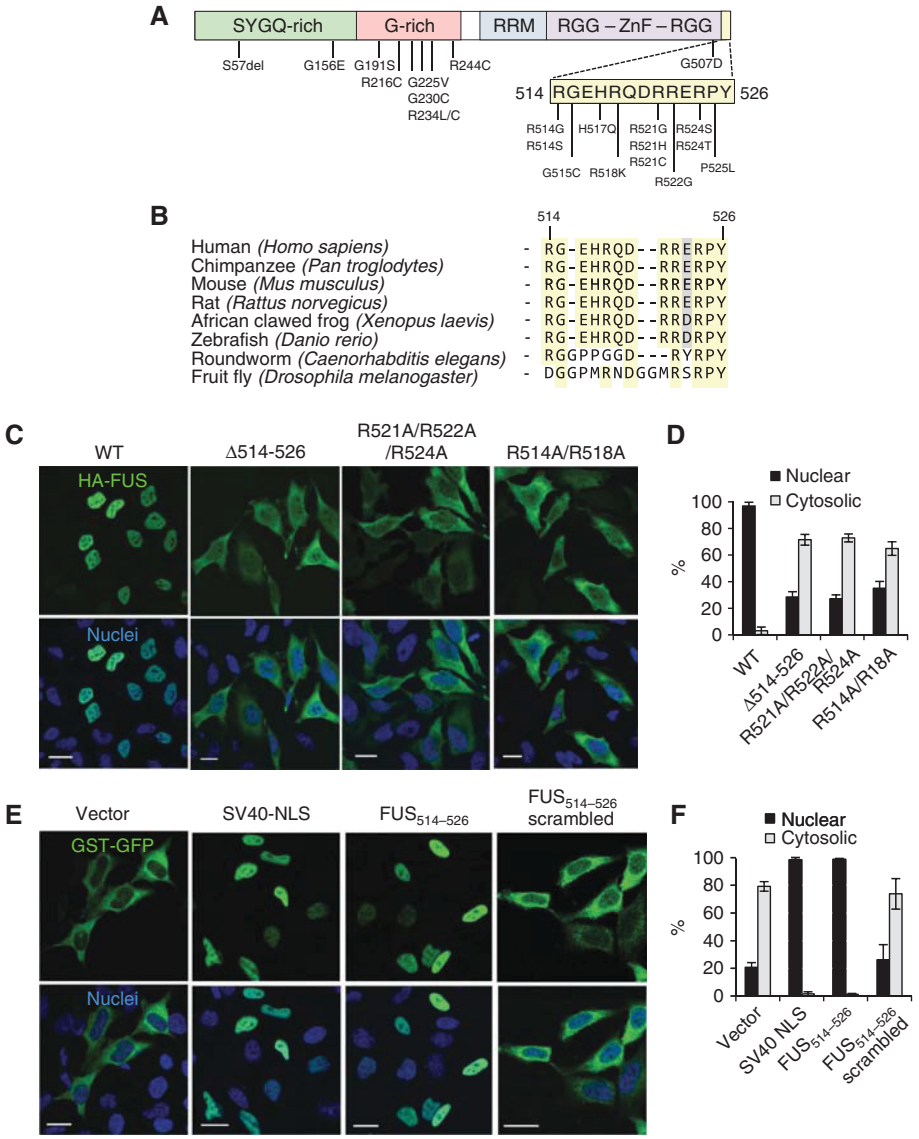

Figure 1 The C-terminal tail of FUS ($FUS_{514-526}$) is necessary and sufficient for nuclear import. (**A**) Schematic diagram of the domain structure of FUS. Mutations identified in fALS patients are shown below; 12 out of the 22 known mutations are clustered in the C-terminal tail (residues 514–526). (**B**) Alignment of the FUS C-termini of different species shows that the sequence of this domain is well conserved during evolution (identical residues are highlighted in yellow, homologous residues in light grey). (**C**) N-terminally HA-tagged wild-type (WT) FUS and the indicated point mutants were transiently expressed in HeLa cells; 24 h post-transfection cells were stained with an HA-specific antibody (green), a nuclear counter-stain (blue) and analysed by confocal microscopy. Although the WT protein is located almost exclusively in the nucleus, deletion of the C-terminal 13 amino acids (Δ514–526) or replacement of arginine residues by alanine (R521A/R522A/R524A or R514A/R518A) leads to a predominantly cytosolic localization. Scale bar, 20 μm. (**D**) Quantification of nuclear and cytosolic fluorescence intensities. Error bars indicate s.d. (**E**) The indicated sequences were fused to the C-terminus of the cytosolic reporter GST-GFP and reporter constructs were transiently expressed in HeLa cells; 24 h post-transfection cells were stained with a GFP-specific antibody (green) and a nuclear counter-stain (blue) and localization of the reporter proteins was analysed by confocal microscopy. Without active nuclear import, GST-GFP is localized predominantly in the cytosol (first panel), whereas attachment of the well-characterized NLS of the SV40 large T antigen (SV40-NLS) or the last 13 amino acids of FUS ($FUS_{514-526}$) efficiently mediate nuclear import (second and third panel). The same amino acids arranged in random order ($FUS_{514-526}$ scrambled) are not sufficient for mediating nuclear import (last panel). Scale bar, 20 μm. (**F**) Quantification of nuclear and cytosolic fluorescence intensities. Error bars indicate s.d.

and B). The fact that none of the point mutants are completely excluded from the nucleus is consistent with the finding that in fALS patients with *FUS* mutations neurons with cytoplasmic FUS inclusions still show some immunolabelling of the nucleus (Kwiatkowski *et al*, 2009; Vance *et al*, 2009; Rademakers *et al*, 2010). The observed cytoplasmic mislocalization cannot be attributed to a higher expression level of the point mutants, as similar expression levels were observed for all mutants (Figure 2C). Thus, R522 and P525 are important residues in the C-terminal NLS of FUS, whereas R521 and R524 have a less important function for NLS activity. Another important residue is the highly conserved tyrosine at the C-terminus, which is predicted to have an important function in a PY-NLS (Lee *et al*, 2006), as its mutation to an alanine results in a dramatic relocalization of FUS (Supplementary Figure S1C and D). Furthermore, it is remarkable that the P525L and R522G mutations, which show the strongest degree of cytosolic mislocalization, were

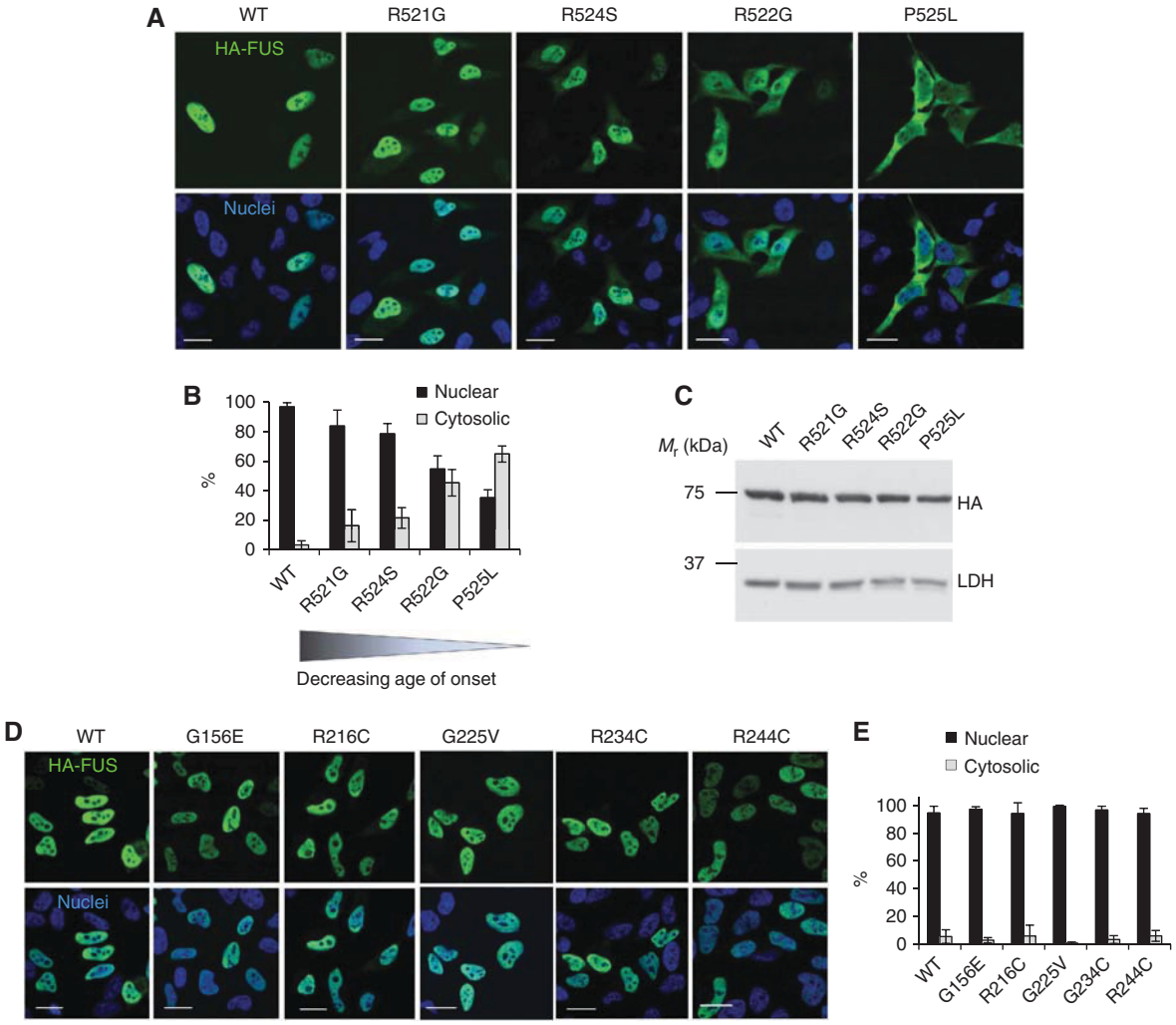

Figure 2 fALS-associated mutations in important residues of the FUS NLS disrupt nuclear import. (**A**) HA-tagged wild-type (WT) FUS or FUS carrying the indicated C-terminal point mutations was transiently expressed in HeLa cells. Cells were stained with an HA-specific antibody (green) and a nuclear counter-stain (blue) and were analysed by confocal microscopy. R521G and R524S show a mild, R522G and P525L a strong cytosolic mislocalization, suggesting that these mutations disrupt important residues of the FUS NLS. Scale bar, 20 μm. (**B**) Quantification of nuclear and cytosolic fluorescence intensities. Error bars indicate s.d. The degree of cytoplasmic mislocalization inversely correlates with the age of onset of the individual point mutations. (**C**) HA-FUS protein levels in HeLa cells transiently transfected with the indicated HA-FUS constructs were analysed by immunoblotting with an HA-specific antibody (upper panel). LDH served as a loading control (lower panel). (**D**) HA-tagged wild-type (WT) FUS or FUS carrying the indicated N-terminal point mutations was transiently expressed in HeLa cells. Cells were stained with an HA-specific antibody (green) and a nuclear counter-stain (blue) and were analysed by confocal microscopy. The nuclear/cytosolic distribution of the N-terminal point mutants is indistinguishable from the WT protein. Scale bar, 20 μm. (**E**) Quantification of nuclear and cytosolic fluorescence intensities. Error bars indicate s.d.

reported to cause especially aggressive forms of fALS, with a mean disease onset at 24 and 28.5 years, respectively (Chio *et al*, 2009; Kwiatkowski *et al*, 2009). Thus, the degree of cytosolic mislocalization is inversely correlated to the age of disease onset (Figure 2B).

As deletion or mutation of the C-terminal NLS did not eliminate nuclear import completely (see Figures 1B and 2B), we investigated whether any of the point mutations located in the N-terminal SYGQ- and G-domains (Figure 1A) might affect a putative second NLS. However, all of the investigated N-terminal point mutants (G156E, R216C, G225V, R234C, R244C) showed an almost exclusive nuclear localization, indistinguishable from the WT protein (Figure 2D, see E for quantification). Furthermore, N-terminal point mutations did not further aggravate mislocalization of the P525L mutant (Supplementary Figure S2A and B), making it unlikely that they affect a second, weaker NLS, which might become important when the C-terminal NLS is impaired. Together, these findings show that C-terminal fALS-associated *FUS* mutations affect the protein's major NLS and thus impair its nuclear import, whereas the so far identified N-terminal *FUS* mutations do not impair nuclear localization. The latter suggests that these mutations cause disease through a different cellular mechanism.

FUS-P525L mutation disrupts nuclear import in primary neurons and prevents import of a cytosolic reporter in vitro and in vivo

As fALS-associated *FUS* mutations specifically cause degeneration of neurons in the cortex and spinal cord (Kwiatkowski *et al*, 2009; Vance *et al*, 2009), we wanted to confirm that these mutations also affect FUS import in neuronal cells.

We, therefore, prepared primary neuronal cultures from embryonic (E19) rat hippocampus and frontal cortex and examined the subcellular localization of the WT protein and the strong P525L mutant on transfection of the corresponding cDNA constructs. As in HeLa cells, FUS-WT was located almost exclusively in the nucleus, whereas the P525L mutant was strongly redistributed to the cytosol, extending even into the neuronal processes in both cortical and hippocampal neurons (Figure 3A, see B for quantification). Thus, fALS-associated C-terminal *FUS* mutations disrupt nuclear

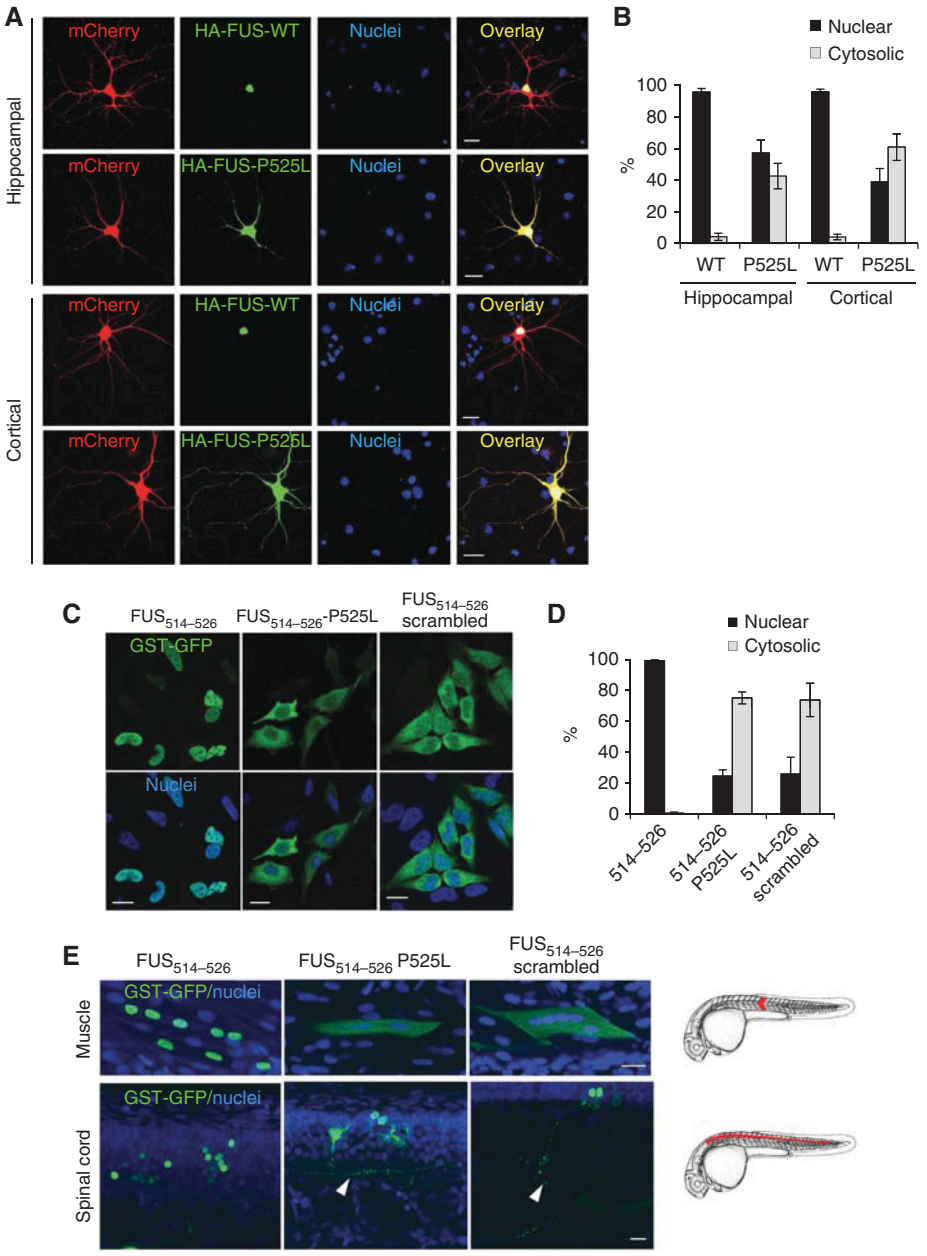

Figure 3 The *FUS*-P525L mutation disrupts nuclear import in primary neurons and prevents import of a cytosolic reporter *in vitro* and *in vivo*. (**A**) Cultured neurons from E19 rat hippocampus or frontal cortex were transfected with HA-tagged FUS-WT or P525L, mCherry (red) was co-expressed to visualize neuron morphology. Two days post-transfection, cells were stained with an HA-specific antibody (green) and a nuclear counter-stain (blue) and were analysed by confocal microscopy. FUS-WT is mostly confined to the nucleus, whereas the P525L mutant shows abundant staining in the whole cell body and in neurites. Scale bar, 20 μm. (**B**) Quantification of nuclear and cytosolic fluorescence intensities. Z-stacks were taken and all planes were projected into a single image along the *z* axis (maximal projection). Ten fields were analysed for each sample and mean values were calculated. Error bars indicate s.d. (**C**) To confirm that fALS-associated point mutations disrupt nuclear import, the P525L mutation was introduced into the GST-GFP-$FUS_{514-526}$ reporter and was analysed for its effect on nuclear import activity. Localization of the P525L-containing reporter is identical to that of the $FUS_{514-526}$ scrambled reporter, showing that this point mutation completely disrupts activity of the C-terminal NLS. Scale bar, 20 μm. (**D**) Quantification of nuclear and cytosolic fluorescence intensities. Error bars indicate s.d. (**E**) To confirm functionality of the FUS-NLS *in vivo*, the indicated GST-GFP reporter constructs were injected into fertilized zebrafish eggs. On day 2 post-fertilization, embryos were stained with a GFP-specific antibody (green) and a nuclear counter-stain (blue), and subcellular localization of the reporter constructs was analysed in muscle cells and spinal cord neurons by confocal microscopy. In both cell types, the $FUS_{514-526}$ WT sequence mediates efficient nuclear import (left panels), whereas reporter proteins carrying the P525L mutation or scrambled NLS remain cytosolic (middle and right panels). Arrowheads indicate axonal localization of reporter proteins in spinal cord neurons. Scale bar, 10 μm.

import not only in transformed cell lines, but also in primary neuronal cells, the cell type primarily affected in FUS-opathies.

To further support that cytosolic mislocalization of the fALS mutants was due to a disrupted NLS activity, the P525L mutation was introduced into the GST-GFP-$FUS_{514-526}$ reporter construct and analysed for its effect on nuclear import. Consistent with the data shown in Figures 2A and 3A, the proline mutation efficiently blocked nuclear import of the reporter protein, as its localization was indistinguishable from that of the $FUS_{514-526}$ scrambled reporter (Figure 3C and D). This further supports that fALS-associated point mutations disrupt the $FUS_{514-526}$ NLS. To provide *in vivo* evidence for these findings, we injected the same reporter constructs into zebrafish eggs and analysed their subcellular localization in zebrafish embryos on day 2 post-fertilization. In both myocytes and spinal cord neurons, the $FUS_{514-526}$ WT sequence mediated efficient nuclear import, whereas reporter proteins carrying the P525L mutation or scrambled NLS remained cytosolic and were detectable in axonal processes of spinal cord neurons (Figure 3E). These data corroborate that fALS-associated point mutations in the FUS-NLS disrupt nuclear import in a living animal in different cell types, including spinal cord neurons.

Nuclear import receptor Transportin is required for nuclear import of FUS

Next, we searched for the cellular mechanism of nuclear transport affected by the fALS mutations described above. The NLS of FUS bears some homology to other NLSs with a PY motif, which have been shown to be recognized by the nuclear transport receptor Transportin (Trp), also known as Karyopherin β2 (Lee *et al*, 2006; Imasaki *et al*, 2007). As FUS has been shown to interact with Trp in *in vitro* pull down assays (Guttinger *et al*, 2004; Lee *et al*, 2006), we speculated that Trp may mediate nuclear import of FUS by binding to its C-terminal NLS and that fALS-associated point mutations might interfere with this import pathway. To test whether Trp is responsible for nuclear import of FUS, we performed siRNA-mediated knockdown of the two Trp homologues, Trp1 and Trp2, two closely related proteins shown to have redundant function as nuclear import receptors (Guttinger *et al*, 2004; Rebane *et al*, 2004). Whereas knockdown of either Trp1 or Trp2 alone had not effect on nuclear import of FUS (data not shown), knockdown of both Trp variants significantly impaired nuclear import of endogenous FUS, as about 25% of the protein was found outside the nucleus on Trp1/2 silencing (Figure 4A, see B for quantification). The fact that substantial amounts of FUS are still detectable in the nucleus may be due to residual Trp1 remaining in siRNA-transfected cells (Figure 4C, middle panel) or could indicate that additional import receptors are involved in nuclear import of FUS. To test whether Trp is the predominant import receptor for the C-terminal NLS, we expressed the two FUS mutants R521G and P525L in cells that had been transfected with Trp1/2-specific siRNAs. As a control, we examined the behaviour of HA-tagged WT FUS. Similar to endogenous FUS (Figure 4A), HA-tagged FUS-WT showed a moderate redistribution to the cytoplasm on Trp knockdown (Figure 4D and E, see F for knockdown efficiency and HA-FUS protein levels). Interestingly, the FUS-R521G mutant, which showed only a mild cytosolic mislocalization in non-siRNA transfected (Figure 2A) or control siRNA-transfected cells (Figure 4D, upper panel), was strongly affected by Trp silencing, as $>60\%$ of the protein redistributed to the cytosol under these conditions (Figure 4D and E). This shows that the R521G mutation indeed interferes with the Trp pathway and strongly suggests that Trp is the major import receptor for the C-terminal NLS of FUS. In line with this, the severe cytosolic mislocalization of the P525L mutant was only slightly, if at all, aggravated by Trp silencing (Figure 4D and E). This further corroborates that Trp is the major import receptor recognizing the FUS PY-NLS.

The structures of several non-classical PY-NLSs bound to Trp have been solved and converge to a consensus-binding geometry consisting of an N-terminal hydrophobic/basic motif and the C-terminal motif $R/H/KX_{2-5}PY$ (Lee *et al*, 2006; Cansizoglu *et al*, 2007; Imasaki *et al*, 2007). On the basis of these data, we modelled the FUS C-terminal sequence as subtype RXXPY bound to Trp (Figure 4G). Interestingly, our model shows two distinct binding areas within this RXXPY motif: R522 makes strong charged H-bond/ion-pair interactions with the side chain carboxylates of E509 and D543 of Trp1. The second area of tight binding comprises residues P525 and Y526. As in the experimental structures, the proline allows a particular kinked main chain geometry between these two residues, enabling a specific surface recognition, consisting of a hydrophobic pocket that engulfs the proline side chain and the phenyl ring of Y526 and an H-bond contact to Y526. In contrast, no specific interaction partner can be found for R521, resulting most likely in a somewhat flexible conformation, and only a weak attractive force between the receptor surface and R521 because of the negative electrostatic potential of the Trp surface in this region can be predicted. Similarly, R524 points away from the receptor surface and should not contribute significantly to recognition. Thus, our model is consistent with our analysis of the fALS-associated FUS mutations (Figure 2A and B), as changes in amino acids that are responsible for strong contacts between the FUS C-terminal sequence and Trp (R522 and P525) resulted in a severe cytosolic relocalization and early disease onset, whereas mutation of either R521 or R524 to glycine or serine only resulted in a mild mislocalization and later disease onset.

As siRNA-mediated silencing of Trp did not result in a complete block of the Trp pathway (see residual Trp1 levels in Figure 4C and F) and only led to a moderate cytosolic redistribution of WT-FUS, we searched for a more efficient way of blocking Trp-mediated nuclear import. To this end, we took advantage of a Trp-specific inhibitor peptide (M9M) designed to bind Trp with high affinity by joining the N-terminal half of the hnRNP A1 NLS (called M9) with the C-terminal half of the PY-NLS of hnRNP M (Cansizoglu *et al*, 2007). By combining these two high-affinity-binding sites, the M9M peptide efficiently competes with natural substrates of Trp, such as hnRNP A1, HuR and hnRNP M (Cansizoglu *et al*, 2007). We reasoned that if Trp mediates nuclear import of FUS by binding to its C-terminal PY-NLS, the high-affinity peptide inhibitor should compete for this interaction and thus should prevent or reduce nuclear import of endogenous FUS. Indeed, when we expressed a GFP-M9M construct in cortical neurons (Figure 5A), hippocampal neurons (Supplementary Figure S3A) and HeLa cells (Figure 5B and C), the transfected cells showed a striking redistribution of endogenous FUS to the cytosol. In contrast, TDP-43, which is imported through

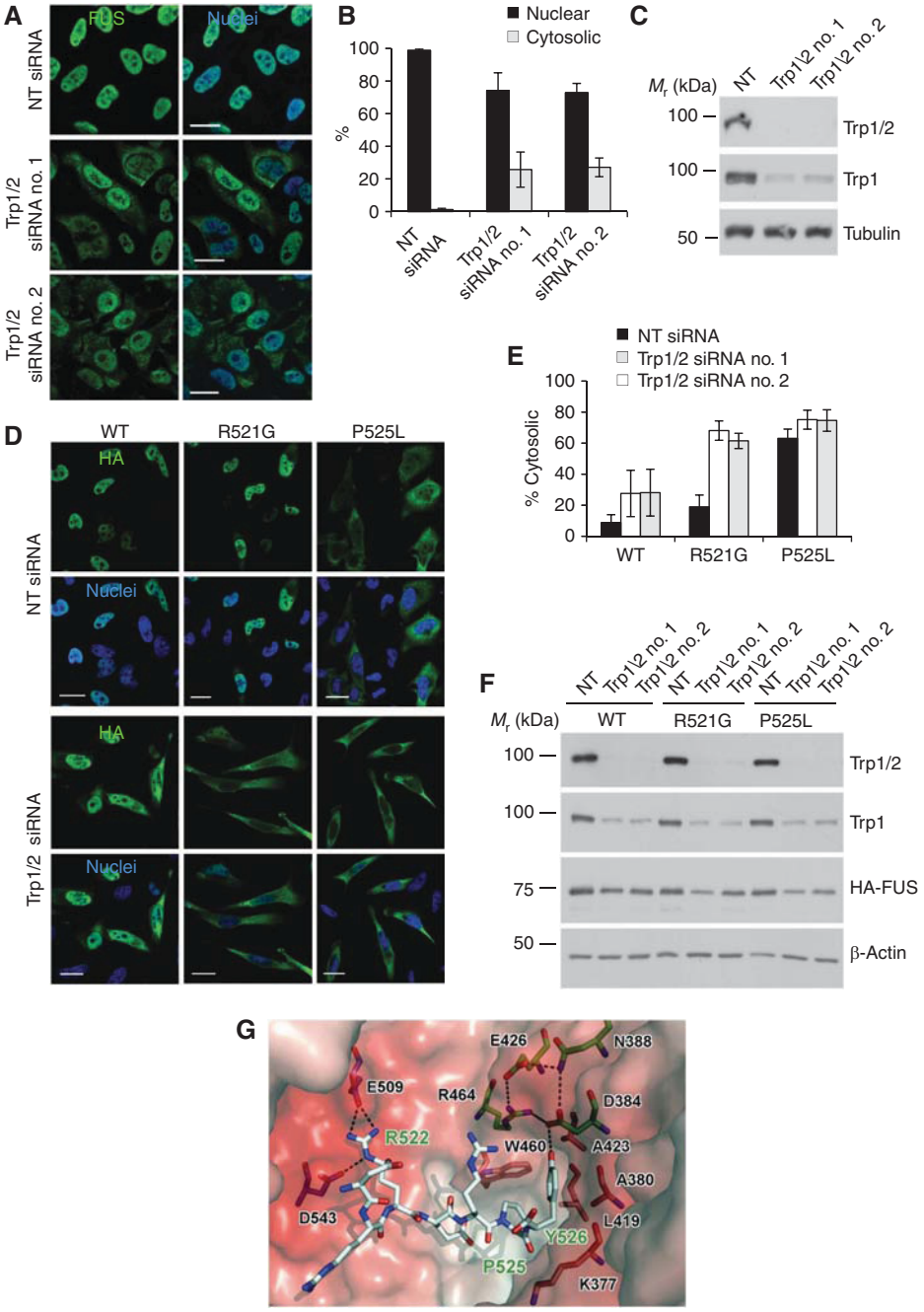

Figure 4 Transportin is required for nuclear import of FUS. (**A**) The two Trp homologues, Trp1 and Trp2, were silenced by siRNA-mediated knockdown, using two different siRNA pools (no. 1 and no. 2). A non-targeting (NT) siRNA was used as a negative control; 72 h post-transfection, cells were stained with an FUS-specific antibody (green) and a nuclear counter-stain (blue) and were analysed by confocal microscopy. Trp1/2 double knockdown leads to a partial cytoplasmic redistribution, showing that Trp is involved in nuclear import of FUS. Scale bar, 20 μm. (**B**) Quantification of nuclear and cytosolic fluorescence intensities. Error bars indicate s.d. (**C**) Verification of knockdown efficiency by immunoblot. Total cell lysates were examined with a pan-Trp (Trp1/2)- and a Trp1-specific antibody (upper two panels). α-Tubulin served as a loading control (lower panel). Note that the Trp1-specific antibody is more sensitive than the pan-Trp antiserum and detects residual levels of Trp1 (middle panel). (**D**) HeLa cells were transfected with NT siRNA or Trp1/2-specific siRNA pool no. 1 or no. 2 and 24 h later with the indicated HA-tagged FUS constructs. Another 24 h later, cells were stained with an HA-specific antibody (green) and a nuclear counter-stain (blue) and were analysed by confocal microscopy. Trp silencing leads to a dramatic cytosolic mislocalization of the otherwise weakly mislocalized R521G mutant, but has almost no further effect on the already strongly mislocalized P525L mutant. Scale bar, 20 μm. (**E**) Quantification of nuclear and cytosolic fluorescence intensities. Error bars indicate s.d. (**F**) Verification of knockdown efficiency and expression of HA constructs by immunoblot. Total cell lysates were examined with antibodies specific for Trp1/2, Trp1 and HA (upper three panels). β-actin served as a loading control (lowest panel). (**G**) Model of the FUS PY-NLS (stick model with grey carbons, red oxygens, blue nitrogens, important amino-acid residues labelled in green) bound to the semitransparent electrostatic surface of Trp coloured according to its calculated negative (−25 e/kT, red) and positive (+25 e/kT, blue) electrostatic surface potential. Underlying amino-acid residues of special importance for binding of the FUS-NLS are depicted as stick model and labelled in black. Residues responsible for the charged H-bond/salt-bridge contact to FUS-R522 and residues forming the hydrophobic pocked for FUS-PY526 and the H-bond network connecting to FUS-Y526 OH are shown with blue, orange and green carbons, respectively. H-bonds are indicated as broken black lines. This figure was made with pymol (DeLano Scientific LLC, USA, http://www.pymol.org).

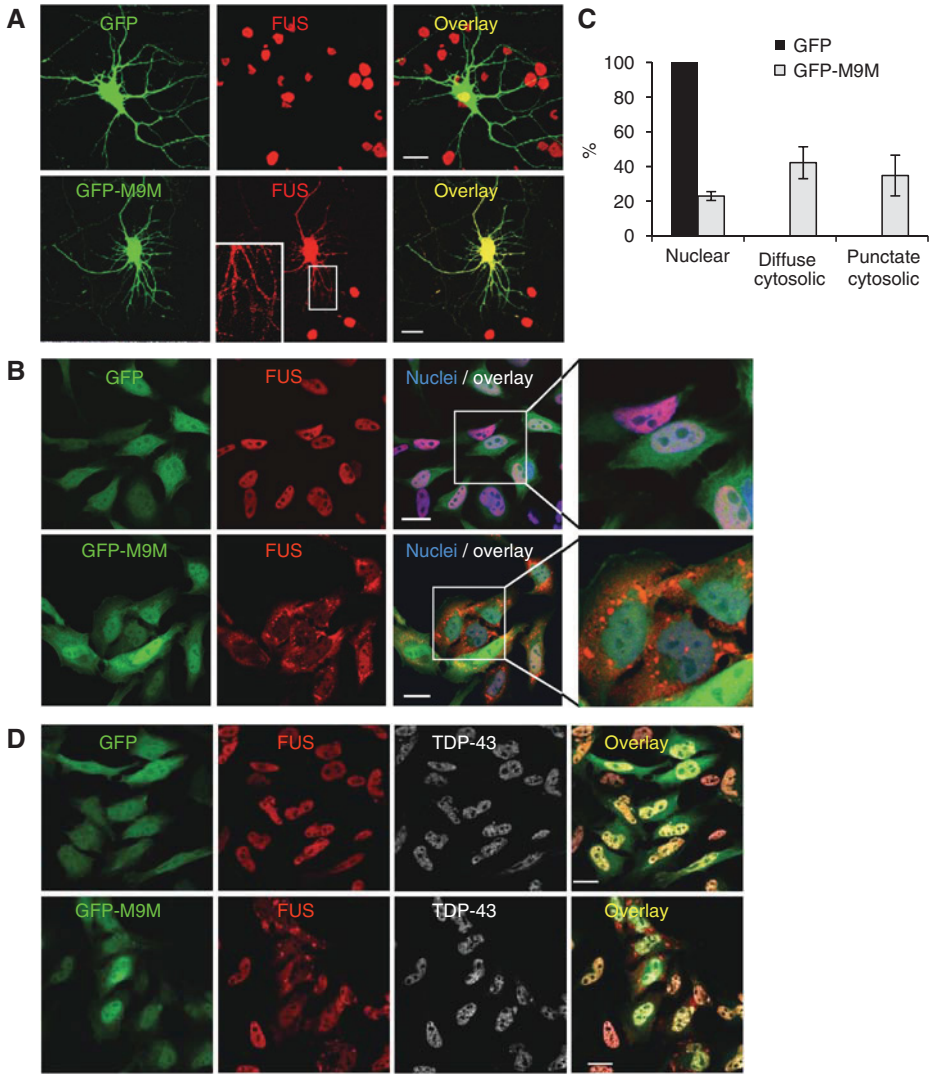

Figure 5 Expression of a Trp-specific peptide inhibitor leads to the cytosolic redistribution of FUS, but not TDP-43. (**A**, **B**) A peptide competitor (M9M) designed to bind to the PY-NLS-binding site in Trp with very high affinity was expressed in primary rat cortical neurons (**A**) or HeLa cells (**B**) as a GFP-fusion protein (green). After staining with an FUS-specific antibody (red), cells were analysed by confocal microscopy. Expression of the Trp-specific inhibitor construct causes a marked cytoplasmic redistribution and localization of endogenous FUS in cytoplasmic punctate structures. Scale bar, 20 μm. Insert in (**A**) and panels on the right of (**B**) show magnifications of the boxed regions. (**C**) Quantification of the percentage of HeLa cells with exclusively nuclear, diffuse cytosolic and punctuate cytosolic FUS staining. Error bars indicate s.d. (**D**) To show selectivity of the M9M peptide inhibitor, GFP or GFP-M9M (green)-transfected HeLa cells were co-stained for endogenous FUS (red) and TDP-43 (white) and were analysed by confocal microscopy. In contrast to FUS, nuclear localization of TDP-43 is not affected by expression of the M9M construct. Scale bar, 20 μm.

the classical NLS-dependent importin α/β (karyopherin α/β1) pathway (Winton *et al*, 2008), was not affected by expression of the M9M inhibitor and remained nuclear even in cells with cytoplasmic FUS staining (Figure 5D). As an additional control, we expressed an importin α/β-specific inhibitor construct (GFP-Bimax2), designed to bind to importin α with high affinity (Kosugi *et al*, 2008). As expected, the importin α/β-specific inhibitor interfered with the nuclear import of TDP-43, but not of FUS (Supplementary Figure S3B). These data show that Trp, but not the classical import receptor importin α/β, is required for nuclear import of FUS. Taken together, our knockdown and competition experiments and structural modelling of the FUS PY-NLS indicate that FUS is imported into the nucleus through the Trp receptor and suggest that the pathogenic mechanism underlying the C-terminal *FUS* mutations is an impairment of Trp-dependent nuclear import of FUS.

Redistribution of FUS into cytoplasmic stress granules

Interestingly, we noted that after GFP-M9M expression, HeLa cells and primary neurons with cytosolic FUS redistribution often showed a punctuate localization pattern of FUS (magnifications in Figure 5A and B, see for quantification). As FUS is an RNA-binding protein (Zinszner *et al*, 1997b), we wondered whether the observed puncta might be stress granules, cytoplasmic RNP structures that temporarily store translationally arrested mRNAs during cellular stress (Anderson and Kedersha, 2006). In addition to stalled mRNAs, stress granules contain characteristic proteins, such as proteins of the small ribosomal subunit, translation initiation factors

including eIF3 and eIF4G and a large variety of RNA-binding proteins, such as the PolyA-binding protein (PABP-1), the translational silencer T cell intracellular antigen-1 (TIA-1), TIA-1-related protein (TIAR) and the Ras-GAP-SH3-binding protein (G3BP1). These proteins specifically associate with stress granules and not with other types of cytoplasmic RNA granules, such as processing bodies (P bodies) associated with mRNA decay (Kiebler and Bassell, 2006). Therefore, they are commonly used as specific markers of stress granules (Anderson and Kedersha, 2008). Co-staining with antibodies specific to PABP-1, TIA-1, TIAR and G3BP1 showed that indeed FUS was localized to stress granules in GFP-M9M-transfected cells (Figure 6A, rows 1–4). In contrast, the P body-specific marker protein Dcp1 did not co-stain with FUS (Figure 6A, row 5), excluding that the FUS-positive granules observed after GFP-M9M expression correspond to P bodies. Furthermore, on addition of the polysome-stabilizing drug cycloheximide, a well-known inhibitor of stress granule assembly (Kedersha and Anderson, 2007), FUS remained diffusely distributed in the cytosol and no FUS-positive G3BP1-positive granules could be observed (Figure 6B). This confirms that the FUS-positive granules observed after GFP-M9M expression are stress granules. Together, our data suggest that cytoplasmically mislocalized FUS may be recruited into stress granules under conditions of cellular stress, such as strong inhibition of Trp-dependent transport by GFP-M9M over-expression.

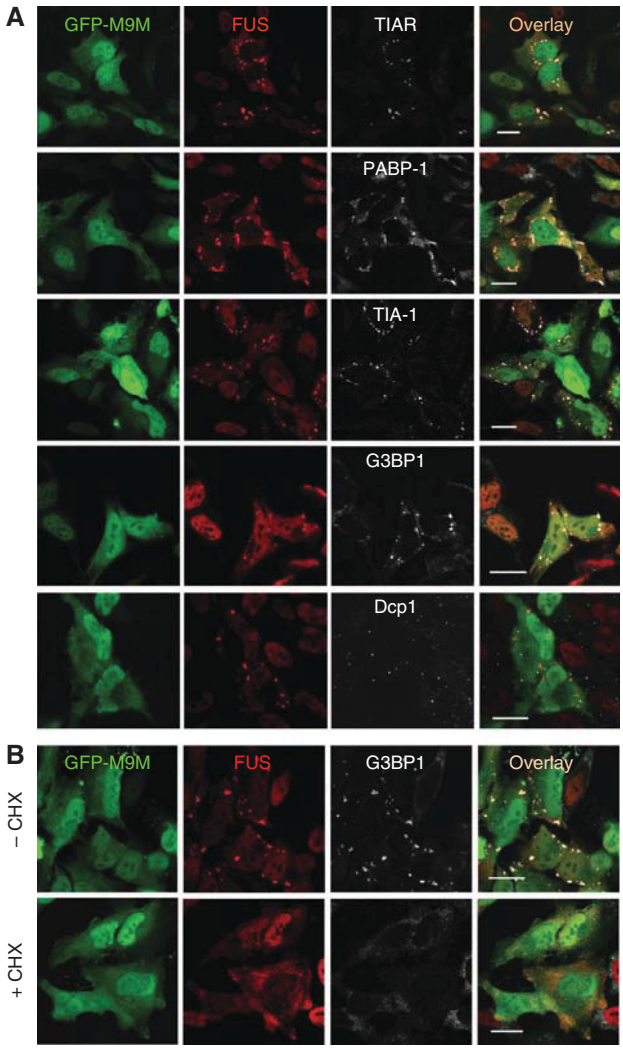

Figure 6 Redistribution of FUS into cytoplasmic stress granules. (**A**) GFP-M9M (green)-transfected HeLa cells were co-stained for endogenous FUS (red) and the stress granule marker proteins TIAR, PABP-1, TIA-1, G3BP1 or the P body marker Dcp1 (white). Co-staining of FUS with TIAR, PABP-1, TIA-1 and G3BP1 shows that the punctate FUS-positive structures are stress granules. Note that there is no co-localization with the P body marker Dcp1. Scale bar, 20 μm. (**B**) GFP-M9M (green)-transfected HeLa cells were stained for endogenous FUS (red) and the stress granule marker G3BP1 (white). Where indicated, the polysome-stabilizing drug cycloheximide (CHX) was added for 1 h before fixation to prevent stress granule formation. Cycloheximide prevents formation of G3BP1- and FUS-positive cytosolic structures, confirming their stress granule identity. Scale bar, 20 μm.

Pathologic inclusions in fALS and FTLD-FUS patients contain marker proteins of stress granules

As stress granules dynamically grow and coalesce on prolonged stress exposure (Kedersha *et al*, 2000), we wondered whether the FUS-containing stress granules might be related to the large FUS-positive inclusions present in brains of fALS and FTLD-FUS patients. We, therefore, analysed sections of post-mortem brain and spinal cord tissue from an fALS case carrying an FUS-R521C mutation and from cases with sporadic FTLD-FUS, including aFTLD-U ($n=3$), NIFID ($n=3$) and BIBD ($n=1$), by immunohistochemistry and double-label immunofluorescence for the presence of the stress granule marker PABP-1 in neuronal cytoplasmic inclusions (NCIs). Strikingly, all cases with FUS pathology revealed strong labelling for PABP-1 in NCIs in affected brain regions such as spinal cord and hippocampus (Figure 7A, upper panels). This was further confirmed by double-label immunofluorescence with anti-p62 (green), a robust marker of NCIs in FUS-opathies (Neumann *et al*, 2009a, b; Munoz *et al*, 2009), and anti-PABP-1 (red), which showed a clear co-localization in NCIs of all tested FUS-opathy cases (Figure 7A, lower panels). Furthermore, NCIs in all cases examined showed an enrichment for another stress granule marker protein, eIF4G (Figure 7B). Notably, cases with FTLD-TDP pathology ($n=2$) included as neurologic controls showed no staining of NCIs with PABP-1 or eIF4G (Figure 7A and B). This suggests that co-sequestration of stress granule-associated proteins is a specific feature of FUS inclusions and that stress granule formation might be involved in inclusion body formation in FUS-opathies.

C-terminal fALS mutations favour recruitment of FUS into stress granules

It is important to note that in our cellular models FUS-positive stress granules were observed after GFP-M9M expression (Figure 6), but not on expression of mutations interfering with the NLS of FUS, despite their substantial redistribution to the cytosol (Figures 1 and 2). This suggests that cytosolic mislocalization by itself is not sufficient for the formation of FUS-containing granules, but that additional cellular stress (e.g. strong inhibition of Trp-dependent transport by GFP-M9M expression) is required for this to occur. To test this hypothesis, we expressed FUS-WT and the above-examined C-terminal *FUS* mutants (R521G, R522G, R524S, P525L) in HeLa cells (Figure 8A) and primary neurons (Figure 8B), subjected them to heat shock and analysed

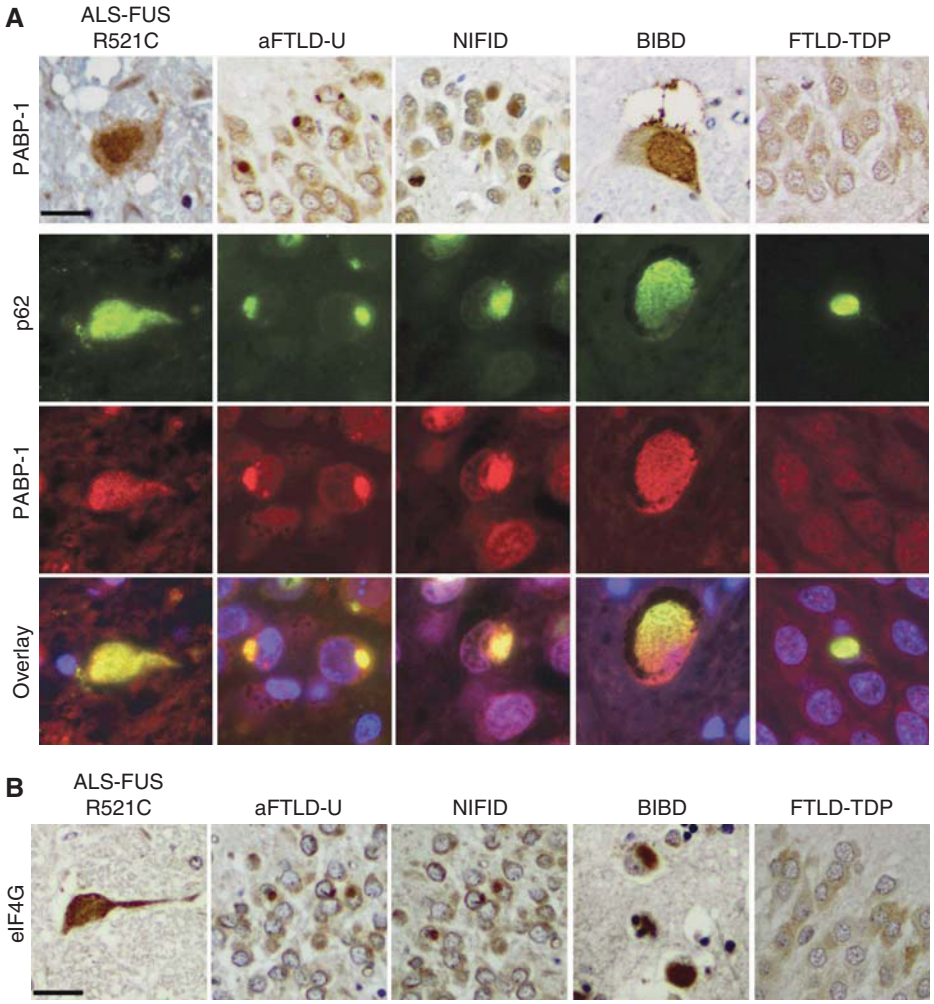

Figure 7 Neuronal cytoplasmic inclusions (NCIs) in patients with FUS pathology contain the stress granule marker proteins PABP-1 and eIF4G. (**A**) Upper panels: PABP-1 immunohistochemistry performed on sections of post-mortem tissue reveals strongly immunoreactive NCIs in motor neurons in the spinal cord in fALS-R521C, in dentate granule cells of the hippocampus in aFTLD-U and NIFID as well as in motor neurons in the spinal cord in BIBD. In contrast, no PABP-1-labeled inclusions were detectable in dentate granule cells of the hippocampus in FTLD-TDP. Scale bar, 25 μm. Lower panels: double-label immunofluorescence stainings of the same cases and brain regions show co-localization of PABP-1 (red) with p62-positive inclusions (green) in fALS-R521C, aFTLD-U, NIFID and BIBD, but no PABP-1 staining in FTLD-TDP inclusions. Note that p62 is a robust marker of FUS and TDP-43 NCIs and was used because double labelling for FUS and PABP-1 was technically not possible, as available antibodies working on paraffin-embedded tissue were both rabbit polyclonal antisera. Scale bar, 12.5 μm. (**B**) eIF4G immunohistochemistry reveals labelling of NCIs in motor neurons in the spinal cord in fALS-R521C, in dentate granule cells of the hippocampus in aFTLD-U and NIFID and neurons in frontal cortex in BIBD. No NCIs were detectable in dentate granule cells in FTLD-TDP. Scale bar, 25 μm.

whether the proteins would be recruited to stress granules. In the absence of heat stress, the expressed proteins showed the above-described localization pattern and no stress granules could be detected with a PABP-1 or TIAR antibody (Figure 8A and B, left panels). In contrast, after heat shock, all FUS mutants localized to cytoplasmic stress granules (Figure 8A and B, right panels, for additional stress granule markers, see Supplementary Figure S4A), confirming our hypothesis that additional cellular stress is required for the recruitment of FUS into stress granules. The presence of cycloheximide during heat shock completely prevented the granular localization of the FUS-P525L mutant (Supplementary Figure S4B), confirming that the FUS mutant-containing granules observed after heat shock correspond to stress granules. Consistent with the GFP-M9M experiment (Figure 5D) and the pathology data shown in Figure 7, TDP-43 was not detectable in FUS-P525L-positive stress granules after heat shock (Figure 8C). Interestingly, FUS-WT also remained exclusively nuclear after heat shock and was not detectable in cytoplasmic stress granules (Figure 8A and B, right panels). This suggests that only cytoplasmically mislocalized FUS is recruited into stress granules. In line with this, the amount of mutant FUS in stress granules correlated with the degree of cytoplasmic mislocalization of the point mutants and inversely with their age of disease onset (Figure 8A). This suggests that cytosolic mislocalization strongly facilitates the formation of FUS-positive stress granules.

In conclusion, our data suggest that two pathological hits, namely cytosolic mislocalization of FUS and cellular stress, are required for the formation of FUS-positive stress granules, both in peripheral and neuronal cells (Figure 9). Furthermore, recruitment of cytoplasmic FUS into stress granules might be an important cellular mechanism leading

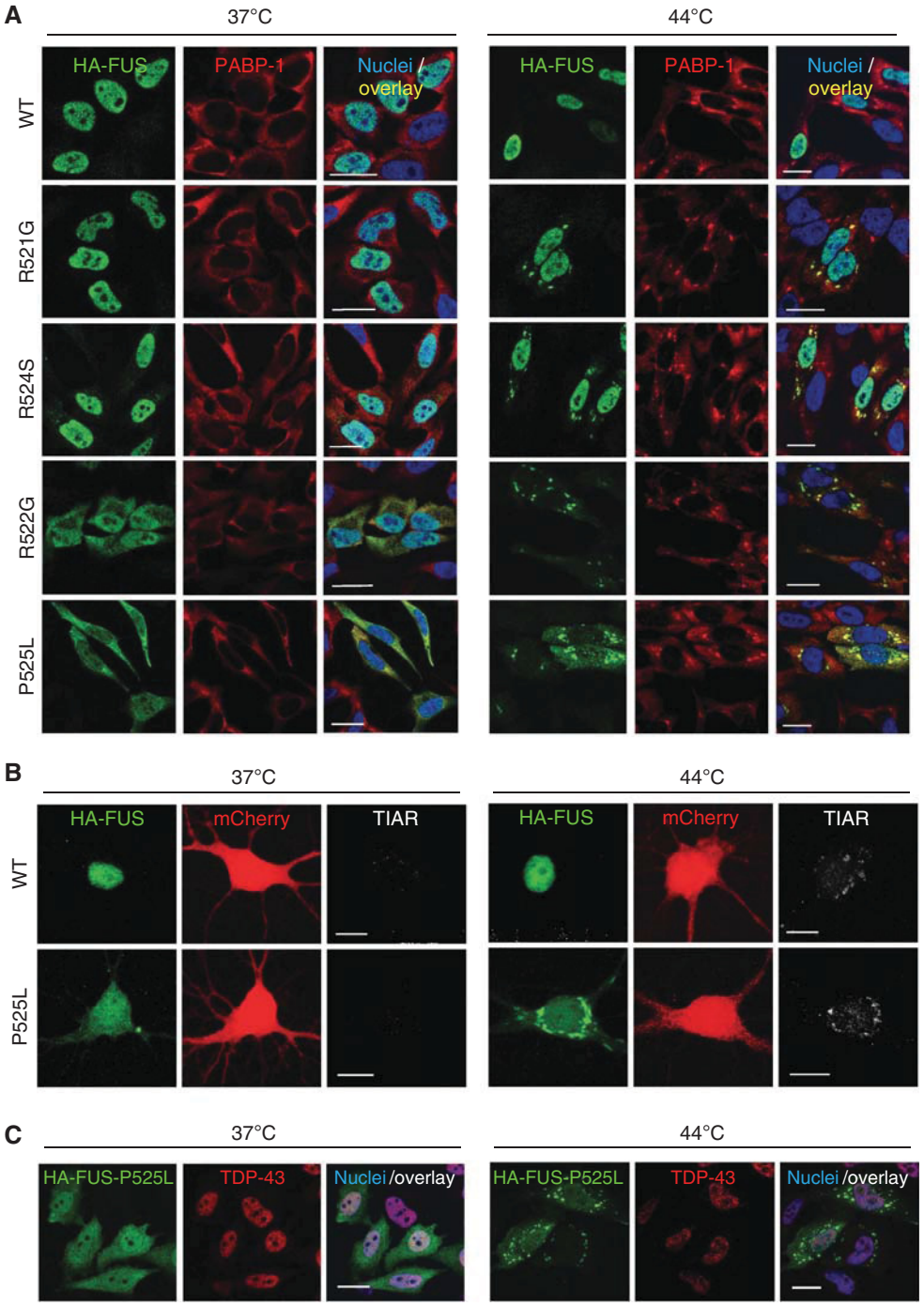

Figure 8 C-terminal fALS-associated *FUS* mutations favour recruitment of FUS into stress granules. (**A**) HeLa cells were transiently transfected with the indicated HA-tagged FUS constructs; 24 h post-transfection, cells were subjected to heat shock (44°C for 1 h, right panels) or were kept at control temperature (37°C, left panels). Cells were fixed, stained with an HA-specific antibody (green), a PABP-1-specific antibody (red) and a nuclear counter-stain (blue) and analysed by confocal microscopy. In contrast to WT-FUS, which remains almost exclusively nuclear on heat shock, all FUS mutants are recruited into PABP-1-positive stress granules. The amount of FUS in stress granules correlates with the cytoplasmic mislocalization and average age of disease onset of the individual point mutations, suggesting that cytoplasmic mislocalization favours recruitment of FUS to stress granules. Scale bar, 20 μm. (**B**) Primary rat hippocampal neurons were transiently transfected with HA-tagged FUS-WT or the P525L mutant, mCherry (red) was co-transfected to visualized neuron morphology. Two days post-transfection, cells were subjected to heat shock (44°C for 1 h) or were kept at control temperature (37°C) and were stained with an HA-specific antibody (green) and a TIAR-specific antibody (white). WT-FUS remains almost exclusively nuclear on heat shock, whereas the P525L mutant shows a mostly granular localization and co-localizes with TIAR-positive stress granules. Scale bar, 10 μm. (**C**) HeLa cells transiently transfected with the HA-tagged FUS-P525L mutant were subjected to heat shock (44°C for 1 h) or were kept at control temperature (37°C). Cells were stained with an HA-specific antibody (green), a TDP-43-specific antibody (red) and a nuclear counter-stain (blue) and analysed by confocal microscopy. TDP-43 is not recruited into FUS-P525L-containing stress granules. Scale bar, 20 μm.

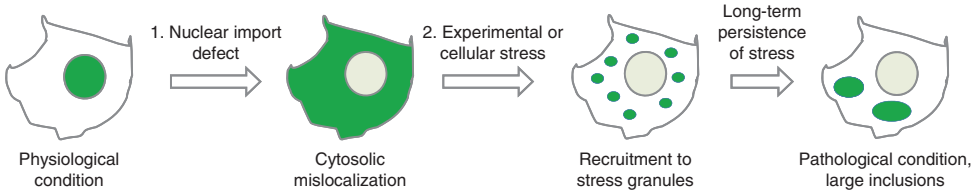

Figure 9 A two hit model of FUS pathology. Green colour represents FUS distribution. For details see Discussion.

to FUS pathology, as stress granule marker proteins also co-deposit with FUS in brains of fALS and FTLD-FUS patients (Figure 7).

Discussion

Our data show that the C-terminal domain of FUS harbours the protein's major NLS, which mediates Trp-dependent nuclear import. Furthermore, we show that several fALS-associated point mutations in the C-terminus of FUS disrupt this import mechanism, leading to cytoplasmic mislocalization of the protein. As the loss of nuclear import correlates with the age of disease onset of the individual point mutations, it seems likely that the nuclear import defect is causally linked to the disease. However, we could also show that additional cellular stress, such as heat shock, is necessary to cause a clustering of cytosolic FUS in the form of stress granules. As we consistently found the stress granule markers PABP-1 and eIF4G co-deposited with FUS inclusions in the whole spectrum of FUS-opathies, including fALS-FUS, aFTLD-U, NIFID and BIBD, we implicate cellular stress in the pathogenesis of these FUS-opathies and propose that two pathological hits, namely a nuclear import defect and cellular stress, are involved in the pathogenesis of FUS-associated diseases.

The identified NLS in the C-terminus of FUS corresponds to the class of non-classical PY-NLSs, which are recognized by the nuclear transport receptor Trp (Lee *et al*, 2006). PY-NLSs typically are 20–30 residue signals with a C-terminal $R/H/KX_{2-5}PY$ consensus motif preceded by a hydrophobic or basic motif, which both make important contacts with Trp (Lee *et al*, 2006; Imasaki *et al*, 2007). The C-terminal tail of FUS fulfils the criteria of this consensus motif and indeed we could show that import of FUS depends on Trp (Figures 4 and 5). Our mutational analysis suggests that R522, P525 and Y526 are the important residues of the $R/H\text{-}X_{2-5}PY$ consensus motif and that R514 and/or R518 may constitute the N-terminal basic motif required for interaction with Trp (Figures 1 and 2; Supplementary Figure S1). This is supported by our three-dimensional model of the FUS-NLS bound to Trp (Figure 4G), explaining why mutations in residues R522, P525 and Y526 specifically affect Trp interaction and, therefore, show the most severe impairment of nuclear transport. To our knowledge, this is the first case in which mutations within a PY-NLS cause a human disease. The only other known example of disease-causing mutations in an NLS is Swyer syndrome, in which mutations in the classical NLS of SRY, the testes-determining transcription factor encoded by the human Y chromosome, lead to a reduced activation of testes-specific genes and thus male-to-female sex reversal (Li *et al*, 2001; Harley *et al*, 2003). Considering the large number of important nuclear proteins, it seems likely that other human diseases can be attributed to nuclear import defects because of mutations within different types of NLSs.

Our data show that mutations in R522 and P525 lead to a strong cytosolic mislocalization of FUS, however, without a complete exclusion of mutant proteins from the nucleus (Figure 2A and B). This is consistent with the observations that neurons of fALS patients with *FUS* mutations still show some immunolabelling in the nucleus (Kwiatkowski *et al*, 2009; Vance *et al*, 2009; Rademakers *et al*, 2010). Although the reported number of patients is still small, it is striking that mutations in R522 and P525 cause an especially aggressive form of ALS. The five reported patients with a P525L mutation all had a very early onset of disease (mean age of onset: 24 years) and an unusually rapid disease progression, with death in <12 months (Chio *et al*, 2009; Kwiatkowski *et al*, 2009). R522G ($n=2$) was the second most aggressive mutation reported by Kwiatkowski *et al* (2009) (mean age of onset: 28.5 years; mean duration: 25 months). Thus, the two mutations that showed the most severe nuclear import defect (Figure 2A and B) and were most readily recruited into stress granules on heat shock (Figure 7A) caused the most aggressive disease course of all reported *FUS* mutations. Furthermore, the R521G ($n=19$) and R524S ($n=1$) mutations, which showed a much weaker import defect (Figure 2A and B) and were recruited into heat-induced stress granules to a lesser degree (Figure 7A), on average caused disease at a much later age (average age of onset: 43 and 34 years, respectively). Interestingly, the weak R521G mutation showed incomplete penetrance, as two members of an R521G family lived well past the average age of onset without developing disease (Kwiatkowski *et al*, 2009). This is consistent with our hypothesis that environmental stress contributes to disease initiation. Different exposure of individuals to environmental stress might also explain the variation in the age of onset reported for other fALS-associated *FUS* mutations (Kwiatkowski *et al*, 2009). Although the number of *FUS* mutation carriers reported to date is still small, Alzheimer's disease (AD) research has shown that the *in vitro* effects of *presenilin* mutations can be clearly correlated with the age of disease onset (Duering *et al*, 2005; Page *et al*, 2008), and in some cases, cell culture experiments have even predicted familial AD mutations and their disease onset. Given the severe effect of the Y526A mutation on nuclear import of FUS, it seems possible that fALS patients carrying FUS-Y526 mutations may be identified in the near future and one would predict a similarly early age of onset as for the P525L mutation. Consistent with this hypothesis, a novel frameshift mutation, which leads to a premature stop codon and thus truncation of the C-terminal 60 amino acids of FUS, was recently reported with a disease onset of 20 years (DeJesus-Hernandez *et al*, 2010).

In addition to mutations in the C-terminal tail of FUS, several point mutations have been identified in the N-terminal SYGQ- or G-rich domains of FUS (Belzil *et al*, 2009; Kwiatkowski *et al*, 2009; Ticozzi *et al*, 2009; Corrado *et al*, 2010) (Figure 1A). As deletion of the C-terminal NLS did not completely eliminate nuclear import (Figure 1C and D) and an N-terminal fragment comprising the SYGQ- and G-domains was described to localize to the nucleus (Zinszner *et al*, 1997a, b), it seemed possible that the N-terminal fALS-associated mutations disrupt a putative second NLS. However, our mutational analysis (Figure 2D and E; Supplementary Figure S2A and B) suggests that N-terminal fALS mutations act through a different cellular mechanism. As the SYGQ- and G-rich domains are involved in transcriptional activation and have been shown to interact with RNA polymerase II and various transcription factors (Zinszner *et al*, 1994; Yang *et al*, 2000; Law *et al*, 2006), the mutations instead might modulate FUS function as a transcriptional activator, either impairing or aberrantly activating transcription of neuronal target genes. The finding that different clusters of mutations within one gene may affect different cellular mechanisms is not too surprising, given the fact that familial AD-causing mutations in three different regions within and around the amyloid β (Aβ) peptide domain have fundamentally different consequences on Aβ metabolism and aggregation (Haass, 2004).

Strikingly, we found a co-deposition of cytosolic FUS with various stress granule marker proteins in cells subjected to cellular stress as well as in brains of fALS-FUS and FTLD-FUS patients. However, some differences exist between the FUS-positive stress granules observed in our cellular models (primary neurons and HeLa cells) and the FUS inclusions present in fALS and FTLD-FUS patients: GFP-M9M-expressing cells or cells exposed to heat shock contain multiple small FUS granules in the perinuclear region or in neuritic processes (Figures 6 and 8). In contrast, NCIs in brains of FTLD-FUS patients are usually much larger (see Figure 7; Neumann *et al*, 2009a). However, the granules in our *in vitro* cultures and the inclusions in brains of patients also share important properties: first, they resemble each other ultrastructurally, as both stress granules and inclusions in BIBID and NIFID patients appear as fibrillogranular aggregates in electron microscopy (Munoz-Garcia and Ludwin, 1984; Mosaheb *et al*, 2005; Souquere *et al*, 2009). A second common property is their protein composition: they both contain FUS and the stress granule markers PABP-1 and eIF4G, but not TDP-43. Interestingly, before the discovery of FUS in ALS and FTLD, Fujita *et al* (2008) described that the basophilic inclusions in BIBD patients contain markers of stress granules. Stress granules are known to be dynamic entities that can enlarge and coalesce on prolonged stress exposure (Kedersha *et al*, 2000). Hence, it seems possible that in the presence of chronic stress, such as oxidative stress, viral infections or proteasome inhibition (Anderson and Kedersha, 2008), small stress granules give rise to larger granules and eventually to large, insoluble inclusions. It will, therefore, be interesting to see if indeed RNA and further RNA-binding proteins commonly found in stress granules in *in vitro* cultures are present in FUS inclusions in fALS and FTLD-FUS patients.

Several reports recently described that TDP-43 can be found in stress granules under various experimental conditions (Colombrita *et al*, 2009; Moisse *et al*, 2009; Volkening *et al*, 2009; Freibaum *et al*, 2010). First, sciatic axotomy in adult mice was reported to cause a marked increase of cytoplasmic TDP-43 and its co-localization with the RNA-binding proteins Staufen and TIA-1 (Moisse *et al*, 2009). In cellular models, oxidative stress and proteasome inhibition were reported to lead to a partial recruitment of TDP-43 into stress granules (Colombrita *et al*, 2009; Freibaum *et al*, 2010), and Freibaum *et al* identified numerous components of stress granules as TDP-43-interacting proteins (Freibaum *et al*, 2010). Although our data clearly show that the FUS-containing stress granules observed after GFP-M9M expression or heat shock do not contain TDP-43 (Figures 5D and 8C), this might be explained by the fact that TDP-43 was predominantly nuclear under these experimental conditions. According to our two hit model, it seems possible that similar to FUS, cytosolic relocalization of TDP-43 is a prerequisite for efficient stress granule recruitment. Thus, it can be speculated that in the studies mentioned above, TDP-43 was at least partially mislocalized to the cytosol before cellular stress.

What remains controversial is the data on stress granule markers in patients with TDP-43 pathology. One study reported a stronger TIA-1 (stress granule) and XRN-1 (P body) staining in sALS patients compared with healthy controls (Volkening *et al*, 2009), whereas another study found a lack of stress granule markers in TDP-43 inclusions of sALS patients (Colombrita *et al*, 2009). Consistent with the latter study, inclusions of FTLD-TDP patients were consistently negative for the stress granule markers PABP-1 and eIF4G in our study (Figure 7). Further studies with larger number of patients are needed to clarify this issue.

Although we did not observe HA-tagged WT-FUS (Figure 8A and B) or endogenous FUS (data not shown) in stress granules on heat shock, it is possible that very small amounts of FUS, undetectable by our antibodies, are present in stress granules even in untransfected or FUS-WT-transfected cells. That this might be the case is suggested by the report of Andersson *et al* (2008), showing a recruitment of endogenous FUS to stress granules on exposure of cell lines to oxidative stress. Nevertheless, our analysis of fALS-associated *FUS* mutations strongly suggests that cytosolic mislocalization of FUS favours recruitment of the protein into stress granules, as the degree of stress granule recruitment correlated with the cytoplasmic mislocalization of the individual point mutations (Figure 8A). Thus, our data suggest that cytosolic FUS is recruited to stress granules, and furthermore, imply that an increased presence of FUS in the cytosol favours the formation of FUS-positive stress granules. In the light of these data, one may postulate that at least small amounts of FUS have to accumulate in the cytosol to trigger the onset of sporadic FTLD-FUS. As not only fALS patients with *FUS* mutations but also sporadic FTLD-FUS patients show a neuronal cytoplasmic redistribution of FUS (Munoz *et al*, 2009; Neumann *et al*, 2009a, b) and a co-deposition of FUS and stress granule marker proteins in NCIs (this study), the question arises what causes the abnormal cytoplasmic accumulation of FUS in cases without *FUS* mutations. Subtle alterations in the Trp pathway, for example caused by reduced Trp expression or post-translational modifications of FUS, might lead to an increase of FUS in the cytosol even in the absence of *FUS* mutations. Indeed, weak cytosolic FUS staining is

consistently observed in post-mortem brain tissue from healthy controls (Neumann *et al*, 2009a), indicating that cytosolic FUS may accumulate during ageing. In combination with environmental stress, a small increase in cytosolic FUS may then be sufficient to initiate clustering of FUS in stress granules and eventually larger inclusions (Figure 9).

Materials and methods

Cell culture and transfection

Human cervical carcinoma cells (HeLa) were cultured in Dulbecco's modified Eagle's medium with Glutamax (Invitrogen) supplemented with 10% (vol/vol) foetal calf serum (FCS, Invitrogen) and penicillin/streptomycin (PAA). Transfection of HeLa cells was carried out with Fugene 6 (Roche) or Lipofectamine 2000 (Invitrogen) according to the manufacturer's instructions. Hippocampal and cortical neurons were cultured from embryonic day 19 rat embryos as described earlier (Tada *et al*, 2007). Neurons were transfected on day *in vitro* (DIV) 5 using Lipofectamine 2000 (Invitrogen) and were analysed on DIV 7. When mCherry was used as a filler to visualize neuron morphology, the mCherry:HA-FUS DNA ratio was 1:10.

Antibodies and inhibitors

A complete list of all antibodies used can be found in the Supplementary data. Cycloheximide (Sigma) was used at a concentration of 20 μg/ml.

cDNA constructs and primers

The cDNA sequence of human FUS (NM_004960) was amplified from a human brain cDNA library and was cloned by XhoI/BamHI restriction digest into the pcDNA3.1/Hygro(−) vector (Invitrogen) with an N-terminal HA-tag. HA-FUS-P525L was generated from the FUS-WT construct by QuikChange mutagenesis (Stratagene), all other FUS mutations were introduced through conventional PCR primers and PCR products were cloned into pcDNA3.1/Hygro(−) through restriction digest. The pGST-EGFP-C1 vector was generated by inserting the GST sequence with a Kozak sequence into the NheI/AgeI restriction sites of the pEGFP-C1 vector (Clontech). NLS reporter constructs were generated by ligating annealed oligos into the XhoI/BamHI restriction sites of pGST-EGFP-C1. The nuclear import inhibitor constructs (GFP-M9M, GFP-Bimax2) were generated by ligating annealed oligos into the XhoI/BamHI restriction sites of pEGFP-C1. For all constructs, sequence integrity was verified by sequencing. Oligonucleotides sequences are available on request.

Zebrafish husbandry and embryo injection

All of the experiments were performed in compliance with the guidelines of the German Council on Animal Care. WT AB zebrafish were kept at 28°C and raised and mated as described (Mullins *et al*, 1994). GST-EGFP constructs (25 ng/μl) were injected into fertilized eggs at the one-cell stage; 48 h old embryos were stained as described in the Supplementary data.

Human post-mortem tissue

Cases with confirmed FUS pathology used in this study have been earlier described and included a case of fALS with an FUS-R521C mutation (Rademakers *et al*, 2010) and cases of aFTLD-U ($n=3$) (Neumann *et al*, 2009a), NIFID ($n=3$) (Neumann *et al*, 2009b) and BIBD ($n=1$) (Munoz *et al*, 2009). In addition, FTLD-TDP ($n=2$) as neurologic controls and cases with no history of neurologic diseases ($n=2$) were included.

Immunocytochemistry and immunohistochemistry

For immunocytochemistry on HeLa cells and neurons, cells were fixed for 15 min in 4% paraformaldehyde in PBS, permeabilized for 5 min in 0.2% Triton X-100 with 50 mM NH_4Cl and subsequently blocked for 20–30 min in blocking buffer (5% goat serum or 2% BSA in PBSS = PBS with 0.1% saponin). Cells were stained with the indicated primary and secondary antibodies diluted in blocking buffer for 30 min and were washed 5 × in PBSS. To visualize nuclei, cells were stained with TO-PRO-3 iodide (Invitrogen) for 15 min and were washed 3 × in PBS. Coverslips were mounted onto glass slides using ProLong Gold Antifade Reagent (Invitrogen). All steps were carried out at RT.

Immunohistochemistry on human post-mortem material was performed on 5 μm thick sections of formalin fixed, paraffin-embedded tissue from spinal cord, medulla or hippocampus with the indicated antibodies (after microwave antigen retrieval) and the avidin–biotin complex detection system (Vector Laboratories) with 3,3′-diaminobenzidine as chromogen. Double-label immunofluorescence for PABP-1 and p62 (after microwave antigen retrieval) was performed using Alexa-488 and -594-conjugated secondary antibodies; 4′-6-diamidino-2-phenylindol (Vector Laboratories) was used for nuclear counter-staining.

Image acquisition and quantification

Confocal images of HeLa cells, primary neurons and zebrafish embryos were obtained with an inverted laser scanning confocal microscope (Zeiss Axiovert 200M) with a 63 × /1.4 NA oil immersion lens, using a pinhole diameter of 1 Airy unit. Pictures were taken and analysed with the LSM 510 confocal software (Zeiss), and, if necessary, for printing, brightness and contrast were linearly enhanced using the LSM image browser (Zeiss). For HeLa cells, single confocal images were taken in the plane of the largest cytosolic area. For neuronal cultures and zebrafish embryos, a series of images along the *z* axis was taken and projected into a single image using the maximal projection tool of the LSM 510 software. Immunofluorescence images of brain sections were obtained by wide-field fluorescence microscopy (BX61 Olympus with digital camera F-view, Olympus).

Nuclear and cytosolic localization was quantified with the LSM 510's co-localization tool as follows: total fluorescence intensities of the green channel were calculated from the mean fluorescence intensity and the number of pixels. Pixels that were co-localized with TO-PRO-3 were considered 'nuclear' and pixels that did not overlap with TO-PRO-3 were considered 'cytosolic'. For each sample, 7–12 randomly selected fields were analysed, containing a total of 50–100 transfected cells. Means across all fields were calculated and s.d. are indicated by error bars. Pictures and quantification shown are from one experiment, but are representative of several experiments.

siRNA-mediated knockdown of Trp1 and Trp2

Trp1/2 knockdown was achieved using two different siRNA pools: Trp1/2 pool #1 consisted of the Trp1-specific siGENOME siRNA D-011308-01 (target sequence: 5′-guauagagaugcagccuua-3′) and the Trp2-specific siGENOME SMART pool M-020491-01 (target sequences: 5′-gggcagagaugcagccuua-3′; 5′-gcaguucucugagcaauuc-3′; 5′-aaacaggagugucucaaca-3′; 5′-gcgcugauggacaauauug-3′), both from Dharmacon. Trp1/2 pool #2 consisted of the Trp1-specific siGENOME siRNA D-011308-04 from Dharmacon (target sequence: 5′-caauuggucgucuugguua-3′) and the Trp2-specific siGENOME SMART pool M-020491-01 (see above). A non-targeting (NT) siRNA (ON-TARGET plus NT siRNA #3, D-001810-03 from Dharmacon) was used as a negative control. Cells were reverse transfected using a total of 50 pmol siRNA and 5 μl Lipofectamine 2000 (Invitrogen) per six well. Medium was changed 4–6 h post-transfection and effect of knockdown was analysed 48–72 h post-transfection.

Cell lysates and immunoblotting

Cells were washed twice in PBS, scraped off and pelleted at 1000 *g*, 5 min. Total cell lysates were prepared in ice cold RIPA buffer freshly supplemented with complete EDTA-free protease inhibitor cocktail (Roche). After 15 min lysis on ice, lysates were sonicated in a bioruptor (Diagenode, 45 s on high) and protein concentration was determined by BCA protein assay (Pierce); 4 × SDS–PAGE sample buffer was added and samples were boiled for 5 min. Proteins were separated by SDS–PAGE, transferred onto a PVDF membrane (Immobilon-P, Millipore) and analysed by immunoblotting using the indicated antibodies. Bound antibodies were detected with the chemiluminescence detection reagents ECL (Amersham) or Immobilon (Millipore).

Structural modelling

The C-terminal amino-acid residues D520–Y526 of FUS were modelled manually into the Trp-binding pocket. Residues of the non-classical NLSs of subtype RXXPY (pdb-entries 2OT8 (Cansizoglu *et al*, 2007) and 2Z5K (Imasaki *et al*, 2007) differing between the experimental structures and the FUS C-terminal sequence were

exchanged obeying standard amino-acid conformations (Engh and Huber, 1991) and the resulting structure was locally energy minimized using MAIN (Turk, 1992), keeping the Trp molecule rigid.

Supplementary data

Supplementary data are available at *The EMBO Journal* Online (http://www.embojournal.org).

Acknowledgements

We thank Drs Harald Steiner, Richard Page and Stefan Lichtenthaler for critical discussion, Dr Sven Lammich for providing human brain cDNA and the Hans and Ilse Breuer Foundation for the confocal microscope. This work was supported by the Center for Integrated Protein Science Munich (CIPSM), the Competence Network of Neurodegenerative Diseases (KNDD) of the Bundesministerium für Bildung und Forschung (BMBF), the Sonderforschungsbereich Molecular Mechanisms of Neurodegeneration (SFB 596) and an EMBO postdoctoral fellowship (to DD). DE is supported by the Helmholtz Young Investigator Program. MN is supported by the Stavros-Niarchos Foundation and the Synapsis Foundation. IRAM is supported by the Canadian Institutes of Health Research and the Pacific Alzheimer's Research Foundation. CH is supported by a 'Forschungsprofessur' of the Ludwig-Maximilians University.

Conflict of interest

The authors declare that they have no conflict of interest.

References

Anderson P, Kedersha N (2006) RNA granules. *J Cell Biol* **172:** 803–808

Anderson P, Kedersha N (2008) Stress granules: the Tao of RNA triage. *Trends Biochem Sci* **33:** 141–150

Andersson MK, Stahlberg A, Arvidsson Y, Olofsson A, Semb H, Stenman G, Nilsson O, Aman P (2008) The multifunctional FUS, EWS and TAF15 proto-oncoproteins show cell type-specific expression patterns and involvement in cell spreading and stress response. *BMC Cell Biol* **9:** 37–53

Arai T, Hasegawa M, Akiyama H, Ikeda K, Nonaka T, Mori H, Mann D, Tsuchiya K, Yoshida M, Hashizume Y, Oda T (2006) TDP-43 is a component of ubiquitin-positive tau-negative inclusions in frontotemporal lobar degeneration and amyotrophic lateral sclerosis. *Biochem Biophys Res Commun* **351:** 602–611

Ayala YM, Zago P, D'Ambrogio A, Xu YF, Petrucelli L, Buratti E, Baralle FE (2008) Structural determinants of the cellular localization and shuttling of TDP-43. *J Cell Sci* **121:** 3778–3785

Belzil VV, Valdmanis PN, Dion PA, Daoud H, Kabashi E, Noreau A, Gauthier J, Hince P, Desjarlais A, Bouchard JP, Lacomblez L, Salachas F, Pradat PF, Camu W, Meininger V, Dupre N, Rouleau GA (2009) Mutations in FUS cause FALS and SALS in French and French Canadian populations. *Neurology* **73:** 1176–1179

Boillee S, Vande Velde C, Cleveland DW (2006) ALS: a disease of motor neurons and their nonneuronal neighbors. *Neuron* **52:** 39–59

Buratti E, Baralle FE (2008) Multiple roles of TDP-43 in gene expression, splicing regulation, and human disease. *Front Biosci* **13:** 867–878

Cansizoglu AE, Lee BJ, Zhang ZC, Fontoura BM, Chook YM (2007) Structure-based design of a pathway-specific nuclear import inhibitor. *Nat Struct Mol Biol* **14:** 452–454

Chio A, Restagno G, Brunetti M, Ossola I, Calvo A, Mora G, Sabatelli M, Monsurro MR, Battistini S, Mandrioli J, Salvi F, Spataro R, Schymick J, Traynor BJ, La Bella V (2009) Two Italian kindreds with familial amyotrophic lateral sclerosis due to FUS mutation. *Neurobiol Aging* **30:** 1272–1275

Colombrita C, Zennaro E, Fallini C, Weber M, Sommacal A, Buratti E, Silani V, Ratti A (2009) TDP-43 is recruited to stress granules in conditions of oxidative insult. *J Neurochem* **111:** 1051–1061

Corrado L, Del Bo R, Castellotti B, Ratti A, Cereda C, Penco S, Soraru G, Carlomagno Y, Ghezzi S, Pensato V, Colombrita C, Gagliardi S, Cozzi L, Orsetti V, Mancuso M, Siciliano G, Mazzini L, Comi GP, Gellera C, Ceroni M *et al* (2010) Mutations of FUS gene in sporadic amyotrophic lateral sclerosis. *J Med Genet* **47:** 190–194

DeJesus-Hernandez M, Kocerha J, Finch N, Crook R, Baker M, Desaro P, Johnston A, Rutherford N, Wojtas A, Kennelly K, Wszolek ZK, Graff-Radford N, Boylan K, Rademakers R (2010) *De novo* truncating FUS gene mutation as a cause of sporadic amyotrophic lateral sclerosis. *Human Mutat* **31:** E1377–E1389

Drepper C, Herrmann T, Wessig C, Beck M, Sendtner M (2009) C-terminal FUS/TLS mutations in familial and sporadic ALS in Germany. *Neurobiol Aging* (advance online publication)

Duering M, Grimm MO, Grimm HS, Schroder J, Hartmann T (2005) Mean age of onset in familial Alzheimer's disease is determined by amyloid beta 42. *Neurobiol Aging* **26:** 785–788

Engh RA, Huber R (1991) Accurate bond and angle parameters for X-ray protein-structure refinement. *Acta Crystallogr A* **47:** 329–400

Freibaum BD, Chitta RK, High AA, Taylor JP (2010) Global analysis of TDP-43 interacting proteins reveals strong association with RNA splicing and translation machinery. *J Proteome Res* **9:** 1104–1120

Fujii R, Okabe S, Urushido T, Inoue K, Yoshimura A, Tachibana T, Nishikawa T, Hicks GG, Takumi T (2005) The RNA binding protein TLS is translocated to dendritic spines by mGluR5 activation and regulates spine morphology. *Curr Biol* **15:** 587–593

Fujii R, Takumi T (2005) TLS facilitates transport of mRNA encoding an actin-stabilizing protein to dendritic spines. *J Cell Sci* **118:** 5755–5765

Fujita K, Ito H, Nakano S, Kinoshita Y, Wate R, Kusaka H (2008) Immunohistochemical identification of messenger RNA-related proteins in basophilic inclusions of adult-onset atypical motor neuron disease. *Acta Neuropathol* **116:** 439–445

Gitcho MA, Baloh RH, Chakraverty S, Mayo K, Norton JB, Levitch D, Hatanpaa KJ, White III CL, Bigio EH, Caselli R, Baker M, Al-Lozi MT, Morris JC, Pestronk A, Rademakers R, Goate AM, Cairns NJ (2008) TDP-43 A315T mutation in familial motor neuron disease. *Ann Neurol* **63:** 535–538

Guttinger S, Muhlhausser P, Koller-Eichhorn R, Brennecke J, Kutay U (2004) Transportin2 functions as importin and mediates nuclear import of HuR. *Proc Natl Acad Sci USA* **101:** 2918–2923

Haass C (2004) Take five—BACE and the gamma-secretase quartet conduct Alzheimer's amyloid beta-peptide generation. *EMBO J* **23:** 483–488

Harley VR, Layfield S, Mitchell CL, Forwood JK, John AP, Briggs LJ, McDowall SG, Jans DA (2003) Defective importin beta recognition and nuclear import of the sex-determining factor SRY are associated with XY sex-reversing mutations. *Proc Natl Acad Sci USA* **100:** 7045–7050

Iijima M, Suzuki M, Tanabe A, Nishimura A, Yamada M (2006) Two motifs essential for nuclear import of the hnRNP A1 nucleocytoplasmic shuttling sequence M9 core. *FEBS Lett* **580:** 1365–1370

Imasaki T, Shimizu T, Hashimoto H, Hidaka Y, Kose S, Imamoto N, Yamada M, Sato M (2007) Structural basis for substrate recognition and dissociation by human transportin 1. *Mol Cell* **28:** 57–67

Johnson BS, Snead D, Lee JJ, McCaffery JM, Shorter J, Gitler AD (2009) TDP-43 is intrinsically aggregation-prone, and amyotrophic lateral sclerosis-linked mutations accelerate aggregation and increase toxicity. *J Biol Chem* **284:** 20329–20339

Kabashi E, Valdmanis PN, Dion P, Spiegelman D, McConkey BJ, Vande Velde C, Bouchard JP, Lacomblez L, Pochigaeva K, Salachas F, Pradat PF, Camu W, Meininger V, Dupre N, Rouleau GA (2008) TARDBP mutations in individuals with sporadic and familial amyotrophic lateral sclerosis. *Nat Genet* **40:** 572–574

Kalderon D, Roberts BL, Richardson WD, Smith AE (1984) A short amino acid sequence able to specify nuclear location. *Cell* **39:** 499–509

Kedersha N, Anderson P (2007) Mammalian stress granules and processing bodies. *Methods Enzymol* **431:** 61–81

Kedersha N, Cho MR, Li W, Yacono PW, Chen S, Gilks N, Golan DE, Anderson P (2000) Dynamic shuttling of TIA-1 accompanies the

recruitment of mRNA to mammalian stress granules. *J Cell Biol* **151:** 1257–1268

Kiebler MA, Bassell GJ (2006) Neuronal RNA granules: movers and makers. *Neuron* **51:** 685–690

Kosugi S, Hasebe M, Entani T, Takayama S, Tomita M, Yanagawa H (2008) Design of peptide inhibitors for the importin alpha/beta nuclear import pathway by activity-based profiling. *Chem Biol* **15:** 940–949

Kwiatkowski Jr TJ, Bosco DA, Leclerc AL, Tamrazian E, Vanderburg CR, Russ C, Davis A, Gilchrist J, Kasarskis EJ, Munsat T, Valdmanis P, Rouleau GA, Hosler BA, Cortelli P, de Jong PJ, Yoshinaga Y, Haines JL, Pericak-Vance MA, Yan J, Ticozzi N *et al* (2009) Mutations in the FUS/TLS gene on chromosome 16 cause familial amyotrophic lateral sclerosis. *Science* **323:** 1205–1208

Lagier-Tourenne C, Cleveland DW (2009) Rethinking ALS: the FUS about TDP-43. *Cell* **136:** 1001–1004

Lai SL, Abramzon Y, Schymick JC, Stephan DA, Dunckley T, Dillman A, Cookson M, Calvo A, Battistini S, Giannini F, Caponnetto C, Mancardi GL, Spataro R, Monsurro MR, Tedeschi G, Marinou K, Sabatelli M, Conte A, Mandrioli J, Sola P *et al* (2010) FUS mutations in sporadic amyotrophic lateral sclerosis. *Neurobiol Aging* (advance online publication)

Law WJ, Cann KL, Hicks GG (2006) TLS, EWS and TAF15: a model for transcriptional integration of gene expression. *Brief Funct Genomic Proteomic* **5:** 8–14

Lee BJ, Cansizoglu AE, Suel KE, Louis TH, Zhang Z, Chook YM (2006) Rules for nuclear localization sequence recognition by karyopherin beta 2. *Cell* **126:** 543–558

Li B, Zhang W, Chan G, Jancso-Radek A, Liu S, Weiss MA (2001) Human sex reversal due to impaired nuclear localization of SRY. A clinical correlation. *J Biol Chem* **276:** 46480–46484

Mackenzie IR, Bigio EH, Ince PG, Geser F, Neumann M, Cairns NJ, Kwong LK, Forman MS, Ravits J, Stewart H, Eisen A, McClusky L, Kretzschmar HA, Monoranu CM, Highley JR, Kirby J, Siddique T, Shaw PJ, Lee VM, Trojanowski JQ (2007) Pathological TDP-43 distinguishes sporadic amyotrophic lateral sclerosis from amyotrophic lateral sclerosis with SOD1 mutations. *Ann Neurol* **61:** 427–434

Mackenzie IR, Neumann M, Bigio EH, Cairns NJ, Alafuzoff I, Kril J, Kovacs GG, Ghetti B, Halliday G, Holm IE, Ince PG, Kamphorst W, Revesz T, Rozemuller AJ, Kumar-Singh S, Akiyama H, Baborie A, Spina S, Dickson DW, Trojanowski JQ *et al* (2010) Nomenclature and nosology for neuropathologic subtypes of frontotemporal lobar degeneration: an update. *Acta Neuropathol* **119:** 1–4

Mackenzie IR, Rademakers R (2008) The role of transactive response DNA-binding protein-43 in amyotrophic lateral sclerosis and frontotemporal dementia. *Curr Opin Neurol* **21:** 693–700

Moisse K, Volkening K, Leystra-Lantz C, Welch I, Hill T, Strong MJ (2009) Divergent patterns of cytosolic TDP-43 and neuronal progranulin expression following axotomy: implications for TDP-43 in the physiological response to neuronal injury. *Brain Res* **1249:** 202–211

Mosaheb S, Thorpe JR, Hashemzadeh-Bonehi L, Bigio EH, Gearing M, Cairns NJ (2005) Neuronal intranuclear inclusions are ultrastructurally and immunologically distinct from cytoplasmic inclusions of neuronal intermediate filament inclusion disease. *Acta Neuropathol* **110:** 360–368

Mullins MC, Hammerschmidt M, Haffter P, Nusslein-Volhard C (1994) Large-scale mutagenesis in the zebrafish: in search of genes controlling development in a vertebrate. *Curr Biol* **4:** 189–202

Munoz-Garcia D, Ludwin SK (1984) Classic and generalized variants of Pick's disease: a clinicopathological, ultrastructural, and immunocytochemical comparative study. *Ann Neurol* **16:** 467–480

Munoz DG, Neumann M, Kusaka H, Yokota O, Ishihara K, Terada S, Kuroda S, Mackenzie IR (2009) FUS pathology in basophilic inclusion body disease. *Acta Neuropathol* **118:** 617–627

Neumann M, Igaz LM, Kwong LK, Nakashima-Yasuda H, Kolb SJ, Dreyfuss G, Kretzschmar HA, Trojanowski JQ, Lee VM (2007) Absence of heterogeneous nuclear ribonucleoproteins and survival motor neuron protein in TDP-43 positive inclusions in frontotemporal lobar degeneration. *Acta Neuropathol* **113:** 543–548

Neumann M, Rademakers R, Roeber S, Baker M, Kretzschmar HA, Mackenzie IR (2009a) A new subtype of frontotemporal lobar degeneration with FUS pathology. *Brain* **132:** 2922–2931

Neumann M, Roeber S, Kretzschmar HA, Rademakers R, Baker M, Mackenzie IR (2009b) Abundant FUS-immunoreactive pathology in neuronal intermediate filament inclusion disease. *Acta Neuropathol* **118:** 605–616

Neumann M, Sampathu DM, Kwong LK, Truax AC, Micsenyi MC, Chou TT, Bruce J, Schuck T, Grossman M, Clark CM, McCluskey LF, Miller BL, Masliah E, Mackenzie IR, Feldman H, Feiden W, Kretzschmar HA, Trojanowski JQ, Lee VM (2006) Ubiquitinated TDP-43 in frontotemporal lobar degeneration and amyotrophic lateral sclerosis. *Science* **314:** 130–133

Nonaka T, Kametani F, Arai T, Akiyama H, Hasegawa M (2009) Truncation and pathogenic mutations facilitate the formation of intracellular aggregates of TDP-43. *Hum Mol Genet* **18:** 3353–3364

Page RM, Baumann K, Tomioka M, Perez-Revuelta BI, Fukumori A, Jacobsen H, Flohr A, Luebbers T, Ozmen L, Steiner H, Haass C (2008) Generation of Abeta38 and Abeta42 is independently and differentially affected by familial Alzheimer disease-associated presenilin mutations and gamma-secretase modulation. *J Biol Chem* **283:** 677–683

Rademakers R, Stewart H, DeJesus-Hernandez M, Krieger C, Graff-Radford N, Fabros M, Briemberg H, Cashman N, Eisen A, Mackenzie IRA (2010) FUS gene mutations in familial and sporadic amyotrophic lateral sclerosis. *Muscle Nerve* (advance online publication)

Rebane A, Aab A, Steitz JA (2004) Transportins 1 and 2 are redundant nuclear import factors for hnRNP A1 and HuR. *RNA* **10:** 590–599

Souquere S, Mollet S, Kress M, Dautry F, Pierron G, Weil D (2009) Unravelling the ultrastructure of stress granules and associated P-bodies in human cells. *J Cell Sci* **122:** 3619–3626

Sreedharan J, Blair IP, Tripathi VB, Hu X, Vance C, Rogelj B, Ackerley S, Durnall JC, Williams KL, Buratti E, Baralle F, de Belleroche J, Mitchell JD, Leigh PN, Al-Chalabi A, Miller CC, Nicholson G, Shaw CE (2008) TDP-43 mutations in familial and sporadic amyotrophic lateral sclerosis. *Science* **319:** 1668–1672

Suzuki N, Aoki M, Warita H, Kato M, Mizuno H, Shimakura N, Akiyama T, Furuya H, Hokonohara T, Iwaki A, Togashi S, Konno H, Itoyama Y (2010) FALS with FUS mutation in Japan, with early onset, rapid progress and basophilic inclusion. *J Hum Genet* **55:** 252–254

Tada T, Simonetta A, Batterton M, Kinoshita M, Edbauer D, Sheng M (2007) Role of Septin cytoskeleton in spine morphogenesis and dendrite development in neurons. *Curr Biol* **17:** 1752–1758

Talbot K, Ansorge O (2006) Recent advances in the genetics of amyotrophic lateral sclerosis and frontotemporal dementia: common pathways in neurodegenerative disease. *Hum Mol Genet* **15** (Spec No 2)**:** R182–R187

Terry LJ, Shows EB, Wente SR (2007) Crossing the nuclear envelope: hierarchical regulation of nucleocytoplasmic transport. *Science* **318:** 1412–1416

Ticozzi N, Silani V, LeClerc AL, Keagle P, Gellera C, Ratti A, Taroni F, Kwiatkowski Jr TJ, McKenna-Yasek DM, Sapp PC, Brown Jr RH, Landers JE (2009) Analysis of FUS gene mutation in familial amyotrophic lateral sclerosis within an Italian cohort. *Neurology* **73:** 1180–1185

Turk D (1992) *Weiterentwicklung eines Programms für Molekülgraphik und Elektronendichte-Manipulation und seine Anwendung auf verschiedene Proteinstrukturaufklärungen*. Munich, Germany: Technische Universität München, PhD thesis

Valdmanis PN, Rouleau GA (2008) Genetics of familial amyotrophic lateral sclerosis. *Neurology* **70:** 144–152

Vance C, Rogelj B, Hortobagyi T, De Vos KJ, Nishimura AL, Sreedharan J, Hu X, Smith B, Ruddy D, Wright P, Ganesalingam J, Williams KL, Tripathi V, Al-Saraj S, Al-Chalabi A, Leigh PN, Blair IP, Nicholson G, de Belleroche J, Gallo JM *et al* (2009) Mutations in FUS, an RNA processing protein, cause familial amyotrophic lateral sclerosis type 6. *Science* **323:** 1208–1211

Volkening K, Leystra-Lantz C, Yang W, Jaffee H, Strong MJ (2009) Tar DNA binding protein of 43 kDa (TDP-43), 14-3-3 proteins and copper/zinc superoxide dismutase (SOD1) interact to modulate NFL mRNA stability. Implications for altered RNA processing in amyotrophic lateral sclerosis (ALS). *Brain Res* **1305:** 168–182

Winton MJ, Igaz LM, Wong MM, Kwong LK, Trojanowski JQ, Lee VM (2008) Disturbance of nuclear and cytoplasmic TAR DNA-

binding protein (TDP-43) induces disease-like redistribution, sequestration, and aggregate formation. *J Biol Chem* **283:** 13302–13309

Yang L, Embree LJ, Hickstein DD (2000) TLS-ERG leukemia fusion protein inhibits RNA splicing mediated by serine-arginine proteins. *Mol Cell Biol* **20:** 3345–3354

Zakaryan RP, Gehring H (2006) Identification and characterization of the nuclear localization/retention signal in the EWS proto-oncoprotein. *J Mol Biol* **363:** 27–38

Zinszner H, Albalat R, Ron D (1994) A novel effector domain from the RNA-binding protein TLS or EWS is required for oncogenic transformation by CHOP. *Genes Dev* **8:** 2513–2526

Zinszner H, Immanuel D, Yin Y, Liang FX, Ron D (1997a) A topogenic role for the oncogenic N-terminus of TLS: nucleolar localization when transcription is inhibited. *Oncogene* **14:** 451–461

Zinszner H, Sok J, Immanuel D, Yin Y, Ron D (1997b) TLS (FUS) binds RNA *in vivo* and engages in nucleo-cytoplasmic shuttling. *J Cell Sci* **110** (Pt 15)**:** 1741–1750

Supplementary data

Figure S1:

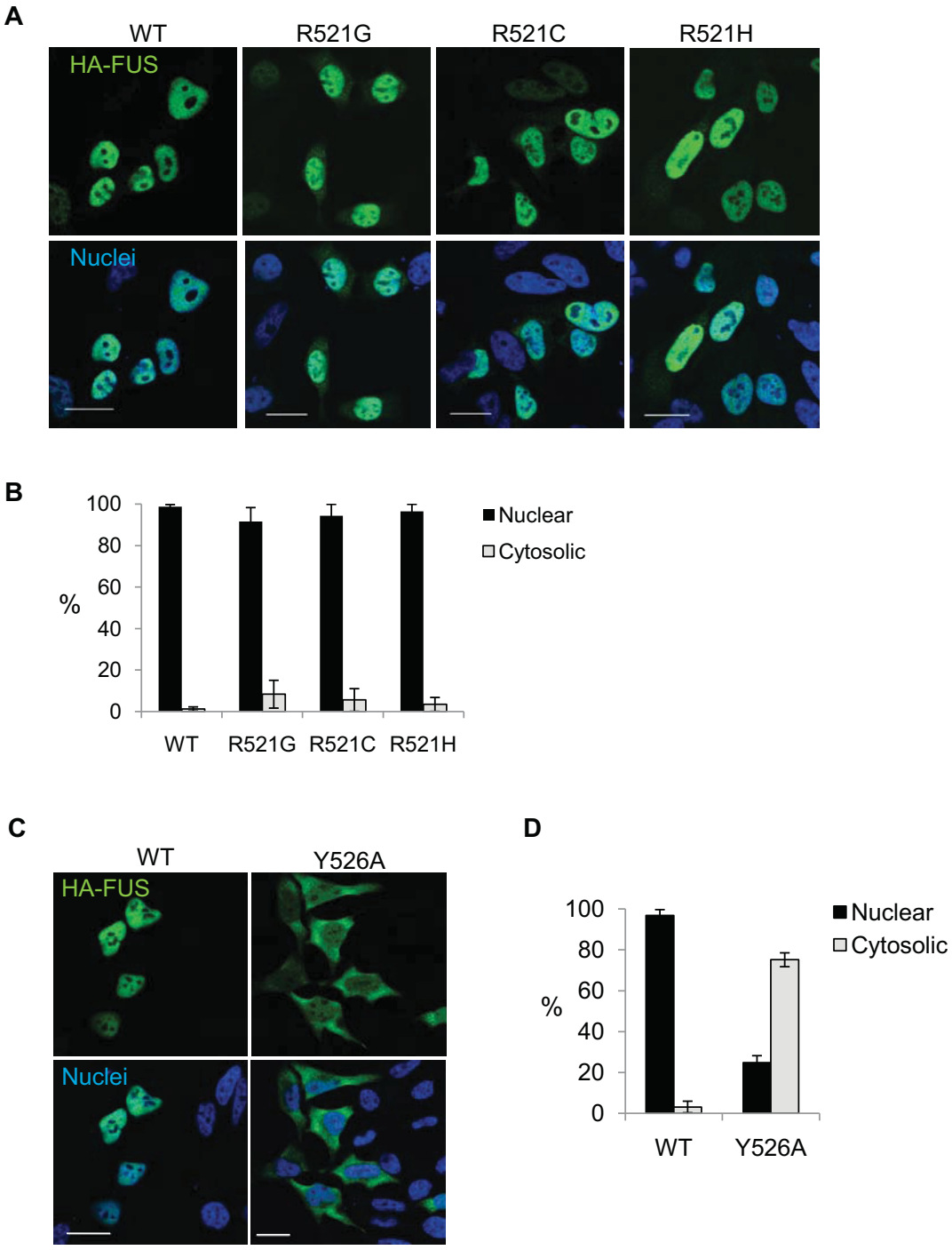

Figure S1: *FUS* mutants R521C and R521H cause a mild cytosolic mislocalization similar R521G, whereas mutation of Y526 causes a strong nuclear import block

(A) HA-tagged wild-type (WT) FUS, FUS-R521G, -R521C, or -R521H were transiently expressed in Hela cells. Cells were stained with an HA-specific antibody (green) and a nuclear counterstain (blue)

and were analyzed by confocal microscopy. Both R521C and R521H show a mild cytosolic mislocalization similar to R521G. Scale bar: 20 μm.

(B) Quantification of nuclear and cytosolic fluorescence intensities. Error bars indicate standard deviations.

(C) HA-tagged FUS-WT or FUS-Y526A were transiently expressed in Hela cells. Cells were stained with an HA-specific antibody (green), a nuclear counterstain (blue) and analyzed by confocal microscopy. The Y526A mutant shows a strong cytosolic mislocalization, demonstrating that the C-terminal tyrosine residue is a key residue of the FUS NLS. Scale bar: 20 μm.

(D) Quantification of nuclear and cytosolic fluorescence intensities. Error bars indicate standard deviations.

Figure S2:

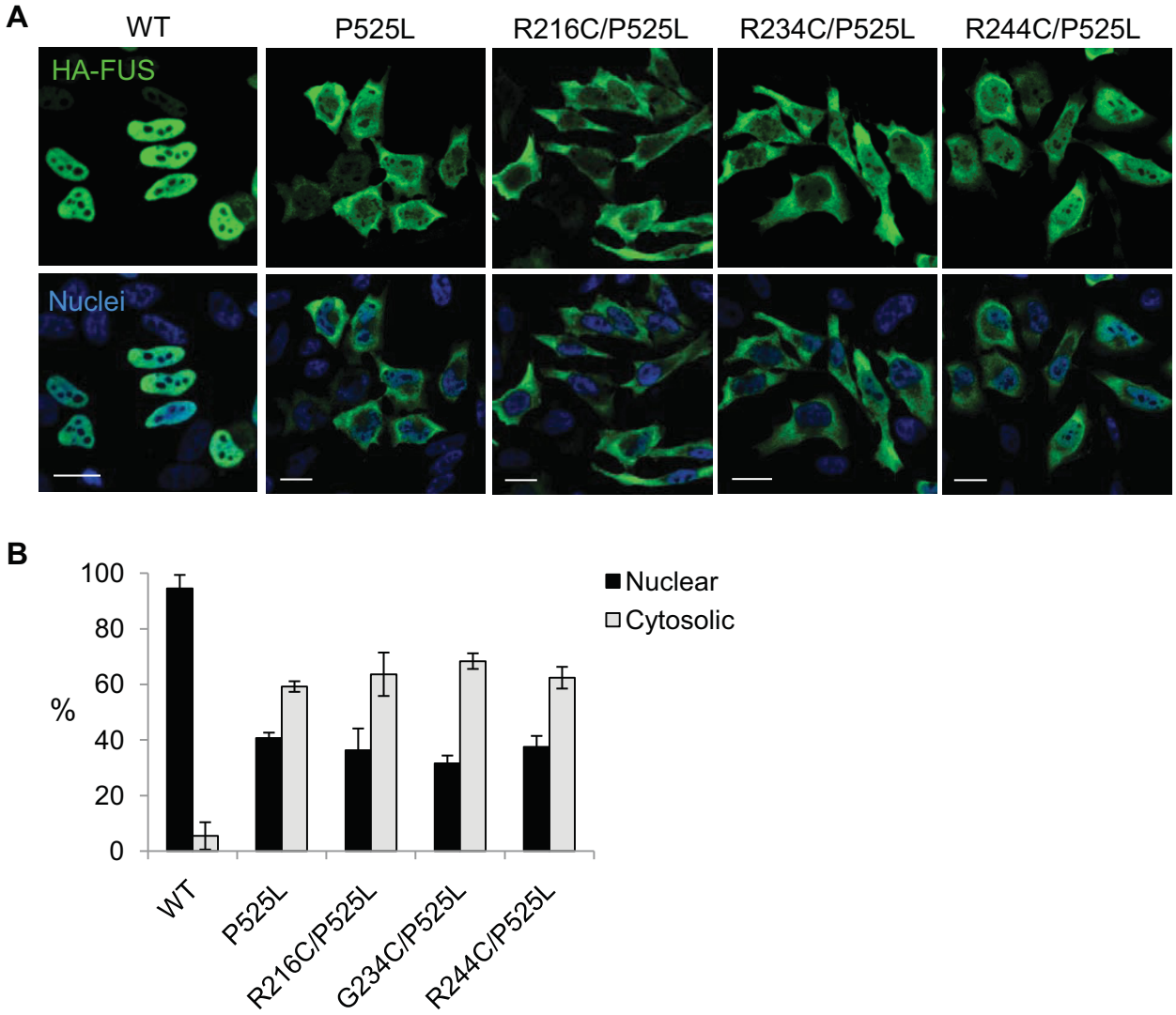

Figure S2: N-terminal fALS-associated *FUS* mutations do not further impair mislocalization of the P525L mutant

(A) HA-tagged wild-type (WT) FUS, FUS-P525L or FUS-P525L carrying the additional N-terminal mutations R216C, R234C or R244C were transiently expressed in Hela cells. Cells were stained with an HA-specific antibody (green) and a nuclear counterstain (blue) and were analyzed by confocal microscopy. The P525L mutant shows a strong cytosolic mislocalization, which is not further exacerbated by any of the N-terminal fALS-associated point mutations. Scale bar: 20 µm.

(B) Quantification of nuclear and cytosolic fluorescence intensities. Error bars indicate standard deviations.

Figure S3:

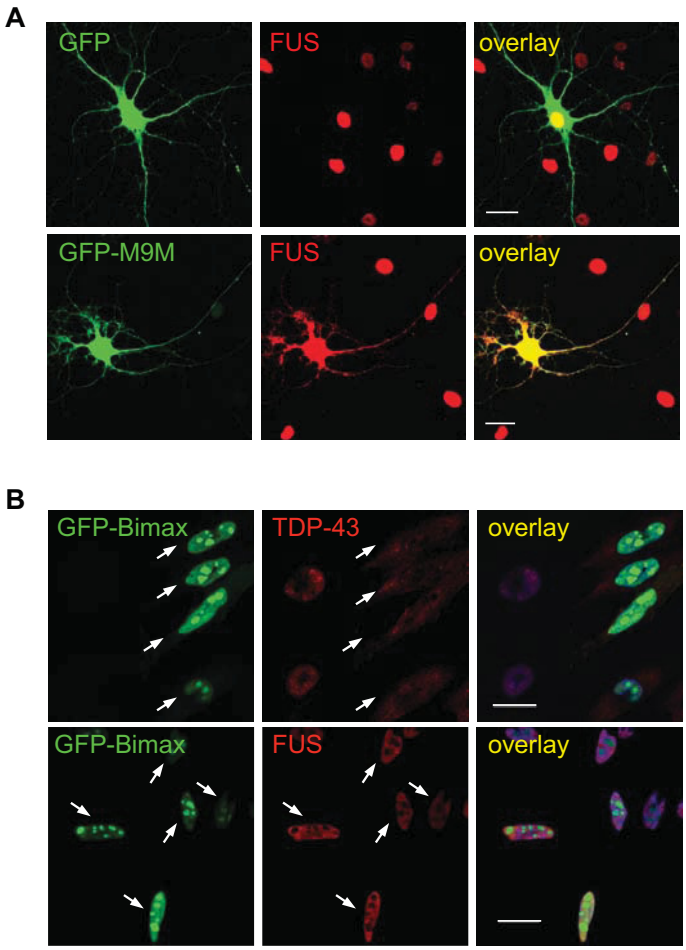

Figure S3: Inhibition of the Trp pathway leads to cytosolic relocalization of FUS, while inhibition of the importin α/β pathway causes mislocalization of TDP-43 but not FUS.

(A) The Trp-specific inhibitor (GFP-M9M) or GFP as a control were expressed in primary rat hippocampal neurons (green). After staining with a FUS-specific antibody (red), cells were analyzed by confocal microscopy. Expression of the Trp-specific inhibitor causes a marked cytoplasmic redistribution and localization of FUS in cytoplasmic punctate structures. Scale bar: 20 μm.

(B) To exclude that FUS is imported via the importin α/β receptor, an importin-specific inhibitor construct (GFP-Bimax2) was expressed in HeLa cells (green). Cells were stained for endogenous TDP-43 or FUS (red) and a nuclear counterstain (blue) and were analyzed by confocal microscopy. TDP-43, which carries a classical bipartite NLS, redistributes to the cytosol upon inhibition of the importin α/β pathway, whereas FUS remains completely nuclear. Cells expressing GFP-Bimax2 are labeled with a white arrow. Scale bar: 20 μm.

Figure S4:

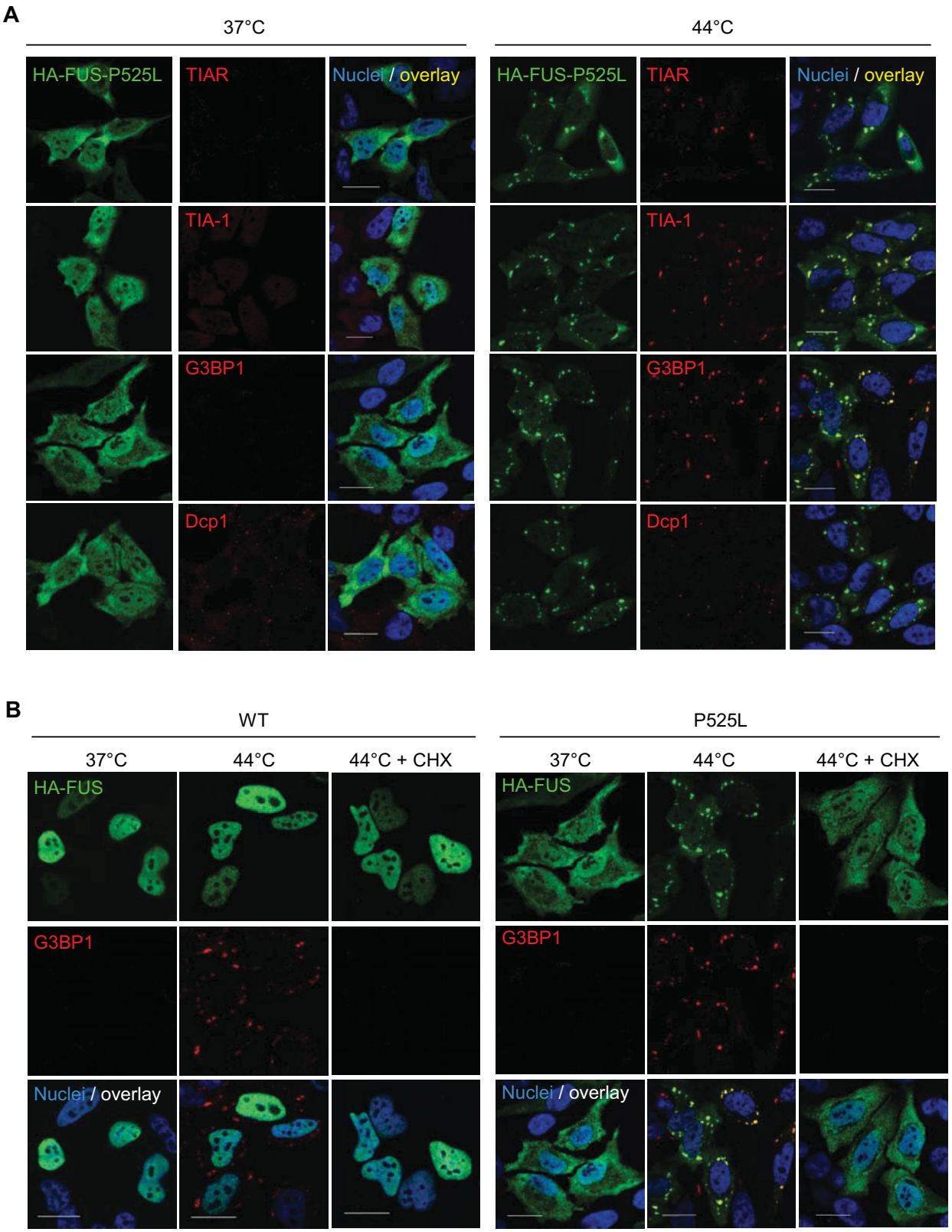
A
37°C
44°C
HA-FUS-P525L
TIAR
Nuclei / overlay
TIA-1
G3BP1
Dcp1
B
WT
P525L
37°C
44°C
44°C + CHX
HA-FUS
G3BP1
Nuclei / overlay

Figure S4: C-terminal fALS-associated *FUS* mutations are recruited into *bona fide* stress granules upon heat shock.

(A) HeLa cells transiently transfected with the HA-tagged FUS-P525L mutant were subjected to heat shock (44°C for 1 h, right panels) or were kept at control temperature (37°C, left panels). Cells were fixed, co-stained with an HA-specific antibody (green) and antibodies specific for the stress granule marker proteins TIAR, TIA-1, G3BP1 or the P body marker protein Dcp1 (red) and a nuclear counterstain (blue) and were analyzed by confocal microscopy. FUS-P525L colocalizes with all stress granule marker proteins, but not with Dcp1, indicating that FUS-P525L-containing granules are indeed stress granules. Scale bar: 20 μm.

(B) HeLa transiently transfected with the HA-tagged FUS-P525L mutant were subjected to heat shock (44°C for 1h) in the presence or absence of the polysome-stabilizing drug cycloheximide (CHX) or were kept at control temperature (37°C). Cells were fixed, co-stained with an HA-specific antibody (green) and a G3BP1-specific antibody (red) and a nuclear counterstain (blue) and were analyzed by confocal microscopy. Cycloheximide completely prevents formation of G3BP1- and FUS-P525L-positive stress granules, demonstrating that the granular FUS-P525L-positive structures observed after heat shock indeed correspond to stress granules. Scale bar: 20 μm.

Supplementary materials and methods

Antibodies

The following antibodies were used: HA-specific mouse monoclonal antibody HA.11 (Covance) or horseradish peroxidase (HRP)-coupled rat monoclonal anti-HA antibody 3F10 (Roche); GFP-specific rabbit polyclonal antiserum BD Living Colors (BD Biosciences); FUS-specific mouse monoclonal antibody 4H11 (Santa Cruz) or rabbit polyclonal A300-294A (Bethyl) or rabbit polyclonal (HPA008784, Sigma); TDP-43-specific rabbit polyclonal antibody (TARDBP, Proteintech); LDH-specific rabbit polyclonal antibody (Santa Cruz); pan-Trp (Trp1/2)-specific goat polyclonal antibody N-19 (Santa Cruz); Trp1-specific mouse monoclonal clone D45 (Sigma); α-Tubulin-specific mouse monoclonal antibody clone B-5-1-2 (Sigma); β-actin specific mouse monoclonal antibody clone AC-74 (Sigma); TIAR-specific rabbit polyclonal antibody (Cell Signaling); PABP-1-specific mouse monoclonal antibody clone 10E10 (Sigma); TIA-1-specific rabbit polyclonal antibody (AV40981, Sigma); TIA-1-specific goat polyclonal antibody (C-20, Santa Cruz); G3BP1-specific rabbit polyclonal antibody (HPA004052, Sigma); Dcp1-specific rabbit polyclonal antibody (HPA013202, Sigma); PABP-1-specific rabbit polyclonal antibody (Cell Signaling); p62-specific mouse monoclonal antibody (BD Transduction Laboratories); eIF4G-specific rabbit polyclonal antibody (Cell Signaling). Secondary antibodies for immunoblotting were HRP-coupled goat anti-mouse or anti-rabbit IgG (Promega) or HRP-coupled donkey anti-goat IgG (Santa Cruz). For immunocytochemistry and immunohistochemistry Alexa-488, Alexa-555, Alexa-594 and Alexa-647-conjugated goat anti-mouse or anti-rabbit IgG (Invitrogen) were used.

Whole mount staining of zebrafish embryos

Embryos were fixed with 4% paraformaldehyde overnight at 4°C. Fixed embryos were dehydrated through a methanol series, kept in methanol overnight at -20°C, subsequently rehydrated through a methanol series and washed 3 times in PBS containing 0.1% Tween-20 (PBST). Embryos were then permeabilized in 1 mg/ml collagenase (Sigma) for 15 min and washed 5 times with PBST. After

blocking for 1 h in newborn calf serum with 0.1% Tween-20 (NCST), embryos were stained with the anti-GFP-antibody overnight at 4°C and washed 2 x 30 min with PBST. The secondary antibody goat anti-rabbit-Alexa-488 was added for 2 h at RT and washed 4 x 30 min with PBST. TO-PRO-3 iodide (Invitrogen) was incubated for 1 h at RT and subsequently rinsed with PBST. Embryos were then mounted in low melting agarose (BioWhittaker) for confocal imaging.

The EMBO Journal (2012) 31, 4258–4275 | © 2012 European Molecular Biology Organization | All Rights Reserved 0261-4189/12
www.embojournal.org

THE EMBO JOURNAL

Arginine methylation next to the PY-NLS modulates Transportin binding and nuclear import of FUS

Dorothee Dormann[1,*], Tobias Madl[2,3,4,13], Chiara F Valori[5,6,13], Eva Bentmann[1], Sabina Tahirovic[7], Claudia Abou-Ajram[1], Elisabeth Kremmer[8], Olaf Ansorge[9], Ian RA Mackenzie[10], Manuela Neumann[5,6,11] and Christian Haass[1,7,12,*]

[1]Adolf-Butenandt-Institute, Biochemistry, Ludwig-Maximilians-University, Munich, Germany, [2]NMR Spectroscopy, Karl-Franzens University, Graz, Austria, [3]Institute of Structural Biology, Helmholtz Zentrum München, Neuherberg, Germany, [4]Biomolecular NMR, Department of Chemistry, Technische Universität München, Garching, Germany, [5]Institute of Neuropathology, University Hospital Zurich, Zurich, Switzerland, [6]DZNE—German Center for Neurodegenerative Diseases, Tübingen, Germany, [7]DZNE—German Center for Neurodegenerative Diseases, Munich, Germany, [8]Institute of Molecular Immunology, Helmholtz Zentrum München, Munich, Germany, [9]Department of Neuropathology, John Radcliffe Hospital, Oxford, UK, [10]Department of Pathology, Vancouver General Hospital, Vancouver, Canada, [11]Department of Neuropathology, University of Tübingen, Tübingen, Germany and [12]Munich Cluster for Systems Neurology (SyNergy), Munich, Germany

Fused in sarcoma (FUS) is a nuclear protein that carries a proline-tyrosine nuclear localization signal (PY-NLS) and is imported into the nucleus via Transportin (TRN). Defects in nuclear import of FUS have been implicated in neurodegeneration, since mutations in the PY-NLS of FUS cause amyotrophic lateral sclerosis (ALS). Moreover, FUS is deposited in the cytosol in a subset of frontotemporal lobar degeneration (FTLD) patients. Here, we show that arginine methylation modulates nuclear import of FUS via a novel TRN-binding epitope. Chemical or genetic inhibition of arginine methylation restores TRN-mediated nuclear import of ALS-associated FUS mutants. The unmethylated arginine–glycine–glycine domain preceding the PY-NLS interacts with TRN and arginine methylation in this domain reduces TRN binding. Inclusions in ALS-FUS patients contain methylated FUS, while inclusions in FTLD-FUS patients are not methylated. Together with recent findings that FUS co-aggregates with two related proteins of the FET family and TRN in FTLD-FUS but not in ALS-FUS, our study provides evidence that these two diseases may be initiated by distinct pathomechanisms and implicates alterations in arginine methylation in pathogenesis.

*Corresponding authors. D Dormann or C Haass, Adolf-Butenandt-Institute, Biochemistry, Ludwig-Maximilians-University, DZNE—German Center for Neurodegenerative Diseases, Schillerstr 44, Munich 80336, Germany. Tel.: +49 89 218075474; Fax: +49 89 218075415; E-mail: dorothee.dormann@dzne.lmu.de or Tel.: +49 89 218075471; Fax: +49 89 218075415; E-mail: christian.haass@dzne.lmu.de
[13]These two authors contributed equally to this work

Received: 26 March 2012; accepted: 17 August 2012; published online: 11 September 2012

The EMBO Journal (2012) **31,** 4258–4275. doi:10.1038/emboj.2012.261; Published online 11 September 2012
Subject Categories: neuroscience
Keywords: amyotrophic lateral sclerosis (ALS); arginine methylation; frontotemporal lobar degeneration (FTLD); fused in sarcoma (FUS); Transportin (TRN)

Introduction

Fused in sarcoma (FUS), also known as translocated in liposarcoma (TLS), is a nucleic acid-binding protein that is predominantly localized in the nucleus and has been implicated in various nuclear processes, such as transcription, splicing and microRNA processing (Lagier-Tourenne *et al*, 2010). Recently, mutations in *FUS* have been described as a cause of familial amyotrophic lateral sclerosis (ALS) (Kwiatkowski *et al*, 2009; Vance *et al*, 2009). ALS is an incurable adult-onset neurodegenerative disease of the human motor system. It is characterized by motor neuron degeneration in the brainstem and spinal cord, leading to progressive paralysis and eventually death due to respiratory muscle failure, typically within 1–5 years of disease onset (Kiernan *et al*, 2011). The majority of ALS cases are sporadic, but about 10% are inherited in a dominant manner (familial ALS, fALS) (Da Cruz and Cleveland, 2011). Of these, about 4% are caused by mutations in the *FUS* gene on chromosome 16 (ALS-FUS). Most pathogenic mutations identified so far are located at the very C-terminus of the FUS protein and affect a proline-tyrosine nuclear localization signal (PY-NLS) (Lee *et al*, 2006) (Figure 1A). This non-classical NLS is bound by the nuclear import receptor Transportin (TRN), also known as Karyopherin β2 (Kapβ2), which translocates PY-NLS-containing cargo proteins across the nuclear pore complex (Chook and Suel, 2011). Pathogenic *FUS* mutations affect key residues of the PY-NLS or completely delete the signal sequence and thus impair nuclear import of FUS (Bosco *et al*, 2010; Dormann *et al*, 2010; Kino *et al*, 2010; Gal *et al*, 2011; Ito *et al*, 2011; Zhang and Chook, 2012). This nuclear transport defect is directly involved in pathogenesis, since mutations that cause a very severe nuclear import block (e.g., FUS-P525L) cause an unusually early disease onset and rapid disease course (Chio *et al*, 2009; Baumer *et al*, 2010; Bosco *et al*, 2010; DeJesus-Hernandez *et al*, 2010; Dormann *et al*, 2010; Waibel *et al*, 2010; Yan *et al*, 2010). Moreover, the FUS protein is deposited in abnormal protein inclusions in neurons and glia of ALS-FUS patients and nuclei often show a reduced FUS staining (Kwiatkowski *et al*, 2009; Vance *et al*, 2009; Blair *et al*, 2010; Groen *et al*, 2010; Hewitt *et al*, 2010; Rademakers *et al*, 2010; Mackenzie *et al*, 2011), further supporting the idea that nuclear import of FUS might be disturbed in this disease.

After the discovery of *FUS* mutations in familial ALS, FUS was studied in a related neurodegenerative disorder, frontotemporal lobar degeneration (FTLD), since ALS and FTLD share many clinical and pathological features (Lomen-Hoerth *et al*, 2002; Murphy *et al*, 2007; Mackenzie *et al*, 2010b). This revealed that FUS is also a component of the abnormal protein inclusions in several subtypes of FTLD, subsequently termed FTLD-FUS (Mackenzie *et al*, 2010a). In contrast to ALS-FUS, which is caused by *FUS* mutations, no genetic alterations in the *FUS* gene have so far been identified in FTLD-FUS cases (Neumann *et al*, 2009a, b; Urwin *et al*, 2010; Snowden *et al*, 2011). Thus, the pathological redistribution of FUS in these cases cannot be explained by a mutant PY-NLS, suggesting that a more general dysregulation of TRN-mediated transport may underlie FUS pathology and neurodegeneration in FTLD-FUS. This is supported by the recent finding that in addition to FUS, two related PY-NLS-containing proteins, Ewing sarcoma protein (EWS) and TATA-binding protein-associated factor 15 (TAF15), which belong to the same protein family (FET family), as well as TRN, are present in inclusions of FTLD-FUS patients (Brelstaff *et al*, 2011; Neumann *et al*, 2011, 2012; Davidson *et al*, 2012). How this pathological redistribution and co-deposition of FUS, EWS and TAF15 and TRN occurs in FTLD-FUS is currently unknown.

Nucleocytoplasmic transport can be regulated at multiple levels, including post-translational modifications of transport cargo, such as phosphorylation or ubiquitination (Terry *et al*, 2007). In addition, arginine methylation, which is a common post-translational modification of nuclear RNA-binding proteins, has been described to affect nuclear localization of several proteins, although the regulatory mechanism(s) are still largely unknown (Bedford and Clarke, 2009). Arginine methylation involves transfer a methyl group from *S*-adenosyl-L-methionine (SAM) onto one or both of the guanidinium nitrogens of the arginine side chain with the help of protein *N*-arginine methyltransferases (PRMTs), resulting in monomethylarginine, symmetric or asymmetric dimethylarginine residues (Pahlich *et al*, 2006). This alters the hydrophobicity and hydrogen bonding capacity of the modified arginine residues and can affect protein–protein interactions (Bedford and Clarke, 2009; Pahlich *et al*, 2006). FUS, EWS and TAF15 have been described to undergo extensive asymmetric dimethylation in their arginine–glycine–glycine (RGG) domains (Figure 1A) (Belyanskaya *et al*, 2001; Lee and Bedford, 2002; Rappsilber *et al*, 2003; Ong *et al*, 2004; Araya *et al*, 2005; Pahlich *et al*, 2005; Hung *et al*, 2009; Jobert *et al*, 2009; Du *et al*, 2011), and there is evidence that arginine methylation can affect their nucleocytoplasmic localization (Araya *et al*, 2005; Jobert *et al*, 2009; Tradewell *et al*, 2012). However, the molecular mechanism by which arginine methylation may affect nuclear localization of the FET proteins is unknown and it is unclear whether arginine methylation is involved in the pathology of ALS/FTLD-FUS.

We now show that arginine methylation impairs TRN-dependent nuclear import of FUS, by decreasing binding of TRN to a novel TRN-binding motif next to the PY-NLS of FUS. Furthermore, immunohistochemistry with novel methyl-FUS-specific antibodies revealed that inclusions in ALS-FUS patients contain methylated FUS, while deposited FUS in FTLD-FUS cases is unmethylated. Our findings provide new insights into the mechanism of TRN-cargo recognition in general and suggest that altered arginine methylation of FET proteins may be involved in the pathological co-deposition of FET proteins and TRN in FTLD-FUS.

Results

Inhibition of methylation restores nuclear localization of ALS-associated FUS mutants

To test if arginine methylation affects the nuclear localization of FUS, we treated HeLa cells with the general methylation inhibitor, adenosine-2,3-dialdehyde (AdOx), which inhibits all SAM-dependent enzymatic reactions, including protein arginine methylation (Chen *et al*, 2004), and analysed its effect on localization of HA-tagged wild-type FUS (WT) and four cytoplasmically mislocalized ALS-associated FUS mutants (Dormann *et al*, 2010). Consistent with our previous findings, FUS-WT was located almost exclusively in the nucleus in untreated cells, whereas the ALS-associated FUS mutants showed a varying degree of cytoplasmic mislocalization, ranging from a very mild mislocalization for R521G, over an intermediate phenotype for R524S and R522G, to a severe mislocalization for P525L (Figure 1B upper panels, see C for quantification). Strikingly, upon treatment of cells with AdOx, all FUS mutants showed a predominant nuclear localization and were almost indistinguishable from the WT protein (Figure 1B lower panels and C). This could not be attributed to altered expression levels, since similar HA–FUS protein levels were observed in untreated and AdOx-treated cells (Figure 1D). Thus, inhibition of methylation with AdOx restores nuclear localization of ALS-associated FUS mutants, suggesting that nuclear import of FUS might be modulated by arginine methylation.

The same phenomenon could also be observed in primary rat hippocampal neurons, where FUS-WT was located almost exclusively in the nucleus (0% cells with mislocalized FUS), while the P525L mutant was partially mislocalized to the cytosol, including neuritic processes, in the majority of neurons ($89 \pm 1\%$) (Figure 1E). AdOx treatment significantly reduced the cytoplasmic mislocalization of FUS-P525L ($26 \pm 12\%$ cells with mislocalized FUS, $P < 0.05$). Thus, nuclear localization of mutant FUS is affected by methylation not only in transformed cell lines, but also in primary neurons, demonstrating that this is not a cell-type-specific phenomenon.

Methylation affects nuclear localization of FET protein mutants

Since not only FUS but also the other FET family members, EWS and TAF15, are subject to arginine methylation (Belyanskaya *et al*, 2001; Ong *et al*, 2004; Araya *et al*, 2005; Pahlich *et al*, 2005; Jobert *et al*, 2009) and the three proteins share a very similar domain structure (Figure 2A), we speculated that arginine methylation may regulate nuclear import of all FET proteins in a similar manner and may contribute to their pathological deposition in FTLD-FUS (Neumann *et al*, 2011; Davidson *et al*, 2012). To test this hypothesis, we mutated the PY-NLS of EWS (EWS-P655L) and TAF15 (TAF-P591L) to generate cytoplasmic point mutants analogous to FUS-P525L. In contrast to WT EWS and TAF15, EWS-P655L and TAF-P591L were partially mislocalized to the cytoplasm (Figure 2B, see C for quantification). Upon treatment with

AdOx, all three FET protein mutants became predominantly nuclear, suggesting that nuclear localization of all FET family members is affected by methylation in a similar manner.

Silencing of protein N-arginine methyltransferase 1 (PRMT1) causes nuclear localization of FUS-P525L

AdOx inhibits all SAM-dependent pathways including DNA, lipid and protein methylation (Bartel and Borchardt, 1984; Liteplo and Kerbel, 1986). Therefore, the above-described relocalization of FUS mutants by AdOx could depend on any of these mechanisms. FUS has been previously reported to be asymmetrically dimethylated on arginine residues (Rappsilber *et al*, 2003; Ong *et al*, 2004) and it is known that protein arginine methylation can affect subcellular localization of various proteins (reviewed in Bedford and Clarke, 2009). We therefore speculated that

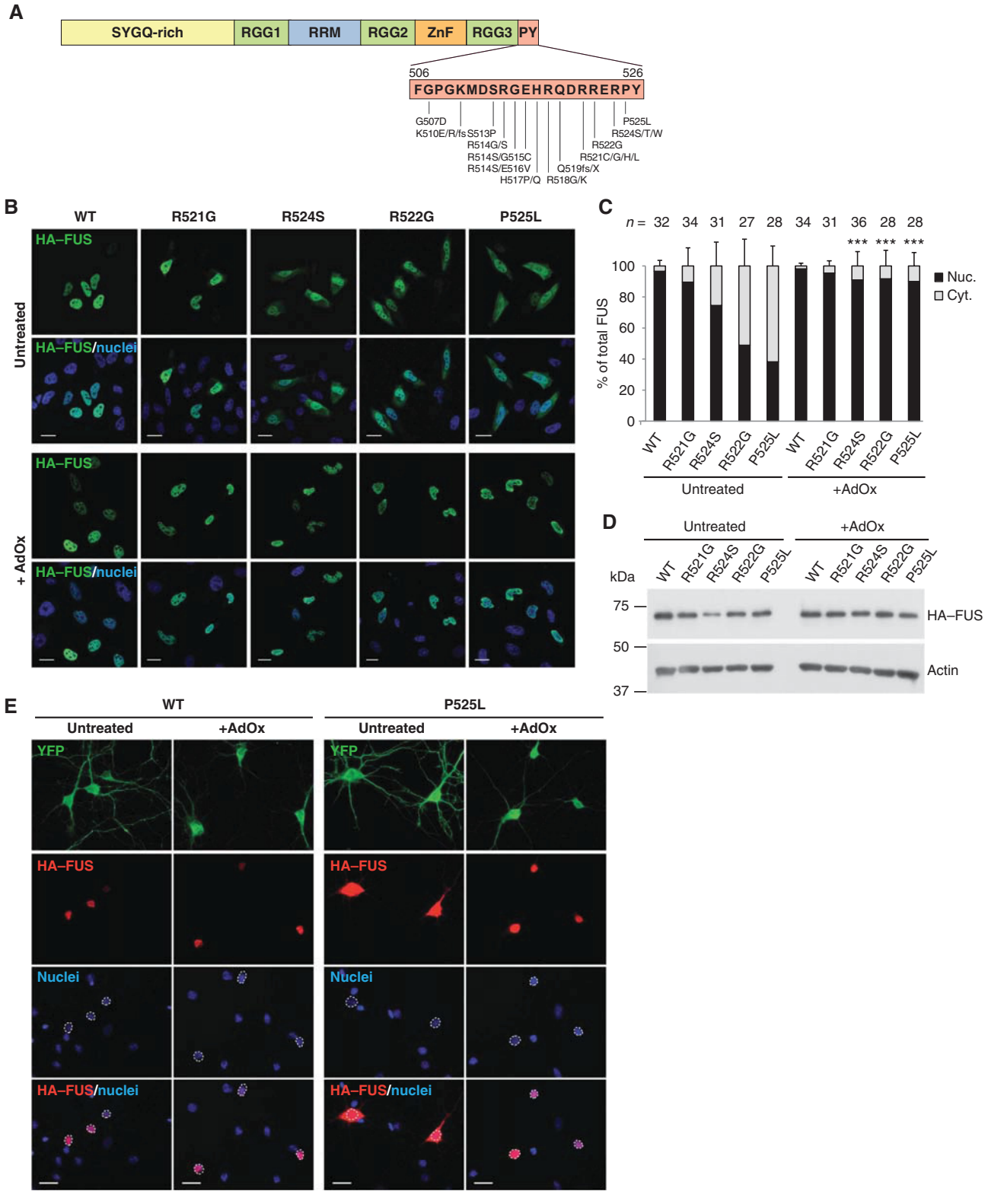

specifically inhibition of arginine methylation could be responsible for the striking relocalization of FUS mutants upon AdOx treatment.

To test this hypothesis, we silenced the major protein arginine methyltransferase predominantly responsible for most asymmetric arginine dimethylation, protein *N*-arginine methyltrasferase 1 (PRMT1) (Pawlak *et al*, 2000; Tang *et al*, 2000), using two different PRMT1-specific siRNAs. Two days after siRNA delivery, HA-tagged FUS-WT or FUS-P525L was transfected into cells and their localization was examined by confocal microscopy. Consistent with our hypothesis, silencing of PRMT1 caused a predominantly nuclear localization of FUS-P525L, whereas the typical partially cytoplasmic localization could be observed in control siRNA-transfected cells (Figure 3A and B). Rescue of nuclear localization of FUS-P525L, although significant ($P<0.001$), was not as efficient as with AdOx treatment, which could be due to residual amounts of PRMT1 in PRMT1 siRNA-transfected cells (see immunoblot in Figure 3A) or to the methylation of FUS by other PRMTs. Nevertheless, siRNA-mediated silencing of PRMT1 mimicked the effect of AdOx treatment, demonstrating that nuclear localization of mutant FUS is modulated by PRMT1-dependent arginine methylation.

Nuclear import of mutant FUS upon AdOx treatment is Transportin dependent

Nuclear import of FUS has been shown to be mediated by the nuclear import receptor TRN. To test if nuclear localization of FUS-P525L upon AdOx treatment or PRMT1 knockdown is still dependent on TRN, we utilized a TRN-specific inhibitor peptide (M9M), which binds to TRN with high affinity and thus efficiently competes with nuclear import of regular TRN substrates (Cansizoglu *et al*, 2007). In addition, we utilized a similar high-affinity peptide inhibitor (Bimax) for the classical nuclear import receptor Importin α (Kosugi *et al*, 2008), since it is also conceivable that arginine methylation masks a so far unidentified NLS, which would become accessible to Importin α upon methylation inhibition.

We expressed these competitor peptides as GFP fusion proteins (GFP–M9M and GFP–Bimax) together with HA-tagged FUS-P525L in HeLa cells and analysed cellular localization of mutant FUS upon AdOx or mock treatment.

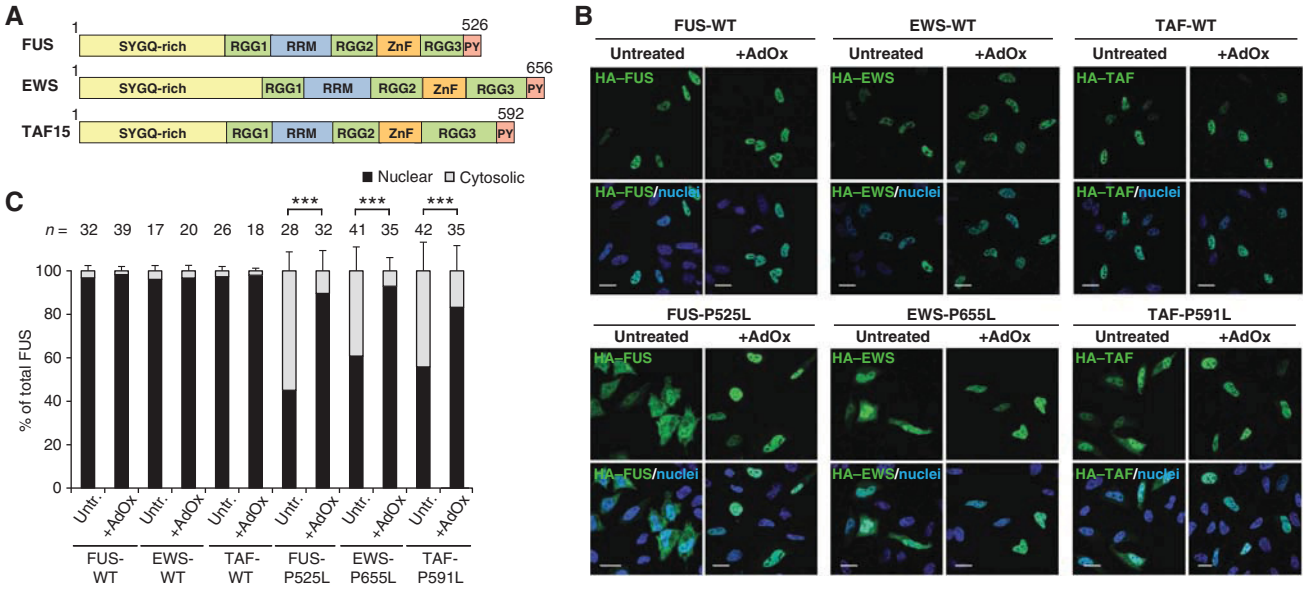

Figure 2 Methylation affects nuclear localization of EWS and TAF15 mutants. (**A**) Schematic diagram showing the domain structures of FUS, EWS and TAF15 (FET proteins). (**B**) Localization of HA-tagged FUS, EWS or TAF15 (WT or with mutant PY-NLS) in untreated or AdOx-treated HeLa cells. Cytoplasmic FET protein mutants become predominantly nuclear upon AdOx treatment, suggesting that methylation affects nuclear import of all FET family members in a similar fashion. Scale bars: 20 μm. (**C**) Quantification of nuclear and cytosolic fluorescence intensities. Values are means across *n* cells, error bars indicate s.d. Statistical significance is displayed as *** ($P<0.001$) (one-way ANOVA).

Figure 1 Cytoplasmic mislocalization of ALS-associated FUS mutants is abrogated upon inhibition of methylation. (**A**) Schematic diagram showing the domain structure of FUS. Sequence of the C-terminal PY-NLS and ALS-causing point mutations within the NLS are given below. ALS-associated mutations outside the PY-NLS are described elsewhere (Mackenzie *et al*, 2010b). SYGQ-rich = serine, tyrosine, glycine, glutamine-rich domain; RRM = RNA recognition motif; ZnF = zinc finger. (**B**) Localization of HA-tagged FUS WT or the indicated ALS-associated FUS mutants in untreated (upper panels) or AdOx-treated (lower panels) HeLa cells. ALS-associated FUS mutants become predominantly nuclear upon AdOx treatment, suggesting that methylation modulates nuclear import of FUS. Scale bars: 20 μm. (**C**) Quantification of nuclear and cytosolic fluorescence intensities. Values are means across *n* cells, error bars indicate standard deviations (s.d.). Statistical significance between untreated and AdOx-treated is displayed as *** ($P<0.001$; one-way ANOVA). (**D**) HA–FUS protein levels in untreated and AdOx-treated HeLa cells were analysed by immunoblotting with an HA-specific antibody (upper panel). Actin served as a loading control (lower panel). AdOx treatment does not affect expression of HA–FUS constructs. (**E**) Localization of HA-tagged FUS-WT or P525L (red) in untreated or AdOx-treated primary rat hippocampal neurons. YFP (green) served as a cytosolic filler protein to visualize neuronal morphology, nuclei were visualized with DAPI. In contrast to untreated neurons, AdOx-treated neurons rarely show cytoplasmic mislocalization of FUS-P525L. Scale bars: 20 μm. Figure source data can be found with the Supplementary data.

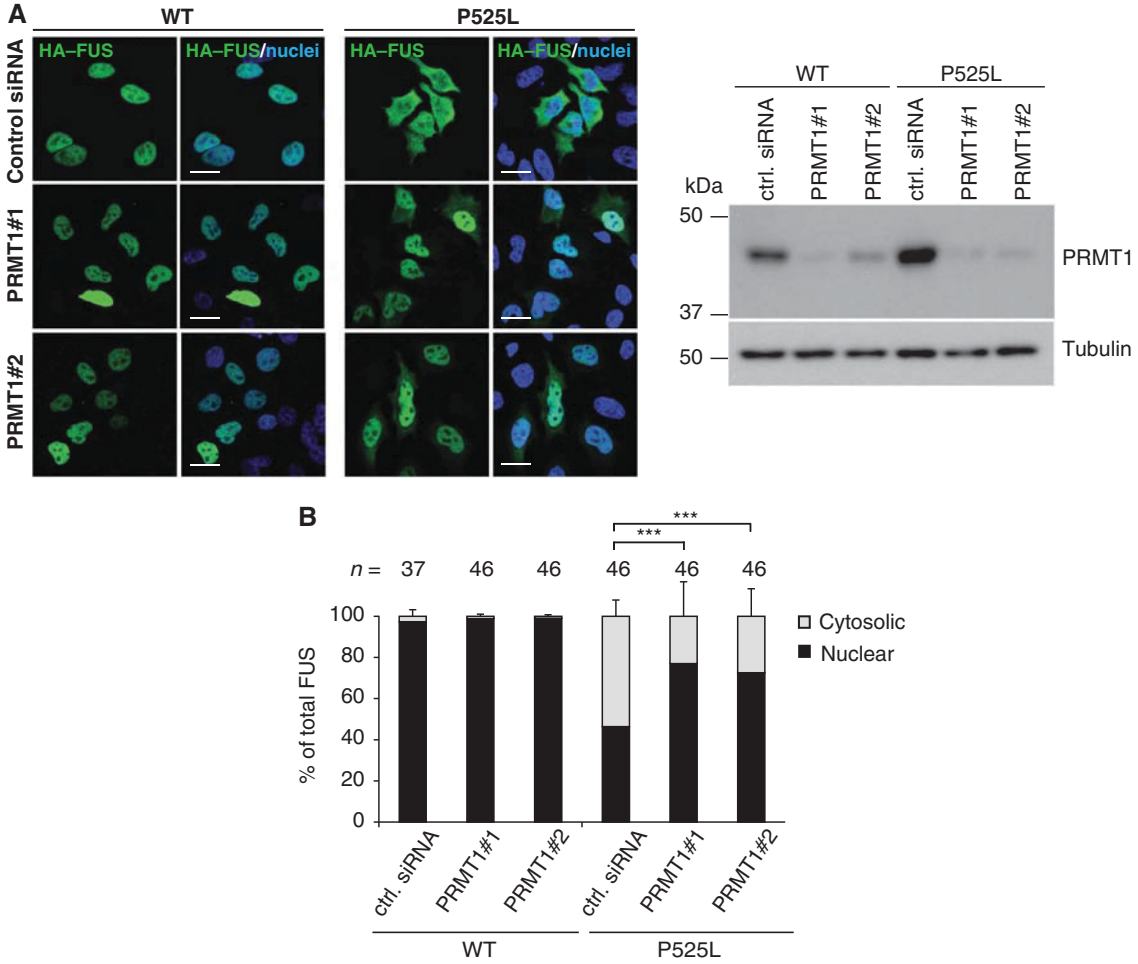

Figure 3 PRMT1 silencing causes increased nuclear localization of FUS-P525L. (**A**) Protein N-arginine methyltransferase 1 (PRMT1) expression was silenced in HeLa cells by transfection of two different siRNAs (PRMT1#1 and PRMT1#2), a control (ctrl.) siRNA was used as a negative control. In all, 48 h after siRNA delivery, cells were transfected with HA-tagged FUS-WT or P525L and localization of these proteins was examined by HA immunostaining (green) and confocal microscopy. PRMT1 knockdown causes a predominantly nuclear localization of the FUS-P525L mutant, suggesting that arginine methylation by PRMT1 modulates nuclear import of FUS. Scale bars: 20 μm. Immunoblots on the right show PRMT1 knockdown efficiency. Total cell lysates were examined with a PRMT1-specific antibody (upper panel) and a tubulin-specific antibody (lower panel). (**B**) Quantification of nuclear and cytosolic fluorescence intensities. Values are means across *n* cells, error bars indicate s.d. Statistical significance is displayed as *** ($P<0.001$) (one-way ANOVA). Figure source data can be found with the Supplementary data.

As expected, in control (GFP)-transfected cells, FUS-P525L showed the above described nuclear localization upon AdOx treatment (Figure 4A, left panels). Consistent with our previous data (Dormann *et al*, 2010), GFP–M9M expression led to recruitment of FUS-P525L into cytosolic stress granules in about half of the cells (Figure 4A, middle panels). However, both in cells with and without stress granules, nuclear accumulation of FUS-P525L upon AdOx treatment was blocked by GFP–M9M expression, demonstrating that TRN activity is required for nuclear import of mutant FUS. In contrast, the classical Importin α-dependent nuclear import pathway does not seem to be involved, since AdOx-mediated nuclear import of FUS-P525L still occurred in cells transfected with the Importin α inhibitor (GFP–Bimax) (Figure 4A, right panels). Thus, nuclear localization of mutant FUS upon AdOx treatment is dependent on TRN, but not Importin α activity.

To investigate whether TRN mediates the above-described relocalization by direct binding of mutant FUS or indirectly via another TRN substrate, we analysed a FUS deletion mutant lacking the most essential amino acids of the FUS PY-NLS (Δ514–526, see schematic diagram in Figure 4B) (Dormann *et al*, 2010; Zhang and Chook, 2012). In contrast to FUS-P525L, which was mostly nuclear upon AdOx treatment, the C-terminal deletion mutant was strongly mislocalized to the cytosol in both untreated and AdOx-treated cells (Figure 4B). This demonstrates that the mutant PY-NLS of FUS is required for nuclear relocalization upon AdOx treatment, suggesting that TRN directly binds to and imports mutant FUS upon inhibition of methylation.

Arginines in the RGG3 domain of FUS are required for nuclear import of mutant FUS

Next, we searched for the mechanism how arginine methylation may regulate TRN-dependent nuclear import of FUS. One possibility would be that, similar to the nuclear poly(A)-binding protein (PABPN1) (Fronz *et al*, 2011), arginine methylation within the PY-NLS of FUS (on residues R514, R518, R521, R522 and/or R524) may affect TRN binding.

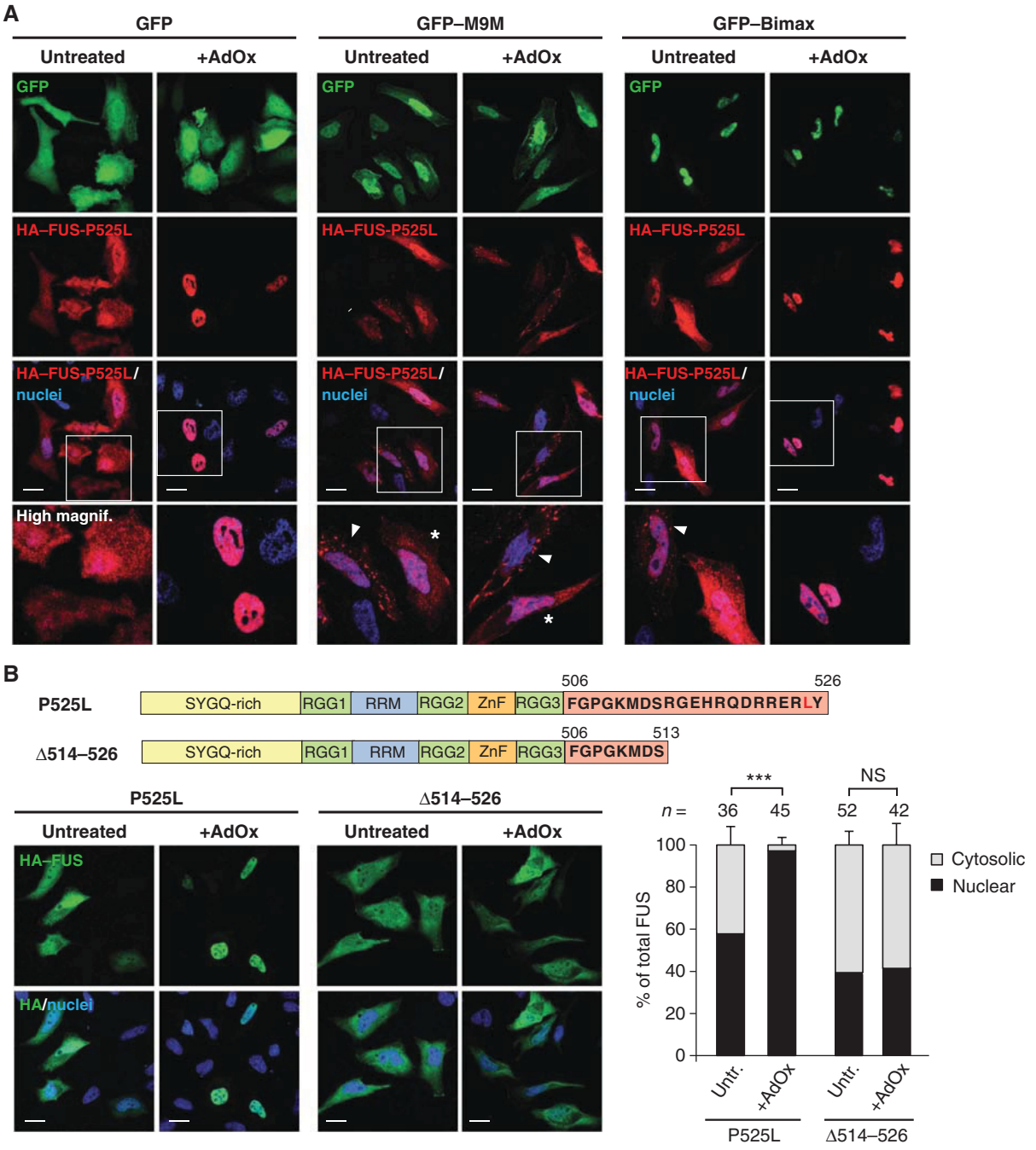

Figure 4 Nuclear import of FUS-P525L upon AdOx treatment is dependent on TRN. (**A**) Localization of HA–FUS-P525L in untreated or AdOx-treated HeLa cells after co-expression of GFP as a control, a competitor of the TRN pathway (GFP–M9M) or a competitor of the Importin α pathway (GFP–Bimax) (green). After HA immunostaining (red), localization of mutant FUS was examined by confocal microscopy. The bottom row shows a higher magnification of the boxed regions. GFP–M9M expressing cells with stress granules are labelled with an arrowhead, cells without stress granules are labelled with an asterisk. Both in cells with and without stress granules, GFP–M9M prevents nuclear import of FUS-P525L upon AdOx treatment, demonstrating that import of FUS-P525L is TRN dependent. Scale bars: 20 μm. (**B**) Localization of a FUS deletion mutant lacking the core amino acids of the C-terminal PY-NLS (Δ514–526, see schematic diagram) in untreated or AdOx-treated HeLa cells. Nuclear relocalization upon AdOx treatment requires the FUS PY-NLS, suggesting that it requires direct TRN binding. Scale bars: 20 μm. Quantification shows nuclear and cytosolic fluorescence intensities. Values are means across *n* cells, error bars indicate s.d. Statistical significance is displayed as *** ($P<0.001$) (one-way ANOVA); NS = not significant.

Another possibility would be that the RGG motifs N-terminal of the PY-NLS could be involved in modulating TRN binding and nuclear import of FUS. The latter scenario would be consistent with the fact that methylated arginines have been exclusively identified in the RGG domains and not the PY-NLS of FUS (Rappsilber *et al*, 2003; Ong *et al*, 2004).

To find out if arginine residues in the PY-NLS or the RGG3 domain mediate the differential localization of mutant FUS upon methylation inhibition, we attached the mutant PY-NLS ($514–526_{P525L}$) alone or with the RGG3 domain ($455–526_{P525L}$) to the C-terminus of the cytosolic reporter protein GST–GFP (see Figure 5A for a schematic diagram). As shown

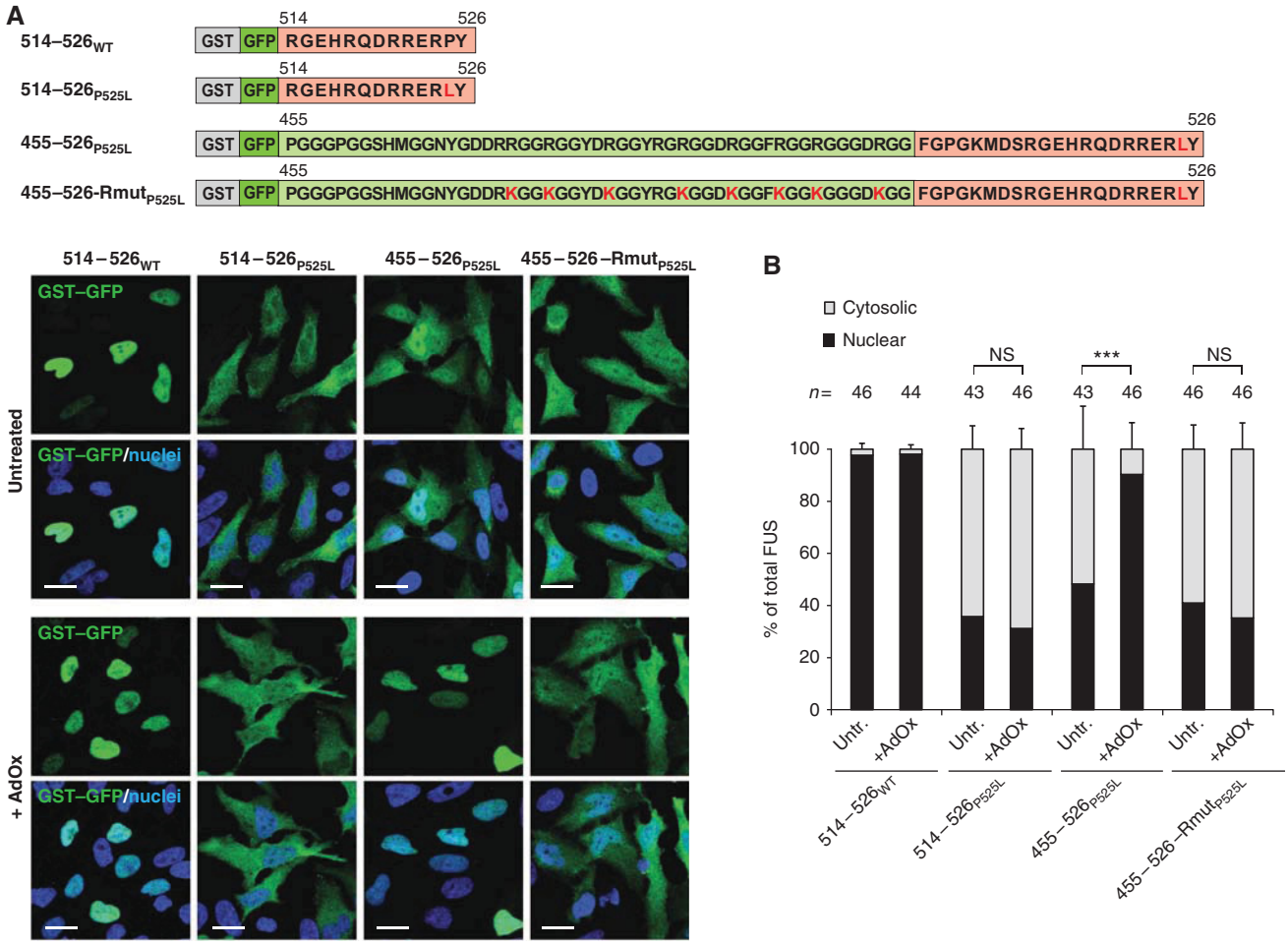

Figure 5 Arginine residues in the RGG3 domain of FUS are required for nuclear import of mutant FUS. (**A**) GST–GFP reporter proteins with the indicated FUS sequences at the C-terminus were transiently expressed in untreated or AdOx-treated HeLa cells. Localization of reporter constructs was examined after GFP (green) immunostaining by confocal microscopy. Arginine residues in the PY-NLS (amino acids 514–526) are not sufficient for restoring nuclear import of the mutant reporter protein upon AdOx treatment, while arginines in the RGG3 domain (amino acids 455–505) are necessary and sufficient for this effect. Scale bars: 20 μm. (**B**) Quantification shows nuclear and cytosolic fluorescence intensities. Values are means across *n* cells, error bars indicate s.d. Statistical significance is displayed as *** ($P<0.001$) (one-way ANOVA); NS = not significant.

previously (Dormann *et al*, 2010), GST–GFP carrying the intact PY-NLS (514–526$_{WT}$) was efficiently imported into the nucleus, while a reporter protein carrying the mutant PY-NLS (514–526$_{P525L}$) failed to be imported efficiently (Figure 5A, see B for quantification). Upon AdOx treatment, the GST–GFP–514–526$_{P525L}$ reporter protein remained predominantly cytoplasmic, demonstrating that the five arginines within the PY-NLS do not mediate nuclear import upon AdOx treatment. In contrast, the reporter protein encompassing the RGG3 domain plus the PY-NLS (455–526$_{P525L}$) fully recapitulated the AdOx-mediated nuclear localization phenotype observed for the full-length protein (Figure 5A and B). A mutant version of this reporter construct, where all arginines within RGG motifs where replaced by lysines (455–526-Rmut$_{P525L}$, see schematic diagram in Figure 5A) and therefore cannot be methylated by PRMT1 (Butler *et al*, 2011), failed to localize to the nucleus upon AdOx treatment. Thus, arginines within the RGG3 domain are necessary and sufficient for restoring nuclear import of the mutant reporter protein upon methylation inhibition.

The RGG3 domain of FUS interacts tightly with TRN and rescues weaker binding of the mutant PY-NLS

To prove that the RGG repeats in the RGG3 domain of FUS directly bind to TRN, we analysed the interaction of recombinant FUS comprising residues 454–526 (FUS454–526$_{WT}$ and FUS454–526$_{P525L}$, see Figure 6A for a schematic diagram) with recombinant TRN by NMR spectroscopy. NMR spectra of FUS454–526$_{WT}$ and FUS454–526$_{P525L}$ in isolation showed that the two proteins are intrinsically disordered, given the distribution of signals in regions characteristic for random coil proteins (Figure 6B). Lack of stable tertiary and secondary structure is a common feature of known PY-NLSs and allows for highly specific binding of a great variety of different transportin cargo proteins (Chook and Suel, 2011). Upon addition of TRN, most NMR signals that are characteristic for glycine residues disappeared both in FUS454–526$_{WT}$ as well as in FUS454–526$_{P525L}$ (Figure 6C, left panels), demonstrating that the RGG motifs indeed bind to TRN. The NMR signal of the C-terminal tyrosine residue (Y526) disappeared upon addition of TRN in the WT protein,

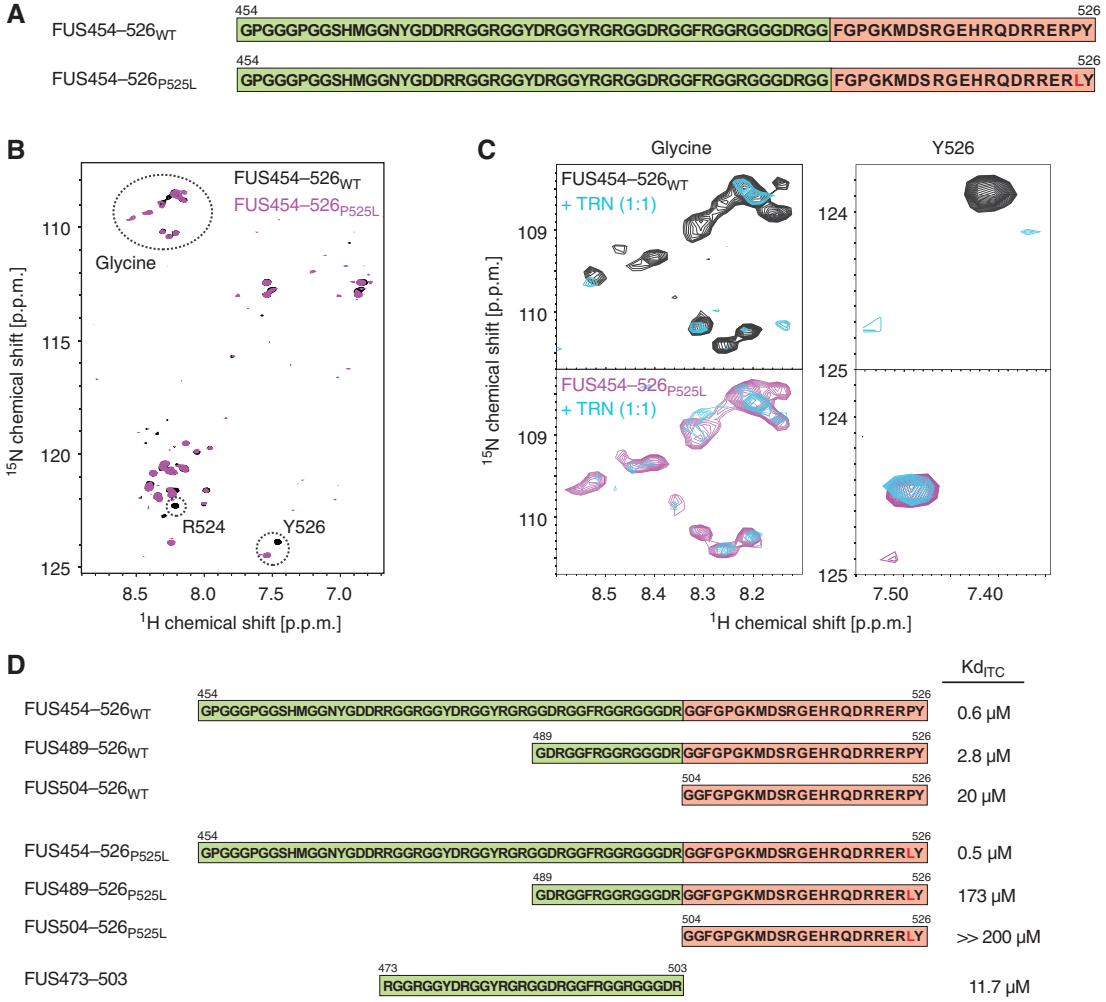

Figure 6 Both the RGG3 domain and the PY-NLS of FUS interact with TRN. (**A**) Schematic diagram of recombinant FUS proteins analysed by NMR spectroscopy. (**B**) Overlay of 2D ^{1}H,^{15}N HSQC NMR spectra recorded for FUS454–526$_{WT}$ (black) and FUS454–526$_{P525L}$ (magenta). Regions characteristic for glycine residues, position R524 and the C-terminal Y526 are encircled (dotted line). The distribution of NMR signals in regions characteristic for random coil proteins indicates that both proteins are intrinsically disordered in solution. (**C**) Overlay of selected regions (glycine and Y526) of 2D ^{1}H,^{15}N HSQC NMR spectra recorded for FUS454–526$_{WT}$ (black) and FUS454–526$_{P525L}$ (magenta) in isolation and in the presence of an equimolar stoichiometric equivalent of TRN (blue). NMR signals characteristic for glycine residues disappear upon addition of TRN, indicating binding of RGG repeats to TRN. The NMR signal of Y526 disappears upon addition of TRN in the WT protein, but is only slightly affected in the P525L mutant, indicating tight binding of TRN to the WT PY but not the mutant LY. (**D**) Schematic diagram of recombinant FUS proteins and synthetic FUS peptides analysed for TRN binding by ITC. Binding constants (Kd$_{ITC}$) are shown on the right. Both the PY-NLS and the N-terminal RGG repeats contribute to TRN binding. The RGG3 repeat domain can bind TRN in the absence of a C-terminal PY-NLS and can compensate for the lack of binding of the mutant C-terminus in the P525L mutant.

but was only slightly affected in FUS454–526$_{P525L}$ (Figure 6C, right panels), demonstrating binding of TRN to the C-terminal PY but not the mutant C-terminus. Thus, the P525L mutation disrupts binding of the C-terminal tyrosine to TRN, while the RGG3 repeat region interacts tightly with TRN in both WT and mutant FUS.

To quantitatively assess binding of the RGG3 repeat region to TRN, we studied the interaction of recombinant FUS454–526 or synthetic FUS peptides with TRN by isothermal titration calorimetry (ITC) (Figure 6D). This showed that both FUS454–526$_{WT}$ and FUS454–526$_{P525L}$ formed high-affinity complexes with TRN, with virtually identical dissociation constants below micromolar Kd (Supplementary Figure S1; Figure 6D). Thus, the binding affinity is unaffected by the C-terminal P525L mutation, suggesting that tight interaction between the unmethylated RGG3 domain and TRN can rescue weak binding of the C-terminus in the P525L mutant. Shorter FUS peptides lacking the N-terminal part of the RGG3 repeat region (FUS489–526$_{WT}$) or the entire RGG3 domain (FUS504–526$_{WT}$) bound to TRN with reduced affinities compared to FUS454–526$_{WT}$ (Figure 6D), confirming that the RGG3 repeats next to the PY-NLS stabilize the FUS–TRN interaction. The importance of the RGG3 repeat region for TRN binding became even more apparent in the context of the P525L mutation, where shortening or deletion of the RGG3 repeat region (FUS489–526$_{P525L}$ or FUS 504–526$_{P525L}$) severely impaired or completely prevented TRN binding (Figure 6D). Finally, we tested if the RGG3 domain alone was able to bind to TRN in the absence of a C-terminal PY-NLS. Indeed, a synthetic FUS peptide comprising the RGG3

repeat domain only (FUS473–503) bound to TRN with an affinity comparable to the WT PY-NLS (FUS504–526$_{WT}$) (Figure 6D). Taken together, our NMR and ITC analysis demonstrate that the unmethylated RGG3 domain of FUS binds tightly to TRN and that this interaction can even rescue weak binding of the mutant C-terminus in the ALS-associated P525L mutant.

Arginine methylation in the RGG3 domain of FUS impairs TRN binding

Based on our cellular assays, we speculated that arginine methylation in the RGG3 domain should impair TRN binding. To test this hypothesis, we performed *in vitro* pulldown assays with recombinant TRN and synthetic FUS peptides comprising the RGG3 domain either unmethylated or with asymmetrically dimethylated (me) arginine residues (FUS473–526 and meFUS473–503; see schematic diagram in Figure 7A). Biotinylated FUS peptides were immobilized on streptavidin beads and were incubated with varying amounts of recombinant His$_6$-tagged TRN or His$_6$–GST as a control. Consistent with our hypothesis, the unmethylated RGG3 peptide efficiently pulled down TRN, while TRN binding was undetectable for the methylated RGG3 peptide (Figure 7A). In line with these data, ITC and NMR showed TRN binding for the unmethylated FUS473–503 peptide, whereas no TRN binding could be observed for the methylated peptide (Figure 7A; Supplementary Figure S2A). Thus, arginine methylation in the RGG3 repeat domain of FUS strongly interferes with TRN binding.

We next investigated the effect of arginine methylation on TRN binding in the context of the C-terminal PY-NLS and thus performed *in vitro* pulldown assays with peptides comprising the WT or mutant PY-NLS preceded by four unmethylated or asymmetrically dimethylated RGG repeats (FUS489–526$_{WT}$, meFUS489–526$_{WT}$, FUS489–526$_{P525L}$ and meFUS489–526$_{P525L}$; see schematic diagrams in Figure 7B and C; these peptide were used since synthesis of longer peptides comprising the entire methylated RGG3 domain plus PY-NLS was not successful and *in vitro* methylation of the recombinant FUS454–526 proteins was very inefficient). We expected that arginine methylation would be especially detrimental for TRN binding of the P525L mutant, where binding of the C-terminal residues to TRN is strongly impaired (Figure 6C). Consistent with this hypothesis, arginine methylation strongly interfered with TRN binding of the mutant peptide in our pulldown assay (Figure 7B), and ITC and NMR showed weak TRN binding of the unmethylated FUS489–526$_{P525L}$ peptide and no binding of meFUS489–526$_{P525L}$ (Figure 7B; Supplementary Figure S2B). Interestingly, methylation also slightly impaired TRN binding of the WT peptide (Figure 7C), and ITC and NMR confirmed a reduced TRN binding affinity ($\sim$3-fold higher Kd) for meFUS489–526$_{WT}$ in comparison to FUS489–526$_{WT}$ (Figure 7C; Supplementary Figure S2C). Considering that the (me)FUS489–526$_{WT}$ peptides comprise only four RGG repeats and not the entire RGG3 domain, it seems likely that arginine methylation has a more dramatic effect on TRN binding in the presence of the entire RGG3 domain. Thus, arginine methylation in the RGG3 repeat domain not only impairs TRN binding of the FUS-P525L mutant, but also slightly modulates TRN binding of the WT protein.

Methylated FUS-P525L is recruited to stress granules upon cellular stress

Our finding that ALS-associated FUS mutants become nuclear upon inhibition of arginine methylation implies that mutant FUS must be methylated, since otherwise the mutant protein should be imported into the nucleus and it would be difficult to explain the correlation between nuclear transport defect and clinical phenotype (Dormann *et al*, 2010; Dormann and Haass, 2011). To test if FUS and ALS-associated FUS mutants are indeed methylated, we raised monoclonal antibodies specific to the methylated RGG3 domain (epitope meFUS473–503; Figure 8A). Two monoclonal antibodies (14H5 and 9G6) selectively recognized endogenous methylated FUS, since signals obtained by immunoblotting (Figure 8B) and immunofluorescence (Figure 8C) disappeared upon AdOx treatment or FUS knockdown. Methylated FUS was located exclusively in the nucleus both in HeLa cells (Figure 8C) and primary rat hippocampal neurons (Supplementary Figure S3C). In addition, cytosolic FUS mutants, such as FUS-P525L, were also recognized by the meFUS-specific antibodies (Figure 8D), which is consistent with our finding that inhibition of methylation restores nuclear localization of mutant FUS.

Stress granules have been suggested to be precursors of pathological FUS inclusions, since inclusions in ALS-FUS and FTLD-FUS patients are immunoreactive for stress granule marker proteins (Fujita *et al*, 2008; Dormann *et al*, 2010). We therefore used stress granules as a pathological surrogate for FUS inclusions and examined whether they contain methylated FUS-P525L. Consistent with our previous findings (Dormann *et al*, 2010; Bentmann *et al*, 2012), cytosolic FUS-P525L was recruited to stress granules in HeLa cells exposed to heat shock (Figure 8D). FUS-P525L-positive granules were not only co-stained with an antibody specific for the stress granule marker protein TIA-1, but also were co-labelled with a meFUS-specific antibody (Figure 8D). This demonstrates that methylated FUS-P525L is recruited to stress granules, the potential precursors of pathological FUS inclusions in ALS-FUS patients.

Inclusions in ALS-FUS contain methylated FUS, while inclusions in FTLD-FUS are hypomethylated

To investigate the methylation status of FUS in human brain, we analysed post mortem tissue from ALS-FUS, FTLD-FUS and healthy controls by immunohistochemistry and double-label immunofluorescence with the newly generated meFUS-specific antibodies. Like in cultured cells, the physiological staining pattern for meFUS was predominantly nuclear in controls and FUS-opathies (Supplementary Figure S3B and C). Consistent with our hypothesis that arginine methylation contributes to the pathological mislocalization of mutant FUS proteins, we revealed a very strong and consistent co-labelling of all FUS-positive cytoplasmic neuronal and glial inclusions with the meFUS antibody in all ALS-FUS cases investigated, including four different *FUS* mutations (Figure 9A). Thus, inclusions in ALS-FUS patients contain methylated FUS.

Next, we investigated the spectrum of FTLD-FUS, including atypical FTLD-U (aFTLD-U), neuronal intermediate filament inclusion body disease (NIFID) and basophilic inclusion body disease (BIBD). Surprisingly, FUS-positive neuronal and glial cytoplasmic inclusions as well as intranuclear inclusions in all

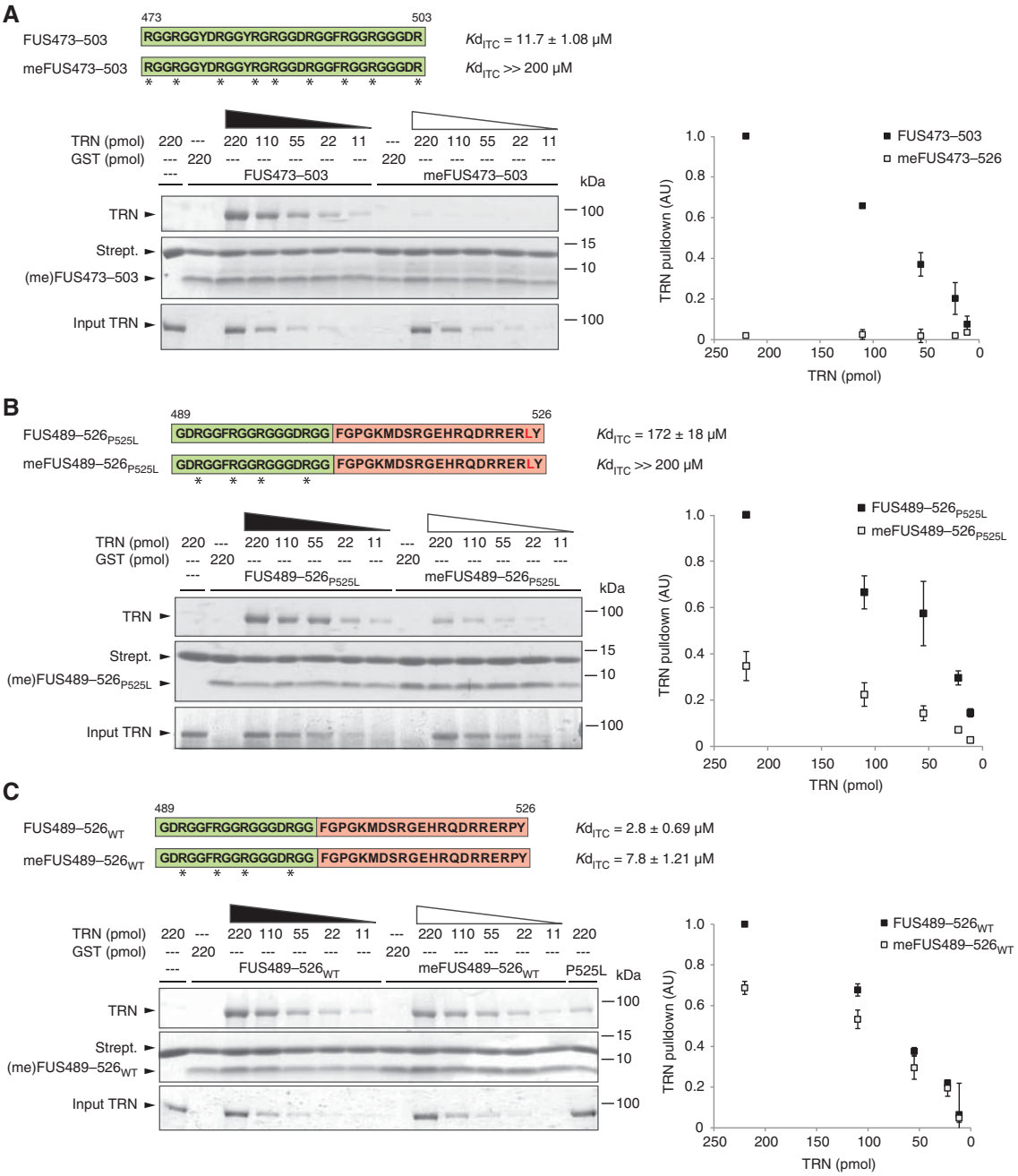

Figure 7 Arginine methylation in the RGG3 domain of FUS weakens TRN binding. *In vitro* pull-down assays with unmethylated and methylated (me) synthetic FUS peptides (see schematic diagrams for sequences, asterisks indicate asymmetric dimethyl groups) and recombinant TRN. Biotinylated peptides were immobilized on streptavidin beads and were incubated with the indicated amount of TRN–His_6 or His_6–GST as a control. Bound TRN was visualized by SDS–PAGE after Coomassie staining (upper panel). The middle panel shows the amount of streptavidin and peptide that was boiled off the streptavidin beads. Lower panel shows input of TRN. Plots on the right show a quantification of the TRN pulldown efficiency. The band with the highest intensity was set to 1.0 AU (arbitrary units) and relative intensities of other bands were calculated. Plots show means from two independent experiments, error bars indicate s.d. (**A**) The unmethylated RGG3 domain (FUS473–503) binds TRN in the absence of a PY-NLS and methylation abrogates this interaction. (**B**) Methylation strongly impairs TRN binding of the FUS489–526_{P525L} peptide. (**C**) Methylation slightly reduces TRN binding of the FUS489–526_{WT} peptide (~3-fold difference in Kd). Note that both FUS489–526_{WT} and meFUS489–526_{WT} bind TRN more tightly than FUS489–526_{P525L} (reference lane labelled 'P525L' on the right). Figure source data can be found with the Supplementary data.

FTLD-FUS subtypes were not labelled with the meFUS-specific antibody (Figure 9B), while a physiological nuclear staining was observed in all cases (Supplementary Figure S3B and C). Thus, in striking contrast to ALS-FUS, inclusions in FTLD-FUS appear to contain unmethylated FUS. This suggests hypomethylation of FUS (and potentially the other FET proteins) as a potential pathomechanism that might contribute to the co-deposition of FET proteins with TRN in FTLD-FUS.

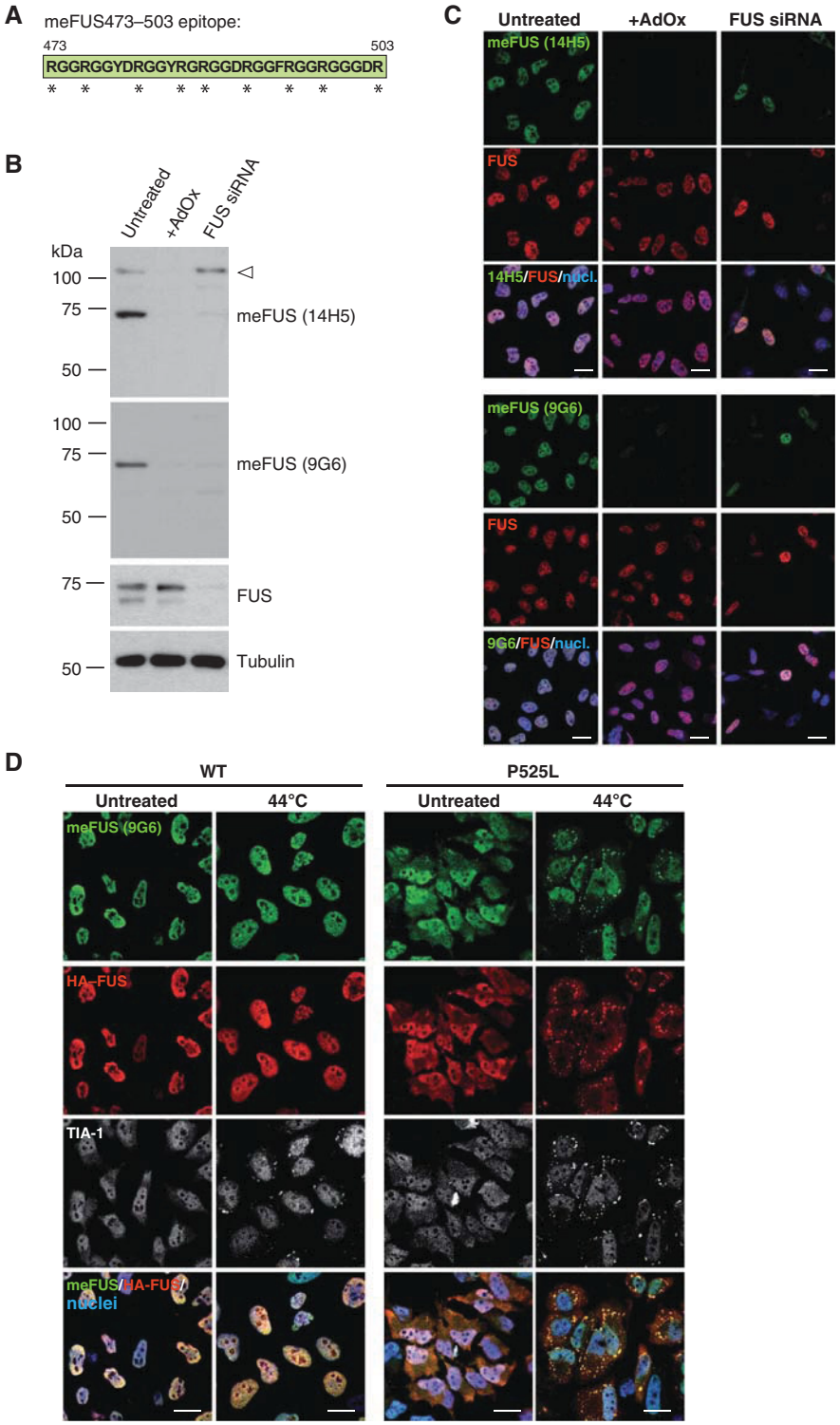

Figure 8 meFUS-specific monoclonal antibodies label ALS-associated FUS mutants in stress granules. (**A**) Schematic diagram of the peptide epitope (meFUS473–503) used for generation of meFUS-specific monoclonal antibodies. Asterisks denote asymmetric dimethyl groups. (**B**) Immunoblots show that monoclonal antibodies 14H5 and 9G6 are specific for methylated FUS, since staining is abrogated upon AdOx treatment and FUS knockdown. Open arrowhead indicates a non-specific methylated protein recognized by 14H5. Lower panels show FUS knockdown efficiency and Tubulin as a loading control. (**C**) Double-label immunocytochemistry of untransfected HeLa cells with meFUS-specific monoclonal antibodies 14H5 or 9G6 (green) and a polyclonal pan-FUS antibody (red). Both 14H5 and 9G6 specifically stain endogenous methylated FUS in the nuclei (blue). This staining is abrogated upon AdOx treatment and FUS knockdown. Scale bars: 20 μm. (**D**) HeLa cells stably expressing HA-tagged FUS-WT or HA–FUS-P525L were exposed to heat shock (44 °C) for 1 h prior to fixation or were kept at 37°C (untreated). Localization of methylated FUS was examined by confocal microscopy by co-labelling with a meFUS-specific antibody 9G6 (green), an HA-specific antibody (red), a TIA-1-specific antibody (white) and a nuclear counterstain (blue). Methylated FUS-P525L is recruited to TIA-1-positive stress granules after heat shock. Scale bars: 20 μm. Figure source data can be found with the Supplementary data.

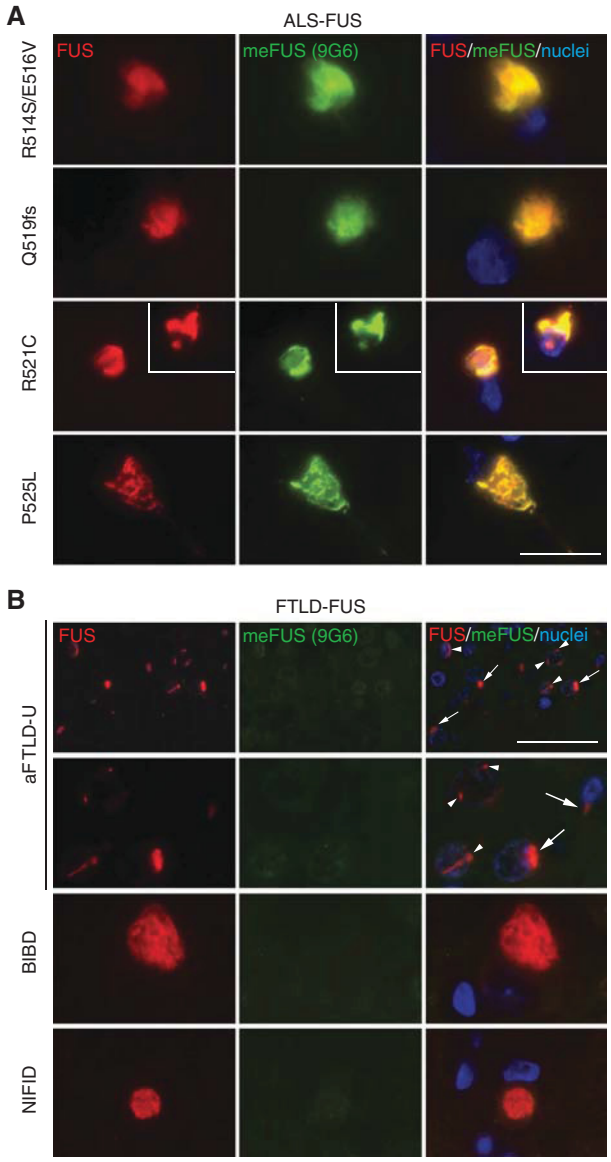

Figure 9 meFUS-specific monoclonal antibodies label FUS inclusions in ALS-FUS, but not in FTLD-FUS. (**A**) Double-label immunofluorescence of spinal cord sections from four ALS patients carrying different *FUS* mutations with a monoclonal antibody against meFUS (9G6, green), a polyclonal pan-FUS antibody (red) and nuclear counterstaining (blue). The characteristic FUS-positive neuronal cytoplasmic inclusions (rows 1–4) and glial inclusions (insert in row 3) in all ALS-FUS cases were intensely co-labelled by the meFUS-specific antibody. Scale bar: 20 μm. (**B**) Double-label immunofluorescence with a monoclonal antibody against meFUS (9G6, green), a polyclonal pan-FUS antibody (red) and nuclear counterstaining (blue) in the spectrum of FTLD-FUS, including aFTLD-U, BIBD and NIFID. In striking contrast to ALS-FUS, the meFUS-specific antibody did not label FUS-positive neuronal cytoplasmic inclusions (arrows in row 1 and 2) and neuronal intranuclear inclusions (arrowheads in row 1 and 2), as shown in dentate granule cells in aFTLD-U and the brainstem in BIBD and NIFID. Scale bar: 50 μm (row 1) or 20 μm (rows 2–4).

Discussion

By studying ALS-associated *FUS* mutations, we have uncovered a novel TRN-binding epitope, which is sensitive to arginine methylation. This broadens our perspective of TRN-cargo recognition, which classically has been thought to be determined by three modular, linear TRN-binding epitopes: (1) The PY of the C-terminal $R/K/H/X_{2-5}PY$ motif, (2) the basic residue of the $R/K/H/X_{2-5}PY$ motif and (3) an N-terminal hydrophobic or basic motif (Suel *et al*, 2008). Together, these three epitopes were described to constitute a signal of ~30 residues with intrinsic structural disorder and overall basic character (Lee *et al*, 2006; Suel *et al*, 2008). Based on these rules, Lee *et al* (2006) predicted a PY-NLS in the C-terminus of FUS and later on FUS residues 514–526 were shown to be necessary and sufficient for nuclear import in cultured cells and *in vivo* (Bosco *et al*, 2010; Dormann *et al*, 2010). Structural modelling of FUS residues 520–526 into the TRN-binding pocket showed that residues R522 and Y526 make strong H-bond interactions with TRN and that P525 allows a particular kinked geometry between P525 and Y526, leading to specific surface recognition of the two C-terminal residues by TRN (Dormann *et al*, 2010). Recently, the crystal structure of the FUS PY-NLS (residues 498–526) bound to TRN has been solved (Zhang and Chook, 2012). This revealed that the FUS PY-NLS consists of a C-terminal PY motif (1), an atypical arginine-rich polarized α-helix (2) and an N-terminal hydrophobic motif (3) (see schematic diagram in Figure 10A) and showed that residues mutated in ALS, for example, P525, make numerous contacts with TRN.

We studied longer recombinant FUS proteins ($FUS454–526_{WT}$ and $FUS454–526_{P525L}$) in complex with TRN and surprisingly found that the RGG repeat domain preceding the PY-NLS interacts tightly with TRN and is even able to rescue weak binding of the C-terminus in the P525L mutant (Figure 6D). Moreover, the RGG3 domain can even bind to TRN independently of the PY-NLS, with an affinity comparable to the PY-NLS itself ($Kd_{ITC} = 11.7$ μM for FUS473–503 versus 20 μM for $FUS504–526_{WT}$). This defines the RGG repeat region adjacent to the PY-NLS of FUS as a novel TRN-binding motif and extends the classical PY-NLS consensus sequence with a fourth binding epitope (Figure 10A). Thus, at least for certain cargo proteins such as the FET proteins, the TRN-binding site can be much larger than previously anticipated. Interestingly, TRN also binds multiple proteins without a PY-NLS, such as ribosomal proteins, histones, c-Fos, HIV-Rev and others (Chook and Suel, 2011), suggesting that TRN can recognize different classes of NLSs. Our data suggest that unmethylated RGG repeats might be such a signal. Supporting this idea, the RGG domain of a putative TRN substrate, Cold-inducible RNA-binding protein (CIRP), is required for nuclear import of CIRP and arginine methylation causes cytoplasmic accumulation of CIRP (Aoki *et al*, 2002).

Nevertheless, our data have shown that epitope 1 and 2 of the (mutant) PY-NLS of FUS are still required for TRN binding, since a FUSΔ514–526 deletion mutant failed to be imported under conditions of methylation inhibition (Figure 4B). This suggests that the C-terminal TRN-binding epitopes might anchor the protein for further interaction of the RGG repeats with the negatively charged surface in the interior of TRN. In line with this hypothesis, addition of either the WT or mutant PY-NLS to the unmethylated RGG3 domain led to high-affinity interactions below micromolar Kd (Figure 6D). Taken together, our data suggest a novel model of FUS-TRN recognition (Figure 10B), where epitopes 1–3 of the PY-NLS anchor the FUS C-terminus to TRN and the adjacent RGG repeats stabilize the interaction, presumably

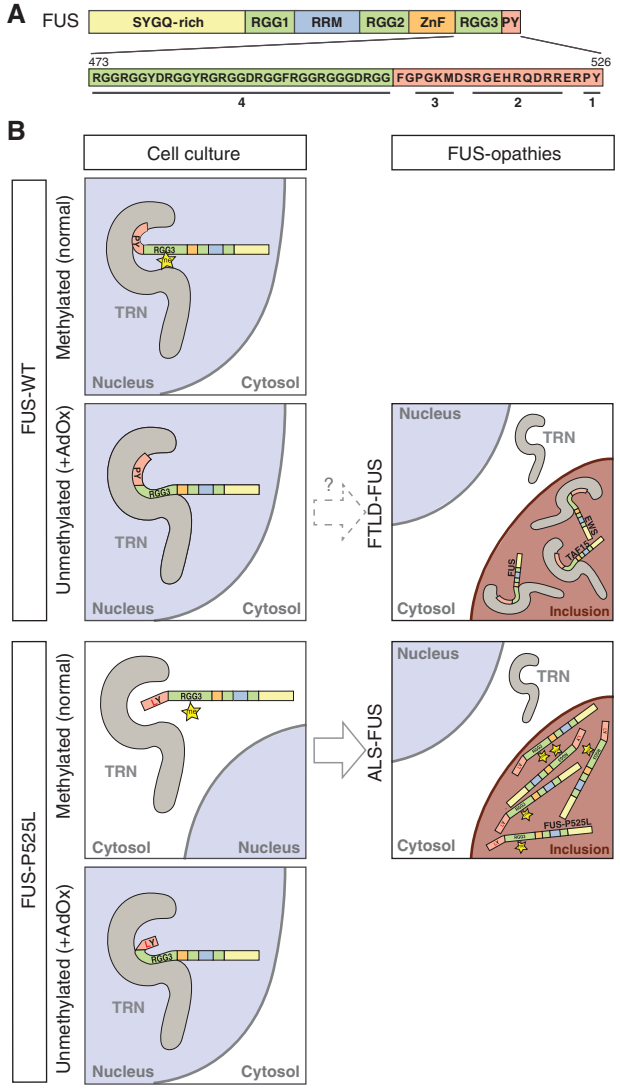

Figure 10 Model of the FUS–TRN interaction in cellular models and human FUSopathies. (**A**) Schematic diagram of FUS with sequences of the C-terminal PY-NLS (light red) and RGG3 domain (light green). Numbers indicate epitopes that contribute to TRN binding: 1 = C-terminal PY motif; 2 = central basic motif forming a polarized helix; 3 = N-terminal hydrophobic motif; 4 = RGG repeat region as a novel TRN-binding epitope. (**B**) Panels on the left show the interaction of methylated and unmethylated FUS-WT and FUS-P525L with TRN and the consequences for nuclear import in cultured cells. The PY-NLS of FUS is shown in light red and the RGG3 repeat region in light green. The yellow star denotes asymmetric dimethylation of the RGG3 domain. Panels on the right show the pathological situation in post mortem brains of FTLD-FUS and ALS-FUS patients. In FTLD-FUS, neuronal cytoplasmic inclusions contain all three FET proteins and TRN, but are not immunoreactive with meFUS-specific antibodies, suggesting that hypomethylation of the FET proteins and thus increased TRN binding may possibly be involved in the co-deposition of these proteins in FTLD-FUS. In contrast, ALS-FUS caused by *FUS* mutations is characterized by neuronal cytoplasmic inclusions that contain methylated FUS, but are negative for EWS, TAF15 and TRN. This suggests that the selective nuclear import defect of the FUS protein is caused by combination of a genetic defect (point mutation in TRN-binding epitopes 1–3) and post-translational modification (arginine methylation in TRN-binding epitope 4).

by interacting with the negatively charged surface in the interior of TRN. Methylation of the RGG repeats interferes strongly with TRN binding, probably due to changing hydrogen bonding and local hydrophobicity. In the methylated WT protein, the C-terminal epitopes nevertheless bind tightly enough to allow nuclear import, while in the methylated P525L mutant, weak binding of both epitopes 1 and 4 abrogates nuclear import, leading to cytoplasmic accumulation (Figure 10B).

It seems possible that other TRN substrates are modulated by arginine methylation in a similar fashion. Indeed, a recent study reported that arginine methylation of the nuclear poly(A) binding protein (PABPN1) weakens its interaction with TRN and that several nuclear proteins, including FUS, show increased TRN binding in PRMT1 knockout cells (Fronz *et al*, 2011). PABPN1 is methylated on key residues within the PY-NLS, such as the N-terminal basic cluster and the C-terminal RX_6PY motif (Smith *et al*, 1999; Lee *et al*, 2006), suggesting that in the case of PABPN1 arginine methylation within epitopes 2 and 3 of the PY-NLS might interfere with TRN binding. In contrast, FUS and the other FET proteins are methylated exclusively on arginine residues in epitope 4 (Belyanskaya *et al*, 2001; Rappsilber *et al*, 2003; Ong *et al*, 2004; Pahlich *et al*, 2005; Jobert *et al*, 2009) and our analysis has shown that arginine methylation within the RGG3 domain and not in other epitopes of the PY-NLS modulates TRN binding (Figure 5). Beyond the FET family proteins, several confirmed or predicted PY-NLS-containing proteins (Lee *et al*, 2006) contain methylated RGG motifs within the vicinity of the PY-NLS. Whether TRN-dependent nuclear import of these proteins is regulated by arginine methylation in a similar fashion remains to be shown.

Although ALS-FUS and FTLD-FUS have an overlapping clinical phenotype and neuropathology, the pathological inclusions in these two disorders were recently found to have a significantly different protein composition: Inclusions in ALS-FUS contain only the FUS protein, while inclusions in FTLD-FUS show a co-deposition of all FET proteins (FUS, EWS, and TAF15) and TRN (Brelstaff *et al*, 2011; Neumann *et al*, 2011, 2012; Davidson *et al*, 2012) (Figure 10B). Our study has revealed additional striking differences in the neuropathology of ALS-FUS and FTLD-FUS (Figure 9), further supporting the idea that the two disorders are caused by different pathomechanisms (Mackenzie and Neumann, 2012; Rademakers *et al*, 2012). In ALS-FUS, pathological inclusions contain methylated FUS, in line with the severe nuclear import defect observed for methylated FUS mutants in our cellular models (Figure 10B). Thus, arginine methylation seems to be required for the pathological mislocalization of ALS-associated FUS mutants and it is tempting to speculate that differences in arginine methylation might determine the age of disease onset, which can vary substantially between patients with the same point mutation (Kwiatkowski *et al*, 2009; Rademakers *et al*, 2010; Yan *et al*, 2010). Accordingly, we propose that ALS-FUS is a dominantly inherited human disease that might be modulated by a post-translational modification.

In contrast to ALS-FUS, which seems to be restricted to a dysfunction of FUS, FTLD-FUS appears to involve a more general defect in TRN-mediated nuclear import (Dormann and Haass, 2011; Mackenzie and Neumann, 2012; Rademakers *et al*, 2012). However, a general dysfunction or reduced expression of TRN seems unlikely, since none of 13 additional TRN cargo proteins investigated (e.g., heterogenous ribonucleoprotein A1, Sam68 and PABPN1) co-accumulate

with the FET proteins and TRN in FTLD-FUS (Neumann *et al*, 2012). Our data suggest that instead, defective arginine methylation of the FET proteins selectively alters their TRN-binding affinity (Figure 10B). Such hypomethylation of the FET proteins may lead to enhanced binding of the FET proteins to TRN and may hamper dissociation of FET–TRN transport complexes. Even though differences in TRN-binding affinity of methylated versus unmethylated FUS-WT may be small, it seems possible that over long periods of time, a slight increase in FET–TRN binding may lead to a co-deposition of FET proteins and TRN in cytoplasmic and nuclear inclusions in this late-onset neurodegenerative disease. It is also interesting to note that arginine methylation can affect protein aggregation, and in all reported cases hypomethylation favoured protein oligomerization/aggregation (Yu *et al*, 2004; Ostareck-Lederer *et al*, 2006; Perreault *et al*, 2007). Thus, hypomethylation might contribute to the pathological deposition of the FET proteins by affecting both their nuclear import and their aggregation behaviour.

What remains to be answered is how and why hypomethylation of the FET proteins might arise. The fact that PABPN1, which also binds to TRN with higher affinity in PRMT1 knockout cells (Fronz *et al*, 2011), is not co-deposited with FET proteins and TRN in FTLD-FUS (Neumann *et al*, 2012) argues against a general defect in arginine methylation and rather points to a selective hypomethylation of FET proteins. The question why hypomethylation of FET proteins might arise in FTLD-FUS brings up a related question, namely what is the physiological role of FET protein methylation in the first place? It can be speculated that arginine methylation of FET proteins reduces their affinity for TRN to a degree that allows for efficient dissociation of the import complex by RanGTP in the nucleus. Overly tight binding of hypomethylated FET proteins to TRN might hamper their dissociation from TRN in the nucleus, leading to re-export of FET–TRN complexes and ultimately to a reduction of FET proteins in the nucleus and co-deposition of FET and TRN in the cytoplasm (Figure 10B). Alternatively, it can be envisaged that arginine methylation of FET proteins is a fine-tuning mechanism to ensure that small amounts of newly synthesized FET proteins stay behind in the cytoplasm to fulfil important cytosolic functions. This would be in agreement with the findings that small amounts of cytosolic FUS are present in human and mouse brain (Neumann *et al*, 2009a; Aoki *et al*, 2012) and that FUS seems to play a role in mRNA transport to dendritic spines (Fujii and Takumi, 2005; Fujii *et al*, 2005; Liu-Yesucevitz *et al*, 2011). Additionally, FUS has been identified at focal adhesions and was shown to function in cell spreading (de Hoog *et al*, 2004). Finally, it cannot be excluded that arginine methylation regulates additional features of FET proteins, such as RNA binding or additional protein–protein interactions. The physiological role of arginine methylation of FET proteins and the mechanism behind a potential hypomethylation in FTLD-FUS certainly warrant further studies.

Materials and methods

Cell culture, transfection, inhibitor and stress treatment

Human cervical carcinoma cells (HeLa) were cultured and transfected as described previously (Dormann *et al*, 2010). HeLa cells stably expressing HA–FUS-WT or HA–FUS-P525L were generated by lentiviral transduction as described in Kuhn *et al* (2010), followed by selection with 0.5 μg/ml puromycin (Sigma). Hippocampal neurons were isolated from embryonic day 18 rats as described previously (Kaech and Banker, 2006). Neurons were plated at densities of 18 000 cells/cm^2 in 6 cm tissue culture dishes containing poly-L-lysine (1 mg/ml; Sigma-Aldrich)-coated glass coverslips and Neurobasal medium supplemented with 2% B27 and 0.5 mM glutamine (all from Invitrogen). On day *in vitro* (DIV) 7, cultured neurons were transfected with HA–FUS constructs using Lipofectamine 2000 (Invitrogen). YFP was co-transfected as a marker to visualize neuronal morphology. For all transient transfections, cells were analysed 24 h post-transfection. AdOx (Sigma) was dissolved in water and was used at a concentration of 20 μM (HeLa) or 10 μM (neurons) and was added to cells upon plating (HeLa) or DIV 7 (neurons) 9 h prior to transfection. Heat shock was performed by incubating cells for 1 h in a tissue culture incubator heated to 44°C.

Antibodies

A list of all commercially available antibodies used can be found in the Supplementary data. Rat monoclonal antibodies against an ovalbumin-conjugated meFUS473–503 peptide epitope were generated at the Institute of Molecular Immunology, Helmholtz Center Munich by standard procedures.

cDNA constructs and primers

All HA-tagged FUS, EWS and TAF15 constructs used for transient transfections were in pcDNA3.1/Hygro(−) (Invitrogen) and all GFP and GST–GFP constructs were in pEGFP–C1 (Clontech). Lentiviral HA–FUS constructs used for generation of stable HeLa cell lines were in pCDH-Ef1-MCS-IRES-Puro (System Biosciences). The cDNA encoding full-length human TRN with a C-terminal His_6-tag was in a pQE-60 vector (pQE-60-TRN–His_6) and was a generous gift of Dirk Görlich. The cDNA encoding His_6-tagged FUS454–526 (WT or P525L) was in a petM11-ZZ–His_6 vector. Details on cloning of mutant constructs can be found in the Supplementary data (Rydzanicz *et al*, 2005).

Recombinant proteins and synthetic peptides

Details on expression and purification of recombinant proteins can be found in the Supplementary data. Synthetic peptides (FUS473–503, meFUS473–503, FUS489–526$_{WT}$ and meFUS489–526$_{WT}$, FUS489–526$_{P525L}$, meFUS489–526$_{P525L}$, FUS504–526$_{WT}$ and FUS504–526$_{P525L}$) were synthesized and HPLC-purified by Peptide Specialty Laboratories GmbH, Heidelberg, Germany and were dissolved in TRN-binding buffer (20 mM sodium phosphate buffer, pH 6.8, 50 mM NaCl, 1 mM EDTA, 1 mM DTT).

Immunocytochemistry

Immunocytochemistry on HeLa cells was performed as described in Dormann *et al* (2010). Hippocampal neurons were fixed with 4% paraformaldehyde, quenched in 50 mM ammonium chloride for 10 min and permeabilized with 0.1% Triton X-100 for 3 min. After blocking with 2% fetal bovine serum (Invitrogen), 2% bovine serum albumin (Sigma-Aldrich) and 0.2% fish gelatin (Sigma-Aldrich) dissolved in phosphate-buffered saline, neurons were incubated with respective primary and secondary antibodies diluted in 10% blocking solution. DAPI (Invitrogen) was used as a nuclear counterstain.

Immunohistochemistry and immunofluorescence on human post mortem tissue

Immunohistochemistry conditions for meFUS antibodies were optimized using a tissue microarray that included formalin-fixed, paraffin-embedded biopsy material from a glioblastoma and a brain metastasis from a colon carcinoma as well as post mortem tissue from hippocampus and temporal cortex of three controls with no history of neurological disease. Studied FUS-opathy cases with robust pathology in selected neuroanatomical regions included aFTLD-U ($n=3$), BIBD ($n=1$), NIFID ($n=1$) and four ALS-FUS cases with three different missense and one truncation mutation, described in detail in previous studies (Neumann *et al*, 2011). Immunohistochemistry was performed on 5 μm thick paraffin sections using the NovoLinkTM Polymer Detection Kit and developed with 3,3′-diaminobenzidine. For double-label immunofluorescence, the secondary antibodies Alexa Fluor 594 and Alexa Fluor 488-conjugated anti-rabbit and anti-rat IgG (Invitrogen, 1:500) were used with Hoechst 33 342 (Sigma) for

nuclear counterstaining. Incubation with primary antibodies meFUS 9G6 (dilution 1:30) and anti-FUS HPA008784 (Sigma, 1:1000) was performed for 1 h at room temperature following microwave antigen retrieval.

Fluorescence image acquisition

Two or three-colour confocal images of HeLa cells were obtained with an inverted laser scanning confocal microscope (Zeiss LSM510) with a $\times 63/1.4$ oil immersion lens, using a pinhole diameter of 1 Airy unit. An image series along the z axis was taken and projected into a single image using the maximal projection tool of the LSM 510 software (Zeiss). Four-colour confocal images of HeLa cells were taken with an inverted laser scanning confocal microscope (Zeiss LSM710) with a $\times 40/1.4$ oil immersion lens. Using the Zen 2011 software (Zeiss), single confocal images were taken in the plane of the largest cytosolic area. For neurons, images were acquired with a wide-field fluorescence microscope (Axio Imager A2 inverted microscope and AxioVision software, both from Zeiss). For human post mortem tissue, immunofluorescence images were obtained by wide-field fluorescence microscopy (BX61 Olympus with digital camera F-view, Olympus). If necessary for printing, brightness and contrast were linearly enhanced using Adobe Photoshop's Level tool. Images and quantification shown are from one experiment, but are representative of at least three independent experiments.

Image quantification and statistics

Nuclear and cytosolic localization was quantified with the LSM 510 colocalization tool as follows: Total fluorescence intensities of the green channel were calculated from the mean fluorescence intensity (MFI) and the number of pixels. Pixels that were colocalized with the nuclear counterstain were considered 'nuclear' and pixels that did not overlap with the nuclear counterstain were considered 'cytosolic'. Typically 30–50 randomly selected cells (n) were analysed and mean values ± s.d. across n cells were calculated. Statistical analysis was carried out using the one-way ANOVA test with a Tukey post test. Images and quantification shown are from one experiment, but are representative of at least three independent experiments. For quantification of HA–FUS localization in neurons, 300 randomly selected cells per experiment ($n = 3$) were scored for cytoplasmic mislocalization of transfected HA–FUS constructs and the percentage of cells with mislocalized FUS ± s.d. were calculated. Statistical analysis was carried out using the unpaired two-tailed t-test.

siRNA-mediated knockdown

PRMT1 knockdown was achieved using two different PRMT1-specific siRNAs from Qiagen (Hs_HRMT1L2_7 and Hs_HRMT1L2_8). Negative control siRNA (Cat. No. 1022076, Qiagen) was used as a control. FUS knockdown was achieved using the ON-TARGET plus SMARTpool L-009497 from Dharmacon. Cells were reverse transfected using 20 pmol siRNA and 5 µl Lipofectamine 2000 (Invitrogen) per six-well. Medium was changed 4–6 h post-transfection and effect of knockdown was analysed 48 h (FUS knockdown) or 72 h (PRMT1 knockdown) post-transfection.

Cell lysates and immunoblotting

Total cell lysates were prepared in ice-cold RIPA buffer freshly supplemented with Complete Protease Inhibitor Cocktail (Roche). Lysates were sonicated (Bioruptor from Diagenode) and protein concentration was determined by BCA protein assay (Pierce). In all, 4 × SDS–PAGE sample buffer was added and samples were boiled for 5 min. Proteins were separated by SDS–PAGE, transferred onto a PVDF membrane (Immobilon-P, Millipore) and analysed by immunoblotting using the indicated antibodies. Bound antibodies were detected with the chemiluminescence detection reagents ECL or ECL prime (both from Amersham) or Immobilon (Millipore).

In vitro pulldown assay

N-terminally biotinylated peptides were immobilized on streptavidin sepharose beads (GE Healthcare, 440 pmol peptide/5 µl beads) and were blocked in wash buffer (20 mM sodium phosphate buffer pH 7.4, 150 mM KCl, 0.5 mM EDTA, 5 mM $MgCl_2$, 10% glycerol, 1 mM DTT) supplemented with 0.5 mg/ml BSA. In all, 5 µl peptide-loaded beads were incubated with the indicated amounts of recombinant TRN–His_6 or His_6–GST in 500 µl of the same buffer for 1–3 h at 4°C. Beads were washed three times in wash buffer and boiled for 3 min in 2 × SDS–PAGE sample buffer. Eluted proteins were separated by SDS–PAGE (10–20%) and visualized by staining with GelCode Blue Stain Reagent (Thermo Scientific). Band intensities were quantified using the MultiGaugeV3.0 programme. After background subtraction, the band with the highest pixel number was set to 1.0 AU (arbitrary units).

Isothermal titration calorimetry

Binding affinities of FUS peptides and recombinant proteins to TRN were determined using ITC on a VP-ITC Microcal calorimeter (Microcal, Northhampton, USA) at 25°C or 10°C (FUS473–503; due to entropy–enthalpy compensation at 25°C) with 35 rounds of 12 µl injections. All proteins/peptides were dialyzed or dissolved in TRN-binding buffer. The ITC data were analysed with the program MicroCal Origin software version 7.0 and single site binding model.

NMR experiments

Samples for NMR measurements contained 0.008–0.012 mM protein in TRN-binding buffer with 10% ^2H_2O added for the lock signal. For the TRN bound measurements, ^{15}N isotope labelled FUS454–526_{WT} and FUS454–526_{P525L} were titrated with increasing amounts of unlabelled TRN to stoichiometric ratios (FUS:TRN) of 1:0.1, 1:0.3, 1:0.5, 1:0.7, 1:1 and 1:2.6. Spectral changes were monitored by 1D ^1H and 2D ^1H,^{15}N HSQC spectra in each step of the titration. For the FUS peptide bound measurements, unlabelled TRN was titrated with increasing amounts of FUS peptides (FUS473–503, meFUS473–503, FUS489–526_{P525L}, meFUS489–$526_{P525L,}$ FUS489–526_{WT}, meFUS489–526_{WT}) to stoichiometric ratios (TRN:FUS) of 1:0.25, 1:0.5, 1:1. Spectral changes were monitored by 1D ^1H spectra in each step of the titration. Details on NMR spectra recording and processing can be found in the Supplementary data.

Supplementary data

Supplementary data are available at *The EMBO Journal* Online (http://www.embojournal.org).

Acknowledgements

We thank Dirk Görlich for generous gifts of plasmids, Sven Lammich for providing human brain cDNA, Julia Strathmann for help with statistics, Harald Steiner for reagents, Sebastian Hogl and Stefan Lichtenthaler for purified His_6–GST. We thank Rita Kemkes, Brigitte Nuscher, Andrea Seibel and Stephanie Kunath for technical assistance. We are grateful to Peter Macheroux and Silvia Wallner for access to the ITC instrument and technical assistance and to Maria Funke and Konstanze Winklhofer for lentiviral vectors and virus production protocols. We thank Anja Capell, Dieter Edbauer, Bettina Schmid and Harald Steiner for critically reading the manuscript and helpful discussion. This work was supported by the Sonderforschungsbereich Molecular Mechanisms of Neurodegeneration (SFB 596, CH and EK), the Competence Network for Neurodegenerative Diseases (KNDD) of the Bundesministerium für Bildung und Forschung (BMBF, CH and MN) and the Swiss National Science Foundation (31003A-132864, MN). DD was supported by the Robert Bosch Foundation. TM was supported by the Austrian Academy of Sciences (APART-fellowship), the Bavarian Ministry of Sciences, Research and the Arts in the framework of the Bavarian Molecular Biosystems Research Network and the German Research Foundation (DFG, Emmy Noether program MA 5703/1-1). EB was supported by the Elite Network of Bavaria. OA was supported by the NIHR Oxford Biomedical Research Centre. IM was funded by the Canadian Institutes of Health Research Grants 179009 and 74580 and the Pacific Alzheimer's Research Foundation centre Grant C06-01. CH was supported by a 'Forschungsprofessur' of the Ludwig-Maximilians University. We thank the Hans and Ilse Breuer Foundation for the Confocal Microscope.

Author contributions: DD cloned most constructs, performed and analysed most cell culture experiments, purified recombinant FUS proteins, performed *in vitro* pulldown assays and characterized meFUS-specific antibodies. TM purified recombinant TRN and performed and analysed NMR and ITC experiments. CV and MN characterized meFUS-specific antibodies on human tissue and

performed the immunohistochemistry and immunofluorescence analysis on human brain tissue. EB generated stable HeLa cell lines, cloned EWS and TAF15 constructs and analysed FET protein localization upon AdOx treatment. ST performed experiments with primary neuronal cultures. CA provided technical assistance and screened monoclonal antibodies. EK generated meFUS-specific monoclonal antibodies. OA and IM provided human post mortem material from FTLD-FUS and ALS-FUS cases and were involved in the interpretation of data. DD and CH designed and supervised the project and DD wrote the manuscript with input from all authors. CH applied for and obtained a grant from an anonymous foundation for this project.

Conflict of interest

The authors declare that they have no conflict of interest.

References

Aoki K, Ishii Y, Matsumoto K, Tsujimoto M (2002) Methylation of Xenopus CIRP2 regulates its arginine- and glycine-rich region-mediated nucleocytoplasmic distribution. *Nucleic Acids Res* **30:** 5182–5192

Aoki N, Higashi S, Kawakami I, Kobayashi Z, Hosokawa M, Katsuse O, Togo T, Hirayasu Y, Akiyama H (2012) Localization of fused in sarcoma (FUS) protein to the post-synaptic density in the brain. *Acta Neuropathol* **124:** 383–394

Araya N, Hiraga H, Kako K, Arao Y, Kato S, Fukamizu A (2005) Transcriptional down-regulation through nuclear exclusion of EWS methylated by PRMT1. *Biochem Biophys Res Commun* **329:** 653–660

Bartel RL, Borchardt RT (1984) Effects of adenosine dialdehyde on S-adenosylhomocysteine hydrolase and S-adenosylmethionine-dependent transmethylations in mouse L929 cells. *Mol Pharmacol* **25:** 418–424

Baumer D, Hilton D, Paine SM, Turner MR, Lowe J, Talbot K, Ansorge O (2010) Juvenile ALS with basophilic inclusions is a FUS proteinopathy with FUS mutations. *Neurology* **75:** 611–618

Bedford MT, Clarke SG (2009) Protein arginine methylation in mammals: who, what, and why. *Mol Cell* **33:** 1–13

Belyanskaya LL, Gehrig PM, Gehring H (2001) Exposure on cell surface and extensive arginine methylation of ewing sarcoma (EWS) protein. *J Biol Chem* **276:** 18681–18687

Bentmann E, Neumann M, Tahirovic S, Rodde R, Dormann D, Haass C (2012) Requirements for stress granule recruitment of fused in sarcoma (FUS) and TAR DNA-binding protein of 43 kDa (TDP-43). *J Biol Chem* **287:** 23079–23094

Blair IP, Williams KL, Warraich ST, Durnall JC, Thoeng AD, Manavis J, Blumbergs PC, Vucic S, Kiernan MC, Nicholson GA (2010) FUS mutations in amyotrophic lateral sclerosis: clinical, pathological, neurophysiological and genetic analysis. *J Neurol Neurosurg Psychiatry* **81:** 639–645

Bosco DA, Lemay N, Ko HK, Zhou H, Burke C, Kwiatkowski Jr TJ, Sapp P, McKenna-Yasek D, Brown Jr. RH, Hayward LJ (2010) Mutant FUS proteins that cause amyotrophic lateral sclerosis incorporate into stress granules. *Hum Mol Genet* **19:** 4160–4175

Brelstaff J, Lashley T, Holton JL, Lees AJ, Rossor MN, Bandopadhyay R, Revesz T (2011) Transportin1: a marker of FTLD-FUS. *Acta Neuropathol* **122:** 591–600

Butler JS, Zurita-Lopez CI, Clarke SG, Bedford MT, Dent SY (2011) Protein-arginine methyltransferase 1 (PRMT1) methylates Ash2L, a shared component of mammalian histone H3K4 methyltransferase complexes. *J Biol Chem* **286:** 12234–12244

Cansizoglu AE, Lee BJ, Zhang ZC, Fontoura BM, Chook YM (2007) Structure-based design of a pathway-specific nuclear import inhibitor. *Nat Struct Mol Biol* **14:** 452–454

Chen DH, Wu KT, Hung CJ, Hsieh M, Li C (2004) Effects of adenosine dialdehyde treatment on in vitro and in vivo stable protein methylation in HeLa cells. *J Biochem* **136:** 371–376

Chio A, Restagno G, Brunetti M, Ossola I, Calvo A, Mora G, Sabatelli M, Monsurro MR, Battistini S, Mandrioli J, Salvi F, Spataro R, Schymick J, Traynor BJ, La Bella V (2009) Two Italian kindreds with familial amyotrophic lateral sclerosis due to FUS mutation. *Neurobiol Aging* **30:** 1272–1275

Chook YM, Suel KE (2011) Nuclear import by karyopherin-betas: recognition and inhibition. *Biochim Biophys Acta* **1813:** 1593–1606

Da Cruz S, Cleveland DW (2011) Understanding the role of TDP-43 and FUS/TLS in ALS and beyond. *Curr Opin Neurobiol* **21:** 904–919

Davidson YS, Robinson AC, Hu Q, Mishra M, Baborie A, Jaros E, Perry RH, Cairns NJ, Richardson A, Gerhard A, Neary D, Snowden JS, Bigio EH, Mann DM (2012) Nuclear carrier and RNA binding proteins in frontotemporal lobar degeneration associated with fused in sarcoma (FUS) pathological changes. *Neuropathol Appl Neurobiol* doi:10.1111/j.1365-2990.2012.01274.x

de Hoog CL, Foster LJ, Mann M (2004) RNA and RNA binding proteins participate in early stages of cell spreading through spreading initiation centers. *Cell* **117:** 649–662

DeJesus-Hernandez M, Kocerha J, Finch N, Crook R, Baker M, Desaro P, Johnston A, Rutherford N, Wojtas A, Kennelly K, Wszolek ZK, Graff-Radford N, Boylan K, Rademakers R (2010) De novo truncating FUS gene mutation as a cause of sporadic amyotrophic lateral sclerosis. *Hum Mutat* **31:** E1377–E1389

Dormann D, Haass C (2011) TDP-43 and FUS: a nuclear affair. *Trends Neurosci* **34:** 339–348

Dormann D, Rodde R, Edbauer D, Bentmann E, Fischer I, Hruscha A, Than ME, Mackenzie IR, Capell A, Schmid B, Neumann M, Haass C (2010) ALS-associated fused in sarcoma (FUS) mutations disrupt Transportin-mediated nuclear import. *EMBO J* **29:** 2841–2857

Du K, Arai S, Kawamura T, Matsushita A, Kurokawa R (2011) TLS and PRMT1 synergistically coactivate transcription at the survivin promoter through TLS arginine methylation. *Biochem Biophys Res Commun* **404:** 991–996

Fronz K, Guttinger S, Burkert K, Kuhn U, Stohr N, Schierhorn A, Wahle E (2011) Arginine methylation of the nuclear poly(a) binding protein weakens the interaction with its nuclear import receptor, transportin. *J Biol Chem* **286:** 32986–32994

Fujii R, Okabe S, Urushido T, Inoue K, Yoshimura A, Tachibana T, Nishikawa T, Hicks GG, Takumi T (2005) The RNA binding protein TLS is translocated to dendritic spines by mGluR5 activation and regulates spine morphology. *Curr Biol* **15:** 587–593

Fujii R, Takumi T (2005) TLS facilitates transport of mRNA encoding an actin-stabilizing protein to dendritic spines. *J Cell Sci* **118:** 5755–5765

Fujita K, Ito H, Nakano S, Kinoshita Y, Wate R, Kusaka H (2008) Immunohistochemical identification of messenger RNA-related proteins in basophilic inclusions of adult-onset atypical motor neuron disease. *Acta Neuropathol* **116:** 439–445

Gal J, Zhang J, Kwinter DM, Zhai J, Jia H, Jia J, Zhu H (2011) Nuclear localization sequence of FUS and induction of stress granules by ALS mutants. *Neurobiol Aging* **32:** e2327–e2340

Groen EJ, van Es MA, van Vught PW, Spliet WG, van Engelen-Lee J, de Visser M, Wokke JH, Schelhaas HJ, Ophoff RA, Fumoto K, Pasterkamp RJ, Dooijes D, Cuppen E, Veldink JH, van den Berg LH (2010) FUS mutations in familial amyotrophic lateral sclerosis in the Netherlands. *Arch Neurol* **67:** 224–230

Hewitt C, Kirby J, Highley JR, Hartley JA, Hibberd R, Hollinger HC, Williams TL, Ince PG, McDermott CJ, Shaw PJ (2010) Novel FUS/TLS mutations and pathology in familial and sporadic amyotrophic lateral sclerosis. *Arch Neurol* **67:** 455–461

Hung CJ, Lee YJ, Chen DH, Li C (2009) Proteomic analysis of methylarginine-containing proteins in HeLa cells by two-dimensional gel electrophoresis and immunoblotting with a methylarginine-specific antibody. *Protein J* **28:** 139–147

Ito D, Seki M, Tsunoda Y, Uchiyama H, Suzuki N (2011) Nuclear transport impairment of amyotrophic lateral sclerosis-linked mutations in FUS/TLS. *Ann Neurol* **69:** 152–162

Jobert L, Argentini M, Tora L (2009) PRMT1 mediated methylation of TAF15 is required for its positive gene regulatory function. *Exp Cell Res* **315:** 1273–1286

Kaech S, Banker G (2006) Culturing hippocampal neurons. *Nat Protoc* **1:** 2406–2415

Kiernan MC, Vucic S, Cheah BC, Turner MR, Eisen A, Hardiman O, Burrell JR, Zoing MC (2011) Amyotrophic lateral sclerosis. *Lancet* **377:** 942–955

Kino Y, Washizu C, Aquilanti E, Okuno M, Kurosawa M, Yamada M, Doi H, Nukina N (2010) Intracellular localization and splicing regulation of FUS/TLS are variably affected by amyotrophic lateral sclerosis-linked mutations. *Nucleic Acids Res* **39:** 2781–2798

Kosugi S, Hasebe M, Entani T, Takayama S, Tomita M, Yanagawa H (2008) Design of peptide inhibitors for the importin alpha/beta nuclear import pathway by activity-based profiling. *Chem Biol* **15:** 940–949

Kuhn PH, Wang H, Dislich B, Colombo A, Zeitschel U, Ellwart JW, Kremmer E, Rossner S, Lichtenthaler SF (2010) ADAM10 is the physiologically relevant, constitutive alpha-secretase of the amyloid precursor protein in primary neurons. *EMBO J* **29:** 3020–3032

Kwiatkowski Jr TJ, Bosco DA, Leclerc AL, Tamrazian E, Vanderburg CR, Russ C, Davis A, Gilchrist J, Kasarskis EJ, Munsat T, Valdmanis P, Rouleau GA, Hosler BA, Cortelli P, de Jong PJ, Yoshinaga Y, Haines JL, Pericak-Vance MA, Yan J, Ticozzi N *et al* (2009) Mutations in the FUS/TLS gene on chromosome 16 cause familial amyotrophic lateral sclerosis. *Science* **323:** 1205–1208

Lagier-Tourenne C, Polymenidou M, Cleveland DW (2010) TDP-43 and FUS/TLS: emerging roles in RNA processing and neurodegeneration. *Hum Mol Genet* **19:** R46–R64

Lee BJ, Cansizoglu AE, Suel KE, Louis TH, Zhang Z, Chook YM (2006) Rules for nuclear localization sequence recognition by karyopherin beta 2. *Cell* **126:** 543–558

Lee J, Bedford MT (2002) PABP1 identified as an arginine methyltransferase substrate using high-density protein arrays. *EMBO Rep* **3:** 268–273

Liteplo RG, Kerbel RS (1986) Periodate-oxidized adenosine induction of murine thymidine kinase: role of DNA methylation in the generation of tumor cell heterogeneity. *Cancer Res* **46:** 577–582

Liu-Yesucevitz L, Bassell GJ, Gitler AD, Hart AC, Klann E, Richter JD, Warren ST, Wolozin B (2011) Local RNA translation at the synapse and in disease. *J Neurosci* **31:** 16086–16093

Lomen-Hoerth C, Anderson T, Miller B (2002) The overlap of amyotrophic lateral sclerosis and frontotemporal dementia. *Neurology* **59:** 1077–1079

Mackenzie IR, Ansorge O, Strong M, Bilbao J, Zinman L, Ang LC, Baker M, Stewart H, Eisen A, Rademakers R, Neumann M (2011) Pathological heterogeneity in amyotrophic lateral sclerosis with FUS mutations: two distinct patterns correlating with disease severity and mutation. *Acta Neuropathol* **122:** 87–98

Mackenzie IR, Neumann M (2012) FET proteins in frontotemporal dementia and amyotrophic lateral sclerosis. *Brain Res* **1462:** 40–43

Mackenzie IR, Neumann M, Bigio EH, Cairns NJ, Alafuzoff I, Kril J, Kovacs GG, Ghetti B, Halliday G, Holm IE, Ince PG, Kamphorst W, Revesz T, Rozemuller AJ, Kumar-Singh S, Akiyama H, Baborie A, Spina S, Dickson DW, Trojanowski JQ *et al* (2010a) Nomenclature and nosology for neuropathologic subtypes of frontotemporal lobar degeneration: an update. *Acta Neuropathol* **119:** 1–4

Mackenzie IR, Rademakers R, Neumann M (2010b) TDP-43 and FUS in amyotrophic lateral sclerosis and frontotemporal dementia. *Lancet Neurol* **9:** 995–1007

Murphy JM, Henry RG, Langmore S, Kramer JH, Miller BL, Lomen-Hoerth C (2007) Continuum of frontal lobe impairment in amyotrophic lateral sclerosis. *Arch Neurol* **64:** 530–534

Neumann M, Bentmann E, Dormann D, Jawaid A, DeJesus-Hernandez M, Ansorge O, Roeber S, Kretzschmar HA, Munoz DG, Kusaka H, Yokota O, Ang LC, Bilbao J, Rademakers R, Haass C, Mackenzie IR (2011) FET proteins TAF15 and EWS are selective markers that distinguish FTLD with FUS pathology from amyotrophic lateral sclerosis with FUS mutations. *Brain* **134:** 2595–2609

Neumann M, Rademakers R, Roeber S, Baker M, Kretzschmar HA, Mackenzie IR (2009a) A new subtype of frontotemporal lobar degeneration with FUS pathology. *Brain* **132:** 2922–2931

Neumann M, Roeber S, Kretzschmar HA, Rademakers R, Baker M, Mackenzie IR (2009b) Abundant FUS-immunoreactive pathology in neuronal intermediate filament inclusion disease. *Acta Neuropathol* **118:** 605–616

Neumann M, Valori CF, Ansorge O, Kretzschmar HA, Munoz DG, Kusaka H, Yokota O, Ishihara K, Ang LC, Bilbao JM, Mackenzie IR (2012) Transportin 1 accumulates specifically with FET proteins but no other transportin cargos in FTLD-FUS and is absent in FUS inclusions in ALS with FUS mutations. *Acta Neuropathol* doi:10.1007/s00401-012-1020-6

Ong SE, Mittler G, Mann M (2004) Identifying and quantifying in vivo methylation sites by heavy methyl SILAC. *Nat Methods* **1:** 119–126

Ostareck-Lederer A, Ostareck DH, Rucknagel KP, Schierhorn A, Moritz B, Huttelmaier S, Flach N, Handoko L, Wahle E (2006) Asymmetric arginine dimethylation of heterogeneous nuclear ribonucleoprotein K by protein-arginine methyltransferase 1 inhibits its interaction with c-Src. *J Biol Chem* **281:** 11115–11125

Pahlich S, Bschir K, Chiavi C, Belyanskaya L, Gehring H (2005) Different methylation characteristics of protein arginine methyltransferase 1 and 3 toward the Ewing Sarcoma protein and a peptide. *Proteins* **61:** 164–175

Pahlich S, Zakaryan RP, Gehring H (2006) Protein arginine methylation: Cellular functions and methods of analysis. *Biochim Biophys Acta* **1764:** 1890–1903

Pawlak MR, Scherer CA, Chen J, Roshon MJ, Ruley HE (2000) Arginine N-methyltransferase 1 is required for early postimplantation mouse development, but cells deficient in the enzyme are viable. *Mol Cell Biol* **20:** 4859–4869

Perreault A, Lemieux C, Bachand F (2007) Regulation of the nuclear poly(A)-binding protein by arginine methylation in fission yeast. *J Biol Chem* **282:** 7552–7562

Rademakers R, Neumann M, Mackenzie IR (2012) Advances in understanding the molecular basis of frontotemporal dementia. *Nat Rev Neurol* **8:** 423–434

Rademakers R, Stewart H, Dejesus-Hernandez M, Krieger C, Graff-Radford N, Fabros M, Briemberg H, Cashman N, Eisen A, Mackenzie IR (2010) Fus gene mutations in familial and sporadic amyotrophic lateral sclerosis. *Muscle Nerve* **42:** 170–176

Rappsilber J, Friesen WJ, Paushkin S, Dreyfuss G, Mann M (2003) Detection of arginine dimethylated peptides by parallel precursor ion scanning mass spectrometry in positive ion mode. *Anal Chem* **75:** 3107–3114

Rydzanicz R, Zhao XS, Johnson PE (2005) Assembly PCR oligo maker: a tool for designing oligodeoxynucleotides for constructing long DNA molecules for RNA production. *Nucleic Acids Res* **33:** W521–W525

Smith JJ, Rucknagel KP, Schierhorn A, Tang J, Nemeth A, Linder M, Herschman HR, Wahle E (1999) Unusual sites of arginine methylation in Poly(A)-binding protein II and in vitro methylation by protein arginine methyltransferases PRMT1 and PRMT3. *J Biol Chem* **274:** 13229–13234

Snowden JS, Hu Q, Rollinson S, Halliwell N, Robinson A, Davidson YS, Momeni P, Baborie A, Griffiths TD, Jaros E, Perry RH, Richardson A, Pickering-Brown SM, Neary D, Mann DM (2011) The most common type of FTLD-FUS (aFTLD-U) is associated with a distinct clinical form of frontotemporal dementia but is not related to mutations in the FUS gene. *Acta Neuropathol* **122:** 99–110

Suel KE, Gu H, Chook YM (2008) Modular organization and combinatorial energetics of proline-tyrosine nuclear localization signals. *PLoS Biol* **6:** e137

Tang J, Frankel A, Cook RJ, Kim S, Paik WK, Williams KR, Clarke S, Herschman HR (2000) PRMT1 is the predominant type I protein arginine methyltransferase in mammalian cells. *J Biol Chem* **275:** 7723–7730

Terry LJ, Shows EB, Wente SR (2007) Crossing the nuclear envelope: hierarchical regulation of nucleocytoplasmic transport. *Science* **318:** 1412–1416

Tradewell ML, Yu Z, Tibshirani M, Boulanger MC, Durham HD, Richard S (2012) Arginine methylation by PRMT1 regulates nuclear-cytoplasmic localization and toxicity of FUS/TLS harbouring ALS-linked mutations. *Hum Mol Genet* **21:** 136–149

Urwin H, Josephs KA, Rohrer JD, Mackenzie IR, Neumann M, Authier A, Seelaar H, Van Swieten JC, Brown JM, Johannsen P, Nielsen JE, Holm IE, Dickson DW, Rademakers R, Graff-Radford NR, Parisi JE, Petersen RC, Hatanpaa KJ, White 3rd CL, Weiner MF *et al* (2010) FUS pathology defines the majority of tau- and TDP-43-negative frontotemporal lobar degeneration. *Acta Neuropathol* **120:** 33–41

Vance C, Rogelj B, Hortobagyi T, De Vos KJ, Nishimura AL, Sreedharan J, Hu X, Smith B, Ruddy D, Wright P, Ganesalingam J, Williams KL, Tripathi V, Al-Saraj S, Al-Chalabi A, Leigh PN, Blair IP, Nicholson G, de Belleroche J, Gallo JM *et al* (2009) Mutations in FUS, an RNA processing protein, cause familial amyotrophic lateral sclerosis type 6. *Science* **323:** 1208–1211

Waibel S, Neumann M, Rabe M, Meyer T, Ludolph AC (2010) Novel missense and truncating mutations in FUS/TLS in familial ALS. *Neurology* **75:** 815–817

Yan J, Deng HX, Siddique N, Fecto F, Chen W, Yang Y, Liu E, Donkervoort S, Zheng JG, Shi Y, Ahmeti KB, Brooks B, Engel WK, Siddique T (2010) Frameshift and novel mutations in FUS in familial amyotrophic lateral sclerosis and ALS/dementia. *Neurology* **75:** 807–814

Yu MC, Bachand F, McBride AE, Komili S, Casolari JM, Silver PA (2004) Arginine methyltransferase affects interactions and recruitment of mRNA processing and export factors. *Genes Dev* **18:** 2024–2035

Zhang ZC, Chook YM (2012) Structural and energetic basis of ALS-causing mutations in the atypical proline-tyrosine nuclear localization signal of the Fused in Sarcoma protein (FUS). *Proc Natl Acad Sci USA* **109:** 12017–12021

Supplementary Information

Supplementary Material and Methods

Antibodies

The following commercial antibodies were used: HA-specific mouse monoclonal HA.11 (Covance) or horseradish peroxidase (HRP)-coupled HA-specific rat monoclonal 3F10 (Roche); GFP-specific rabbit polyclonal (BD Living Colors from BD Biosciences or Fitzgerald Industries International); PRMT1-specific rabbit monoclonal EPR3292 (Abcam); FUS-specific mouse monoclonal antibody 4H11 (Santa Cruz) and rabbit polyclonal A300-294A (Bethyl) and HPA008784 (Sigma); TIA-1-specific goat polyclonal antibody (C-20, Santa Cruz); β-Tubulin III-specific rabbit polyclonal antibody (Tuj1, Sigma); α-Tubulin-specific mouse monoclonal antibody clone B-5-1-2 (Sigma); β-actin specific mouse monoclonal antibody clone AC-74 (Sigma). Secondary antibodies for immunoblotting were HRP-coupled goat anti-mouse, anti-rabbit or anti-rat IgG (Promega). For immunocytochemistry, Alexa-488, Alexa-555 or Alexa647-conjugated goat or donkey anti-mouse, anti-rabbit or anti-rat IgG (Invitrogen) were used.

Cloning of cDNA constructs

The pcDNA3.1/Hygro(-) constructs encoding HA-tagged FUS-WT, R521G, R522G, R524S, P525L, ΔPY-NLS (Δ514-526), GFP-M9M, GFP-Bimax, GST-GFP-514-526$_{WT}$ and GST-GFP-514-526$_{P525L}$ have been described previously (Dormann et al, 2010). For generation of lentiviral constructs, HA-FUS-WT and HA-FUS-P525L were subcloned from pcDNA3.1/Hygro(-) into pCDH-Ef1-MCS-IRES-Puro via NheI/BamHI restriction digest. For generation of the GST-GFP455-526$_{P525L}$ reporter construct, the respective FUS sequence was PCR amplified and cloned via XhoI/BamHI restriction digest into the pGST-EGFP-C1 vector

described in Dormann et al, 2010. The FUS455-526-Rmut$_{P525L}$ sequence was assembled from 6 oligonucleotides according to Rydzanicz et al., 2005 and was subsequently cloned into pGST-EGFP-C1. The cDNA sequence of human EWS (NM_005243.3) was amplified from an human brain cDNA and was cloned by XhoI/HindIII restriction digest into pcDNA3.1/Hygro(-) with an N-terminal HA-tag. The cDNA sequence of human TAF15 (BC046099) was amplified from an I.M.A.G.E. full length cDNA clone (IRATp970A0976D, Source BioScience) and was cloned by XbaI/BamHI restriction digest into pcDNA3.1/Hygro(-) with an N-terminal HA-tag. Point mutations (EWS-P665L and TAF15-P591L) were introduced by conventional PCR via the reverse primer. For bacterial expression constructs, the sequences encoding FUS454-526$_{WT}$ or FUS454-526$_{P525L}$ were PCR amplified and cloned into the petM11-ZZ-His$_6$ vector via NcoI/BamHI restriction digest. For all constructs, sequence integrity was verified by sequencing. Oligonucleotide sequences are available upon request.

Recombinant protein expression and purification

For expression of recombinant ZZ-His$_6$-FUS454-526$_{WT}$ or FUS454-526$_{P525L}$, the bacterial expression vectors petM11-FUS454-526 (WT or P525L) were transformed into BL21-DE3-Rosetta cells and 1 l expression cultures were grown in modified M9 minimal medium supplemented with $^{15}NH_4Cl$. For expression of His$_6$-tagged TRN, the pQE-60-TRN-His$_6$ vector was transformed into *E.coli* BL21(DE3)pLysS cells and cells were grown in standard lysogeny broth (LB) medium. Cells were induced at an OD(600 nm) of 0.7 - 0.8 with 0.5 mM IPTG followed by protein expression for 16 h at 20°C (TRN-His$_6$) or 4 h at 37°C (FUS-454-526). Unlabeled or ^{15}N-labeled His$_6$-tagged proteins were purified under native conditions using Ni-NTA agarose (Qiagen) according to the QIAexpressionist protocol (Qiagen). For FUS454-526, the eluted proteins were subjected to a brief heat shock (10 min at 90°C) to denature contaminating proteases. All proteins were dialyzed against TRN binding buffer (20 mM sodium phosphate buffer, pH 6.8, 50 mM NaCl, 1 mM EDTA, 1 mM DTT). To obtain

untagged FUS454-526 proteins, the ZZ-His_6 tag was cleaved off with TEV protease. After 10-fold dilution in the buffer used for Ni-NTA purification, the tag, TEV protease and uncleaved protein were removed by a second affinity purification on Ni-NTA resin. For NMR measurements samples were buffer exchanged to TRN binding buffer using a PD10^{TM} column (GE Healthcare) and concentrated using Amicon Ultra-15 (Millipore) centrifugal filter units.

NMR spectra recording and processing

NMR spectra were recorded at 298 K on an Avance III 900 Bruker NMR spectrometer equipped with a cryogenic triple resonance gradient probe. All spectra were recorded with a recycle delay of 1.0 s, spectral widths of 20/30 ppm centered at 4.7/118.5 ppm in $^{1}H/^{15}N$, with 1024 and 128 points, respectively, using 64 scans per increment. Spectra were processed with NMRPipe/Draw and analyzed with Sparky 3 (T. D. Goddard & D. G. Kneller, University of California, San Francisco, USA). Chemical shift assignment of the C-terminal residue was confirmed with a standard ^{15}N-edited TOCSY-HSQC spectrum.

Supplementary Figures

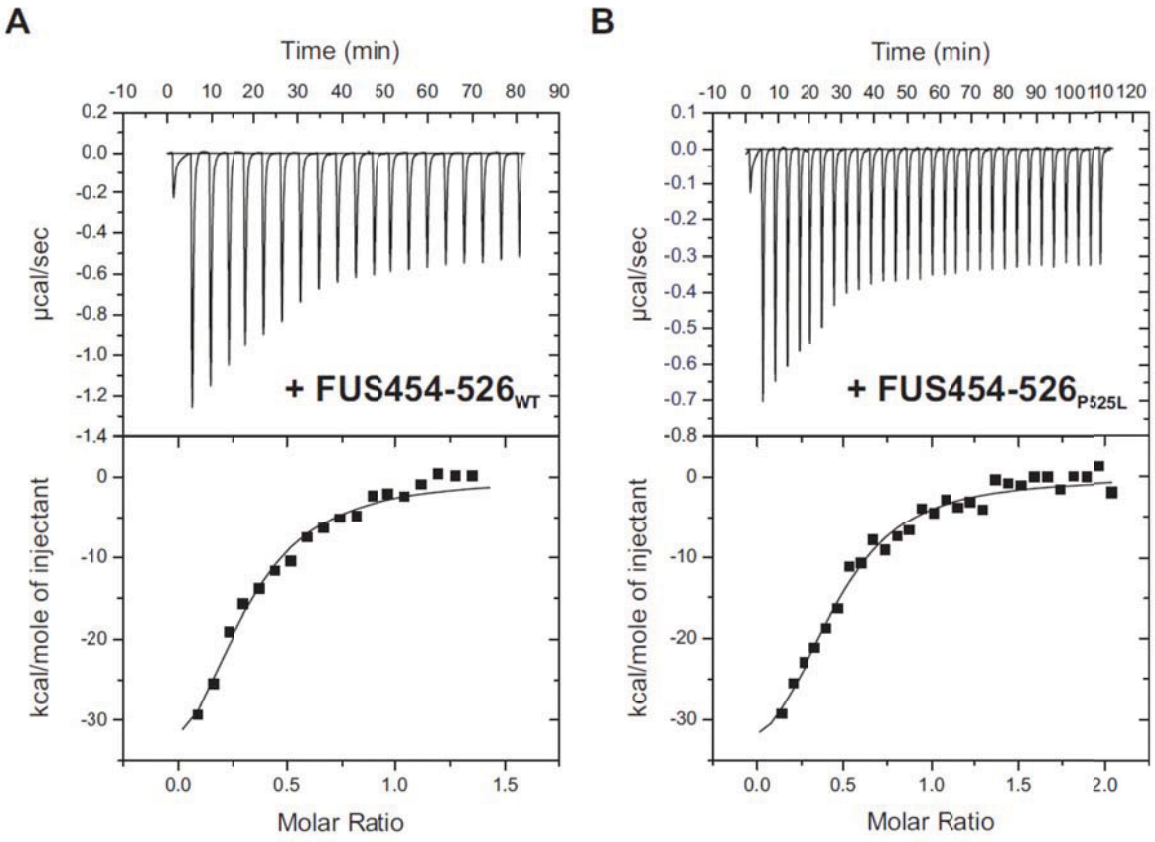

Supplementary Figure S1: ITC titrations of TRN with recombinant FUS.

Experimental calorimetric data of the binding of FUS FUS454-526$_{WT}$ **(A)** and FUS454-526$_{P525L}$ **(B)** to TRN. The experiment was carried out at 25 °C. Dilution heats measured by titrating FUS into the corresponding buffer were in the range of the heat effects observed at the end of the titration (data not shown) and were subtracted for the analysis.

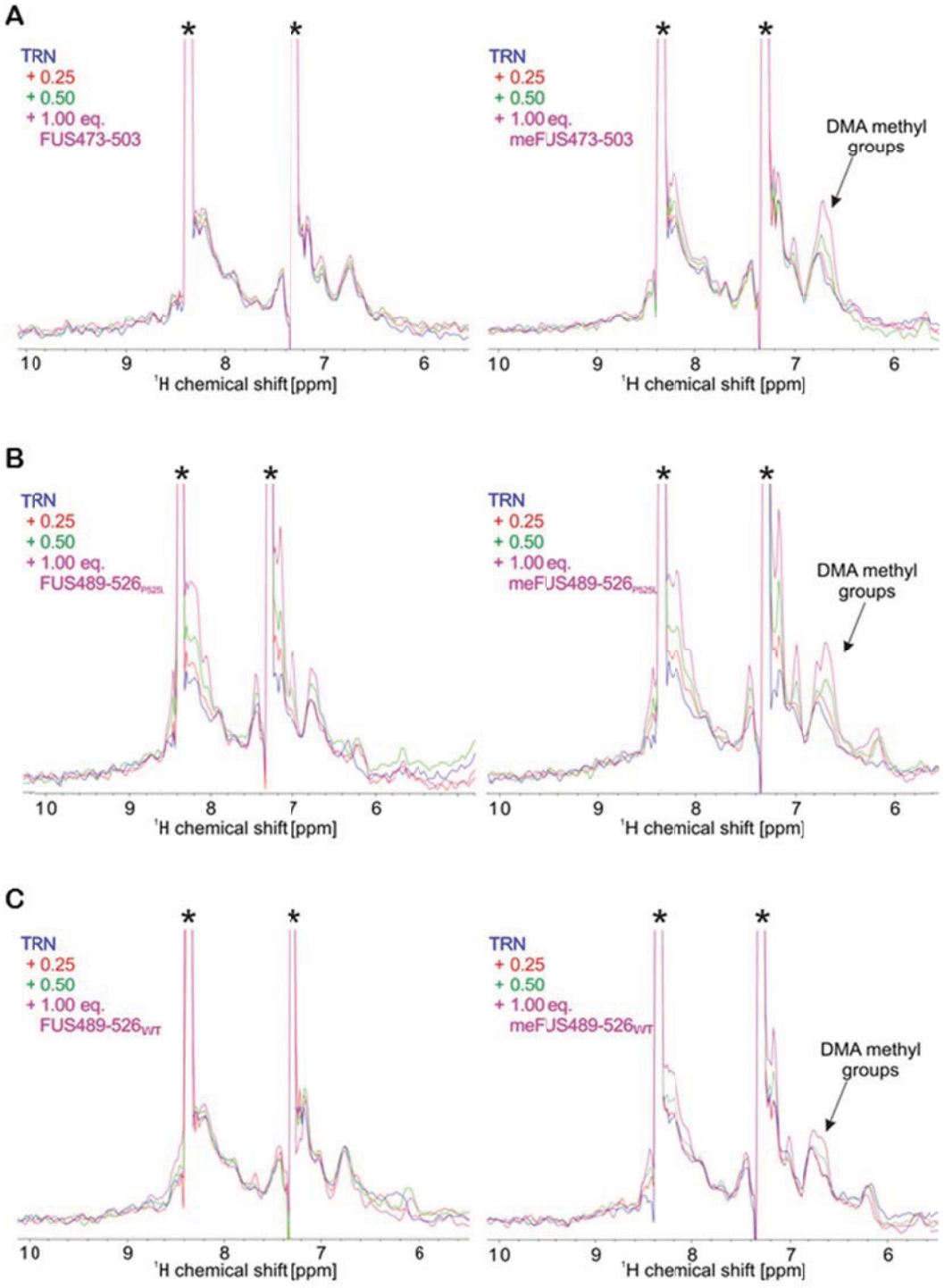

Supplementary Figure S2: NMR titrations of TRN with FUS peptides.

(A) Overlay of 1D ^{1}H NMR spectra recorded for TRN with increasing amounts of FUS473-503 and meFUS473-503 peptides. In agreement with the binding observed by ITC (Kd_{ITC} = 11.7 µM), a weak increase in NMR signals is observed for the unmethylated peptide, whereas a strong increase in NMR signal characteristic for unbound FUS was observed for the methylated peptide (Kd_{ITC} >> 200 µM).

(B) Overlay of 1D ^{1}H NMR spectra recorded for TRN with increasing amounts of FUS489-526$_{P525L}$ and meFUS489-526$_{P525L}$ peptides. The increase in signal intensity corresponds to the amount of unbound FUS peptide. In agreement with the weak binding observed by ITC, a strong increase in NMR signals characteristic for unbound FUS is observed.

(C) Overlay of 1D ^{1}H NMR spectra recorded for TRN with increasing amounts of FUS489-526$_{WT}$ and meFUS489-526$_{WT}$ peptides. In agreement with the binding observed by ITC (Kd_{ITC} = 2.8 μM), a weak increase in NMR signals is observed for the unmethylated peptide. The increase in signal intensity for the methylated peptide (Kd_{ITC} = 7.8 μM) was significantly lower than for meFUS489-526$_{P525L}$, but stronger than for FUS489-526$_{WT.}$

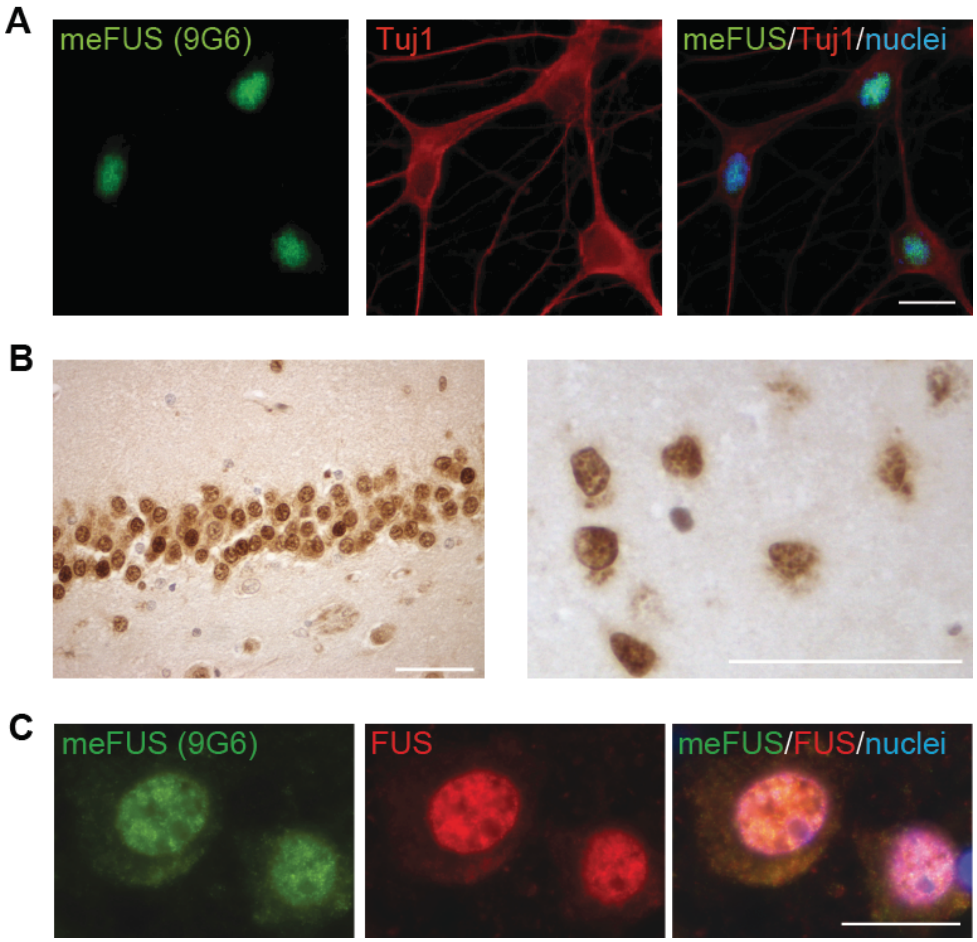

Supplementary Figure S3: Physiological staining of methylated FUS in primary neurons and human post mortem tissue

(A) Primary rat hippocampal neurons were co-labeled with a meFUS-specific antibody (9G6, green), the neuronal marker antibody Tuj1 (red) to visualize neuronal morphology and a nuclear counterstain (blue). Methylated FUS is located in nuclei of neurons. Scale bar: 20 µm.

(B) Immunohistochemistry with a meFUS-specific antibody (9G6) revealed strong nuclear and faint cytoplasmic physiological staining as shown in the dentate granule cells of a control case (left) and an unaffected cortical brain region of a BIBD case (right). Scale bars: 50 µm.

(C) Double-label immunofluorescence with a meFUS antibody (9G6, green), a polyclonal pan-FUS antibody (red) and nuclear counterstaining (blue) of unaffected neurons in the brainstem of a BIBD case demonstrating predominant nuclear staining with both antibodies. Scale bar: 20 µm.

the FEBS Journal
MINIREVIEW

Stress granules in neurodegeneration – lessons learnt from TAR DNA binding protein of 43 kDa and fused in sarcoma

Eva Bentmann[1], Christian Haass[1,2,3] and Dorothee Dormann[1]

1 Adolf Butenandt Institute, Department of Biochemistry, Ludwig Maximilians University, Munich, Germany
2 German Center for Neurodegenerative Diseases (DZNE), Munich, Germany
3 Munich Cluster for Systems Neurology (SyNergy), Munich, Germany

Keywords
ALS; FTLD; FUS; neurodegeneration; RNA-binding proteins; stress granules; TDP-43; TLS

Correspondence
D. Dormann or E. Bentmann, Adolf Butenandt Institute, Biochemistry, Ludwig Maximilians University, Munich, Schillerstrasse 44, 80336 Munich, Germany
Fax: +49 89 2180 75415
Tel: +49 89 2180 75474
E-mail: dorothee.dormann@dzne.lmu.de; eva.bentmann@dzne.lmu.de

(Received 3 January 2013, revised 28 March 2013, accepted 8 April 2013)

doi:10.1111/febs.12287

Stress granules (SGs) are cytoplasmic foci that rapidly form when cells are exposed to stress. They transiently store mRNAs encoding house-keeping proteins and allow the selective translation of stress-response proteins (e.g. heat shock proteins). Besides mRNA, SGs contain RNA-binding proteins, such as T cell internal antigen-1 and poly(A)-binding protein 1, which can serve as characteristic SG marker proteins. Recently, some of these SG marker proteins were found to label pathological TAR DNA binding protein of 43 kDa (TDP-43)- or fused in sarcoma (FUS)-positive cytoplasmic inclusions in patients with amyotrophic lateral sclerosis and frontotemporal lobar degeneration. In addition, protein aggregates in other neurodegenerative diseases (e.g. tau inclusions in Alzheimer's disease) show a co-localization with T cell internal antigen-1 as well. Moreover, several RNA-binding proteins that are commonly found in SGs have been genetically linked to neurodegeneration. This suggests that SGs might play an important role in the pathogenesis of these proteinopathies, either by acting as a seed for pathological inclusions, by mediating translational repression or by trapping essential RNA-binding proteins, or by a combination of these mechanisms. This minireview gives an overview of the general biology of SGs and highlights the recently identified connection of SGs with TDP-43, FUS and other proteins involved in neurodegenerative diseases. We propose that pathological inclusions containing RNA-binding proteins, such as TDP-43 and FUS, might arise from SGs and discuss how SGs might contribute to neurodegeneration via toxic gain or loss-of-function mechanisms.

Abbreviations
ALS, amyotrophic lateral sclerosis; ANG, angiogenin; ATXN2, ataxin-2; CTF, C-terminal fragment; DYRK3, dual specificity tyrosine-phosphorylation-regulated kinase 3; eIF, eukaryotic translation initiation factor; EWS, Ewing sarcoma protein; FMRP, fragile X mental retardation protein; FTLD, frontotemporal lobar degeneration; FUS, fused in sarcoma; G3BP, Ras-GTPase-activating protein SH3-domain-binding protein; Htt, huntingtin; mRNP, messenger ribonucleoprotein; mTORC1, mammalian target of rapamycin complex 1; NLS, nuclear localization signal; PABP-1, poly(A)-binding protein 1; P-bodies, processing bodies; PTM, post-translational modification; RGG, arginine-glycine-glycine; RRM, RNA recognition motif; SCA2, spinocerebellar ataxia type 2; SG, stress granule; siRNA, small interfering RNA; SMA, spinal muscular atrophy; SMN, survival of motor neurone; SOD1, superoxide dismutase 1; SYGQ, serine-tyrosine-glycine-glutamine; TAF15, TATA-binding protein-associated factor 15; TDP-43, TAR DNA binding protein of 43 kDa; TIAR, TIA-1-related; TIA-1, T cell internal antigen-1; TLS, translocated in liposarcoma; ZnF, zinc finger.

Introduction

Abnormal neuronal inclusions consisting of disease-characterizing protein aggregates are key features of almost all neurodegenerative diseases [1]. In many of these disorders (e.g. in Alzheimer's disease), the identification of the proteinaceous components of the pathological inclusions was an important step in understanding the associated disease mechanisms. Similarly, research in amyotrophic lateral sclerosis (ALS) and frontotemporal lobar degeneration (FTLD) was tremendously advanced by the discovery that the RNA-binding proteins TAR DNA-binding protein of 43 kDa (TDP-43) or fused in sarcoma (FUS) are abnormally deposited in neuronal and glial cytoplasmic inclusions in the majority of ALS and FTLD patients [2–4]. This has led to the concept that defects in RNA metabolism are an important pathomechanism in ALS and FTLD [5–7].

Recently, stress granule (SG) marker proteins were found to be additional components of the TDP-43- or FUS-positive cytoplasmic inclusion in ALS and FTLD patients [8–12], a finding that has lead to an entirely new mechanism of inclusion formation. Moreover, several other proteins associated with neurodegenerative diseases [e.g. tau, ataxin-2, survival of motor neurone (SMN) and angiogenin (ANG)] are recruited into SGs upon noxious conditions and/or regulate SG assembly [13]. Thus, SGs have not only emerged as a new player in ALS and FTLD, but also possibly play an important role in other neurodegenerative disorders.

Because TDP-43 and FUS were the first proteins shown to be co-deposited with SG proteins in human post mortem brains, we use the case of TDP-43 and FUS to highlight the newly-identified role of SGs in neurodegenerative diseases. We first provide a brief introduction into FTLD and ALS and the pathobiology of TDP-43 and FUS. We then provide an overview of SGs in general and present what is known about their connection to TDP-43, FUS and other RNA-binding proteins linked to neurodegenerative diseases. Finally, we discuss the different mechanisms by which SGs may contribute to the formation of pathological protein inclusions and neurodegeneration in general.

ALS and FTLD: related but not identical neurodegenerative diseases

ALS and FTLD are related neurodegenerative disorders that are connected by overlapping clinical phenotypes [14]. ALS, also known as Lou Gehrig's disease, is the most common motor neurone disease and is caused by selective degeneration of motor neurones. This results in gradual muscle weakness and atrophy that ultimately leads to death [15]. FTLD is the second most common dementia below the age of 65 years and is characterized by atrophy of the frontal and temporal lobe [16]. Because these brain regions control behaviour and cognitive function (e.g. language), patients suffering from FTLD exhibit progressive changes in their personality and/or language [16]. FTLD is accompanied by motor neurone symptoms in a significant proportion of patients and cognitive and behavioural impairment is observed in up to 75% of ALS patients [17]. This has led to the view that ALS and FTLD form a clinical disease continuum, in which both entities are linked by overlapping syndromes [14].

Over the last few years, seminal discoveries in the neuropathology and genetics of ALS and FTLD have revealed a common molecular basis of the two diseases. In 2006, the DNA/RNA-binding protein TDP-43 was identified as major component of the ubiquitinated inclusions found in the brain and spinal cord in the vast majority of ALS patients (ALS-TDP). Additionally, TDP-43 was found to be the pathological hallmark protein in approximately 50% of FTLD patients (FTLD-TDP) [2,3], whereas most of the remaining FTLD cases show TDP-43-negative, but tau-positive neuropathology (FTLD-tau) [14]. Shortly afterwards, mutations in *TARDBP*, the gene encoding TDP-43, were identified in rare cases of familial ALS [18–21], demonstrating that TDP-43 is not just an innocent bystander, but also plays a crucial role in the pathogenesis of ALS/FTLD. Up to now, more than 40 dominant mutations in the *TARDBP* gene have been identified in ALS and occasionally in FTLD patients [22] (http://www.molgen.vib-ua.be/FTDMutations) (Fig. 1). In 2009, another DNA/RNA-binding protein called FUS was found in pathological protein aggregates in rare familial ALS cases with a *FUS* mutation [23,24] (Fig. 1) and in approximately 5–10% of sporadic FTLD cases (FTLD-FUS) [4,25,26]. Recently, the most common genetic cause of ALS and FTLD could be linked to a GGGGCC repeat expansion in the *C9ORF72* gene [27–29]. The expanded hexanucleotide repeat is translated into aggregating dipeptide repeat proteins, which are deposited in the brains of *C9ORF72* mutation carriers [30,31]. Noteworthy, the *C9ORF72* mutation was also identified in patients with a combined ALS/FTLD phenotype, further confirming the genetic and clinical overlap of these two disorders. Thus, the genetics and neuropathology of FTLD and ALS, which are reviewed in more detail elsewhere [14,22], clearly demonstrate a link between the two diseases and suggest that they are caused by similar pathomechanisms.

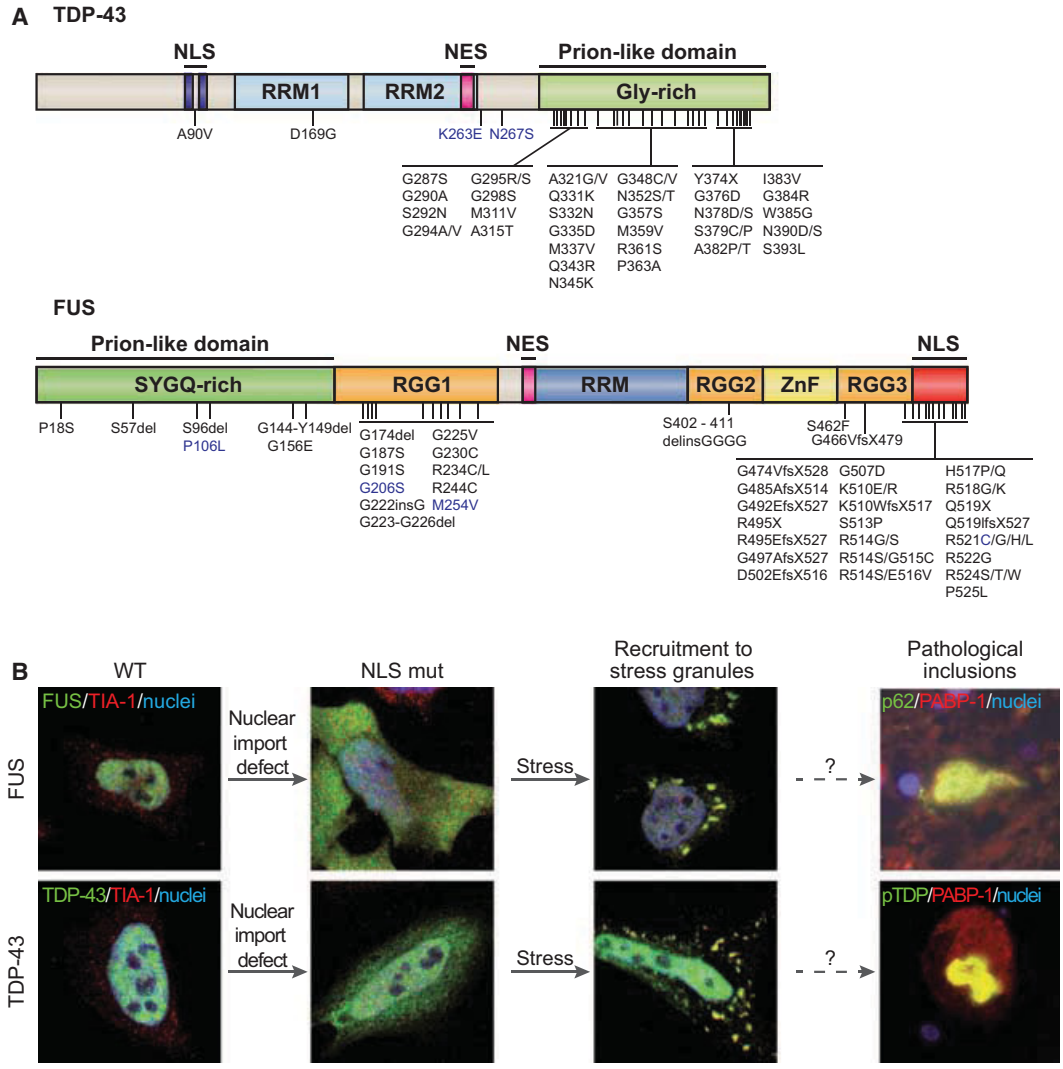

Fig. 1. Schematic diagram and SG recruitment of TDP-43 and FUS. (A) Domain structure of TDP-43 and FUS and disease-associated mutations. Mutations in *TARDBP*, the gene encoding TDP-43, and *FUS* were identified in familial cases of ALS (shown in black) and FTLD (shown in blue). Besides missense mutations, premature stop codons (X), deletions (del), insertions (ins) and frameshift (fs) mutations are designated. The most frequently identified FUS mutations cluster in the protein's NLS and disrupt the interaction with the nuclear import factor transportin. Mutations in the N-terminal prion-like domain termed the SYGQ-rich domain in FUS are considered to be risk factors because they were mainly found in sporadic cases [22]. By contrast, all disease-causing TDP-43 mutations cluster in a prion-like domain termed the glycine-rich (Gly-rich) domain. Both FUS and TDP-43 contain a nuclear export signal (NES) and RRMs. FUS contains additional RNA-binding motifs, as well as a ZnF and RGG repeats. (B) Wild-type (WT) TDP-43 and FUS are localized in the nucleus (left row), whereas mutants with a defective NLS (NLS mut) accumulate in the cytosol (second row). Upon cellular stress (e.g. heat shock, 1 h at 44 °C), cytosolic TDP-43 and FUS are recruited into TIA-1-positive SGs (third row). Pathological TDP-43 and FUS inclusions in ALS/FTLD patients also contain SG marker proteins, such as PABP-1 (right row), suggesting that they might originate from SGs. Note that p62 is an established marker of FUS-positive pathological inclusions and was used because double-labelling for FUS and PABP-1 was technically not possible, and the available antibodies that work on paraffin-embedded tissue were both rabbit polyclonals. This research was published previously [9,12] and is reproduced with permission.

TDP-43 and FUS: multifunctional RNA-binding proteins with pivotal roles in ALS and FTLD

TDP-43 was initially discovered as a protein that binds to the TAR regulatory element in the HIV long terminal repeat [32]. Subsequently, it was shown that TDP-43 can also bind to RNA and regulates splicing of the cystic fibrosis transmembrane conductance regulator [33]. Today, we know that TDP-43 has apparently several thousand RNA targets in the brain

[34,35]. Moreover, TDP-43 is involved in microRNA processing [36,37] and plays a role in mRNA transport and local translation in dendritic spines [38–41]. TDP-43 has two RNA recognition motifs (RRMs) (Fig. 1A), of which only RRM1 is necessary and sufficient for specific binding to nucleic acids [33]. Moreover, TDP-43 has a C-terminal glycine-rich domain that mediates protein–protein interactions [42–44]. Interestingly, this domain is intrinsically disordered and was shown to have similarity to yeast prions, which exhibit ordered, self-perpetuating aggregation [45–47]. Conspicuously, almost all disease-associated *TARDBP* mutations are clustered in the C-terminal glycine-rich domain (Fig. 1A). Despite extensive research over the last few years, the pathomechanism of these mutations is still unclear. One study reported an increased protein–protein interaction with FUS [48], whereas other studies could not confirm these results [44,49]. Some *TARDBP* mutations were reported to cause cytosolic mislocalization [10,50,51], whereas other studies reported an unchanged nuclear localization of mutant TDP-43 [12,48,52]. Moreover, *TARDBP* mutations have been described to increase and accelerate TDP-43 aggregation and toxicity [10,50,51,53–58]. Finally, wild-type but not mutant TDP-43 stimulates the growth of dendrites and axons in *Drosophila* [40,59], suggesting that *TARDBP* mutations may be partial loss-of-function alleles. This is also supported by the finding that *TARDBP* mutations are slightly less efficient in rescuing the phenotype of zebrafish null mutants [60]. Thus, the mechanism(s) by which *TARDBP* mutations cause disease are still controversial and remain to be clarified.

FUS, also known as translocated in liposarcoma (TLS), was initially discovered in characteristic chromosomal translocations in human sarcomas, giving FUS/TLS its name [61,62]. Similar to TDP-43, FUS is a DNA/RNA-binding protein that regulates transcription and splicing of hundreds of target genes [63–65] and is involved in mRNA transport and local translation [66–69]. FUS contains an N-terminal serine-tyrosine-glycine-glutamine (SYGQ)-rich transcriptional activation domain [70,71] (Fig. 1A), which is intrinsically unfolded and, similar to the TDP-43 glycine-rich domain, was predicted to have prion-like properties [45]. Additionally, FUS contains several RNA-binding elements, such as arginine-glycine-glycine (RGG) domains, an RRM and a zinc finger (ZnF) (Fig. 1A). Although it has not been fully determined whether all of these domains are necessary and sufficient for RNA-binding, several *in vitro* studies have suggested that the C-terminal RGG2-ZnF-RGG3 domain is most likely the major RNA-binding domain [12,72,73]. Many ALS-associated *FUS* mutations are clustered in the very C-terminal region and disrupt the interaction of the nonclassical proline-tyrosine nuclear localization signal (NLS) with the nuclear import receptor transportin/karyopherin β2 [9,74–78]. This causes a reduced nuclear import of FUS and results in cytosolic mislocalization of mutant FUS. Notably, the degree of cytoplasmic mislocalization correlates negatively with the age of onset and disease severity (i.e. strong mutations, such as P525L, that show a severe cytosolic accumulation cause an unusually early disease onset and a rapid disease progression, whereas mutations that cause a mild cytosolic mislocalization show an incomplete penetrance) [9,23,78]. Thus, defective nuclear import and/or the cytosolic accumulation of FUS appear to be key events in ALS pathogenesis [79].

Both TDP-43 and FUS are predominantly nuclear proteins, yet the pathological inclusions containing TDP-43 or FUS are frequently found in the cytosol [3,4]. This has led to the idea that defects in nuclear import are involved in this pathological redistribution [79] (Fig. 1B). In the case of ALS-FUS, mutations in the NLS of FUS obviously explain the cytosolic mislocalization. In TDP-43-proteinopathies, reduced levels of nuclear import factors were proposed to contribute to the cytosolic distribution of TDP-43 [80]. However, FUS and TDP-43 variants with a defective NLS (NLS mut) are homogenously distributed in the cytosol (Fig. 1B), indicating that their presence in the cytosol does not automatically cause aggregation of these proteins. Instead, environmental stress appears to be required to initiate clustering of cytosolic FUS or TDP-43 in SGs [9,10,12,74–76,81] (Fig. 1B). Because SG marker proteins [e.g. poly(A)-binding protein 1 (PABP-1)] are present in cytosolic TDP-43/FUS inclusions in ALS/FTLD patients (Fig. 1B), it can be hypothesized that SGs are precursors of these pathological inclusions and thus may be relevant in the pathomechanism of TDP-43- and FUS-proteinopathies.

SGs: cytoplasmic messenger ribonucleoprotein (mRNP) particles with cytoprotective function

Function and composition of SGs

SGs are cytoplasmic non-membrane covered mRNP particles composed of poly(A)+ mRNAs and RNA-binding proteins. They are formed by eukaryotic cells in response to environmental stress and facilitate cell survival by prioritizing the synthesis of stress-protective proteins, such as heat shock proteins and

chaperones, at the same time as transiently storing mRNAs encoding house-keeping proteins [82,83]. Thus, SGs are considered to be storage/sorting stations, where transcripts can be stored in a translationally silent form, sorted for translation re-entry or degraded in interacting processing bodies (P-bodies), which are extensively reviewed elsewhere [83–85]. With this triage, cellular anabolic energy is saved because a portion of the already synthesized mRNAs can be translated at a later time-point and they are not nonselectively degraded. Additionally, SGs sequester important signalling molecules and thereby enhance cell survival during stress [86]. SGs sequester regulatory apoptotic proteins (e.g. TRAF2 and RACK1) and thereby inhibit apoptosis [87–89]. Moreover, the mammalian target of rapamycin complex 1 (mTORC1), a central regulator of cell growth and metabolism, is sequestered into SGs upon cellular stress, which protects cells from DNA damage [90].

How are certain mRNAs recruited into SGs, whereas others escape the translational arrest in SGs? mRNAs found in SGs often contain 5′-terminal oligopyrimidine tracts, which are commonly found in mRNAs encoding ribosomal proteins and translation elongation factors. The inclusion of these 5′-terminal oligopyrimidine tract-containing mRNAs into SGs ensures that energy-consuming processes, such as ribosome formation, are suppressed during cellular stress [91–93]. Additionally, transcripts that require eukaryotic translation initiation factor (eIF)4A-dependent 5′ UTR scanning are preferentially included into SGs, because eIF4A is inactivated during SG assembly [83]. By contrast, mRNAs encoding for proteins necessary for stress adaption escape the translational arrest in SGs by using noncanonical translation initiation motifs [92,94–97].

Besides mRNA, SGs comprise mRNA-bound 48S pre-initiation complexes composed of small ribosomal subunits and translation initiation factors (e.g. eIF3, eIF4E and eIF4G). Moreover, SGs contain proteins involved in mRNA stabilization, processing and transport, such as PABP-1, T cell internal antigen-1 (TIA-1), TIA-1-related (TIAR) and Ras-GTPase-activating protein SH3-domain-binding protein (G3BP) [84,89,98–101]. These proteins can promote SG assembly [83] and serve as specific SG markers because they are only found in SGs, and not in other cytoplasmic mRNP granules, such as P-bodies or transport granules [100,102].

SG assembly and disassembly

Under acute stress conditions, actively-translating polysomes are rapidly disassembled and, simultaneously, SGs are assembled (Fig. 2). Experimental stress conditions that induce SGs include oxidative stress induced by arsenite or H_2O_2, osmotic shock induced by exposure to sorbitol, mitochondrial stress induced by carbonyl cyanide *p*-(trifluoromethoxy)-phenylhydrazon (FCCP) or clotrimazole, UV irradiation, viral infection, cellular acidosis and thermal stress [102–107]. These toxic environmental stimuli impair translation initiation via an eIF2α-dependent or -independent pathway, ultimately leading to translational arrest.

eIF2α-dependent SG assembly is induced when stress stimuli activate specific serine/threonine kinases (PKR, PERK, HRI, GCN) [108]. These kinases subsequently phosphorylate and thereby inactivate the α subunit of eIF2 [98] (Fig. 2), which is usually required for translation initiation in its unphosphorylated state. Phosphorylation of eIF2α results in decreased production of the ternary complex composed of eIF2-GTP-Met-$tRNA_i^{Met}$ (Fig. 2), which must bind to the 40S small ribosomal subunit to initiate mRNA scanning and start codon selection. As a result of the decreased availability of eIFs and ternary complexes, a further round of translation cannot be initiated [83]. Other chemicals (e.g. hippuristanol, pateamine A) initiate SG assembly independently of eIF2α. They interfere with translation initiation by blocking eIF4A helicase, which is required for the ribosome recruitment phase of translation initiation. When the eIF4A helicase is impaired, translation initiation is stalled and SGs are formed in an eIF2α-independent manner [109–113]. Both the eIF2α-dependent and the eIF2α-independent pathways prevent translation initiation and, thus, actively-translating ribosomes finish their round and then run-off from the transcript. Nevertheless, the so-called 48S pre-initiation complex, consisting of one 40S small ribosomal subunit, several eIFs and PABP-1, remains bound to the 5′ UTR of the mRNA [83] (Fig. 2). Although the next step (SG nucleation) is not yet fully understood, it has been suggested that aggregation-prone RNA-binding proteins, such as G3BP, TIA-1, fragile X mental retardation protein (FMRP) and tristetraprolin [83], associate with mRNPs and promote their aggregation (Fig. 2). After this primary aggregation step, protein–protein interactions and especially mRNA-bound PABP-1 cross-link individual aggregated mRNPs to initiate clustering into microscopically visible SGs [83] (Fig. 2). However, it should be noted that SGs do not have all the properties of aggregates typically associated with neurodegenerative diseases because their formation is fully reversible upon recovery from stress and they do not contain the insoluble, fibrous β-sheet-containing aggregates typically found in most neurodegenerative disorders.

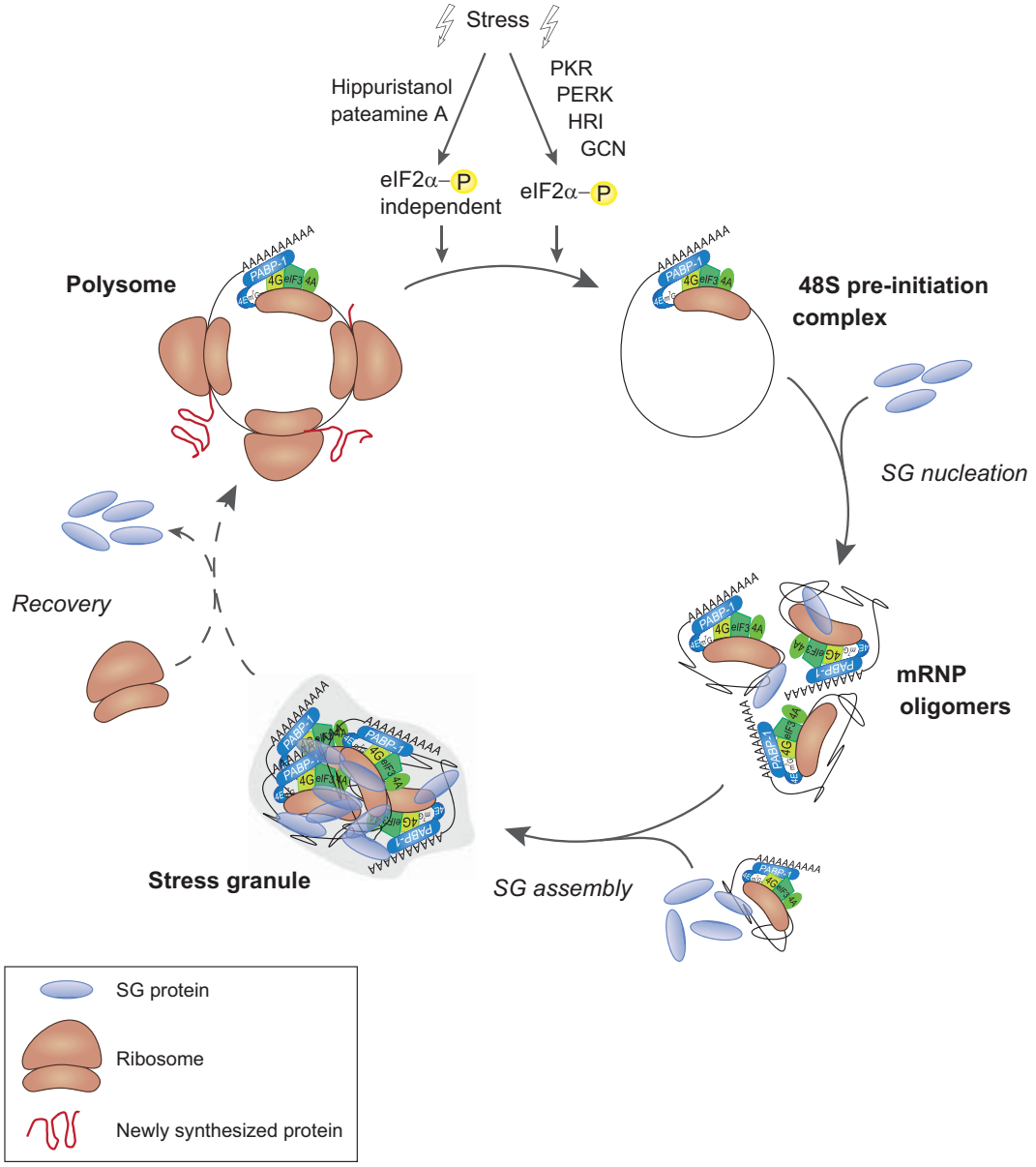

Fig. 2. SG life cycle. Under physiological conditions, several ribosomes that translate mRNA into protein are bound to an mRNA molecule, forming a polysome. Upon cellular stress, elongating ribosomes run-off the transcript as a result of the reduced availability of eIFs, leaving behind a circularized mRNP (48S pre-initiation complex). SG nucleation is initiated by the recruitment of SG-associated proteins, such as TIA-1, G3BP and tristetraprolin (blue), which triggers the aggregation of mRNPs. Subsequently, protein–protein interactions and cross-linking via PABP-1, as well as O-glycosylation of the small ribosomal subunit, facilitate the assembly of the aggregated mRNPs into SGs. During recovery from stress, SG proteins dissociate from the SG, allowing ribosomes to bind and re-form a translating polysome.

Besides eIF2α phosphorylation, other post-translational modifications play an important role in regulating SG assembly or the recruitment of RNA-binding proteins to SGs. O-linked *N*-acetylglucosamine (O-GlcNAc)-modified proteins accumulate in SGs and the depletion of key enzymes of the glucose to GlcNAc conversion abolishes SG formation, suggesting that *O*-GlcNAc modifications are important for proper SG formation [114]. Possible functional explanations are that these sugars act as molecular glue in the aggregation process of untranslated mRNPs or that *O*-GlcNAc modifications promote translational repression via interference with ribosomal subunits [115]. Another post-translational modification linked to SGs is

methylation of arginine residues by peptidylarginine methyltransferases. The RNA-binding proteins FMRP, CIRP and FUS can be methylated in their RGG repeat motifs and localize to SGs in the methylated state [116–119]. Global inhibition of methylation decreases the recruitment of these proteins into SGs, either by altering the protein's subcellular localization and therefore its availability for SGs [118,119], or possibly by changing its RNA-binding affinity or so far unknown mechanisms.

When sublethal stress has passed, SGs are rapidly disassembled and polysomes are re-formed [98] (Fig. 2). Because 48S pre-initiation complexes are preserved in SGs in an assembled state, translation can be rapidly reactivated upon stress recovery. The re-formation of polysomes from SGs requires chaperones and can be promoted by the overexpression of staufen [120] or heat shock protein 70 [121]. Moreover, this step is regulated by the dual specificity tyrosine-phosphorylation-regulated kinase 3 (DYRK3), which cycles between SGs and the cytosol and regulates SG assembly/disassembly [122]. When DYRK3 kinase activity is inhibited, DYRK3 remains associated with SGs and prevents their dissolution and the release of sequestered mTORC1. When stress signals are gone, the kinase activity of DYRK3 is required for disassembly of SGs and reactivation of mTORC1 signalling. These recent findings revealed an interesting mechanism of how a kinase couples SG assembly/disassembly to translational control via mTORC1 signalling and may have implications for neurodegenerative diseases. Additionally, the drugs cycloheximide and emetine were shown to actively dissolve pre-formed SGs [123,124]. Both chemicals freeze ribosomes on translating mRNA, thereby inhibiting ribosome run-off and SG formation. Because SGs and polysomes are in dynamic equilibrium, this leads to the disassembly of pre-formed SGs.

Stressors that initiate SG formation *in vivo*

SGs were not only observed in cultured cells after various experimental stress conditions, but also in embryonic muscles of *Drosophila* after hypoxia [125] and in the brains of rats and mice after experimentally-induced brain injury. Mechanical injury in the hippocampus of rats causes a shift of FMRP from polysomes to SGs, supporting the idea that SGs form after brain injury [126]. Moreover, sciatic axotomy in mice induces the redistribution of TDP-43 to the cytosol, where it co-localizes with TIA-1 [127]. Additionally, global brain ischaemia leads to rapid eIF2α phosphorylation, SG formation and translational inhibition in hippocampal CA3 neurones [128,129]. Forty-eight hours later, translation is completely restored and CA3 neurones are protected from cell death [129]. By contrast, hippocampal CA1 neurones show persistent SGs and irreversible translational arrest, which is correlated with the increased cell death of CA1 pyramidal neurones [128,129]. At later time-points, some SGs co-localize with ubiquitin [130], suggesting that they might give rise to the ubiquitin-positive protein aggregates that are found in many neurodegenerative diseases.

Interestingly, oxidative stress, damage to the vasculature, mechanical head injury and chronic viral infections were all reported to be risk factors for motor neurone disease and dementia [131–137]. Thus, it is possible that these physiological stressors may trigger the sequestration of RNA-binding proteins (e.g. TDP-43 and FUS) into SGs and thus contribute to neurodegeneration.

SGs in neurodegeneration

In the past few years, dysfunction in RNA metabolism has been recognized as a common theme in several neurodegenerative diseases [6,7,138]. Neurones appear to be especially vulnerable to disturbances in RNA processing and transport, possibly as a result of their long processes, which requires spatial and temporal separation of translation [41,139]. It is conspicuous that several proteins associated with neurodegenerative diseases are RNA-binding proteins and are recruited into SGs (Table 1). The best studied examples are TDP-43 and FUS. Other examples are the 'cousins' of FUS, Ewing sarcoma protein (EWS) and TATA-binding protein-associated factor 15 (TAF15), which are genetically linked to ALS and are co-deposited with FUS in the pathological inclusions in FTLD-FUS patients. Moreover, mutations in the RNA-binding proteins ANG and ataxin-2 (ATXN2) cause ALS, and mutations in the protein SMN lead to ALS or spinal muscular atrophy (SMA). Interestingly, all of these proteins have been found in SGs and/or regulate SG assembly (Table 1). Moreover, SG marker proteins have been identified as components of pathological TDP-43 and FUS inclusions and other proteins involved in different neurodegenerative disorders (Table 2). This suggests that SGs play an important role in neurodegeneration, either as precursors of the pathological inclusions or by the depletion of essential transcripts or RNA-binding proteins, or by a combination of these mechanisms.

TDP-43: an important player in SG formation?

As already noted above, TDP-43 is recruited to SGs in cell lines and primary neurones exposed to different

Table 1. Summary of RNA-binding proteins linked to neurodegenerative diseases and their presence in SGs

Protein	Link to disease [Reference]	Presence in SGs [Reference]
Angiogenin (ANG)	Mutations in ALS [7,186]	Yes [185,188]
Ataxin-2 (ATXN2)	Poly Q expansions in ALS and SCA2 [11,163]	Yes [145,169–172]
Ewing sarcoma protein (EWS)	Mutations in ALS, inclusions in FTLD-FUS [154,155,158]	Yes [150,151]
Fused in sarcoma (FUS)	Mutations and inclusions in ALS/FTLD-FUS, inclusions in polyQ diseases [4,23–25,222–225]	Yes [9,74–76,81,150]
Survival of motor neurone (SMN)	Mutations in ALS and SMA [180]	Yes [181]
TATA-binding protein-associated factor 15 (TAF15)	Mutations in ALS, inclusions in FTLD-FUS [154,155,158]	Yes [150,151,159]
TAR DNA binding protein of 43 kDa (TDP-43)	Mutations and inclusions in ALS/FTLD-TDP [18–20,226–229], inclusions in a subset of Alzheimer's disease [230–232] and Huntington's disease [233]	Yes [10,12,44,127,140–144,146]

experimental stressors [10,12,44,140–144]. Nuclear wild-type TDP-43 is found in SGs only to a minor extent, whereas cytosolic TDP-43 mutants with a defective NLS are efficiently recruited to SGs upon cellular stress [10,12]. Thus, not unexpectedly, TDP-43 needs to be present in the cytosol before being recruited to SGs. Whether TDP-43 can nucleate SGs and how ALS-linked *TARDBP* mutations influence SGs has been intensely investigated over the past few years; however, no clear picture has emerged so far. Some studies have reported that TDP-43 overexpression itself is sufficient to induce SG formation [10,44,51,141,145–147], which would put TDP-43 together with G3BP and TIA-1/TIAR in the group of SG-nucleating proteins. However, other studies have shown that a low level expression of TDP-43 *per se* does not induce SGs, although additional stress is needed for SG formation and recruitment of TDP-43 into SGs [12,140–143]. Thus, experiments with TDP-43 overexpression should be interpreted with caution because it is possible that SG formation in these studies is induced not by the protein itself, but rather by the accompanying transfection stress.

It is still a matter of controversy as to whether small interfering RNA (siRNA)-mediated silencing of TDP-43 affects SGs. One group reported that siRNA-mediated depletion of TDP-43 decelerates initial SG nucleation via TIA-1 and hinders the secondary aggregation of SGs upstream of G3BP [142,148]. However, other groups have observed no change in SG formation upon TDP-43 knockdown [10,140]. Moreover, it is still a matter of debate if and how ALS-associated *TARDBP* mutations affect SG formation. Two groups found that the G348C and R361S mutations lead to fewer SGs [141,142], whereas another group reported more SGs in cells expressing different *TARDBP* mutations (G294A, A315T, Q331K, Q333R) [10]. By contrast, a further study found no differences in SG recruitment of mutant TDP-43 (A315T, M337V or G348C) compared to wild-type TDP-43 [12]. However, the region in which these mutations are clustered (Fig. 1) appears to be crucial for SG recruitment because the deletion of the C-terminal glycine-rich domain abolishes the association of TDP-43 with SGs [12,140,141]. Besides the C-terminal region, the N-terminal domain comprising the major RNA-binding domain (RRM1) (Fig. 1) is also necessary for SG incorporation of TDP-43 because C-terminal fragments (CTFs) of TDP-43 fail to show SG association [12]. Thus, only full-length TDP-43 (and not N- or CTFs) is efficiently recruited to SGs, indicating that efficient SG recruitment of TDP-43 requires both RNA-binding and protein–protein interactions.

Cytosolic FUS is recruited to SGs

Similar to TDP-43, only cytosolically mislocalized FUS but not nuclear wild-type FUS is efficiently sequestered into SGs [9,12,75,81,149]. Thus, although small amounts of endogenous FUS are occasionally found in SGs [150,151], nuclear import defects caused by ALS-associated *FUS* mutations in the proline-tyrosine NLS (Fig. 1) strongly enhance the incorporation of FUS into SGs. Whether cytosolic FUS induces SGs or not remains controversial. Transient overexpression of cytosolic FUS mutants was reported to induce SG formation [74–76]. However, upon mild overexpression or stable expression of FUS mutants, additional stress is needed to induce SGs and to recruit cytosolic FUS into SGs in cell lines, cultured primary neurones or zebrafish embryos [9,12,81,149]. Thus, SGs observed upon the overexpression of mutant FUS (in the absence of exogenous stress) are most likely induced by transfection stress and thus should be interpreted with caution. Furthermore, the finding that siRNA-mediated depletion of FUS does not affect the number

Table 2. SG marker proteins in pathological protein aggregates

Disease	Deposited protein	SG	SG marker(s) analyzed	Analyzed tissue [Reference]
ALS	TDP-43	+	TIA-1, staufen	Spinal cord (sALS) [8]
	TDP-43	–	TIAR, HuR	Spinal cord (sALS) [140]
	TDP-43	+	TIA-1	Spinal cord (sALS) [10]
	TDP-43[a]	+	Ataxin-2	Spinal cord (sALS) [11]
	TDP-43 (full-length)	+	PABP-1	Spinal cord (sALS) [12]
	FUS[b]	+	PABP-1, eIF4G	Spinal cord (fALS-FUS) [9]
	FUS[b]	+	PABP-1	Spinal cord (fALS-FUS) [199]
	SOD-1	+	TIA-1, HuR	Spinal cord extracts (murine) [189]
FTLD	TDP-43	+	eIF3	Frontal cortex (FTLD-TDP) [10]
	TDP-43	+	Ataxin-2	Temporal lobe (FTLD-TDP) [11]
	TDP-43 (full-length)	+	PABP-1	Spinal cord (FTLD-TDP) [12]
	TDP-43 (CTF)	–	PABP-1	Hippocampus (FTLD-TDP) [9,12]
	FUS[b]	+	TIA-1, PABP-1	Motor cortex and spinal cord (FTLD-FUS) [198]
	FUS[b]	+	PABP-1, eIF4G	Hippocampus and spinal cord (FTLD-FUS) [9]
	Tau	+	TIA-1	Frontal cortex (FTLD-tau) [192]
Alzheimer's disease	Tau	+	TIA-1	Frontal cortex (Alzheimer's disease) [192]
SCA2	TDP-43	+	Ataxin-2	Brain stem (SCA2) [11]
Huntington's disease	Htt (poly Q)	+	TIA-1	HEK293 Tet-off cells [190]

[a] Analyzed cases were TDP-proteinopathies; therefore, the deposited protein is presumed to be TDP-43. [b] Analyzed cases were FUS-proteinopathies; therefore, the deposited protein is presumed to be FUS.

or size of SGs [148,151] demonstrates that FUS is not required for SG formation.

Similar to TDP-43, RNA-binding appears to be crucial for SG recruitment of FUS because the main RNA-binding domain of the protein, the C-terminal RGG2-ZnF-RGG3 domain (Fig. 1), is the most important domain for SG recruitment [12]. By contrast, the prion-like SYGQ-domain (Fig. 1) was shown to be dispensable for SG incorporation of FUS [12]. Recently, *in vitro* and yeast studies suggested that the SYGQ-domain confers aggregation propensity and is able to form amyloid-like fibres at high concentrations [149,152], confirming former *in silico* predictions [45]. Mutation of tyrosine residues in this domain prevents the recruitment of cytosolic FUS into SGs [149]. This appears to contradict the finding that the SYGQ-domain is dispensable for SG recruitment of FUS. However, the possibility cannot be excluded that tyrosine mutations convert the resulting protein into a dominant negative mutant, which forms aberrant protein–protein interactions and therefore can no longer be recruited into SGs.

The FET family proteins EWS and TAF15

EWS and TAF15 are two DNA/RNA-binding proteins that are closely related to FUS. Together, these three proteins form a protein family of structurally and functionally related proteins called the FET (FUS, EWS, TAF15) family [153]. Recently, EWS and TAF15 have been implicated in ALS/FTLD because they were found to accumulate together with FUS in pathological protein inclusions in brains of FTLD-FUS patients [154,155]. Additionally, mutations in *EWS* and *TAF15* were identified in ALS patients, although the underlying pathomechanism is still unclear because the mutations do not alter the protein NLS [156–158]. Similar to FUS, both proteins are mainly nuclear, although minor amounts can be incorporated into SGs [150,151,159]. Upon inhibition of transportin-mediated nuclear import, TAF15 accumulates in the cytosol and a substantial fraction is incorporated into SGs [154]. As in FUS, the C-terminal RGG2-ZnF-RGG3 domain of TAF15 was shown to mediate SG recruitment [160]. Thus, cytosolic TAF15 (and possibly EWS) appears to be recruited to SGs by the same mechanisms as FUS.

Ataxin-2, SMN and ANG: linked to ALS and important for SG?

Two genes that encode RNA-binding proteins and are considered to be risk factors for ALS are *ATXN2* and *SMN*. Both proteins appear to play an important role in SG formation. Another protein that is important for SG assembly is ANG, which is mutated in ALS patients.

Ataxin-2 is involved in several RNA processing events and directly interacts with polyribosomes [161,162]. Trinucleotide repeat expansions (> 35 CAG) in the *ATXN2* gene cause a progressive neurodegenerative disease: spinocerebellar ataxia type 2 (SCA2) [163]. An intermediate length repeat expansion (27–33

CAG) in *ATXN2* was found to be a risk factor for sporadic ALS with TDP-43 inclusions [11], a finding that was subsequently reproduced in several other studies [164–167]. In cells overexpressing TDP-43, ataxin-2 forms large cytosolic inclusions and interacts with TDP-43 in an RNA-dependent manner [11]. In ALS-TDP patients, ataxin-2 is found in cytoplasmic inclusions in approximately 25% of spinal cord neurones. Recently, ataxin-2 was also found to co-localize with FUS in cytoplasmic inclusions of ALS-FUS patients [168]. Upon oxidative stress or heat shock, endogenous Ataxin-2 accumulates in SGs, whereas depletion of ataxin-2 strongly reduces the number of SG-positive cells upon arsenite treatment [145,169–172], indicating that ataxin-2 may be necessary for proper SG formation. Whether ataxin-2 inclusions in ALS-TDP and ALS-FUS patients contain SG markers and whether mutant ataxin-2 affects SG formation and the recruitment of TDP-43 or FUS to SGs has not yet been reported.

SMN has important functions in RNA metabolism (e.g. assembly of pre-mRNA splicing complexes and axonal transport of mRNAs) [173]. Initially, mutations in the *SMN* gene were identified in patients suffering from the motor neurone disorder SMA. Disease-causing mutations are loss-of-function mutations resulting in decreased SMN mRNA and protein levels [174–177]. Remarkably, SMN levels correlate with disease severity (i.e. SMN levels are dramatically reduced in severe SMA, although they are decreased only modestly in mild forms of the disease) [176]. Additionally, reduced SMN levels were identified as a risk factor for ALS [178,179]. Upon cellular stress, endogenous SMN is recruited to SGs and, interestingly, fibroblasts from SMA patients or SMN-depleted cells show reduced SG formation [180,181]. This suggests that defects in SG formation might contribute to SMA pathogenesis.

ANG is a ribonuclease with angiogenic and cytoprotective functions [182]. Stress initiates the secretion of ANG by motor neurones to adjacent astrocytes, which take up ANG by clathrin-mediated endocytosis [183]. ANG can cleave tRNAs [184], thus inducing eIF2α-phosphorylation and SG assembly [185]. It has been proposed that this might change the protein profile in astrocytes, which in turn could secrete protective molecules and/or prevent the astrocytic production of toxic factors [182]. Mutations in ANG were identified in ALS patients [7,186] and found to disrupt its RNase activity and subcellular localization [186,187]. Expression of an ALS-associated *ANG* mutant (K40I) with reduced RNAse A activity results in slightly reduced SG formation upon exposure of cells to oxidative stress [188]. Whether this is indeed a pathomechanism of *ANG* mutations remains to be determined.

Non-RNA-binding proteins related to neurodegenerative diseases and SGs

Besides RNA-binding proteins, some non-RNA-binding proteins related to neurodegenerative diseases appear to have a connection to SGs. One example is mutant superoxide dismutase 1 (SOD1), which interacts with SG-associated proteins and co-localizes with SG markers in cell culture and murine spinal cord extracts [189] (Table 2). Another example is mutant huntingtin (Htt) with pathological poly Q expansion, which co-localizes with TIA-1 in different cell lines [190] (Table 2). Moreover, cells expressing an aggresome-forming cytosolic variant of the prion protein are deficient in SG formation [191]. Finally, the microtubule-associated protein tau was shown to facilitate SG formation when co-expressed with TIA-1 in cultured cells, and TIA-1 overexpression enhances the formation of tau aggregates [192]. Based on these findings, it has been proposed that aggregating proteins, such as tau, may stimulate SG formation and cross-seeding of SG aggregation around the primary protein aggregates [13].

SG markers co-localize with pathological protein inclusions in neurodegenerative diseases

Pathological inclusions in several neurodegenerative diseases were reported to co-localize with SG marker proteins (Table 2), suggesting that these inclusions might originate from SGs. First, TDP-43 inclusions in ALS patients were found to co-localize with various SG markers (e.g. TIA-1, PABP-1 and staufen) [8,10–12], although one study reported a lack of TIAR and HuR co-labelling of TDP-43 inclusions [140] (Table 2). Possible explanations for these conflicting results could be variations in SG composition and/or the use of different SG marker antibodies. Similar discrepancies exist for FTLD patients because two studies confirmed the presence of SG marker proteins in FTLD-TDP patients [10,11], whereas another study did not detect SG markers in hippocampal TDP-43 inclusions [9]. These discrepancies might be explained by the finding that different TDP-43 species are present in different brain regions [12,193,194]. Although cortical and hippocampal inclusions are enriched for TDP-43 CTFs and are not co-labelled with PABP-1, inclusions in the spinal cord contain full-length TDP-43 and are positive for SG markers [12]. This suggests that SG marker

co-labelling depends on the presence of full-length TDP-43, which is much more abundant in spinal cord inclusions than in cortical/hippocampal TDP-43 inclusions. Consistently, the cell culture experiments described above show that CTFs of TDP-43 are not incorporated into SGs, probably because they lack the protein's main RNA-binding motif [12]. This observation might be explained by the fact that TDP-43 CTFs are particularly aggregation prone [195–197] and might start to aggregate and form inclusions without the contribution of SGs. This could indicate that CTFs of TDP-43 cause neurotoxicity independently of SGs and challenges the concept that SGs play a pathogenic role in neurodegeneration.

In addition to TDP-43 proteinopathies, all FUSopathies examined show robust co-localization of several SG markers (TIA-1, PABP-1 or eIF4G) with pathological FUS inclusions [9,198,199] (Table 2). Moreover, the co-localization of SG markers with protein aggregates is not only limited to ALS and FTLD, but also has been observed for tau inclusions in Alzheimer's disease and FTLD-tau patients [13,192] and TDP-43-positive inclusions of SCA2 cases [11] (Table 2). These findings strongly suggest that SGs are involved in the formation of pathological protein inclusions in different neurodegenerative diseases. Possible scenarios for how SGs may be connected to pathological protein inclusions are discussed below.

Possible pathomechanims involving SGs

Are SGs precursors of pathological protein inclusions in neurodegenerative diseases?

A key question that remains to be answered is whether pathological protein inclusions originate from SGs (Fig. 3, left), from protein aggregates that fuse with SGs (Fig. 3, middle) or from protein aggregates that secondarily sequester SG marker proteins (Fig. 3, right). The first scenario appears more likely for RNA-binding proteins, such as TDP-43 and FUS, whereas the second and third scenarios appear more plausible for non-RNA-binding proteins, such as tau, SOD1 and Htt.

In the first scenario, cellular stress causes sequestration of TDP-43 or FUS into SGs together with its mRNA targets (Fig. 3, left). Several mutually non-exclusive mechanisms may then contribute to inclusion formation. First, high local concentrations of mRNA-bound TDP-43 or FUS may be reached in SGs. Interestingly, high concentrations of FUS were recently shown to initiate polymerization into amyloid-like fibres *in vitro* [149]. Second, the aggregation of TDP-43 or FUS within SGs might be assisted by the presence of RNA, which was shown to stimulate aggregation of purified tau and PrP [200,201]. Third, SG dissolution might be impaired (e.g. by chronic inhibition of DYRK3 kinase activity) [122]. Additionally, reduced heat shock protein 70 levels [121,202], cellular acidosis [104] or chronic stress [143] may impair SG disassembly. All of these mechanisms could convert reversible SGs into permanent structures and facilitate seeding of TDP-43 or FUS aggregation (Fig. 3, left) [13,203].

In the second scenario, the formation of pathological TDP-43 or FUS inclusions depends on both aggregation and SG formation. (Fig. 3, middle). According to this scenario, TDP-43 or FUS aggregate because they are intrinsically aggregation-prone proteins that rapidly aggregate *in vitro*, yeast and cultured cells [53,149,152,204–206]. *TARDBP* mutations might even increase the aggregation propensity of TDP-43 [10,53–55,205] and the phosphorylation status may furthermore influence the aggregation of TDP-43 [207]. In the case of FUS, defects in arginine methylation might enhance its aggregation, as previously described for other proteins [208–210]. Environmental stress or stress provoked by TDP-43 or FUS aggregates then may elicit SGs, which subsequently may be sequestered by TDP-43 or FUS aggregates (Fig. 3, middle). Such a model has recently been proposed by Wolozin [13], who suggests that protein aggregates stimulate SG formation and serve as a nidus for further aggregation of SGs by binding to other RNA-binding proteins or RNA in SGs. Whether such a cross-seeding mechanism between aggregation-prone proteins and SG components can indeed occur remains to be tested in cellular and animal models.

In the third model, pathological inclusion formation occurs completely independently of SGs (Fig. 3, right). As described in the previous model, TDP-43 or FUS may form protein aggregates as a result of mutations or post-translational modifications (PTMs). Protein–protein interactions between the prion-like domain of TDP-43 or FUS and the prion-like domain of other SG-associated proteins, such as TIA-1 [10,121,149], may secondarily incorporate SG marker proteins into pre-formed TDP-43 or FUS aggregates (Fig. 3, right). In this scenario, the formation of pathological protein inclusions only depends on protein aggregation and further protein–protein interactions, although it is independent of stress and SG formation. To distinguish between the different models, it may be essential to identify the entire set of mRNAs and SG proteins in pathological protein inclusions.

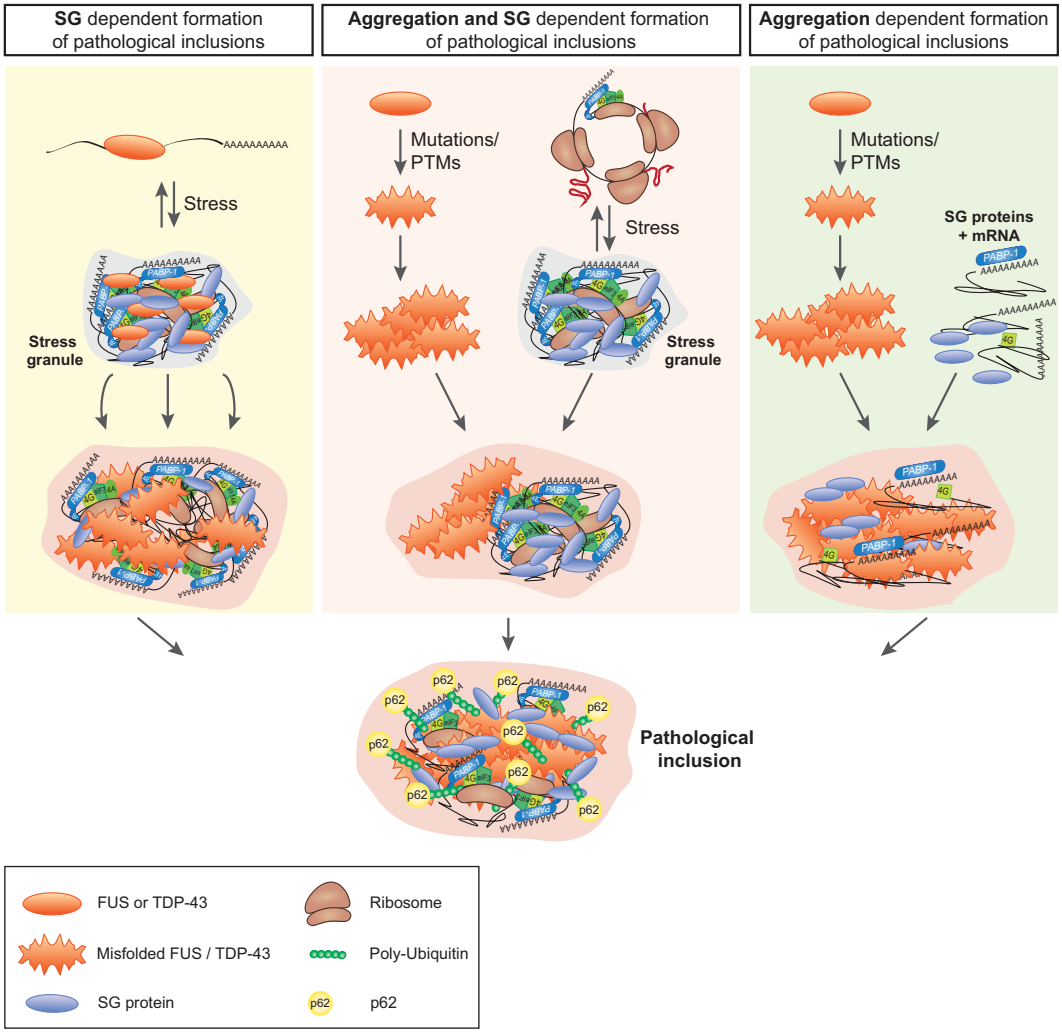

Fig. 3. Alternative models for the formation of SG marker-positive pathological inclusions. The first model (left) proposes that SGs are the origin of pathological TDP-43/FUS inclusions. Upon cellular stress, TDP-43/FUS are sequestered into SGs together with their mRNA targets. This is a reversible process, although the high local concentration of these aggregation-prone proteins within SGs and/or the presence of RNA as a templating agent might trigger the aggregation of TDP-43/FUS. Additionally, defects in SG disassembly (e.g. caused by inhibition of DYRK3 or Hsp70 or by chronic stress) could contribute to the conversion of SGs into pathological inclusions. In the alternative second model (middle), aggregation of FUS/TDP-43 or other aggregation-prone proteins, such as tau, SOD1 and poly Q Htt, is triggered by mutations or post-translational modifications (PTMs). These aggregates and/or external stress stimuli elicit the formation of SGs, which are then sequestered by pre-formed FUS/TDP-43 aggregates via protein–protein or protein–RNA interactions. In the third model (right), inclusions form completely independently of stress and SGs. Mutations and/or PTMs that enhance the intrinsic aggregation propensity of FUS, TDP-43 and other aggregation-prone proteins result in misfolded protein aggregates. Subsequently, SG marker proteins, such as TIA-1 or PABP-1, may be recruited into these aggregates together with their bound mRNA. The presence of ubiquitin and p62 in these SG marker-positive pathological inclusions (bottom) may indicate that a defect in the clearance of these aggregates by the protein degradation machinery contributes to inclusion formation.

Because pathological TDP-43/FUS inclusions also contain ubiquitin and p62/sequestosome 1 [211–213] (Fig. 3, bottom), defects in protein degradation may furthermore contribute to the formation of pathological protein inclusions. TDP-43 or FUS aggregates might become polyubiquitinated and thus tagged for degradation. Subsequently, p62/sequestosome 1 may bind the ubiquitin chains and target these protein aggregates for autophagic degradation [214,215]. However, this pathway may be functionally impaired or overwhelmed [216], leading to persistent ubiquitin and p62-positive inclusions (Fig. 3, bottom).

Are SGs protective or detrimental?

As explained earlier in this minireview, SG formation is generally considered to be a protective mechanism because SGs enable the preferential synthesis of stress-protective proteins and sequester pro-apoptotic proteins. For example, the chemical inhibition of SG formation after cold shock results in increased cell death [107]. Moreover, neurones that mount an efficient stress response (i.e. transient formation of SGs followed by a complete recovery of translation) are protected from ischaemia-induced cell death [128,129], further supporting the notion that SGs have an important neuroprotective function. This also could explain why mutations in genes that play a role in SG formation, such as *ATXN2*, *SMN* and *ANG*, are associated with neurodegenerative diseases (Table 1).

Even though SGs may initially be cytoprotective, they may become neurotoxic when the SG pathway is overactive [13] or when SGs fail to dissolve and translational repression persists for too long. This appears to be the case in hippocampal CA1 neurones, which show an irreversible translational arrest and increased cell death after global brain ischaemia [128,129]. Another example is prion replication, in which persistent eIF2α-mediated translational repression causes synaptic loss and neurotoxicity in mice [217]. Overexpression of GADD34, a eIF2α-phosphatase, reduces the levels of phosphorylated eIF2α and rescues neuronal loss and survival. Although SG formation was not examined in that study, it is possible that SGs induced by phosphorylated eIF2α may contribute to neurodegeneration in this model.

Nevertheless, because SGs have important stress-protective functions, pharmacological inhibition of SG formation, recently proposed as a therapeutic approach [13], might not be a viable strategy for therapeutic intervention because severe side effects are to be expected.

How may aberrant SGs cause toxicity?

The permanent trapping of TDP-43, FUS or other aggregation-prone proteins together with SG proteins (Fig. 3) may cause toxicity through a variety of loss-of-function or gain-of-function mechanisms. TDP-43 and FUS both have a multitude of different functions, such as regulating pre-mRNA splicing, transcription and mRNA transport into dendritic spines [5,69,218], and so it would not be unexpected if trapping of TDP-43 or FUS in persistent SGs or mature inclusions resulted in a detrimental loss-of-function. Moreover, the other RNA-binding proteins that are recruited into SGs and are found in pathological inclusions in neurodegenerative diseases, such as EWS, TAF15 and ATXN2 (Tables 1 and 2), may also not be able to fulfill their physiological function. Finally, permanent trapping of SG marker proteins and mRNAs in persistent SGs or inclusions may further contribute to a toxic loss-of-function. Besides trapping of essential RNA-binding proteins or SG proteins, sustained translational arrest may cause a toxic loss-of-function of all kinds of essential cellular proteins.

Alternatively, or additionally, deposition of TDP-43, FUS or other aggregation-prone proteins together with SG proteins in irreversible cytosolic aggregates might provoke toxicity through gain-of-function mechanisms. Aggregated TDP-43 or FUS or SG proteins may have altered protein–protein or protein–RNA interactions (e.g. they may lose or gain interaction partners or display altered binding kinetics). Furthermore, permanent trapping of TDP-43 in SGs may initiate a toxic feed-forward mechanism that enhances TDP-43 expression because TDP-43 autoregulates its own levels [34,219].

Concluding remarks

Over the past 6 years, we have rapidly increased our knowledge about the key genes and pathological proteins in two fatal neurodegenerative diseases: FTLD and ALS. Nevertheless, cellular and animal models that mimic the human pathology are still missing. Interestingly, many stressors that can elicit SG formation in cultured cells or animal models (e.g. oxidative stress, mitochondrial dysfunction, viral infection, brain injury and damage to the vasculature) have been implicated in neurodegeneration [131,132,137,220,221]. Given the evidence that SGs might play an important role in ALS/FTLD pathogenesis, it will be essential to incorporate these stressors (or even a combination of different stressors) into our current cellular and animal models. This may more faithfully recapitulate the human neuropathology and the neurodegenerative process. Long-term *in vivo* imaging in such models may eventually allow us to visualize the conversion of SGs into pathological protein aggregates. Additionally, it will be important to gain a deeper understanding of the basic cell biology of SGs. Identifying the factors and mechanisms that are involved in the dissolution of SGs or their conversion into permanent structures will be the next big enigma that requires a solution.

Acknowledgements

We thank Marc Suarez-Calvet, Maria Funke, Katrin Strecker, Bettina Schmid and Anja Capell for critically

reading the manuscript. This work was supported by the Competence Network for Neurodegenerative Diseases (KNDD) of the Bundesministerium für Bildung und Forschung (BMBF, to C.H.) and the Consortium of Centers of Excellence in Neurodegenerative Brain Diseases (CoEN, to C.H.). The research leading to these results has received funding from the European Research Council under the European Union's Seventh Framework Programme (FP7/2007-2013)/ERC grant agreement no. 321366-Amyloid (to C.H.). E.B. is supported by the Elite Network of Bavaria and D.D. is supported by the Robert Bosch Foundation. We regret that we were unable to cite every important reference owing to limitations of space.

References

1 Haass C & Selkoe DJ (2007) Soluble protein oligomers in neurodegeneration: lessons from the Alzheimer's amyloid beta-peptide. *Nat Rev Mol Cell Biol* **8**, 101–112.
2 Arai T, Hasegawa M, Akiyama H, Ikeda K, Nonaka T, Mori H, Mann D, Tsuchiya K, Yoshida M, Hashizume Y *et al*. (2006) TDP-43 is a component of ubiquitin-positive tau-negative inclusions in frontotemporal lobar degeneration and amyotrophic lateral sclerosis. *Biochem Biophys Res Commun* **351**, 602–611.
3 Neumann M, Sampathu DM, Kwong LK, Truax AC, Micsenyi MC, Chou TT, Bruce J, Schuck T, Grossman M, Clark CM *et al*. (2006) Ubiquitinated TDP-43 in frontotemporal lobar degeneration and amyotrophic lateral sclerosis. *Science* **314**, 130–133.
4 Neumann M, Rademakers R, Roeber S, Baker M, Kretzschmar HA & Mackenzie IR (2009) A new subtype of frontotemporal lobar degeneration with FUS pathology. *Brain* **132**, 2922–2931.
5 Lagier-Tourenne C, Polymenidou M & Cleveland DW (2010) TDP-43 and FUS/TLS: emerging roles in RNA processing and neurodegeneration. *Hum Mol Genet* **19**, R46–R64.
6 Polymenidou M, Lagier-Tourenne C, Hutt KR, Bennett CF, Cleveland DW & Yeo GW (2012) Misregulated RNA processing in amyotrophic lateral sclerosis. *Brain Res* **1462**, 3–15.
7 van Blitterswijk M & Landers JE (2010) RNA processing pathways in amyotrophic lateral sclerosis. *Neurogenetics* **11**, 275–290.
8 Volkening K, Leystra-Lantz C, Yang W, Jaffee H & Strong MJ (2009) Tar DNA binding protein of 43 kDa (TDP-43), 14–3-3 proteins and copper/zinc superoxide dismutase (SOD1) interact to modulate NFL mRNA stability. Implications for altered RNA processing in amyotrophic lateral sclerosis (ALS). *Brain Res* **1305**, 168–182.
9 Dormann D, Rodde R, Edbauer D, Bentmann E, Fischer I, Hruscha A, Than ME, Mackenzie IR, Capell A, Schmid B *et al*. (2010) ALS-associated fused in sarcoma (FUS) mutations disrupt transportin-mediated nuclear import. *EMBO J* **29**, 2841–2857.
10 Liu-Yesucevitz L, Bilgutay A, Zhang YJ, Vanderwyde T, Citro A, Mehta T, Zaarur N, McKee A, Bowser R, Sherman M *et al*. (2010) Tar DNA binding protein-43 (TDP-43) associates with stress granules: analysis of cultured cells and pathological brain tissue. *PLoS One* **5**, e13250.
11 Elden AC, Kim HJ, Hart MP, Chen-Plotkin AS, Johnson BS, Fang X, Armakola M, Geser F, Greene R, Lu MM *et al*. (2010) Ataxin-2 intermediate-length polyglutamine expansions are associated with increased risk for ALS. *Nature* **466**, 1069–1075.
12 Bentmann E, Neumann M, Tahirovic S, Rodde R, Dormann D & Haass C (2012) Requirements for stress granule recruitment of fused in Sarcoma (FUS) and TAR DNA binding protein of 43 kDa (TDP-43). *J Biol Chem* **287**, 23079–23094.
13 Wolozin B (2012) Regulated protein aggregation: stress granules and neurodegeneration. *Mol Neurodegener* **7**, 56.
14 van Langenhove T, van der Zee J & van Broeckhoven C (2012) The molecular basis of the frontotemporal lobar degeneration-amyotrophic lateral sclerosis spectrum. *Ann Med* **8**, 817–828.
15 Kiernan MC, Vucic S, Cheah BC, Turner MR, Eisen A, Hardiman O, Burrell JR & Zoing MC (2011) Amyotrophic lateral sclerosis. *Lancet* **377**, 942–955.
16 Snowden JS, Neary D & Mann DM (2002) Frontotemporal dementia. *Br J Psychiatry* **180**, 140–143.
17 Strong MJ, Grace GM, Freedman M, Lomen-Hoerth C, Woolley S, Goldstein LH, Murphy J, Shoesmith C, Rosenfeld J, Leigh PN *et al*. (2009) Consensus criteria for the diagnosis of frontotemporal cognitive and behavioural syndromes in amyotrophic lateral sclerosis. *Amyotroph Lateral Scler* **10**, 131–146.
18 Gitcho MA, Baloh RH, Chakraverty S, Mayo K, Norton JB, Levitch D, Hatanpaa KJ, White CL III, Bigio EH, Caselli R *et al*. (2008) TDP-43 A315T mutation in familial motor neuron disease. *Ann Neurol* **63**, 535–538.
19 Sreedharan J, Blair IP, Tripathi VB, Hu X, Vance C, Rogelj B, Ackerley S, Durnall JC, Williams KL, Buratti E *et al*. (2008) TDP-43 mutations in familial and sporadic amyotrophic lateral sclerosis. *Science* **319**, 1668–1672.
20 Kabashi E, Valdmanis PN, Dion P, Spiegelman D, McConkey BJ, Vande Velde C, Bouchard JP, Lacomblez L, Pochigaeva K, Salachas F *et al*. (2008) TARDBP mutations in individuals with sporadic and

familial amyotrophic lateral sclerosis. *Nat Genet* **40**, 572–574.
21 Van Deerlin VM, Leverenz JB, Bekris LM, Bird TD, Yuan W, Elman LB, Clay D, Wood EM, Chen-Plotkin AS, Martinez-Lage M *et al.* (2008) TARDBP mutations in amyotrophic lateral sclerosis with TDP-43 neuropathology: a genetic and histopathological analysis. *Lancet Neurol* **7**, 409–416.
22 Mackenzie IR, Rademakers R & Neumann M (2010) TDP-43 and FUS in amyotrophic lateral sclerosis and frontotemporal dementia. *Lancet Neurol* **9**, 995–1007.
23 Kwiatkowski TJ Jr, Bosco DA, Leclerc AL, Tamrazian E, Vanderburg CR, Russ C, Davis A, Gilchrist J, Kasarskis EJ, Munsat T *et al.* (2009) Mutations in the FUS/TLS gene on chromosome 16 cause familial amyotrophic lateral sclerosis. *Science* **323**, 1205–1208.
24 Vance C, Rogelj B, Hortobagyi T, De Vos KJ, Nishimura AL, Sreedharan J, Hu X, Smith B, Ruddy D, Wright P *et al.* (2009) Mutations in FUS, an RNA processing protein, cause familial amyotrophic lateral sclerosis type 6. *Science* **323**, 1208–1211.
25 Munoz DG, Neumann M, Kusaka H, Yokota O, Ishihara K, Terada S, Kuroda S & Mackenzie IR (2009) FUS pathology in basophilic inclusion body disease. *Acta Neuropathol* **118**, 617–627.
26 Neumann M, Roeber S, Kretzschmar HA, Rademakers R, Baker M & Mackenzie IR (2009) Abundant FUS-immunoreactive pathology in neuronal intermediate filament inclusion disease. *Acta Neuropathol* **118**, 605–616.
27 Dejesus-Hernandez M, Mackenzie IR, Boeve BF, Boxer AL, Baker M, Rutherford NJ, Nicholson AM, Finch NA, Flynn H, Adamson J *et al.* (2011) Expanded GGGGCC hexanucleotide repeat in noncoding region of C9ORF72 causes chromosome 9p-linked FTD and ALS. *Neuron* **72**, 245–256.
28 Renton AE, Majounie E, Waite A, Simon-Sanchez J, Rollinson S, Gibbs JR, Schymick JC, Laaksovirta H, van Swieten JC, Myllykangas L *et al.* (2011) A hexanucleotide repeat expansion in C9ORF72 is the cause of chromosome 9p21-linked ALS-FTD. *Neuron* **72**, 257–268.
29 Gijselinck I, Van Langenhove T, van der Zee J, Sleegers K, Philtjens S, Kleinberger G, Janssens J, Bettens K, Van Cauwenberghe C, Pereson S *et al.* (2012) A C9orf72 promoter repeat expansion in a Flanders-Belgian cohort with disorders of the frontotemporal lobar degeneration-amyotrophic lateral sclerosis spectrum: a gene identification study. *Lancet Neurol* **11**, 54–65.
30 Mori K, Weng SM, Arzberger T, May S, Rentzsch K, Kremmer E, Schmid B, Kretzschmar HA, Cruts M, Van Broeckhoven C *et al.* (2013) The C9orf72 GGGGCC repeat is translated into aggregating dipeptide-repeat proteins in FTLD/ALS. *Science* **339**, 1335–1338.
31 Ash PE, Bieniek KF, Gendron TF, Caulfield T, Lin WL, Dejesus-Hernandez M, van Blitterswijk MM, Jansen-West K, Paul JW III, Rademakers R *et al.* (2013) Unconventional translation of C9ORF72 GGGGCC expansion generates insoluble polypeptides specific to c9FTD/ALS. *Neuron* **77**, 639–646.
32 Ou SH, Wu F, Harrich D, Garcia-Martinez LF & Gaynor RB (1995) Cloning and characterization of a novel cellular protein, TDP-43, that binds to human immunodeficiency virus type 1 TAR DNA sequence motifs. *J Virol* **69**, 3584–3596.
33 Buratti E & Baralle FE (2001) Characterization and functional implications of the RNA binding properties of nuclear factor TDP-43, a novel splicing regulator of CFTR exon 9. *J Biol Chem* **276**, 36337–36343.
34 Polymenidou M, Lagier-Tourenne C, Hutt KR, Huelga SC, Moran J, Liang TY, Ling SC, Sun E, Wancewicz E, Mazur C *et al.* (2011) Long pre-mRNA depletion and RNA missplicing contribute to neuronal vulnerability from loss of TDP-43. *Nat Neurosci* **14**, 459–468.
35 Tollervey JR, Curk T, Rogelj B, Briese M, Cereda M, Kayikci M, Konig J, Hortobagyi T, Nishimura AL, Zupunski V *et al.* (2011) Characterizing the RNA targets and position-dependent splicing regulation by TDP-43. *Nat Neurosci* **14**, 452–458.
36 Buratti E & Baralle FE (2010) The multiple roles of TDP-43 in pre-mRNA processing and gene expression regulation. *RNA Biol* **7**, 420–429.
37 Kawahara Y & Mieda-Sato A (2012) TDP-43 promotes microRNA biogenesis as a component of the Drosha and Dicer complexes. *Proc Natl Acad Sci USA* **109**, 3347–3352.
38 Elvira G, Wasiak S, Blandford V, Tong XK, Serrano A, Fan X, del Rayo Sanchez-Carbente M, Servant F, Bell AW, Boismenu D *et al.* (2006) Characterization of an RNA granule from developing brain. *Mol Cell Proteomics* **5**, 635–651.
39 Wang IF, Wu LS, Chang HY & Shen CK (2008) TDP-43, the signature protein of FTLD-U, is a neuronal activity-responsive factor. *J Neurochem* **105**, 797–806.
40 Lu Y, Ferris J & Gao FB (2009) Frontotemporal dementia and amyotrophic lateral sclerosis-associated disease protein TDP-43 promotes dendritic branching. *Mol Brain* **2**, 30.
41 Liu-Yesucevitz L, Bassell GJ, Gitler AD, Hart AC, Klann E, Richter JD, Warren ST & Wolozin B (2011) Local RNA translation at the synapse and in disease. *J Neurosci* **31**, 16086–16093.
42 Buratti E, Brindisi A, Giombi M, Tisminetzky S, Ayala YM & Baralle FE (2005) TDP-43 binds heterogeneous nuclear ribonucleoprotein A/B through its C-terminal tail: an important region for the

inhibition of cystic fibrosis transmembrane conductance regulator exon 9 splicing. *J Biol Chem* **280**, 37572–37584.
43 D'Ambrogio A, Buratti E, Stuani C, Guarnaccia C, Romano M, Ayala YM & Baralle FE (2009) Functional mapping of the interaction between TDP-43 and hnRNP A2 *in vivo*. *Nucleic Acids Res* **37**, 4116–4126.
44 Freibaum BD, Chitta RK, High AA & Taylor JP (2010) Global analysis of TDP-43 interacting proteins reveals strong association with RNA splicing and translation machinery. *J Proteome Res* **9**, 1104–1120.
45 Cushman M, Johnson BS, King OD, Gitler AD & Shorter J (2010) Prion-like disorders: blurring the divide between transmissibility and infectivity. *J Cell Sci* **123**, 1191–1201.
46 Fuentealba RA, Udan M, Bell S, Wegorzewska I, Shao J, Diamond MI, Weihl CC & Baloh RH (2010) Interaction with polyglutamine aggregates reveals a Q/N-rich domain in TDP-43. *J Biol Chem* **285**, 26304–26314.
47 Udan M & Baloh RH (2011) Implications of the prion-related Q/N domains in TDP-43 and FUS. *Prion* **5**, 1–5.
48 Ling SC, Albuquerque CP, Han JS, Lagier-Tourenne C, Tokunaga S, Zhou H & Cleveland DW (2010) ALS-associated mutations in TDP-43 increase its stability and promote TDP-43 complexes with FUS/TLS. *Proc Natl Acad Sci USA* **107**, 13318–13323.
49 Kim SH, Shanware NP, Bowler MJ & Tibbetts RS (2010) Amyotrophic lateral sclerosis-associated proteins TDP-43 and FUS/TLS function in a common biochemical complex to co-regulate HDAC6 mRNA. *J Biol Chem* **285**, 34097–34105.
50 Ritson GP, Custer SK, Freibaum BD, Guinto JB, Geffel D, Moore J, Tang W, Winton MJ, Neumann M, Trojanowski JQ *et al*. (2010) TDP-43 mediates degeneration in a novel *Drosophila* model of disease caused by mutations in VCP/p97. *J Neurosci* **30**, 7729–7739.
51 Barmada SJ, Skibinski G, Korb E, Rao EJ, Wu JY & Finkbeiner S (2010) Cytoplasmic mislocalization of TDP-43 is toxic to neurons and enhanced by a mutation associated with familial amyotrophic lateral sclerosis. *J Neurosci* **30**, 639–649.
52 Voigt A, Herholz D, Fiesel FC, Kaur K, Muller D, Karsten P, Weber SS, Kahle PJ, Marquardt T & Schulz JB (2010) TDP-43-mediated neuron loss *in vivo* requires RNA-binding activity. *PLoS One* **5**, e12247.
53 Johnson BS, Snead D, Lee JJ, McCaffery JM, Shorter J & Gitler AD (2009) TDP-43 is intrinsically aggregation-prone, and amyotrophic lateral sclerosis-linked mutations accelerate aggregation and increase toxicity. *J Biol Chem* **284**, 20329–20339.
54 Nonaka T, Kametani F, Arai T, Akiyama H & Hasegawa M (2009) Truncation and pathogenic mutations facilitate the formation of intracellular aggregates of TDP-43. *Hum Mol Genet* **18**, 3353–3364.
55 Arai T, Hasegawa M, Nonoka T, Kametani F, Yamashita M, Hosokawa M, Niizato K, Tsuchiya K, Kobayashi Z, Ikeda K *et al*. (2010) Phosphorylated and cleaved TDP-43 in ALS, FTLD and other neurodegenerative disorders and in cellular models of TDP-43 proteinopathy. *Neuropathology* **30**, 170–181.
56 Kabashi E, Lin L, Tradewell ML, Dion PA, Bercier V, Bourgouin P, Rochefort D, Bel Hadj S, Durham HD, Vande Velde C *et al*. (2010) Gain and loss of function of ALS-related mutations of TARDBP (TDP-43) cause motor deficits *in vivo*. *Hum Mol Genet* **19**, 671–683.
57 Liachko NF, Guthrie CR & Kraemer BC (2010) Phosphorylation promotes neurotoxicity in a *Caenorhabditis elegans* model of TDP-43 proteinopathy. *J Neurosci* **30**, 16208–16219.
58 Zhou H, Huang C, Chen H, Wang D, Landel CP, Xia PY, Bowser R, Liu YJ & Xia XG (2010) Transgenic rat model of neurodegeneration caused by mutation in the TDP gene. *PLoS Genet* **6**, e1000887.
59 Wang JW, Brent JR, Tomlinson A, Shneider NA & McCabe BD (2011) The ALS-associated proteins FUS and TDP-43 function together to affect *Drosophila* locomotion and life span. *J Clin Invest* **121**, 4118–4126.
60 Schmid B, Hruscha A, Hogl S, Banzhaf-Strathmann J, Strecker K, van der Zee J, Teucke M, Eimer S, Hegermann J, Kittelmann M *et al*. (2013) Loss of ALS-associated TDP-43 in zebrafish causes muscle degeneration, vascular dysfunction, and reduced motor neuron axon outgrowth. *Proc Natl Acad Sci USA* **110**, 4986–4991.
61 Crozat A, Aman P, Mandahl N & Ron D (1993) Fusion of CHOP to a novel RNA-binding protein in human myxoid liposarcoma. *Nature* **363**, 640–644.
62 Rabbitts TH, Forster A, Larson R & Nathan P (1993) Fusion of the dominant negative transcription regulator CHOP with a novel gene FUS by translocation t(12;16) in malignant liposarcoma. *Nat Genet* **4**, 175–180.
63 Lagier-Tourenne C, Polymenidou M, Hutt KR, Vu AQ, Baughn M, Huelga SC, Clutario KM, Ling SC, Liang TY, Mazur C *et al*. (2012) Divergent roles of ALS-linked proteins FUS/TLS and TDP-43 intersect in processing long pre-mRNAs. *Nat Neurosci* **15**, 1488–1497.
64 Ishigaki S, Masuda A, Fujioka Y, Iguchi Y, Katsuno M, Shibata A, Urano F, Sobue G & Ohno K (2012) Position-dependent FUS-RNA interactions regulate alternative splicing events and transcriptions. *Sci Rep* **2**, 529.

65 Rogelj B, Easton LE, Bogu GK, Stanton LW, Rot G, Curk T, Zupan B, Sugimoto Y, Modic M, Haberman N *et al.* (2012) Widespread binding of FUS along nascent RNA regulates alternative splicing in the brain. *Sci Rep* **2**, 603.
66 Kanai Y, Dohmae N & Hirokawa N (2004) Kinesin transports RNA: isolation and characterization of an RNA-transporting granule. *Neuron* **43**, 513–525.
67 Fujii R, Okabe S, Urushido T, Inoue K, Yoshimura A, Tachibana T, Nishikawa T, Hicks GG & Takumi T (2005) The RNA binding protein TLS is translocated to dendritic spines by mGluR5 activation and regulates spine morphology. *Curr Biol* **15**, 587–593.
68 Yoshimura A, Fujii R, Watanabe Y, Okabe S, Fukui K & Takumi T (2006) Myosin-Va facilitates the accumulation of mRNA/protein complex in dendritic spines. *Curr Biol* **16**, 2345–2351.
69 Dormann D & Haass C (2013) Fused in sarcoma (FUS): an oncogene goes awry in neurodegeneration. *Mol Cell Neurosci*, doi:10.1016/j.mcn.2013.03.006.
70 Zinszner H, Albalat R & Ron D (1994) A novel effector domain from the RNA-binding protein TLS or EWS is required for oncogenic transformation by CHOP. *Genes Dev* **8**, 2513–2526.
71 Prasad DD, Ouchida M, Lee L, Rao VN & Reddy ES (1994) TLS/FUS fusion domain of TLS/FUS-erg chimeric protein resulting from the t(16;21) chromosomal translocation in human myeloid leukemia functions as a transcriptional activation domain. *Oncogene* **9**, 3717–3729.
72 Lerga A, Hallier M, Delva L, Orvain C, Gallais I, Marie J & Moreau-Gachelin F (2001) Identification of an RNA binding specificity for the potential splicing factor TLS. *J Biol Chem* **276**, 6807–6816.
73 Iko Y, Kodama TS, Kasai N, Oyama T, Morita EH, Muto T, Okumura M, Fujii R, Takumi T, Tate S *et al.* (2004) Domain architectures and characterization of an RNA-binding protein, TLS. *J Biol Chem* **279**, 44834–44840.
74 Gal J, Zhang J, Kwinter DM, Zhai J, Jia H, Jia J & Zhu H (2011) Nuclear localization sequence of FUS and induction of stress granules by ALS mutants. *Neurobiol Aging* **32**, 2323.e27–e40.
75 Ito D, Seki M, Tsunoda Y, Uchiyama H & Suzuki N (2011) Nuclear transport impairment of amyotrophic lateral sclerosis-linked mutations in FUS/TLS. *Ann Neurol* **69**, 152–162.
76 Kino Y, Washizu C, Aquilanti E, Okuno M, Kurosawa M, Yamada M, Doi H & Nukina N (2010) Intracellular localization and splicing regulation of FUS/TLS are variably affected by amyotrophic lateral sclerosis-linked mutations. *Nucleic Acids Res* **39**, 2781–2798.
77 Zhang ZC & Chook YM (2012) Structural and energetic basis of ALS-causing mutations in the atypical proline-tyrosine nuclear localization signal of the fused in sarcoma protein (FUS). *Proc Natl Acad Sci USA* **109**, 12017–12021.
78 Niu C, Zhang J, Gao F, Yang L, Jia M, Zhu H & Gong W (2012) FUS-NLS/Transportin 1 complex structure provides insights into the nuclear targeting mechanism of FUS and the implications in ALS. *PLoS One* **7**, e47056.
79 Dormann D & Haass C (2011) TDP-43 and FUS: a nuclear affair. *Trends Neurosci* **34**, 339–348.
80 Nishimura AL, Zupunski V, Troakes C, Kathe C, Fratta P, Howell M, Gallo JM, Hortobagyi T, Shaw CE & Rogelj B (2010) Nuclear import impairment causes cytoplasmic trans-activation response DNA-binding protein accumulation and is associated with frontotemporal lobar degeneration. *Brain* **133**, 1763–1771.
81 Bosco DA, Lemay N, Ko HK, Zhou H, Burke C, Kwiatkowski TJ Jr, Sapp P, McKenna-Yasek D, Brown RH Jr & Hayward LJ (2010) Mutant FUS proteins that cause amyotrophic lateral sclerosis incorporate into stress granules. *Hum Mol Genet* **19**, 4160–4175.
82 Kedersha N & Anderson P (2002) Stress granules: sites of mRNA triage that regulate mRNA stability and translatability. *Biochem Soc Trans* **30**, 963–969.
83 Anderson P & Kedersha N (2008) Stress granules: the tao of RNA triage. *Trends Biochem Sci* **33**, 141–150.
84 Kedersha N, Stoecklin G, Ayodele M, Yacono P, Lykke-Andersen J, Fritzler MJ, Scheuner D, Kaufman RJ, Golan DE & Anderson P (2005) Stress granules and processing bodies are dynamically linked sites of mRNP remodeling. *J Cell Biol* **169**, 871–884.
85 Kulkarni M, Ozgur S & Stoecklin G (2010) On track with P-bodies. *Biochem Soc Trans* **38**, 242–251.
86 Buchan JR, Capaldi AP & Parker R (2012) TOR-tured yeast find a new way to stand the heat. *Mol Cell* **47**, 155–157.
87 Kim WJ, Back SH, Kim V, Ryu I & Jang SK (2005) Sequestration of TRAF2 into stress granules interrupts tumor necrosis factor signaling under stress conditions. *Mol Cell Biol* **25**, 2450–2462.
88 Arimoto K, Fukuda H, Imajoh-Ohmi S, Saito H & Takekawa M (2008) Formation of stress granules inhibits apoptosis by suppressing stress-responsive MAPK pathways. *Nat Cell Biol* **10**, 1324–1332.
89 Buchan JR & Parker R (2009) Eukaryotic stress granules: the ins and outs of translation. *Mol Cell* **36**, 932–941.
90 Takahara T & Maeda T (2012) Transient sequestration of TORC1 into stress granules during heat stress. *Mol Cell* **47**, 242–252.
91 Hamilton TL, Stoneley M, Spriggs KA & Bushell M (2006) TOPs and their regulation. *Biochem Soc Trans* **34**, 12–16.

92 Spriggs KA, Bushell M & Willis AE (2010) Translational regulation of gene expression during conditions of cell stress. *Mol Cell* **40**, 228–237.
93 Damgaard CK & Lykke-Andersen J (2011) Translational coregulation of 5'TOP mRNAs by TIA-1 and TIAR. *Genes Dev* **25**, 2057–2068.
94 Stohr N, Lederer M, Reinke C, Meyer S, Hatzfeld M, Singer RH & Huttelmaier S (2006) ZBP1 regulates mRNA stability during cellular stress. *J Cell Biol* **175**, 527–534.
95 Bornes S, Boulard M, Hieblot C, Zanibellato C, Iacovoni JS, Prats H & Touriol C (2004) Control of the vascular endothelial growth factor internal ribosome entry site (IRES) activity and translation initiation by alternatively spliced coding sequences. *J Biol Chem* **279**, 18717–18726.
96 Sherrill KW, Byrd MP, Van Eden ME & Lloyd RE (2004) BCL-2 translation is mediated via internal ribosome entry during cell stress. *J Biol Chem* **279**, 29066–29074.
97 Bornes S, Prado-Lourenco L, Bastide A, Zanibellato C, Iacovoni JS, Lacazette E, Prats AC, Touriol C & Prats H (2007) Translational induction of VEGF internal ribosome entry site elements during the early response to ischemic stress. *Circ Res* **100**, 305–308.
98 Kedersha NL, Gupta M, Li W, Miller I & Anderson P (1999) RNA-binding proteins TIA-1 and TIAR link the phosphorylation of eIF-2 alpha to the assembly of mammalian stress granules. *J Cell Biol* **147**, 1431–1442.
99 Kimball SR, Horetsky RL, Ron D, Jefferson LS & Harding HP (2003) Mammalian stress granules represent sites of accumulation of stalled translation initiation complexes. *Am J Physiol Cell Physiol* **284**, C273–C284.
100 Anderson P & Kedersha N (2006) RNA granules. *J Cell Biol* **172**, 803–808.
101 Moser JJ & Fritzler MJ (2010) Cytoplasmic ribonucleoprotein (RNP) bodies and their relationship to GW/P bodies. *Int J Biochem Cell Biol* **42**, 828–843.
102 Kedersha N & Anderson P (2007) Mammalian stress granules and processing bodies. *Methods Enzymol* **431**, 61–81.
103 Lloyd RE (2012) How do viruses interact with stress-associated RNA granules? *PLoS Pathog* **8**, e1002741.
104 Chudinova EM, Nadezhdina ES & Ivanov PA (2012) Cellular acidosis inhibits assembly, disassembly, and motility of stress granules. *Biochemistry* **77**, 1277–1284.
105 Pothof J, Verkaik NS, Hoeijmakers JH & van Gent DC (2009) MicroRNA responses and stress granule formation modulate the DNA damage response. *Cell Cycle* **8**, 3462–3468.
106 Emara MM, Fujimura K, Sciaranghella D, Ivanova V, Ivanov P & Anderson P (2012) Hydrogen peroxide induces stress granule formation independent of eIF2alpha phosphorylation. *Biochem Biophys Res Commun* **423**, 763–769.
107 Hofmann S, Cherkasova V, Bankhead P, Bukau B & Stoecklin G (2012) Translation suppression promotes stress granule formation and cell survival in response to cold shock. *Mol Biol Cell* **23**, 3786–3800.
108 Anderson P & Kedersha N (2009) Stress granules. *Curr Biol* **19**, R397–R398.
109 Bordeleau ME, Mori A, Oberer M, Lindqvist L, Chard LS, Higa T, Belsham GJ, Wagner G, Tanaka J & Pelletier J (2006) Functional characterization of IRESes by an inhibitor of the RNA helicase eIF4A. *Nat Chem Biol* **2**, 213–220.
110 Bordeleau ME, Matthews J, Wojnar JM, Lindqvist L, Novac O, Jankowsky E, Sonenberg N, Northcote P, Teesdale-Spittle P & Pelletier J (2005) Stimulation of mammalian translation initiation factor eIF4A activity by a small molecule inhibitor of eukaryotic translation. *Proc Natl Acad Sci USA* **102**, 10460–10465.
111 Low WK, Dang Y, Schneider-Poetsch T, Shi Z, Choi NS, Merrick WC, Romo D & Liu JO (2005) Inhibition of eukaryotic translation initiation by the marine natural product pateamine A. *Mol Cell* **20**, 709–722.
112 Mazroui R, Sukarieh R, Bordeleau ME, Kaufman RJ, Northcote P, Tanaka J, Gallouzi I & Pelletier J (2006) Inhibition of ribosome recruitment induces stress granule formation independently of eukaryotic initiation factor 2alpha phosphorylation. *Mol Biol Cell* **17**, 4212–4219.
113 Mokas S, Mills JR, Garreau C, Fournier MJ, Robert F, Arya P, Kaufman RJ, Pelletier J & Mazroui R (2009) Uncoupling stress granule assembly and translation initiation inhibition. *Mol Biol Cell* **20**, 2673–2683.
114 Ohn T, Kedersha N, Hickman T, Tisdale S & Anderson P (2008) A functional RNAi screen links O-GlcNAc modification of ribosomal proteins to stress granule and processing body assembly. *Nat Cell Biol* **10**, 1224–1231.
115 Ohn T & Anderson P (2010) The role of posttranslational modifications in the assembly of stress granules. *Wiley Interdiscip Rev RNA* **1**, 486–493.
116 Dolzhanskaya N, Merz G, Aletta JM & Denman RB (2006) Methylation regulates the intracellular protein–protein and protein–RNA interactions of FMRP. *J Cell Sci* **119**, 1933–1946.
117 De Leeuw F, Zhang T, Wauquier C, Huez G, Kruys V & Gueydan C (2007) The cold-inducible RNA-binding protein migrates from the nucleus to cytoplasmic stress granules by a methylation-dependent mechanism and acts as a translational repressor. *Exp Cell Res* **313**, 4130–4144.

118 Dormann D, Madl T, Valori CF, Bentmann E, Tahirovic S, Abou-Ajram C, Kremmer E, Ansorge O, Mackenzie IR, Neumann M *et al*. (2012) Arginine methylation next to the PY-NLS modulates transportin binding and nuclear import of FUS. *EMBO J* **31**, 4258–4275.
119 Tradewell ML, Yu Z, Tibshirani M, Boulanger MC, Durham HD & Richard S (2011) Arginine methylation by PRMT1 regulates nuclear-cytoplasmic localization and toxicity of FUS/TLS harbouring ALS-linked mutations. *Hum Mol Genet* **21**, 136–149.
120 Thomas MG, Martinez Tosar LJ, Desbats MA, Leishman CC & Boccaccio GL (2009) Mammalian staufen 1 is recruited to stress granules and impairs their assembly. *J Cell Sci* **122**, 563–573.
121 Gilks N, Kedersha N, Ayodele M, Shen L, Stoecklin G, Dember LM & Anderson P (2004) Stress granule assembly is mediated by prion-like aggregation of TIA-1. *Mol Biol Cell* **15**, 5383–5398.
122 Wippich F, Bodenmiller B, Trajkovska MG, Wanka S, Aebersold R & Pelkmans L (2013) Dual specificity kinase DYRK3 couples stress granule condensation/dissolution to mTORC1 signaling. *Cell* **152**, 791–805.
123 Kedersha N, Cho MR, Li W, Yacono PW, Chen S, Gilks N, Golan DE & Anderson P (2000) Dynamic shuttling of TIA-1 accompanies the recruitment of mRNA to mammalian stress granules. *J Cell Biol* **151**, 1257–1268.
124 Kozak SL, Marin M, Rose KM, Bystrom C & Kabat D (2006) The anti-HIV-1 editing enzyme APOBEC3G binds HIV-1 RNA and messenger RNAs that shuttle between polysomes and stress granules. *J Biol Chem* **281**, 29105–29119.
125 van der Laan AM, van Gemert AM, Dirks RW, Noordermeer JN, Fradkin LG, Tanke HJ & Jost CR (2012) mRNA cycles through hypoxia-induced stress granules in live *Drosophila* embryonic muscles. *Int J Dev Biol* **56**, 701–709.
126 Kim SH, Dong WK, Weiler IJ & Greenough WT (2006) Fragile X mental retardation protein shifts between polyribosomes and stress granules after neuronal injury by arsenite stress or *in vivo* hippocampal electrode insertion. *J Neurosci* **26**, 2413–2418.
127 Moisse K, Volkening K, Leystra-Lantz C, Welch I, Hill T & Strong MJ (2009) Divergent patterns of cytosolic TDP-43 and neuronal progranulin expression following axotomy: implications for TDP-43 in the physiological response to neuronal injury. *Brain Res* **1249**, 202–211.
128 Kayali F, Montie HL, Rafols JA & DeGracia DJ (2005) Prolonged translation arrest in reperfused hippocampal cornu Ammonis 1 is mediated by stress granules. *Neuroscience* **134**, 1223–1245.
129 Jamison JT, Kayali F, Rudolph J, Marshall M, Kimball SR & DeGracia DJ (2008) Persistent redistribution of poly-adenylated mRNAs correlates with translation arrest and cell death following global brain ischemia and reperfusion. *Neuroscience* **154**, 504–520.
130 DeGracia DJ, Rudolph J, Roberts GG, Rafols JA & Wang J (2007) Convergence of stress granules and protein aggregates in hippocampal cornu ammonis 1 at later reperfusion following global brain ischemia. *Neuroscience* **146**, 562–572.
131 Barber SC & Shaw PJ (2010) Oxidative stress in ALS: key role in motor neuron injury and therapeutic target. *Free Radical Biol Med* **48**, 629–641.
132 Quaegebeur A, Lange C & Carmeliet P (2011) The neurovascular link in health and disease: molecular mechanisms and therapeutic implications. *Neuron* **71**, 406–424.
133 Gavett BE, Stern RA & McKee AC(2011) Chronic traumatic encephalopathy: a potential late effect of sport-related concussive and subconcussive head trauma. *Clin Sports Med* **30**, 179–188, xi.
134 Abel EL (2007) Football increases the risk for Lou Gehrig's disease, amyotrophic lateral sclerosis. *Percept Mot Skills* **104**, 1251–1254.
135 Chen H, Richard M, Sandler DP, Umbach DM & Kamel F (2007) Head injury and amyotrophic lateral sclerosis. *Am J Epidemiol* **166**, 810–816.
136 Chio A, Calvo A, Dossena M, Ghiglione P, Mutani R & Mora G (2009) ALS in Italian professional soccer players: the risk is still present and could be soccer-specific. *Amyotroph Lateral Scler* **10**, 205–209.
137 De Chiara G, Marcocci ME, Sgarbanti R, Civitelli L, Ripoli C, Piacentini R, Garaci E, Grassi C & Palamara AT (2012) Infectious agents and neurodegeneration. *Mol Neurobiol* **46**, 614–638.
138 Renoux AJ & Todd PK (2012) Neurodegeneration the RNA way. *Prog Neurobiol* **97**, 173–189.
139 Ferraiuolo L, Kirby J, Grierson AJ, Sendtner M & Shaw PJ (2011) Molecular pathways of motor neuron injury in amyotrophic lateral sclerosis. *Nat Rev Neurol* **7**, 616–630.
140 Colombrita C, Zennaro E, Fallini C, Weber M, Sommacal A, Buratti E, Silani V & Ratti A (2009) TDP-43 is recruited to stress granules in conditions of oxidative insult. *J Neurochem* **111**, 1051–1061.
141 Dewey CM, Cenik B, Sephton CF, Dries DR, Mayer P III, Good SK, Johnson BA, Herz J & Yu G (2011) TDP-43 Is directed to stress granules by sorbitol, a novel physiological osmotic and oxidative stressor. *Mol Cell Biol* **31**, 1098–1108.
142 McDonald KK, Aulas A, Destroismaisons L, Pickles S, Beleac E, Camu W, Rouleau GA & Vande Velde C (2011) TAR DNA-binding protein 43 (TDP-43) regulates stress granule dynamics via differential

regulation of G3BP and TIA-1. *Hum Mol Genet* **20**, 1400–1410.
143 Meyerowitz J, Parker SJ, Vella LJ, Ng D, Price KA, Liddell JR, Caragounis A, Li QX, Masters CL, Nonaka T *et al.* (2011) C-Jun N-terminal kinase controls TDP-43 accumulation in stress granules induced by oxidative stress. *Mol Neurodegener* **6**, 57.
144 Parker SJ, Meyerowitz J, James JL, Liddell JR, Crouch PJ, Kanninen KM & White AR (2012) Endogenous TDP-43 localized to stress granules can subsequently form protein aggregates. *Neurochem Int* **60**, 415–424.
145 Nihei Y, Ito D & Suzuki N (2012) Roles of ataxin-2 in pathological cascades mediated by TAR DNA-binding protein 43 (TDP-43) and fused in sarcoma (FUS). *J Biol Chem* **287**, 41310–41323.
146 Dammer EB, Fallini C, Gozal YM, Duong DM, Rossoll W, Xu P, Lah JJ, Levey AI, Peng J, Bassell GJ *et al.* (2012) Coaggregation of RNA-binding proteins in a model of TDP-43 proteinopathy with selective RGG motif methylation and a role for RRM1 ubiquitination. *PLoS One* **7**, e38658.
147 Nishimoto Y, Ito D, Yagi T, Nihei Y, Tsunoda Y & Suzuki N (2010) Characterization of alternative isoforms and inclusion body of the TAR DNA-binding protein-43. *J Biol Chem* **285**, 608–619.
148 Aulas A, Stabile S & Vande Velde C (2012) Endogenous TDP-43, but not FUS, contributes to stress granule assembly via G3BP. *Mol Neurodegener* **7**, 54.
149 Kato M, Han TW, Xie S, Shi K, Du X, Wu LC, Mirzaei H, Goldsmith EJ, Longgood J, Pei J *et al.* (2012) Cell-free formation of RNA granules: low complexity sequence domains form dynamic fibers within hydrogels. *Cell* **149**, 753–767.
150 Andersson MK, Stahlberg A, Arvidsson Y, Olofsson A, Semb H, Stenman G, Nilsson O & Aman P (2008) The multifunctional FUS, EWS and TAF15 proto-oncoproteins show cell type-specific expression patterns and involvement in cell spreading and stress response. *BMC Cell Biol* **9**, 37–53.
151 Blechingberg J, Luo Y, Bolund L, Damgaard CK & Nielsen AL (2012) Gene expression responses to FUS, EWS, and TAF15 reduction and stress granule sequestration analyses identifies FET-protein non-redundant functions. *PLoS One* **7**, e46251.
152 Sun Z, Diaz Z, Fang X, Hart MP, Chesi A, Shorter J & Gitler AD (2011) Molecular determinants and genetic modifiers of aggregation and toxicity for the ALS disease protein FUS/TLS. *PLoS Biol* **9**, e1000614.
153 Tan AY & Manley JL (2009) The TET family of proteins: functions and roles in disease. *J Mol Cell Biol* **1**, 82–92.
154 Neumann M, Bentmann E, Dormann D, Jawaid A, DeJesus-Hernandez M, Ansorge O, Roeber S, Kretzschmar HA, Munoz DG, Kusaka H *et al.* (2011) FET proteins TAF15 and EWS are selective markers that distinguish FTLD with FUS pathology from amyotrophic lateral sclerosis with FUS mutations. *Brain* **134**, 2595–2609.
155 Davidson YS, Robinson AC, Hu Q, Mishra M, Baborie A, Jaros E, Perry RH, Cairns NJ, Richardson A, Gerhard A *et al.* (2012) Nuclear carrier and RNA binding proteins in frontotemporal lobar degeneration associated with fused in sarcoma (FUS) pathological changes. *Neuropathol Appl Neurobiol*, doi:10.1111/j.1365-2990.
156 Couthouis J, Hart MP, Shorter J, DeJesus-Hernandez M, Erion R, Oristano R, Liu AX, Ramos D, Jethava N, Hosangadi D *et al.* (2011) A yeast functional screen predicts new candidate ALS disease genes. *Proc Natl Acad Sci USA* **108**, 20881–20890.
157 Ticozzi N, Vance C, Leclerc AL, Keagle P, Glass JD, McKenna-Yasek D, Sapp PC, Silani V, Bosco DA, Shaw CE *et al.* (2011) Mutational analysis reveals the FUS homolog TAF15 as a candidate gene for familial amyotrophic lateral sclerosis. *Am J Med Genet B Neuropsychiatr Genet* **156B**, 285–290.
158 Couthouis J, Hart MP, Erion R, King OD, Diaz Z, Nakaya T, Ibrahim F, Kim HJ, Mojsilovic-Petrovic J, Panossian S *et al.* (2012) Evaluating the role of the FUS/TLS-related gene EWSR1 in amyotrophic lateral sclerosis. *Hum Mol Genet* **21**, 2899–2911.
159 Jobert L, Argentini M & Tora L (2009) PRMT1 mediated methylation of TAF15 is required for its positive gene regulatory function. *Exp Cell Res* **315**, 1273–1286.
160 Marko M, Vlassis A, Guialis A & Leichter M (2012) Domains involved in TAF15 subcellular localisation: dependence on cell type and ongoing transcription. *Gene* **506**, 331–338.
161 Albrecht M, Golatta M, Wullner U & Lengauer T (2004) Structural and functional analysis of ataxin-2 and ataxin-3. *Eur J Biochem* **271**, 3155–3170.
162 Satterfield TF & Pallanck LJ (2006) Ataxin-2 and its *Drosophila* homolog, ATX2, physically assemble with polyribosomes. *Hum Mol Genet* **15**, 2523–2532.
163 Pulst SM, Nechiporuk A, Nechiporuk T, Gispert S, Chen XN, Lopes-Cendes I, Pearlman S, Starkman S, Orozco-Diaz G, Lunkes A *et al.* (1996) Moderate expansion of a normally biallelic trinucleotide repeat in spinocerebellar ataxia type 2. *Nat Genet* **14**, 269–276.
164 Lee T, Li YR, Ingre C, Weber M, Grehl T, Gredal O, de Carvalho M, Meyer T, Tysnes OB, Auburger G *et al.* (2011) Ataxin-2 intermediate-length polyglutamine expansions in European ALS patients. *Hum Mol Genet* **20**, 1697–1700.
165 Corrado L, Mazzini L, Oggioni GD, Luciano B, Godi M, Brusco A & D'Alfonso S (2011) ATXN-2 CAG

repeat expansions are interrupted in ALS patients. *Hum Genet* **130**, 575–580.
166 Ross OA, Rutherford NJ, Baker M, Soto-Ortolaza AI, Carrasquillo MM, DeJesus-Hernandez M, Adamson J, Li M, Volkening K, Finger E *et al.* (2011) Ataxin-2 repeat-length variation and neurodegeneration. *Hum Mol Genet* **20**, 3207–3212.
167 Van Damme P, Veldink JH, van Blitterswijk M, Corveleyn A, van Vught PW, Thijs V, Dubois B, Matthijs G, van den Berg LH & Robberecht W (2011) Expanded ATXN2 CAG repeat size in ALS identifies genetic overlap between ALS and SCA2. *Neurology* **76**, 2066–2072.
168 Farg MA, Soo KY, Warraich ST, Sundaramoorthy V, Blair IP & Atkin JD (2013) Ataxin-2 interacts with FUS and intermediate-length polyglutamine expansions enhance FUS-related pathology in amyotrophic lateral sclerosis. *Hum Mol Genet* **22**, 717–728.
169 Nonhoff U, Ralser M, Welzel F, Piccini I, Balzereit D, Yaspo ML, Lehrach H & Krobitsch S (2007) Ataxin-2 interacts with the DEAD/H-box RNA helicase DDX6 and interferes with P-bodies and stress granules. *Mol Biol Cell* **18**, 1385–1396.
170 Ariumi Y, Kuroki M, Kushima Y, Osugi K, Hijikata M, Maki M, Ikeda M & Kato N (2011) Hepatitis C virus hijacks P-body and stress granule components around lipid droplets. *J Virol* **85**, 6882–6892.
171 Buchan JR, Muhlrad D & Parker R (2008) P bodies promote stress granule assembly in *Saccharomyces cerevisiae*. *J Cell Biol* **183**, 441–455.
172 Ralser M, Albrecht M, Nonhoff U, Lengauer T, Lehrach H & Krobitsch S (2005) An integrative approach to gain insights into the cellular function of human ataxin-2. *J Mol Biol* **346**, 203–214.
173 Fallini C, Bassell GJ & Rossoll W (2012) Spinal muscular atrophy: the role of SMN in axonal mRNA regulation. *Brain Res* **1462**, 81–92.
174 Lefebvre S, Burglen L, Reboullet S, Clermont O, Burlet P, Viollet L, Benichou B, Cruaud C, Millasseau P, Zeviani M *et al.* (1995) Identification and characterization of a spinal muscular atrophy-determining gene. *Cell* **80**, 155–165.
175 Gennarelli M, Lucarelli M, Capon F, Pizzuti A, Merlini L, Angelini C, Novelli G & Dallapiccola B (1995) Survival motor neuron gene transcript analysis in muscles from spinal muscular atrophy patients. *Biochem Biophys Res Commun* **213**, 342–348.
176 Lefebvre S, Burlet P, Liu Q, Bertrandy S, Clermont O, Munnich A, Dreyfuss G & Melki J (1997) Correlation between severity and SMN protein level in spinal muscular atrophy. *Nat Genet* **16**, 265–269.
177 Coovert DD, Le TT, McAndrew PE, Strasswimmer J, Crawford TO, Mendell JR, Coulson SE, Androphy EJ, Prior TW & Burghes AH (1997) The survival motor neuron protein in spinal muscular atrophy. *Hum Mol Genet* **6**, 1205–1214.
178 Veldink JH, van den Berg LH, Cobben JM, Stulp RP, De Jong JM, Vogels OJ, Baas F, Wokke JH & Scheffer H (2001) Homozygous deletion of the survival motor neuron 2 gene is a prognostic factor in sporadic ALS. *Neurology* **56**, 749–752.
179 Corcia P, Mayeux-Portas V, Khoris J, de Toffol B, Autret A, Muh JP, Camu W & Andres C (2002) Abnormal SMN1 gene copy number is a susceptibility factor for amyotrophic lateral sclerosis. *Ann Neurol* **51**, 243–246.
180 Hua Y & Zhou J (2004) Survival motor neuron protein facilitates assembly of stress granules. *FEBS Lett* **572**, 69–74.
181 Zou T, Yang X, Pan D, Huang J, Sahin M & Zhou J (2011) SMN deficiency reduces cellular ability to form stress granules, sensitizing cells to stress. *Cell Mol Neurobiol* **31**, 541–550.
182 Aparicio-Erriu IM & Prehn JH (2012) Molecular mechanisms in amyotrophic lateral sclerosis: the role of angiogenin, a secreted RNase. *Front Neurosci* **6**, 167.
183 Skorupa A, King MA, Aparicio IM, Dussmann H, Coughlan K, Breen B, Kieran D, Concannon CG, Marin P & Prehn JH (2012) Motoneurons secrete angiogenin to induce RNA cleavage in astroglia. *J Neurosci* **32**, 5024–5038.
184 Fu H, Feng J, Liu Q, Sun F, Tie Y, Zhu J, Xing R, Sun Z & Zheng X (2009) Stress induces tRNA cleavage by angiogenin in mammalian cells. *FEBS Lett* **583**, 437–442.
185 Emara MM, Ivanov P, Hickman T, Dawra N, Tisdale S, Kedersha N, Hu GF & Anderson P (2010) Angiogenin-induced tRNA-derived stress-induced RNAs promote stress-induced stress granule assembly. *J Biol Chem* **285**, 10959–10968.
186 Greenway MJ, Andersen PM, Russ C, Ennis S, Cashman S, Donaghy C, Patterson V, Swingler R, Kieran D, Prehn J *et al.* (2006) ANG mutations segregate with familial and 'sporadic' amyotrophic lateral sclerosis. *Nat Genet* **38**, 411–413.
187 Crabtree B, Thiyagarajan N, Prior SH, Wilson P, Iyer S, Ferns T, Shapiro R, Brew K, Subramanian V & Acharya KR (2007) Characterization of human angiogenin variants implicated in amyotrophic lateral sclerosis. *Biochemistry* **46**, 11810–11818.
188 Thiyagarajan N, Ferguson R, Subramanian V & Acharya KR (2012) Structural and molecular insights into the mechanism of action of human angiogenin-ALS variants in neurons. *Nat Commun* **3**, 1121.
189 Lu L, Wang S, Zheng L, Li X, Suswam EA, Zhang X, Wheeler CG, Nabors LB, Filippova N & King PH (2009) Amyotrophic lateral sclerosis-linked mutant SOD1 sequesters Hu antigen R (HuR) and TIA-1-

related protein (TIAR): implications for impaired post-transcriptional regulation of vascular endothelial growth factor. *J Biol Chem* **284**, 33989–33998.
190 Waelter S, Boeddrich A, Lurz R, Scherzinger E, Lueder G, Lehrach H & Wanker EE (2001) Accumulation of mutant huntingtin fragments in aggresome-like inclusion bodies as a result of insufficient protein degradation. *Mol Biol Cell* **12**, 1393–1407.
191 Goggin K, Beaudoin S, Grenier C, Brown AA & Roucou X (2008) Prion protein aggresomes are poly (A)+ ribonucleoprotein complexes that induce a PKR-mediated deficient cell stress response. *Biochim Biophys Acta* **1783**, 479–491.
192 Vanderweyde T, Yu H, Varnum M, Liu-Yesucevitz L, Citro A, Ikezu T, Duff K & Wolozin B (2012) Contrasting pathology of the stress granule proteins TIA-1 and G3BP in tauopathies. *J Neurosci* **32**, 8270–8283.
193 Igaz LM, Kwong LK, Xu Y, Truax AC, Uryu K, Neumann M, Clark CM, Elman LB, Miller BL, Grossman M *et al.* (2008) Enrichment of C-terminal fragments in TAR DNA-binding protein-43 cytoplasmic inclusions in brain but not in spinal cord of frontotemporal lobar degeneration and amyotrophic lateral sclerosis. *Am J Pathol* **173**, 182–194.
194 Neumann M, Kwong LK, Lee EB, Kremmer E, Flatley A, Xu Y, Forman MS, Troost D, Kretzschmar HA, Trojanowski JQ *et al.* (2009) Phosphorylation of S409/410 of TDP-43 is a consistent feature in all sporadic and familial forms of TDP-43 proteinopathies. *Acta Neuropathol* **117**, 137–149.
195 Igaz LM, Kwong LK, Chen-Plotkin A, Winton MJ, Unger TL, Xu Y, Neumann M, Trojanowski JQ & Lee VM (2009) Expression Of TDP-43 C-terminal fragments *in vitro* recapitulates pathological features of TDP-43 proteinopathies. *J Biol Chem* **284**, 8516–8524.
196 Zhang YJ, Xu YF, Cook C, Gendron TF, Roettges P, Link CD, Lin WL, Tong J, Castanedes-Casey M, Ash P *et al.* (2009) Aberrant cleavage of TDP-43 enhances aggregation and cellular toxicity. *Proc Natl Acad Sci USA* **106**, 7607–7612.
197 Yang C, Tan W, Whittle C, Qiu L, Cao L, Akbarian S & Xu Z (2010) The C-terminal TDP-43 fragments have a high aggregation propensity and harm neurons by a dominant-negative mechanism. *PLoS One* **5**, e15878.
198 Fujita K, Ito H, Nakano S, Kinoshita Y, Wate R & Kusaka H (2008) Immunohistochemical identification of messenger RNA-related proteins in basophilic inclusions of adult-onset atypical motor neuron disease. *Acta Neuropathol* **116**, 439–445.
199 Baumer D, Hilton D, Paine SM, Turner MR, Lowe J, Talbot K & Ansorge O (2010) Juvenile ALS with basophilic inclusions is a FUS proteinopathy with FUS mutations. *Neurology* **75**, 611–618.
200 Kampers T, Friedhoff P, Biernat J, Mandelkow EM & Mandelkow E (1996) RNA stimulates aggregation of microtubule-associated protein tau into Alzheimer-like paired helical filaments. *FEBS Lett* **399**, 344–349.
201 Deleault NR, Lucassen RW & Supattapone S (2003) RNA molecules stimulate prion protein conversion. *Nature* **425**, 717–720.
202 Mazroui R, Di Marco S, Kaufman RJ & Gallouzi IE (2007) Inhibition of the ubiquitin-proteasome system induces stress granule formation. *Mol Biol Cell* **18**, 2603–2618.
203 Polymenidou M & Cleveland DW (2011) The seeds of neurodegeneration: prion-like spreading in ALS. *Cell* **147**, 498–508.
204 Furukawa Y, Kaneko K, Watanabe S, Yamanaka K & Nukina N (2011) A seeding reaction recapitulates intracellular formation of sarkosyl-insoluble TAR DNA binding protein-43 inclusions. *J Biol Chem* **286**, 18664–18672.
205 Guo W, Chen Y, Zhou X, Kar A, Ray P, Chen X, Rao EJ, Yang M, Ye H, Zhu L *et al.* (2011) An ALS-associated mutation affecting TDP-43 enhances protein aggregation, fibril formation and neurotoxicity. *Nat Struct Mol Biol* **18**, 822–830.
206 Johnson BS, McCaffery JM, Lindquist S & Gitler AD (2008) A yeast TDP-43 proteinopathy model: exploring the molecular determinants of TDP-43 aggregation and cellular toxicity. *Proc Natl Acad Sci USA* **105**, 6439–6444.
207 Brady OA, Meng P, Zheng Y, Mao Y & Hu F (2011) Regulation of TDP-43 aggregation by phosphorylation and p62/SQSTM1. *J Neurochem* **116**, 248–259.
208 Yu MC, Bachand F, McBride AE, Komili S, Casolari JM & Silver PA (2004) Arginine methyltransferase affects interactions and recruitment of mRNA processing and export factors. *Genes Dev* **18**, 2024–2035.
209 Ostareck-Lederer A, Ostareck DH, Rucknagel KP, Schierhorn A, Moritz B, Huttelmaier S, Flach N, Handoko L & Wahle E (2006) Asymmetric arginine dimethylation of heterogeneous nuclear ribonucleoprotein K by protein-arginine methyltransferase 1 inhibits its interaction with c-Src. *J Biol Chem* **281**, 11115–11125.
210 Perreault A, Lemieux C & Bachand F (2007) Regulation of the nuclear poly(A)-binding protein by arginine methylation in fission yeast. *J Biol Chem* **282**, 7552–7562.
211 Kuusisto E, Kauppinen T & Alafuzoff I (2008) Use of p62/SQSTM1 antibodies for neuropathological diagnosis. *Neuropathol Appl Neurobiol* **34**, 169–180.
212 Mizuno Y, Amari M, Takatama M, Aizawa H, Mihara B & Okamoto K (2006) Immunoreactivities of p62, an ubiqutin-binding protein, in the spinal anterior horn cells of patients with amyotrophic lateral sclerosis. *J Neurol Sci* **249**, 13–18.

213 Zatloukal K, Stumptner C, Fuchsbichler A, Heid H, Schnoelzer M, Kenner L, Kleinert R, Prinz M, Aguzzi A & Denk H (2002) p62 Is a common component of cytoplasmic inclusions in protein aggregation diseases. *Am J Pathol* **160**, 255–263.
214 Bjorkoy G, Lamark T, Brech A, Outzen H, Perander M, Overvatn A, Stenmark H & Johansen T (2005) p62/SQSTM1 forms protein aggregates degraded by autophagy and has a protective effect on huntingtin-induced cell death. *J Cell Biol* **171**, 603–614.
215 Pankiv S, Clausen TH, Lamark T, Brech A, Bruun JA, Outzen H, Overvatn A, Bjorkoy G & Johansen T (2007) p62/SQSTM1 binds directly to Atg8/LC3 to facilitate degradation of ubiquitinated protein aggregates by autophagy. *J Biol Chem* **282**, 24131–24145.
216 Wong E & Cuervo AM (2010) Autophagy gone awry in neurodegenerative diseases. *Nat Neurosci* **13**, 805–811.
217 Moreno JA, Radford H, Peretti D, Steinert JR, Verity N, Martin MG, Halliday M, Morgan J, Dinsdale D, Ortori CA *et al.* (2012) Sustained translational repression by eIF2alpha-P mediates prion neurodegeneration. *Nature* **485**, 507–511.
218 Fiesel FC & Kahle PJ (2011) TDP-43 and FUS/TLS: cellular functions and implications for neurodegeneration. *FEBS J* **278**, 3550–3568.
219 Ayala YM, De Conti L, Avendano-Vazquez SE, Dhir A, Romano M, D'Ambrogio A, Tollervey J, Ule J, Baralle M, Buratti E *et al.* (2011) TDP-43 regulates its mRNA levels through a negative feedback loop. *EMBO J* **30**, 277–288.
220 Saxena S & Caroni P (2011) Selective neuronal vulnerability in neurodegenerative diseases: from stressor thresholds to degeneration. *Neuron* **71**, 35–48.
221 McKee AC, Cantu RC, Nowinski CJ, Hedley-Whyte ET, Gavett BE, Budson AE, Santini VE, Lee HS, Kubilus CA & Stern RA (2009) Chronic traumatic encephalopathy in athletes: progressive tauopathy after repetitive head injury. *J Neuropathol Exp Neurol* **68**, 709–735.
222 Aguzzi A & Haass C (2003) Games played by rogue proteins in prion disorders and Alzheimer's disease. *Science* **302**, 814–818.
223 Woulfe J, Gray DA & Mackenzie IR (2010) FUS-immunoreactive intranuclear inclusions in neurodegenerative disease. *Brain Pathol* **20**, 589–597.
224 Doi H, Okamura K, Bauer PO, Furukawa Y, Shimizu H, Kurosawa M, Machida Y, Miyazaki H, Mitsui K, Kuroiwa Y *et al.* (2008) RNA-binding protein TLS is a major nuclear aggregate-interacting protein in huntingtin exon 1 with expanded polyglutamine-expressing cells. *J Biol Chem* **283**, 6489–6500.
225 Doi H, Koyano S, Suzuki Y, Nukina N & Kuroiwa Y (2010) The RNA-binding protein FUS/TLS is a common aggregate-interacting protein in polyglutamine diseases. *Neurosci Res* **66**, 131–133.
226 Benajiba L, Le Ber I, Camuzat A, Lacoste M, Thomas-Anterion C, Couratier P, Legallic S, Salachas F, Hannequin D, Decousus M *et al.* (2009) TARDBP mutations in motoneuron disease with frontotemporal lobar degeneration. *Ann Neurol* **65**, 470–473.
227 Borroni B, Bonvicini C, Alberici A, Buratti E, Agosti C, Archetti S, Papetti A, Stuani C, Di Luca M, Gennarelli M *et al.* (2009) Mutation within TARDBP leads to frontotemporal dementia without motor neuron disease. *Hum Mutat* **30**, E974–E983.
228 Gitcho MA, Bigio EH, Mishra M, Johnson N, Weintraub S, Mesulam M, Rademakers R, Chakraverty S, Cruchaga C, Morris JC *et al.* (2009) TARDBP 3′-UTR variant in autopsy-confirmed frontotemporal lobar degeneration with TDP-43 proteinopathy. *Acta Neuropathol* **118**, 633–645.
229 Kovacs GG, Murrell JR, Horvath S, Haraszti L, Majtenyi K, Molnar MJ, Budka H, Ghetti B & Spina S (2009) TARDBP variation associated with frontotemporal dementia, supranuclear gaze palsy, and chorea. *Mov Disord* **24**, 1843–1847.
230 Amador-Ortiz C, Lin WL, Ahmed Z, Personett D, Davies P, Duara R, Graff-Radford NR, Hutton ML & Dickson DW (2007) TDP-43 immunoreactivity in hippocampal sclerosis and Alzheimer's disease. *Ann Neurol* **61**, 435–445.
231 Youmans KL & Wolozin B (2012) TDP-43: a new player on the AD field? *Exp Neurol* **237**, 90–95.
232 Wilson AC, Dugger BN, Dickson DW & Wang DS (2011) TDP-43 in aging and Alzheimer's disease – a review. *Int J Clin Exp Pathol* **4**, 147–155.
233 Schwab C, Arai T, Hasegawa M, Yu S & McGeer PL (2008) Colocalization of transactivation-responsive DNA-binding protein 43 and huntingtin in inclusions of Huntington disease. *J Neuropathol Exp Neurol* **67**, 1159–1165.